frontiers | Research Topics

Soil microbial communities to promote suppressiveness against soil-borne pathogens and diseases

Edited by
Jesus Fernandez Bayo, Massimo Pugliese, Francesco Di Gioia, Dongdong Yan and Jose Ignacio Marín-Guirao

Published in
Frontiers in Microbiology

ISSN 1664-8714
ISBN 978-2-8325-6922-1
DOI 10.3389/978-2-8325-6922-1

Generative AI statement
Any alternative text (Alt text) provided alongside figures in the articles in this ebook has been generated by Frontiers with the support of artificial intelligence and reasonable efforts have been made to ensure accuracy, including review by the authors wherever possible. If you identify any issues, please contact us.

About Frontiers

Frontiers is more than just an open access publisher of scholarly articles: it is a pioneering approach to the world of academia, radically improving the way scholarly research is managed. The grand vision of Frontiers is a world where all people have an equal opportunity to seek, share and generate knowledge. Frontiers provides immediate and permanent online open access to all its publications, but this alone is not enough to realize our grand goals.

Frontiers journal series

The Frontiers journal series is a multi-tier and interdisciplinary set of open-access, online journals, promising a paradigm shift from the current review, selection and dissemination processes in academic publishing. All Frontiers journals are driven by researchers for researchers; therefore, they constitute a service to the scholarly community. At the same time, the *Frontiers journal series* operates on a revolutionary invention, the tiered publishing system, initially addressing specific communities of scholars, and gradually climbing up to broader public understanding, thus serving the interests of the lay society, too.

Dedication to quality

Each Frontiers article is a landmark of the highest quality, thanks to genuinely collaborative interactions between authors and review editors, who include some of the world's best academicians. Research must be certified by peers before entering a stream of knowledge that may eventually reach the public - and shape society; therefore, Frontiers only applies the most rigorous and unbiased reviews. Frontiers revolutionizes research publishing by freely delivering the most outstanding research, evaluated with no bias from both the academic and social point of view. By applying the most advanced information technologies, Frontiers is catapulting scholarly publishing into a new generation.

What are Frontiers Research Topics?

Frontiers Research Topics are very popular trademarks of the *Frontiers journals series*: they are collections of at least ten articles, all centered on a particular subject. With their unique mix of varied contributions from Original Research to Review Articles, Frontiers Research Topics unify the most influential researchers, the latest key findings and historical advances in a hot research area.

Find out more on how to host your own Frontiers Research Topic or contribute to one as an author by contacting the Frontiers editorial office: frontiersin.org/about/contact

Soil microbial communities to promote suppressiveness against soil-borne pathogens and diseases

Topic editors
Jesus Fernandez Bayo — University of Granada, Spain
Massimo Pugliese — University of Turin, Italy
Francesco Di Gioia — The Pennsylvania State University (PSU), United States
Dongdong Yan — Chinese Academy of Agricultural Sciences (CAAS), China
Jose Ignacio Marín-Guirao — IFAPA Centro La Mojonera, Spain

Citation
Fernandez Bayo, J., Pugliese, M., Di Gioia, F., Yan, D., Marín-Guirao, J. I., eds. (2025). *Soil microbial communities to promote suppressiveness against soil-borne pathogens and diseases*. Lausanne: Frontiers Media SA.
doi: 10.3389/978-2-8325-6922-1

Table of contents

frontiers | Frontiers in Microbiology

TYPE Editorial
PUBLISHED 16 September 2025
DOI 10.3389/fmicb.2025.1677158

OPEN ACCESS

EDITED AND REVIEWED BY
Jeanette M. Norton,
Utah State University, United States

*CORRESPONDENCE
Jesus D. Fernandez-Bayo
✉ jdfbayo@ugr.es

RECEIVED 31 July 2025
ACCEPTED 26 August 2025
PUBLISHED 16 September 2025

CITATION
Marín-Guirao JI, Yan D, Di Gioia F, Pugliese M and Fernandez-Bayo JD (2025) Editorial: Soil microbial communities to promote suppressiveness against soil-borne pathogens and diseases. *Front. Microbiol.* 16:1677158. doi: 10.3389/fmicb.2025.1677158

Editorial: Soil microbial communities to promote suppressiveness against soil-borne pathogens and diseases

Jose Ignacio Marín-Guirao[1], Dongdong Yan[2], Francesco Di Gioia[3], Massimo Pugliese[4] and Jesus D. Fernandez-Bayo[5]*

[1]Andalusian Institute of Agricultural and Fisheries Research Training (IFAPA) La Mojonera, Almería, Spain, [2]Chinese Academy of Agricultural Sciences (CAAS), Beijing, China, [3]The Pennsylvania State University (PSU), University Park, PA, United States, [4]University of Turin – Agroinnova, Grugliasco, Italy, [5]Department of Soil Science and Agricultural Chemistry, University of Granada, Granada, Spain

KEYWORDS

suppressive soils, soil fumigation alternative, beneficial soil microbes, sustainable agricultural practices, soil biosolarization

Editorial on the Research Topic
Soil microbial communities to promote suppressiveness against soil-borne pathogens and diseases

Introduction

The phaseout of methyl bromide, stringent regulations on fumigant application, and the consumer demand for safer food are leading farmers toward the adoption of more sustainable soil management practices for the control of soil-borne pathogens (Rosskopf et al., 2024). In this context, organic amendment-based approaches such as soil biofumigation, biosolarization, and anaerobic soil disinfestation have emerged as promising alternatives to the use of synthetic soil fumigants, especially for their ability to suppress soilborne pathogens while preserving soil health and the environment. However, their widespread adoption is still limited by technical and sustainability constraints, such as the variability in efficacy across soils and climates, relatively high costs, amendment type, and use of impermeable plastic barriers. Given these limitations, new approaches aimed at enhancing natural soil suppressiveness and shifting soil microbial communities against soil-borne pathogens have gained increasing attention. Soil microorganisms, whether native or introduced *ex novo*, play a pivotal role in providing ecosystem services that can contribute to this goal by enhancing both soil and plant health. Thus, harnessing this biological potential offers a promising way to reduce agrochemical dependency and increase the resilience of cropping systems.

The main aim of this Research Topic was to expand knowledge on how soil management practices influence microbial communities and their ability to suppress soil-borne pathogens. The contributions span both fundamental understanding and practical implications, addressing the effects of soil amendments, microbial community shifts associated with disease suppression, interactions with plant defense mechanisms, and the overall effects on soil health and crop yield. Together, the 12 articles included reflect a growing body of evidence that shows how soil microbial communities can contribute to

the sustainable management of soil-borne pathogens and enhance soil health and productivity (Table 1).

Outline of contributions

Several contributions emphasized the use of native beneficial microbes with biocontrol potential, while underscoring the importance of single and mixed microbial inoculants in disease suppression strategies. Correa-Delgado et al. provided a detailed inventory of *Trichoderma* spp. from banana rhizospheres, identifying 10 species, six of which were reported for the first time in the Canary Islands, along with two putative novel taxa. Their findings revealed distinct distribution patterns across agroecosystems and a strong correlation with soil chemical properties, particularly pH and phosphorus levels. This comprehensive survey offers a foundation for the development of future biocontrol strategies against *Fusarium oxysporum* f. sp. *cubense* subtropical race 4. Li et al. demonstrated that *Bacillus velezensis* NT35, a strain isolated from the rhizosphere soil of *Panax ginseng*, exhibited antifungal activity and enhanced resistance to *Ilyonectria robusta* by modulating the expression of defense-related genes and shaping the rhizosphere microbiota. Similarly, focusing on *Bacillus velezensis* BF-237, a strain isolated from wheat rhizosphere soils, Wang Y. et al. demonstrated its efficacy in reducing wheat crown rot (WCR) severity and in supporting beneficial microbes under pathogen pressure. Furthermore, functional predictions suggest that microbial communities adapt to WCR by enhancing signaling pathways and decreasing anabolic activity. Conversely, a native mixed inoculant composed of *Serratia marcescens* and *Paenibacillus polymyxa* promoted *Cajanus cajan* growth (Liu et al.). This inoculant caused more pronounced changes in the soil fungal community than in bacterial communities, indicating that soil fungi are more sensitive to the inoculation of non-native biocontrol agents. Changes in the abundance of both beneficial and potentially pathogenic fungi were detected, alongside improved nutrient availability and plant development. Finally, Yin et al. reported that the cyanobacterium *Nostoc punctiforme* mitigated the soybean cyst nematode by indirectly reshaping the rhizosphere microbiota, rather than directly triggering host-defense mechanisms. The inoculation altered bacterial and fungal community composition in the soybean rhizosphere, increasing the relative abundance of taxa with potential nematicidal activity.

Other studies explored the interaction between soil amendments and microbial communities in the context of disease suppression. Bian-Hong et al. reported that lime, biochar, and a combination of the two reduced the tobacco bacterial wilt caused by *Ralstonia solanacearum* and improved tobacco yield in acidified soils. Biochar and lime-biochar treatments improved soil pH, and nutrient availability, while reducing acidity and bulk density. All treatments expanded niche breadth, enhanced positive microbial interactions, and intensified negative interactions involving *R. solanacearum*. Huang et al. showed that bio-organic fertilizers, based on prickly ash seed meal enriched with beneficial microorganisms such as *T. asperellum*, *B. amyloliquefaciens*, and *B. subtilis*, significantly reduced root rot and improved *Codonopsis pilosula* yield and quality compared to synthetic fertilizers. These effects were attributed to modifications in the structure of the rhizosphere bacterial community, enhanced stability of the microbial network, and enrichment of key taxa such as *Microlunatus*, *Rubrobacter*, and *Nakamurella*. Functional

TABLE 1 Summary of beneficial organisms added to the soil or agronomic practices, target pathogens and target crops included in the Research Topic.

Beneficial organisms added to the soil or agronomic practices	Target pathogen	Target crop	References
Trichoderma sp	*Fusarium oxysporum* f. sp. *cubense* subtropical race 4 (Foc-STR4)	Banana (*Musa acuminata*)	Correa-Delgado et al.
Bacillus velezensis NT35	*Ilyonectria robusta*	*Panax ginseng*	Li et al.
Bacillus velezensis BF-237	Wheat crown rot (WCR). *Fusarium* sp	Wheat	Wang Y. et al.
Serratia marcescens and Paenibacillus polymyxa	NA	*Cajanus cajan*	Liu et al.
Nostoc punctiforme	*Heterodera glycines Ichinohe*	Soybean [Glycine max (L.) Merr.]	Yin et al.
Application of biochar, lime or both	*Ralstonia solanacearum*	Tobacco (*Nicotiana tabacum* L.)	Bian-hong et al.
Bio-organic fertilizers enriched with *T. asperellum, B. amyloliquefaciens*, and *B. subtilis*	Unidentified root disease	*Codonopsis pilosula*	Huang et al.
Native bacteria from biosolarized soil with fresh sheep manure	*Colletotrichum gloeosporioides*, *F. proliferatum*, F. *oxysporum* f. sp. *radicis-cucumerinum, Botrytis cinerea* and *Phytophthora capsici*	Tomato (*Solanum lycopersicum* L)	Marín-Guirao and de Cara-García
Functional rhizosphere microbiomes associated with plant genetic factors	Fungal plant pathogens. I.e. *F. oxysporum*	*Panax notoginseng*	Shi et al.
Fumigation with allyl isothiocyanate	NA	Peppers *(Capsicum annuum L.)*	Tian et al.
Crop rotation	*F. oxysporum*	*Vanilla (Vanilla planifolia)* *black pepper (Piper nigrum L.)* *sweet rice tea (Strobilanthes tonkinensis Lindau)*	Hong et al.
Intercropping	NA	*Torreya grandis cv Merrillii* *Polygonatum sibiricum*	Wang Q. et al.

analyses indicated that bacterial signal transduction and amino acid metabolism may play a central role during the early and mid-growth stages. The study by Marín-Guirao and de Cara-García, conducted over two seasons in an organic Mediterranean tomato greenhouse, demonstrated that native bacterial diversity, shaped by biosolarization with fresh sheep manure, may enhance natural suppressiveness but also interfere with the performance of introduced biocontrol agents. A notable finding of the study was the high prevalence of native bacteria with antagonistic properties, primarily *Streptomyces* spp. and *Bacillus* spp., which inhibited the growth of both pathogenic and beneficial fungi sourced from commercial products.

Crop genotype and previous cultivation practices have also been identified as major factors influencing the composition and assembly of soil and rhizosphere microbial communities. Shi et al. demonstrated that the deterministic assembly of biocontrol-associated microbial communities in the rhizosphere of *Panax notoginseng* was particularly evident during the third year of root development and was influenced by plant genetic pathways. Transcriptomic analyses revealed that genes involved in protein export, alkaloid and amino acid biosynthesis, along with associated transcription factors, contributed to the recruitment of beneficial microbial taxa. Tian et al. showed that allyl-isothiocyanate fumigation significantly alters soil microbial diversity and composition, notably promoting Actinomycetota and suppressing Pseudomonadota. However, its effects on endophytic bacterial communities differed among pepper genotypes, highlighting the complex interactions among fumigation, soil microbiota, and plant internal microbiomes.

Finally, crop rotation and intercropping have proven to be effective strategies for disease management linked to soil microbiome modulation. Hong et al. showed that rotating vanilla with pandan or sweet rice tea significantly reduced *Fusarium* wilt by decreasing *F. oxysporum* abundance, enhancing fungal diversity, and enriching beneficial microbial taxa. In addition, the raised soil pH along with the altered microbial communities, was directly associated with pathogen suppression and enhanced vanilla disease resistance. Wang Q. et al. demonstrated that intercropping *Torreya grandis* with *Polygonatum sibiricum* enhanced soil microbial diversity, reduced the relative abundance of fungal genera, including potential soil-borne pathogens (e.g., *Cladosporium*, *Fusarium*, *Neocosmospora*), and enriched microbial groups involved in carbon and nitrogen cycling. These findings further support the role of diversified plant systems in fostering microbial diversity and pathogen suppression.

Conclusion

The studies in this Research Topic offer valuable frameworks for transitioning to more sustainable alternatives in the management of soil-borne pathogens. Together, they underscore the importance of managing soil microbial communities as a cornerstone of any sustainable strategy aimed at improving soil and plant health. These contributions provide compelling evidence that biotic and abiotic interventions, including microbial inoculants, organic amendments, genotype selection, and cropping system diversification, can enhance pathogen suppression by promoting beneficial taxa and restructuring microbial networks. Nevertheless, the complexity of microbial interactions, underlying mechanisms and key microbial traits in disease-suppressive soils remains largely elusive. Therefore, recognizing that each agroecosystem presents unique conditions and challenges, tailored approaches are required for the successful generation of disease-suppressive soils.

Author contributions

JM-G: Writing – original draft. DY: Writing – review & editing. FD: Writing – review & editing. MP: Writing – review & editing. JF-B: Conceptualization, Supervision, Writing – review & editing.

Conflict of interest

The authors declare that the research was conducted in the absence of any commercial or financial relationships that could be construed as a potential conflict of interest.

The author(s) declared that they were an editorial board member of Frontiers, at the time of submission. This had no impact on the peer review process and the final decision.

Generative AI statement

The author(s) declare that no Gen AI was used in the creation of this manuscript.

Any alternative text (alt text) provided alongside figures in this article has been generated by Frontiers with the support of artificial intelligence and reasonable efforts have been made to ensure accuracy, including review by the authors wherever possible. If you identify any issues, please contact us.

Publisher's note

References

Rosskopf, E., Gioia, F. D., Vincent, I., Hong, J., and Zhao, X. (2024). Impacts of the ban on the soil-applied fumigant methyl bromide. *Phytopathology* 114, 1161–1175. doi: 10.1094/PHYTO-09-23-0345-IA

frontiers | Frontiers in Microbiology

TYPE Original Research
PUBLISHED 10 May 2024
DOI 10.3389/fmicb.2024.1376602

OPEN ACCESS

EDITED BY
Jesus Fernandez Bayo,
University of Granada, Spain

REVIEWED BY
Dewa Ngurah Suprapta,
Udayana University, Indonesia
Ahmad Fakhoury,
Southern Illinois University Carbondale,
United States

*CORRESPONDENCE
Federico Laich
✉ flaich@icia.es

RECEIVED 25 January 2024
ACCEPTED 12 April 2024
PUBLISHED 10 May 2024

CITATION
Correa-Delgado R, Brito-López P, Jaizme Vega MC and Laich F (2024) Biodiversity of *Trichoderma* species of healthy and *Fusarium* wilt-infected banana rhizosphere soils in Tenerife (Canary Islands, Spain).
Front. Microbiol. 15:1376602.
doi: 10.3389/fmicb.2024.1376602

Biodiversity of *Trichoderma* species of healthy and *Fusarium* wilt-infected banana rhizosphere soils in Tenerife (Canary Islands, Spain)

Raquel Correa-Delgado, Patricia Brito-López, María C. Jaizme Vega and Federico Laich*

Unidad de Protección Vegetal, Instituto Canario de Investigaciones Agrarias, Valle de Guerra, Santa Cruz de Tenerife, Canary Islands, Spain

Banana (*Musa acuminata*) is the most important crop in the Canary Islands (38.9% of the total cultivated area). The main pathogen affecting this crop is the soil fungal *Fusarium oxysporum* f. sp. *cubense* subtropical race 4 (*Foc*-STR4), for which there is no effective control method under field conditions. Therefore, the use of native biological control agents may be an effective and sustainable alternative. This study aims to: (i) investigate the diversity and distribution of *Trichoderma* species in the rhizosphere of different banana agroecosystems affected by *Foc*-STR4 in Tenerife (the island with the greatest bioclimatic diversity and cultivated area), (ii) develop and preserve a culture collection of native *Trichoderma* species, and (iii) evaluate the influence of soil chemical properties on the *Trichoderma* community. A total of 131 *Trichoderma* isolates were obtained from 84 soil samples collected from 14 farms located in different agroecosystems on the northern (cooler and wetter) and southern (warmer and drier) slopes of Tenerife. Ten *Trichoderma* species, including *T. afroharzianum, T. asperellum, T. atrobrunneum, T. gamsii, T. guizhouense, T. hamatum, T. harzianum, T. hirsutum, T. longibrachiatum*, and *T. virens*, and two putative novel species, named *T.* aff. *harzianum* and *T.* aff. *hortense*, were identified based on the *tef1*-α sequences. *Trichoderma virens* (35.89% relative abundance) and *T.* aff. *harzianum* (27.48%) were the most abundant and dominant species on both slopes, while other species were observed only on one slope (north or south). Biodiversity indices (Margalef, Shannon, Simpson, and Pielou) showed that species diversity and evenness were highest in the healthy soils of the northern slope. The Spearman analysis showed significant correlations between *Trichoderma* species and soil chemistry parameters (mainly with phosphorus and soil pH). To the best of our knowledge, six species are reported for the first time in the Canary Islands (*T. afroharzianum, T. asperellum, T. atrobrunneum, T. guizhouense, T. hamatum, T. hirsutum*) and in the rhizosphere of banana soils (*T. afroharzianum, T. atrobrunneum, T. gamsii, T. guizhouense, T. hirsutum, T. virens*). This study provides essential information on the diversity/distribution of native *Trichoderma* species for the benefit of future applications in the control of *Foc*-STR4.

KEYWORDS

banana *Fusarium* wilt, Panama disease, *Fusarium oxysporum* f. sp. *cubense* subtropical race 4, *Trichoderma*, biodiversity, soil rhizosphere, biological control agent, *Musa acuminata*

Introduction

The Canary Island archipelago comprises eight islands located in the subtropical region of the Atlantic Ocean near the Tropic of Cancer, off the African coast of Western Sahara (between 27°37′-29°25′N and 13°20′-18°10′W). Its climate is characterized by low annual thermal variations, mainly due to the influence of cold ocean currents and trade winds from the NE (cold and humid) that blow for most of the year (Carracedo et al., 2002). The Canary Islands are one of the most biodiverse areas in the European Union and one of the most outstanding in the world for its endemism. This region contains half of Spain's endemic flora and provides the right conditions for the cultivation of a wide variety of subtropical and tropical species (Madruga et al., 2016). Banana (*Musa acuminata*) is the most important crop in the Canary Islands. It covers a total area of 8,891 ha (38.9% of the cultivated area of the whole archipelago) and provides 63% of the total banana production in Europe (Food and Agriculture Organization of the United Nations, 2022; Instituto Canario de Estadística [ISTAC], 2022). Due to the commercial importance of the crop, since 2013, it has been included in the Register of Protected Designations of Origin (PDO) and Protected Geographical Indications (PGI) (EUR-Lex, 2013).

Various pests and diseases affect banana crops in subtropical areas. Among these, *Fusarium* wilt of musaceae, also known as Panama disease is worth highlighting. This disease is caused by the soil fungus *Fusarium oxysporum* f. sp. *cubense* (*Foc*) and is one of the most destructive diseases for the musaceae (Ploetz, 2015a). Tropical race 4 (*Foc*-TR4) is the most pathogenic among the major commercial cultivars of the Cavendish subgroup (AAA) (Ploetz, 2006). In the Canary Islands, studies carried out at the Department of Plant Protection of the Canary Institute of Agricultural Research (ICIA)[1] from the 1980s to the present have shown that the causal agent of Panama disease is the subtropical race 4 of *Foc* (*Foc*-STR4) and that *Foc*-TR4 has not been detected. Perera-González et al. (2023) showed that 23% of banana farms on Tenerife had plants with *Foc* symptoms (yellowing of leaves, drying of leaves, and xylem necrosis on corm and pseudostem). Nevertheless, the incidence of the disease is generally low (3.4% of plants on affected farms present symptoms of the disease), and these plants are usually found in places with poor drainage, acid pH, soil compaction, excessive humidity, and/or shady areas. In other (minority) cases, the incidence of the disease is higher (49.1% of plants with symptoms) and leads to abandonment or change in crops.

A large number of publications describe different alternatives to control the pathogen, however, several reasons make control difficult (Ploetz, 2015b; Dita et al., 2018; Siamak and Zheng, 2018). Among them are: (a) the ability of the pathogen to survive in the soil for long periods of time (more than 40 years) (Buddenhagen, 2009); (b) the spread of the pathogen through contaminated materials (plants, tools, farm equipment, irrigation water, etc.); (c) the endophytic properties of the fungus, which protect it from the action of contact fungicides or non-endophyte biological control agents (Bubici et al., 2019); (d) the lack of rotation in most commercial crops of intensive production (monoculture) cause the pathogen to multiply in a continuous cycle, increasing the inoculum in the soil over time (Dita et al., 2018). Considering these factors, probably, the most effective alternative for its control could be the use of resistant cultivars, although the appearance of new pathogenic variants of the fungus can overcome this resistance (Ploetz, 2015b; Dita et al., 2018). Nevertheless, the key measures to control the disease and prevent the spread of the pathogen in those regions free of the fungus or with low infestation levels are pathogen exclusion, contingency plans and destroying infected materials (Ploetz, 2015b; Dita et al., 2018).

Other management alternatives aimed at improving soil health are mainly based on the application of appropriate agronomic practices, the use of cover crops or the application of organic amendments and biological control agents (BCA) (Dita et al., 2018). In this sense, soil microorganisms have a fundamental role in plant health and protection, especially those that colonize the rhizosphere zone, by enhancing nutrient uptake, disease resistance, plant defense response, and tolerance to various biotic and abiotic stresses (Raaijmakers et al., 2009; Liu et al., 2021). A well-researched example is the genus *Trichoderma* (syn. Hypocrea, Hypocreales), which consist of more than 400 species (Cai and Druzhinina, 2021) divided into three representative groups, *Harzianum*, *Trichoderma*, and *Longibrachiatum* (Kubicek et al., 2019), known as linages (Gutiérrez et al., 2021). *Trichoderma* is a cosmopolitan and opportunistic filamentous fungus and a ubiquitous colonizer in almost all environments, commonly found in agriculture soils (Woo et al., 2023). Of particular interest in this genus are the processes involved in the biological control of plant diseases, with direct action on plant pathogens and indirect mechanisms through the induction of local and systemic plant defenses (Harman et al., 2004). Due to these characteristics, *Trichoderma* has remained a notable BCA and has become a popular protagonist as the key component of plant biostimulants, bioprotectants, biofertilizers, and soil amendments (Woo et al., 2023).

In relation to the biological control of *Foc*, a wide variety of scientific articles describe the biocontrol potential of *Trichoderma* against this pathogen (mainly on *Foc*-TR4) (Bubici et al., 2019; Izzati et al., 2019; Damodaran et al., 2020). However, there are few studies that evaluate *Trichoderma* isolates obtained from banana soils or plants (Thangavelu et al., 2004; Thangavelu and Mustaffa, 2010; Caballero et al., 2013; Galarza et al., 2015; Thangavelu and Gopi, 2015; Chaves et al., 2016; Taribuka et al., 2017; Damodaran et al., 2020; Olowe et al., 2022). In many cases, the reduced efficacy of BCAs under field conditions could be due to their inability to grow under local biotic and abiotic environmental conditions. For this reason, it is extremely important to know the natural microbial biodiversity in the different ecosystems and to have a wide collection of native strains adapted to the specific agroclimatic conditions of the crop where it is to be applied.

The main purpose of this study was to collect a representative number of rhizosphere soil samples from healthy and *Foc*-STR4-affected banana plants in different agroecosystems on Tenerife, in order to: (i) describe the diversity and distribution of *Trichoderma* species in different agroecosystems, (ii) develop and preserve a culture collection of native *Trichoderma* species, and (iii) evaluate the influence of soil chemical properties on *Trichoderma* community composition. The practical importance of this study is to provide an initial knowledge base about the diversity and distribution of *Trichoderma* species in different banana ecosystems of Tenerife, and to preserve a culture collection of native *Trichoderma* as a reservoir of potential beneficial microorganisms

1 www.icia.es

to develop sustainable agro-biotechnological alternatives. Indeed, it is important to highlight the role of the microbial culture collection as an essential source for the selection of potential BCA against *Foc*-STR4 or plant growth promoting microorganisms (PGPM) naturally adapted to the agroclimatic conditions of banana crops in the Canary Islands.

This is the first work that describes the *Trichoderma* community in the rhizosphere soil of banana plants with and without symptoms of Panama disease in the different bioclimatic conditions and growing areas of the island of Tenerife. In addition, six species of *Trichoderma* are reported for the first time in the Canary Islands (*T. afroharzianum, T. asperellum, T. atrobrunneum, T. guizhouense, T. hamatum*, and *T. hirsutum*) and six species that have not been previously reported associated with banana rhizosphere (*T. afroharzianum, T. atrobrunneum, T. gamsii, T. guizhouense, T. hirsutum*, and *T. virens*). Furthermore, we detected two groups of isolates, which we identified as *T.* aff. *harzianum* and *T.* aff. *hortense*, corresponding to putative novel endemic species to be described in the near future.

Materials and methods

Crop distribution and agroclimatic characteristics of Tenerife

Approximately 9,000 farmers cultivate bananas in the Canary Islands on an area of about 8,891.2 ha. The island with the largest cultivated area is Tenerife (4,002.9 ha), followed by La Palma (2,727.6 ha), and Gran Canaria (1,936.6 ha) (Instituto Canario de Estadística [ISTAC], 2022). In addition, Tenerife (situated near the center of the archipelago) is the largest (2,034 km^2) and highest island (3,718 m.a.s.l.) of the archipelago and has the largest number of bioclimatic belts (26): from the hyperarid desertic inframediterranean in the southern zone of the coast to the dry pluviseasonal oromediterranean at higher altitudes (3,718 m.a.s.l., Mount Teide) (Del-Arco et al., 2006).

In Tenerife, banana crops are distributed around almost the entire perimeter of the island, mainly at altitudes below 300 m.a.s.l. The main environmental difference is observed when comparing the northern and southern slopes. The northern slope is wetter and cooler (due to the trade winds and annual rainfall of up to 500 mm), while the southern slope is drier and warmer (exposed to heatwaves from the Sahara and with less than 200 mm annual rainfall) (**Supplementary Table 1**). These differences affect crop development, with significant differences between slopes in terms of leaf emission and bunch emergence intervals because of temperature (Galán-Sauco et al., 1984). Also, on both slopes, altitude (related to temperature) has a significant effect. As altitude increases, the emergence interval becomes longer. The soil type in both slope is Andisols (Tejedor et al., 2009).

Characteristics of the sampling points and experimental design

The sampling points were selected considering the following factors: (a) the agroclimatic characteristics, (b) the distribution of banana production areas, and (c) the distribution of *Foc*-STR4-affected banana plants. As a reference for the distribution of Panama disease (*Foc*-STR4) in Tenerife, we used the analysis of a previous work in which 100 farms spread randomly and proportionally over the cultivated area in each of the banana production zones were studied (Perera-González et al., 2023). For this purpose, a grid (500 m × 500 m) was implemented over the entire cultivated area of banana crops and several squares proportional to the cultivated area of each zone were randomly selected. In each square (approximately one per 40 ha), the largest farm was selected and an assessment of Panama disease was carried out (Perera-González et al., 2023). Taking into account the results of this study and the factors mentioned above, 14 farms (8 on the north slope and 6 on the south) with plants affected by *Foc*-STR4 distributed representatively in each production zone were selected. All selected farms had a history of banana monoculture of more than 15 years. The geographical, bioclimatic data, and the cropping history of each farm are given in **Table 1**.

Soil and plant sample collection

Six plants per farm were selected: three plants with visible symptoms of *Foc*-STR4 disease and three asymptomatic plants. Plants with symptoms were selected as far apart as possible. The selection of asymptomatic plants was carried out on specimens with the same growing conditions and phenological state as the plants with symptoms, at 5–10 m from them.

Rhizosphere soil samples were collected around each plant (50 cm from the pseudostem) at four opposite points, discarding the upper plant remains and using a 45-mm diameter soil auger at 0–20 cm depth. Before each sampling, the auger was disinfected with alcohol and burned with a butane torch. Subsequently, the four subsamples from each plant were mixed into a single sample (approximately 1,000 g) and kept in a sterile plastic bag to be transported to the laboratory. In this way, a total of 84 samples (6 plants × 14 farms) were obtained (42 from rhizospheric soil of plants with symptoms and 42 from asymptomatic plants). At the same time, vascular tissue samples were extracted from the inner part of the rhizome and the pseudostem of each plant to verify the presence or absence of *Foc*-STR4 in plants with and without symptoms, respectively. In this case, the samples (500–1,000 g/plant) were extracted with a sterile scalpel knife and wrapped in absorbent filter paper. Both types of samples (soil and plant) were transported refrigerated to the laboratory.

Determination of soil chemical properties

Five hundred grams of each soil sample were processed. The soils were air-dried at room temperature, sieved through a 2 mm sieve and homogenized. Oxidizable organic matter (%) was analyzed by oxidation with potassium dichromate in an acid medium and titrated with Mohr's salt, using a protocol modified from Walkley and Black (1934). Total nitrogen (%) content was determined by the Kjeldahl method. Assimilable phosphorus (mg/kg) was analyzed according to the colorimetric method of

TABLE 1 Geographical, bioclimatic data, and cropping history of the 14 sampling farms in Tenerife (Canary Islands).

Farm code	Municipality	Location	Slope	Thermotype[a]	Bioclimatic belt[a]	Coordinates	Years of planting[b]	Altitude (m.a.s.l.)
BN47	Buenavista del Norte	Las Toscas	North	Inframediterranean	Lower-semiarid xeric inframediterranean	28°22′ 13.52″N 16°50′ 37.76″W	35	124.69
IV72	Icod de Los Vinos	Las Granaderas	North	Inframediterranean	Lower-semiarid xeric inframediterranean	28°23′ 26.83″N 16°32′ 06.74″W	15	164.02
IV37	Icod de los Vinos	Valois	North	Inframediterranean	Lower-semiarid xeric inframediterranean	28°22′ 32.54″N 16°43′ 31.47″W	20	109.71
VO78	La Orotava	El Rincón	North	Inframediterranean	Lower-semiarid xeric inframediterranean	28°25′ 09.73″N 16°30′ 34.49″W	50–60	105.59
VO64	La Orotava	San Miguel	North	Inframediterranean	Upper-semiarid xeric inframediterranean	28°22′ 16.60″N 16°43′ 27.16″W	70	278.12
BN4	Los Silos	Hoya Matos	North	Inframediterranean	Lower-semiarid xeric inframediterranean	28°22′ 40.08″N 16°49′ 16.25″W	25	47.71
TV26	San Cristóbal de La Laguna	La Cardonera (Tejina)	North	Inframediterranean	Lower-semiarid xeric inframediterranean	28°32′ 29.91″N 16°21′ 55.07″W	40	103.56
PH1	San Cristóbal de La Laguna	Punta Hidalgo	North	Inframediterranean	Lower-semiarid xeric inframediterranean	28°34′ 13.98″N 16°19′ 08.72″W	50–60	73.21
AD46	Adeje	La Tiñosa (Barranco Las Moradas)	South	Inframediterranean	Arid desertic inframediterranen	28°09′ 04.23″N 16°46′53.99″W	15	177.33
AR51	Arona	Llanos de Guargacho	South	Inframediterranean	Arid desertic inframediterranen	28°02′ 23.23″N 16°38′ 23.56″W	15	101.03
AR68	Arona	Buzanada	South	Inframediterranean	Arid desertic inframediterranen	28°04′ 29.14″N 16°39′ 17.31″W	40	304.83
CPE	Guía de Isora	Cueva del Polvo	South	Inframediterranean	Arid desertic inframediterranen	28°13′ 47.11″N 16°49′ 58.73″W	30	104.86
GUI	Güímar	Hoya del Cerco	South	Inframediterranean	Arid desertic inframediterranen	28°18′ 39.40″N 16°23′ 03.31″W	25	115.03
SM109	San Miguel de Abona	Montaña de Los Gorones	South	Inframediterranean	Arid desertic inframediterranen	28°03′ 11.28″N 16°37′ 54.31″W	35	159.03

[a] Del-Arco et al. (2006). [b] Years of the farm with banana crop (monoculture).

Olsen et al. (1954). Soil exchange cations (mEq/kg), calcium, magnesium, potassium and sodium were extracted with neutral 1N ammonium acetate and determined by flame atomic absorption spectrophotometry (Bower et al., 1952). The pH and the electrical conductivity (EC) were determined in a 1:5 (v:v) aqueous extract according to Norma UNE-EN 77308:2001 (2001) and Norma UNE-ISO 10390:2012 (2012), respectively. The analyses of these parameters were carried out by the Laboratory Unit of the Canary Institute of Agricultural Research (ICIA).

Microbiological analysis

Isolation and preservation of *Trichoderma* isolates from soil samples

Each soil sample was air-dried and sieved (3 mm) to separate the soil conglomerates and larger organic matter remains. Subsequently, 20 g of soil were mixed with 180 ml of sterile 0.85% KCl (potassium chloride, PanReac AppliChem, Barcelona, Spain) in 250 ml capacity bottles and homogenized using an orbital shaker (Orbital, J.P. Selecta) at 150 rpm during 20 min. A serial of decimal dilutions was prepared and 0.1 ml of each dilution was streaked onto the following culture mediums for *Trichoderma* isolation: *Trichoderma* Selective Medium (TSM) (Askew and Laing, 1993) and Dichloran Rose Bengal Chloramphenicol Agar (DRBC, Condalab, Laboratory Conda S.A., Madrid, Spain).

Petri dishes were incubated at 25°C for 7–10 days in the dark. Putative *Trichoderma* colonies were quantified and purified by subculturing on Blakeeslee's Malt Extract Agar (MEAbl; Blakeslee, 1915; Visagie et al., 2014) for 7 days at 25°C. All isolates described in this study were maintained at −80°C in 30% glycerol solution.

Species were identified by a combination of morphological analysis and molecular methods. Morphological characteristics were based on the key of Gams and Bissett (1998). Colony characteristics were also examined on cultures grown on MEAbl after 7 days of incubation at 25°C. Microscopic observations were made on cultures grown on Corn Meal Agar (CMD; CM0103, Oxoid Ltd., Basingstoke, Hampshire, United Kingdom) and on Spezieller Nährstoffarmer Agar (SNA) after 10 days at 25°C. Observations were made with a Nikon Eclipse 80i optical microscope using differential interference contrast (DIC).

Soil and plant pathogen analysis

The quantification of *Foc* was carried out by planting (in triplicate) a serial dilution of the rhizosphere soil suspensions onto Petri dishes containing the Komada selective medium (Komada,

1975). After planting, the Petri dishes were incubated at 25°C for 7–10 days in the dark, and the colonies with microscopic characteristics of *Fusarium* were counted to obtain the number of colony forming units per gram of soil (cfu/g) (Leslie and Summerell, 2006).

The analysis of the plant tissue samples was carried out using the following procedure: four pieces of each type of tissue (corm and pseudostem from each plant) were obtained and surface disinfected. From each of them, a 15–20 mm long portion of the vascular bundles was extracted aseptically and deposited on the surface of a Petri dish with Potato Dextrose Agar (PDA, Condalab, Laboratory Conda S.A., Madrid, Spain), supplemented with streptomycin (300 mg/L) and chloramphenicol (250 mg/L). After incubation at 25°C for 7 days in the dark, putative *Fusarium* colonies were purified by subculturing on PDA. Subsequently, macroscopic (colony diameter, surface appearance, colony edge, coloring, pigmentation in the medium, exudates formation, etc.) and microscopic (shape and arrangement of micro- and macroconidia, length of conidiophores, chlamydospore formation, etc.) characteristics of each isolate were recorded (Leslie and Summerell, 2006) and stored at −80°C in 30% glycerol solution.

DNA extraction and PCR amplification

DNA from all *Trichoderma* and *Fusarium* isolates was obtained according to the following protocol. Each isolate was grown in PDA for 7–10 days at 25°C. Subsequently, the mycelium was collected and transferred to a microtube (approximately 50–70 mg) with 500 μl of lysis buffer (400 mM Tris–HCl, 60 mM EDTA, 150 mM NaCl, 1% SDS) containing glass beads. The mixture was shaken in a Retsch MM400 shaker (Retsch, Düsseldorf, Germany) for 10 min, incubated at 65°C for 40 min and centrifuged at 15,000 rcf for 10 min. The supernatant was recovered in a sterile microtube and an equal volume of chloroform/isoamyl alcohol [24:1 (v/v)] was added. After homogenization of the mixture and centrifugation at 17,000 rcf (4°C for 10 min), the supernatant was recovered in a sterile microtube. The DNA was precipitated with 2.5 volumes of cold absolute ethanol at −20°C for 2–4 h and collected by centrifugation at 20,000 rcf (4°C for 15 min). The pellet was washed with 500 μl of 70% ethanol, air-dried and resuspended in 50 μl of sterile DNase/RNase-free water. The DNA was quantified using a spectrophotometer (NanoDrop 2000c, Wilmington, NC, USA), and stored at −20°C until use.

For molecular identification of *Trichoderma* species, a 1,200 bp fragment of the translation elongation factor 1-α region (*tef1*-α) gene was amplified by conventional PCR using the following primers pairs: EF1-728F (5′-CAT CGA GAA GTT CGA GAA GG-3′) (Carbone and Kohn, 1999) and TEF1LLErev (5′-AAC TTG CAG GCA ATG TGG-3′) (Jaklitsch et al., 2005). PCR reactions were performed in a volume of 25 μl at the following final concentrations: 1.6 ng/μl of DNA, 1× buffer [Tris–HCl pH 8.5, $(NH_4)_2SO_4$, and 1% Tween 20], 1.5 mM $MgCl_2$, 0.15 mM dNTP, 0.3 μM of each primer, 0.05 U/μl Taq DNA Polymerase (VWR Taq DNA Polymerase). Amplification was carried out in a conventional Thermal Cycler (Eppendorf Mastercycler X50s) under the following conditions: initial denaturation of 5 min at 94°C; 30 cycles of 45 s at 95°C, 45 s at 57°C, 1:10 min at 72°C; with a final extension of 10 min at 72°C.

The PCR product was electrophoresed at 90 $V \cdot cm^{-1}$ for about 2.5 h on agarose gels (1.5% w/v) with 1 × TAE buffer (PanReac AppliChem) and stained with gel red (Gel Red Nucleic Acid Gel Stain, Biotium). A 50-bp DNA Step Ladder (S7025, Sigma-Aldrich) was used as a size standard. The PCR products were visualized under UV light and photographed (Nikon D3500 DX, Nikon).

For the molecular identification of the *Foc* isolates obtained from the plant tissue samples (rhizome and pseudostem), a PCR amplification was performed using secreted in xylem (SIX) specific primers to detect the different *Foc* races: STR4: *Foc*-SIX8b-F/*Foc*-SIX8b-R (Fraser-Smith et al., 2014) and SIX8b-206-F/SIX8b-206-R (Carvalhais et al., 2019); TR4: SIX1a-266-F/SIX1a-266-R (Carvalhais et al., 2019). Subsequently, all the isolates with positive results in the specific amplifications were confirmed and identified by partial sequencing of the translation elongation factor 1-α gene (*tef1*-α) using the primers EF-1 and EF-2 (O'Donnell et al., 1998). The PCR conditions used for each primer set were those recommended by the respective authors. The fragments were evaluated by electrophoresis in agarose gel as described above.

Sequence and phylogenetic analysis

The PCR products were purified with exonuclease I (M0293S, BioLabs) and shrimp alkaline phosphatase (M0371S, BioLabs) according to the manufacturer instructions [Shrimp Alkaline Phosphatase (rSAP), BioLabs]. Purified amplicons were sequenced through Sanger sequencing methods by Macrogen sequencing service (Macrogen Inc., Spain) in both directions (forward and reverse complimentary DNA strands). The sequence data assembly and editing were performed using MEGA 11 software (Tamura et al., 2021).

All the *Trichoderma* sequences were deposited in GenBank database with the accession numbers from OQ858692 to OQ858800 (**Supplementary Table 2**). Comparisons with sequences from GenBank were performed using BLASTN (Altschul et al., 1997). Moreover, sequences of the *tef1*-α region were compared with those available at the TrichOKEY databases (TrichOKEY v2 software), accessed online at the International Subcommittee on *Trichoderma* and *Hypocrea* taxonomy (ISTH)[2] (Druzhinina et al., 2005). For phylogenetic analysis, sequences of the representative species of the *Trichoderma* genus were retrieved from the NCBI GenBank database[3] and are listed in **Supplementary Table 3**. Multiple sequence (*tef1*-α dataset) alignments were performed with MUSCLE and phylogenetic trees were reconstructed using maximum-likelihood (ML) analysis using MEGA 11 software. The robustness of branches was assessed by bootstrap analysis of 1,000 replicates. For ML analyses, the best-fit nucleotide substitution model for each dataset was selected with MEGA 11, according to the Bayesian information criterion (BIC) values (Schwarz, 1978). In this context, the best models (lowest BIC scores) were Kimura 2-parameter model with a gamma distribution (+G) and invariable sites (+I) for the *Trichoderma* lineage, *Longibrachiatum* lineage and *Harzianum-Virens* lineage.

Fusarium sequences (*tef1*-α) were analyzed using a procedure similar to that described for *Trichoderma*. In this case, the best

2 www.isth.info

3 http://www.ncbi.nlm.nih.gov/genbank/

model for the ML analysis of the *F. oxysporum* species complex (FOSC; Lombard et al., 2019) was the Kimura 2-parameter model with a gamma distribution (+G).

Diversity analysis of *Trichoderma* species

Different indices were analyzed to quantitatively determine the diversity of *Trichoderma* species in the different bioclimatic zones (northern and southern slopes) according to the origin of the samples (soil rhizosphere of plants with and without *Foc*-STR4).

The occurrence frequency (OF) percentage at the species level was calculated using the following formula:

$$OF\ (\%) = \frac{n}{N}\,100$$

where "*n*" is the number of rhizospheric soil samples with one *Trichoderma* species and "*N*" is the total number of rhizospheric soil samples.

The relative abundance (RA) percentage for every species was calculated as:

$$RA\ (\%) = \frac{ni}{Nt}\,100$$

where "ni" is the number of isolated of *Trichoderma* belonging to species *i* and "Nt" is the total number of isolates.

The isolation rate (IR) was calculated by the total number of isolates of *Trichoderma* (nt) divided by the total number of soil samples (Ns).

$$IR = \frac{nt}{Ns}$$

Margalef's (E) index was used to measure the richness (Margalef, 1958), Shannon–Wiener (H), and Simpson (D) indices were used to measure the diversity (Shannon, 1948; Simpson, 1949), and Pielou index (J) was used to measure evenness (Pielou, 1966). These indices were calculated using the following formulas:

$$E = \frac{S-1}{\ln N}$$

$$H = -\sum_{i=1}^{N} P_i lnP_i,\ P_i = \frac{n_i}{N}$$

$$D = 1 - (\Sigma \mathrm{Pi}^2)$$

$$J = \frac{H}{lnS}$$

where "*S*" represents the number of *Trichoderma* species, "*N*" is the sum of all *Trichoderma* species isolates, "P_i" is the ratio of the number of isolates of *Trichoderma* belonging to species *i* (n_i) to the total number of isolates in the community (*N*).

Data processing

Microsoft Excel version 2016 software was used to calculate the diversity indices. Statgraphics Centurion 18 V18.1.14 software was used for statistical analysis of the data. One-way analysis of variance (ANOVA) and LSD ($p < 0.05$) multiple comparisons were used to analyze the variance and test the significance of differences in soil chemical properties and *Foc* population. The hierarchical location of the *Trichoderma* species detected in the rhizospheric soil samples, was determined using the Olmstead-Tukey correlation method. The graphical representation used a quadrant graph based on the occurrence frequency and the relative abundance [expressed as Log (RA + 1)] values (Sokal and Rohlf, 1995). Each species was classified as dominant (OF and RA higher than the average values), frequent (OF above average and RA below average), occasional (OF below average and RA above average), and rare (OF and RA lower than the average values). The Spearman correlation coefficient method was used to analyze the correlation between soil chemical properties and *Trichoderma* community composition.

Results

Analysis of *Fusarium oxysporum* f. sp. *cubense* in plant samples and quantification in soil

To test the absence and presence of the pathogen on healthy and *Foc*-STR4-affected banana plants, respectively, rhizome and pseudostem samples were obtained from all banana plants selected for soil sampling. Endophytic fungi were isolated from these samples and all colonies with macro and microscopic characteristics typical of *Fusarium* were identified at species and race level by molecular and phylogenetic analysis of the *tef1*-α gene and specific-race SIX primers (O'Donnell et al., 1998; Fraser-Smith et al., 2014; Carvalhais et al., 2019). The results of this analysis determined that the causal agent of the disease in plants with symptoms was *Foc*-STR4 (*Fusarium phialophorum*), while in plants without symptoms, the pathogen was not detected in any case.

The abundance of *Foc* in the rhizosphere of healthy and diseased plants was analyzed in each soil sample. No significant difference ($p < 0.05$) was observed between the population of *Foc* (ufc/g) of the healthy and diseased soils on both slopes (north and south). However, significant differences ($p < 0.05$) were detected between northern and southern soils samples (**Figure 1**). Our results showed that population of *Foc* in northern soils ranged from 3.67×10^2 to 3.63×10^3 cfu/g (average 1.41×10^3 cfu/g) and 1.50×10^2 to 2.20×10^3 cfu/g (average 1.43×10^3 cfu/g) in healthy and diseased plants, respectively, and in southern soils ranged from 0.83×10^2 to 1.68×10^3 cfu/g (average 9.21×10^2 cfu/g) and 9.75×10^2 to 1.46×10^3 cfu/g (average 1.05×10^3 cfu/g) in healthy and diseased plants, respectively (**Figure 1**). The lowest *Foc* population in the rhizosphere of healthy plants was detected in CPE (Cueva del Polvo, southern slope) and the highest was in VO78 (Valle de La Orotava, northern slope). The lowest and highest populations in diseased plants were detected in BN47 and BN4 (Buenavista del Norte, north slope), respectively.

Trichoderma isolation and species identification

The most appropriate culture medium for *Trichoderma* isolation was DRBC. This was mainly due to the following reasons:

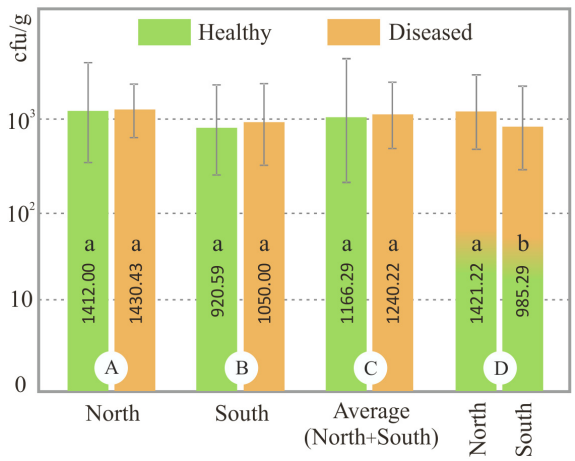

FIGURE 1
Fusarium oxysporum f. sp. *cubense* (*Foc*) population in soil samples. Columns in group A and B show the *Foc* population (cfu/g) in soils from healthy and diseased plants from the northern and southern slopes, respectively. Columns in group C show the *Foc* population of healthy and diseased plants from all soil samples (north + south). Columns of group D show the *Foc* population in all soils (healthy + diseased) of the north and south slope. Equal letters in the same group of data (A, B, C or D) indicate no significant difference ($p < 0.05$). Errors bars represent the standard deviations of the means.

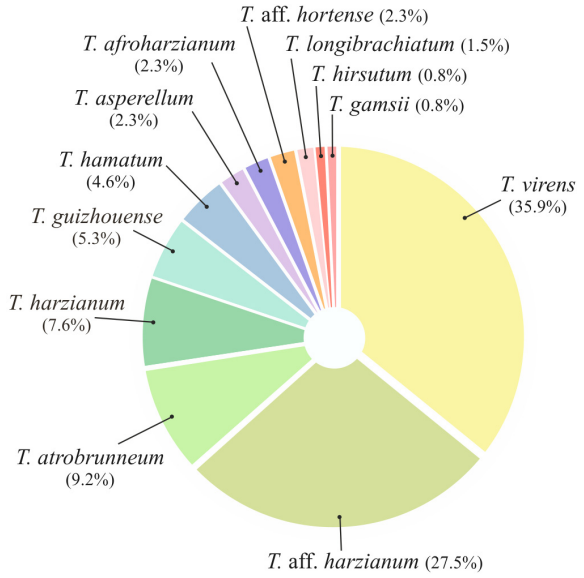

FIGURE 2
Pie chart showing the relative abundance (%) of each *Trichoderma* species isolated in this study from banana rhizosphere soil in Tenerife (Canary Islands).

(a) the development and sporogenesis of *Trichoderma* colonies on DRBC was significantly higher than on TSM, (b) the contrasting color of the rose bengal of DRBC facilitated the recognition of *Trichoderma* colonies, and (c) most of the colonies corresponding to the soil mycobiota population did not show abundant growth. Therefore, the *Trichoderma* colonies in DRBC were quickly located and identified by micromorphological characteristics.

No significant differences ($p < 0.05$) in *Trichoderma* population were observed between healthy and diseased soils, and between northern and southern soils. Nevertheless, *Trichoderma* quantification (cfu/g) on samples from healthy plants was higher than in diseased plants (3.4×10^3 and 2.1×10^3 cfu/g, respectively). Likewise, the cfu/g from soils on the northern slope were slightly higher than those from soils on the southern slope (2.9×10^3 and 2.7×10^3 cfu/g, respectively). Regarding the relationship between *Trichoderma* and *Fusarium* populations in soil, no significant correlation was observed between both populations in any of the conditions tested (north and south slope or healthy and diseased plants).

Taking into account the morphological (macro and microscopic) diversity of the colonies and the origin of the samples, a total of 131 *Trichoderma* isolates were obtained from 84 soil samples collected from 14 farms located in different banana-production areas of Tenerife (8 farms from the north slope and 6 from the south). All *Trichoderma* isolates were identified at species level by the sequence analysis of *tef1*-α gene. Twelve species were identified: *T. virens* (47 isolates), *T.* aff. *harzianum* (36), *T. atrobrunneum* (12), *T. harzianum* (10), *T. guizhouense* (7), *T. hamatum* (6), *T.* aff. *hortense* (3), *T. afroharzianum* (3), *T. asperellum* (3), *T. longibrachiatum* (2), *T. gamsii* (1), and *T. hirsutum* (1) (**Figure 2**).

Phylogenetic analysis

One hundred nine isolates were selected for taxonomy studies according to the macro and micromorphological characteristics of the 131 isolates initially obtained from the soil samples of banana plants in Tenerife. The phylogenetic relationship of the 109 representative isolates of *Trichoderma* was constructed from the sequence analysis of *tef1*-α gene using the ML method. The 12 identified species were distributed among three different evolutionary lineages of the *Trichoderma* genus namely: *Harzianum-Virens* (8 species, 90.84% of the isolates), *Trichoderma* (3 species, 7.63% of the isolates), and *Longibrachiatum* (1 species, 1.53% of the isolates) (Cai and Druzhinina, 2021; Gutiérrez et al., 2021).

Ninety-seven isolates were identified into six known species belonging to the linage *Harzianum-Virens* (Jaklitsch and Voglmayr, 2015); *T. afroharzianum, T. atrobrunneum, T. guizhouense, T. harzianum, T. hirsutum*, and *T. virens* (**Figure 3**). Ten isolates were identified in the *Trichoderma* linage (Jaklitsch and Voglmayr, 2015) as *T. asperellum, T. gamsii*, and *T. hamatum* (**Figure 4**), and two isolates were identified in the *Longibrachiatum* linage as *T. longibrachiatum* (Jaklitsch and Voglmayr, 2015; **Figure 5**).

Interestingly, 34 isolates could not be grouped in previously described *Trichoderma* species. In these cases, the term *affinis* (aff.) was used to indicate that these OTUs are similar but not necessarily identical to the described species. Thus, 31 isolates were named *T.* aff. *harzianum* and 3 isolates as *T.* aff. *hortense*, both belonging to the *Harzianum-Virens* lineage. The phylogram showed that *T.* aff. *harzianum* formed a subclade with *T. afarasin, T. austroindianum, T. camerunense, T. endophyticum, T. lixii, T. neotropicale, T. rifaii, T. simmonsii*, and *T. syagri*, and *T.* aff. *hortense* formed a subclade with *T. hortense*. *Trichoderma* aff.

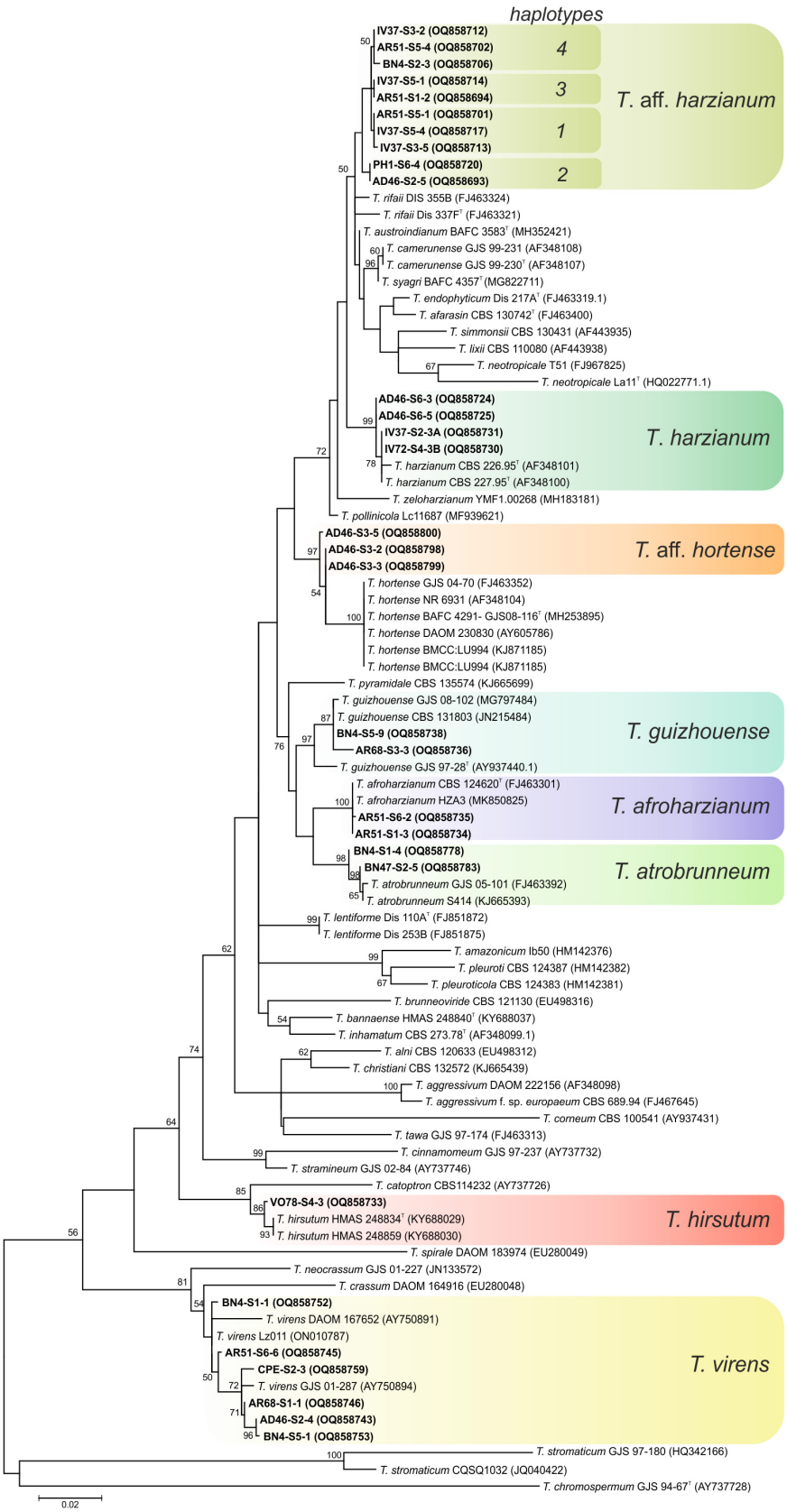

FIGURE 3
Maximum likelihood phylogenetic tree of the *Harzianum-Virens* lineage (Jaklitsch and Voglmayr, 2015) showing the position of seven *Trichoderma* species isolated from banana rhizosphere soils in Tenerife (Canary Islands) based on the nucleotide sequences of the *tef1-α* gene. Sequences obtained in this work are indicated in bold. ML bootstrap support above 50% is given on each node. The type strains are indicated with "T". GenBank accession numbers are shown in parentheses.

harzianum tef1-α sequence allowed the detection of four haplotypes (haplotype 1: 13 isolates; haplotype 2: 9 isolates; haplotype 3: 5 isolates; and haplotype 4: 4 isolates). The comparison with sequences of the type strains of the related species showed 98.2% similarity (4 substitutions + 2 gaps) with *T. austroindianum* VAB T050^T (accession no. MH352421), 97.2% similarity (9 substitutions + 1 gaps) with *T. syagri* BAFC 4357^T (MG822711), 97.0% similarity (10 substitutions + 1 gaps) with *T. camerunense* GJS99 230^T (AF348107), 96.1% similarity (8 substitutions + 7 gaps) with *T. rifaii* DIS 37F^T (FJ463321), and 94.46% similarity (12 substitutions + 3 gaps) with *T. harzianum* CBS 226.95^T (AF348101). In addition, *T.* aff. *hortense* showed 95.6% similarity (4 substitutions + 10 gaps) with the type strain of *T. hortense* G.J.S. 08-116^T (accession no. MH253895).

Diversity and distribution of *Trichoderma* species in the rhizosphere of healthy and *Foc*-STR4-affected banana plants in different agroecosystems

Trichoderma isolates were obtained from all the farms analyzed and from 65.48% of soil samples examined (70.83% in the soils of the northern slope and 58.33% in soils of the southern slope). In relation to the number of isolates (131 in total), 75 isolates were obtained from the soils of the northern slope (57.25% of the total isolates) and 56 from the soils of the south of the island (42.75% of the total isolates) (**Table 2**). In general terms, it can be observed that the percentage of soil samples with *Trichoderma* and the percentage of isolates obtained is higher on the northern slope than on the southern slope. In addition, on both slopes, the percentage of isolates obtained from healthy plants is higher than that of diseased plants (51.91% and 48.09%, respectively).

Regarding the number of species identified (12 in total), no differences were observed between the different origins of the samples. In the northern soils, a total of eight species were identified, while from the southern soils, nine species were identified. *Trichoderma virens* and *T. harzianum* group (identified as *T.* aff. *harzianum* and *T. harzianum*) were the most abundant species. *Trichoderma virens* represent 35.9% of isolates and was detected in 11 of the 14 farms (78.6% of the farms). *Trichoderma* aff. *harzianum* and *T. harzianum* represent 35.1% of all isolates and were detected in 12 and 6 farms, respectively (85.7% and 42.8% of the farms). It is interesting to note that *T.* aff. *harzianum* was the only species isolated in all farms on the southern slope from the soil of healthy plants (**Figure 6**). *Trichoderma atrobrunneum* (9.2% of isolates) and *T. guizhouense* (5.3%) were the most abundant species after *T. virens* and *T.* aff. *harzianum*, being observed in 5 and 6 farms, respectively. *Trichoderma hamatum* and *T. asperellum* (4.6% and 2.3% of isolates, respectively) were detected on two farms and *T. hirsutum* (0.76%) on one farm on the northern slope, while none of these species were detected on the southern slope (**Figures 6, 7**). Unlike *T. afroharzianum* (2.3% of isolated), *T.* aff. *hortense* (2.3%), *T. longibrachiatum* (1.5%), and *T. gamsii* (0.76%) were detected in one farm on the southern slope, while no isolates were obtained from northern slope (**Figures 6, 7**).

The Olmstead-Tukey scattergram shows *T. virens* and *T.* aff. *harzianum* are the dominant species in the northern and southern soils of healthy and *Foc*-STR4-affected banana plants (**Figure 8**). Similarly, *T. atrobrunneum* and *T. hamatum* occur as dominant species in the northern soils of healthy plants, while the rest of the species were classified as occasional or rare. The Margalef (E), Shannon (H), Simpson (D), and Pielou (J) diversity indices show a different performance of the species on each slope (**Table 3**). The richness index (Margalef) of the northern slope was higher in healthy plants (E: 1.91) than in diseased plants (E: 1.82). While on the southern slope, this tendency was not observed. The Simpson index was close to 1, indicating a high diversity of *Trichoderma* species in the banana rhizosphere soils of Tenerife. In northern soils, the diversity of *Trichoderma* of the healthy plants (D: 0.81) were higher than those from diseased plants (D: 0.69). Likewise, the Shannon index showed the same trend (H: 1.82 in healthy plants and H: 1.53 in diseased plants). However, on the southern slope, the diversity indices of healthy plants were lower than those of diseased plants. Pielou's index measures evenness. It can vary between 0 and 1, where 0 means that there is only one species (no evenness) and 1 means that all species are equally abundant (complete evenness). In this study, we observed that northern soils showed higher species evenness in healthy plants (J: 0.87) than in diseased plants (J: 0.78). However, the trend in the southern soils is the opposite: soils of healthy plants (J: 0.75) have a lower index than soils of diseased plants (J: 0.80). With regard to the relationship between soil *Foc* population (cfu/g) and the *Trichoderma* biodiversity indices, no significant correlation was detected between both parameters.

Effect of soil chemical properties on *Trichoderma* community

To evaluate the effect of the soil chemical properties on the relative frequency of the different *Trichoderma* species, the oxidizable organic matter, total nitrogen, assimilable phosphorus, calcium, magnesium, potassium, sodium, electrical conductivity, and pH were determined in the soil samples of each of the farms. No significant differences ($p < 0.05$) were observed (on both slopes) between the chemical properties of healthy and diseased soils. However, the comparison of the soils from the northern and southern slopes showed significant differences ($p < 0.05$) in the content of oxidizable organic matter (%), sodium (mEq/kg) and pH (**Table 4**).

The Spearman analysis showed that certain *Trichoderma* species present significant correlations with some soil chemical parameters. For example, on the northern slope, *T. virens* (the species isolated with the highest occurrence frequency) showed a significant positive correlation with phosphorus content and a negative correlation with calcium and magnesium content, while on the southern slope these correlations were not significant (**Figure 9**). *Trichoderma* aff. *harzianum* (another species isolated with high occurrence frequency) and *T. atrobrunneum* showed a significant positive correlation with soil pH on the northern slope, while on the southern slope none of the correlations were significant. Likewise, *T. atrobrunneum* showed a significant negative correlation with total nitrogen on the

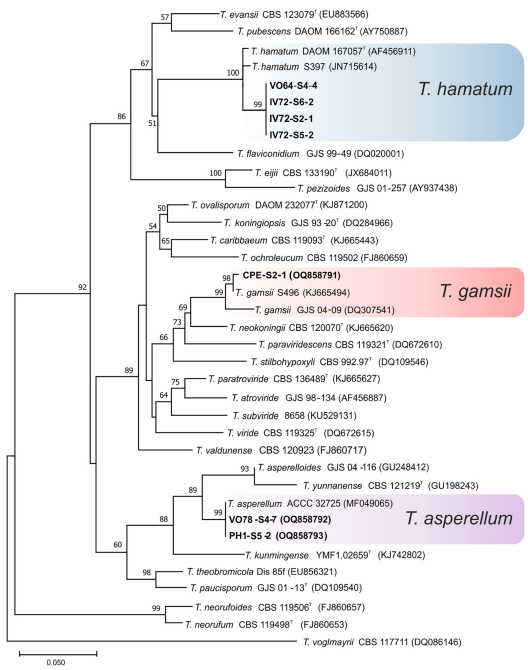

FIGURE 4
Maximum likelihood phylogenetic tree of the *Trichoderma* lineage (Jaklitsch and Voglmayr, 2015) showing the position of three *Trichoderma* species isolated from banana rhizosphere soils in Tenerife (Canary Islands) based on the nucleotide sequences of the *tef1*-α gene. Sequences obtained in this work are indicated in bold. ML bootstrap support above 50% is given on each node. The type strains are indicated with "T". GenBank accession numbers are shown in parentheses.

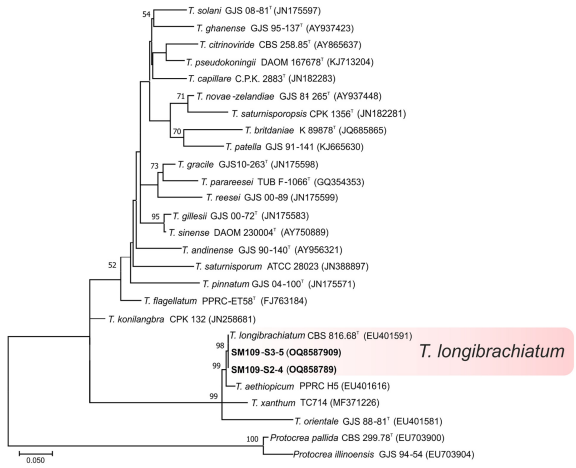

FIGURE 5
Maximum likelihood phylogenetic tree of the *Longibrachiatum* lineage (Jaklitsch and Voglmayr, 2015) showing the position of one *Trichoderma* species isolated from banana rhizosphere soils in Tenerife (Canary Islands) based on the nucleotide sequences of the *tef1*-α gene. Sequences obtained in this work are indicated in bold. ML bootstrap support above 50% is given on each node. The type strains are indicated with "T". GenBank accession numbers are shown in parentheses.

northern slope. *Trichoderma harzianum* showed a significant positive correlation with the potassium content on the southern slope and a negative correlation with calcium on the northern slope. *Trichoderma guizhouense* showed a significant positive correlation with the phosphorous content on both slopes and with magnesium on the southern slope of the island. *Trichoderma hamatum* showed a positive correlation with oxidizable organic matter and total nitrogen and a negative correlation with sodium, potassium, and pH. According to these results, the parameters that significantly affect the *Trichoderma* population were the phosphorus and soil pH.

Discussion

It is widely recognized that soil features, plant characteristics, microorganism diversity, agronomic management, and environmental factors significantly influence the plant/root-microorganism relationship (Lemanceau et al., 1995). Likewise, the amount of phytopathogen in the soil and its relationship with BCA microorganisms is another important aspect to consider. Xue et al. (2015) found significantly lower colony forming unit numbers of *F. oxysporum* f. sp. *cubense* in the disease-suppressive rhizospheric soil (no disease plants) (approximately 5×10^3 cfu/g) compared to the wilted banana rhizosphere (disease plants) (approximately 1×10^5 cfu/g). Likewise, Zhou et al. (2019) quantified a *F. oxysporum* f. sp. *cubense* population less than

TABLE 2 ***Trichoderma*** **isolates' distribution in the different banana rhizosphere soils in Tenerife.**

	Northern slope		Southern slope	
	Diseased plants	Healthy plants	Diseased plants	Healthy plants
Number of farms	8		6	
Number of soil samples	24	24	18	18
Percentage of soil samples with *Trichoderma* isolates	70.83		58.33	
	62.50	79.17	55.56	61.11
Number of *Trichoderma* species	7	8	8	8
Number of *Trichoderma* isolates	75		56	
	36	39	27	29
Isolation rates (IR)	1.50	1.62	1.50	1.61
Percentage of isolates	57.25(1)		42.75(1)	
	27.48(1)	29.77(1)	20.61(1)	22.14(1)
	48.00(2)	52.00(2)	48.21(3)	51.79(3)

(1)In relation to the total number of isolates (131). (2)In relation to the number of isolates from northern soils (75). (3)In relation to the number of isolates from southern soils (56).

1.3×10^3 cfu/g in disease-free soils and more than 1.7×10^3 cfu/g in diseased soil samples of three banana farms in China. Based on these results, the authors indicate that a *Foc* population lower than 1.3×10^3 cfu/g does not cause *Fusarium* wilt banana in the field. However, these data are not in agreement with our results where 41.6% of diseased soil samples had less than 1.3×10^3 cfu/g, and no significant differences were detected between the rhizosphere *Fusarium* population of healthy and diseased plants (**Figure 1**). On the other hand, soil chemical parameters can play an important role in the amount of the pathogen. In this regard, Senechkin

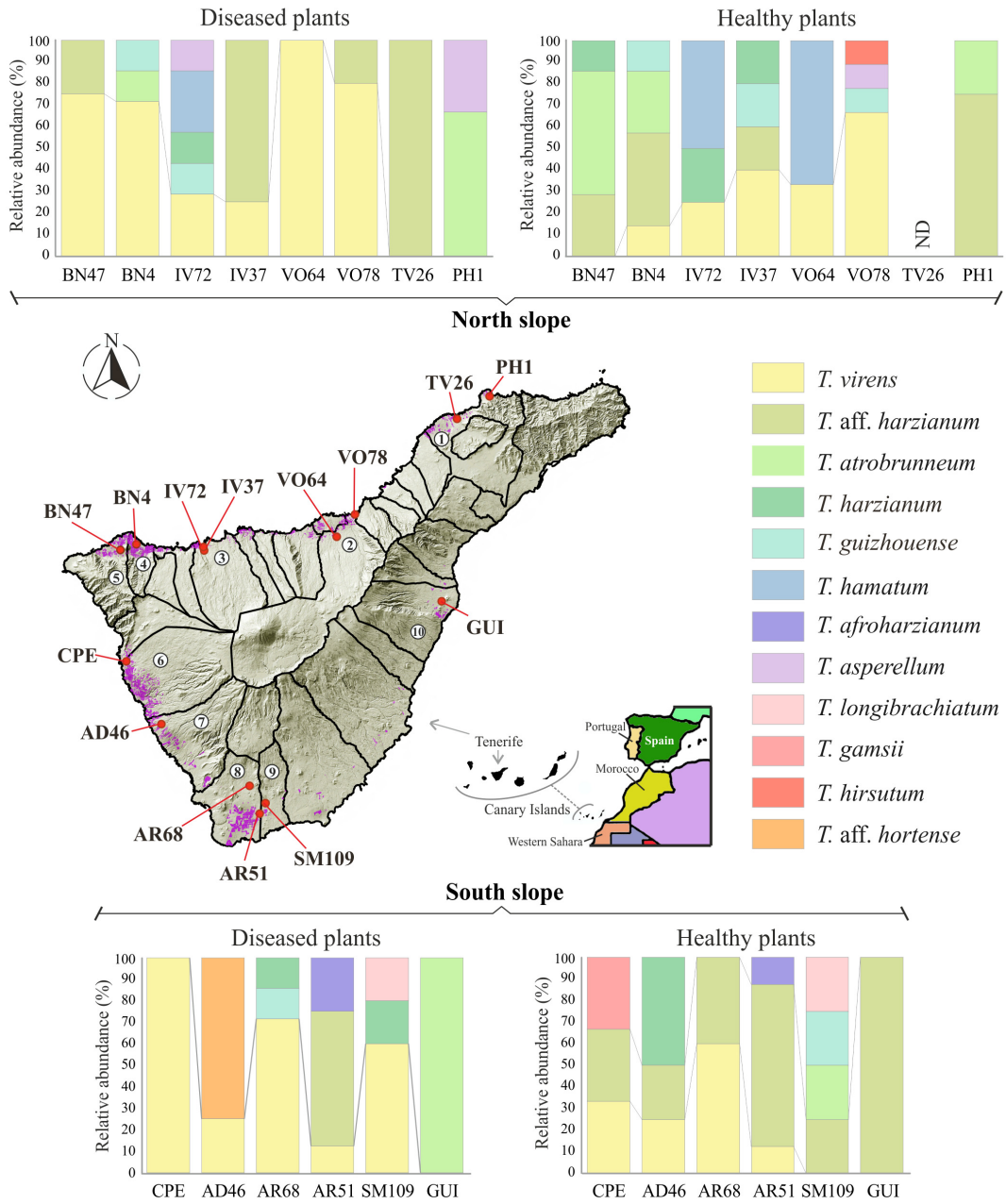

FIGURE 6
Diversity and distribution of *Trichoderma* species in banana rhizosphere soil in Tenerife (Canary Islands). Sampling points and farm locations are indicated with a red circle. Banana growing areas are indicated in purple. Municipalities are indicated with numbers: 1, San Cristóbal de La Laguna; 2, Valle de La Orotava; 3, Icod de los Vinos; 4, Los Silos; 5, Buenavista del Norte; 6, Guía de Isora; 7, Adeje; 8, Arona; 9, San Miguel de Abona; 10, Güímar; ND: *Trichoderma* was not detected.

et al. (2014) and Zhou et al. (2019) describe a positive correlation between soil organic matter and *Fusarium* abundance, and a negative correlation for pH. In this aspect, the results of our work are consistent with these authors: the *Foc* population in the soils of the northern slope was significantly higher than in the southern soils, where organic matter and pH were higher and lower, respectively (**Figure 1** and **Table 4**).

Trichoderma is a fungus with a worldwide distribution and widely studied in different natural and agricultural ecosystems of the world. However, there are few works related to *Trichoderma* distribution and biodiversity in banana rhizosphere soils under different environmental conditions or in relation to the health status of the plant. In the specific case of the Canary Islands, Zachow et al. (2009) analyzed the fungal diversity in the rhizosphere of endemic plants of six different climatic and vegetation zones in Tenerife, indicating that it is an interesting place to study biodiversity and species diversification. However, in contrast to other fungi analyzed, the *Trichoderma* species described were ubiquitous and widely distributed and no significant differences were detected between the biodiversity of the different sampling areas. Moreover, Jaklitsch and Voglmayr (2015) analyzed *Trichoderma* populations in Tenerife, La Palma, and La Gomera

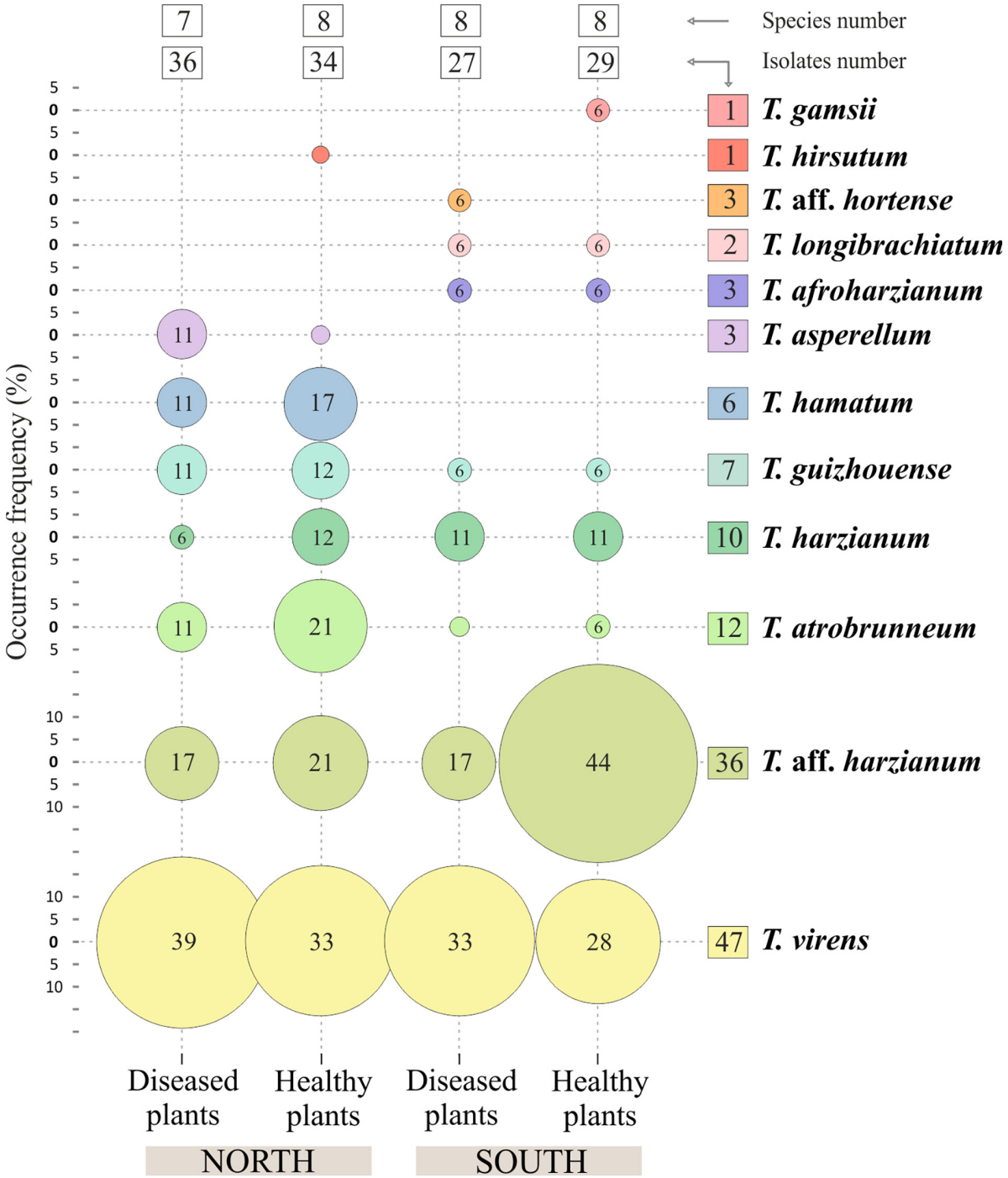

FIGURE 7
Occurrence frequency (OF), number of isolates and species of *Trichoderma* spp. in banana rhizosphere soils in Tenerife (Canary Islands). OF above 5% are indicated inside the circles.

(the western Canary Islands) and identified 17 described species and 3 putatively new *Trichoderma* species, of which 62% belonged to the Viride clade and 16.7% to *Trichoderma harzianum* s.l.

Trichoderma harzianum is a cosmopolitan species widely distributed in different parts of the world, such as Tunisia (Sadfi-Zouaoui et al., 2009), Sardinia (Migheli et al., 2009), Egypt (Gherbawy et al., 2004), South America (Barrera et al., 2021), Canary Islands (Tenerife) (Zachow et al., 2009), etc. Moreover, it is the species with the highest number of citations in soil samples from banana crops: China (Yang et al., 2016; Du et al., 2020), India (Thangavelu et al., 2004; Thangavelu and Gopi, 2015), Malaysia (Naher et al., 2019), Mexico (Hernández-Domínguez et al., 2019), and Tenerife (Canary Islands) (Ciancio et al., 2022). In our study, this species was detected in healthy and *Foc*-STR4 diseased plants on both slopes of the island (**Figures 6–8**). Likewise, *T.* aff. *harzianum* (a putatively new species) was one

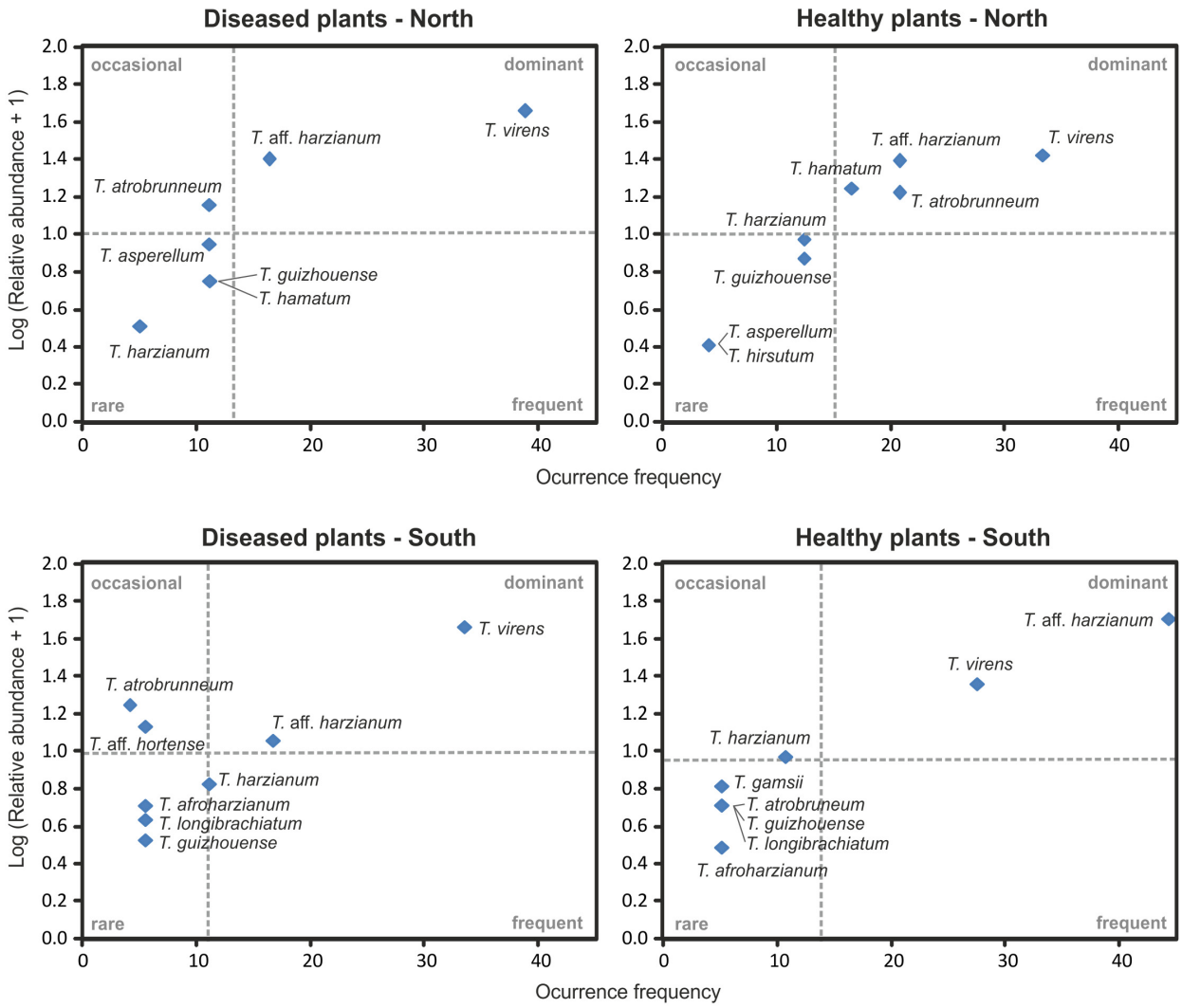

FIGURE 8
Olmstead-Tukey diagram relationship between the occurrence frequency and the relative abundance of *Trichoderma* species identified from banana rhizosphere soil on the north and the south slopes of Tenerife. The dashed lines correspond to the mean relative abundance (horizontal) and occurrence frequency (vertical) and are used to define the dominant, frequent, occasional, and rare species.

TABLE 3 **Diversity indices of *Trichoderma* species isolated from healthy and diseased banana plants of the northern and southern slope of the island of Tenerife.**

Slope	Plants	Margalef (E)	Simpson (D)	Shannon (H)	Pielou (J)
North	Healthy	1.91	0.81	1.82	0.87
	Diseased	1.82	0.69	1.53	0.78
South	Healthy	2.08	0.72	1.56	0.75
	Diseased	2.12	0.74	1.67	0.80

of the dominant species (27.48% of the isolates) (Figures 2, 8) and was detected on both slopes of the island in healthy and diseased plants (Figure 7). Notably, it was the only species detected in 100% of the southern farms in the rhizosphere of healthy plants (Figure 6). Additionally, a positive correlation ($p < 0.05$) with the soil pH was detected on the northern slope (Figure 9). These results agree with those described by Mayo-Prieto et al. (2021), who observed an increase in the development of *T. harzianum* T059 in Esla-Campo's soils with high pH values.

Trichoderma virens was the most frequently isolated species (35.89% RA) (Figure 2). On the northern slope, it was detected in 62.5% and 75.0% of the farms (from healthy and diseased soils samples, respectively), while on the southern slope it was observed in 66.7% and 83.3% of the farms (healthy and diseased soils, respectively) (Figures 6, 7). According to the Olmstead-Tukey test,

TABLE 4 Chemical properties of the different rhizosphere soil samples (healthy and diseased banana plants) obtained from farms located on the northern and southern slopes of Tenerife.

Slope	Plants	Organic matter (%)	Total nitrogen (%)	Phosphorus (mg/kg)	Calcium (mEq/Kg)	Magnesium (mEq/Kg)	Sodium (mEq/Kg)	Potassium (mEq/Kg)	pH	Conductivity (mS/cm)
North	Diseased	5.72 a	0.256 a	36.00 a	232.50 a	134.01 a	34.16 a	42.75 a	7.43 a	0.68 a
	Healthy	5.44 a	0.255 a	34.75 a	241.88 a	123.88 a	33.81 a	36.70 a	7.40 a	0.65 a
	Average	5.58 A	0.256 A	35.38 A	237.19 A	128.94 A	33.99 A	39.73 A	7.41 A	0.67 A
South	Diseased	3.53 a	0.208 a	28.25 a	233.50 a	143.23 a	56.23 a	42.68 a	8.08 a	1.72 a
	Healthy	3.56 a	0.207 a	30.42 a	230.50 a	147.22 a	54.28 a	34.48 a	8.00 a	1.68 a
	Average	3.55 B	0.208 A	29.33 A	232.00 A	145.23 A	55.26 B	38.58 A	8.04 B	1.70 A

Different letters in each column indicate that there are statistically significant differences (Tukey HSD test, $p < 0.05$) between soils from healthy and diseased plants from the same slope (north or south) (lowercase) or between soils from different slopes (uppercase). Each experiment was repeated three times. See section "Materials and methods" for details on chemical analysis of soil samples.

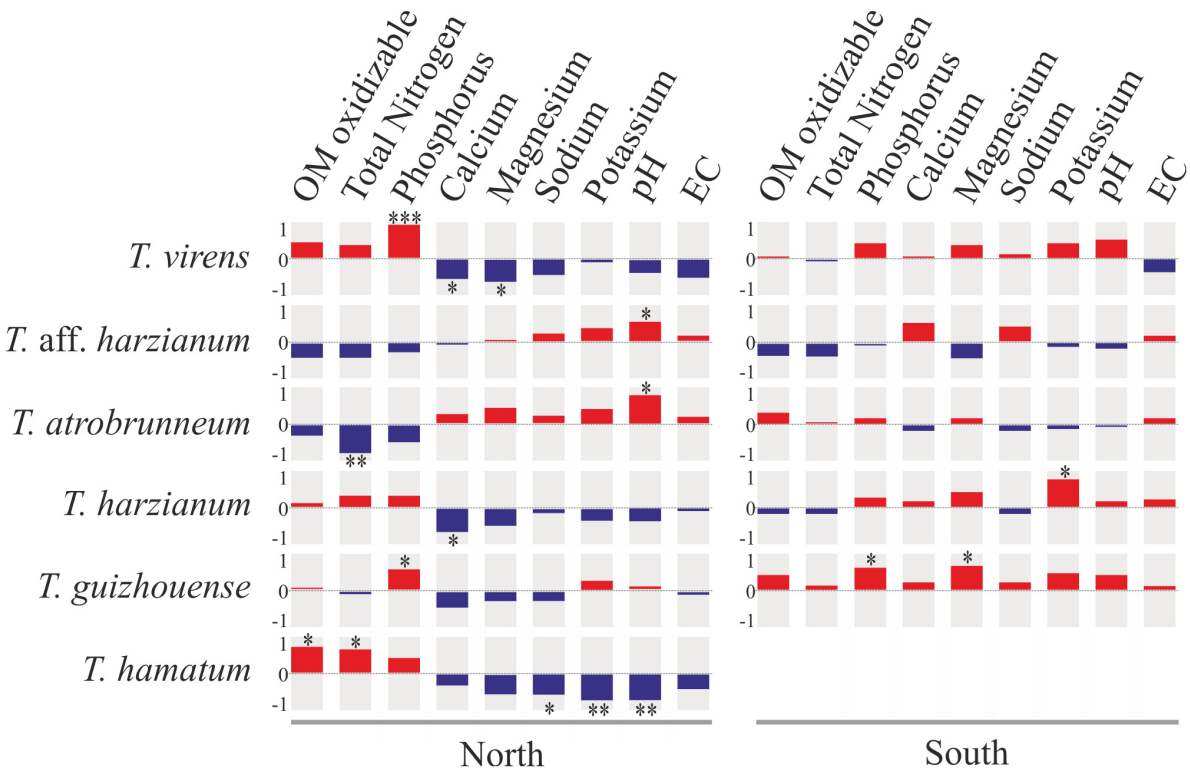

FIGURE 9
Spearman's rank correlation matrix between the occurrence frequency of the top six *Trichoderma* species and soil chemical parameters on the northern and southern slopes of Tenerife. Square size reflects the magnitude of the correlation coefficient (red, positive correlation; blue, negative correlation). *$p < 0.05$; **$p < 0.01$; ***$p < 0.001$.

T. virens was classified as a dominant species on both slopes of the island (Figure 8) and in the north, its abundance was significantly positively correlated ($p < 0.001$) with the phosphorus content in the soil (Figure 9). Surprisingly, this species has not been previously described in banana soils elsewhere in the world and, in Tenerife, it was identified by Ciancio et al. (2022) from a "control" sample of rhizospheric soil free of banana roots. *Trichoderma virens* is a potent bioeffector for plant protection (biofungicide) and plant growth promotion (biofertilizers) (Harman et al., 2004) and is currently marketed as a BCA in organic farming (Woo et al., 2023). Muthukathan et al. (2020) identified *T. virens* proteins involved in banana/root-*Trichoderma* interaction that could be relevant for disease management in banana. These proteins are associated with penetration, colonization and induction of the plant defense response. For this reason, finding this dominant species in the banana soils rhizosphere in Tenerife opens a promising avenue of research into the selection of potential *Foc*-STR4 biocontrol agents adapted to the environmental and crop conditions of the Canary Islands.

Trichoderma atrobrunneum is a widely distributed species and has been described in different parts of the world in soil samples or decaying wood of North America, Europe (Jaklitsch and Voglmayr, 2015), and Africa (Haouhach et al., 2020; Nyang'au et al., 2023). However, none of the previous works performed in the Canary

Islands or in banana soils in other parts of the world describe this species. In our work, the highest occurrence frequency in the rhizosphere of healthy plants from the northern slope was observed (**Figures 6–8**) and a significant positive correlation ($p < 0.05$) with the soil pH of the northern slope was detected (**Figure 9**). Therefore, this is the first time it has been described in Tenerife and in banana rhizosphere.

The ability of *T. atrobrunneum* as BCA has been demonstrated in many studies. The genomic analysis reveals the presence of different genes encoding for carbohydrate-active enzymes, proteins associated with the synthesis of secondary metabolites, peptaboils, epidithiodioxopiperazines, and siderophores potentially involved in parasitism, saprophytic degradation as well as in biocontrol and antagonistic activities (Fanelli et al., 2018). Pavlovskaya et al. (2020) demonstrate the ability to control *Fusarium* wilt in cucumber through an efficient protective effect and growth stimulation. Natsiopoulos et al. (2022) report the efficacy of an isolate obtained in Serres (Northern Greece) from corn cobs to significantly reduce the *in vitro* development of *F. oxysporum* f. sp. *lycopersici* and to decrease the incidence of the disease in tomato plants grown in pots. This background demonstrates the biocontrol capacity of *T. atrobrunneum* and its potential use in the control of *Foc*-STR4 on banana crops in the Canary Islands.

Trichoderma guizhouense was first described in soil samples from two different regions in Guizhou province in China (Li et al., 2013) and has subsequently been detected in different countries in southern Europe (Croatia, Italy, Greece, and Spain) and South America (Argentina) (Jaklitsch and Voglmayr, 2015; Barrera et al., 2021). However, in the Canary Islands, previous works do not describe this species, whereas in our study, we obtained isolates from both slopes of the island in the rhizosphere of healthy and diseased plants (**Figures 6–8**). Furthermore, a significant positive correlation ($p < 0.05$) was detected with the phosphorus content of the soil on both slopes (**Figure 9**). Regarding its agronomic utility, several studies have demonstrated the ability of this species to promote plant growth, produce volatile compounds and antioxidants, and control the development of phytopathogens (Wang and Zhuang, 2019; Liu et al., 2021). In this regard, the NJAU 4,742 strain isolated in China from aromatic plant tissue has been intensively studied for its antifungal capacity against different plant pathogens of different crops, including *Foc*-TR4 (Zhang et al., 2016, 2019; Pang et al., 2020).

Trichoderma hamatum has been described in banana soils in Mexico with a relative abundance of 5% (referring to the total number of *Fusarium* and *Trichoderma* isolates evaluated) (Hernández-Domínguez et al., 2019). In our work, this species constituted 4.6% (RA) of the *Trichoderma* isolates (**Figure 2**) and was only detected in samples from the northern slope as a dominant species in healthy plants and rare in diseased plants (**Figures 7, 8**). Previous works in the Canary Islands have not reported this species, while in other parts of the world it is described as a widely distributed species in different environmental conditions. Danielson and Davey (1973) and Jiang et al. (2016) highlight the ability of *T. hamatum* to tolerate excessive moisture conditions in forest soils in the United States (North Carolina, Virginia, and Washington) and in farmland soils of East China, respectively. However, Sadfi-Zouaoui et al. (2009) found *T. hamatum* to be a dominant species in all areas of Tunisia and detected no differences in its distribution with respect to different climatic conditions. By contrast, in Tenerife, the distribution of this species seems to be affected by the climatic and soil conditions of the slope, with the northern area being more favorable for its development (**Figures 6–8**). Additionally, highlighting the significant negative correlation ($p < 0.01$) with the soil pH (**Figure 9**) could explain its non-detection in the soils of the southern slope (significantly more alkaline than those of the north) (**Table 4**). This result would agree with that described by Danielson and Davey (1973), who define *T. hamatum* as one of the most widely distributed species in North American acid forest soils. Another aspect to highlight in our study is the significant positive correlation ($p < 0.05$) with the total nitrogen and the organic matter content (**Figure 9**), which could also contribute to the non-detection in the southern slope soils (with a significantly lower amount of organic matter) (**Table 4**). These results concur with those described by Migheli et al. (2009) on Sardinia (Italy), where they describe a positive correlation with the content of organic compounds in the soil.

Trichoderma asperellum is a species widely used as a BCA against different pathogens, including the different "special forms" (f. sp.) of *F. oxysporum* (Patel and Saraf, 2017; Sehim et al., 2023). Therefore, this species is part of the active ingredient of several microbial fungicides marketed in different countries around the world (Woo et al., 2023). In banana soils, it is cited in different places, such as: India (Thangavelu and Gopi, 2015; Damodaran et al., 2020), Nigeria (Akinyele et al., 2019), and China (Win et al., 2021). Some authors also describe it as an endophytic species of banana (Xia et al., 2011; Thangavelu and Gopi, 2015; Olowe et al., 2022). However, in the Canary Islands, previous works do not describe this species in any of the bioclimatic conditions, while in our study, it was detected as a rare species on the northern slope of healthy and diseased plants (**Figures 6–8**). The non-detection in the southern soils could be due to the inability to establish in the warmer and drier conditions of this slope of the island. In this sense, similar results were observed by Migheli et al. (2009) on the island of Sardinia (Italy).

Trichoderma afroharzianum is an opportunistic environmental species with an outstanding aptitude for biocontrol, plant growth promotion and enzyme production (Chaverri et al., 2016; Xiao et al., 2023). Previous studies do not report this species in the Canary Islands or in the banana rhizosphere in other parts of the world. In this study, this species was detected with a low occurrence frequency (rare species) on the southern slope of both types of plants (healthy and diseased) (**Figures 6–8**).

Trichoderma longibrachiatum has been previously described in banana soils in different parts of the world: Mexico (Hernández-Domínguez et al., 2019), Brazil (Sanó et al., 2022), and Tenerife (Spain) (Ciancio et al., 2022). In our work, this species has been detected as rare (**Figure 8**) in soils from the southern slope (**Figures 6, 7**), which agrees with what was previously described by Ciancio et al. (2022).

Trichoderma aff. *hortense* was first described in Argentina from horticultural soil samples. However, isolates of this species previously identified under other names (*T. harzianum, T. aureoviride, Hypocrea lixii*) have been described in Japan, Italy, and New Zealand, suggesting a cosmopolitan distribution (Barrera et al., 2021). In our study, the *tef1*-α gene sequences obtained from banana soil isolates from Tenerife were related to the same clade as the *T. hortense* sequences. However, these sequences were not identical to those deposited in the GenBank database (95.6%

similarity), therefore, we use the term *affinis* (aff.) to indicate that the OTUs are similar but not identical to the assigned species (accession no. MH253895). According to the Olmstead-Tukey test, this species is classified as rare in the banana crops of Tenerife (**Figure 8**), with a low number of isolates (3) from the rhizosphere of diseased plants from a single farm on the southern slope (**Figures 6**, **7**).

Trichoderma gamsii has been described in Greece, Italy, Spain, Africa, India, and China (Migheli et al., 2009; Ding et al., 2012; Rinu et al., 2014; Jaklitsch and Voglmayr, 2015). Zachow et al. (2009) describes this species in Tenerife in soil/rhizosphere samples from different vegetation zones: Arico (Cardonal/Tabaibal; subtropical, arid) and Buenavista del Norte (Laurisilva/Fayal-Brezal; subtropical, subhumid). In our study, a single isolate was obtained from the rhizosphere of a healthy plant from the southern slope of Tenerife (Guía de Isora) (**Figures 6**, **7**) and to our knowledge, there are no previous records associated with banana crops in other parts of the world. *Trichoderma gamsii* has already demonstrated it can reduce the growth of *Fusarium* head blight in wheat and *F. oxysporum* rot and wilt black gram (*Vigna mungo*) (Alukumbura et al., 2022; Valan-Arasu et al., 2023). Consequently, the ability of *T. gamsii* to control *F. oxysporum* f. sp. *cubense* STR4 under the environmental conditions of the Canary Islands should be analyzed.

Trichoderma hirsutum was first described in China in the Shennongjia Natural Reserve in soil samples at 1,200 m.a.s.l. (Chen and Zhuang, 2017) and subsequently in northern Algeria (Sub-humid bioclimate) at very low frequency from the tomato rhizosphere (Benttoumi et al., 2020). In Tenerife, a single isolate was obtained from the rhizosphere of a healthy plant from the northern slope (La Orotava) (**Figures 6**, **7**).

Conclusion

This work represents the first investigation of the biodiversity of *Trichoderma* species in the soil rhizosphere of the Canary Island banana agroecosystem. The results presented here mainly concern the taxonomic analysis of *Trichoderma* and the distribution of the species in the rhizosphere of healthy and *Foc*-STR4 diseased plants in different bioclimatic conditions of Tenerife (Canary Islands, Spain). The findings demonstrate the biodiversity of *Trichoderma* in banana crops. Many of the species identified (6 out of 12 total) had not been previously described in the Canary Islands (*T. afroharzianum, T. asperellum, T. atrobrunneum, T. guizhouense, T. hamatum*, and *T. hirsutum*) or associated to banana rhizosphere (*T. afroharzianum, T. atrobrunneum, T. gamsi, T. guizhouense, T. hirsutum*, and *T. virens*). Therefore, to the best of our knowledge, this work is the first report of these species in the Canary Islands or in banana ecosystems. In addition, two putative novel species, named *T.* aff. *harzianum* and *T.* aff. *hortense*, were detected. The analysis of species distribution showed that *T. virens* and *T.* aff. *harzianum* were the most abundant (35.89% and 27.48% RA, respectively) (**Figure 2**) and dominant species in the rhizosphere of banana soils on both slopes of Tenerife (north and south) (**Figures 7**, **8**). While other species were mainly associated with a particular bioclimatic condition: *T. hamatum, T. asperellum*, and *T. hirsutum* were isolated only on the northern slope, and *T. afroharzianum, T. longibrachiatum, T. gamsii*, and *T.* aff. *hortense* on the southern slope (**Figures 6**, **7**). Probably, the species associated with the northern slope are better adapted to lower temperatures and higher humidity, while the species associated with the southern slope are better adapted to higher temperatures and lower humidity. Likewise, the edaphic characteristics could influence species distribution: soils on the southern slope had a significantly higher pH than those on the north, while the relationship of the organic matter was the opposite.

Trichoderma species have long been recognized as agents for the control of plant diseases and for their ability to enhance root growth and development, crop productivity, resistance to abiotic stresses, and nutrient uptake and utilization (Berg et al., 2005). Knowledge and understanding of the biodiversity of the rhizosphere microbiota in relation to plant health and the environment is essential for the prevention and treatment of plant diseases (Xue et al., 2015). For this reason, it is recommended to select potential biocontrol agents from native *Trichoderma* isolates obtained under similar conditions (soil or plant parts) to those encountered during pathogen control (Howell, 2003). These isolates will be naturally adapted to the specific environmental conditions of biocontrol (temperature, humidity, nutrient availability, microbiota, etc.) and represent a suitable strategy to overcome problems related to the introduction of exogenous microorganisms (Howell, 2003; Anees et al., 2010). In this context, the analysis of the *Trichoderma* population distribution and the culture collection developed in this study will contribute to the future selection of new isolates or novel native species as BCAs against the most important banana disease in the Canary Islands (*Foc*-STR4). In this sense, our work demonstrates the existence of a high number of *Trichoderma* species with biocontrol potential and that are naturally adapted to the environmental and agronomic conditions of banana cultivation in the Canary Islands. This is in line with the ultimate goal of finding a cost-effective and environmentally friendly alternative for disease control.

Data availability statement

The datasets generated for this study can be found in the GenBank (https://www.ncbi.nlm.nih.gov/genbank/) accession number (OQ858692 to OQ858800).

Author contributions

RC-D: Data curation, Formal analysis, Investigation, Software, Visualization, Writing – original draft. PB-L: Data curation, Investigation, Writing – original draft. MJV: Funding acquisition, Resources, Supervision, Writing – review & editing. FL: Formal analysis, Funding acquisition, Methodology, Project administration, Resources, Supervision, Validation, Visualization, Writing – review & editing.

Funding

The author(s) declare financial support was received for the research, authorship, and/or publication of this article. This study was financially supported by the Consejería de Agricultura, Ganadería, Pesca y Aguas del Gobierno de Canarias (Project: CAIA 2023-001-04 "Estrategias agroecológicas para el manejo de sistemas plataneros").

Acknowledgments

The authors are thankful to Patricia C. Pérez Parrado for her technical assistance and dedication to this work. The authors wish to thank the Laboratory Unit of the Canary Institute of Agricultural Research (ICIA) for the physical-chemical analysis of soil samples, and to the farmers for allowing this research to be carried out on their banana crops. Finally, the authors would like to thank for the Grant PRE2019-089319 funded by MCIN/AEI/10.13039/501100011033 and, as appropriate, by "ESF Investing in your future" or by "European Union Next Generation EU/PRTR" from the Spanish Government.

Conflict of interest

The authors declare that the research was conducted in the absence of any commercial or financial relationships that could be construed as a potential conflict of interest.

Publisher's note

All claims expressed in this article are solely those of the authors and do not necessarily represent those of their affiliated organizations, or those of the publisher, the editors and the reviewers. Any product that may be evaluated in this article, or claim that may be made by its manufacturer, is not guaranteed or endorsed by the publisher.

Supplementary material

The Supplementary Material for this article can be found online at: https://www.frontiersin.org/articles/10.3389/fmicb.2024.1376602/full#supplementary-material

References

Akinyele, H. A., Gabriel-Ajobiewe, R. A. O., Ukhureigbe, O. M., Adebesin, A. A., and Omotayo, T. L. (2019). Xylanase-production potential of *Trichoderma asperellum* NG-T161 and NG-T163 isolated from banana farm soils in South Western Nigeria. *Curr. Res. Environ. Appl. Mycol. Fungal Biol.* 9, 301–312. doi: 10.5943/cream/9/1/25

Altschul, S. F., Madden, T. L., Schäffer, A. A., Zhang, J., Zhang, Z., Miller, W., et al. (1997). Gapped BLAST and PSI-BLAST: A new generation of protein database search programs. *Genetics* 156, 1997–2005. doi: 10.1093/genetics/156.4.1997

Alukumbura, A. S., Bigi, A., Sarrocco, S., Fernando, W. G. D., Vannacci, G., Mazzoncini, M., et al. (2022). Minimal impacts on the wheat microbiome when *Trichoderma gamsii* T6085 is applied as a biocontrol agent to manage *Fusarium* head blight disease. *Front. Microbiol.* 13:972016. doi: 10.3389/fmicb.2022.972016

Anees, M., Tronsmo, A., Edel-Hermann, V., Hjeljord, L. G., Héraud, C., and Steinberg, C. (2010). Characterization of field isolates of *Trichoderma* antagonistic against *Rhizoctonia solani*. *Fungal Biol.* 114, 691–701. doi: 10.1016/j.funbio.2010.05.007

Askew, D. J., and Laing, M. D. (1993). An adapted selective medium for the quantitative isolation of *Trichoderma* species. *Plant Pathol.* 42, 686–690. doi: 10.1111/j.1365-3059.1993.tb01553.x

Barrera, V. A., Iannone, L., Romero, A. I., and Chaverri, P. (2021). Expanding the *Trichoderma harzianum* species complex: Three new species from *Argentina* natural and cultivated ecosystems. *Mycologia* 113, 1136–1155. doi: 10.1080/00275514.2021.1947641

Benttoumi, N., Colagiero, M., Sellami, S., Boureghda, H., Keddad, A., and Ciancio, A. (2020). Diversity of nematode microbial antagonists from Algeria shows occurrence of nematotoxic *Trichoderma* spp. *Plants* 9, 1–14. doi: 10.3390/plants9080941

Berg, G., Zachow, C., Lottmann, J., Götz, M., Costa, R., and Smalla, K. (2005). Impact of plant species and site on rhizosphere-associated fungi antagonistic to *Verticillium dahliae* Kleb. *Appl. Environ. Microbiol.* 71, 4203–4213. doi: 10.1128/AEM.71.8.4203-4213.2005

Blakeslee, A. (1915). Lindner's roll tube method of separation cultures. *Phytopathology* 5, 68–69.

Bower, C., Reitemeier, R., and Fireman, M. (1952). Exchangeable cation analysis of saline and alkali soils. *Soil Sci.* 73, 251–261. doi: 10.1097/00010694-195204000-00001

Bubici, G., Kaushal, M., Prigigallo, M. I., Cabanás, C. G. L., and Mercado-Blanco, J. (2019). Biological control agents against *Fusarium* wilt of banana. *Front. Microbiol.* 10:616. doi: 10.3389/fmicb.2019.00616

Buddenhagen, I. (2009). Understanding strain diversity in *Fusarium oxysporum* f. sp. cubense and history of introduction of 'tropical race 4' to better manage banana production. *Acta Hortic.* 828, 193–204.

Caballero, H., Pocasangre, E., Casanoves, F., Avelin, J., Tapia, F., Ortiz, J. L., et al. (2013). Uso de aislamientos endofíticos de *Trichoderma* spp., para el biocontrol del *Fusarium oxysporum* f. sp. cubense (Mal de Panamá) raza 1 en vitro plantas de banano del cultivar Gros Michel (AAA) en condiciones de invernadero. *Univ. Rev. Cient. UNAN León* 4, 71–82. doi: 10.5377/universitas.v4i1.1676

Cai, F., and Druzhinina, S. I. (2021). In honor of John Bissett: Authoritative guidelines on molecular identification of *Trichoderma*. *Fungal Divers.* 107, 1–69. doi: 10.1007/s13225-020-00464-4

Carbone, I., and Kohn, L. M. (1999). A method for designing primer sets for speciation studies in filamentous ascomycetes. *Mycologia* 91, 553–556. doi: 10.1080/00275514.1999.12061051

Carracedo, J. C., Pérez-Torrado, F. J., Ancochea, E., Meco, J., Hernán, F., Cubas, C. R., et al. (2002). Cenozoic volcanism: II. The Canary Islands. In F. A. W. Gibbons & T. Moreno (Eds.), The geology of Spain (pp. 439–472). Geological Society of London: London.

Carvalhais, L. C., Henderson, J., Rincon-Florez, V. A., O'Dwyer, C., Czislowski, E., Aitken, E. A. B., et al. (2019). Molecular diagnostics of banana *Fusarium* wilt targeting secreted-in-xylem genes. *Front. Plant Sci.* 10:547. doi: 10.3389/fpls.2019.00547

Chaverri, P., Building, S., Park, C., Rica, U. D. C., De, E., and Branco-rocha, F. (2016). Systematics of the *Trichoderma harzianum* species complex and the re-identification of commercial biocontrol strains. *Mycologia* 107, 558–590. doi: 10.3852/14-147.Systematics

Chaves, N. P., Staver, C., and Dita, M. A. (2016). Potential of *Trichoderma asperellum* for biocontrol of *Fusarium* wilt in banana. *Act. Hortic.* 25, 261–266. doi: 10.17660/ActaHortic.2016.1114.35

Chen, K., and Zhuang, W. Y. (2017). Discovery from a large-scaled survey of *Trichoderma* in soil of China. *Sci. Rep.* 7, 1–37. doi: 10.1038/s41598-017-07807-3

Ciancio, A., Rosso, L. C., and Lopez-Cepero, J. (2022). Rhizosphere 16S-ITS metabarcoding profiles in banana crops are affected by nematodes, cultivation and local climatic variations. *Front. Microbiol.* 13:1–18. doi: 10.3389/fmicb.2022.855110

Damodaran, T., Rajan, S., Muthukumar, M., Ram Gopal, Yadav, K., Kumar, S., et al. (2020). Biological management of banana *Fusarium* wilt caused by *Fusarium oxysporum* f. sp. cubense tropical race 4 using antagonistic fungal isolate CSR-T-3 (*Trichoderma reesei*). *Front. Microbiol.* 11:1–19. doi: 10.3389/fmicb.2020.595845

Danielson, R. M., and Davey, C. B. (1973). The abundance of *Trichoderma propagules* and the distribution of species in forest soils. *Soil Biol. Biochem.* 5, 485–494. doi: 10.1016/0038-0717(73)90038-2

Del-Arco, M., Pérez-de-Paz, P. L., Acebes, J. R., González-Mancebo, J. M., Reyes Betancort, J. A., Bermejo, J. A., et al. (2006). Bioclimatology and climatophilous vegetation of Tenerife (Canary Islands). *Ann. Bot. Fenn.* 43, 167–192.

Ding, G., Wang, H., Lou, Chen, L., Chen, A. J., Lan, J., et al. (2012). Cytochalasans with different amino-acid origin from the plant endophytic fungus *Trichoderma gamsii*. *J. Antibiot.* 65, 143–145. doi: 10.1038/ja.2011.124

Dita, M., Barquero, M., Heck, D., Mizubuti, E. S. G., and Staver, C. P. (2018). *Fusarium* wilt of banana: Current knowledge on epidemiology and research needs toward sustainable disease management. *Front. Plant Sci.* 871:1468. doi: 10.3389/fpls.2018.01468

Druzhinina, I. S., Kopchinskiy, A. G., Komoń, M., Bissett, J., Szakacs, G., and Kubicek, C. P. (2005). An oligonucleotide barcode for species identification in *Trichoderma* and *Hypocrea*. *Fungal Genet. Biol.* 42, 813–828. doi: 10.1016/j.fgb.2005.06.007

Du, W., Yao, Z., Li, J., Sun, C., Xia, J., Wang, B., et al. (2020). Diversity and antimicrobial activity of endophytic fungi isolated from *Securinega suffruticosa* in the Yellow River Delta. *PLoS One* 15:e0229589. doi: 10.1371/journal.pone.0229589

EUR-Lex (2013). *Reglamento de ejecución (UE) n° 1084/2013 de la comisión, de 30 de octubre de 2013, por el que se inscribe una denominación en el registro de denominaciones de origen Protegidas y de indicaciones geográficas protegidas [Plátano de Canarias (IGP)]*. Available online at: http://data.europa.eu/eli/reg_impl/2013/1084/oj (accessed March 22, 2023).

Fanelli, F., Liuzzi, V. C., Logrieco, A. F., and Altomare, C. (2018). Genomic characterization of *Trichoderma atrobrunneum* (*T. harzianum* species complex) ITEM 908: Insight into the genetic endowment of a multi-target biocontrol strain. *BMC Genom.* 19:662. doi: 10.1186/s12864-018-5049-3

Food and Agriculture Organization of the United Nations (2022). *Banana: Market review – Preliminary results 2022*. Rome: Food and Agriculture Organization of the United Nations.

Fraser-Smith, S., Czislowski, E., Meldrum, R. A., Zander, M., O'Neill, W., Balali, G. R., et al. (2014). Sequence variation in the putative effector gene SIX8 facilitates molecular differentiation of *Fusarium oxysporum* f. sp. cubense. *Plant Pathol.* 63, 1044–1052. doi: 10.1111/ppa.12184

Galán-Sauco, V., García Samarín, J., and Carbonell, E. (1984). Estudio de la práctica del deshijado y la fenología de la platanera (*Musa acuminata* Colla (AAA), cv. "Pequeña enana") en la isla de Tenerife. *Fruits* 39, 595–605.

Galarza, L., Akagi, Y., Takao, K., Kim, C. S., Maekawa, N., Itai, A., et al. (2015). Characterization of *Trichoderma* species isolated in Ecuador and their antagonistic activities against phytopathogenic fungi from Ecuador and Japan. *J. Gen. Plant Pathol.* 81, 201–210. doi: 10.1007/s10327-015-0587-x

Gams, W., and Bissett, J. (1998). *Morphology and identification of Trichoderma. Trichoderma and Gliocladium*. Milton Park: Taylor & Francis Ltd.

Gherbawy, Y., Druzhinina, I., Shaban, G. M., Wuczkowsky, M., Yaser, M., El-Naghy, M. A., et al. (2004). Trichoderma populations from alkaline agricultural soil in the Nile valley, Egypt, consist of only two species. *Mycol. Prog.* 3, 211–218. doi: 10.1007/s11557-006-0091-y

Gutiérrez, S., McCormick, S. P., Cardoza, R. E., Kim, H. S., Yugueros, L. L., Vaughan, M. M., et al. (2021). Distribution, function, and evolution of a gene essential for trichothecene toxin biosynthesis in *Trichoderma*. *Front. Microbiol.* 12:791641. doi: 10.3389/fmicb.2021.791641

Haouhach, S., Karkachi, N., Oguiba, B., Sidaoui, A., Chamorro, I., Kihal, M., et al. (2020). Three new reports of *Trichoderma* in Algeria: *T. atrobrunneum*, (south) *T. longibrachiatum* (south), and *T. afroharzianum* (northwest). *Microorganisms* 8, 1–14. doi: 10.3390/microorganisms8101455

Harman, G. E., Howell, C. R., Viterbo, A., Chet, I., and Lorito, M. (2004). *Trichoderma* species – Opportunistic, avirulent plant symbionts. *Nat. Rev. Microbiol.* 2, 43–56. doi: 10.1038/nrmicro797

Hernández-Domínguez, C., Vázquez Benito, J. A., Vázquez Moreno, F., Berdeja Arbeu, R., Morales Fernández, S. D., and Reyes López, D. (2019). Abundance and genetic diversity of *Fusarium oxysporum* and *Trichoderma* sp. in muse AAB. *Rev. Mex. Cienc. Agríc.* 10, 1783–1796.

Howell, C. R. (2003). Mechanisms employed by *Trichoderma* species in the biological control of plant diseases: The history and evolution of current concepts. *Plant Dis.* 87, 4–10. doi: 10.1094/PDIS.2003.87.1.4

Instituto Canario de Estadística [ISTAC] (2022). Available online at: https://www3.gobiernodecanarias.org/istac/statistical-visualizer/visualizer/data.html?resourceTypedataset&agencyId=ISTAC&resourceId=E01135A_000004&version=~{}latest#visualization/table. (accesed March 22, 2023).

Izzati, N. A. M. Z., Maryam, S. S. S. A. R., and Azwady, N. A. A. (2019). *International Conference on Agriculture, Environment, and Food Security 2018 24-25 October 2018*, Medan. doi: 10.1088/1755-1315/260/1/012119

Jaklitsch, W. M., and Voglmayr, H. (2015). Biodiversity of *Trichoderma* (Hypocreaceae) in Southern Europe and Macaronesia. *Stud. Mycol.* 80, 1–87. doi: 10.1016/j.simyco.2014.11.001

Jaklitsch, W. M., Komon, M., Kubicek, C. P., and Druzhinina, I. S. (2005). *Hypocrea voglmayrii* sp. nov. from the Austrian Alps represents a new phylogenetic clade in *Hypocrea*/*Trichoderma*. *Mycologia* 97, 1365–1378. doi: 10.3852/mycologia.97.6.1365

Jiang, Y., Wang, J. L., Chen, J., Mao, L. J., Feng, X. X., Zhang, C. L., et al. (2016). *Trichoderma* biodiversity of agricultural fields in East China reveals a gradient distribution of species. *PLoS One* 11:e0160613. doi: 10.1371/journal.pone.0160613

Komada, H. (1975). Development of a selective medium for quantitative isolation of *Fusarium oxysporum* from natural soil. *Rev. Plant Prot. Res.* 8, 114–124.

Kubicek, C. P., Steindorff, A. S., Chenthamara, K., Manganiello, G., Henrissat, B., Zhang, J., et al. (2019). Evolution and comparative genomics of the most common *Trichoderma* species. *BMC Genomics* 20:485. doi: 10.1186/s12864-019-5680-7

Lemanceau, P., Corberand, T., Gardan, L., Latour, X., Laguerre, G., Boeufgras, J. M., et al. (1995). Effect of two plant species, flax (*Linum usitatissinum* L.) and tomato (*Lycopersicon esculentum* Mill.), on the diversity of soilborne populations of fluorescent pseudomonads. *Appl. Environ. Microbiol.* 61, 1004–1012. doi: 10.1128/aem.61.3.1004-1012.1995

Leslie, J. F., and Summerell, B. A. (2006). *The Fusarium laboratory manual*. Hoboken, NJ: John Wiley and Sons, doi: 10.1002/9780470278376

Li, Q. R., Tan, P., Jiang, Y. L., Hyde, K. D., Mckenzie, E. H. C., Bahkali, A. H., et al. (2013). A novel *Trichoderma* species isolated from soil in Guizhou, *T. guizhouense*. *Mycol. Prog.* 12, 167–172. doi: 10.1007/s11557-012-0821-2

Liu, H., Li, J., Carvalhais, L. C., Schenk, P. M., Singh, B. K., Percy, C. D., et al. (2021). Evidence for the plant recruitment of beneficial microbes to suppress soil-borne pathogens. *New Phytol.* 229, 2873–2885. doi: 10.1111/nph.17057

Lombard, L., Sandoval-Denis, M., Lamprecht, S. C., and Crous, P. W. (2019). Epitypification of *Fusarium oxysporum* – Clearing the taxonomic chaos. *Pers. Mol. Phylogeny Evol. Fungi* 43, 1–47. doi: 10.3767/persoonia.2019.43.01

Madruga, L., Wallenstein, F., and Azevedo, J. M. N. (2016). *Regional ecosystem profile –Macaronesian region; Technical report for European commission*. Brussels: European Commission.

Margalef, R. (1958). Information theory in ecology. *Int. J. Gen. Syst.* 3, 36–71.

Mayo-Prieto, S., Porteous-Álvarez, A. J., Mezquita-García, S., Rodríguez-González, Á, Carro-Huerga, G., Del Ser-Herrero, S., et al. (2021). Influence of physicochemical characteristics of bean crop soil in *Trichoderma* spp. development. *Agronomy* 11:274. doi: 10.3390/agronomy11020274

Migheli, Q., Balmas, V., Komoñ-Zelazowska, M., Scherm, B., Fiori, S., Kopchinskiy, A. G., et al. (2009). Soils of a Mediterranean hot spot of biodiversity and endemism (Sardinia, Tyrrhenian Islands) are inhabited by pan-European, invasive species of *Hypocrea*/*Trichoderma*. *Environ. Microbiol.* 11, 35–46. doi: 10.1111/j.1462-2920.2008.01736.x

Muthukathan, G., Mukherjee, P., Salaskar, D., Pachauri, S., Tak, H., Ganapathi, T. R., et al. (2020). Secretome of *Trichoderma virens* induced by banana roots-identification of novel fungal proteins for enhancing plant defence. *Physiol. Mol. Plant Pathol.* 110:101476. doi: 10.1016/j.pmpp.2020.101476

Naher, L., Syawani, N., Amieza, N., and Kamarudin, A. B. (2019). Trichoderma species diversity in rhizosphere soils and potential antagonism with *Fusarium oxysporum*. *Biosci J.* 256, 13–26. doi: 10.14393/BJ-v35n1a2019-41605

Natsiopoulos, D., Tziolias, A., Lagogiannis, I., Mantzoukas, S., and Eliopoulos, P. A. (2022). Growth-Promoting and protective effect of *Trichoderma atrobrunneum* and *T. simmonsii* on tomato against soil-borne fungal pathogens. *Crops* 2, 202–217. doi: 10.3390/crops2030015

Norma UNE-EN 77308:2001 (2001). *Calidad del suelo. Determinación de la conductividad eléctrica específica*. Madrid: AENOR.

Norma UNE-ISO 10390:2012 (2012). *Calidad del suelo. Determinación del pH*. Madrid: AENOR.

Nyang'au, M. N., Akutse, K. S., Fathiya, K., Charimbu, M. K., and Haukeland, S. (2023). Biodiversity and efficacy of fungal isolates associated with Kenyan populations of potato cyst nematode (*Globodera* spp.). *Biol. Control* 186:105328. doi: 10.1016/j.biocontrol.2023.105328

O'Donnell, K., Kistlerr, H. C., Cigelnik, E., and Ploetz, R. C. (1998). Multiple evolutionary origins of the fungus causing Panama disease of banana: Concordant evidence from nuclear and mitochondrial gene genealogies. *Proc. Natl. Acad. Sci. U.S.A.* 95, 2044–2049. doi: 10.1073/pnas.95.5.2044

Olowe, O. M., Nicola, L., Asemoloye, M. D., Akanmu, A. O., Sobowale, A. A., and Babalola, O. O. (2022). Characterization and antagonistic potentials of selected rhizosphere *Trichoderma* species against some *Fusarium* species. *Front. Microbiol.* 13:985874. doi: 10.3389/fmicb.2022.985874

Olsen, S. R., Cole, C. V., Watanabe, F. S., and Dean, L. A. (1954). Estimation of available phosphorus in soils by extraction with sodium bicarbonate. *Circular* 939:19.

Pang, G., Sun, T., Yu, Z., Yuan, T., Liu, W., Zhu, H., et al. (2020). Azaphilones biosynthesis complements the defence mechanism of *Trichoderma guizhouense* against oxidative stress. *Environ. Microbiol.* 22, 4808–4824. doi: 10.1111/1462-2920.15246

Patel, S., and Saraf, M. (2017). Biocontrol efficacy of *Trichoderma asperellum* MSST against tomato wilting by *Fusarium oxysporum* f. sp. lycopersici. *Arch. Phytopathol. Plant Prot.* 50, 228–238. doi: 10.1080/03235408.2017.1287236

Pavlovskaya, N., Gneusheva, I., Solokhina, I., and Ageeva, N. (2020). The biological activity of subspecies *Trichoderma harzianum* against *Fusarium oxysporum*, the causative agent of fusarium wilt cucumber in vitro. *BIO Web Conf.* 21:00021. doi: 10.1051/bioconf/20202100021

Perera-González, S., Brito-López, P., Hernández-Hernández, D., Laich, F. S., and Siverio de la Rosa, F. (2023). Estudio sobre el mal de Panamá causado por *Fusarium oxysporum* f. sp. cubense en cultivos de platanera de Tenerife. Informe técnico n°5. *GMR Canarias* 72:56.

Pielou, E. C. (1966). The measurement of diversity in different types of biological collections. *J. Theoretical Biol.* 13, 131–144. doi: 10.1016/0022-5193(66)90013-0

Ploetz, R. C. (2006). *Fusarium* wilt of banana is caused by several pathogens referred to as *Fusarium oxysporum* f. sp. cubense. *Phytopathology* 96, 653–656. doi: 10.1094/PHYTO-96-0653

Ploetz, R. C. (2015a). *Fusarium* wilt of banana. *Phytopathology* 105, 1512–1521. doi: 10.1094/PHYTO-04-15-0101-RVW

Ploetz, R. C. (2015b). Management of *Fusarium* wilt of banana: A review with special reference to tropical race 4. *Crop Prot.* 73, 7–15. doi: 10.1016/j.cropro.2015.01.007

Raaijmakers, J. M., Paulitz, T. C., Steinberg, C., Alabouvette, C., and Moënne-Loccoz, Y. (2009). The rhizosphere: A playground and battlefield for soilborne pathogens and beneficial microorganisms. *Plant Soil* 321, 341–361. doi: 10.1007/s11104-008-9568-6

Rinu, K., Sati, P., and Pandey, A. (2014). *Trichoderma gamsii* (NFCCI 2177): A newly isolated endophytic, psychrotolerant, plant growth promoting, and antagonistic fungal strain. *J. Basic Microbiol.* 54, 408–417. doi: 10.1002/jobm.201200579

Sadfi-Zouaoui, N., Hannachi, I., Rouaissi, M., Hajlaoui, M. R., Rubio, M. B., Monte, E., et al. (2009). Biodiversity of *Trichoderma* strains in Tunisia. *Can. J. Microbiol.* 55, 154–162. doi: 10.1139/W08-101

Sanó, L., de Oliveira, L. L. B., Leão, M. D. M., de Santos, J. E. Á, de Medeiros, S. C., Schneider, F., et al. (2022). *Trichoderma longibrachiatum* as a biostimulant of micropropagated banana seedlings under acclimatization. *Plant Physiol. Biochem.* 190, 184–192. doi: 10.1016/j.plaphy.2022.09.008

Schwarz, G. (1978). Estimating the dimension of a model. *Ann. Stat.* 6, 461–464.

Sehim, A. E., Hewedy, O. A., Altammar, K. A., Alhumaidi, M. S., and Abd Elghaffar, R. Y. (2023). *Trichoderma asperellum* empowers tomato plants and suppresses *Fusarium oxysporum* through priming responses. *Front. Microbiol.* 14:1140378. doi: 10.3389/fmicb.2023.1140378

Senechkin, I. V., Van Overbeek, L. S., and Van Bruggen, A. H. C. (2014). Greater *Fusarium* wilt suppression after complex than after simple organic amendments as affected by soil pH, total carbon and ammonia-oxidizing bacteria. *Appl. Soil Ecol.* 73, 148–155. doi: 10.1016/j.apsoil.2013.09.003

Shannon, C. E. (1948). A mathematical theory of communication. *Bell Syst. Tech. J.* 27, 623–656. doi: 10.1002/j.1538-7305.1948.tb00917.x

Siamak, S. B., and Zheng, S. (2018). Banana *Fusarium* wilt (*Fusarium oxysporum* f. sp. cubense) control and resistance, in the context of developing wilt-resistant bananas within sustainable production systems. *Hortic. Plant J.* 4, 208–218. doi: 10.1016/j.hpj.2018.08.001

Simpson, E. (1949). Measurement of diversity. *Nature* 163:688. doi: 10.1038/163688a0

Sokal, R. R., and Rohlf, F. J. (1995). *Biometry: The principles and practice of statistics in biological research*, 3rd Edn. New York, NY: W.H. Freeman and Co.

Tamura, K., Stecher, G., and Kumar, S. (2021). MEGA11: Molecular evolutionary genetics analysis version 11. *Mol. Biol. Evol.* 38, 3022–302738. doi: 10.1093/molbev/msab120

Taribuka, J., Wibowo, A., Widyastuti, S., and Sumardiyono, C. (2017). Potency of six isolates of biocontrol agents endophytic *Trichoderma* against *Fusarium* wilt on banana. *J. Degrad. Min. Land Manag.* 4, 723–731. doi: 10.15243/jdmlm.2017.042.723

Tejedor, M., Jiménez, C., Armas-Espinel, S., and Hernández-Moreno, J. M. (2009). Classification of anthropogenic soils with andic properties. *Soil Sci. Soc. Am. J.* 73, 170–175. doi: 10.2136/sssaj2008.0100

Thangavelu, R., and Gopi, M. (2015). Combined application of native *Trichoderma* isolates possessing multiple functions for the control of *Fusarium* wilt disease in banana cv. Grand Naine. *Biocontrol Sci. Technol.* 25, 1147–1164. doi: 10.1080/09583157.2015.1036727

Thangavelu, R., and Mustaffa, M. (2010). A potential isolate of *Trichoderma viride* NRCB1 and its mass production for the effective management of *Fusarium* wilt disease in banana. *Tree For. Sci. Biotechnol.* 4, 76–84.

Thangavelu, R., Palaniswami, A., and Velazhahan, R. (2004). Mass production of *Trichoderma harzianum* for managing *Fusarium* wilt of banana. *Agric. Ecosyst. Environ.* 103, 259–263. doi: 10.1016/j.agee.2003.09.026

Valan-Arasu, M., Vijayaraghavan, P., Al-Dhabi, N. A., Choi, K. C., and Moovendhan, M. (2023). Biocontrol of *Trichoderma gamsii* induces soil suppressive and growth-promoting impacts and rot disease-protecting activities. *J. Basic Microbiol.* 63, 801–813. doi: 10.1002/jobm.202300016

Visagie, C. M., Houbraken, J., Frisvad, J. C., Hong, S. B., Klaassen, C. H. W., Perrone, G., et al. (2014). Identification and nomenclature of the genus *Penicillium*. *Stud. Mycol.* 78, 343–371. doi: 10.1016/j.simyco.2014.09.001

Walkley, A., and Black, I. A. (1934). An examination of the Degtjareff method for determining soil organic matter, and a proposed modification of the chromic acid titration method. *Soil Sci.* 37, 29–38. doi: 10.1097/00010694-193401000-00003

Wang, C., and Zhuang, W. (2019). Evaluating effective *Trichoderma* isolates for biocontrol of *Rhizoctonia solani* causing root rot of *Vigna unguiculata*. *J. Integr. Agric.* 18, 2072–2079. doi: 10.1016/S2095-3119(19)62593-1

Win, T. T., Bo, B., Malec, P., Khan, S., and Fu, P. (2021). Newly isolated strain of *Trichoderma asperellum* from disease suppressive soil is a potential bio-control agent to suppress *Fusarium* soil borne fungal phytopathogens. *J. Plant Pathol.* 103, 549–561. doi: 10.1007/s42161-021-00780-x

Woo, S. L., Hermosa, R., Lorito, M., and Monte, E. (2023). *Trichoderma*: A multipurpose, plant-beneficial microorganism for eco-sustainable agriculture. *Nat. Rev. Microbiol.* 21, 312–326. doi: 10.1038/s41579-022-00819-5

Xia, X., Lie, T. K., Qian, X., Zheng, Z., Huang, Y., and Shen, Y. (2011). Species diversity, distribution, and genetic structure of endophytic and epiphytic *Trichoderma* associated with banana roots. *Microb. Ecol.* 61, 619–625. doi: 10.1007/s00248-010-9770-y

Xiao, Z., Zhao, Q., Li, W., Gao, L., and Liu, G. (2023). Strain improvement of *Trichoderma harzianum* for enhanced biocontrol capacity: Strategies and prospects. *Front. Microbiol.* 14:1146210. doi: 10.3389/fmicb.2023.1146210

Xue, C., Penton, C. R., Shen, Z., Zhang, R., Huang, Q., Li, R., et al. (2015). Manipulating the banana rhizosphere microbiome for biological control of Panama disease. *Sci. Rep.* 5, 2–11. doi: 10.1038/srep11124

Yang, J., Li, B., Liu, S. W., Biswas, M. K., Liu, S., Wei, Y. R., et al. (2016). Fermentation of Foc TR4-infected bananas and *Trichoderma* spp. *Genet. Mol. Res.* 15:2278. doi: 10.4238/gmr15048494

Zachow, C., Berg, C., Mu, H., Komon-zelazowska, M., Druzhinina, I. S., Kubicek, C. P., et al. (2009). Fungal diversity in the rhizosphere of endemic plant species of Tenerife (Canary Islands): Relationship to vegetation zones and environmental factors. *ISME J.* 3, 79–92. doi: 10.1038/ismej.2008.87

Zhang, J., Bayram Akcapinar, G., Atanasova, L., Rahimi, M. J., Przylucka, A., Yang, D., et al. (2016). The neutral metallopeptidase NMP1 of *Trichoderma guizhouense* is required for mycotrophy and self-defence. *Environ. Microbiol.* 18, 580–597. doi: 10.1111/1462-2920.12966

Zhang, Y., Wang, X., Pang, G., Cai, F., Zhang, J., Shen, Z., et al. (2019). Two-step genomic sequence comparison strategy to design *Trichoderma* strain-specific primers for quantitative PCR. *AMB Expr* 9:179. doi: 10.1186/s13568-019-0904-4

Zhou, D., Jing, T., Chen, Y., Wang, F., Qi, D., Feng, R., et al. (2019). Deciphering microbial diversity associated with *Fusarium* wilt-diseased and disease-free banana rhizosphere soil. *BMC Microbiol.* 19:161. doi: 10.1186/s12866-019-1531-6

frontiers | Frontiers in Microbiology

TYPE Original Research
PUBLISHED 30 July 2024
DOI 10.3389/fmicb.2024.1447488

OPEN ACCESS

EDITED BY
Dongdong Yan,
Chinese Academy of Agricultural Sciences (CAAS), China

REVIEWED BY
Zhiqiang Kong,
Chinese Academy of Agricultural Sciences (CAAS), China
Zhongwei Zou,
Wilfrid Laurier University, Canada

*CORRESPONDENCE
Yun Jiang
✉ yunj@jlau.edu.cn
Changqing Chen
✉ chenchangqing@jlau.edu.cn

†These authors have contributed equally to this work

RECEIVED 11 June 2024
ACCEPTED 10 July 2024
PUBLISHED 30 July 2024

CITATION
Li X, Wang J, Shen H, Xing C, Kong L, Song Y, Hou W, Gao J, Jiang Y and Chen C (2024) Biocontrol and growth promotion potential of *Bacillus velezensis* NT35 on *Panax ginseng* based on the multifunctional effect. *Front. Microbiol.* 15:1447488. doi: 10.3389/fmicb.2024.1447488

Biocontrol and growth promotion potential of *Bacillus velezensis* NT35 on *Panax ginseng* based on the multifunctional effect

Xueqing Li[1†], Jiarui Wang[2†], Hang Shen[1], Chenxi Xing[1], Lingxin Kong[1], Yu Song[2], Wanpeng Hou[3], Jie Gao[1], Yun Jiang[2*] and Changqing Chen[1*]

[1]College of Plant Protection, Jilin Agricultural University, Changchun, China, [2]College of Life Science, Jilin Agricultural University, Changchun, China, [3]Jilin Shenwang Plant Protection Co., Ltd., Fusong, China

The *Bacillus velezensis* strain NT35, which has strong biocontrol ability, was isolated from the rhizosphere soil of *Panax ginseng*. The antifungal effects of the NT35 strain against the mycelium and spore growth of *Ilyonectria robusta*, which causes ginseng rusty root rot, were determined. The inhibitory rate of *I. robusta* mycelial growth was 94.12% when the concentration of the NT35 strain was 10^7 CFU·mL^{-1}, and the inhibitory rates of *I. robusta* sporulation and spore germination reached 100 and 90.31%, respectively, when the concentration of the NT35 strain was 10^4 and 10^8 CFU·mL^{-1}, respectively. Strain NT35 had good prevention effects against ginseng rust rot indoors and in the field with the control effect 51.99%, which was similar to that of commercial chemical and biocontrol agents. The labeled strain NT35-Rif^{160}-Stre^{400} was obtained and colonized ginseng roots, leaves, stems and rhizosphere soil after 90 days. *Bacillus velezensis* NT35 can induce a significant increase in the expression of five defensive enzyme-encoding genes and ginsenoside biosynthesis-related genes in ginseng. In the rhizosphere soil, the four soil enzymes and the microbial community improved during different periods of ginseng growth in response to the biocontrol strain NT35. The NT35 strain can recruit several beneficial bacteria, such as *Luteimonas*, *Nocardioides*, *Sphingomonas*, and *Gemmatimonas*, from the rhizosphere soil and reduce the relative abundance of *Ilyonectria*, *Fusarium*, *Neonectria* and *Dactylonectria*, which cause root rot and rusty root rot in ginseng plants. The disease indices were significantly negatively correlated with the abundances of *Sphingomonas* and *Trichoderma*. Additionally, *Sphingomonadales*, *Sphingomonadaceae* and actinomycetes were significantly enriched under the NT35 treatment according to LEfSe analysis. These results lay the foundation for the development of a biological agent based on strain NT35.

KEYWORDS

***Bacillus velezensis*, *Panax ginseng*, biocontrol, plant growth promotion, multifunctional mechanisms**

Highlights

- The strain NT35 has ability to control rusty root rot and promote growth of ginseng.
- Increasing gene expression of defense enzymes and ginsenoside biosynthesis of ginseng.
- To colonize and significantly improve microbial community in rhizosphere soil of ginseng.

1 Introduction

Panax ginseng, one of the most well-known Chinese herbal medicinal plants, is now grown in the northeastern region of China (You et al., 2022). Rusty root rot disease caused by *Ilyonectria robusta* is the most common and serious root disease that occurs during *P, ginseng* cultivation in China (Lee et al., 2015; Farh et al., 2018). At present the general incidence of ginseng rusty root rot in China is 20%–30%, and more seriously, some more than 70%. The quality and yield of ginseng were severely affected, resulting in huge property losses (Wang et al., 2019; Guan et al., 2020). For a long time, this disease has been controlled mainly by chemical fungicides. However, chemical control is not ideal for treating soil-borne diseases in perennial plants. Additionally, prolonged use of chemical fungicides results in pathogen resistance, residue risk, soil microecological imbalance and environmental pollution (Wołejko et al., 2020).

Biocontrol can reduce or prevent the occurrence of plant diseases and has the benefits of being environmentally friendly, safe, and highly efficient (Sharma and Manhas, 2022). For instance, *Bacillus amyloliquefaciens* was reported to be effective at controlling *Phytophthora capsica* (Bhusal and Mmbaga, 2020). Fu et al. (2010) reported the biocontrol potential of *B. subtilis* against banana leaf spot caused by *Pseudocercospora musae* and postharvest anthracnose caused by *Colletotrichum musae*. The *B. velezensis* strain B19 can control Fusarium root rot in *Panax notoginseng* (Wang C. X. et al., 2023). Thus, biocontrol by beneficial microorganisms may be chosen as an alternative means of reducing ginseng rusty root rot without negatively impacting the environment compared to chemical control with fungicides. Previous studies have shown that the rhizosphere acts as an important bridge between plants and soil for the exchange of substances through plant roots and helps establish mutual relationships (Ahkami et al., 2017). The bacteria in rhizospheric soil are responsible for many important ecological functions, such as disease control (Linden et al., 2022) and resistance induction (Zhang et al., 2022). System induction resistance is an important mechanism for plants to fight pathogens. *Bacillus velezensis* effective against *Botrytis cinerea* by inducing systemic resistance in tomato (Stoll et al., 2021). And biocontrol bacteria have been reported to improve rhizosphere soil microecology by recruiting beneficial microorganisms, reducing the abundance of harmful communities, and increasing microbial communities diversity (Zhao et al., 2022). Using rhizospheric soil bacteria has been a good strategy for the efficient biocontrol of soil-borne diseases. The objective of this study was to determine the ability of the *B. velezensis* strain NT35 to inhibit *I. robusta* growth and control ginseng rusty root rot via *in vitro* and field experiments. The expression of defense enzyme-encoding genes in ginseng induced by the biocontrol bacterium was also analyzed. The high-throughput sequence technique was used to study the microbial community structure, which may improve rhizosphere soil microecology through the strain NT35. The results lay a foundation for the development and application of the biocontrol bacterium NT35 on ginseng plants.

2 Materials and methods

2.1 Strains and culture

The *B. velezensis* strain NT35 was previously isolated from the rhizosphere soil of *P. ginseng* in Ji'an, Jilin Province, China, and the eight pathogens causing ginseng diseases including *I. robusta*, *Sclerotinia schinseng*, *Phytophthora cactorum*, *Rhizoctonia solani*, *Alternaria panax*, *Botrytis cinerea*, *Colletotrichum panacicola*, *Fusarium solani* were obtained was obtained from the Laboratory of Integrated Management of Plant Diseases, Jilin Agricultural University, Changchun, Jilin Province, China, and stored at −80°C. The plant pathogens were incubated on potato dextrose agar (PDA) at 25°C for 5 days. *Bacillus velezensis* NT35 was cultured on lysogeny broth agar medium (LB) and incubated at 28°C for 2 days in dark.

2.2 Inhibition of *Ilyonectria robusta* mycelial growth by strain NT35

A dual culture assay was used to evaluate the ability of *B. velezensis* NT35 against *I. robusta* CBLJ-3 (Wang J. et al., 2023). The concentrations of *B. velezensis* NT35 were 10^9, 10^8, 10^7, 10^6, 10^5, 10^4, 10^3, 10^2, and 10^1 CFU·mL^{-1}. In the control, only the *I. robusta* CBLJ-3 mycelium plug was inoculated, and sterile agar was added to the Petri dishes; three replicates were used for each treatment. Then, the plates were incubated at 25°C for 7 days. Measurements were calculated by the formula $I\ (\%) = [(C - T)/C] \times 100$ (I: percentage of inhibition, C: growth of pathogen in control plate, T: growth of pathogen in treatment plate). Additionally, the antifungal efficacy of the NT35 strain against 14 other plant pathogens was determined by the confrontation culture method.

The effect of *B. velezensis* NT35 on the mycelial weight of *I. robusta* was evaluated as described below (Wang C. X. et al., 2023). An 8 mm diameter of the fungal agar plug of *I. robusta* CBLJ-3 was inoculated into 90 mL of PD fluid in a 250 mL flask and cultured at 150 rpm and 28°C for 2 days, after which 10 mL of 1×10^8 CFU/mL NT35 fermentation broth was added. The mixture was further cultured with shaking at 25°C, and the mycelia of *I. robusta* were sampled at 1, 2, 3, 4, 5, 6, and 7 dpi after inoculation with *B. velezensis* NT35. The mycelial samples were filtered and washed three times with sterile water. The mycelial dry weight of each treatment was determined after drying at 80°C for 24 h. Three replicates were performed for each group.

2.3 Inhibition of *Ilyonectria robusta* spore production and germination by the NT35 strain

The hemocytometer method was used to determine the inhibitory effect of the NT35 strain on the spore production and germination of *I. robusta* (Wang J. et al., 2023). The strain CBLJ-3 was inoculated on plates mixed with serially diluted fermentation broth as described above and cultured at 25°C. The conidia were flushed with 5 mL of sterile water after the colonies reached more than 60 mm in diameter, and the plates were mixed with sterile water as a control. The conidia yield was determined using a hemocytometer, and the inhibition rate was calculated as follows: inhibition rate (%) = 100 × (control conidia production − treatment conidia production)/control conidia production. When the CBLJ-3 spore germination rate of the control group reached greater than 90%, the germinated conidia were counted using a hemocytometer, and the inhibition rate was calculated as follows: inhibition rate (%) = 100 × (control germination rate − treatment germination rate)/control germination rate. Each treatment was replicated three times.

2.4 *In vivo* effect of the NT35 strain on inhibiting *Ilyonectria robusta* growth in ginseng roots

An *in vitro* inhibition test was also performed in ginseng roots according to Wang C. X. et al. (2023). The three-year-old healthy ginseng roots were disinfected with 2% sodium hypochlorite solution for 90 s, rinsed twice with sterile distilled water and dried at room temperature for 2 h. A total of 10 μL of 1×10^8 CFU·mL^{-1} NT35 fermentation broth was inoculated at each site, at which three wound sites with a depth of 3 mm were generated on each ginseng root by using a sterile pipette tip with a diameter of 2 mm. The four treatments included the following: (A) water as a negative control; (B) *I. robusta* as a positive control; (C) Prevention treatment: inoculation with NT35 for 1 day and then with *I. robusta*; and (D) Therapeutic treatment: inoculation with *I. robusta* for 1 day and then with NT35. All the inoculated plants were incubated at 25°C.

2.5 Growth-promoting effect of strain NT35 on ginseng plants

The Salkowski method was used to screen for high IAA production by the strain NT35 (Ait Bessai et al., 2022). The phosphate solubilization ability of the strains was determined by cultivation on Pikovskaya's agar medium and by the Mo-Sb colorimetric method (Liu et al., 2021). Potassium solubilization was tested by using Aleksandrow's agar medium and a flame atomic absorption spectrometer (Iyer et al., 2017). The nitrogen fixation potency was determined after the strain NT35 was inoculated in ASHBY nitrogen-free agar medium and incubated at 30°C for 24 h (Xu et al., 2001). Siderophore production was determined by the CAS method (Delaporte-Quintana et al., 2020), and ACC deaminase activity was determined by the Honma method (Tiwari et al., 2016).

The NT35 strain was inoculated in LB liquid, cultured at 160 rpm at 28°C for 12 h and subsequently centrifuged at 10,000 × g for 5 min. The collected cells were dissolved in distilled water, and the original cells were diluted to 1×10^8 CFU·mL^{-1}. Ginseng seeds were first sterilized by soaking in 70% ethanol for 5 min and then in 0.5% sodium hypochlorite for 3 min and rinsed three times with distilled water. These disinfected seeds were immersed in the above bacterial suspension of strain NT35 for 4 h. Seeds treated with distilled water served as the control. All the seeds were then transferred to plates containing wetted sand (10 seeds per plate) and incubated at 25°C for 10–15 days (Jiang et al., 2022).

2.6 Colonization ability of strain NT35 in *Panax ginseng* and rhizosphere soil

Preparation of rifampicin solutions (2×10^4 μg·mL^{-1}) and streptomycin solutions (5×10^4 μg·mL^{-1}), The NT35 strain was activated by LB medium and incubated at 28°C and 160 rpm for 12 h. Rifampicin was uniformly mixed into the LB solid medium to make a plate containing rifampicin at a concentration of 40 μg·mL^{-1}, and 0.1 mL of NT35 bacterial solution was coated on the plate, and the plate was incubated at 28°C for 3–4 days. Single colonies with the same or similar morphology as that of the original NT35 were picked for streaking and incubation. After incubation for 2–3 days, the single colonies were streaked and inoculated onto LB medium containing rifampicin at a concentration of 80 μg·mL^{-1}, and antibiotic-resistant mutant strains with good growth and the same colony morphology as that of the original bacterium were always selected to obtain the mutant NT35-Rif^{160}, which was able to tolerate rifampicin at a concentration of 160 μg·mL^{-1}. The concentration of streptomycin of NT35 was increased step by step according to the same method from 50 μg·mL^{-1} to 400 μg·mL^{-1} to obtain the double-resistant strain NT35-Rif^{160}-Stre^{400}, which has the same colony characteristics as the original strain and stable drug resistance (Cohen et al., 1989). Ginseng roots were inoculated with the NT35-Rif^{160}-Stre^{400} strain at 10^8 CFU/mL, and 50 mL of liquid was added to each root. The ginseng roots, stems, leaves and rhizosphere soil were sampled after inoculation for 3, 7, 15, 30, 45, 60, or 90 days, and each treatment was repeated three times. The colonization of various parts of ginseng and soil by the NT35-Rif^{160}-Stre^{400} strain was determined via the plate colony counting method. Each treatment was repeated three times.

2.7 qRT–PCR analysis of defense enzyme-encoding gene expression

After leaf spreading, three-year-old healthy ginseng plants were inoculated with a bacterial suspension of *B. velezensis* NT35 at a concentration of 1×10^8 CFU·mL^{-1} in pots in the greenhouse, and water was inoculated as the control. The ginseng roots were sampled at 1, 3, 5, 7, 9 and 11 days after treatment and were soaked in liquid nitrogen. The total RNA of ginseng roots was extracted using the RNAiso Plus method. Reverse transcription was conducted using M-MLV reverse transcriptase (TaKaRa Biotechnology Co., Ltd., Dalian, China). The qRT-PCR assay was performed on a fluorescent quantitative PCR instrument LC96 (Roche) using Fast SYBR Mixture (Company) for qRT-PCR reactions. The 10 μL PCR mixture contained 1 μL of cDNA, 0.2 μL each of 10 μmol/L upstream and downstream primers, 5 μL of 2 × Fast SYBR mixture, 0.2 μL of 50 × Low ROX and

3.4 μL of ddH_2O. The qRT–PCR conditions were 95°C predenaturation for 10 min, 95°C denaturation for 10 s, 60°C annealing and extension for 30 s, for a total of 40 cycles. Five genes, phenylalanine ammonia-lyase (*PAL*), β-1.3 glucanase (*β-1,3-GLU*), chitinase (*CHI*), superoxide dismutase (*SOD*) and peroxidase (*POD*), of NT35-treated ginseng plants were analyzed by using qRT–PCR (Jiang et al., 2022). Each gene was conducted with three biological and technical replicates. The relative gene expression was analyzed using the $2^{-\triangle\triangle Ct}$ method (Livak and Schmittgen, 2001; Kim et al., 2019).

2.8 Efficacy of strain NT35 for controlling rusty root rot in ginseng in the field

The field experiment was carried out in 2021 in Choushui township, Fusong county, Jilin Province, China. The control effect of 1×10^8 cfu/g NT35 WP (Jilin Agricultural University) was evaluated in a field where ginseng rusty root rot occurs frequently. The ginseng field was divided into different plots of 1.5 m^2 following a completely random design on 25th April. The soil of all plots was treated by mixing 8 g/m^2 NT35 WP with commercial agents, including 8 g/m^2 3×10^{11} cfu/g YIWEI WP (Shandong Jingqing Agriculture Science and Technology Co., China), 8 g/m^2 2×10^{11} cfu/g ZNLK WP (Zhongnong Lvkang Biotechnology Co., China) and 5 g/m^2 50% carbendazim WP (Jiangsu Wansheng International Chemical Group, China), with no agent serving as a control. Two-year-old ginseng plants of uniform size were planted at a 7 cm depth in the soil and treated consistently. The row spacing was 20 cm, the plant spacing was 10 cm, and there were approximately 60 plants in each plot and the three random plots were sampled. All ginseng roots were harvested at the maturity stage, and disease severity was investigated (Rahman and Punja, 2005).

2.9 Effect of strain NT35 on soil enzyme activity

After the ginseng roots were inoculated with the NT35 bacterial suspension at a concentration of 1×10^8 CFU·mL^{-1}, rhizosphere soil samples were collected at four different periods of ginseng growth: leaf spread stage (13 June), fruit stage (15 July), root expansion stage (16 August), and mature stage (15 September). The soil urease activity was determined by using the method described by Kandeler and Gerber (1988). The catalase activity was tested according to Lúcia et al. (2016). The alkaline phosphatase activity was determined using the protocol described by Rahul and Anita (2016). The invertase activity was measured using the method described by Sun et al. (2021). Three replicates were carried out for each treatment.

2.10 qRT–PCR analysis of ginsenoside synthesis-related gene expression

Three-year-old healthy ginseng roots were inoculated with an NT35 bacterial suspension at a concentration of 1×10^8 CFU·mL^{-1}, and water was used as a control. Total RNA was extracted from ginseng roots using the RNAiso Plus method. Reverse transcription was conducted using M-MLV reverse transcriptase (TaKaRa Biotechnology Co., Ltd., Dalian, China). The three genes encoding squalene synthase, squalene epoxidase, and dammarediol synthase were analyzed by qRT–PCR as described above, and the *β-actin* gene was used as the internal reference. The primers used were synthesized by Sangon Biotech (Shanghai) Co., Ltd., in China (Supplementary Table S1). Each gene was conducted with three biological and technical replicates.

2.11 Effects of strain NT35 on the rhizosphere microbial community of ginseng

2.11.1 Soil samples

The rhizosphere soil samples and sampling method for this experiment were consistent with those described in section 2.8 above. The soil microbial community was analyzed during three periods: leaf spreading, fruiting and root expansion. Three samples were taken as one replicate, and a total of 18 soil samples were obtained. Soil samples with no added agent were used as a control group.

2.11.2 DNA extraction, sequencing, and data analysis

The total DNA of the soil samples was extracted by the CTAB method (Niemi et al., 2001). The V3–V4 regions of the bacterial 16S rRNA gene (Zhang et al., 2018) and the fungal ITS2 gene (Huang J. et al., 2022) were amplified. Library construction and sequence analysis were performed on an Illumina NovaSeq 6000 platform by Novogene Co., Ltd. (Beijing, China). Spearman correlation was used to analyze the relationships between soil enzymes, disease indices and the microbial community.

2.11.3 Sequence processing and data analysis

After the chimeric sequences were removed, the operational taxonomic units (OTUs) were clustered at 97% sequence identity using UPARSE (Uparse v7.0.1001, http://www.drive5.com/uparse/; Edgar, 2013). The taxonomic identities of the microbiome were determined using the SSUrRNA database of Silva138[1] (Quast et al., 2013). The alpha diversity and abundances of the OTUs were calculated between the different treatments. PCoA dimensionality reduction was performed to analyze the differences in community structure between the groups at different stages. Spearman correlation was used to study the relationships among soil enzymes, disease indices and microbial communities. Pairwise correlation and significance *p*-values were obtained.

2.12 Statistical analysis

Three replicates were analyzed for each treatment. The significant differences between means were calculated using Tukey's multiple range test, followed by one-way ANOVA ($*p<0.05$, $**p<0.01$, $***p<0.001$). For each trial, the results were subjected to analysis of variance (ANOVA), and treatment means were compared by Fisher's protected least significant difference (LSD) test at 5% probability. Before the ANOVA, the normality of the distribution of residuals and

1 http://www.arb-silva.de

homogeneity of variance were verified. The statistical analyzes were performed with SPSS 26.0 (Ning et al., 2022).

3 Results

3.1 Effects of strain NT35 on the growth of *Ilyonectria robusta* and other pathogens in *Panax ginseng*

All nine concentrations of *B. velezensis* NT35 inhibited the hyphal growth of *I. robusta* with different efficacies. Among the concentrations, the inhibition rate of the treatment with a concentration greater than 10^7 CFU·mL^{-1} was more than 94.12%, which was significantly greater than that of the other treatments, and the highest inhibition rate was observed for the treatment with 10^9 CFU·mL^{-1}, which reached 99.51% (Supplementary Table S2).

The NT35 strain not only inhibited *I. robusta* but also had a broad-spectrum inhibitory effect on seven other plant pathogens, including *Sclerotinia sclerotiorum*, *Phytophthora cactorum*, *Alternaria panax*, *Rhizoctonia solani*, *Fusarium solani*, *Botrytis cinerea*, and *Colletotrichum panacicola* (Figure 1).

The weight of *I. robusta* mycelia also decreased 7 days after inoculation with NT35 (Supplementary Figure S1). At 3 dpi and 4 dpi, there were significantly greater inhibition rates against *I. robusta* than at the other time points, and the highest rate reached 77.21% at 4 dpi. The NT35 strain was found to have a good inhibitory effect on the amount of sporulation of *I. robusta* (Supplementary Table S3). The inhibition rates exceeded 90% at all concentrations greater than 10^1 CFU·mL^{-1}. When the concentration of *B. velezensis* NT35 was greater than 10^4 CFU·mL^{-1}, the sporulation inhibition rate was 100%. Moreover, when the spore germination rate of the control group reached 91.4%, the spore germination rates of *I. robusta* treated with different concentrations of NT35 decreased. With increasing concentration, the inhibition rate increased, and the highest inhibition rate reached 93.28% at 10^9 CFU·mL^{-1}, indicating that *B. velezensis* NT35 has a good inhibitory effect on *I. robusta* sporulation and spore germination.

3.2 *In vivo* effect of the NT35 strain on inhibiting *Ilyonectria robusta* growth in ginseng roots

The positive control with only pathogen inoculation (Figure 2B) showed typical discolouration around the inoculation site on the fifth day after inoculation with *I. robusta*. No significant discolouration was observed in the preventive treatment (Figure 2C) or the therapeutic treatment (Figure 2D) with strain NT35. The ginseng in water treatment (Figure 2A) showed only slight oxidation of the wound and its interior after inoculation, with no ginseng rusty root rot symptoms, which proves that the ginseng lesions in this experiment could only be caused by inoculation with CBLJ-3. With increasing days after inoculation, the disease spots in the pathogen-positive control gradually became larger, darker and more decomposed. However, there was no obvious deterioration in the ginseng roots after the NT35 treatment. On the 11th day after inoculation, the ginseng roots were dissected lengthwise, and the extent and area invaded by the pathogen *I. robusta* inside the roots were significantly lower than those of the control plants. The preventive treatment (Figure 2C) had the greatest effect.

3.3 Growth-promoting effect of strain NT35 on ginseng plants

The four indicators of growth-promoting abilities of strain NT35 were determined in this study (Supplementary Figure S2). The NT35 strain has the potential for nitrogen fixation and siderophore activity, but it cannot solubilize phosphorus or potassium. The levels of IAA

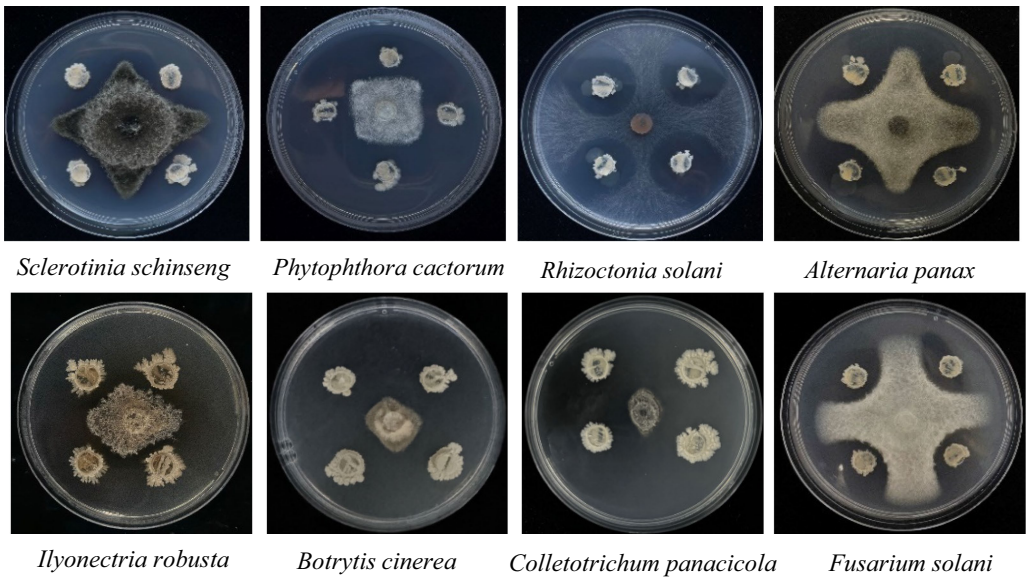

FIGURE 1
Inhibitory effect of NT35 on eight pathogenic fungi of *Panax ginseng*.

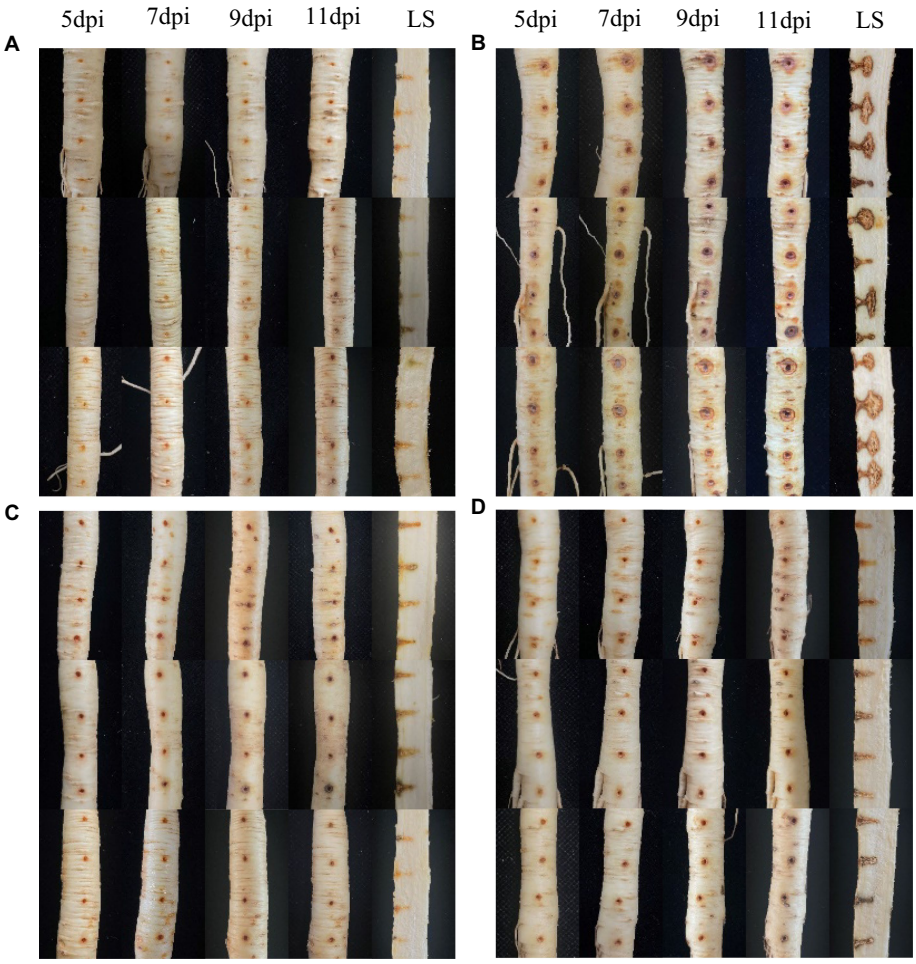

FIGURE 2
In vivo effect of strain NT35 inhibiting *Ilyonectria robusta* on ginseng root. LS, Longitudinal section; **(A)** Water treatment; **(B)** *I. robusta* CBLJ-3; **(C)** Prevention treatment: inoculation with NT35 for 1 day and then with *I. robusta*; **(D)** Therapeutic treatment: inoculation with *I. robusta* for 1 day and then with NT35.

FIGURE 3
The promoting effect of strain NT35 on ginseng seed germination. **(A)** Water control; **(B)** NT35 treatment; **(C)** Seed bud length ($n = 3$ independent replicates). p-values were indicated by * symbol: $^{**}p < 0.01$; $^{*}p < 0.05$.

and ACC deaminase produced by strain NT35 were 1.392 and 0.0197 μmoL/mg·h, respectively. After 15 days, the average bud length of the ginseng plants soaked in water was 1.56 cm, while that of the plants in the NT35 treatment was 2.25 cm, which was significantly (1.44 times) greater than that of the water control. The results showed that the bacterium NT35 could promote ginseng seed germination (Figure 3).

3.4 Colonization of strain NT35 in ginseng and its rhizosphere soil

The labeled strain NT35-Rif^{160}-Stre^{400} was obtained, and its ability to colonize ginseng roots, leaves, stems and rhizosphere soil was maintained for 90 days (Figure 4). In the ginseng roots and leaves, the trend first increased and then decreased, while it gradually decreased

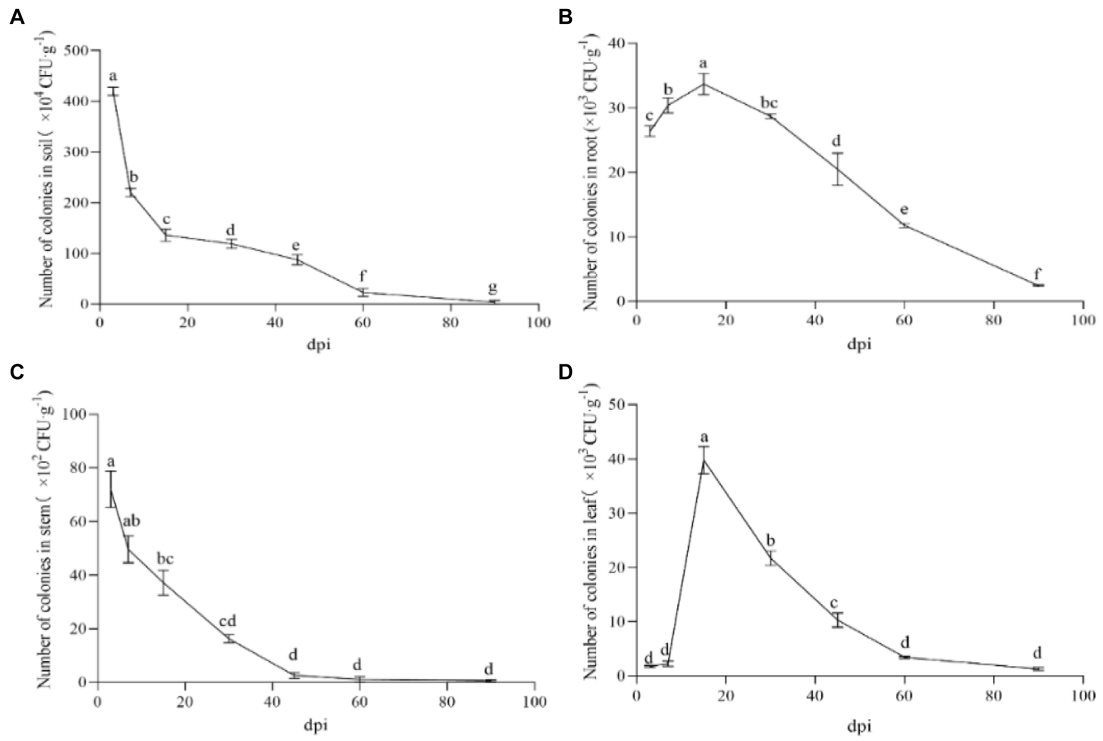

FIGURE 4
Colonization of strain NT35 in ginseng and rhizosphere soil. **(A)** rhizosphere soil; **(B)** ginseng root; **(C)** ginseng stem; **(D)** ginseng leave. $n = 3$; different values (a, b, c, d, e, f, g) between different dpi are significantly different ($p < 0.05$).

in the rhizosphere soil and stems. The colonization of NT35 in rhizosphere soil was greater than that in the roots, stems and leaves of ginseng. On the 3rd day after inoculation, the colonization level of the NT35-Rif^{160}-Stre^{400} population was 4.20×10^6 CFU/g in rhizosphere soil, 2.64×10^4 CFU/g in roots, 7.20×10^3 CFU/g in stems, and 1.77×10^3 CFU/g in leaves. At 15 days after inoculation, the colonization population in the ginseng roots and leaves peaked. Up to 90 days after inoculation, the colonization amounts in the rhizosphere soil, roots, stems and leaves were 3.7×10^4, 2.46×10^3, 0.67×10^2, and 1.29×10^3 CFU/g, respectively.

3.5 Expression of the defense enzyme-encoding gene induced by *Bacillus velezensis* NT35

Similarly, the expression of all five defense genes (*β-1.3-GA*, *CHI*, *PAL*, *SOD* and *CAT*) in ginseng roots inoculated with *B. velezensis* NT35 tended to increase compared to that in the control (Figure 5). The transcript expression of the *β-1.3-GA* and *CAT* genes significantly increased in response to treatment with strain NT35 from 1 to 9 dpi and peaked at 3 and 7 dpi, respectively (Figures 5C,D). *CHI* and *SOD* were significantly expressed from 3 to 9 dpi, with peaks occurring at 7 and 5 dpi, respectively (Figures 5B,E). The *PAL* genes were significantly upregulated throughout the sampling period and peaked at 9 dpi (Figure 5A). In addition, the expression of all five genes showed a decreasing trend from 9 to 11 dpi.

3.6 Control effect of strain NT35 on rusty root rot in ginseng in the field

In the field experiment, the disease index of the NT35 WP treatment (2.333) was lower than that of the negative control (4.859), and the control effect reached 51.99% in the NT35 WP treatment, which was not significant different from the control effects of the YIWEI WP and ZNLK biological agents and carbendazim chemical fungicide (Supplementary Figure S3). For yield, the weight of ginseng roots (191.16 g) treated with NT35 WP was significantly greater than that of those treated with the ZNLK agent or water control.

3.7 Effect of strain NT35 on ginseng soil enzyme activity

In general, the soil enzyme activity in ginseng plants treated with strain NT35 increased to some degree during different growth stages compared with that in plants treated with water. However, the change trend of the activity of each enzyme was different. The change in invertase activity showed a trend of increasing first and then decreasing overall, with the maximum value occurring at the fruit stage (Supplementary Figure S4A). The phosphatase activity increased continuously and peaked during the mature period of ginseng. The maximum phosphatase activity after NT35 treatment was 1988.94 μg g^{-1}, which was significantly greater than that in the water control and YIWEI treatment groups (Supplementary Figure S4B). After the NT35 treatment, the soil urease activity first increased and then decreased.

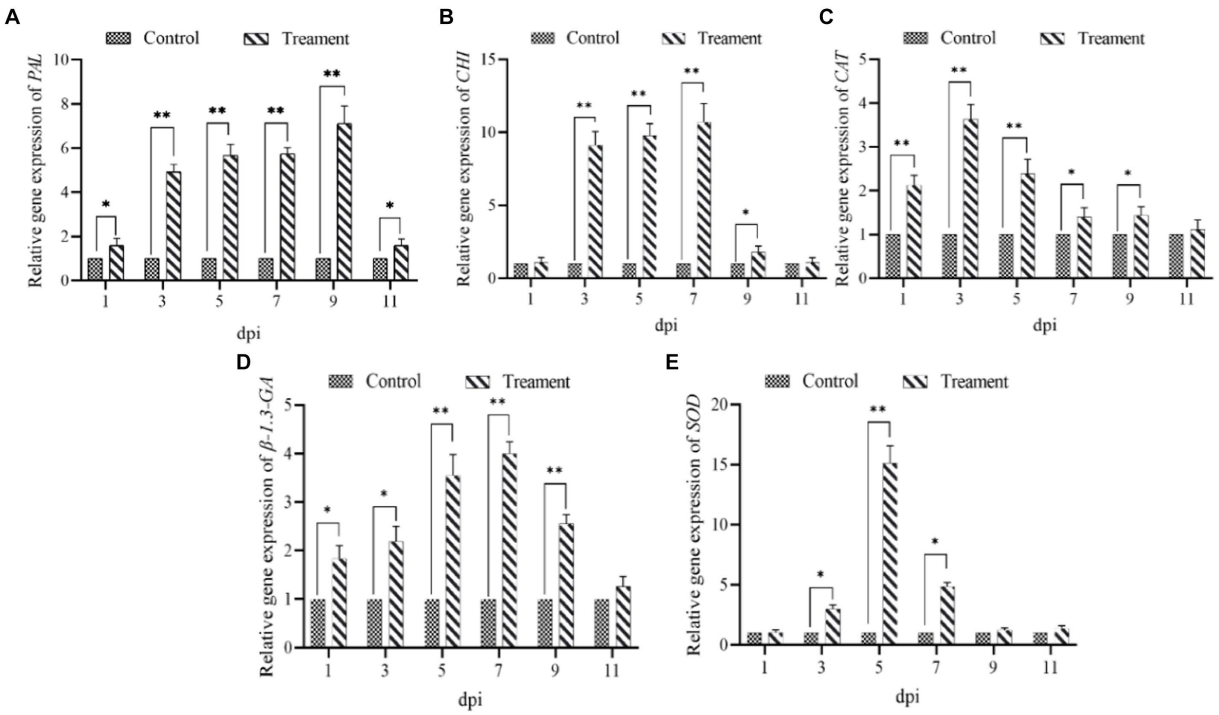

FIGURE 5
Relative expression levels of five defense genes of ginseng **(A)** PAL; **(B)** CHI; **(C)** CAT; **(D)** β-1.3-GA; **(E)** SOD.

During the fruiting period, a maximum value of 572.26 μg/g was reached, which was almost twice as high as that of the Yiwei treatment (Supplementary Figure S4C). The maximum value of catalase activity was reached during the root expansion period and was significantly greater than that in the YIWEI treatment and water control groups (Supplementary Figure S4D).

3.8 Effect of NT35 on the expression of ginsenoside biosynthesis-related genes

After NT35 treatment, the expression of ginsenoside biosynthesis-related genes was upregulated. The relative expression levels of the squalene synthase gene (*PgSS*), squalene epoxidase gene (*PgSE*) and dammarenediol synthase gene (*PgDDS*) in response to treatment with strain NT35 were 25.11, 12.82, and 2.85 times greater than those in response to treatment with water, respectively. The relative expression of *PgDDS* and *PgSS* in the NT35 treatment group was extremely significantly greater than that in the water control group, and the relative expression of *PgSE* was significantly greater than that in the water control group (Figure 6).

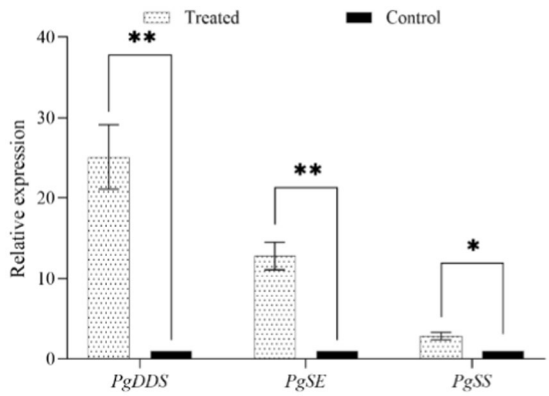

FIGURE 6
Effect of strain NT35 on relative expression of ginsenoside synthesis genes. Values represent mean ± standard deviation ($n = 3$), p-values were indicated by * symbol: $^{**}p < 0.01$; $^{*}p < 0.05$.

3.9 Effect of strain NT35 on the rhizosphere microbial community of *Panax ginseng*

3.9.1 Alpha diversity and PCoA analysis

During the four stages of ginseng growth, the Shannon, Simpson, Chao1 and ACE indices of the bacterial and fungal communities changed to different degrees. The Simpson and Shannon indices of the soil bacterial and fungal communities treated with strain NT35 were significantly greater than those of the control at the flowering and root-expanding stages and significantly lower than those of the control at the leaf-spreading stage (Supplementary Figures S5A,B,E,F). The Chao1 and ACE indices of the bacterial and fungal communities were not significantly different among the three stages throughout the growth cycles (Supplementary Figures S5C,D,G,H).

According to the PCoA analysis based on the Bray–Curtis distance, the diversity of the soil microbial communities changed in

response to the antagonistic bacteria NT35 treatment, as reflected by the coordinate axes. The bacterial communities produced by the *B. velezensis* NT35 treatment and the water control treatment were significantly different on the horizontal axis at the fruiting and root expansion stages, and the fungal communities at the fruiting stage were significantly different on both the horizontal and vertical axes (Supplementary Figures S6A,B).

3.9.2 Phylum- and genus-level composition of the microbial community

The dominant bacterial phyla were Myxococcota, Crenarchaeota, Chloroflexi, Actinobacteria, Verrucomicrobiota, and Proteobacteria, and the dominant fungal phyla were Ascomycota, Basidiomycota and Mortierellomycota. During the three stages of ginseng growth, there were differences in the proportions of the dominant microbial groups at the phylum level between the treatment with strain NT35 and the negative control and between the different growth stages under the same treatment (Figure 7).

In terms of the genus-level composition of the bacterial microbial communities (Figure 7A), *Mycobacterium*, *Luteimonas*, *Ellin6055*, *Nocardioides*, *Sphingomonas*, *Galella* and *Gemmatimonas* were the dominant genera in the rhizosphere soil treated with *B. velezensis* NT35 during the three stages of ginseng growth. For the control, the dominant genera consisted of *Candidatus solibacter*, *C. xiphinematobacter*, *C. nitrosotalea*, *C. udaeobacter*, RB41, *Aeromicrobium*, *Bradyrhizobium*, *Massilia*, *Rhodanobacter*, *Luteibacter*, *Pseudolabrys*, *Luteibacter* and *Massillia*. However, the abundances of some microorganisms also decreased. Without the NT35 treatment, the abundances of *Sphingomonas*, *Nocardioides*, *Ellin6055*, *Luteimonas*, *Galella*, *Mycobacterium* and *Jatrophihabitans* were always low. Additionally, the abundances of *Candidatus Solibacter*, *C. xiphinematobacter*, *C. nitrosotalea*, *C. udaeobacter*, *Bradyrhizobium*, *Pseudolabrys* and *Rhodanobacter* in the rhizosphere soil decreased significantly after treatment with the biocontrol bacterial strain NT35. For the genus composition of the fungal microbial community (Figure 7B), the fungal community treated without NT35 was composed mainly of *Fusarium*, *Neonectria*, *Thelonectria*, *Geomyces*, *Ilyonectria*, *Dactylonectria*, *Chaetomiun*, *Trichoderma*, and *Botryotrichum*. After treatment with *B. velezensis* NT35, *Penicillium*, *Pseudogymnoascus*, *Epicoccum*, *unidentified Sodariales* sp., *Cercophora*, *Cephalotrichum*, *Mortierella*, *Aspergillus*, *Apodus*, *Saitozyma* and *Trichoderma* became the dominant genera.

3.9.3 Correlation analysis between the microbial community, soil enzymes and ginseng growth

The correlation between the bacterial community composition and the four soil enzymes activity was shown in Figure 8A. There was a significant negative correlation between the abundance of the genus *Massilia* and catalase activity. The alkaline phosphatase activity was significantly negatively related to the abundances of *Aeromicrobium*, *Candidatus_xiphinematobacter* and *Luteimonas* and was significantly positively related to the abundances of *Gemmatimonas*, *C. solibacter*, *C. nitrosotalea*, *Bryobacter*, and *Pseudolabrys*. The invertase activity was significantly negatively related to the abundance of RB41 but significantly positively related to the abundances of *Gemmatimonas* and *Sphigomonas*.

On the other hand, the correlations between fungal community composition at the genus level and the activities of the four soil enzymes are shown in Figure 8C. The abundance of the genus *Cercophora* was significantly negatively correlated with catalase activity, and that of *Neonectria* was significantly positively correlated with catalase activity. Alkaline phosphatase activity was significantly negatively related to the abundances of *Fusarium* and *Epicoccum* and significantly positively related to the abundances of *Botryotrichia, Trichoderma*, *Saitozyma*, *Apodus* and *Chaetomium*. The abundances of *Neonectria* and *Pseudogymnoascus* were significantly negatively related to urease activity. Invertase activity was extremely significantly negatively related to the abundances of *Dacylonectria*, *Ilyonectria* and *Neonectria*; significantly negatively related to the abundances of *Geomyces* and *Pseudogymnoascus*; and significantly positively related to the abundance of the genus *Cercophora*.

The correlations between the microbial community at the genus level and the disease indices of rusty root rot and root growth in ginseng and bacterial composition are shown in Figure 8B. The abundances of *Acidothermus*, *Nocardioides*, *Bradyrhizobium*, *Sphingominas*, and *Psedolabrys* were significantly negatively related to the disease index of ginseng and were extremely significantly negatively related to *Gaiella*, *Jatrophihabitans* and *Luteimonas*, while the abundances of RB41 and *Candidatus udaeobacter* were significantly positively related to the disease index of ginseng rusty root rot. In terms of abundance, the length of the roots of the ginseng plants was strongly negatively related to *Acidothermus*, *Mycobacterium* and *Psedolabrys*; significantly negatively related to *Jatrophihabitans* and *Gaiella*; and significantly positively related to *C. nitrosotalea*, *Bryobacter* and *C. xiphinematobacter*. For the fungal community (Figures 8C,D), the disease index associated with ginseng rusty root rot was significantly negatively related to the abundance of *Geminibasidium* and *Trichoderma*. In terms of abundance, the ginseng root length was strongly negatively related to *Trichosporiella* and significantly negatively related to *Pleotrichocladium* but was extremely significantly positively related to *Botryotrichum*. The ginseng taproot diameter was strongly negatively related to the abundance of *Torula* and significantly negatively related to the abundances of *Tetracladium* and *Thelonectria*.

3.9.4 LEfSe analysis of rhizosphere soil

The analysis of the bacterial community LEfSe in rhizosphere soil showed that *Acidobacteriota* was enriched in the soil without NT35 treatment, and *Alphaproteobacteria*, *Actinobacteria*, *Sphingomonadales* and *Sphingomonadaceae* were enriched in the NT35 treatment during the leaf-spreading period (Figure 9A). During the fruiting period, *Proteobacteria* and *Acidobacteria* were enriched in the control group, and in the NT35 treatment, *Actinobacteriota, Nitrososphaeraceae* and *Nitrososphaerales* were enriched (Figure 9B). During the root expansion stage, *Acidobacteria* and *Acidobacteriota* were enriched in the control group, and *Actinobacteriota*, *Actinobacteria* and *Thermoleophilia* were enriched in the NT35 treatment (Figure 9C).

According to the results of the fungal community LEfSe analysis, the soil not subjected to biocontrol bacterial treatment was enriched in *Fusarium*, *Dactylonectria*, *Dactylonectria_estremocensis*, *Geomyces*, *Geomyces_luteus*, *Thelonectria*, *Ilyonectria*, *Neonectria*, *Neonectria_lugdunensis*, *Nectriaceae*_sp., *Nectriaceae*, *Hypocreales* and *Sordariomycetes*. However, *Leotiomycetes*, *Pseudogymnoascus_pannorum*, *Thelebolales*, *Psedugymnascus*, *Pseudeurotiaceae* and *Ascomycota* were enriched after the NT35 treatment during the leaf-spreading stage (Figure 9E). There was

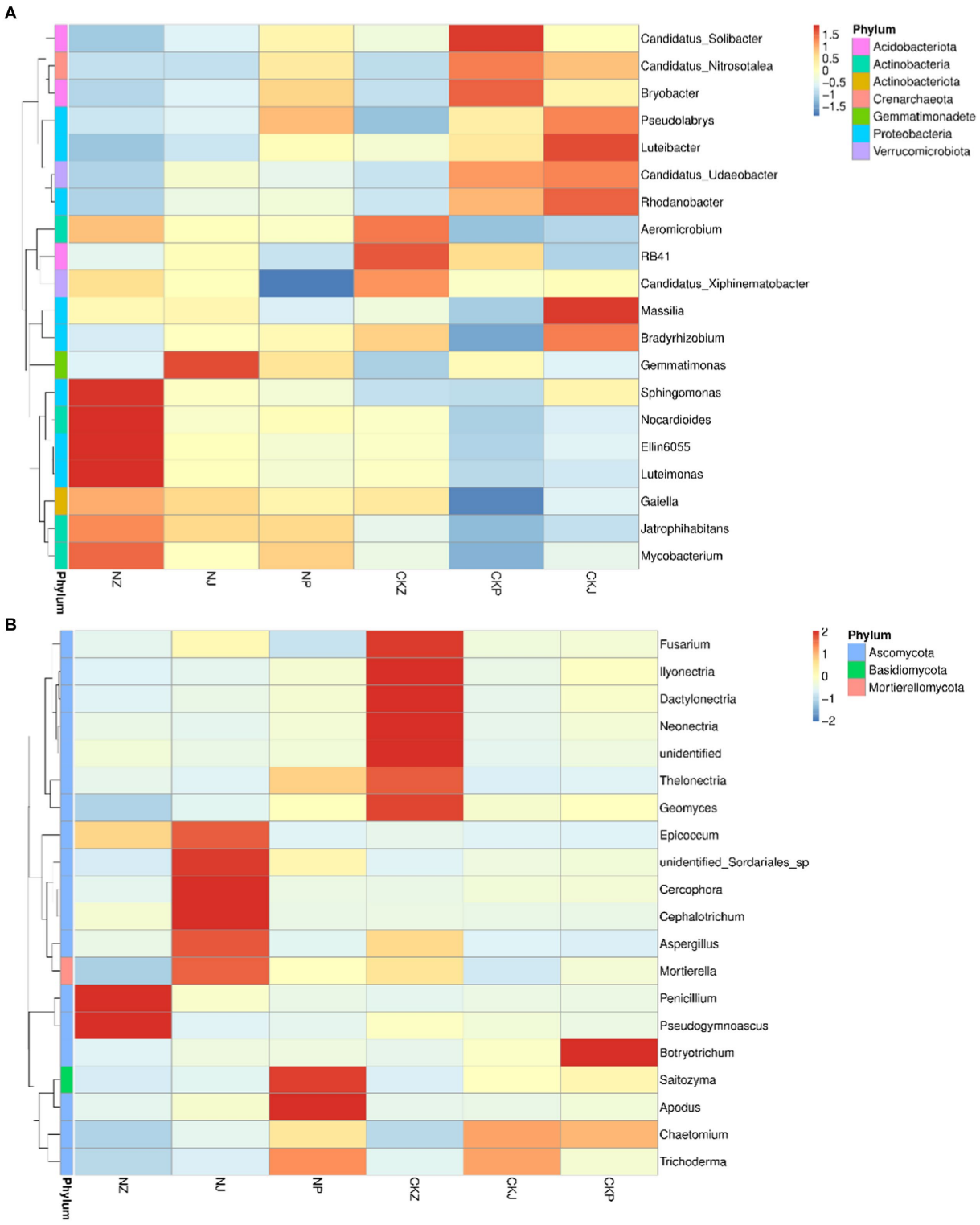

FIGURE 7
Composition of bacteria and fungi at different ginseng growth stages. **(A)** Bacterial community composition; **(B)** Fungal community composition. NZ, leaf spread of NT35 treatment; NJ, Fruit of NT35 treatment; NP, Root expansion of NT35 treatment; CKZ, leaf spread of control; CKJ, Fruit of control; CKP, Root expansion of control.

enrichment of *Sordariales*, *Chaetomium*, *Chaetomium*_sp., and *Chaetomiaceae* in the control treatment at the fruiting stage, while the fungi *Microascales*, *Cephalotrichum_stemonitis*, *Cephalotrichum*, *Microascaceae*, *Lasiosphaeriaceae*, *Cercophora*, *Epicoccum_nigrum*, *Epicoccum*, *Mortierellaceae*, *Mortierella*, *Mortierellales*, *Mortierellomycota*, *Mortierellomycetes*, *Eurotiales*, *Aspergillaceae*, *Aspergillus*, *Eurotiomycetes* and *Aspergillus_capsici* were enriched in the NT35 treatment (Figure 9F). During the root expansion stage, the

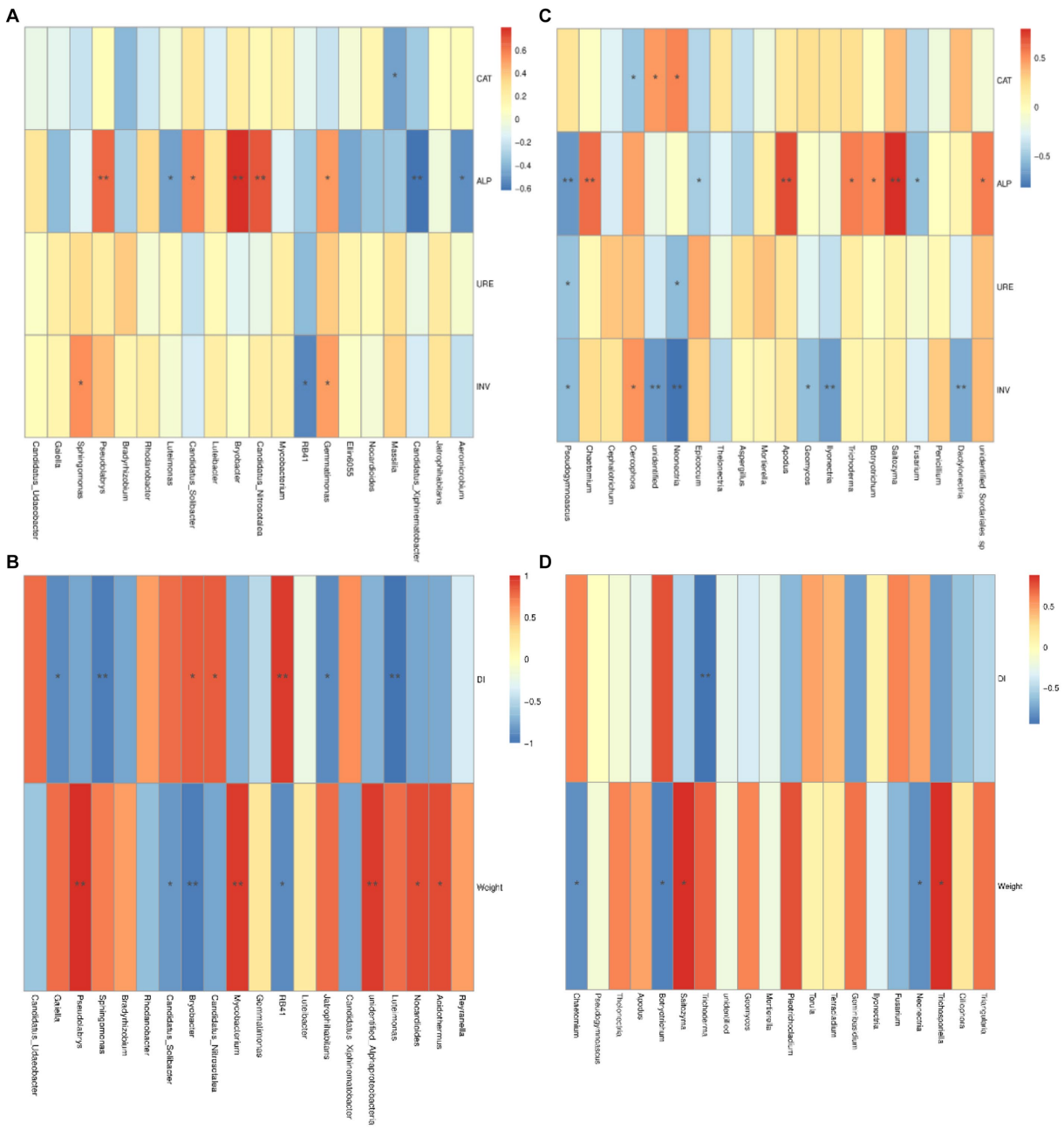

FIGURE 8
Associations between bacterial and fungal communities and relative factors. Correlation among bacterial microbial community and soil enzyme activity **(A)**, and disease index and root growth of ginseng **(B)**; Correlation among fungal microbial community and soil enzyme activity **(C)**; Disease index and root growth of ginseng **(D)**. CAT, catalase; ALP, alkaline phosphatase; URE, urease; INV, invertase. DI, disease index of ginseng rusty root rot; RL, root length of ginseng; RD, root diameter of ginseng. *p*-values were indicated by * symbol: $^{**}p < 0.01$; $^{*}p < 0.05$.

control group was enriched in *Chaetomium*_sp., *Chaetomiaceae*, *Sordariales* and *Chaetomium*, and *Basidiomycota* was enriched in the NT35 treatment (Figure 9D).

4 Discussion

In nature, *Bacillus* species exist widely and can be isolated from plant stems, leaves, roots and soil (Dinesh et al., 2015; Ali et al., 2020). Many articles have reported that *B. velezensis* can inhibit plant pathogens and be used as a biocontrol agent (Peng et al., 2019; Chen et al., 2020; Mta et al., 2020). In the field of biological control, research on screening antagonistic strains and control mechanisms is ongoing (Dimkić et al., 2022). The biocontrol bacterium *B. velezensis* strain NT35 was isolated from the rhizosphere soil of *P. ginseng*. In this study, the mechanism by which the *B. velezensis* strain NT35 controls ginseng rusty root rot was clarified by determining antagonistic effects and improvements in soil enzymes and microbial communities; however, these effects have rarely been described before in the field of controlling ginseng disease. Disease biocontrol mechanisms can

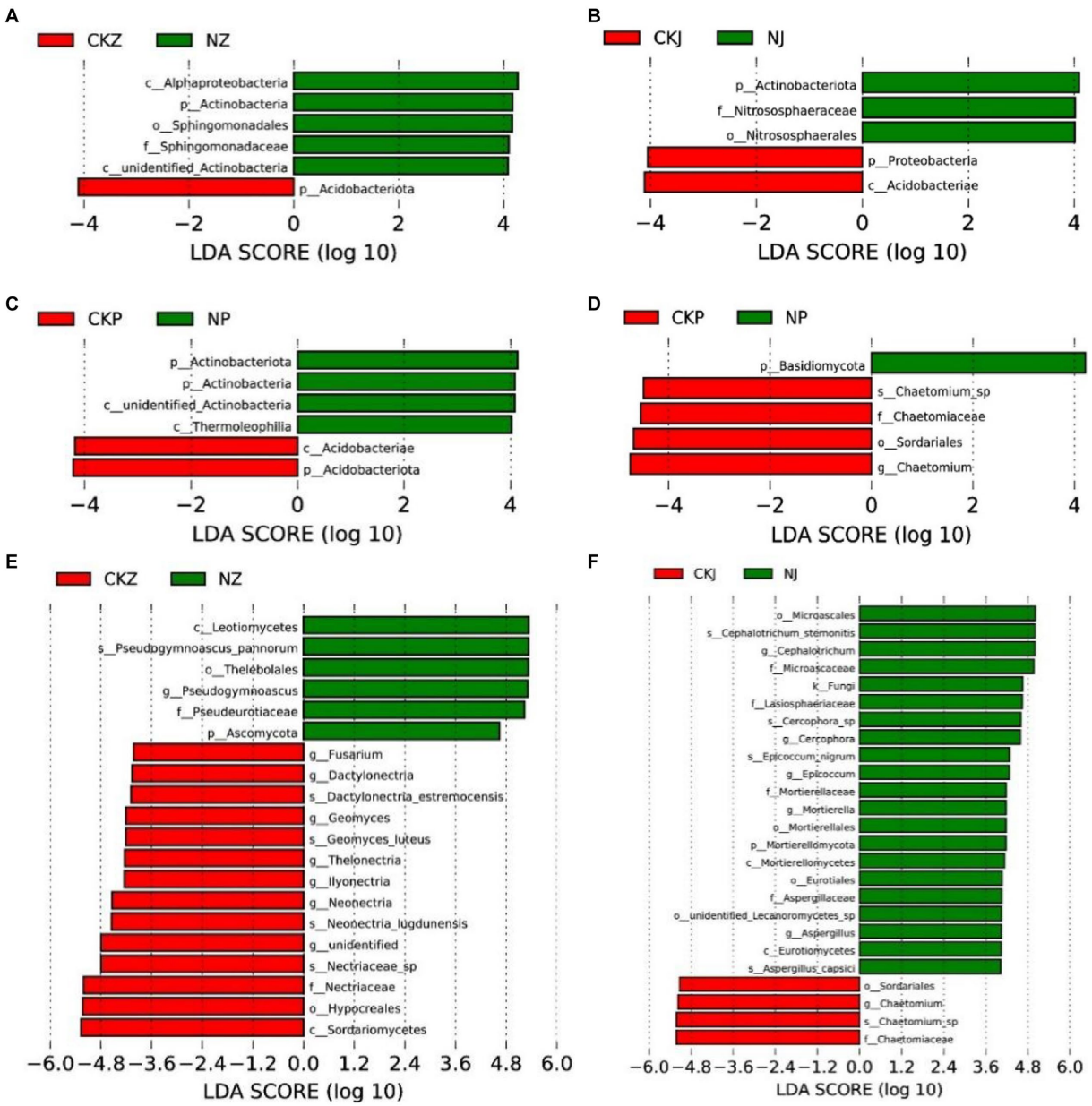

FIGURE 9
Linear discriminant effect size identified differentially abundant taxa of different periods of NT35 and control treatment (LDA significance threshold of 4.0). Bacterial community at the period of leaf spread **(A)**, fruit **(B)**, and root-expansion **(C)**; Fungal community at the period of leaf spread **(E)**, fruit **(F)**, and root expansion **(D)**. NZ, leaf-spread of NT35 treatment; NJ, fruit of NT35 treatment; NP, root expansion of NT35 treatment; CKZ, leaf-spreading of control; CKJ, fruiting of control; CKP, root expansion of control. The letters of k, p, c, o, f, g, and s were used to represent the kingdom, phylum, class, order, family, genus, and species, respectively.

be summarized as competition, antagonism and induction of plant resistance (Márquez et al., 2020; Ribeiro et al., 2021). The NT35 strain had a significant antagonistic effect on the mycelial growth, sporulation and spore germination of *I. robusta*, which causes ginseng rusty root rot.

The defense enzymes can increase plant resistance to biological stress and abiotic stress. *PAL* can prevent pathogen infection in the cell walls of host plants, and *CHI* combined with *β-1,3-GA* can induce a plant defense response to inhibit the growth of filamentous pathogenic fungi. *SOD* and *CAT* can eliminate endogenous free radicals to prevent cell death, which results in free radicals maintaining a normal dynamic level in plants to improve plant stress resistance (Manikandan et al., 2021; Wang Q. et al., 2023). For example, *B. velezensis* YYC induces an increase in the enzyme activity of *PAL*, *POD*, and *SOD* in tomato plants, resulting in resistance to bacterial wilt (Yan et al., 2022). Strawberry and grape plants can also obtain systemic resistance to external pathogens by increasing defense enzyme activity (Apaliya et al., 2017; Tang et al., 2022). Ginseng can also resist the invasion of pathogens by increasing the expression of defense-related enzyme-encoding genes (Em et al., 2020). The NT35 strain could significantly

increase the expression of the *PAL*, *β-1,3-GA*, *CHI*, *SOD* and *CAT* genes in ginseng roots to increase systemic resistance to ginseng rusty root rot, and the control effect reached 51.99%.

In recent years, research on the rhizospheric soil microbial community structure has become a popular topic in the research of biological control mechanisms. The role of biocontrol bacteria in the early stage of microecology was mainly to cause microbial community changes in plant rhizosphere soil. The *B. velezensis* strain NT35 can change the alpha and beta diversity of the microbial community in ginseng rhizosphere soil, especially the Shannon and Simpson indices, according to PCoA. Notably, the NT35 strain can recruit several beneficial bacteria, such as *Luteimonas*, *Nocardioides*, *Sphingomonas*, and *Gemmatimonas,* from the rhizosphere soil. *Gemmatimonas* contains chlorophyll phototrophic species that can support plant life processes (Chen et al., 2022). Isolates of *Luteimonas* are associated with plant growth promotion and plant resistance to pathogens and have shown antifungal activity against wheat scab, wood brown rot and ash seedling pathogens (Xiao et al., 2017; Ulrich et al., 2022). *Nocardioides* can repair pesticides or other chemically contaminated soils (Benedek et al., 2022). *Sphingomonas* can metabolize prothioconazole and has a soil remediation function (Huang Z. et al., 2022). However, in the soil not treated with strain NT35, the enriched fungal community included *Fusarium*, *Neonectria*, *Ilyonectria*, and *Dactylonectria*, which cause ginseng root rot and rusty root rot (Farh et al., 2020; Fang et al., 2022; Walsh et al., 2022). *Ilyonectria robusta* is the main pathogenic fungus of ginseng studied in this paper. The relative abundance of *Ilyonectria* significantly decreased in the rhizosphere soil after the NT35 treatment. We also found that NT35 not only reduced the abundance of *Ilyonectria* in ginseng rhizosphere soil but also reduced the abundance of *Fusarium,* which causes root rot in ginseng plants. These results suggested that the NT35 strain has a strong biocontrol effect on ginseng rusty root rot. There is evidence that the introduction of biocontrol agents can increased soil enzyme activity and improved soil nutrient, provide a suitable environment for microorganisms in soil, generate a signature microbial composition (Tian et al., 2022). In addition, it has been reported that plants alter the rhizosphere microbial composition through root secretions (Lu et al., 2018). Here we also speculate that the strain NT35 improved soil nutritional conditions and might stimulate the formation of a special secretion pattern from ginseng root which recruit the beneficial microbes to affect the composition and structure of the rhizospheric soil microbial community.

The microbial community structure is affected by biological or abiotic factors, such as the seasonal climate, soil physical and chemical properties, microtopography, and plant activities, which affect the production of enzymes and enzyme reaction kinetics in soil (Bell et al., 2014). There was a close relationship between the microbial community and soil enzyme activity and plant roots (Bell et al., 2014). However, there have been few reports about the relationships among the disease indices of ginseng rusty root rot, root growth, soil enzyme activity and the microbial community after treatment with biocontrol agent. Among the four soil enzyme activities in this study, the bacterial community was strongly correlated with ALP activity, and the fungal community was highly correlated with both ALP and INV activity. However, the abundances of *Ilyonectria* and *Fusarium* were significantly negatively correlated with INV activity, indicating that INV activity could significantly affect the abundance of pathogenic fungi in ginseng rhizosphere soil (Figure 8C).

The effects on the disease index and root length were influenced mainly by the bacterial community. For example, the disease index was significantly negatively correlated with the abundance of *Sphingomonas,* which increased after the addition of strain NT35 (Figure 8B). The fungal community represented by *Trichoderma* was similar to that represented by *Sphingomonas* (Figure 8D). Therefore, the treatment with the *B. velezensis* strain NT35 can affect the rhizosphere microbial community, thereby reducing the disease index of ginseng rusty root rot. The effects of the biocontrol agent NT35 on ginseng rhizosphere soil are summarized as follows. First, strain NT35 can recruit beneficial bacteria and fungi, which not only have biocontrol functions but also degrade pesticides or even improve soil. Second, NT35 treatment can directly reduce the relative abundance of target pathogens in soil and control soil-borne diseases. Finally, the NT35 strain increased the correlations among soil enzyme activity, disease indices and microbial communities. LEfSe analysis revealed that the bacteria beneficial to plants, such as *Sphingomonadales* and *Sphingomonadaceae,* were enriched in the rhizosphere soil (Levy et al., 2018). Additionally, the NT35 treatment significantly enriched some actinomycetes that can secrete secondary metabolites to inhibit pathogens. The abundance of pathogenic fungi in the treatment inoculated with NT35 was significantly lower than that in the noninoculated NT35 treatment (Figure 9E).

Data availability statement

The original contributions presented in the study are included in the article/Supplementary material, further inquiries can be directed to the corresponding authors.

Author contributions

XL: Writing – original draft, Methodology, Investigation, Formal analysis, Data curation. JW: Writing – original draft, Methodology, Investigation, Formal analysis, Data curation. HS: Writing – original draft, Methodology, Investigation, Data curation. CX: Writing – original draft, Methodology, Data curation. LK: Writing – original draft, Methodology. YS: Writing – original draft, Data curation. WH: Writing – original draft, Resources. JG: Writing – review & editing, Resources, Project administration, Conceptualization. YJ: Writing – review & editing, Resources, Project administration, Funding acquisition, Conceptualization. CC: Writing – review & editing, Writing – original draft, Supervision, Project administration, Funding acquisition, Conceptualization.

Funding

The author(s) declare that financial support was received for the research, authorship, and/or publication of this article. This work was supported by the earmarked fund for China Agriculture Research System (CARS-21), Jilin Science and Technology Development Project (20230204008YY and 20210202075NC), and Jilin Provincial Natural Science Foundation (20240101240JC).

Acknowledgments

Thanks to Jilin Shenwang Plant Protection Co., Ltd., China for its support in field trials and samples of ginseng plant and soil.

Conflict of interest

WH was employed by Jilin Shenwang Plant Protection Co., Ltd.

The remaining authors declare that the research was conducted in the absence of any commercial or financial relationships that could be construed as a potential conflict of interest.

Publisher's note

All claims expressed in this article are solely those of the authors and do not necessarily represent those of their affiliated organizations, or those of the publisher, the editors and the reviewers. Any product that may be evaluated in this article, or claim that may be made by its manufacturer, is not guaranteed or endorsed by the publisher.

Supplementary material

The Supplementary material for this article can be found online at: https://www.frontiersin.org/articles/10.3389/fmicb.2024.1447488/full#supplementary-material

References

Ahkami, A. H., Allen White, R., Handakumbura, P. P., and Jansson, C. (2017). Rhizosphere engineering: enhancing sustainable plant ecosystem productivity. *Rhizosphere.* 3, 233–243. doi: 10.1016/j.rhisph.2017.04.012

Ait Bessai, S., Bensidhoum, L., and Nabti, E. (2022). Optimization of IAA production by telluric bacteria isolated from northern Algeria. *Biocatal. Agric. Biotechnol.* 41:102319. doi: 10.1016/j.bcab.2022.102319

Ali, S., Hameed, S., Shahid, M., Iqbal, M., Lazarovits, G., and Imran, A. (2020). Functional characterization of potential PGPR exhibiting broad-spectrum antifungal activity. *Microbiol. Res.* 232:126389. doi: 10.1016/j.micres.2019.126389

Apaliya, M. T., Zhang, H., Yang, Q., Zheng, X., Zhao, L., and Kwaw, E. (2017). *Hanseniaspora uvarum* enhanced with trehalose induced defense-related enzyme activities and relative genes expression levels against aspergillus tubingensis in table grapes. *Postharvest Biol. Technol.* 132, 162–170. doi: 10.1016/j.postharvbio.2017.06.008

Bell, C. W., Tissue, D. T., Loik, M. E., Wallenstein, M. D., and Zak, J. C. (2014). Soil microbial and nutrient responses to 7 years of seasonally altered precipitation in a Chihuahuan Desert grassland. *Glob. Chang. Biol.* 20, 1657–1673. doi: 10.1111/gcb.12418

Benedek, T., Pápai, M., Gharieb, K., Bedics, A., Táncsics, A., Tóth, E., et al. (2022). Nocardioides carbamazepini sp. nov., an ibuprofen degrader isolated from a biofilm bacterial community enriched on carbamazepine. *Syst. Appl. Microbiol.* 45:126339. doi: 10.1016/j.syapm.2022.126339

Bhusal, B., and Mmbaga, M. T. (2020). Biological control of Phytophthora blight and growth promotion in sweet pepper by Bacillus species. *Biol. Control* 150:104373. doi: 10.1016/j.biocontrol.2020.104373

Chen, M., Author, W. N. C., Author, L. F. C., Zhu, Y., and Chen, Z. (2020). Biocontrol of tomato bacterial wilt by the new strain *Bacillus velezensis* FJAT-46737 and its lipopeptides. *BMC Microbiol.* 20, 160–112. doi: 10.1186/s12866-020-01851-2

Chen, L., Zhao, Z., Li, J., Wang, H., Guo, G., and Wu, W. (2022). Effects of muddy water irrigation with different sediment particle sizes and sediment concentrations on soil microbial communities in the Yellow River Basin of China. *Agric Water Manag* 270:107750. doi: 10.1016/j.agwat.2022.107750

Cohen, Y., Eyal, H., and Hanania, J. (1989). Ultrastructure of Pseudoperonospora cubensis, in muskmelon genotypes susceptible and resistant to downy mildew. *Physiol. Mol. Plant Pathol.* 34, 27–40. doi: 10.1016/0885-5765(89)90014-3

Delaporte-Quintana, P., Lovaisa, C. N., Rapisarda, A. V., and Pedraza, R. O. (2020). The plant growth promoting bacteria Gluconacetobacter diazotrophicus and *Azospirillum brasilense* contribute to the iron nutrition of strawberry plants through siderophores production. *Plant Growth Regul.* 91, 185–199. doi: 10.1007/s10725-020-00598-0

Dimkić, I., Janakiev, T., Petrović, M., Degrassi, G., and Fira, D. (2022). Plant-associated Bacillus and Pseudomonas antimicrobial activities in plant disease suppression via biological control mechanisms—a review. *Physiol. Mol. Plant Pathol.* 117:101754. doi: 10.1016/j.pmpp.2021.101754

Dinesh, R., Anandaraj, M., Kumar, A., Bini, Y. K., Subila, K. P., and Aravind, R. (2015). Isolation, characterization, and evaluation of multi-trait plant growth promoting rhizobacteria for their growth promoting and disease suppressing effects on ginger. *Microbiol. Res.* 173, 34–43. doi: 10.1016/j.micres.2015.01.014

Edgar, R. C. (2013). UPARSE: highly accurate OTU sequences from microbial amplicon reads. *Nat. Methods* 10, 996–998. doi: 10.1038/nmeth.2604

Em, A., Tat, B., and Kah, A. (2020). Role of plant-growth promoting fungi (PGPF) in defensive genes expression of *Triticum aestivum* against wilt disease. *Rhizosphere.* 15:100223. doi: 10.1016/j.rhisph.2020.100223

Fang, W., Liu, X., Song, Z., Jin, X., Yan, D., Wang, Q., et al. (2022). Mechanism of the antifungal action of chloropicrin fumigation against Panax notoginseng root rot caused by fusarium solani. *Physiol. Mol. Plant Pathol.* 121:101859. doi: 10.1016/j.pmpp.2022.101859

Farh, M. E.-A., Kim, Y.-J., Abbai, R., Singh, P., Jung, K.-H., Kim, Y.-J., et al. (2020). Pathogenesis strategies and regulation of ginsenosides by two species of Ilyonectria in *Panax ginseng*: power of speciation. *J. Ginseng Res.* 44, 332–340. doi: 10.1016/j.jgr.2019.02.001

Farh, M. E.-A., Kim, Y.-J., Kim, Y.-J., and Yang, D.-C. (2018). Cylindrocarpon destructans/Ilyonectria radicicola-species complex: causative agent of ginseng root-rot disease and rusty symptoms. *J. Ginseng Res.* 42, 9–15. doi: 10.1016/j.jgr.2017.01.004

Fu, G., Huang, S., Ye, Y., Wu, Y., Cen, Z., and Lin, S. (2010). Characterization of a bacterial biocontrol strain B106 and its efficacies on controlling banana leaf spot and post-harvest anthracnose diseases. *Biol. Control* 55, 1–10. doi: 10.1016/j.biocontrol.2010.05.001

Guan, Y. M., Ma, Y. Y., Jin, Q., Wang, Q. X., Liu, N., Fu, Y. P., et al. (2020). Multi-locus phylogeny and taxonomy of the fungal complex associated with rusty root rot of *Panax ginseng* in China. *Front. Microbiol.* 11:618942. doi: 10.3389/fmicb.2020.618942

Huang, Z., Li, Q., Gai, X., Zhang, X., Zhong, Z., Bian, F., et al. (2022). Corrigendum: effects of on-and off-year management practices on the soil organic C fractions and microbial community in a Moso bamboo (*Phyllostachys edulis*) forest in subtropical China. *Front. Plant Sci.* 13:1020344. doi: 10.3389/fpls.2022.1020344

Huang, J., Li, M., Jin, F., Wang, Z., Li, W., Pan, D., et al. (2022). Isolation of Sphingomonas sp. AJ-1 and its enantioselective S-methylation of the triazole fungicide prothioconazole. *Sci. Total Environ.* 851:158220. doi: 10.1016/j.scitotenv.2022.158220

Iyer, B., Rajput, S. M., and Rajkumar, S. (2017). Effect of succinate on phosphate solubilization in nitrogen fixing bacteria harbouring chick pea and their effect on plant growth. *Microbiol. Res.* 202, 43–50. doi: 10.1016/j.micres.2017.05.005

Jiang, Y., Song, Y., Jiang, C. Y., Li, X., Liu, T. T., Wang, J., et al. (2022). Identification and characterization of *Arthrobacter nicotinovorans* JI39, a novel plant growth-promoting Rhizobacteria strain from *Panax ginseng*. *Front. Plant Sci.* 13:873621. doi: 10.3389/fpls.2022.873621

Kandeler, E., and Gerber, H. (1988). Short-term assay of soil urease activity using colorimetric determination of ammonium. *Biol. Fertil. Soils* 6, 68–72. doi: 10.1007/BF00257924

Kim, Y., Lim, J., Sukweenadhi, J., Seok, W. J., Lee, S. W., Park, J. C., et al. (2019). Genomic characterization of a newly isolated Rhizobacteria Sphingomonas panacis reveals plant growth promoting effect to Rice. *Biotechnol. Bioprocess Eng.* 24, 119–125. doi: 10.1007/s12257-018-0386-2

Lee, J.-H., Lee, J.-S., Kwon, W.-S., Kang, J.-Y., Lee, D.-Y., In, J.-G., et al. (2015). Characteristics of Korean ginseng varieties of Gumpoong, Sunun, Sunpoong, Sunone, Cheongsun, and Sunhyang. *J. Ginseng Res.* 39, 94–104. doi: 10.1016/j.jgr.2014.06.007

Levy, A., Salas, G. I., Mittelviefhaus, M., Clingenpeel, S., Herrera, P. S., Miao, J., et al. (2018). Genomic features of bacterial adaptation to plants. *Nat. Genet.* 50, 138–150. doi: 10.1038/s41588-017-0012-9

Linden, C., Fatouros, N. E., and Kammenga, J. E. (2022). The potential of entomopathogenic nematodes to control moth pests of ornamental plantings. *Biol. Control* 165:104815. doi: 10.1016/j.biocontrol.2021.104815

Liu, X. Y., Chen, C. Y., Wang, J., Zhou, S. H., and Long, X. X. (2021). Phosphorus solubilizing bacteria Bacillus thuringiensis and *Pantoea ananatis* simultaneously

promote soil inorganic phosphate dissolution and soil Pb immobilization. *Rhizosphere* 20, 100448–102198. doi: 10.1016/j.rhisph.2021.100448

Livak, K. J., and Schmittgen, T. D. (2001). Analysis of relative gene expression data using real-time quantitative PCR and the $2^{-\Delta\Delta Ct}$ method. *Methods* 25, 402–408. doi: 10.1006/meth.2001.1262

Lu, T., Ke, M. J., Lavoie, M., Jin, Y. J., Fan, X. J., Zhang, Z. Y., et al. (2018). Rhizosphere microorganisms can influence the timing of plant flowering. *Microbiome* 6, 1–12. doi: 10.1186/s40168-018-0615-0

Lúcia, R. R. B., Newton, P. S., Lilia, G. W., Delson, L., Marcos, A. B. L., Samuel, M. M. M., et al. (2016). Cowpea resistance induced against fusarium oxysporum f. sp. tracheiphilum by crustaceous chitosan and by biomass and chitosan obtained from Cunninghamella elegans. *Biol. Control* 92, 45–54. doi: 10.1016/j.biocontrol.2015.09.006

Manikandan, A., Parthasarathy, R., Anusuya, S., and Huang, J. (2021). An overview of plant defense-related enzymes responses to biotic stresses. *Plant Gene.* 27:100302. doi: 10.1016/j.plgene.2021.100302

Márquez, R., Blanco, E. L., and Aranguren, Y. (2020). Bacillus strain selection with plant growth-promoting mechanisms as potential elicitors of systemic resistance to gray mold in pepper plants. *Saudi J Biol Sci.* 27, 1913–1922. doi: 10.1016/j.sjbs.2020.06.015

Mta, B., Ila, B., Bt, C., Lt, C., Isa, B., and Vba, B. (2020). Growth promotion on horticultural crops and antifungal activity of *Bacillus velezensis* XT1. *Appl. Soil Ecol.* 150:103453. doi: 10.1016/j.apsoil.2019.103453

Niemi, R. M., Heiskanen, I., Wallenius, K., and Lindström, K. (2001). Extraction and purification of DNA in rhizosphere soil samples for PCR-DGGE analysis of bacterial consortia. *J. Microbiol. Methods* 45, 155–165. doi: 10.1016/S0167-7012(01)00253-6

Ning, Z. Y., Li, Y. L., Zhao, X. Y., Han, D., and Zhan, J. (2022). Comparison of leaf and fine root traits between annuals and perennials, implicating the mechanism of species changes in desertified grasslands. *Front. Plant Sci.* 12:778547. doi: 10.3389/fpls.2021.778547

Peng, G., Zhao, X. Y., Li, Y. Z., Wang, R., Huang, Y., and Qi, G. F. (2019). Engineering *Bacillus velezensis* with high production of acetoin primes strong induced systemic resistance in *Arabidopsis thaliana*. *Microbiol. Res.* 227:126297. doi: 10.1016/j.micres.2019.126297

Quast, C., Pruesse, E., Yilmaz, P., Gerken, J., Schweer, T., Yarza, P., et al. (2013). The SILVA ribosomal RNA gene database project: improved data processing and web-based tools. *Nucleic Acids Res.* 41, D590–D596. doi: 10.1093/nar/gks1219

Rahman, M., and Punja, Z. K. (2005). Factors influencing development of root rot on ginseng caused by Cylindrocarpon destructans. *Phytopathology* 95, 1381–1390. doi: 10.1094/PHYTO-95-1381

Rahul, J., and Anita, P. (2016). Soil enzymes and microbial endophytes as indicators of climate variation along an altitudinal gradient with respect to wheat rhizosphere under mountain ecosystem. *Rhizosphere.* 2, 75–84. doi: 10.1016/j.rhisph.2016.07.007

Ribeiro, I., Bach, E., Moreira, F., Müller, A., and Passaglia, L. (2021). Antifungal potential against Sclerotinia sclerotiorum (lib.) de Bary and plant growth promoting abilities of Bacillus isolates from canola (*Brassica napus* L.) roots. *Microbiol. Res.* 248:126754. doi: 10.1016/j.micres.2021.126754

Sharma, M., and Manhas, R. K. (2022). Biocontrol potential of Streptomyces sp. M4 and salvianolic acid B produced by it against Alternaria black leaf spot. *Microb. Pathog.* 173:105869. doi: 10.1016/j.micpath.2022.105869

Stoll, A., Salvatierra-Martínez, R., González, M., and Araya, M. (2021). The role of Surfactin production by *Bacillus velezensis* on colonization, biofilm formation on tomato root and leaf surfaces and subsequent protection (ISR) against Botrytis cinerea. *Microorganisms.* 9:2251. doi: 10.3390/microorganisms9112251

Sun, X. D., Ye, Y. Q., Ma, Q. X., Guan, Q. W., and Jones, D. L. (2021). Variation in enzyme activities involved in carbon and nitrogen cycling in rhizosphere and bulk soil after organic mulching. *Rhizosphere.* 19:100376. doi: 10.1016/j.rhisph.2021.100376

Tang, Y., Li, R., Jiang, Z. C., Cheng, Z. Y., Li, W., and Shao, Y. Z. (2022). Combined effect of Debaryomyces hansenii and *Bacillus atrophaeus* on the physicochemical attributes, defense-related enzyme activity, and transcriptomic profile of stored litchi fruit. *Biol. Control* 172:104975. doi: 10.1016/j.biocontrol.2022.104975

Tian, Y., Liu, Y., Yue, L., Uwaremwe, C., Zhao, X., Zhou, Q., et al. (2022). Bacterial inoculant and sucrose amendments improve the growth of *Rheum palmatum* L. by reprograming its metabolite composition and altering its soil microbial community. *Int. J. Mol. Sci.* 23:1694. doi: 10.3390/ijms23031694

Tiwari, S., Sarangi, B. K., and Thul, S. T. (2016). Identification of arsenic resistant endophytic bacteria from *Pteris vittata* roots and characterization for arsenic remediation application. *J. Environ. Manage.* 180, 359–365. doi: 10.1016/j.jenvman.2016.05.029

Ulrich, K., Becker, R., Behrendt, U., Kube, M., Schneck, V., and Ulrich, A. (2022). Physiological and genomic characterisation of Luteimonas fraxinea sp. nov., a bacterial species associated with trees tolerant to ash dieback. *Syst. Appl. Microbiol.* 45:126333. doi: 10.1016/j.syapm.2022.126333

Walsh, J. P., McMullin, D. R., Yeung, K. K. C., and Sumarah, M. W. (2022). Resorcylic acid lactones from the ginseng pathogen Ilyonectria mors-panacis. *Phytochem. Lett.* 48, 94–99. doi: 10.1016/j.phytol.2022.02.008

Wang, J., Wang, J. R., Liu, T. T., Li, X., Gao, J., Jiang, Y., et al. (2023). *Bacillus amyloliquefaciens* FG14 as a potential biocontrol strain against rusty root rot of Panax ginseng, and its impact on the rhizosphere microbial community. *Biol. Control* 182:105221. doi: 10.1016/j.biocontrol.2023.105221

Wang, H., Xu, F., Wang, X., Wang, X. Q., Kwon, W. S., and Yang, D. C. (2019). Molecular discrimination of *Panax ginseng* cultivar K-1 using pathogenesis-related protein 5 gene. *J. Ginseng Res.* 43, 482–487. doi: 10.1016/j.jgr.2018.07.001

Wang, C. X., Zhao, X. L., Wu, K., Liang, C. Y., Liu, J., Yang, H., et al. (2023). Isolation and characterization of *Bacillus velezensis* strain B19 for biocontrol of Panax notoginseng root rot. *Biol. Control* 185:105311. doi: 10.1016/j.biocontrol.2023.105311

Wang, Q., Xu, X. Y., Li, X. H., Wang, J. L., et al (2023). Soil enzyme activities, physiological indicators, agronomic traits and yield of common buckwheat under herbicide combined with safeners. *Sci. Total Environ.* 903:166261. doi: 10.1016/j.scitotenv.2023.166261

Wołejko, E., Jabłońska-Trypuć, A., Wydro, U., Butarewicz, A., and Łozowicka, B. (2020). Soil biological activity as an indicator of soil pollution with pesticides – a review. *Appl. Soil Ecol.* 147:103356. doi: 10.1016/j.apsoil.2019.09.006

Xiao, X., Fan, M., Wang, E., Chen, W., and Wei, G. (2017). Interactions of plant growth-promoting rhizobacteria and soil factors in two leguminous plants. *Appl. Microbiol. Biotechnol.* 101, 8485–8497. doi: 10.1007/s00253-017-8550-8

Xu, Y. P., Zang, R. C., Chen, W. L., and Lou, Y. C. (2001). Effect of *Enterobacter cloacae* B8 fermentation broth on plant growth and analysis of IAA. *J Zhejiang Univ.* 49, 1370–1375. doi: 10.1360/04wc0011

Yan, Y. C., Xu, W. H., Hu, Y. L., Tian, R. M., and Wang, Z. G. (2022). *Bacillus velezensis* YYC promotes tomato growth and induces resistance against bacterial wilt. *Biol. Control* 172:104977. doi: 10.1016/j.biocontrol.2022.104977

You, L., Cha, S. H., Kim, M.-Y., and Cho, J. Y. (2022). Ginsenosides are active ingredients in *Panax ginseng* with immunomodulatory properties from cellular to organismal levels. *J. Ginseng Res.* 46, 711–721. doi: 10.1016/j.jgr.2021.12.007

Zhang, J. Y., Ding, X., Guan, R., Zhu, C. M., Xu, C., Zhu, B. C., et al. (2018). Evaluation of different 16S rRNA gene V regions for exploring bacterial diversity in a eutrophic freshwater lake. *Sci. Total Environ.* 618, 1254–1267. doi: 10.1016/j.scitotenv.2017.09.228

Zhang, X. Y., Zhou, Y., Li, J., Gu, X. Y., Zhao, L. N., Li, B., et al. (2022). Pichia caribbica improves disease resistance of cherry tomatoes by regulating ROS metabolism. *Biol. Control* 169:104870. doi: 10.1016/j.biocontrol.2022.104870

Zhao, W., Guo, Q., Li, S., Lu, X. Y., Dong, L. H., Wang, P. P., et al. (2022). Application of *Bacillus subtilis* NCD-2 can suppress cotton verticillium wilt and its effect on abundant and rare microbial communities in rhizosphere. *Biol. Control* 165:104812. doi: 10.1016/j.biocontrol.2021.104812

frontiers | Frontiers in Microbiology

TYPE Original Research
PUBLISHED 01 October 2024
DOI 10.3389/fmicb.2024.1448950

OPEN ACCESS

EDITED BY
Dongdong Yan,
Chinese Academy of Agricultural Sciences (CAAS), China

REVIEWED BY
Yupeng Fan,
University of Oklahoma, United States
Bin Huang,
Chinese Academy of Agricultural Sciences, China

*CORRESPONDENCE
Tang Li-na
704142780@qq.om
Lin Wen-xiong
lwx@fafu.edu.cn
Huang Jin-wen
huangjw1126@sohu.com

RECEIVED 14 June 2024
ACCEPTED 18 September 2024
PUBLISHED 01 October 2024

CITATION
Bian-hong Z, Li-na T, Ri-kun L, Rui-xin P, Lin-dong Y, Xiao-yan C, Kai-wen Y, Wen-xiong L and Jin-wen H (2024) Synergistic co-evolution of rhizosphere bacteria in response to acidification amelioration strategies: impacts on the alleviation of tobacco wilt and underlying mechanisms.
Front. Microbiol. 15:1448950.
doi: 10.3389/fmicb.2024.1448950

Synergistic co-evolution of rhizosphere bacteria in response to acidification amelioration strategies: impacts on the alleviation of tobacco wilt and underlying mechanisms

Zhang Bian-hong[1,2], Tang Li-na[3]*, Li Ri-kun[4], Pan Rui-xin[1,2], You Lin-dong[1,2], Chen Xiao-yan[1,2], Yang Kai-wen[1,2,5], Lin Wen-xiong[1,2,5]* and Huang Jin-wen[1,2]*

[1]Key Laboratory for Genetics Breeding and Multiple Utilization of Crops, Ministry of Education/College of Agriculture, Fujian Agriculture and Forestry University, Fuzhou, Fujian, China, [2]Key Laboratory of Crop Ecology and Molecular Physiology (Fujian Agriculture and Forestry University), Fujian Province University, Fuzhou, Fujian, China, [3]Tobacco Science Research Institute of Fujian Tobacco Monopoly Bureau, Fuzhou, Fujian, China, [4]Ganzhou Tobacco Company Shicheng Branch, Ganzhou, Jiangxi, China, [5]College of JunCao Science and Ecology, Fujian Agriculture and Forestry University, Fuzhou, China

Soil acidification represents a severe threat to tobacco cultivation regions in South China, exacerbating bacterial wilt caused by *Ralstonia solanacearum*. The comprehension of the underlying mechanisms that facilitate the restoration of rhizosphere microbial communities in "healthy soils" is imperative for ecologically managing tobacco bacterial wilt. This study focuses on acidified tobacco soils that have been subjected to continuous cultivation for 20 years. The experimental treatments included lime (L), biochar (B), and a combination of lime and biochar (L+B), in addition to a control group (CK). Utilizing rhizosphere biology and niche theory, we assessed disease suppression effects, changes in soil properties, and the co-evolution of the rhizosphere bacterial community. Each treatment significantly reduced tobacco bacterial wilt by 16.67% to 20.14% compared to the control group (CK) ($p< 0.05$) and increased yield by 7.86% to 27.46% ($p< 0.05$). The biochar treatment (B) proved to be the most effective, followed by the lime-biochar combination (L+B). The key factors controlling wilt were identified through random forest regression analysis as an increase in soil pH and exchangeable bases, along with a decrease in exchangeable acidity. However, lime treatment alone led to an increase in soil bulk density and a decrease in available nutrients, whereas both biochar and lime-biochar treatments significantly improved these parameters ($p<0.05$). No significant correlation was found between the abundance of *Ralstonia* and wilt incidence. Nonetheless, all treatments significantly expanded the ecological niche breadth and average variation degree (AVD), enhanced positive interactions and cohesion within the community, and intensified negative interactions involving *Ralstonia*. This study suggests that optimizing community niches and enhancing pathogen antagonism are key mechanisms for mitigating tobacco wilt in acidified soils. It recommends using lime-biochar mixtures as soil amendments due to their potential ecological and economic benefits. This study offers valuable insights for disease control strategies and presents a novel perspective for research on *Solanaceous* crops.

KEYWORDS

bacterial wilt, acidification amelioration, tobacco, rhizosphere bacteria, synergistic co-evolution

Introduction

Soil-borne bacterial wilt caused by *Ralstonia solanacearum* has led to devastating losses in the yield and profitability of solanaceous crops such as tobacco (*Nicotiana tabacum* L.), potato (*Solanum tuberosum* L.), and tomato (*Solanum lycopersicum* L.) worldwide (Coll and Valls, 2013; Wen et al., 2023; Msabila et al., 2024). Wilt is difficult to control, and its occurrence can result in significant reductions in crop yield and quality, or even total crop failure, hence it is often referred to as "plant cancer" (Yuliar and Toyota, 2015). Tobacco, being one of the most significant economic crops globally, provides substantial employment opportunities in many countries, particularly in developing nations where the tobacco industry is a primary source of income for numerous farmers and laborers. In recent years, soil acidification in tobacco-growing regions of southern China has been exacerbated by factors such as continuous monoculture, environmental pollution, and the application of the use of acidic fertilizers. The rapid proliferation of *R. solanacearum* has resulted in an escalating outbreak of bacterial wilt in these regions, leading to a continuous decline in tobacco yield and quality (Li et al., 2017).

The current measures employed in tobacco production primarily revolve around the development of disease-resistant varieties and the utilization of chemical products for effective control. The disease resistance of the currently selected varieties, however, is not robust enough, rendering them vulnerable to bacterial wilt. The prolonged utilization of chemical agents also poses risks to environmental pollution, pesticide toxicity, and the emergence of pathogen resistance (Meng et al., 2024). The exploration of green control technologies is imperative, necessitating urgent attention. Recent studies have increasingly demonstrated that the occurrence of bacterial wilt is closely associated with imbalances in the microbial community structure within the rhizosphere soil and alterations in rhizosphere microbial diversity. Previous research indicates a negative correlation between higher abundance of beneficial microorganisms in the soil and disease incidence (Dordas, 2008; Dignam et al., 2019; Najeeb and Li, 2023). Consequently, fostering a healthy soil environment and promoting diverse microbial communities are considered highly effective ecological approaches for managing soil-borne diseases. The composition of soil microbial communities is significantly influenced by soil environmental conditions, with soil pH being widely recognized as the most influential predictor, commonly referred to as a key determinant of microbial community structure.

The diversity and stability of bacterial communities are strongly influenced by soil pH (Lauber et al., 2009; Zhalnina et al., 2015). The research findings indicate a significant negative correlation between soil pH and the incidence of bacterial wilt within the pH range of 4.5–6.5 (Yang et al., 2017). This suggests that optimizing soil pH is a fundamental and pivotal strategy for controlling the spread of bacterial wilt. Consequently, there has been a growing interest among researchers in elevating pH levels to mitigate the potential risk associated with bacterial wilt. Lime is a classic soil acidification amendment in agricultural production, and its use is particularly widespread in southern China. Studies have shown that lime application not only increases soil pH but also effectively controls soil-borne diseases such as root rot and fusarium wilt. The key to disease suppression is often attributed to changes in the microbial community, such as reduced pathogen abundance and enhanced microbial community functionality (Chen et al., 2022; Deng et al., 2024). Shen et al. (2018) also found that lime application significantly reduced the incidence of tobacco bacterial wilt, attributing this effect to changes in the rhizosphere microbial community, including decreased abundance of the wilt pathogen and recruitment of disease-suppressive microbes such as *Saccharibacteria* and *Aeromicrobium*. However, the potential long-term risks associated with lime application on soil environments cannot be ignored. Bolo et al. (2021) and Ding et al. (2023) have observed that continuous application of lime may suppress the activity of nutrient-cycling microorganisms, potentially leading to soil "re-acidification." Furthermore, Liu et al. (2023) revealed that while lime significantly reduced the incidence of tobacco bacterial wilt, it also had a notable negative impact on the diversity of rhizosphere soil bacterial communities. Therefore, there is an urgent need to explore alternative soil improvement measures.

In this context, biochar has increasingly attracted attention as a novel soil amendment due to its characteristics such as enhancing soil fertility, improving physicochemical properties, and optimizing the microbial habitat (Lehmann et al., 2011; Blanco-Canqui, 2017). Recent studies have shown that biochar can adsorb toxic substances and harmful compounds (Kumari et al., 2024). The research conducted by Li et al. (2022) on tobacco plants has demonstrated the effective reduction of bacterial wilt incidence, enhancement of rhizosphere microbial diversity, and decrease in the abundance of the wilt pathogen through biochar application. Our preliminary research also indicates that the primary reason for the reduced incidence of bacterial wilt with biochar application is the improvement in microbial community structure, reduction in wilt pathogen abundance, and increased abundance of beneficial bacteria such as *Bacillus* and *Sphingomonas* (Pan et al., 2024). However, the high cost of biochar remains a significant limitation for its widespread use in agriculture. Despite advancements in disease management through soil improvement strategies and the identification of the close relationship between disease suppression mechanisms and rhizosphere microbial communities, practical implementation in agriculture faces numerous challenges that significantly impede widespread adoption. Therefore, to develop appropriate, efficient, and cost-effective measures and products for the control of tobacco bacterial wilt, it is imperative to investigate the mechanisms underlying rhizosphere microbial evolution during disease development and suppression. Furthermore, researchers emphasize the necessity of deepening our understanding of the mechanisms and co-occurrence patterns of bacterial communities involved in disease suppression to establish a sustainable disease management system. A comprehensive understanding of microbial assembly mechanisms and co-occurrence patterns is crucial for the development of more effective management tools, disease prediction models, and control strategies based on microbial mechanisms (Mallon et al., 2015; Batista et al., 2024).

Therefore, we hypothesize that although different strategies for soil acidification amendment may exhibit variations in their impact on disease suppression in both soil and plants, the fundamental abiotic and biotic mechanisms underlying disease suppression remain fundamentally similar. The critical biotic mechanisms primarily arise from alterations in the process of microbial community assembly and microbial interactions. Accordingly, this research focuses on soils

acidified by long-term tobacco monoculture, comparing the efficacy of various amendment strategies in suppressing bacterial wilt and exploring the changes in soil physicochemical properties and the co-evolutionary patterns of rhizosphere bacterial communities during disease suppression. The aim is to elucidate the mechanisms for restoring microbial community equilibrium under "healthy soil" conditions and to provide a scientific basis for establishing sustainable ecological control mechanisms for tobacco bacterial wilt. The findings are expected to offer new theoretical and methodological insights for managing bacterial wilt in other *Solanaceous* crops.

Materials and methods

Experimental design

The Fujian tobacco variety "Yunyan 87," provided by the Tobacco Research Institute of Yunnan Province and the Longyan Tobacco Company of Fujian Province, was utilized in this study. Field trials were conducted over 2 years from 2021 to 2022 at the Fujian Tobacco Agricultural Research Base in Huanxi Town, Jin'an District, Fuzhou City, Fujian Province, China (119°36′86″E, 26°17′33″N). The experimental soil was a red soil paddy field under continuous tobacco-rice rotation for 20 years. From January to August 2021, a randomized block design was implemented, comprising three treatments: a control group without any soil amendments (CK), the application of 1,500 kg·ha^{-1} lime (L), and the application of 30 t·ha^{-1} biochar (B). Each treatment had three replicates, resulting in a total of nine plots with dimensions of 144 m^2 (24 m × 6 m). From January to August 2022, an additional treatment was introduced: the combined application of 750 kg·ha^{-1} lime and 15 t·ha^{-1} biochar (L + B). This led to four treatments, each with three replicates, totaling 12 plots.

One month before tobacco planting, whole top soil layer amendments were conducted, followed by tractor-ploughing and ridging with a height of 35 cm and row spacing of 1.2 m × 0.5 m. All other field management practices adhered to the high-yield and quality cultivation measures of Fujian Province, with fertilization rates set at 127.5 kg·ha^{-1} N, 99 kg·ha^{-1} P_2O_5, and 402 kg·ha^{-1} K_2O. The application rates of the soil amendments were determined based on the results (Zhang B. et al., 2023; Zhang B. H. et al., 2023; Huang J. W. et al., 2023; Huang X. Q. et al., 2023).

During the tobacco growing season in 2021, the accumulated temperature was 2445.59°C and the total rainfall was 459.11 mm. In 2022, the accumulated temperature was 2209.04°C and the total rainfall was 610.43 mm. The initial soil pH was 4.96, with a soil organic matter content of 27.65 g·kg^{-1}, total nitrogen of 2.06 g·kg^{-1}, total phosphorus of 0.88 g·kg^{-1}, total potassium of 24.91 g·kg^{-1}, alkali-hydrolyzable nitrogen of 96.37 mg·kg^{-1}, available phosphorus of 51.10 mg·kg^{-1}, and available potassium of 190.06 mg·kg^{-1}.

The biochar used in the amendment experiment was produced from tobacco stalks by Sanli New Energy Co., Ltd. in Shangqiu, Henan Province, through high-temperature pyrolysis (approximately 450°C) under anaerobic conditions. Its physicochemical properties are as follows: pH of 9.66, fixed carbon content of 475.90 g·kg^{-1}, total nitrogen of 15.00 g·kg^{-1}, total phosphorus of 1.40 g·kg^{-1}, and total potassium of 20.10 g·kg^{-1}. The lime used primarily consists of calcium oxide and calcium carbonate, with a pH of 11.41.

Survey of tobacco bacterial wilt disease

During the tobacco harvest period, investigate the number of diseased plants under various treatments, classify the severity of the disease according to "GB/T 23222–2008" (Supplementary Table S1), and calculate the incidence percentage and disease index Equations 1, 2 (Cai et al., 2021).

$$\text{Incidence percentage}(\%) = (\text{Number of diseased plants} / \text{Total number of plants surveyed}) \times 100\% \quad (1)$$

$$\text{Disease index} = \sum(\text{number of diseased plants at each level} \times \text{corresponding grade value}) / (\text{highest value} \times \text{total number of plants investigated}) \times 100. \quad (2)$$

Survey of tobacco economic traits

The tobacco yield was individually measured based on the plot area during the harvesting period. The cured tobacco leaves were classified according to GB 2635–1992 "Flue-cured Tobacco," and subsequently, the tobacco yield and output value of each plot were calculated.

Soil physicochemical property determination

During the vigorous growth stages of tobacco, a strategically placed sampling point was positioned on the ridge surface between two representative tobacco plants in each plot. According to the five-point sampling method, five soil samples were collected from each plot. Subsequently, a single sample was provided for each repeating plot before mixing the soil of the same layer. Soil bulk density, porosity, and field capacity were subsequently measured at depths of 0–10 cm, 10–20 cm, and 20–30 cm in the topsoil using a ring knife method. The obtained measurements were averaged across three repetitions for each treatment (Zhang et al., 2023; Zhang B. H. et al., 2023). A total of 36 soil samples (3 × 4 × 3) are were collected from the 0–30 cm soil layer for determining soil nutrients. The samples were air-dried indoors and ground using a 1 mm mesh. pH is determined using the potentiometric method with an acidity meter. Soil exchangeable acidity is determined using the KCl exchange-neutralization titration method, and soil exchangeable bases are determined using the CH_3COONH_4 exchange-neutralization titration method. The sum of these two values represents the soil cation exchange capacity. The determination of total nitrogen, phosphorus, and potassium contents was conducted using the $HClO_4$-H_2SO_4 digestion method with the assistance of the Smartchem 2000 fully automated discrete chemical analyzer and the NaOH fusion-flame photometry method. The soil's organic matter content was measured through the H_2SO_4-$K_2Cr_2O_7$ external heating method. Additionally, the levels of alkali-hydrolyzable nitrogen, available phosphorus, available potassium, and readily oxidisable organic carbon in soil were assessed using respective techniques such as alkali hydrolysis diffusion for nitrogen

determination or molybdenum antimony anti-colorimetric for phosphorus measurement (Bao, 2000; Gu et al., 2023).

Rhizosphere soil bacterial DNA extraction and high-throughput sequencing

During the vigorous growth period of tobacco, three representative tobacco plants exhibiting consistent growth patterns were chosen for each experimental treatment. The entire root systems of the tobacco plants were excavated, and the impurities surrounding the root system were eliminated. The soil samples adhered to the root surfaces were homogenized and wrapped in tin foil, followed by rapid freezing in liquid nitrogen and subsequent transfer to a −80°C freezer for storage. Soil DNA extraction, PCR amplification, and sequencing were all completed by Allwegene Technology Co., Ltd. (Beijing, China). After sampling soil and extracting total DNA of soil microorganisms, DNA samples were stored at −20°C following detection using NanoDrop 2000 UV–Vis spectrophotometer and agarose gel electrophoresis. Following total DNA extraction from soil, primers 338F (5'-ACTCCTACGGGAGGCAGCAG-3') and 806R (5'-GGACTA CHVGGGTWTCTAAT-3') with barcodes were used to amplify the V3-V4 region of 16S rDNA sequences. Library construction was performed using the TruSeq® DNA PCR-Free Sample Preparation Kit, and sequencing was carried out on the Illumina Miseq platform. Raw image data from sequencing were processed using the RDP Classifier algorithm and Silva database Release 119 to cluster reads with >97.0% similarity, generating operational taxonomic unit (OTU) representative sequences for comparative analysis. Species information of the community was annotated, and OTU abundance in each sample was normalized for diversity and differential analysis (NCBI accession number: PRJNA1118945).

Bioinformatics analysis

After sequencing the 16S rDNA sequences, raw sequences were filtered and quality-checked using QIIME (v1.8.0). Operational taxonomic units (OTUs) were clustered at 97% similarity using Vsearch (v2.7.1). Clustering was performed with the Uparse method (Edgar, 2013), and denoising was carried out using the Unoise3 method (Rognes et al., 2016). To obtain species classification information for each OTU, the RDP Classifier algorithm was used to evaluate representative sequences with 70% confidence (Wang et al., 2007), and species information was annotated at various taxonomic levels (Kingdom, Phylum, Class, Order, Family, Genus, Species). After normalizing OTU abundance for each sample, diversity and differential analyses were conducted. Alpha species diversity was calculated using the diversity function from the R package "vegan" (Dixon, 2003), while phylogenetic diversity (PD), phylogenetic species variability (PSV), phylogenetic species richness (PSR), and phylogenetic species evenness (PSE) were computed using the R package "picante" (Kembel et al., 2010). Species diversity and phylogenetic diversity were standardized using Z-scores (Equation 3), where x_i represents the observed value for treatment i, and μ and σ denote the mean and standard deviation of the dataset.

$$Z = (x_i - \mu) / \sigma \tag{3}$$

Functional prediction of community species

The bacterial functions were categorized using the Plant-Beneficial Bacteria (PBB) database, which is constructed based on microbial taxonomy and functional traits (Li P. F. et al., 2023).

Community ecology information and assembly mechanisms

The term "niche breadth" refers to the ecological position occupied by a population within an ecosystem and encompasses the entire spectrum of resources it utilizes. It is a key indicator for measuring the diversity of resource use and environmental adaptability of a species. A broader niche breadth indicates greater capability to exploit various resources and higher environmental adaptability, potentially leading to more stable survival across larger temporal or spatial scales. Niche breadth was calculated using the Levin method from the R package "spaa" (Zhang and Ma, 2013) (Equation 4), where P_{ij} represents the proportion of the i-th species at sampling site j, and r is the total number of sampling sites. Microbial community stability was assessed using the Average Variation Degree (AVD) based on the method proposed by Xun et al. (2021) (Equation 5), where k is the number of samples in each group, n is the number of OTUs in each group, a_i represents the variation of OTU_i, and x_i is the abundance of OTU_i in a single sample after rarefaction. x_i and δ_i denote the mean and standard deviation of the abundances of OTU_i across a group of samples after rarefaction. Typically, lower AVD values indicate greater community stability, while higher AVD values suggest increased community activity.

$$\text{Niche breadth} = 1 / r \cdot \sum_{j=1}^{r} (P_{ij}) \tag{4}$$

$$\text{AVD} = \sum_{i=1}^{n} |a_i| \Big/ k \times n, \; |a_i| = x_i - \bar{x}_i \Big/ \delta_i \tag{5}$$

The C-score null model method proposed by Stone and Roberts (1990) was used to assess the randomness of species distributions. The observed C-score was calculated to evaluate species co-occurrence, and a null distribution of the simulated C-scores was generated using a randomization algorithm. By comparing the observed C-score with the null distribution, the standardized effect size (SES) was computed. Higher absolute values of SES indicate stronger relative contributions of deterministic processes. All calculations were performed using the "EcoSimR" package (Mo et al., 2021).

Null model analysis was conducted using the framework described by Stegen et al. (2012) to quantify the relative contributions of different treatments to microbial community assembly processes. Beta Nearest Taxon Index (βNTI) calculations were performed using the R package "picante" (Kembel et al., 2010). When βNTI < −2 or ≥ 2,

it was classified as homogenizing or heterogeneous selection, respectively. For $|\beta NTI| < 2$, RCbray was calculated using the "vegan" package (Dixon, 2003). RCbray < -0.95 indicated homogenizing dispersal, RCbray ≥ 0.95 indicated dispersal limitation, and $|RCbray| < 0.95$ represented drift.

Construction and characteristics of microbial community co-occurrence networks

The OTU table, after rarefaction, was used to independently construct microbial co-occurrence networks for each treatment. The microbial network matrices were created using the "reshape2" and "WGCNA" packages (Wickham, 2007; Langfelder et al., 2008), and network visualizations were generated in Gephi 0.10.1, retaining edges with Spearman correlation coefficients $|r| > 0.65$ and $p < 0.01$. To evaluate the complexity of microbial networks and interspecies interactions, we calculated various network features, including the number of nodes, number of edges, average degree, graph density, modularity index, and the proportion of positive to negative interactions, using the "igraph" package (Yuan et al., 2021). Cohesion is a measure of microbial interactions and was used to understand how positive/negative species interactions or niche similarities/differences affect community connectivity across temporal, spatial, or environmental gradients (Herren and McMahon, 2017). For a given network, the cohesion index is calculated as the sum of significant positive or negative correlations between species, weighted by species abundance (Equation 6), reflecting the extent of cooperative behavior or interactions, and is widely applied in various habitats.

$$\text{Cohesion} = \sum_{i=1}^{n} abundance_i \times connectedness_i \quad (6)$$

Statistical analysis

Principal Coordinates Analysis (PCoA) based on Bray-Curtis distance was performed using the corresponding functions from the "vegan" package (Dixon, 2003). The random forest regression model, built with the "randomForest" package, was employed to predict key soil properties influencing the incidence of tobacco bacterial wilt (Liaw and Wiener, 2002). Spearman's rank correlation coefficient was used to analyze the relationships between community assembly processes, co-occurrence patterns, and tobacco bacterial wilt incidence. Graphs and charts were created using Microsoft Excel 2019, Origin 2024b, and R 4.2.9 software. Statistical significance was assessed using SPSS 22.0, with Duncan's multiple range tests applied at $\alpha = 0.05$.

Results

Effect of different soil amendments on the incidence of tobacco bacterial wilt disease and performance of agronomic traits

As shown in Supplementary Table S2, in the 2021 experiment, the application of lime or biochar (L, B) significantly reduced the incidence percentage and disease index of tobacco bacterial wilt disease compared to the CK treatment. However, in terms of yield and production value, the B treatment outperformed the L treatment. The results from 2022 (Figure 1) indicate that compared to the CK treatment, each treatment significantly reduced the incidence percentage of tobacco bacterial wilt disease by 16.67 to 20.14% ($p < 0.05$) and significantly increased tobacco yield by 7.86 to 27.46% ($p < 0.05$). However, only the B treatment significantly reduced the disease index compared to the CK treatment. Moreover, in terms of yield and production value, the B treatment showed the best improvement, followed by the lime and biochar mixture treatment (L + B). The findings from the 2-year experiment suggested that various soil amendments exhibit significant disease suppression effects; however, they demonstrate diverse impacts on tobacco yield and its economic value.

Changes in the physicochemical properties of tobacco-growing soil and their correlation with the incidence of bacterial wilt disease

As shown in Table 1, compared to the CK treatment, the application of soil amendments significantly increased soil pH, reduced exchangeable acidity, and significantly increased exchangeable base content and cation exchange capacity ($p < 0.05$). In terms of soil bulk density and field capacity, both B and L + B treatments significantly decreased soil bulk density and increased field capacity compared to the CK treatment ($p < 0.05$), while only the lime treatment (L) showed no significant difference in bulk density and field capacity compared to the CK treatment. Regarding soil nutrients, both B and L + B treatments significantly increased soil alkali-hydrolyzable nitrogen, available phosphorus, available potassium, and readily oxidisable organic content compared to the CK treatment ($p < 0.05$), while the L treatment only significantly increased available potassium content ($p < 0.05$). The results suggest that the application of lime alone exhibits limited efficacy in soil improvement, whereas the combination of lime with biochar demonstrates a multifaceted enhancement in soil physicochemical properties.

The random forest regression model, as depicted in Figure 2, demonstrates that soil physicochemical properties exhibit a strong predictive capacity for the incidence percentage and disease index of tobacco bacterial wilt disease, with a total explanation rate exceeding 50%. Available potassium, pH level, and exchangeable acidity display significant correlations with both the incidence percentage and disease index ($p < 0.05$). Cation exchange capacity and exchangeable bases are significantly associated with the disease incidence percentage ($p < 0.05$), while readily oxidizable organic matter exhibits a significant correlation with the disease index ($p < 0.05$).

Changes in rhizosphere bacterial community diversity

To investigate the dynamic characteristics of rhizosphere microbiota in response to reduced incidence of bacterial wilt disease, high-throughput sequencing of the V3-V4 region was

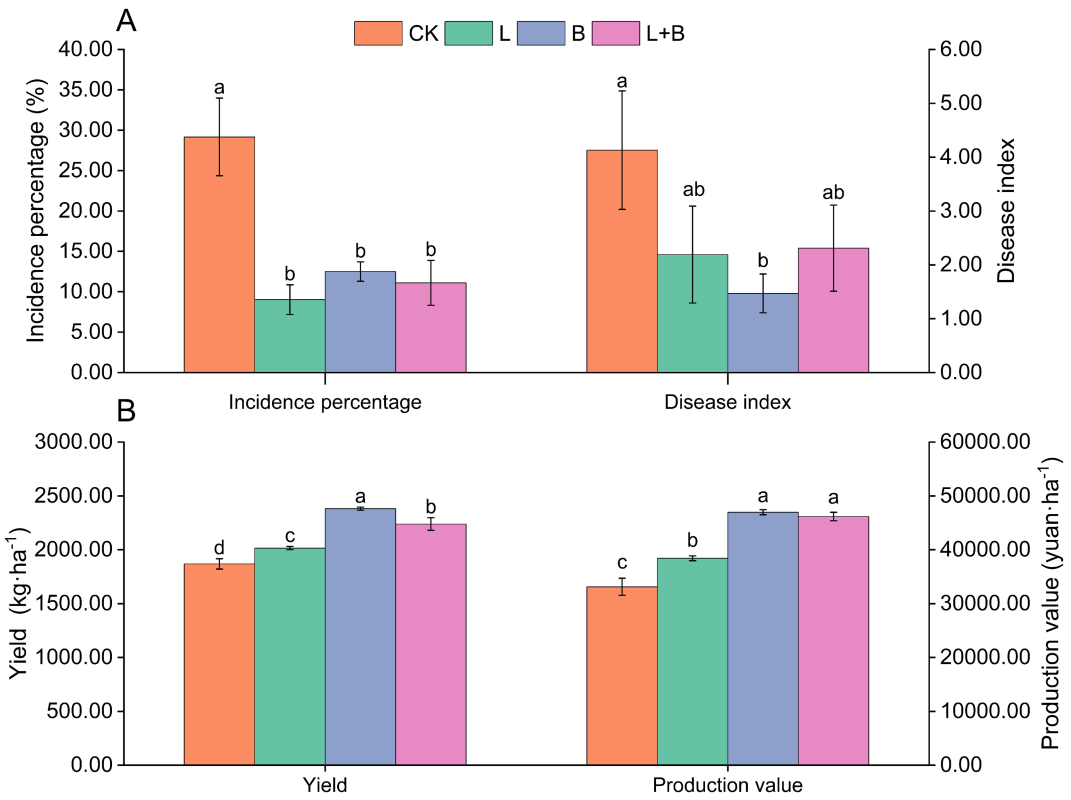

FIGURE 1
Incidence of bacterial wilt **(A)** and economic traits **(B)** of tobacco plants in each treatment (2022). CK, control without soil amendment; L, lime treatment; B, biochar treatment; L + B, lime and biochar mixture treatment. Data depicts means ± SD of three biological replicates. Significant differences between treatments ($p < 0.05$) are illustrated by different lowercase letters.

performed using the Illumina MiSeq platform. A total of 1,867,236 bacterial 16S rDNA sequences were identified, resulting in 9201 operational taxonomic units (OTUs). The rarefaction curves of OTUs at a 97% sequence similarity level exhibited saturation without further increase (Supplementary Figure S1A), indicating that the data accurately represented the composition of rhizosphere bacterial communities and facilitated subsequent data analysis.

The effect of soil amendments on bacterial community species diversity and phylogenetic diversity (Supplementary Figure S1B). Both L and L + B treatments significantly increased species diversity (Observed OTUs, Ace, Chao1, Shannon) and phylogenetic diversity (PD, PSR, PSE) compared to the CK treatment ($p < 0.05$), whereas the B treatment showed no significant difference from the CK treatment in species diversity and phylogenetic diversity.

As depicted in Supplementary Figure S1C, PCoA based on Bray-Curtis distance quantified differences in species composition among treatments, with a cumulative explanatory rate of 63.71%. Only the B treatment significantly separated from the CK treatment along PCoA1 and PCoA2 axes (PERMANOVA, $R^2 = 61.57\%$, $p = 0.001$). However, L and L + B treatments exhibited significant separation from the CK treatment only along the PCoA2 axis (PERMANOVA, $R^2 = 61.57\%$, $p = 0.001$). It is evident that different soil amendments have inconsistent effects on species diversity and composition of rhizosphere bacterial communities.

Changes in the species composition of bacterial communities and the abundance of *Ralstonia* in rhizosphere soil

In this sequencing, a total of 59 bacterial phyla and 818 bacterial genera were annotated. The top 10 dominant bacterial phyla or genera in relative abundance were selected for comparison. The results indicated that different soil amendments had inconsistent effects on the relative abundance of dominant bacterial phyla in rhizosphere bacterial communities (Figure 3A). The L and L + B treatments significantly reduced the relative abundance of Proteobacteria and Bacteroidota, while significantly increasing the relative abundance of Chloroflexi and Acidobacteriota ($p < 0.05$). Conversely, the B treatment significantly increased the relative abundance of Proteobacteria and Bacteroidota, while significantly decreasing the relative abundance of Chloroflexi and Acidobacteriota ($p < 0.05$). With respect to the dominant bacterial genera (Figure 3B), a significant reduction in the relative abundance of *Rhodanobacter* and *Chujaibacter* was detected following the application of soil amendments.

As shown in Figure 3C, compared to the CK treatment, the B and L + B treatments significantly reduced the relative abundance of the main pathogen of bacterial wilt, *Ralstonia*, but there was no significant change compared to the L treatment and CK treatment. Pearson linear regression analysis indicated that the relative abundance of *Ralstonia* was not significantly correlated with the incidence percentage of

TABLE 1 Physicochemical properties of tobacco soil in each treatment.

	CK	L	B	L + B
Bulk density (g·cm^{-3})	1.37 ± 0.03a	1.38 ± 0.04a	1.16 ± 0.01c	1.24 ± 0.01b
Porosity (%)	48.44 ± 0.12c	47.94 ± 0.16c	56.14 ± 0.24a	53.38 ± 0.41b
Field capacity (%)	31.75 ± 0.29c	31.49 ± 0.27c	43.95 ± 0.28a	41.78 ± 0.35b
pH	4.89 ± 0.01d	5.04 ± 0.02c	5.27 ± 0.01a	5.13 ± 0.02b
Exchangeable acidity (mmol·kg^{-1})	12.83 ± 0.17a	8.33 ± 0.01b	7.00 ± 0.17c	7.17 ± 0.17c
Exchangeable bases (mmol·kg^{-1})	29.84 ± 0.04c	35.50 ± 0.07b	37.12 ± 0.11a	37.34 ± 0.04a
Cation exchange capacity (mmol·kg^{-1})	42.67 ± 0.15c	43.84 ± 0.11b	44.32 ± 0.11a	44.50 ± 0.19a
Total nitrogen (g·kg^{-1})	2.15 ± 0.70a	2.21 ± 0.33a	2.18 ± 0.20a	2.19 ± 0.26a
Alkali-hydrolyzable nitrogen (mg·kg^{-1})	169.67 ± 3.33b	170.00 ± 5.04b	190.33 ± 2.33a	186.83 ± 5.41a
Total phosphorus (g·kg^{-1})	0.90 ± 0.02a	0.92 ± 0.02a	0.91 ± 0.04a	0.92 ± 0.02a
Available phosphorus (mg·kg^{-1})	68.58 ± 1.77b	71.27 ± 1.32b	79.72 ± 2.58a	75.56 ± 1.08a
Total potassium (g·kg^{-1})	25.84 ± 0.10c	26.39 ± 0.49bc	27.48 ± 0.11a	26.82 ± 0.30b
Available potassium (mg·kg^{-1})	314.72 ± 7.16d	334.44 ± 5.68c	387.98 ± 7.06a	355.06 ± 7.52b
Soil organic carbon (g·kg^{-1})	16.30 ± 0.10b	16.49 ± 0.19b	16.94 ± 0.20a	16.75 ± 0.10a
Readily oxidisable organic carbon (g·kg^{-1})	3.14 ± 0.14c	3.05 ± 0.07c	4.20 ± 0.16a	3.86 ± 0.06b

CK, control without soil amendment; L, lime treatment; B, biochar treatment; L + B, lime and biochar mixture treatment. Data depicts means ± SD of three biological replicates. Significant differences between different treatments ($P < 0.05$) are illustrated by different lowercase letters.

bacterial wilt ($p > 0.05$) but was significantly positively correlated with the disease index ($p < 0.05$). However, its explanatory power for the disease severity index was only 33.84% ($R^2 = 33.84\%$).

Functional prediction of rhizosphere bacterial communities and their assembly mechanisms

Based on the PBB database, the prediction of the tobacco rhizosphere bacterial community was predicted (Supplementary Figure S2). The results indicated that compared to the CK treatment, the L treatment significantly decreased the relative abundance of PGPR (Plant Growth-Promoting Rhizobacteria), Plant pathogen bacteria, Biocontrol bacteria, and Stress resistance bacteria ($p < 0.05$). However, there was no significant change in these parameters compared to the CK treatment for the B treatment and L + B treatment.

The community assembly mechanisms, as shown in Figure 4, were illustrated through the C-score results. A higher |SES| value indicates a stronger relative contribution of deterministic processes, with the magnitude of |SES| ranked as CK > L > L + B > B (Figure 4A). Using the Beta Nearest Taxon Index (βNTI), the relative contributions of deterministic and stochastic community assembly processes to changes in rhizosphere bacterial communities after applying soil amendments were quantified (Figure 4B). The results indicated that compared to the CK treatment, the assembly process of rhizosphere bacterial communities in the L treatment was primarily dominated by heterogeneous selection (77.78%), while the B treatment and L + B treatment were dominated by dispersal limitation (100, 88.89%). Regarding the ecological niche breadth and average variation degree (AVD) (Figures 4C,D), consistent results were observed across different soil amendment treatments, all showing significant improvements compared to the CK treatment. The ecological niche breadth increased significantly by 45.16 to 140.71% ($p < 0.05$), and AVD increased significantly by 4.45–11.15% ($p < 0.05$).

Co-occurrence patterns and the co-evolutionary rules of rhizosphere bacterial communities

By constructing a bacterial community network to understand the co-evolutionary rules within communities, the results are shown in Figure 5A, indicating that each treatment has increased the modularity index and reduced the graph density in the community network compared to the CK treatment, while significantly increasing the proportion of positive interactions among species. Based on species interactions and species abundance-weighted calculations of community cohesion, the results are shown in Figure 5B, indicating that each treatment significantly enhanced both positive and total community cohesion compared to the CK treatment ($p < 0.05$).

Further analysis of the interactions of *Ralstonia* within the community, as shown in Figure 6, reveals that under the CK treatment, *Ralstonia* interactions within the community are mainly positive (60.63%), with negative interactions accounting for 39.97%. However, after the application of soil amendments, *Ralstonia* interactions within the community are predominantly negative (77.71, 51.70, 51.15%).

Spearman correlation analysis indicated (Figure 7) that the incidence percentage of tobacco bacterial wilt is significantly negatively correlated with niche breadth, network modularity

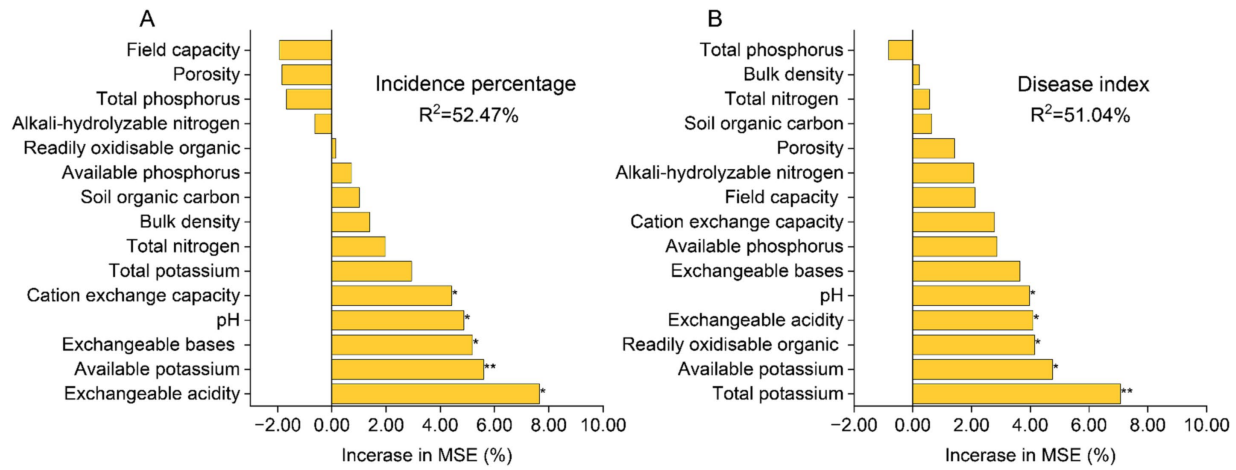

FIGURE 2
Random Forest regression model predicts the correlation between soil physicochemical properties and the incidence percentage of tobacco bacterial wilt **(A)** as well as the disease index **(B)**. The precision importance measures were calculated for each tree in a random forest and averaged over the entire forest (5,000 trees). The percentage increase in the mean squared error (MSE) of the variables was used to estimate the importance of these predictors. "*"at 0.05 level (two-tailed), the correlation was significant; "**" at level 0.01 (two-tailed), the correlation was significant. CK, control without soil amendment; L, lime treatment; B, biochar treatment; L + B, lime and biochar mixture treatment.

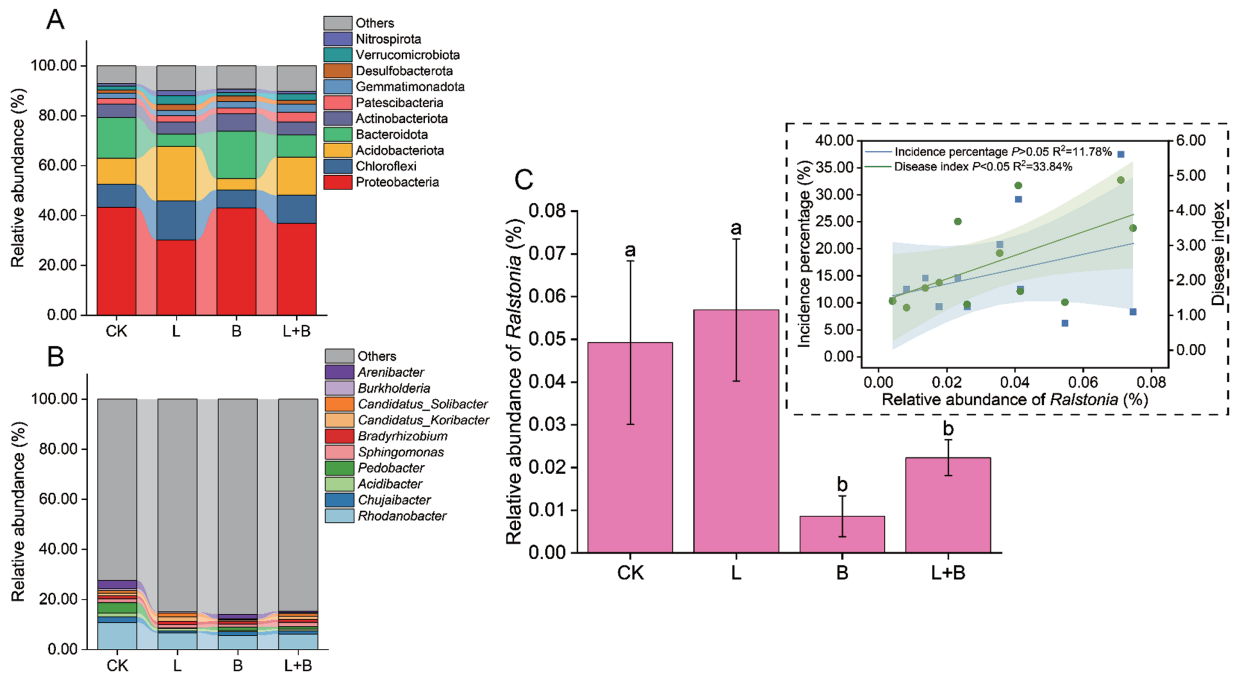

FIGURE 3
Alterations in the relative abundance of dominant bacterial phyla **(A)** and genera **(B)** in the rhizosphere of tobacco, changes in the relative abundance of *Ralstonia*, and its Pearson correlation analysis with tobacco bacterial wilt incidence **(C)**. Both dominant phyla and genera were selected based on the top 10 in relative abundance. CK, control without soil amendment; L, lime treatment; B, biochar treatment; L + B, lime and biochar mixture treatment. Data depicts means ± SD of three biological replicates. Significant differences between treatments ($p < 0.05$) are illustrated by different lowercase letters.

index, and total cohesion ($p < 0.05$). Additionally, the total cohesion is highly negatively correlated with the disease index ($p < 0.01$). There is a highly significant negative correlation between the incidence rate and community average variation degree (AVD) as well as the proportion of positive interactions within the network ($p < 0.01$), whereas it is highly positively correlated with the proportion of negative interactions ($p < 0.01$). Moreover, the proportion of positive interactions of *Ralstonia* within the community shows a significant positive correlation with both the incidence percentage and disease index ($p < 0.05$), while its proportion of negative interactions is significantly negatively correlated with these metrics ($p < 0.05$).

Discussion

Soil acidification is a critical environmental factor influencing the occurrence of bacterial wilt disease, with outbreaks being particularly severe in tobacco-growing regions of southern China where acidification issues are increasingly pronounced (Li et al., 2017). Previous studies have demonstrated that the application of lime or biochar can effectively reduce the incidence of tobacco bacterial wilt disease (Shen et al., 2018; Li et al., 2022). Our two-year field experiment revealed that the application of lime (L), biochar (B), or their combination (L + B) significantly reduces the incidence of tobacco bacterial wilt ($p < 0.05$) (Supplementary Table S2 and Figure 1A). However, in terms of disease severity and economic traits, the B treatment performed better than both the L and L + B treatments (Figures 1A,B). This may be attributed to biochar's additional benefits over lime; besides alleviating soil acidification like lime, biochar's high carbon content, good porosity, strong adsorption capacity, and rich nutrient profile provide a superior "refuge" for microbial habitation and proliferation. It supplies diverse carbon sources, energy, and mineral nutrients, which enhances microbial growth, consequently, modifies the microenvironment of crop growth. This improved microenvironment increases the efficiency of nutrient utilization and disease resistance in crops (Zhang et al., 2021). These findings align with the results of Xie et al. (2013) and Azim et al. (2024), underscoring the importance of selecting appropriate materials for soil remediation and plant disease management.

The exacerbation of soil acidification is often accompanied by the loss of base cations and nutrients in the soil, as well as the accumulation of H^+ and Al^{3+} (Dong et al., 2022). This evidently threatens the plant disease defense mechanisms. The results of this study indicate that the biochar (B) and lime plus biochar (L + B) treatments significantly increased the levels of effective nutrients such as alkali-hydrolyzable nitrogen and readily oxidisable organic carbon, and decreased soil bulk density compared to the control (CK) ($p < 0.05$), while the lime (L) treatment did not show significant differences from the CK treatment (Table 1). All treatments significantly improved soil pH, exchangeable acidity, exchangeable bases, and available potassium compared to the CK treatment ($p < 0.05$) (Table 1), which is consistent with findings by Zhang C. et al. (2017) and Liang et al. (2021). As a major abiotic factor affecting plant disease incidence, increased soil pH can directly or indirectly impact the survival environment of plant pathogens. For instance, higher pH directly inhibits the metabolic activity of *Ralstonia solanacearum* and reduces its colonization rate in the soil (Huang J. W. et al., 2023; Huang X. Q. et al., 2023). Additionally, alkaline soil conditions promote the growth of actinomycetes and

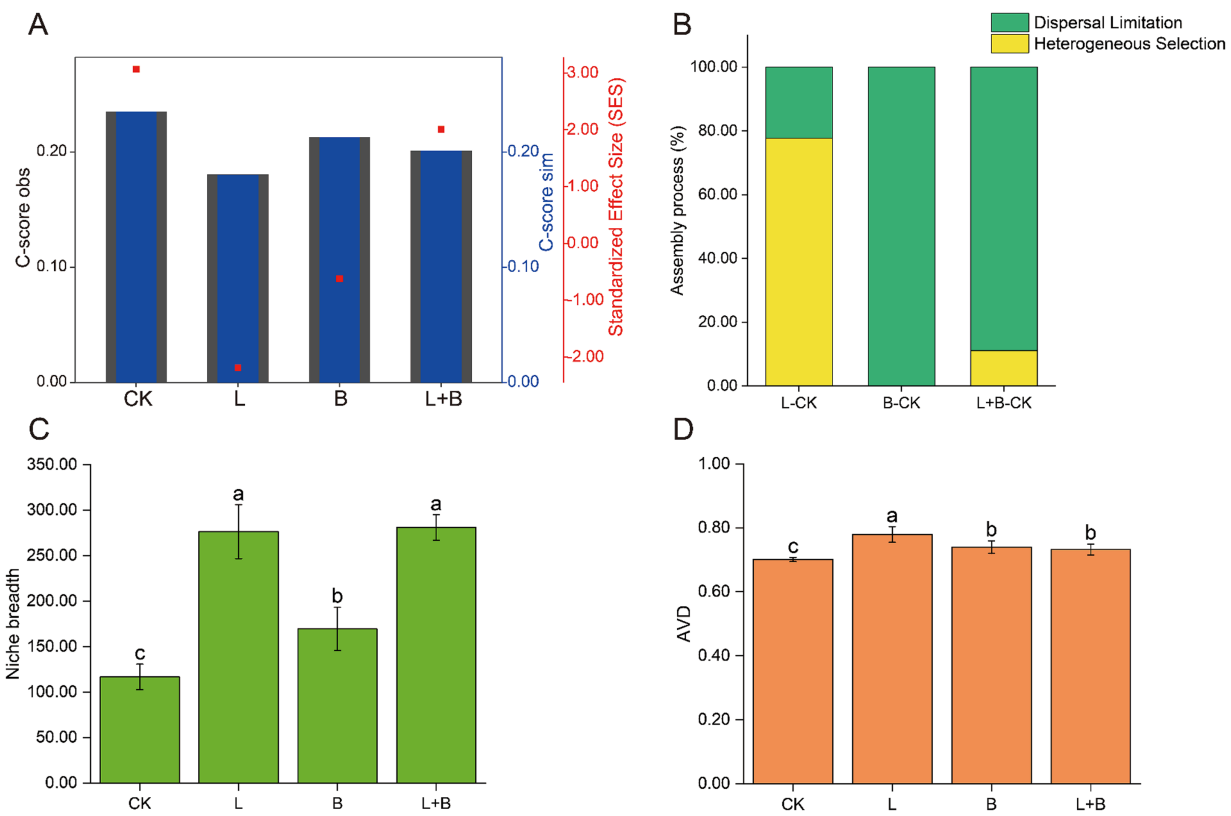

FIGURE 4
Mechanisms of rhizosphere bacterial community assembly, calculated using a phylogenetic null model C-score **(A)** and the relative contributions of different assembly processes to the community assembly mechanisms **(B)**, community niche breadth **(C)**, and AVD **(D)**. C-score metric using null models. The values of observed C-score (C-$score_{obs}$) > simulated C-score (C-$score_{sim}$) indicate non-random co-occurrence patterns. Standardized effect size <−2 and >2 represent aggregation and segregation, respectively. AVD, average variation degree; CK, control without soil amendment; L, lime treatment; B, biochar treatment; L + B, lime and biochar mixture treatment. Data depicts means ± SD of three biological replicates. Significant differences between treatments ($p < 0.05$) are illustrated by different lowercase letters.

certain antagonistic fungi, which produce natural antibiotics or other metabolites that help resist pathogen invasion (Bibi et al., 2018; Lee et al., 2021). Moreover, exchangeable base cations in the soil directly benefit plant root health by aiding in more effective water and nutrient absorption, enhancing cellular structure, and improving disease resistance (Sharma et al., 2018; Niu et al., 2021). Li et al. (2017) demonstrated that increased soil pH enhances the expression of resistance genes in the soil, playing a crucial role in suppressing bacterial wilt. Predictions from the random forest regression model in this study indicate that soil pH, exchangeable acidity, exchangeable bases, and available potassium are the primary soil physicochemical factors affecting the incidence and severity of tobacco diseases ($p < 0.05$) (Figures 2A,B). Thus, increasing soil pH and concentrations of exchangeable bases (Ca^{2+}, K^{+}, Na^{+}, Mg^{2+}) while reducing exchangeable acidity (Al^{3+}, H^{+}) are core strategies for managing bacterial wilt, and maintaining appropriate levels of available nutrients in the soil is essential to ensure crop yield.

The composition of plant rhizosphere microorganisms is an inheritable trait and represents secondary genomics that exert influences on plant growth, development, as well as yield and quality. Soil-borne diseases are closely related to the diversity and species composition of rhizosphere microbial communities (Ling et al., 2022). Several studies have indicated that soil acidification primarily reduces soil suppressive capacity against pathogens by regulating bacterial community structure (Chen et al., 2022; Li X. et al., 2023). Previous studies have demonstrated that the application of lime or biochar to enhance soil pH leads to an increase in soil microbial community diversity and induces alterations in microbial community composition (Gul et al., 2015; Guo et al., 2019). In this study, compared to the control (CK) treatment, the lime (L) and lime mixed biochar (L + B) treatments significantly increased bacterial community species diversity and phylogenetic diversity (Supplementary Figure S1B) ($p < 0.05$). The differences in rhizosphere soil bacterial composition between these treatments and the CK treatment, however, were not as pronounced as those observed with the biochar (B) treatment (Supplementary Figure S1C) (PERMANOVA, $R^2 = 61.57\%$, $p = 0.001$). Notably, there were no significant differences between the B treatment and the CK treatment in terms of community species diversity and phylogenetic diversity. Previous studies have suggested a significant positive correlation between disease severity in plant hosts and pathogen abundance (Zhang H. C. et al., 2017; Qi et al., 2022). In this study, the effects of different treatments on the relative abundance of *Ralstonia* were inconsistent; the L treatment did not significantly reduce the relative abundance of *Ralstonia* compared to the CK treatment ($p < 0.05$) (Figure 3C). Additionally, Pearson linear regression analysis revealed

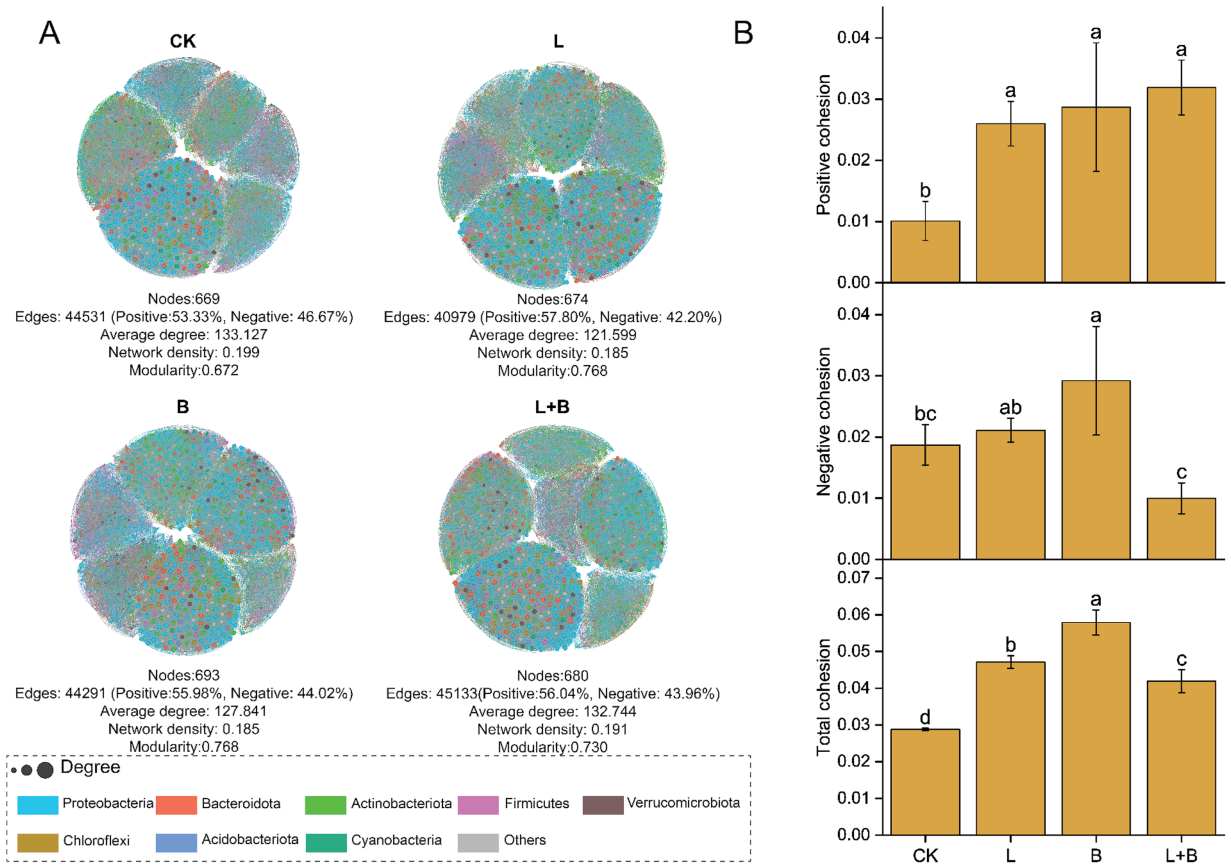

FIGURE 5
Co-occurrence network analysis **(A)** and community cohesion **(B)** of rhizosphere bacterial communities under each treatments. Each node represents a distinct bacterial genus, with node size corresponding to its degree, nodes are colored based on their phylum in the co-occurrence network. CK, control without soil amendment; L, lime treatment; B, biochar treatment; L + B, lime and biochar mixture treatment. Data depicts means ± SD of three biological replicates. Significant differences between treatments ($p < 0.05$) are illustrated by different lowercase letters.

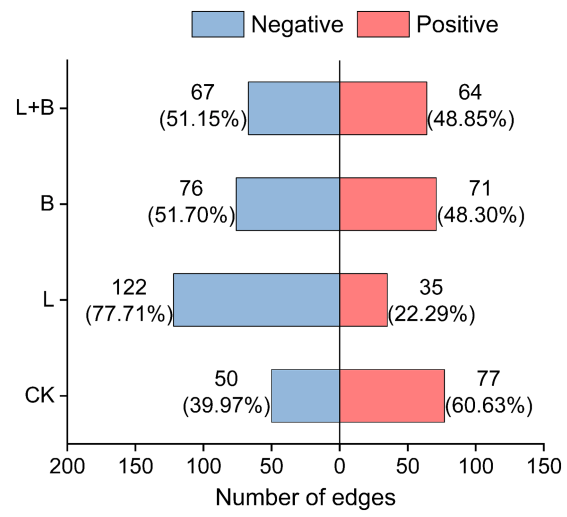

FIGURE 6
In the co-occurrence network analysis of rhizosphere bacterial communities, the interactions between Ralstonia and other bacterial genera are investigated. CK, control without soil amendment; L, lime treatment; B, biochar treatment; L + B, lime and biochar mixture treatment.

no significant correlation between the relative abundance of *Ralstonia* and bacterial wilt incidence ($p < 0.05$) (Figure 3C). Furthermore, functional classification of bacterial communities using the PBB database showed no consistent impact on the abundance of bacterial functional groups compared to the CK treatment, with both the B and L + B treatments not significantly reducing the relative abundance of plant pathogens compared to the CK treatment (Supplementary Figure S2). This result aligns with Yuan et al. (2020), who argued that relying solely on the relative abundance of pathogens, such as *Fusarium*, is insufficient for predicting the likelihood of plant disease. Based on these findings, we hypothesize that the key to suppressing bacterial wilt may involve not only reducing the abundance of *Ralstonia* within bacterial communities but also altering the abundance of various functional groups. This finding that our understanding of the rhizosphere microbial mechanisms in suppressing tobacco bacterial wilt still requires further investigation.

In natural ecosystems, the interactions among microbial species form highly dynamic and complex co-occurrence patterns (Hu et al., 2022). The evolution of community ecology research has rendered simplistic community models inadequate in capturing the entirety of community dynamics. A deeper understanding of community assembly mechanisms is crucial for exploring how different ecological

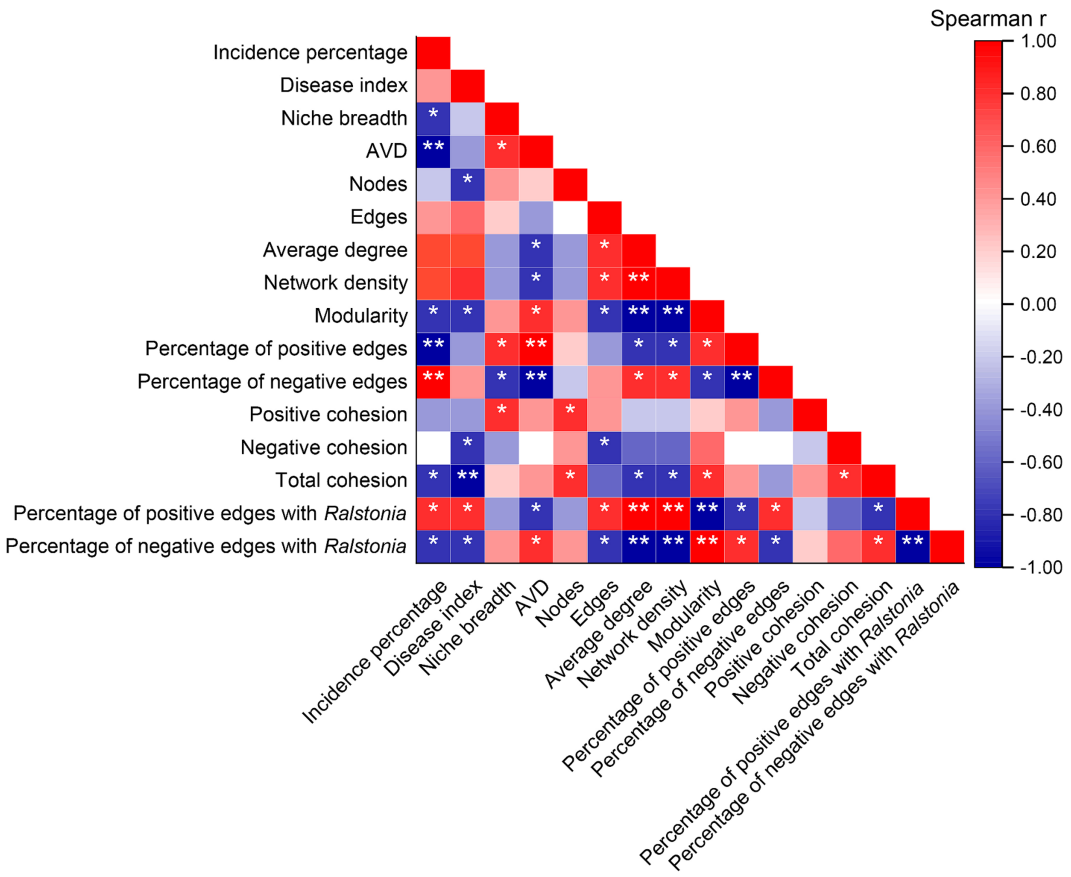

FIGURE 7
Correlations between mechanisms of community assembly and co-occurrence patterns with the incidence of bacterial wilt disease. "*" at 0.05 level (two-tailed), the correlation was significant; "**" at level 0.01 (two-tailed), the correlation was significant. AVD: average variation degree. CK, control without soil amendment; L, lime treatment; B, biochar treatment; L + B, lime and biochar mixture treatment.

processes shape and maintain microbial community composition and diversity patterns in varying soil environments (Stegen et al., 2012). In this study, treatments with soil amendments significantly reduced the relative contribution of deterministic processes to community assembly compared to the control (Figure 4A), indicating a decrease in environmental constraints on bacterial communities (Chase and Myers, 2011). βNTI analysis revealed that the assembly processes of bacterial communities differed by treatment: lime application (L) was primarily driven by heterogeneous selection, whereas biochar application (B) was mainly influenced by dispersal limitation (Figure 4B). Lime affects soil microbial community structure primarily by altering the microbial habitat, while biochar impacts community structure by increasing species turnover rates (Moeller et al., 2017), which is beneficial for improving community structure. Niche breadth measures a species' functional role and status within the community, and a wider niche breadth generally indicates faster species migration and greater environmental adaptability (Slatyer et al., 2013). Community average variation degree (AVD) reflects the activity level of the community (Xun et al., 2021). During plant host infection, soil pathogens must compete for niches or resources with other microorganisms in the rhizosphere (Liu et al., 2021). In this study, all treatments significantly increased community niche breadth and AVD compared to the control ($p < 0.05$) (Figures 4C,D). Spearman correlation analysis showed a significant negative correlation between community niche breadth and disease incidence ($p < 0.05$) (Figure 7), and an extremely significant negative correlation between community AVD and disease incidence ($p < 0.01$) (Figure 7). Thus, we hypothesize that during the suppression of bacterial wilt, the significant increase in soil pH reduces environmental selective pressures on bacteria, improves the rhizosphere nutrient environment, enhances species migration rates, and decreases interspecies competition.

Microbial ecological interactions are crucial for maintaining the stability and functionality of soil microbial communities (Yang et al., 2017). Various soil microbial groups can interact through mutualistic, synergistic, commensal, or parasitic relationships, forming a complex and interconnected ecological network that directly impacts soil and plant health (Van Der Heijden and Hartmann, 2016). Research indicates that a higher diversity of microbial species within a network increases the likelihood of metabolic and informational exchanges among microbes (Qi et al., 2019). Gu et al. (2017) demonstrated that beneficial interspecies relationships are primarily characterized by positive correlations, which promote stable coexistence or mutualistic interactions. This study constructed a community interaction network to reveal the connections and interactions between previously independent microbial communities in the soil (Rillig et al., 2016). The results showed that all treatments significantly increased the number of nodes and the modularity index in the community network compared to the control, as well as the proportion of positive interactions among species (Figure 5A). Qiao et al. (2024) combined network and cohesion analyses and found that microbial networks in healthy soils exhibit higher stability and complexity, which in turn reduce plant disease indices and increase biomass. Additionally, cohesion, which reflects the level of cooperation, also showed a negative correlation with plant disease indices. Our study also found that all treatments significantly enhanced community positive cohesion and total cohesion compared to the control ($p < 0.05$) (Figure 5B). Correlation analysis further revealed significant negative correlations between network modularity index and total cohesion with disease incidence and disease index ($p < 0.05$) (Figure 7). After increasing soil pH, bacterial communities underwent niche differentiation, disrupting and reshaping existing interspecies relationships, thereby enhancing mutualistic interactions. This could be a key rhizomicrobial mechanism in suppressing tobacco bacterial wilt. The previous results showed no significant correlation between the relative abundance of *Ralstonia* and disease incidence (Figure 3C). To further elucidate *Ralstonia*'s role in community co-evolution during disease suppression, we examined co-occurrence relationships between *Ralstonia* and other species in the network. Under the control treatment, *Ralstonia* established more mutualistic positive interactions, while after lime or biochar application, its interactions shifted to competitive or antagonistic relationships (Figure 6). Zhang et al. (2022) suggested that alleviating bacterial wilt can be achieved by recruiting species that antagonize the pathogen, which is supported by our correlation analysis results (Figure 7). Therefore, the key to suppressing tobacco bacterial wilt lies in enhancing interspecies cooperation within the community, strengthening antagonistic relationships with pathogens, and promoting positive evolutionary changes in rhizomicrobial communities. The incorporation of this approach is pivotal in simultaneously enhancing plant productivity and soil fertility. Consequently, the development of efficient control technologies for tobacco bacterial wilt should thoroughly consider these ecological mechanisms to attain optimal integrated prevention outcomes.

Conclusion

In summary, all amendment treatments significantly reduced the incidence of tobacco bacterial wilt and improved tobacco economic traits, with biochar (B) treatment being the most effective and lime + biochar (L + B) treatment being the second most effective. Improving soil pH and exchangeable base concentrations while reducing exchangeable acidity is a core strategy for managing bacterial wilt. Additionally, this study found that the lime + biochar (L + B) treatment more effectively improved soil physicochemical properties compared to lime alone (L). Therefore, this combined approach is recommended for balancing both ecological and economic benefits. Furthermore, in the context of bacterial wilt control mechanisms, the key is not only reducing *Ralstonia* abundance and altering the abundance of different functional groups but also enhancing the rhizosphere nutrient environment. This includes broadening the bacterial community's ecological niche, reducing environmental pressures on bacterial communities, and fostering mutually beneficial symbiotic relationships while recruiting antagonistic species against *Ralstonia* to establish a stable rhizosphere microbial diversity mechanism. The results suggest that further exploration of *Ralstonia* antagonistic mechanisms in soil is needed, with targeted selection of beneficial antagonistic microbial communities suitable for various soil environments. Additionally, employing soil ecological enhancement agents containing diverse antagonistic microorganisms can accelerate the positive evolution of soil microbial communities and restore the diversity and health of soil microbiomes. These findings offer new research perspectives for developing ecological control strategies for *Solanaceous* crop bacterial wilt.

Data availability statement

The datasets presented in this study can be found in online repositories. The names of the repository/repositories and accession number(s) can be found in the article/Supplementary material.

Author contributions

ZB-h: Conceptualization, Data curation, Formal analysis, Methodology, Software, Supervision, Writing – original draft, Writing – review & editing. TL-n: Data curation, Funding acquisition, Project administration, Writing – review & editing. LR-k: Writing – review & editing. PR-x: Investigation, Writing – review & editing. YL-d: Methodology, Writing – review & editing. CX-y: Methodology, Writing – review & editing. YK-w: Writing – review & editing. LW-x: Project administration, Supervision, Writing – review & editing. HJ-w: Funding acquisition, Project administration, Resources, Supervision, Writing – review & editing.

Funding

The author(s) declare that financial support was received for the research, authorship, and/or publication of this article. This study was funded by the Natural Science Foundation of Fujian Province (2021J01467), the Fujian Branch of China National Tobacco Corporation, China (2019350000240143) and the Fujian-Taiwan Joint Innovative Centre for Germplasm Resources and Cultivation of Crop, China (Fujian 2011 Program, No. 2015-75).

Conflict of interest

The authors declare that the research was conducted in the absence of any commercial or financial relationships that could be construed as a potential conflict of interest.

Publisher's note

All claims expressed in this article are solely those of the authors and do not necessarily represent those of their affiliated organizations, or those of the publisher, the editors and the reviewers. Any product that may be evaluated in this article, or claim that may be made by its manufacturer, is not guaranteed or endorsed by the publisher.

Supplementary material

The Supplementary material for this article can be found online at: https://www.frontiersin.org/articles/10.3389/fmicb.2024.1448950/full#supplementary-material

References

Azim, R., Wang, Q., Sadiq, M., Zhou, X. J., Zhang, D. K., Zhao, X. L., et al. (2024). Exploring the potential of straw and biochar application on soil quality indicators and crop yield in semi-arid regions. *J. Soil Sci. Plant Nut.* 24, 1907–1923. doi: 10.1007/s42729-024-01668-2

Bao, S. D. (2000). Soil and agricuiture chemistry analysis. *3rd* Edn. Beijing: China Agricultural Press.

Batista, B. D., Wang, J., Liu, H., Kaur, S., Macdonald, C. A., Qiu, Z., et al. (2024). Biotic and abiotic responses to soilborne pathogens and environmental predictors of soil health. *Soil Biol. Biochem.* 189:109246. doi: 10.1016/j.soilbio.2023.109246

Bibi, F., Strobel, G. A., Naseer, M. I., Yasir, M., Khalaf Al-Ghamdi, A. A., and Azhar, E. I. (2018). Microbial flora associated with the halophyte–salsola imbricate and its biotechnical potential. *Front. Microbiol.* 9:65. doi: 10.3389/fmicb.2018.00065

Blanco-Canqui, H. (2017). Biochar and soil physical properties. *Soil Sci. Soc. Am. J.* 81, 687–711. doi: 10.2136/sssaj2017.01.0017

Bolo, P., Kihara, J., Mucheru-Muna, M., Njeru, E. M., Kinyua, M., and Sommer, R. (2021). Application of residue, inorganic fertilizer and lime affect phosphorus solubilizing microorganisms and microbial biomass under different tillage and cropping systems in a ferralsol. *Geoderma* 390:114962. doi: 10.1016/j.geoderma.2021.114962

Cai, Q., Zhou, G., Ahmed, W., Cao, Y., Zhao, M., Li, Z., et al. (2021). Study on the relationship between bacterial wilt and rhizospheric microbial diversity of flue-cured tobacco cultivars. *Eur. J. Plant Pathol.* 160, 265–276. doi: 10.1007/s10658-021-02237-4

Chase, J. M., and Myers, J. A. (2011). Disentangling the importance of ecological niches from stochastic processes across scales. *Philos. T. R. Soc. B.* 366, 2351–2363. doi: 10.1098/rstb.2011.0063

Chen, D. L., Wang, X. X., Carrion, V. J., Yin, S., Yue, Z. F., Liao, Y., et al. (2022). Acidic amelioration of soil amendments improves soil health by impacting rhizosphere microbial assemblies. *Soil Biol. Biochem.* 167:108599. doi: 10.1016/j.soilbio.2022.108599

Coll, N. S., and Valls, M. (2013). Current knowledge on the *Ralstonia solanacearum* type iii secretion system. *Microb. Biotechnol.* 6, 614–620. doi: 10.1111/1751-7915.12056

Deng, W. P., Gong, J. S., Peng, W. C., Luan, W. J., Liu, Y. X., Huang, H. C., et al. (2024). Alleviating soil acidification to suppress *Panax notoginseng* soil-borne disease by modifying soil properties and the microbiome. *Plant Soil.* 1–17. doi: 10.1007/s11104-024-06577-y

Dignam, B. E. A., O'Callaghan, M., Condron, L. M., Raaijmakers, J. M., Kowalchuk, G. A., and Wakelin, S. A. (2019). Impacts of long-term plant residue management on soil organic matter quality, pseudomonas community structure and disease suppressiveness. *Soil Biol. Biochem.* 135, 396–406. doi: 10.1016/j.soilbio.2019.05.020

Ding, Z. F., Ren, B. L., Chen, Y. H., Yang, Q. Y., and Zhang, M. K. (2023). Chemical and biological response of four soil types to lime application: an incubation study. *Agronomy* 13:504. doi: 10.3390/agronomy13020504

Dixon, P. (2003). Vegan, a package of r functions for community ecology. *J. Veg. Sci.* 14, 927–930. doi: 10.1111/j.1654-1103.2003.tb02228.x

Dong, Y., Yang, J., Zhao, X., Yang, S., Mulder, J., Dörsch, P., et al. (2022). Soil acidification and loss of base cations in a subtropical agricultural watershed. *Sci. Total Environ.* 827:154338. doi: 10.1016/j.scitotenv.2022.154338

Dordas, C. (2008). Role of nutrients in controlling plant diseases in sustainable agriculture. *Agron. Sustain. Dev.* 28, 33–46. doi: 10.1051/agro:2007051

Edgar, R. C. (2013). Uparse: highly accurate otu sequences from microbial amplicon reads. *Nat. Methods* 10, 996–998. doi: 10.1038/nmeth.2604

Gu, L., Gong, Z. W., and Li, W. Z. (2017). Niches and interspecific associations of dominant populations in three changed stages of natural secondary forests on loess plateau, Pr China. *Sci. Rep.* 7:6604. doi: 10.1038/s41598-017-06689-9

Gu, X. J., Yu, Y. H., Liu, Y., Wu, M. J., Liu, L. Y. H., and Mo, Q. F. (2023). Effects of typical plantations on soil readily oxidized carbon in South China. *J. Forest Environ.* 43, 145–151. doi: 10.13324/j.cnki.jfcf.2023.02.005

Gul, S., Whalen, J. K., Thomas, B. W., Sachdeva, V., and Deng, H. Y. (2015). Physico-chemical properties and microbial responses in biochar-amended soils: mechanisms and future directions. *Agric. Ecosyst. Environ.* 206, 46–59. doi: 10.1016/j.agee.2015.03.015

Guo, A., Ding, L., Tang, Z., Zhao, Z., and Duan, G. (2019). Microbial response to caco3 application in an acid soil in southern China. *J. Environ. Sci. China* 79, 321–329. doi: 10.1016/j.jes.2018.12.007

Herren, C. M., and McMahon, K. D. (2017). Cohesion: a method for quantifying the connectivity of microbial communities. *ISME J.* 11, 2426–2438. doi: 10.1038/ismej.2017.91

Hu, J. L., Amor, D. R., Barbier, M., Bunin, G., and Gore, J. (2022). Emergent phases of ecological diversity and dynamics mapped in microcosms. *Science* 378, 85–89. doi: 10.1126/science.abm7841

Huang, J. W., Li, R. K., Chen, Z. C., Zhang, B. H., Lei, H., Pan, R. X., et al. (2023). Effects of straw returning techniques on soil nutrients, organic carbon and microbial

diversity in tobacco-rice rotation system. *Chin. J. Rice Sci.* 37, 415–426. doi: 10.16819/j.1001-7216.2023.220901

Huang, X. Q., Li, S., Xiao, Q., Qu, J. S., Zhao, J., Zhang, J. B., et al. (2023). Soil ph fitness of residents contributes more to the invasion success of *Ralstonis solanacearum* than the invader itself. *Appl. Soil Ecol.* 190:105032. doi: 10.1016/j.apsoil.2023.105032

Kembel, S. W., Cowan, P. D., Helmus, M. R., Cornwell, W. K., Morlon, H., Ackerly, D. D., et al. (2010). Picante: r tools for integrating phylogenies and ecology. *Bioinformatics* 26, 1463–1464. doi: 10.1093/bioinformatics/btq166

Kumari, R., Kumar, V., and Kumar, A. (2024). Soil and biochar: attributes and actions of biochar for reclamation of soil and mitigation of soil borne plant pathogens. *J. Soil Sci. Plant Nut.* 24, 1924–1939. doi: 10.1007/s42729-024-01810-0

Langfelder, P., Horvath, S., Langfelder, P., and Horvath, S. (2008). WGCNA: an R package for weighted correlation network analysis. *BMC Bioinform. J. Statistic. Softw.* 9, 551–559. doi: 10.1186/1471-2105-9-559

Lauber, C. L., Hamady, M., Knight, R., and Fierer, N. (2009). Pyrosequencing-based assessment of soil ph as a predictor of soil bacterial community structure at the continental scale. *Appl. Environ. Microb.* 75, 5111–5120. doi: 10.1128/AEM.00335-09

Lee, S., Kong, H. G., Song, G. C., and Ryu, C. (2021). Disruption of firmicutes and actinobacteria abundance in tomato rhizosphere causes the incidence of bacterial wilt disease. *ISME J.* 15, 330–347. doi: 10.1038/s41396-020-00785-x

Lehmann, J., Rillig, M. C., Thies, J., Masiello, C. A., Hockaday, W. C., and Crowley, D. (2011). Biochar effects on soil biota - a review. *Soil Biol. Biochem.* 43, 1812–1836. doi: 10.1016/j.soilbio.2011.04.022

Li, C., Ahmed, W., Li, D., Yu, L., Xu, L., Xu, T., et al. (2022). Biochar suppresses bacterial wilt disease of flue-cured tobacco by improving soil health and functional diversity of rhizosphere microorganisms. *Appl. Soil Ecol.* 171:104314. doi: 10.1016/j.apsoil.2021.104314

Li, X., Chen, D., Carrión, V. J., Revillini, D., Yin, S., Dong, Y., et al. (2023). Acidification suppresses the natural capacity of soil microbiome to fight pathogenic fusarium infections. *Nat. Commun.* 14:5090. doi: 10.1038/s41467-023-40810-z

Li, S. L., Liu, Y. Q., Wang, J., Yang, L., Zhang, S. T., Xu, C., et al. (2017). Soil acidification aggravates bacterial wilt in South China. *Front. Microbiol.* 8:703. doi: 10.3389/fmicb.2017.00703

Li, P. F., Tedersoo, L., Crowther, T. W., Dumbrell, A. J., Dini-Andreote, F., Bahram, M., et al. (2023). Fossil-fuel-dependent scenarios could lead to a significant decline of global plant-beneficial bacteria abundance in soils by 2100. *Nature Food.* 4, 996–1006. doi: 10.1038/s43016-023-00869-9

Liang, J., Yu, X., Cao, Y., Zhang, J., Yan, N., Xue, L., et al. (2021). Effect of quicklime on microbial community in strong acidic soil. *J. Soil Sci. Plant Nut.* 21, 1771–1781. doi: 10.1007/s42729-021-00478-0

Liaw, A., and Wiener, M. (2002). Classification and regression by randomforest. *R News.* 2, 18–22. doi: 10.1057/9780230509993

Ling, N., Wang, T., and Kuzyakov, Y. (2022). Rhizosphere bacteriome structure and functions. *Nat. Commun.* 13:836. doi: 10.1038/s41467-022-28448-9

Liu, H., Li, J., Carvalhais, L. C., Percy, C. D., Prakash Verma, J., Schenk, P. M., et al. (2021). Evidence for the plant recruitment of beneficial microbes to suppress soil-borne pathogens. *New Phytol.* 229, 2873–2885. doi: 10.1111/nph.17057

Liu, Y. X., Li, H., Li, X., Zhang, H., Zhu, J. W., Peng, Y., et al. (2023). Effect of soil bioremediation on soil microbial community structure aimed at controlling tobacco bacterial wilt. *Appl. Microbiol. Biot.* 107, 7543–7555. doi: 10.1007/s00253-023-12753-4

Mallon, C. A., Van Elsas, J. D., and Salles, J. F. (2015). Microbial invasions: the process, patterns, and mechanisms. *Trends Microbiol.* 23, 719–729. doi: 10.1016/j.tim.2015.07.013

Meng, X., Wang, L., Ma, B., Wei, X., Zhou, Y., Sun, Z., et al. (2024). Screening, identification and evaluation of an acidophilic strain of *Bacillus velezensis* b4-7 for the biocontrol of tobacco bacterial wilt. *Front. Plant Sci.* 15:1360173. doi: 10.3389/fpls.2024.1360173

Mo, Y. Y., Peng, F., Gao, X. F., Xiao, P., Logares, R., Jeppesen, E., et al. (2021). Low shifts in salinity determined assembly processes and network stability of microeukaryotic plankton communities in a subtropical urban reservoir. *Microbiome* 9:128. doi: 10.1186/s40168-021-01079-w

Moeller, A. H., Suzuki, T. A., Lin, D., Lacey, E. A., Wasser, S. K., and Nachman, M. W. (2017). Dispersal limitation promotes the diversification of the mammalian gut microbiota. *Proc. Natl. Acad. Sci. USA* 114, 13768–13773. doi: 10.1073/pnas.1700122114

Msabila, S. E., Nordey, T., Ernest, Z., Mlowe, N., Manickam, R., Ramasamy, S., et al. (2024). Boosting tomato resilience in Tanzania: grafting to combat bacterial wilt and abiotic stress. *Horticulturae* 10:338. doi: 10.3390/horticulturae10040338

Najeeb, S., and Li, Y. (2023). *Parthenium hysterophorus* alleviates wilt stress in tomato plants caused by *Ralstonia solanacearum* through direct antibacterial effect and indirect upregulation of host resistance. *Front. Plant Sci.* 14:1126228. doi: 10.3389/fpls.2023.1126228

Niu, G., Wang, R., Hasi, M., Wang, Y., Geng, Q., Wang, C., et al. (2021). Availability of soil base cations and micronutrients along soil profile after 13-year nitrogen and water addition in a semi-arid grassland. *Biogeochemistry* 152, 223–236. doi: 10.1007/s10533-020-00749-5

Pan, M., Tang, L. N., Wu, C. Z., Yang, M. Y., Zhang, B. H., Huang, J. W., et al. (2024). Effects of biochar dosage on tobacco bacterial wilt and soil bacterial community. *J. Nuclear Agric. Sci.* 6, 1186–1195. doi: 10.11869/j.issn.1000-8551.2024

Qi, Y. Q., Liu, H. L., Zhang, B. P., Geng, M. X., Cai, X. X., Wang, J. H., et al. (2022). Investigating the effect of microbial inoculants frankia f1 on growth-promotion, rhizosphere soil physicochemical properties, and bacterial community of ginseng. *Appl. Soil Ecol.* 172:104369. doi: 10.1016/j.apsoil.2021.104369

Qi, G., Ma, G., Chen, S., Lin, C., and Zhao, X. (2019). Microbial network and soil properties are changed in bacterial wilt-susceptible soil. *Appl. Environ. Microb.* 85, e00119–e00162. doi: 10.1128/AEM.00162-19

Qiao, Y. Z., Wang, T. T., Huang, Q. W., Guo, H. Y., Zhang, H., Xu, Q. C., et al. (2024). Core species impact plant health by enhancing soil microbial cooperation and network complexity during community coalescence. *Soil Biol. Biochem.* 188:109231. doi: 10.1016/j.soilbio.2023.109231

Rillig, M. C., Lehmann, A., Aguilar-Trigueros, C. A., Antonovics, J., Caruso, T., Hempel, S., et al. (2016). Soil microbes and community coalescence. *Pedobiologia* 59, 37–40. doi: 10.1016/j.pedobi.2016.01.001

Rognes, T., Flouri, T., Nichols, B., Quince, C., and Mahé, F. (2016). Vsearch: a versatile open source tool for metagenomics. *PeerJ* 4:e2584. doi: 10.7717/peerj.2584

Sharma, V., Irmak, S., and Padhi, J. (2018). Effects of cover crops on soil quality: part ii. Soil exchangeable bases (potassium, magnesium, sodium, and calcium), cation exchange capacity, and soil micronutrients (zinc, manganese, iron, copper, and boron). *J. Soil Water Conserv.* 73, 652–668. doi: 10.2489/jswc.73.6.652

Shen, G., Zhang, S., Liu, X., Jiang, Q., and Ding, W. (2018). Soil acidification amendments change the rhizosphere bacterial community of tobacco in a bacterial wilt affected field. *Appl. Microbiol. Biot.* 102, 9781–9791. doi: 10.1007/s00253-018-9347-0

Slatyer, R. A., Hirst, M., and Sexton, J. P. (2013). Niche breadth predicts geographical range size: a general ecological pattern. *Ecol. Lett.* 16, 1104–1114. doi: 10.1111/ele.12140

Stegen, J. C., Lin, X. J., Konopka, A. E., and Fredrickson, J. K. (2012). Stochastic and deterministic assembly processes in subsurface microbial communities. *ISME J.* 6, 1653–1664. doi: 10.1038/ismej.2012.22

Stone, L., and Roberts, A. (1990). The checkerboard score and species distributions. *Oecologia* 85, 74–79. doi: 10.1007/BF00317345

Van Der Heijden, M. G., and Hartmann, M. (2016). Networking in the plant microbiome. *PLoS Biol.* 14:e1002378. doi: 10.1371/journal.pbio.1002378

Wang, Q., Garrity, G. M., Tiedje, J. M., and Cole, J. R. (2007). Naive Bayesian classifier for rapid assignment of rRNA sequences into the new bacterial taxonomy. *Appl. Environ. Microb.* 73, 5261–5267. doi: 10.1128/AEM.00062-07

Wen, T., Xie, P., Liu, H., Liu, T., Zhao, M., Yang, S., et al. (2023). Tapping the rhizosphere metabolites for the prebiotic control of soil-borne bacterial wilt disease. *Nat. Commun.* 14:4497. doi: 10.1038/s41467-023-40184-2

Wickham, H. (2007). Reshaping data with the reshape package. *J. Stat. Softw.* 21, 1–20. doi: 10.18637/jss.v021.i12

Xie, Z. B., Xu, Y. P., Liu, G., Liu, Q., Zhu, J. G., Tu, C., et al. (2013). Impact of biochar application on nitrogen nutrition of rice, greenhouse-gas emissions and soil organic carbon dynamics in two paddy soils of China. *Plant Soil* 370, 527–540. doi: 10.1007/s11104-013-1636-x

Xun, W. B., Liu, Y. P., Li, W., Ren, Y., Xiong, W., Xu, Z. H., et al. (2021). Specialized metabolic functions of keystone taxa sustain soil microbiome stability. *Microbiome* 9:35. doi: 10.1186/s40168-020-00985-9

Yang, H., Li, J., Xiao, Y., Gu, Y., Liu, H., Liang, Y., et al. (2017). An integrated insight into the relationship between soil microbial community and tobacco bacterial wilt disease. *Front. Microbiol.* 8:8. doi: 10.3389/fmicb.2017.02179

Yuan, M. M., Guo, X., Wu, L. W., Zhang, Y., Xiao, N. J., Ning, D. L., et al. (2021). Climate warming enhances microbial network complexity and stability. *Nat. Clim. Chang.* 11, 343–348. doi: 10.1038/s41558-021-00989-9

Yuan, J., Wen, T., Zhang, H., Zhao, M., Penton, C. R., Thomashow, L. S., et al. (2020). Predicting disease occurrence with high accuracy based on soil macroecological patterns of fusarium wilt. *ISME J.* 14, 2936–2950. doi: 10.1038/s41396-020-0720-5

Yuliar, N., and Toyota, K. (2015). Recent trends in control methods for bacterial wilt diseases caused by *Ralstonia solanacearum*. *Microbes Environ.* 30, 1–11. doi: 10.1264/jsme2.ME14144

Zhalnina, K., Dias, R., de Quadros, P. D., Davis-Richardson, A., Camargo, F. A. O., Clark, I. M., et al. (2015). Soil ph determines microbial diversity and composition in the park grass experiment. *Microb. Ecol.* 69, 395–406. doi: 10.1007/s00248-014-0530-2

Zhang, B. H., Lei, H., Li, R. K., Yang, M. Y., Pan, R. X., Pan, M. Q., et al. (2023). Effects of deep tillage on the yield and production value of flue cured tobacco and its rhizosphere soil microenvironment. *J. Southern Agric.* 54, 2195–2206. doi: 10.3969/j.issn.2095-1191.2023.08.001

Zhang, C., Lin, Y., Tian, X., Xu, Q., Chen, Z., and Lin, W. (2017). Tobacco bacterial wilt suppression with biochar soil addition associates to improved soil physiochemical properties and increased rhizosphere bacteria abundance. *Appl. Soil Ecol.* 112, 90–96. doi: 10.1016/j.apsoil.2016.12.005

Zhang, S. T., Liu, X. J., Zhou, L. H., Deng, L. Y., Zhao, W. Z., Liu, Y., et al. (2022). Alleviating soil acidification could increase disease suppression of bacterial wilt by recruiting potentially beneficial rhizobacteria. *Microbiol. Spectrum* 10:e02333-21. doi: 10.1128/spectrum.02333-21

Zhang, J., and Ma, K. (2013). Spaa: An r package for computing species association and niche overlap. *Research Progress of Biodiversity Conservation in China*. 10, 165–174.

Zhang, B., Tang, L., Wang, Y., Yang, M., Pan, R., Pan, M., et al. (2023). Effect of reduced nitrogen fertilizer application combined with biochar on nitrogen utilization of flue-cured tobacco and its association with functional gene expressions of the nitrogen cycle in rhizosphere soil. *Technol Agron.* 3:12. doi: 10.48130/TIA-2023-0012

Zhang, H. C., Wang, R., Chen, S., Qi, G. F., He, Z. L., and Zhao, X. Y. (2017). Microbial taxa and functional genes shift in degraded soil with bacterial wilt. *Sci. Rep.* 7:39911. doi: 10.1038/srep39911

Zhang, W., Xiu, L. Q., Wu, D., Sun, Y. Y., Gu, W. Q., Zhang, H. G., et al. (2021). Review of biochar structure and physicochemical properties. *Acta Agron. Sin.* 47, 1–18. doi: 10.3724/SP.J.1006.2021.02021

frontiers | Frontiers in Microbiology

TYPE Original Research
PUBLISHED 21 October 2024
DOI 10.3389/fmicb.2024.1484727

OPEN ACCESS

EDITED BY
Dongdong Yan,
Institute of Plant Protection, Chinese Academy of Agricultural Sciences (CAAS), China

REVIEWED BY
Zhoubin Liu,
Hunan Agricultural University, China
Haitao Yu,
Gansu Academy of Agricultural Sciences (CAAS), China

*CORRESPONDENCE
Yi Cao
✉ yicao1001@163.com
Dong Wang
✉ 9830129@163.com
Jie Wang
✉ wangjie@caas.cn

†These authors have contributed equally to this work

RECEIVED 22 August 2024
ACCEPTED 04 October 2024
PUBLISHED 21 October 2024

CITATION
Huang B, Chen Y, Cao Y, Liu D, Fang H, Zhou C, Wang D and Wang J (2024) The structure and function of rhizosphere bacterial communities: impact of chemical vs. bio-organic fertilizers on root disease, quality, and yield of *Codonopsis pilosula*. *Front. Microbiol.* 15:1484727. doi: 10.3389/fmicb.2024.1484727

The structure and function of rhizosphere bacterial communities: impact of chemical vs. bio-organic fertilizers on root disease, quality, and yield of *Codonopsis pilosula*

Bin Huang[1†], Yuxuan Chen[1†], Yi Cao[2]*, Dongyang Liu[3], Hua Fang[4], Changchun Zhou[4], Dong Wang[5]* and Jie Wang[1*†]

[1]Pest Integrated Management Key Laboratory of China Tobacco, Tobacco Research Institute of Chinese Academy of Agricultural Sciences, Qingdao, China, [2]Guizhou Academy of Tobacco Science, Guiyang, China, [3]Institute and Enterprise Joint Creation of Tobacco Technology Center, Sichuan Provincial Tobacco Company Liangshanzhou Company, Liangshanzhou, China, [4]Shandong Hezhong Kangyuan Biotechnology Co., Ltd, Zibo, Shandong, China, [5]Department of Vector Biology and Contro, Jinan Center for Disease Control and Prevention, Jinan, China

Introduction: Long-term use of chemical fertilizers (CFs) can cause soil compaction and acidification. In recent years, bio-organic fertilizers (BOFs) have begun to replace CFs in some vegetables and cash crops, but the application of CFs or BOFs has resulted in crop quality and disease occurrence.

Methods: This study aimed to analyze the microbial mechanism of differences between CFs and BOFs in root disease, quality, and yield of tuber Chinese herbal medicine. We studied the effects of CFs, organic fertilizers, commercial BOFs, biocontrol bacteria BOFs, and biocontrol fungi BOFs on rhizosphere microbial community structure and function, root rot, quality, and yield of *Codonopsis pilosula* at different periods after application and analyzed the correlation.

Results and discussion: Compared to CFs, the emergence rate and yield in BOF treatments were increased by 21.12 and 33.65%, respectively, and the ash content, water content, and disease index in the BOF treatments were decreased by 17.87, 8.19, and 76.60%, respectively. The structural equation model showed that CFs promoted the quality and yield of *C. pilosula* by influencing soil environmental factors, while BOFs directly drove soil bacterial community to reduce disease index and improve the quality and yield of *C. pilosula*. There was a stronger interaction and stability of soil microbial networks after BOF treatments. *Microlunatus*, *Rubrobacter*, *Luteitalea*, *Nakamurella*, and *Pedomicrobium* were identified as effector bacteria, which were related to disease prevention and yield and quality increase of *C. pilosula*. Microbial functional analysis indicated that the signal transduction and amino acid metabolism of soil bacteria might play a major role in improving the quality and yield of *C. pilosula* in the early and middle growth stages. In conclusion, compared to CFs, BOFs obtained a lower disease index of root rot and a higher quality and yield of *C. pilosula* by changing the structure and function of the rhizosphere bacterial community.

KEYWORDS

chemical and bio-organic fertilizers, *Codonopsis pilosula*, co-occurrence network, microbial community, yield and quality

1 Introduction

Codonopsis pilosula is a perennial herbaceous plant and an important Chinese herbal medicine. Its fleshy roots are widely used in the field of medicine, and they can be used as both medicine and food (Lodi et al., 2023). Perennial continuous cropping can lead to the accumulation of pathogenic bacteria, and this can result in the severe root rot of *C. pilosula*. One of the main goals of current research in the production of Chinese herbal medicines, including *C. pilosula*, is to develop approaches for enhancing yield and quality and the control of plant diseases without compromising soil health.

Bio-organic fertilizers (BOF) are environmentally friendly fertilizers that can be used for the control of pest populations and for enhancing soil properties. Some of the advantages of BOFs include their positive effects on soil microbial activities and their ability to enhance soil properties and prevent soil-borne diseases, as well as some of the problems caused by *CF* application, including soil compaction and acidification and ecological imbalances (Rani et al., 2021). BOF application has been shown to be effective in enhancing the production of agricultural crops. Wang et al. (2022a) reported that *Bacillus subtilis* BOF can promote cabbage growth, with plant height and biomass being 1.20 and 1.93 times greater in the BOF group than in the *CF* group on the 30th day of the experiment. The sugar–acid ratio of apples was greater under BOF application than under organic fertilizer (OF) application, and this is associated with differences in sucrose accumulation and citric acid degradation (Wang et al., 2022b). The efficacy of different crop protection practices has been studied for several crops, including tobacco, bananas, and tomatoes. BOFs have been shown to be more effective than CFs or OFs in minimizing the deleterious effects of tobacco black shank (Chen et al., 2023), banana wilt (Tao et al., 2020), and tomato bacterial wilt (Shen et al., 2021). However, compared to CFs, the mechanism by which BOFs enhances the yield and quality of root herbs at the microbiological level has not yet been elucidated.

Soil microbial structure and function are likely key for mediating differences in the positive effects of BOFs and CFs on the quality and yield of crops or Chinese herbs. The application of CFs is considered an important source of crop nutrient elements, including macroelements and trace elements, which play key roles in diverse processes, including protein synthesis (Khan et al., 2021), energy conversion processes (Wang et al., 2017), water regulation (Hartmann et al., 2021), and regulation of enzyme activity and hormone synthesis (Li et al., 2021). The application of BOFs has various effects on soil microorganisms, including their ability to respond to abiotic and biotic stresses. BOFs have thus received a lot of research attention. BOF application after fumigation has been shown to increase soil pH and the abundance of 13 functional genes related to amino acid metabolism, suggesting that soil ecological health was improved following the application of BOF (Huang et al., 2023). The BOF SQR9 has been shown to increase pear yield by enhancing the abundance and functional diversity of the rhizosphere microbiome. Specifically, the abundance and functional diversity of the rhizosphere were 21 and 8% higher following BOF application compared to *CF* and OF application, respectively (Wang et al., 2023). BOFs have been shown to have indirect and lagged effects (Chen et al., 2023), with fruit quality improving more significantly following BOF application than the application of traditional OFs (Wang et al., 2022a; Wang et al., 2022b; Wang et al., 2022c). This improvement may stem from the diverse functions of soil microorganisms.

In this study, the roots of *C. pilosula*, a Chinese herbal medicine, were explored by conducting an experiment in which plants were subjected to treatments with CFs, OFs, and different BOFs. We (1) measured the emergence rate, incidence rate, yield, and quality of *C. pilosula*; (2) determined soil physicochemical properties at different periods, α and β diversity of soil microorganisms; (3) analyzed the factors leading to the differences between CFs and BOFs using a structural equation model (SEM); (4) identified differential microorganisms and core microorganisms in the rhizosphere soil through network analysis as key microorganisms affecting *C. pilosula*; and (5) employed ternary analysis, correlation analysis, and the Mantel test of microbial function to reveal the potential mechanisms by which BOFs influence the quality and yield of *C. pilosula* through microbial reshaping at different times. This study provides new insights into using different fertilizers to improve the quality and yield of tuber Chinese herbal medicine, highlighting the feasibility of BOFs as an alternative to chemical fertilizers in Chinese herbal medicine cultivation.

2 Materials and methods

2.1 Field experimental design

The experimental site was in Mianliuping Village, Dingxi City, Gansu Province (35.13675°N, 104.215467°E). *C. pilosula* has been continuously cultivated at the experimental site for several years; the incidence of root rot in the field plot was 20–30%. *C. pilosula* seedlings with good growth and no disease were transplanted from the seedling nursery on 20 April 2022. Fertilizers were applied the day before *C. pilosula* transplanting. The experiment comprised five fertilization treatments: CK: 600 kg/ha of conventional chemical fertilizer (total nutrients ≥40%, $N–P_2O_5–K_2O = 15–15–10\%$); T1: 1500 kg/ha of prickly ash seed oil meal OF (without biocontrol bacteria); T2: 1500 kg/ha of commercial BOF (*Bacillus* complex); T3: 1500 kg/ha of *Trichoderma* BOF (prickly ash seed meal OF + *Trichoderma asperellum*); and T4: 1500 kg/ha of *Bacillus* BOF (prickly ash seed meal OF + *Bacillus amyloliquefaciens* + *B. subtilis*). The size of each plot was 200 m^2, and a total of 12,000 plants of *C. pilosula* were transplanted. The plots were randomly arranged, and three replications of each treatment were performed. All plants were cultivated in an open field and cultivated per standard local practices. *C. pilosula* was harvested on 23 October 2024, 5 months after transplanting. The compound chemical fertilizers were obtained from Su Di Fertilizer Co., Ltd. in Gansu Province. The commercial BOFs were obtained from Hebei Rundong Fertilizer Co. Ltd. *Trichoderma* and *Bacillus* BOFs were provided by the Tobacco Research Institute of the Chinese Academy of Agricultural Sciences (Huang et al., 2021).

2.2 Determination of emergence rate, disease index, quality, and yield of *C. pilosula*

The emergence rate of *C. pilosula* in each plot was determined at the seedling stage on 25 May 2024. and *C. pilosula* were considered to

have emerged if they were approximately 2 cm above the ground. The disease index of root rot of *C. pilosula* was measured at the time of harvesting. The disease index was determined using the following four-graded scale: Grade 0, disease spots are absent along the entire root system; Grade 1, the area with lesions is less than one-third of the entire area of the roots; Grade 2, the area with lesions accounts for one-third to two-thirds of the entire root area; and Grade 3, the area with lesions is greater than two-thirds of the entire root area. The formula for the disease index was based on a previous study (Carlos, 2022). During the harvest period, a total of 30\u00B0*C. pilosula* were randomly excavated from each plot, and branches and large pieces of soil were removed. Samples were dried at 50°C to maintain low moisture content. After drying, the yield of *C. pilosula* was weighed and counted for each treatment. The water content of *C. pilosula* samples was determined according to General Rule 0832 from the 2015 edition of the Pharmacopoeia of the People's Republic of China 2015 (Part 4). The total ash content of *C. pilosula* samples was determined according to General Rule 2302 of the Pharmacopoeia of the People's Republic of China (National Pharmacopoeia Commission, 2015). Three parallel experiments were performed. The quality of *C. pilosula* is mainly determined by its ash and water content. According to the first edition of the Pharmacopoeia of the People's Republic of China (2015), the water content of *C. pilosula* should not exceed 16%, with approximately 10% being optimal. Additionally, the total ash content should not exceed 5%; lower total ash content indicates better quality of *C. pilosula*.

2.3 Collection of soil samples and determination of physicochemical properties

Soil samples were collected on the 30th, 90th, and 150th days after fertilization. The *C. pilosula* was uprooted, and most of the soil was shaken off. The soil remaining on the surface of the roots was collected with a brush, which was the rhizosphere soil. A total of three replicate soil samples were taken. The obtained soil samples were stored at −20°C for DNA extraction and physical and chemical analyses. Soil ammonium N (NH_4^+-N) and nitrate nitrogen (NO_3^--N) were extracted using 2 M KCl and then determined using a Flow Analytical System (Yan et al., 2017). A sodium bicarbonate extraction agent was used to extract soil-available phosphorus (AP), and the molybdenum antimony resistance colorimetric method was used to measure AP (Olsen, 1954). Soil-available potassium (AK) was extracted from neutral 1 mol/L ammonium acetate solution and determined using a Model 410 flame photometer (Franz et al., 1996). The soil organic matter (OM) was determined using the potassium dichromate method (Xu et al., 2022). Soil pH and water content were measured in a 1:2.5 soil/water suspension.

2.4 High-throughput sequencing

An E.Z.N.A.® soil DNA kit (Omega Bio-tek, Norcross, GA, USA) was used to extract the total genomic DNA of the rhizosphere soil samples per the manufacturer's instructions. The V3–V4 variable region of the *16S rRNA* gene was sequenced using the forward primer 338F and the reverse primer 806R (Xu et al., 2016) carrying barcode sequences and the extracted DNA as a template. PCR was conducted in 20 μL reactions, and the reaction system and thermal cycling conditions referred to our previous studies (Huang et al., 2023). The samples were then preserved at 4°C. A total of three replicate reactions were performed per sample. PCR products from the same sample were mixed, and 2% agarose gel electrophoresis was performed to recover the samples. The products were purified, recovered, detected, and quantified, and then the PCR library was constructed. Illumina's MiSeq PE300/NovaSeq PE250 platform (Shanghai Meiji Biomedical Technology Co., Ltd.) was used to sequence the libraries.

2.5 Bioinformation and statistical analysis

FLASH software (v1.2.11) was used to splice the sequences derived from the offline raw data. The QIIME (v1.9.1) platform was used for quality control of the original sequences, and the UCHIME algorithm was used to detect and remove chimeric sequences. The Uparse (v11) pipeline was used to cluster operational taxonomic units (OTUs) with at least 97% similarity (Adams et al., 2013). The taxonomic identity of the bacterial and fungal sequences was determined using the SILVA (v138) database for bacteria with the Mothur algorithm and the UNITE (v8.0) database for fungi (Edgar et al., 2011). The abundance of OTUs was standardized relative to the least abundant sequence in the samples; diversity analysis was conducted using standardized OTU abundance data. The α-diversity of the Simpson and Chao1 indices of microbial communities was analyzed using Mothur (v.1.30.0) software (Schloss et al., 2009). Principal coordinate analysis (PCoA) was performed using Bray–Curtis distances. The relative abundances of species were analyzed using Python (v.2.7.0).

The pheatmap package and vegan package in R were used to generate heatmaps and determine statistical correlations. SEM in IBM SPSS Amos 26 was used to evaluate the effects of soil environmental factors and microorganisms on the quality and yield of *C. pilosula* (Chu et al., 2022). Environmental factors with significant effects on soil microbial communities were determined using the Mantel tests (Li et al., 2022). Visual maps for correlation analysis of environmental factors (Pheatmap), Ternary maps for three temporal soil microbial functions (Ternary), and pie maps for contribution of species functions (vegan) were drawn using R (4.3.2). The soil microbial co-occurrence network was constructed using the Hmisc package and visualized with Gephi (0.10.0). PICRUSt was used to predict the microbial function of bacterial *16S rRNA* sequencing data (Huang et al., 2021). After OTUs standardization, the KEGG database annotation was performed to analyze microbial metabolic pathways. The significance of differences in emergence rate, disease index, quality, yield, and soil physicochemical properties was determined using a one-way analysis of variance and Duncan's multiple range test.

3 Results and discussion

3.1 Effects of each treatment on the emergence rate, disease index, quality, and yield of *C. pilosula*

The emergence rate was the lowest in the chemical fertilizer (CK, 67.62%) and the highest in T3 (81.90%). The emergence rate was

significantly higher in T2, T3, and T4 than in the CK (Figure 1A). The exogenous application of BOFs has been shown to promote the metabolic activities of soil microorganisms, including respiration, and the water generated might play a key role in inducing the emergence of *C. pilosula* (Carlos, 2022; Zhao et al., 2019). The disease index was the highest in the CK (11.11) and the lowest in T4 (2.60). The disease index was significantly lower in T1, T2, T3, and T4 than in the CK, and the disease index was significantly lower in T2, T3, and T4 than in T1 (Figure 1B), suggesting that BOFs could effectively control the root rot of *C. pilosula*.

The water content was significantly higher in the CK (11.23%) than in the other four treatments, and the water content was the lowest in T4 (10.31%). The ash content was significantly higher in the CK (4.87%) than in the other four treatments, and the total ash content was the lowest in T4 (4.00%). According to the first edition of the Pharmacopoeia of the People's Republic of China (2020), the water content of *C. pilosula* should not exceed 16%, and the total ash content should not exceed 5%. A previous study has shown that severe worm infestations can occur when the water content of *C. pilosula* is >15%, and worm infestations can be prevented when the water content is <13% (Leng et al., 2023). The quality and ash content of *C. pilosula* are inversely related. The fresh root yield was significantly higher in T3 and T4 than in the other three treatments (Figures 1C–E; Supplementary Table S1).

3.2 Effects of fertilizations on the soil physicochemical properties

At 90 days after treatment, the NH_4^+-N was significantly higher in T1, T2, and T3 than in the CK. The soil NO_3^--N content was significantly higher in T4 than in the CK at 30 days and 90 days after treatment. BOF application has been shown to promote the N fixation of microbes in soil and reduce the loss of N (Rahimi et al., 2021) (Table 1).

The content of AP was significantly lower in all OF treatments than in the CK at 30 days after treatment. The content of AP in all soil samples decreased over time. The content of soil AK was significantly lower in all OF treatments than in the CK at 30 d after treatment; the content of soil AK was the lowest in T3, and it was 18.49% lower in T3 than in the CK. The AK content was the lowest at 90 days after treatment in the CK, and the content of AK was 14.56 and 35.39% higher in T2 and T3 than in the CK, respectively. The AK content was 15.49 and 6.94% lower in T3 and T4 than in the CK at 150 days after treatment, and these differences were significant. Compared to chemical fertilizers, BOF treatments were more slow-release and helped to supplement the AK in the middle and late growth of *C. pilosula* (Yang et al., 2017). The content of OM significantly increased in the OF and BOF treatments during

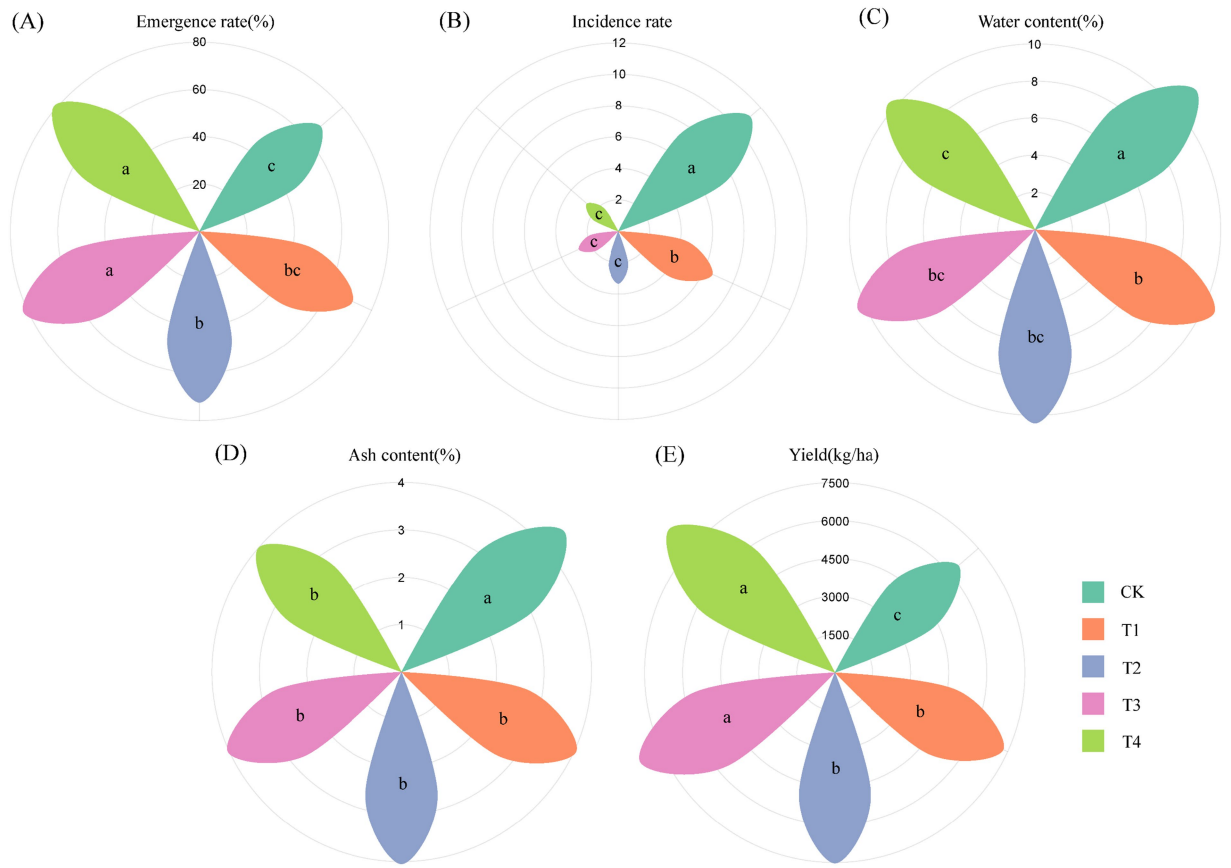

FIGURE 1
Emergence rate, disease index, yield, and quality of *C. pilosula* following treatment with *CF*, OF, and BOF. (A) Emergence rate of *C. pilosula*; (B) incidence of root rot; (C) moisture content of *C. pilosula*; (D) ash content of *C. pilosula*; (E) yield of *C. pilosula*. Specific information on each indicator is provided in Supplementary Table S1. Different letters (a, b, c) indicate significant differences between treatments.

TABLE 1 The physicochemical properties of soil in the chemical fertilizer, OF, and BOF treatments.

Sampling days	Treatment	NH_4^+-N (mg/kg)	NO_3^--N (mg/kg)	Available P (mg/kg)	Available K (mg/kg)	SOM (mg/kg)	pH (1:2.5)	EC (μs/cm)
Day 30	CK	35.07 ± 1.39a	17.07 ± 0.38c	117.97 ± 3.83a	238.37 ± 6.93a	10.77 ± 0.30d	7.06 ± 0.01a	130.13 ± 2.05b
	T1	36.60 ± 1.24a	18.33 ± 0.43bc	78.27 ± 2.12 cd	213.30 ± 2.91b	21.50 ± 0.49b	7.08 ± 0.04a	124.27 ± 3.50b
	T2	36.43 ± 0.46a	19.37 ± 0.50b	83.97 ± 2.99bc	212.00 ± 3.33bc	19.00 ± 0.76c	7.12 ± 0.03a	124.70 ± 6.15b
	T3	36.80 ± 0.81a	16.80 ± 0.67c	90.53 ± 1.92b	194.30 ± 8.79c	17.63 ± 0.43c	7.11 ± 0.03a	115.57 ± 6.99b
	T4	35.80 ± 1.80a	25.10 ± 0.93a	73.80 ± 2.62d	214.83 ± 4.33b	24.63 ± 1.18a	7.03 ± 0.03a	222.93 ± 6.01a
Day 90	CK	58.07 ± 1.79b	20.13 ± 0.68b	69.17 ± 1.75ab	206.70 ± 5.04a	12.53 ± 0.49c	7.32 ± 0.03b	96.83 ± 3.74c
	T1	67.10 ± 0.98a	21.47 ± 1.44b	60.63 ± 1.20b	164.50 ± 5.57bc	16.17 ± 0.45b	7.55 ± 0.04a	86.47 ± 5.80 cd
	T2	64.37 ± 1.58a	24.97 ± 0.87ab	73.53 ± 5.43a	174.90 ± 3.81b	16.43 ± 0.54b	7.40 ± 0.03b	230.23 ± 8.68a
	T3	64.60 ± 1.77a	22.70 ± 2.57b	75.63 ± 2.39a	152.67 ± 5.09c	15.00 ± 0.21b	7.41 ± 0.03b	70.77 ± 5.90d
	T4	58.17 ± 1.67b	27.83 ± 1.28a	62.20 ± 3.35b	149.13 ± 6.73c	21.97 ± 0.64a	7.18 ± 0.03c	129.10 ± 6.62b
Day 150	CK	36.37 ± 1.11a	20.77 ± 1.87b	52.57 ± 2.92ab	212.27 ± 3.15a	11.27 ± 0.26d	6.66 ± 0.04c	330.03 ± 10.32a
	T1	35.50 ± 0.40a	29.30 ± 2.08a	60.47 ± 3.50a	217.80 ± 5.23a	17.10 ± 0.15ab	6.89 ± 0.03b	196.90 ± 7.20bc
	T2	36.47 ± 0.58a	24.53 ± 2.23ab	45.47 ± 1.39b	215.53 ± 4.80a	16.00 ± 0.40c	7.03 ± 0.04a	212.70 ± 5.62b
	T3	34.33 ± 1.07a	24.27 ± 1.32ab	44.77 ± 2.07b	179.37 ± 1.62c	16.30 ± 0.47bc	6.99 ± 0.03a	184.77 ± 6.30c
	T4	35.27 ± 1.60a	23.03 ± 1.21b	44.27 ± 3.59b	197.53 ± 3.17b	17.83 ± 0.15a	7.07 ± 0.03a	181.90 ± 1.12c

Data depicts means ± SD of three biological replicates. Significant differences between treatments ($P < 0.05$) are illustrated by lowercase letters of a-d.

the three periods, and this was driven by the input of exogenous organic carbon (Table 1).

The soil pH was significantly higher in all BOF treatments than in the CK at 150 days after treatment. The excessive application of *CF* can result in the acidification of soil, which stems from the fact that ammonium sulfate and calcium carbonate make *CF* acidic (Kakihara and Ogura, 2022). The mixed application of cow manure and different OFs has been shown to increase soil pH to different degrees, which is consistent with the results of our study (Chen et al., 2023). Tobacco black shank is more common in acidic soil, and alterations in soil acidity can alter the abundance of the pathogens that cause tobacco black shank (Ma et al., 2023). Soil acidification also decreases the number of ammoniating bacteria and N-fixing bacteria in soil and the ammoniating and nitrification capabilities of soil microorganisms (Liu et al., 2023). The EC was significantly higher in T4 than in the other treatments at 30 days after treatment, and the EC was significantly higher in the CK than in the other four treatments at 150 days after treatment (Table 1).

3.3 Variation in the α- and β-diversity of soil microbial communities

The Shannon index of rhizosphere soil bacteria was significantly lower in T1, T2, and T3 than in the CK at 30 days after treatment. The Shannon index of bacteria was significantly higher in the OF and BOF treatments than in the CK at 90 days after treatment (Figure 2A). At 30 days after treatment, the Shannon index of soil fungi was the highest in the CK. At 150 days after treatment, the Shannon index of soil fungi was higher in T2, T3, and T4 than in the CK (Figure 2B). Thus, the diversity of soil microbes in BOF treatments was increased in the middle and later stages of the experiment. It may promote the stability and functional diversity of soil ecosystems (Sharma et al., 2022). The Chao1 index of soil bacteria was significantly higher in T3 and T4 than in the CK at 90 days after treatment (Figure 2C). The Chao1 index of soil fungi was significantly higher in the CK than in T4 at 30 days after treatment (Figure 2D).

The PCoA results indicated that the contribution of PC1 and PC2 to differences in the composition of species among treatments was 18.14%/16.77% (bacteria) and 23.92%/14.4% (fungi), respectively (Figures 2E,F). The community composition of soil bacteria at 150 days after treatment differed from that at 30 days and 90 days after treatment along PC1. The community composition of soil fungi at 90 days after treatment differed from that at 30 days and 150 days after treatment along PC1, which indicates that soil fungi were more vulnerable to the effects of BOFs in the middle of the experimental period compared to conventional fertilizers.

3.4 The driving factors affecting the emergence, disease prevention, yield, and quality of *C. pilosula*

To clarify the direct and indirect effects of soil environmental factors (NH_4^+-N, NO_3^--N, AP, AK, OM, pH, and EC) and soil microorganisms on the emergence, disease prevention, yield, and quality of *C. pilosula*, we established a SEM for the *CF* (CK; Figure 3A) and BOF treatments (T2, T3, and T4; Figure 3B). Soil environmental properties accounted for the majority of the variation in the soil bacterial community (95.4%) in the *CF* treatment. Soil environmental properties were significantly negatively correlated with soil bacteria and yield quality and significantly positively correlated with emergence rate (path coefficient of 1.008). The soil fungal community was significantly negatively correlated with the incidence rate (path coefficient of −0.770).

Soil environmental properties explained the most variation in the soil bacteria community (55.4%) under BOF treatment. Soil

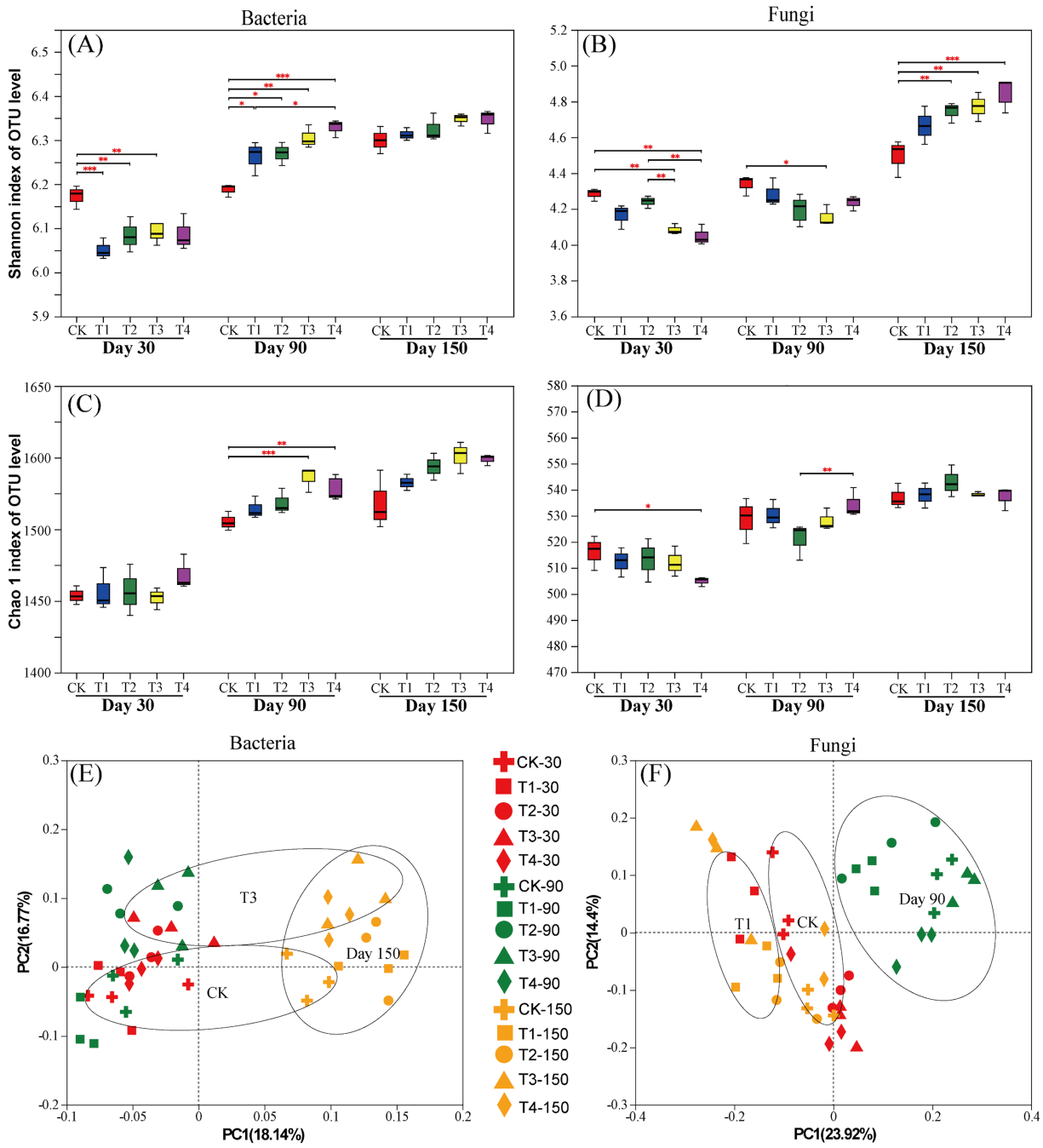

FIGURE 2
α- and β-diversity of rhizosphere soil microorganisms. (A) Shannon index of the soil bacterial community; (B) Shannon index of the soil fungal community; (C) Chao1 index of the soil bacterial community; (D) Chao1 index of the soil fungal community; (E) PCoA of the soil bacterial community; (F) PCoA of the soil fungal community.

environmental factors were significantly positively correlated with the soil bacterial community (path coefficient of 0.232). The soil bacterial and fungal communities were significantly positively correlated with incidence rate. The soil bacteria community showed a significant positive correlation with quality, yield, and emergence rate. Under the *CF* treatment system, soil environmental factors had a significant direct effect on the yield and quality of *C. pilosula*. However, under the BOF treatment, soil environmental factors directly affected the soil bacterial community, which directly drove the yield and quality of *C. pilosula*. CFs had a rapid effect and provided abundant nutrients; these nutrients are key for crops over short time intervals, given that CFs directly determine the yield and quality of crops. BOFs can promote N fixation, P solubilization, and K solubilization through the life processes of microbes; BOFs can also mediate reductions in molecular N in the atmosphere, the decomposition and destruction of mineral crystals through the production of various organic acids, the release of fixed P and K in the soil, and the full utilization of nutrients, which enhances the yield and quality of crops (Peng et al., 2022).

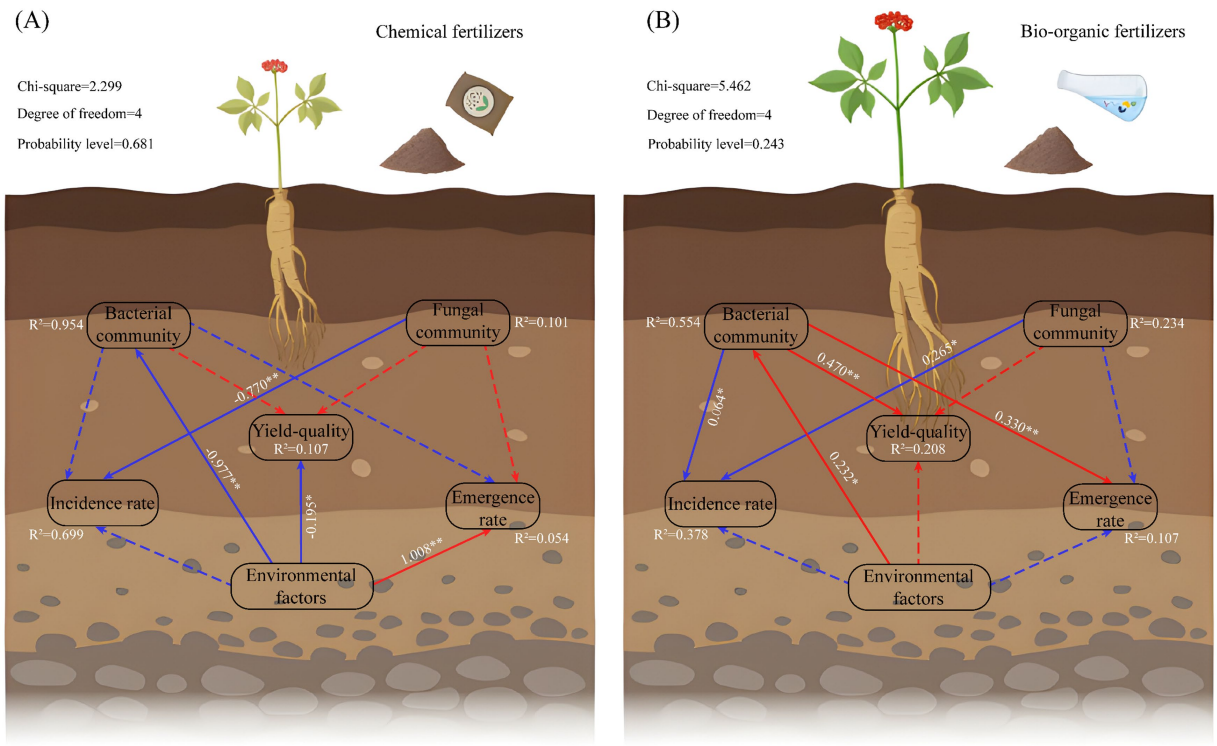

FIGURE 3
SEM of the effects of soil microbial community structure and environmental factors on the emergence rate, disease prevention, yield, and quality of *C. pilosula*. (A) SEM for the *CF* treatment; (B) SEM for the BOF treatment. Continuous and dashed arrows indicate significant and non-significant relationships, respectively. The numbers adjacent to the arrows indicate the path coefficients, and the red and blue arrows indicate negative and positive relationships, respectively. The R^2 value indicates the proportion of the explained variance for each variable. The significance level was expressed as $*p < 0.05$, $**p < 0.01$, and $***p < 0.001$. The total normalized effect of the structural equation model calculations is shown in the upper left. "Yield-quality" represents the yield, ash, and water content of *C. pilosula*; "Environmental factors" represents the soil physicochemical properties; "Bacterial community" represents the rhizosphere bacterial community structure; and "Fungal community" represents the rhizosphere fungal community structure.

3.5 Differential microorganisms in soil bacterial communities

BOFs affect the incidence rate, quality, and yield of *C. pilosula* by influencing the soil bacterial community. Therefore, we focused on the changes in the soil bacterial community. Linear discriminant analysis effect size (LEFSe) was conducted to compare *CF* and BOF treatments (T2, T3, and T4) using data from the phylum to genus level, with an LDA threshold set at 2 (Supplementary Figure S1). In the soil bacterial community, p_unclassified_k_norank_d_Bacteria was significantly enriched in the BOF treatments, and no significant phylum was significantly enriched in the CK treatment. The orders Bryobacterales, Solibacterales, Cyanobacteriales, Acetobacterales, Reyranellales, and Sphingomonadaceae and the genera *Bryobacter*, *Reyranella*, and *Sphingomonas* were significantly enriched in the CK treatments. Solibacterales, Cyanobacteriales, and Sphingomonadaceae are all primitive microorganisms (Supplementary Figure S1). These archaea and bacteria inhabit swamps and volcanoes and prefer using simple nutrients to complete their life processes (Gao et al., 2018), which indicates that they would grow optimally with the direct nutrient supply provided by CFs but grow poorly with the indirect nutrient supply provided by BOFs. The orders Streptosporangiales and Rubrobacterales, and the genera *Microlunatus* and *Rubrobacter* were significantly enriched in BOF treatment. Many genera in Streptosporangiales produce broad-spectrum antibiotics, including *Streptospora rosetta* and *Streptospora virescini*. They can produce polymycin and sporomycin, respectively, and inhibit most plant pathogens. Streptosporangiales may be the key differentiating bacteria in the prevention of the root rot of *C. pilosula*. SG1 strain of Streptosporangiales showed significant positive results in its control effect on cucumber fusarium wilt and its growth promotion effect on durum wheat. Among them, SG1 can reduce the disease index of cucumber wilt from 77.8 to 16% and significantly increase wheat growth and yield, thus having a wide application prospect (Nassira et al., 2018). *Microlunatus* and *Rubrobacter* were isolated from Marine ascidians with obvious antibacterial and anti-inflammatory activities. The former has anti-*Candida albicans* activity, and the ethyl acetate extract of the latter has good cytotoxic activity (Yuan et al., 2014; Chen et al., 2018). They may play a key role in the prevention of the root rot of *C. pilosula*.

3.6 Co-occurrence network analysis of soil bacteria community

Co-occurrence networks for the bacterial communities in the *CF* (CK), OF (T1), and BOF (T4) treatments were constructed to clarify the effects of these fertilizers on the interactions between soil microorganisms. In the soil bacterial co-occurrence network, the CK

network included 73 nodes and 56 edges; the OF network included 95 nodes and 102 edges; and the BOF (T4) network included 193 nodes and 506 edges (Supplementary Table S2). The number of nodes and connections in the co-occurrence network of bacteria increased following the application of OFs and BOFs (T4), and the number of nodes and connections was the highest in the BOF (T4) treatment, suggesting that the soil microbial network was more complex and interactions were stronger in the BOF treatment than in the *CF*/OF treatment. Nodes were classified by their within-module connectivity (*Zi*) and among-module connectivity (*Pi*), and their roles in the network were deduced. In the bacterial network, all nodes of CK and OF were identified as peripherals, with no critical nodes. Under the treatment of BOF, *Luteitalea*, *Nakamurella*, *Pedomicrobium*, *norank_f__Acetobacteraceae*, *unclassified_o__Saccharimonadales*, *norank_f__norank_o__S085*, and *norank_f__norank_o__norank_c__Subgroup_11* were identified as the key class groups (Figure 4). Of these key groups, one is a Module hub, which is *Luteitalea*. The remaining six groups are connectors, which are highly connected nodes between modules and can combine different modules to achieve network functions; therefore, the realization of BOF to reduce the incidence of *C. pilosula* and improve the emergence rate, quality, and yield of *C. pilosula* may require the joint action of different modules to complete.

Luteitalea, as a phosphorus-solving bacterium in soil, contains *ppgC* gene and can produce organic acid and reduce calcium-bound phosphorus, thereby improving the utilization efficiency of phosphorus by plants (Ding et al., 2022). *Nakamurella* is also sensitive to the antibiotic ciprofloxacin and can be used as a marker of environmental ecological health (Kim et al., 2020). *Pedomicrobium* has been shown to degrade some of the microplastics in soil and repair soil pollution (Rong et al., 2021). Current studies believe that the complexity of the microbial co-occurrence network is a key factor reflecting the interrelation and coexistence of microbes in an ecological environment (Kishore et al., 2023).

3.7 Microbial function analysis of driving emergence, disease prevention, yield, and quality change of *C. pilosula* at different times

The differential microorganisms obtained from the LEFSe analysis and the key microbial class identified in network analysis after BOF treatment may be effective microorganisms for reducing root rot of *C. pilosula* and improving yield quality, which we defined as key microorganisms. The relative abundance matrix of their OTU level and the physicochemical properties of soil were used for the Mantel detection (Figure 5B) to characterize the correlation between key microorganisms and soil environmental factors. The results showed that key microorganisms were strongly correlated with NO_3^--N ($p<0.01$) and AK ($p<0.05$), but not strongly correlated with other soil environmental factors. At the same time, there was a significant positive correlation between soil pH and NH_4^+-N ($r=0.79$) and a significant negative correlation between pH and EC ($r=-0.68$), AK and NH_4^+-N ($r=-0.60$), AP and NO_3^--N ($r=-0.64$).

In addition, we constructed a ternary plot of functional genes at level 3 over three time points (Figure 5A) and a correlation analysis

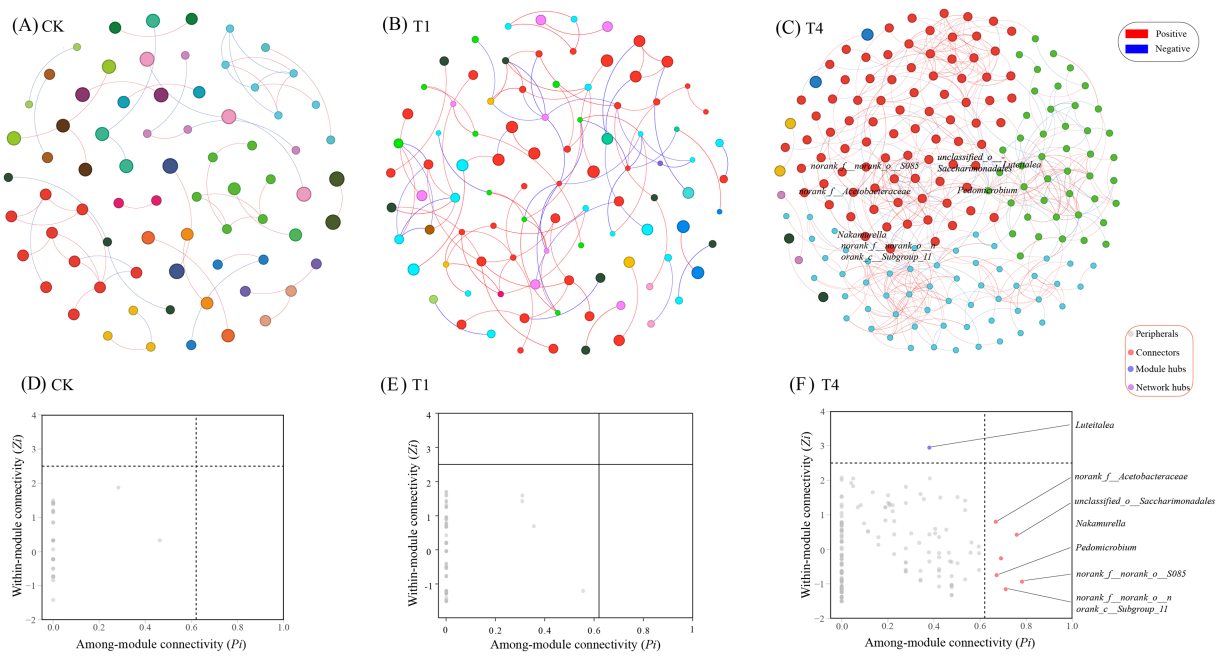

FIGURE 4
Analysis of the co-occurrence network of soil bacteria community induced by CK, OF, and BOF. (A) Co-occurrence network of soil bacterial community after CK (chemical fertilizer). (B) Co-occurrence network of soil bacterial community after organic fertilizer (OF, T1). (C) Co-occurrence network of soil bacterial community after BOF (T4). (D) Distributions of keystone taxa according to the topological properties of CK. (E) Distributions of keystone taxa according to the topological properties of OF. (F) Distributions of keystone taxa according to the topological properties of BOF (T4). The colors of the different nodes indicate different microbial genera, with red edges indicating positive correlations between two nodes and blue edges indicating negative correlations.

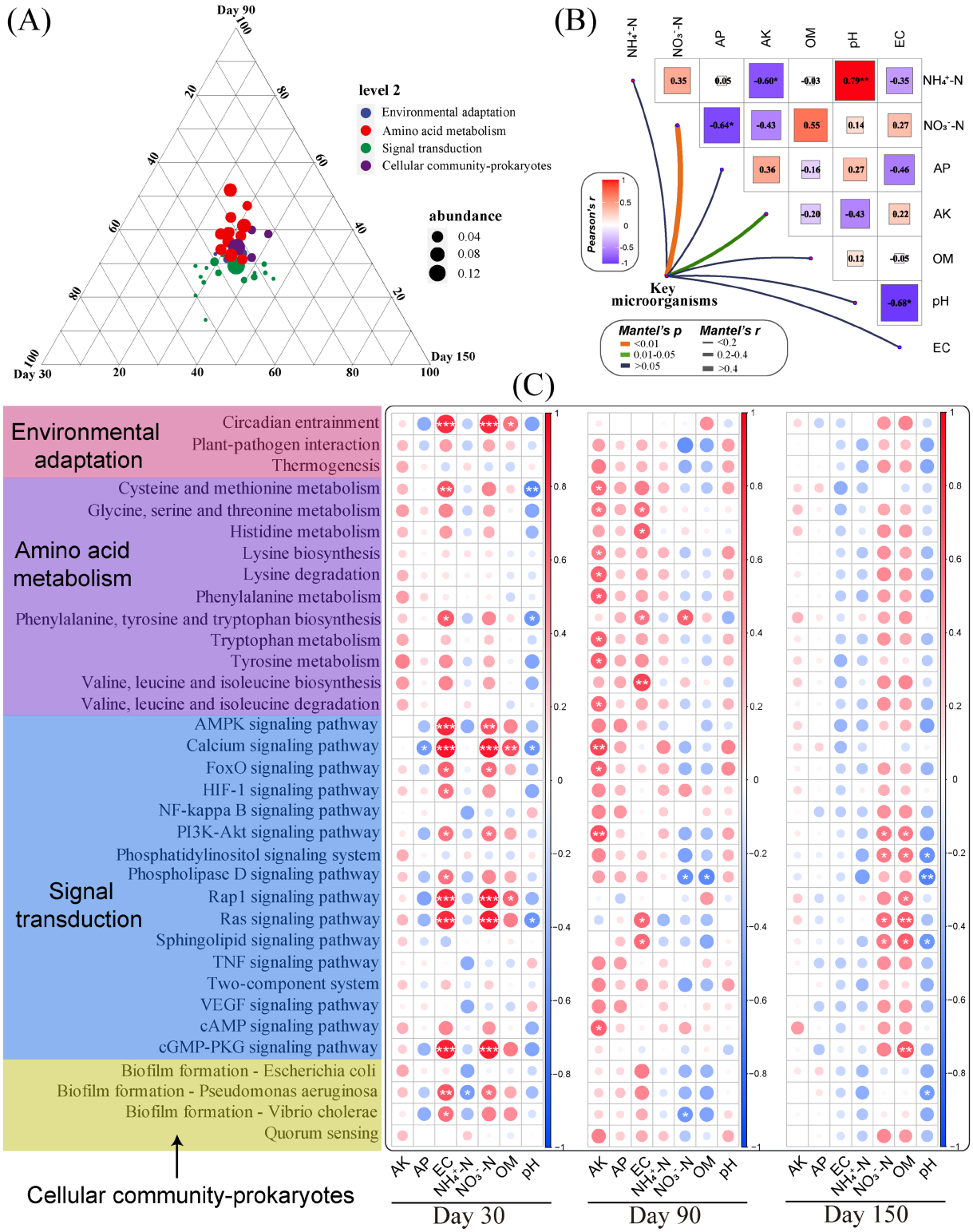

FIGURE 5
Soil microbial function analysis at different times. (A) Ternary phase analysis of the relative abundance of KEGG level 2 functional genes; (B) Mantel detection of key microorganisms and soil environmental factors; (C) Correlation analysis of the relative abundance of KEGG level 3 functional genes and soil environmental factors in three periods. The significance level was expressed as $*p < 0.05$, $**p < 0.01$, and $***p < 0.001$.

between the relative abundance of functional genes and environmental factors (Figure 5C) to explore how different times and functions affect the yield and quality of *C. pilosula*. The results showed that the signal transduction was closer to day 30 and day 150, and the amino acid metabolism was closer to day 90. The results of correlation analysis showed that the function of key microorganisms was positively

correlated with EC on day 30, AK on day 90, and OM on day 150. After that, we selected 10 functional genes with strong correlation at level 3 (5 on day 30, 3 on day 90, and 2 on day 150) for further analysis, and the results showed that, on day 30, the relative abundance of calcium signaling pathway, Rap1 signaling pathway, Ras signaling pathway, and cGMP-PKG signaling pathway in T4 was the highest. Both were significantly higher than the CK treatment (Supplementary Figure S2). During the initial application of the BOF treatment (especially bacteria), a large number of *Bacillus* as "invaders" broke the balance of the soil ecosystem, and the soil native bacterial community maintained the balance of the ecosystem by strengthening signal transduction. Calcium, Rap1, Ras, Cgmp-PKG, and other signal pathways are important intracellular signal transmission systems. They are involved in conducting many hormone signaling pathways (inducing or inhibiting the synthesis of hormones within plants to affect crop yield and quality) (Zhang et al., 2022), metabolite signaling pathways (secreting enzymes directly affect the nutrient absorption and metabolic processes of crops) (Wang et al., 2023), and immune system signaling pathways (regulating the plant immune system to affect crop yield and quality) (Joseph et al., 2019). On day 90, glycine, serine, and threonine metabolism in T2 and T3 were significantly higher than those in CK, and valine, leucine, and isoleucine biosynthesis in T2 were significantly higher than those in CK. The biosynthesis of these amino acids is one of the functions of metabolites and plants to drive the change of diseased soil, and their metabolism may play a certain role in the weakening of the root rot of *C. pilosula* (Li et al., 2018; Wen et al., 2022). On day 150, the sphingolipid signaling pathway in T4 was significantly higher than that in CK. Sphingolipids, as one of the important components of the cell membrane, participate in various physiological processes (Sánchez-Rangel et al., 2015), and play an important role in the stability of the rhizosphere bacterial community at the later stage of the experiment.

Based on the species and functional relative abundance of the samples, the relationship between key microorganisms' abundance and functional abundance was analyzed to explore the specific microorganisms that performed major functions during the three periods (Supplementary Figure S3). The results show that *Nakamurell* contributed most to the calcium signaling pathway, phenylalanine, tyrosine, and tryptophan biosynthesis, Rap1 signaling pathway, cGMP-PKG signaling pathway, and Ras signaling pathway, which were 54.03, 51.17, 50.62, 50.92, and 26.03%, respectively. *Pedomicrobium* contributed most to glycine, serine, and threonine metabolism, phosphatidylinositol signaling system, and sphingolipid signaling pathway, which were 43.85, 33.74, and 27.19%, respectively. *Microlunatus* contributed most to biofilm formation—*Pseudomonas aeruginosa* (32.78%). *Rubrobacter* contributed most to the biosynthesis of valine, leucine, and isoleucine (33.23%).

4 Conclusion

In this study, the yield and quality of *C. pilosula* were higher, and the disease incidence was lower in the BOF treatment than in the *CF* treatment. These findings indicate that soil ecology was enhanced by the application of BOFs. The addition of BOFs promoted the diversity and richness of rhizosphere bacteria in the middle growth stage of *C. pilosula*. The SEM showed that the rhizosphere bacterial community directly drove the yield and quality of *C. pilosula* after BOF application, while the chemical fertilizer increased the yield and quality by influencing soil environmental factors. LEFSe and network analysis showed that *Microlunatus*, *Rubrobacter*, *Luteitalea*, *Nakamurella*, and *Pedomicrobium* as key microorganisms, may play a key role in improving the soil of *C. pilosula*. At the same time, the microbial co-occurrence network revealed stronger interactions between soil microorganisms after the BOF treatment, which are key to soil biodiversity and ecosystem stability. Key microorganisms increase the signal transduction and amino acid metabolism functions of the rhizosphere bacterial community in the early and middle growth period of *C. pilosula*. *Nakamurell* and *Pedomicrobium* made a major contribution to the change in microbial function. These results concluded that BOFs and CFs have different mechanisms for improving the yield and quality of Chinese herbal medicine. BOFs are more beneficial to soil ecological health.

Data availability statement

The datasets presented in this study can be found in online repositories. The names of the repository/repositories and accession number(s) can be found in the article/Supplementary material.

Author contributions

BH: Funding acquisition, Investigation, Writing – original draft, Writing – review & editing. YuC: Methodology, Software, Visualization, Writing – original draft. YiC: Investigation, Visualization, Writing – review & editing. DL: Resources, Writing – review & editing. HF: Funding acquisition, Resources, Writing – review & editing. CZ: Investigation, Writing – review & editing. DW: Supervision, Visualization, Writing – review & editing. JW: Funding acquisition, Supervision, Visualization, Writing – review & editing.

Funding

The author(s) declare that financial support was received for the research, authorship, and/or publication of this article. This study was supported by the National Natural Science Foundation Project of China (32102257), the Science and Technology Cooperation Project of Shandong and Gansu (YDZX2021098), the Science and Technology Project of Guizhou [110202201019 (LS-03)] and Sichuan (SCYC202312), and the Youth Foundation for the Key Open Laboratory of Tobacco Pest Monitoring and Integrated Management (KLTPMIMT2022-10).

Acknowledgments

We thank TopEdit for linguistic assistance during the preparation of this manuscript.

Conflict of interest

DL were employed by the Sichuan Provincial Tobacco Company Liangshanzhou Company. HF and CZ were employed by the Shandong Hezhong Kangyuan Biotechnology Co., Ltd.

The remaining authors declare that the research was conducted in the absence of any commercial or financial relationships that could be construed as a potential conflict of interest.

Publisher's note

All claims expressed in this article are solely those of the authors and do not necessarily represent those of their affiliated organizations, or those of the publisher, the editors and the reviewers. Any product that may be evaluated in this article, or claim that may be made by its manufacturer, is not guaranteed or endorsed by the publisher.

Supplementary material

The Supplementary material for this article can be found online at: https://www.frontiersin.org/articles/10.3389/fmicb.2024.1484727/full#supplementary-material

References

Adams, R., Miletto, M., Taylor, J., and Bruns, T. (2013). Dispersal in microbes: fungi in indoor air are dominated by outdoor air and show dispersal limitation at short distances. *ISME J.* 7, 1262–1273. doi: 10.1038/ismej.2013.28

Carlos, J. (2022). Soil microbial inoculant has no effect on plant growth, fruit yield, fruit disorders, and soilborne diseases in bell pepper. *J. Veg. Sci.* 28, 409–416. doi: 10.1080/19315260.2022.2036888

Chen, Y., Lv, X., Qin, Y., Zhang, D., Zhang, C., Song, Z., et al. (2023). Effects of different botanical oil meal mixed with cow manure organic fertilizers on soil microbial community and function and tobacco yield and quality. *Front. Microbiol.* 14:1191059. doi: 10.3389/fmicb.2023.1191059

Chen, R., Wang, K., Wang, F., He, Y., Long, L., and Tian, X. (2018). Rubrobacter indicoceani sp. nov., a new marine actinobacterium isolated from Indian Ocean sediment. *Int. J. Syst. Evol. Microbiol.* 68, 3487–3493. doi: 10.1099/ijsem.0.003018

Chu, X., Bai, N., Zheng, X., Wang, Q., Pan, X., Li, S., et al. (2022). Effects of straw returning combined with earthworm addition on nitrification and ammonia oxidizers in paddy soil. *Front. Microbiol.* 13:1069554. doi: 10.3389/fmicb.2022.1069554

Ding, Y., Wang, H., Zhang, Q., Chai, B., Lei, X., Ye, M., et al. (2022). Effects of dissolved oxygen on phosphorus transformation in reservoir sediments: novel insights on bacterial community and functional genes. *J. Soils Sediments* 22, 2094–2104. doi: 10.1007/s11368-022-03233-9

Edgar, R., Haas, B., Clemente, J., Quince, C., and Knight, R. (2011). UCHIME improves sensitivity and speed of chimera detection. *Bioinformatics* 27, 2194–2200. doi: 10.1093/bioinformatics/btr381

Franz, S., Richard, Ö., Ellen, K., and Rosa, M. (1996). Methods in soil biology. Berlin: Springer.

Gao, C., Guo, Z., Lu, X., Chen, H., Liu, L., Yu, Z., et al. (2018). Hexaricins, Pradimicin-like polyketides from a marine sediment-derived Streptosporangium sp. and their antioxidant effects. *J. Nat. Prod.* 81, 2069–2074. doi: 10.1021/acs.jnatprod.8b00397

Hartmann, H., Link, R., and Schuldt, B. (2021). A whole-plant perspective of isohydry: stem-level support for leaf-level plant water regulation. *Tree Physiol.* 41, 901–905. doi: 10.1093/treephys/tpab011

Huang, B., Chen, Y., Pei, Z., Jiang, L., Zhang, Y., Wang, J., et al. (2023). Application of microbial organic fertilizers promotes the utilization of nutrients and restoration of microbial community structure and function in rhizosphere soils after dazomet fumigation. *Front. Microbiol.* 13:1122611. doi: 10.3389/fmicb.2022.1122611

Huang, B., Jia, H., Han, X., Gou, J., Huang, C., Wang, J., et al. (2021). Effects of biocontrol Bacillus and fermentation bacteria additions on the microbial community, functions and antibiotic resistance genes of prickly ash seed oil meal-biochar compost. *Bioresour. Technol.* 340:125668. doi: 10.1016/j.biortech.2021.125668

Joseph, O., Hassan, K., Kathy, L., Joseph, K., and Henry, F. (2019). A soil bacterium can shape belowground interactions between maize, herbivores and entomopathogenic nematodes. *Plant Soil* 437, 83–92. doi: 10.1007/s11104-019-03957-7

Kakihara, H., and Ogura, S. (2022). Effect of soil acidification on regrowth of orchardgrass (*Dactylis glomerata*) under application of grazing cattle dung, cattle manure compost, and chemical fertilizer. *Grassl. Sci.* 68, 255–262. doi: 10.1111/grs.12361

Khan, M., Jalil, S., Chopra, P., Chhillar, H., and Ansari, M. (2021). Role of GABA in plant growth, development and senescence. *Plant Gene* 26:100283. doi: 10.1016/j.plgene.2021.100283

Kim, D., Nguyen, L., and Oh, S. (2020). Ecological impact of the antibiotic ciprofloxacin on microbial community of aerobic activated sludge. *Environ. Geochem. Health* 42, 1531–1541. doi: 10.1007/s10653-019-00392-6

Kishore, D., Birzu, G., Hu, Z., DeLisi, C., Korolev, K., and Segrè, D. (2023). Inferring microbial co-occurrence networks from amplicon data: a systematic evaluation. *MSystems.* 8:e0096122. doi: 10.1128/msystems.00961-22

Leng, F., Zhang, B., Zhu, X., Kong, Z., Wang, X., and Wang, Y. (2023). A microecological research reveals seasonal variation in rhizosphere-endophytic bacteria and growth and development of *Codonopsis pilosula* root. *Rhizosphere* 28:100805. doi: 10.1016/j.rhisph.2023.100805

Li, X., Han, G., Eller, F., Hui, D., Zhu, L., Chen, L., et al. (2021). Acclimation of coastal wetland vegetation to salinization results in the asymmetric response of soil respiration along an experimental precipitation gradient. *Agric. For. Meteorol.* 310:108626. doi: 10.1016/j.agrformet.2021.108626

Li, S., Li, Y., and Smolke, C. (2018). Strategies for microbial synthesis of high-value phytochemicals. *Nat. Chem.* 10, 395–404. doi: 10.1038/s41557-018-0013-z

Li, Y., Shi, C., Wei, D., Gu, X., Wang, Y., Sun, L., et al. (2022). Soybean continuous cropping affects yield by changing soil chemical properties and microbial community richness. *Front. Microbiol.* 13:1083736. doi: 10.3389/fmicb.2022.1083736

Liu, Y., Zhang, M., Li, Y., Zhang, Y., Huang, X., Yang, Y., et al. (2023). Influence of nitrogen fertilizer application on soil acidification characteristics of tea plantations in karst areas of Southwest China. *Agriculture* 13:849. doi: 10.3390/agriculture13040849

Lodi, R., Dong, X., Jiang, C., Sun, Z., Deng, P., and Sun, S. (2023). Antimicrobial activity and enzymatic analysis of endophytes isolated from *Codonopsis pilosula*. *FEMS Microbiol. Ecol.* 99:fiad071. doi: 10.1093/femsec/fiad071

Ma, Y., Gu, Y., Liu, J., Zhang, Y., Wang, X., Xia, Z., et al. (2023). Deciphering the rhizosphere bacteriome associated with biological control of tobacco black shank disease. *Front. Plant Sci.* 14:1152639. doi: 10.3389/fpls.2023.1152639

Nassira, B., Yacine, G., Miyada, Z., Fawzia, C., Nasserdine, S., Florence, M., et al. (2018). Biocontrol and plant-growth-promoting capacities of actinobacterial strains from the Algerian Sahara and characterisation of Streptosporangium becharense SG1 as a promising biocontrol agent. *Bio Sci. Tec.* 28, 858–873. doi: 10.1080/09583157.2018.1501466

National Pharmacopoeia Commission (2015). Pharmacopoeia of the People's Republic of China, edition, part 4. Beijing: China Medical Science Press.

Olsen, S. (1954). Estimation of available phosphorus in soils by extraction with sodium bicarbonate. New York, NY: US Department of Agriculture. No, 939.

Peng, L., Zhang, Y., Druzhinina, I., Kubicek, C., Wang, Y., Zhu, Z., et al. (2022). A facultative ectomycorrhizal association is triggered by organic nitrogen. *Curr. Biol.* 32, 5235–5249. doi: 10.1016/j.cub.2022.10.054

Rahimi, A., Amirnia, R., Siavash, M., El, E., Hanapi, S., and Sayyed, R. (2021). Effect of different biological and organic fertilizer sources on the quantitative and qualitative traits of *Cephalaria syriaca*. *Horticulturae* 7:397. doi: 10.3390/horticulturae7100397

Rani, R., Raj, K., and Surindra, S. (2021). Production of compost with biopesticide property from toxic weed Lantana: quantification of alkaloids in compost and bacterial pathogen suppression. *J. Hazard. Mater.* 401:123332. doi: 10.1016/j.jhazmat.2020.123332

Rong, L., Zhao, L., Zhao, L., Cheng, Z., Yao, Y., Yuan, C., et al. (2021). LDPE microplastics affect soil microbial communities and nitrogen cycling. *Sci. Total Environ.* 773:145640. doi: 10.1016/j.scitotenv.2021.145640

Sánchez-Rangel, D., Rivas-San, V., De, L., Nájera-Martínez, M., and Plasencia, J. (2015). Deciphering the link between salicylic acid signaling and sphingolipid metabolism. *Front. Plant Sci.* 6:00125. doi: 10.3389/fpls.2015.00125

Schloss, P., Westcott, S., Ryabin, T., Hall, J., Hartmann, M., Hollister, E., et al. (2009). Introducing mothur: open-source, platform-independent, community-supported software for describing and comparing microbial communities. *Appl. Environ. Microbiol.* 75, 7537–7541. doi: 10.1128/AEM.01541-09

Sharma, D., Shukla, A., and Gupta, M. (2022). Evaluation of bio-control agents against fusarium wilt of cucumber. *Internat J. Eco. Plants.* 9, 334–339. doi: 10.23910/2/2022.0495

Shen, T., Lei, Y., Pu, X., Zhang, S., and Du, Y. (2021). Identification and application of *Streptomyces microflavus* G33 in compost to suppress tomato bacterial wilt disease. *Appl. Soil Ecol.* 157:103724. doi: 10.1016/j.apsoil.2020.103724

Tao, C., Li, R., Xiong, W., Shen, Z., Liu, S., Wang, B., et al. (2020). Bio-organic fertilizers stimulate indigenous soil Pseudomonas populations to enhance plant disease suppression. *Microbiome* 8:137. doi: 10.1186/s40168-020-00892-z

Wang, T., Cheng, K., Huo, X., Meng, P., Cai, Z., Wang, Z., et al. (2022a). Bioorganic fertilizer promotes pakchoi growth and shapes the soil microbial structure. *Front. Plant Sci.* 13:1040437. doi: 10.3389/fpls.2022.1040437

Wang, Y., Xu, C., Zhang, B., Wu, M., and Chen, G. (2017). Physiological and proteomic analysis of rice (*Oryza sativa* L.) in flag leaf during flowering stage and milk stage under drought stress. *Plant Growth Regul.* 82, 201–218. doi: 10.1007/s10725-017-0252-9

Wang, Z., Yang, H., Ma, Y., Jiang, G., Mei, X., Li, X., et al. (2022b). WGCNA analysis revealing molecular mechanism that bio-organic fertilizer improves pear fruit quality by increasing sucrose accumulation and reducing citric acid metabolism. *Front. Plant Sci.* 13:1039671. doi: 10.3389/fpls.2022.1039671

Wang, Z., Yang, T., Mei, X., Wang, N., Li, X., Yang, Q., et al. (2022c). Bio-organic fertilizer promotes pear yield by shaping the rhizosphere microbiome composition and functions. *Microbiol. Spectr.* 10:e0357222. doi: 10.1128/spectrum.03572-22

Wang, C., Yu, Q., Ji, N., Zheng, Y., Taylor, J., Guo, L., et al. (2023). Bacterial genome size and gene functional diversity negatively correlate with taxonomic diversity along a pH gradient. *Nat. Commun.* 14:7437. doi: 10.1038/s41467-023-43297-w

Wen, T., Xie, P., Penton, C., Hale, L., Thomashow, L., Yang, S., et al. (2022). Specific metabolites drive the deterministic assembly of diseased rhizosphere microbiome through weakening microbial degradation of autotoxin. *Microbiome* 10:177. doi: 10.1186/s40168-022-01375-z

Xu, Y., Bi, Z., Zhang, Y., Wu, H., Zhou, L., and Zhang, H. (2022). Impact of wine grape pomace on humification performance and microbial dynamics during pig manurecomposting. *Bioresour. Technol.* 358:127380. doi: 10.1016/j.biortech.2022.127380

Xu, N., Tan, G., Wang, H., and Gai, X. (2016). Effect of biochar additions to soil on nitrogen leaching, microbial biomass and bacterial community structure. *Eur. J. Soil Biol.* 74, 1–8. doi: 10.1016/j.ejsobi.2016.02.004

Yan, D., Wang, Q., Li, Y., Ouyang, C., Guo, M., and Cao, A. (2017). Analysis of the inhibitory effects of chloropicrin fumigation on nitrification in various soil types. *Chemosphere* 175, 459–464. doi: 10.1016/j.chemosphere.2017.02.075

Yang, Y., Li, X., Liu, J., Zhou, Z., Zhang, T., and Wang, X. (2017). Bacterial diversity as affected by application of manure in red soils of subtropical China. *Biol. Fertil. Soils* 53, 639–649. doi: 10.1007/s00374-017-1209-x

Yuan, M., Yu, Y., Li, H., Dong, N., and Zhang, X. (2014). Phylogenetic diversity and biological activity of Actinobacteria isolated from the Chukchi shelf marine sediments in the Arctic Ocean. *Mar. Drugs* 12, 1281–1297. doi: 10.3390/md12031281

Zhang, Q., Yang, J., Zhou, X., Ding, Y., Wang, Y., Zhu, X., et al. (2022). Soil-borne bacterium *Klebsiella pneumoniae* promotes cluster root formation in white lupin through ethylene mediation. *New Phytol.* 237, 1320–1332. doi: 10.1111/nph.18600

Zhao, J., Lu, Y., Tian, H., Jia, H., and Guo, M. (2019). Effects of straw returning and residue cleaner on the soil moisture content, soil temperature, and maize emergence rate in China's three major maize producing areas. *Sustain. For.* 11:5796. doi: 10.3390/su11205796

frontiers | Frontiers in Microbiology

TYPE Original Research
PUBLISHED 04 December 2024
DOI 10.3389/fmicb.2024.1487619

OPEN ACCESS

EDITED BY
Jesus Fernandez Bayo,
University of Granada, Spain

REVIEWED BY
Yigal Achmon,
Guangdong Technion-Israel Institute of Technology (GTIIT), China
Weiliang Zuo,
University of Cologne, Germany
Jiyeun Park,
University of Cologne, Germany

*CORRESPONDENCE
Haonan Wang
✉ haonanwang@zafu.edu.cn
Jianqin Huang
✉ huangjq@zafu.edu.cn

RECEIVED 28 August 2024
ACCEPTED 04 November 2024
PUBLISHED 04 December 2024

CITATION
Wang Q, Peng X, Yuan Y, Zhou X, Huang J and Wang H (2024) The effect of *Torreya grandis* inter-cropping with *Polygonatum sibiricum* on soil microbial community.
Front. Microbiol. 15:1487619.
doi: 10.3389/fmicb.2024.1487619

The effect of *Torreya grandis* inter-cropping with *Polygonatum sibiricum* on soil microbial community

Quanchao Wang, Xiaojie Peng, Yuxuan Yuan, Xudong Zhou, Jianqin Huang* and Haonan Wang*

State Key Laboratory of Subtropical Silviculture, College of Forestry and Biotechnology, Zhejiang A & F University, Hangzhou, Zhejiang, China

Background: Inter-cropping is a reasonable planting pattern between different plants. Inter-cropping of *Torreya grandis* with *Polygonatum sibiricum* is a relatively mature planting pattern in China, which has been applied to improve soil ecological environment and reduce the occurrence of pests and diseases in China. However, there is currently limited knowledge on the response of soil microbial communities to this practice.

Methods: In this study, we employed Illumina MiSeq sequencing coupled with Functional Annotation of Prokaryotic Taxa (FAPROTAX) and Fungi Functional Guild (FUNGuild) analyses to investigate the dynamic changes in soil microbial communities across seven treated groups [the bulk soil of the *T. grandis* inter-cropping with *P. sibiricum* (IB), the bulk soil for mono-cropping of *P. sibiricum* (PB), the bulk soil for mono-cropping of *T. grandis* (TB), the *P. grandis* rhizosphere soil of the *T. grandis* inter-cropping with *P. sibiricum* (IPR), the rhizosphere soil for mono-cropping of *P. sibiricum* (PR), the *T. grandis* rhizosphere soil of the *T. grandis* inter-cropping with *P. sibiricum* (ITR), and the rhizosphere soil for mono-cropping of *T. grandis* (TR)].

Results: The results showed that the rhizosphere soil of *Torreya-Polygonatum* inter-cropping exhibited higher microbial community richness, diversity and evenness than mono-cropping (ITR > TR, IPR > PR). Inter-cropping increased the abundance of Micrococcaceae, Xanthobacteraceae, *Saitozyma*, while decreased *Bacillus*, *Burkholderia*, *Streptomyces*, *Cladosporium*, and *Gibberella* significantly of the rhizosphere soil of *T. grandis.* Further, the abundance of pathogens, such as *Fusarium* and *Neocosmospora*, was higher in mono-cropping samples compared to inter-cropping. There existed distinct variations in bacterial and fungal communities among all groups except for IB and TB. The FAPROTAX and FUNGuild analyses results indicated that inter-cropping significantly enhanced soil microbial function associated with nutrient cycling and exhibited a consistent increase in the relative abundance of nitrogen-cycling and carbon-cycling bacteria, and decreased the abundance of plant pathogen guild in the inter-cropping sample ITR compared to the mono-cropping TR.

Conclusion: Our findings suggest that *T. grandis* inter-cropping with *P. sibiricum* not only enhance the diversity of soil microbial communities, but also improve the nitrogen and carbon cycling functions. In addition, the inter-cropping can effectively reduce the relative abundance of some soil-borne pathogens for

T. grandis and *P. sibiricum*, indicating that this intercropping method may alleviate the impact of pathogens on crops, thus providing assistance for plant disease prevention and sustainable management.

KEYWORDS

plant health, soil microbiota, agroforestry, sustainable development, soil microbial function

1 Introduction

Plant rhizosphere communicating with soil microorganisms represents the important site for the interaction between microbes and plant hosts (Hinsinger et al., 2009). The host can reshape the microbial community structure through root exudates and soil composition has effect on rhizosphere microbial communities (Haichar et al., 2008; Berg and Smalla, 2009). Higher microbial diversity enhances nutrient exchange and resource utilization, and increases plant productivity (Tedersoo et al., 2020). The reduction of soil biodiversity, however, significantly impairs the functioning of ecosystems (Wagg et al., 2014).

Plant cropping practice impacts plant growth, soil physicochemical properties and microbial community. Long-term cropping of the same plant species leads to the decrease of soil enzyme activity, deterioration of physiochemical properties, and change of the soil microbial structure and diversity (Machado et al., 2007; Du et al., 2017; Yu et al., 2017; Bai et al., 2019; Pervaiz et al., 2020). It thus reduces plant growth and yield, and promotes damage from pests, diseases and weeds (Zhang et al., 2017; Zeng et al., 2020). In contrast, inter-cropping of different plant species can improve soil micro-ecological environment by recruiting beneficial microbiota (Li et al., 2007; Wang et al., 2021). The mustard inter-cropping with cucumber increased the diversity of soil microbiota and the abundance of beneficial microorganisms (Li and Wu, 2018). The peanut-tobacco inter-cropping improved soil ecology and microbial structure, increasing the number of beneficial bacteria and decreasing the number of pathogenic bacteria (Gao et al., 2019). Plant inter-cropping can also inhibit the spread of soil-borne diseases such as *Fusarium* wilt and *Phytophthora* blight by changing the content and composition of root exudates and increasing the diversity of rhizosphere microbial community structure (Yu et al., 2019; Lv et al., 2020; Zhang et al., 2020; Song et al., 2022).

Torreya grandis cv Merrillii (Taxaceae, *Torreya*) is a precious economic tree cropped in subtropical mountains in China with various uses such as for fruit, medicine, oil, wood and ornamental purposes. The root system of *T. grandis* exhibits characteristics such as shallow depth, wide distribution, and strong adaptability to drought and nutrient-poor soil conditions. Furthermore, the afforestation process minimizes any potential damage to existing vegetation, rendering it highly suitable for cultivation in forested areas (Chen and Jin, 2019; Chen and Chen, 2021). The perennial herbaceous plant, *Polygonatum sibiricum* (Asparagaceae *Polygonatum*) is a perennial tuberous herb with shallow roots, which can be taken as food, and is rich in chemical components beneficial to human health (Kato et al., 1994; Xian et al., 2012; Luo et al., 2018). Inter-cropping of *T. grandis* with *P. sibiricum* has thus been applied in China for efficient land utilization and yield increase, thereby facilitates the rapid establishment of young *Torreya* forests, thereby expediting forest formation while also yielding short-term economic benefits, and effectively mitigating soil and water erosion resulting from excessive planting (Luo et al., 2023). However, its effect on soil microbial community remains unexplored.

In this study, we collected the rhizosphere and bulk soil samples of inter-cropping and mono-cropping of *T. grandis* and *P. sibiricum*. The high-throughput Illumina MiSeq sequencing coupled with Functional Annotation of Prokaryotic Taxa (FAPROTAX) and Fungi Functional Guild (FUNGuild) analyses were used to address: (a) The effects of *Torreya-Polygonatum* inter-cropping on the composition of rhizosphere and bulk soil bacterial and fungal communities comparing to mono-cropping; (b) The response and function of *Torreya-Polygonatum* inter-cropping to bacterial and fungal communities.

2 Materials and methods

2.1 Site description, experimental design, and soil sample collection

The study areas were located in Chun'an County, Hangzhou, China (29°11′46″N, 118°42′10″E), from where there is subtropical monsoon climate, characterized by high temperature and rainy summer, and mild winter with little rain. The meteorological parameters there were obtained from the China Meteorological Data Service website (http://data.cma.cn/). The average annual sunshine and precipitation are 1,850.3 h and 1,515.1 mm with average temperature of 17.2°C ranging from −5.4°C in winter to 37.6°C in summer. The *T. grandis* plantation was established in 2011, and it has been inter-cropped with *P. sibiricum* since 2015 (Supplementary Table 1).

Seven different sets of samples including the rhizosphere and bulk soil were collected from inter-cropping and mono-cropping of *T. grandis* and *P. sibiricum* (Figure 1): the bulk soil of the *T. grandis* inter-cropping with *P. sibiricum* (IB), the bulk soil for mono-cropping of *P. sibiricum* (PB), the bulk soil for mono-cropping of *T. grandis* (TB), the *P. grandis* rhizosphere soil of the *T. grandis* inter-cropping with *P. sibiricum* (IPR), the rhizosphere soil for mono-cropping of *P. sibiricum* (PR), the *T. grandis* rhizosphere soil of the *T. grandis* inter-cropping with *P. sibiricum* (ITR), and the rhizosphere soil for mono-cropping of *T. grandis* (TR).

The soil samples were collected during the maturation season of *T. grandis* and *P. sibiricum* (September 22, 2022), and arranged in a randomized block design (3 replications). The bulk soil samples

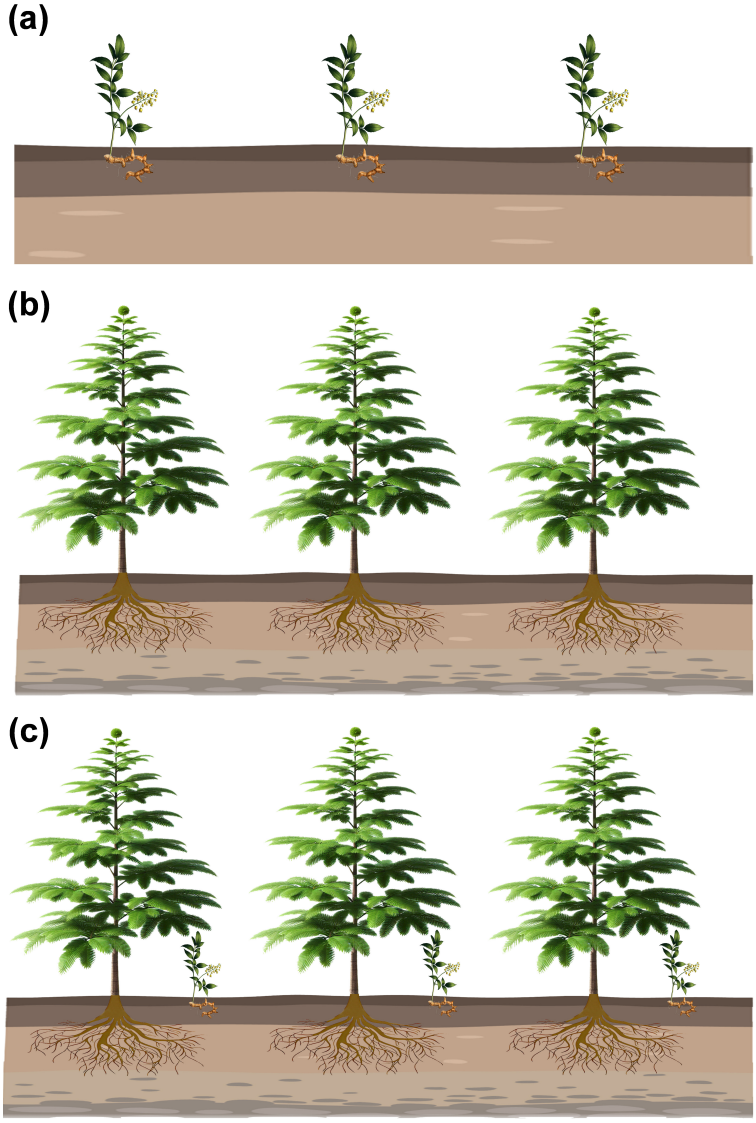

FIGURE 1
Schematic diagram showing different cropping practice. **(a)** *Polygonatum sibiricum* mono-cropping. **(b)** *Torreya grandis* mono-cropping. **(c)** Inter-cropping of *P. sibiricum* and *T. grandis*.

were collected using four-point sampling method to select four square points at a distance of 10 cm away from the plant roots, and passed through a 2-mm sieve to remove plant roots and debris. The rhizosphere soil samples were collected from the roots of *T. grandis* and *P. sibiricum* and rinsed with phosphate buffer solution (PBS; McPherson et al., 2018).

2.2 Soil DNA extraction, PCR amplification, and high-throughput sequencing

Soil DNA was extracted using the Soil DNA kit (OMEGA BIO TEK) following the manufacturer's instruction. DNA concentration and quality were detected by 1% agarose gel electrophoresis with NanoDrop 2000 spectrophotometer (Thermo Fisher Scientific Inc., USA).

The bacterial V3-V4 variable region was amplified with primers 338F (5′-ACTCCTACGGGAGGCAGCAG-3′) and 806R (5′-GGACTACHVGGGTWTCTAAT-3′; Xu et al., 2016). The fungal ITS region was amplified with primers ITS3F (5′-GCATCGATGAAGAACGCAGCGCATCGATGAAGAACGCAGC-3′) and ITS4R (5′-TCCTCCGCTTATTGATATGC-3′; Toju et al., 2012). The PCR reaction condition was as follows: initial denaturation at 95°C for 3 min, 27 cycles of denaturation at 95°C for 30 s, annealing at 55°C for 30 s, 72°C for 30 s, and then a final extension of 10 min at 72°C. The PCR amplification products were mixed and detected by 2% agarose gel electrophoresis. Amplicons were extracted using QuantiFluor™-ST (Promega) and quantified using the AxyPrep DNA Gel Extraction Kit (Axygen Biosciences, Union City, CA, U.S.) according to the manufacturer's protocol. The PCR product was sequenced with paired-end (PE = 300) Illumina MiSeq platform at Majorbio (Shanghai International Medical Zone). The

raw reads were deposited in the Sequence Read Archive database maintained by the National Center for Biotechnology Information (NCBI, Accession Number: PRJNA1150097).

The raw sequences were denoised, quality controlled and clustered into Amplicon Sequence Variant (ASV). The optimized data were then processed using Sequence Denoising Methods (DADA2/Deblur, etc.) to obtain ASV representing sequence and abundance information. Based on the representative ASV sequence and abundance information, analyses including microbial taxa, community diversity, species difference, correlation, and functional prediction were performed.

2.3 Statistical analysis

The bacterial and fungal community richness (Chao1), α-diversity index (Shannon), evenness (Shannoneven), and Pd (Phylogenetic diversity) were calculated using QIIME (Version 1.7.0). The bacterial and fungal indicator taxa were identified using the linear discriminant analysis Effect Size (LEfSe). LEfSe uses non-parametric Kruskal-Wallis rank sum tests to detect significant features and performs LDA to estimate the effect size of each feature ($P < 0.05$, and LDA score > 3.5). Principal coordinate analysis (PCoA) based on Bray–Curtis similarities at ASV level were used to calculate the difference in soil microbial community composition (beta diversity) by R (R v.3.4.4) program. Microbial networks diagrams were drawn using the Gephi software. Ecological function prediction of microorganisms b was performed using the FAPROTAX database (Louca et al., 2016) for bacteria (16s gene) and the FUNGuild database (Nguyen et al., 2016) for fungi (ITS gene).

3 Results

3.1 Bacterial and fungal community diversity in bulk and rhizosphere soil under different cropping patterns

Results showed that there were significant differences among the samples ($P < 0.05$) for bacterial and fungal community richness (Chao1), community diversity (Shannon), community evenness (Shannoneven), and phylogenetic diversity (PD). The rhizosphere soil of *T. grandis* mono-cropping (TR) exhibited the lowest bacterial and fungal community richness (381.70 ± 36.70; 136.47 ± 6.45) as well as phylogenetic diversity (114.25 ± 9.07; 41.48 ± 3.05), along with a lower bacterial community diversity (3.30 ± 0.45) and bacterial community evenness (0.55 ± 0.066; Figure 2, Supplementary Table 2). In contrast, the rhizosphere soil of *Torreya-Polygonatum* inter-cropping samples had higher fungal Chao1, Shannon, Shannoneven, and PD indices than those of mono-cropping (IPR > PR, ITR > TR). These results were consistent with the findings observed in the ITR and TR samples for bacterial communities. However, inter-cropping had minimal impact on the composition of rhizosphere soil bacterial community. Further, the bulk soil of the *T. grandis* inter-cropping with *P. sibiricum* (IB) had the higher fungal community richness, diversity, evenness and Phylogenetic diversity than the bulk soil of *T. grandis* (TB) and *P. sibiricum* (PB), respectively. There was no significant difference in bacterial richness, diversity, evenness and phylogenetic diversity between the rhizosphere and bulk soil samples in the *T. grandis* inter-cropping with *P. sibiricum* and *P. sibiricum* (IB and IPR, ITR; PB and PR), while the rhizosphere soil for mono-cropping of *T. grandis* were lower than bulk soil (TB and TR). After inter-cropping, the richness and phylogenetic diversity of the inter-cropping rhizosphere soil of *P. sibiricum* were significantly higher than bulk soil (IB and IPR), while no significant difference for *T. grandis* (IB and ITR). Moreover, there was no significant difference in fungal richness and phylogenetic diversity between the bulk soil and the rhizosphere soil for mono-cropping of *T. grandis* and *P. sibiricum* (PB and PR; TB and TR; Figure 2, Supplementary Table 2).

3.2 Bacterial and fungal community composition at ASV level under different cropping patterns

All obtained sequences were classified to bacterial and fungal domains. Among them, 74.7% were classified to 39 bacterial phyla and 1,003 genera, and 79.8% were classified to 13 fungal phyla and 545 genera. The bacterial and fungal community coverage is 99.96–100% (Supplementary Table 2), indicating that the sequence data reasonably reflect the species and basic structure.

In Venn diagrams, 19,458 bacterial ASVs (73.2% of the total ASV) and 1,658 fungal ASVs (65.2% of the total ASV) were used to calculate the distribution of soil bacterial and fungal ASVs in the cropping. The seven samples shared 147 ASVs (0.8%) and 83 ASVs (4.9%) of the bacterial and fungal ASVs. The bacterial and fungal ASVs in the rhizosphere soil of *Torreya-Polygonatum* inter-cropping were higher than those in mono-cropping [bacterial: 3,281 (IPR) > 2,804 (PR), 3,189 (ITR) > 1,743 (TR); fungal: 378 (IPR) > 169 (PR), 401 (ITR) > 88 (TR; Figure 3)].

PCoA based on the Bray–Curtis distance was performed to address the bacterial and fungal community structure of seven samples. The two extracted principal coordinates explained 45.38 and 50.7% of the total variation in bacteria and fungi, respectively (Figure 4). The rest five samples showed separation. The R-values of bacterial and fungal communities were 0.9894 and 0.8786, respectively.

3.3 Bacterial and fungal composition diversity under different cropping patterns

The dominant bacterial phyla were Actinobacteriota (33.3%), Proteobacteria (32%), Acidobacteriota (11.5%), Firmicutes (7.4%), and Chloroflexi (6.7%) accounted for most (90.9%) of the bacterial sequences (Figure 5a, Supplementary Figure 1). The dominant fungal phyla were Ascomycota (80.6%) and Basidiomycota (13.8%), Rozellomycota (1.4% and Mortierellomycota (1.4%) accounted for the rest (Figure 5b, Supplementary Figure 1). The abundance of the dominant phyla differed across the samples. Compared to TR sample, ITR increased the relative abundance of phyla

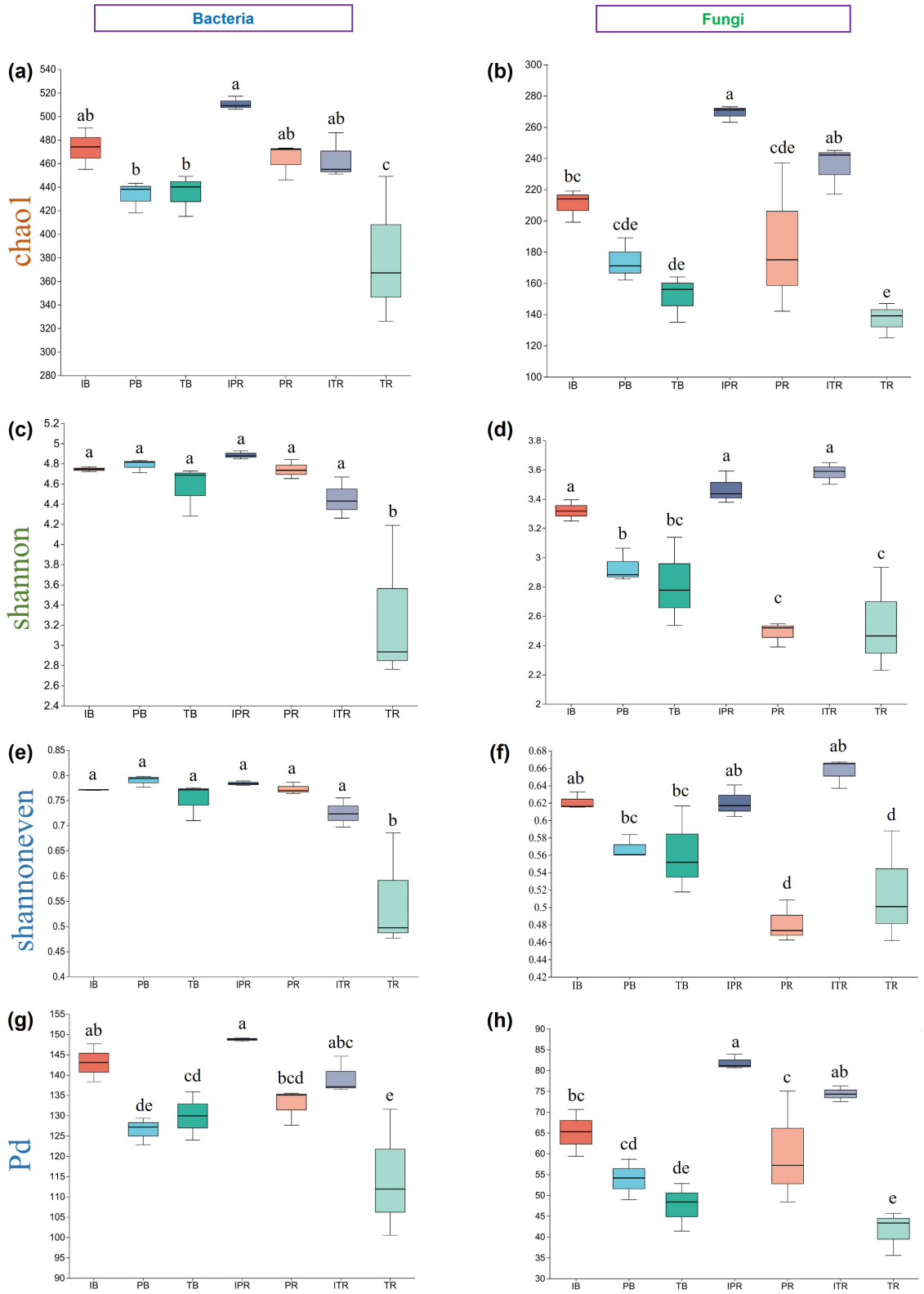

FIGURE 2
Alpha diversity of bacterial and fungal in bulk soil. **(a, b)** Chao1 index in **(a)** bacteria and **(b)** fungi. **(c, d)** Shannon index in **(c)** bacteria and **(d)** fungi. **(e, f)** Shannoneven diversity index in **(e)** bacteria and **(f)** fungi. **(g, h)** Pd diversity index in **(g)** bacteria and **(h)** fungi. Different lowercase letters indicate significant differences among the seven sets of samples. IB: the bulk soil of the *T. grandis* inter-cropping with *P. sibiricum*, PB: the bulk soil for mono-cropping of *P. sibiricum*, TB: the bulk soil for mono-cropping of *T. grandis*, IPR: the *P. grandis* rhizosphere soil of the *T. grandis* inter-cropping with *P. sibiricum*, PR: the rhizosphere soil for mono-cropping of *P. sibiricum*, ITR: the *T. grandis* rhizosphere soil of the *T. grandis* inter-cropping with *P. sibiricum*, and TR: the rhizosphere soil for mono-cropping of *T. grandis*.

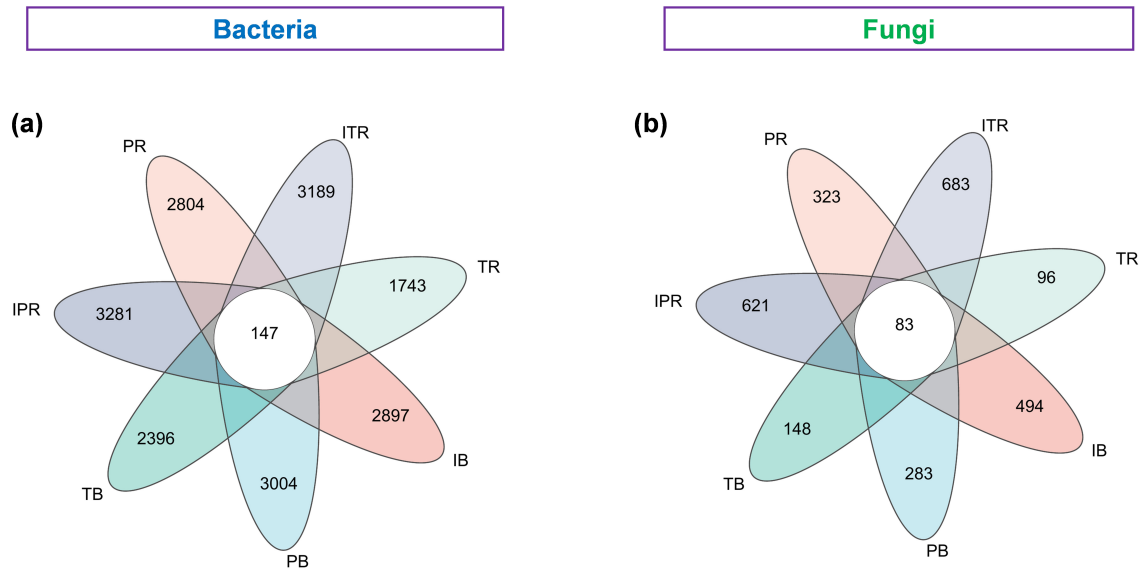

FIGURE 3
Venn diagram showing the bacterial **(a)** and fungal **(b)** unique and shared ASVs among the seven treated groups based on Bray–Curtis distances at the ASV level. IB: the bulk soil of the *T. grandis* inter-cropping with *P. sibiricum*, PB: the bulk soil for mono-cropping of *P. sibiricum*, TB: the bulk soil for mono-cropping of *T. grandis*, IPR: the *P. grandis* rhizosphere soil of the *T. grandis* inter-cropping with *P. sibiricum*, PR: the rhizosphere soil for mono-cropping of *P. sibiricum*, ITR: the *T. grandis* rhizosphere soil of the *T. grandis* inter-cropping with *P. sibiricum*, and TR: the rhizosphere soil for mono-cropping of *T. grandis*.

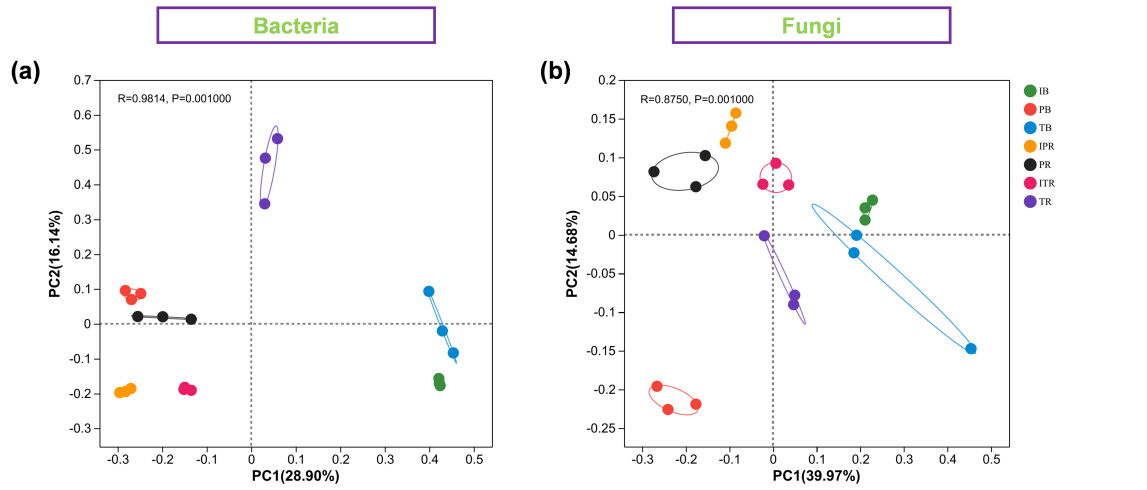

FIGURE 4
Principal coordinate analysis (PCoA) showing the bacterial **(a)** and fungal **(b)** community structure among the seven sets of samples. IB: the bulk soil of the *T. grandis* inter-cropping with *P. sibiricum*, PB: the bulk soil for mono-cropping of *P. sibiricum*, TB: the bulk soil for mono-cropping of *T. grandis*, IPR: the *P. grandis* rhizosphere soil of the *T. grandis* inter-cropping with *P. sibiricum*, PR: the rhizosphere soil for mono-cropping of *P. sibiricum*, ITR: the *T. grandis* rhizosphere soil of the *T. grandis* inter-cropping with *P. sibiricum*, and TR: the rhizosphere soil for mono-cropping of *T. grandis*.

Actinobacteriota, Acidobacteriota, Chloroflexi, Basidiomycota, Rozellomycota, Mortierellomycota, and Glomeromycota, while Proteobacteria, Firmicutes and Ascomycota significantly decreased (Figures 6a, b). However, except for the higher abundance of Chloroflexi within IPR, there was no significant difference in the abundance of other dominant bacterial and fungal phyla between IPR and PR (Figures 6a, b). For the bulk soil samples, the IB samples showed higher abundance of the Chloroflexi, Mortierellomycota, and Glomeromycota compared to TB sample (IB and PB). Each of the bacterial and fungal phyla in the rhizosphere soil (IPR, PR, ITR, and TR) showed similar abundance. The overall phyla composition remained consistent across the different samples, though the abundance was different (Figures 5a, b, 6).

The most abundant bacterial genus was *Bacillus* (belong to Firmicutes, 6.08% of the sequences), followed by Unidentified Micrococcaceae (Actinobacteriota, 5.24% of the sequences)

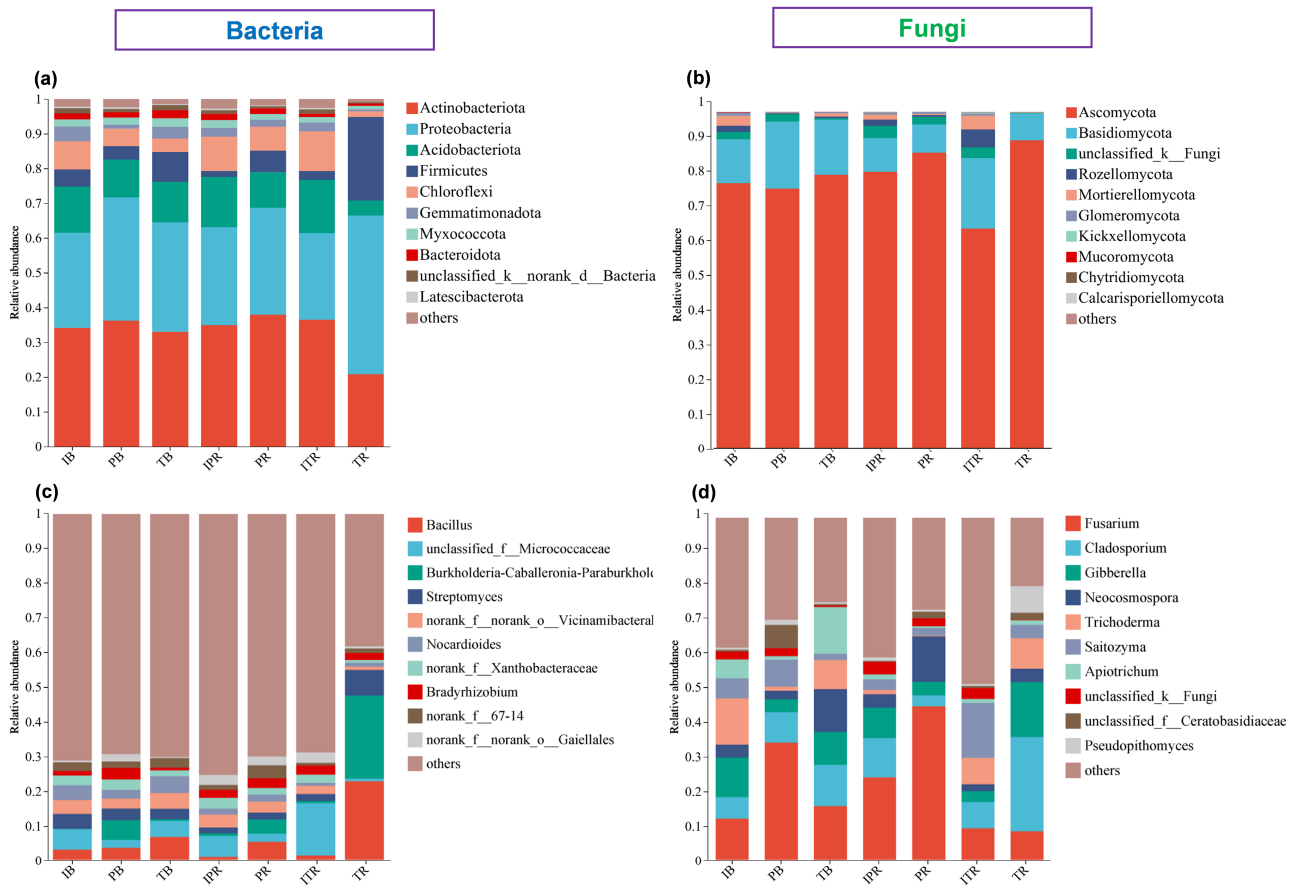

FIGURE 5
The top 10 most abundant bacterial and fungal groups. **(a, b)** Phyla level at **(a)** bacteria and **(b)** fungi. **(c, d)** Genus level at **(c)** bacteria and **(d)** fungi. IB: the bulk soil of the *T. grandis* inter-cropping with *P. sibiricum*, PB: the bulk soil for mono-cropping of *P. sibiricum*, TB: the bulk soil for mono-cropping of *T. grandis*, IPR: the *P. grandis* rhizosphere soil of the *T. grandis* inter-cropping with *P. sibiricum*, PR: the rhizosphere soil for mono-cropping of *P. sibiricum*, ITR: the *T. grandis* rhizosphere soil of the *T. grandis* inter-cropping with *P. sibiricum*, and TR: the rhizosphere soil for mono-cropping of *T. grandis*.

and *Burkholderia* (Proteobacteria, 4.63% of the sequences), *Streptomyces* (Actinobacteriota, 3.32% of the sequences), and unidentified Vicinamibacterales (Actinobacteriota, 3.17% of the sequences; Figure 5c, Supplementary Figure 2). The top five fungal genera were *Fusarium* (Ascomycota, 23.18% of the sequences), *Cladosporium* (Ascomycota, 10.84% of the sequences), *Gibberella* (Ascomycota, 8.22% of the sequences), *Neocosmospora* (Ascomycota, 6.37% of the sequences), and *Trichoderma* (Ascomycota, 5.84% of the sequences; Figure 5d, Supplementary Figure 2).

Among the top 10 genera of bacteria and fungi with high relative abundance, compared to the TR, ITR increased the relative abundance of unidentified Micrococcaceae, unidentified Xanthobacteraceae, unidentified Gaiellales and *Saitozyma*, while the relative abundance of *Bacillus*, *Burkholderia*, *Streptomyces*, *Cladosporium*, *Gibberella Apiotrichum*, and *Pseudopithomyces* decreased significantly (Figures 6c, d, Supplementary Tables 3, 4). For two rhizosphere soil of *P. sibiricum* (IPR and PR), *Fusarium and Neocosmospora* had higher abundance in the PR sample (Figures 6c, d, Supplementary Tables 3, 4). For the bulk and rhizosphere soil samples, *Streptomyces*, *Nocrdioides*, and *Trichoderma* had lower abundance in the rhizosphere soil after inter-croping, while unidentified Gaiellales was higher (IB and IPR, ITR; Figures 6c, d, Supplementary Tables 3, 4). Compare to the TB samples, the TR samples increased the relative abundance of *Bacillus*, *Burkholderia*, *Streptomyces*, *Bradyrhizobium*, *Gibberella*, *Neocosmospora*, and *Penicillium*, while the unidentified vicinamibacterales, *Nocardioides*, *Apiotrichum*, and *Pseudopithomyces* were decreased (Figures 6c, d, Supplementary Tables 3, 4).

3.4 Bacterial community composition of predicted function under different cropping patterns

The FAPROTAX classifier facilitates the annotation and prediction of microorganism functions through the construction of a comprehensive database that correlates microbial classification with their respective functionalities. The total number of 2,517 ASVs (9.46% of the total ASV) was assigned to 46 functional

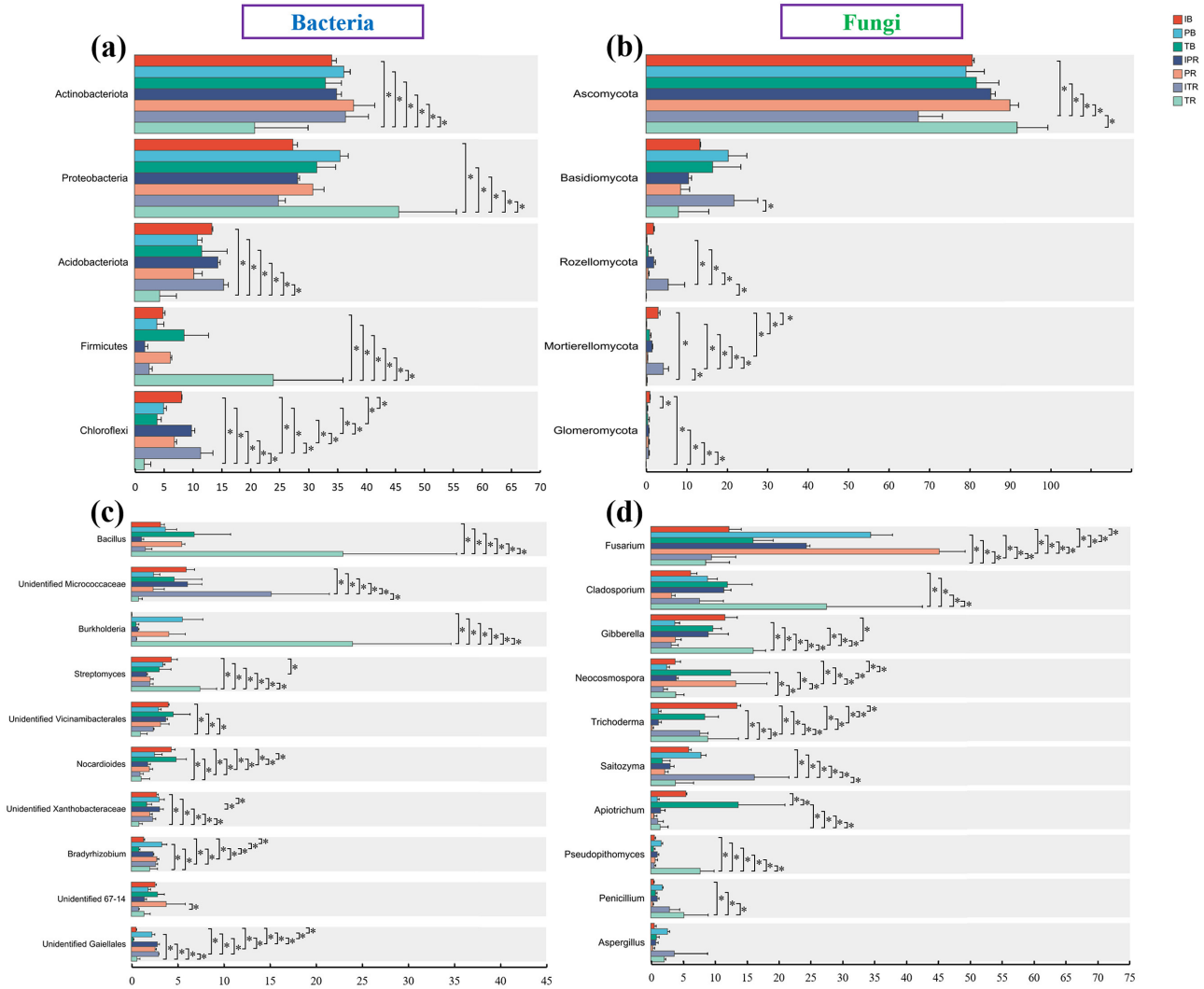

FIGURE 6
Differences in the abundance of the top bacterial **(a, c)** and fungal **(b, d)**. **(a, b)** Top five phyla level at **(a)** bacteria and **(b)** fungi. **(c, d)** Top 10 genus level at **(c)** bacteria and **(d)** fungi. *Indicate significant differences among the seven sets of samples. IB: the bulk soil of the *T. grandis* inter-cropping with *P. sibiricum*, PB: the bulk soil for mono-cropping of *P. sibiricum*, TB: the bulk soil for mono-cropping of *T. grandis*, IPR: the *P. grandis* rhizosphere soil of the *T. grandis* inter-cropping with *P. sibiricum*, PR: the rhizosphere soil for mono-cropping of *P. sibiricum*, ITR: the *T. grandis* rhizosphere soil of the *T. grandis* inter-cropping with *P. sibiricum*, and TR: the rhizosphere soil for mono-cropping of *T. grandis*.

bacterial groups based on 16S rDNA sequence classification using FAPROTAX classifier. The dominant functional groups were associated with biogeochemical cyclings, including chemoheterotrophy (33.6%), aerobic chemoheterotrophy (33.3%), and aromatic_compound_degradation (4.7%) involved with C cycle, followed by the groups in the N cycle associated with nitrogen_fixation (3.9%) and nitrate_reduction (1.8%; Supplementary Table 5).

ANOVA analysis disclosed that the functions with significant differences among samples were mainly concentrated in the C cycle (phototrophy, photoheterotrophy, photoautotrophy, and anoxygenic_photoautotrophy, Figures 7a–d) and N cycle (nitrate_respiration, nitrite_denitrification, nitrite_respiration, and nitrogen_respiration, Figures 7e–h) with the same trend. These functions (Figures 7a–h) had the lowest abundance in the TR, of which was significantly lower than that in the ITR. For the bulk and the rhizosphere soil samples, except for the groups of phototrophy, photoheterotrophy, nitrite_denitrification, and nitrite_respiration, there was no significant difference in the other function groups in between.

3.5 Fungal community composition of predicted function under different cropping patterns

FUNGuild was used to predict the function of the fungal community structure of seven samples, incorporating current literature and authoritative website data for categorizing fungi into distinct functional groups based on their nutritional modes. In total, 3,846 ASVs were assigned to different functional groups

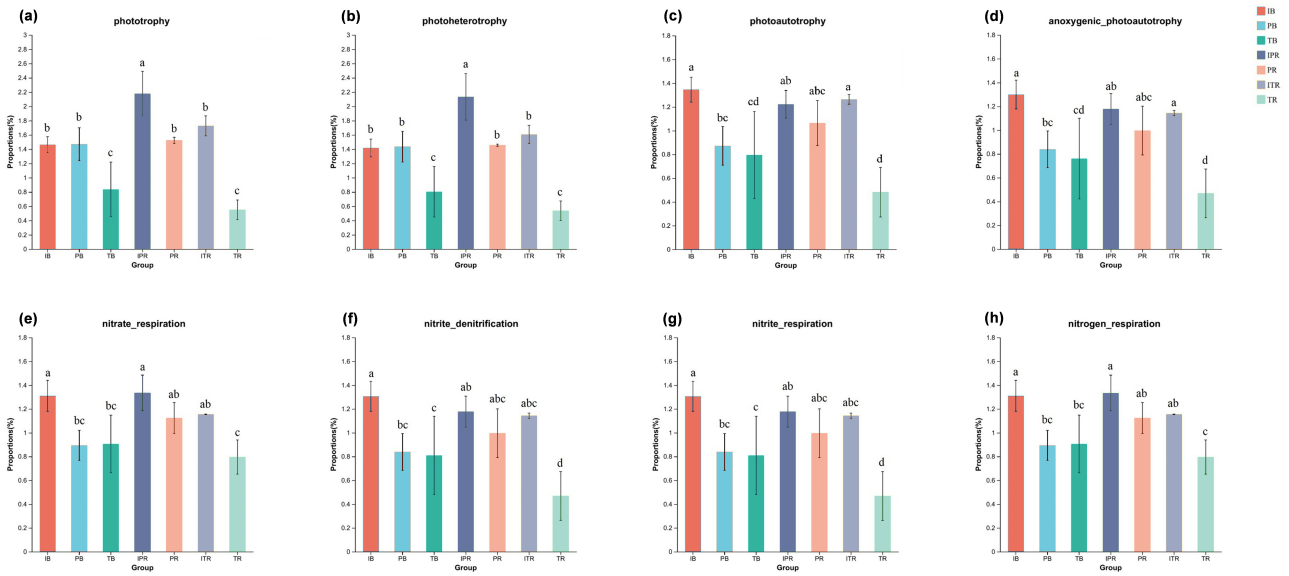

FIGURE 7
Bacterial ecological functions predicted by FAPROTAX under different cropping practice. Bar chart showing the significantly different functional groups involved in C cycle **(a–d)**, N cycle **(e, h)**. C cycle in phototrophy **(a)**; photoheterotrophy **(b)**; photoautotrophy **(c)**; anoxygenic_photoautotrophy **(d)**; N cycle in nitrate_respiration **(e)**; nitrite_denitrification **(f)**; nitrite_respiration **(g)**; nitrogen_respiration **(h)**. Different lowercase letters indicate significant differences among the seven sets of samples. IB: the bulk soil of the *T. grandis* inter-cropping with *P. sibiricum*, PB: the bulk soil for mono-cropping of *P. sibiricum*, TB: the bulk soil for mono-cropping of *T. grandis*, IPR: the *P. grandis* rhizosphere soil of the *T. grandis* inter-cropping with *P. sibiricum*, PR: the rhizosphere soil for mono-cropping of *P. sibiricum*, ITR: the *T. grandis* rhizosphere soil of the *T. grandis* inter-cropping with *P. sibiricum*, and TR: the rhizosphere soil for mono-cropping of *T. grandis*.

according to the annotation of ITS sequence classification. According to the absorption and utilization of environmental resources of the fungal community, the fungi were divided into pathotroph, symbiotroph, and saprotroph. Undefined saprotroph was the most enriched functional group, followed by plant and animal pathogens. Fungi are classified into various guilds based on the three major nutritional methods, encompassing animal pathogens, arbuscular mycorrhizal fungi, ectomycorrhizal fungi, lichenicolous fungi, lichenized fungi, plant pathogens, undefined root endophytes, undefined saprotrophs, and wood saprotrophs as the main functional groups. The seven samples had different effects on the abundance of the functional groups. The results further revealed that inter-cropping significantly enhanced the abundance of plant pathogens and Animal Pathogen-Endophyte-Lichen Parasite-Plant Pathogen-Wood Saprotroph in the rhizosphere soil of *P. sibiricum*, conversely, it resulted in a decrease in the abundance of Animal Pathogen-Endophyte-Lichen Parasite-Plant Pathogen-Soil Saprotroph-Wood Saprotroph (Figure 8, Supplementary Table 6). Simultaneously Fungal Parasite-Undefined Saprotroph function groups exhibited an increase in the rhizosphere soil of *T. grandis* after inter-cropping, while plant pathogens and Animal Pathogen-Endophyte-Lichen Parasite-Plant Pathogen-Wood Saprotroph decreased (Figure 8, Supplementary Table 6).

4 Discussion

The agricultural productivity and stability rely heavily on the richness and diversity of soil microbial communities (Van Der Heijden et al., 2008). They are often reshaped with different cropping practice. Of which, inter-cropping has been demonstrated to have the potential to enhance beneficial soil microbial communities and effectively mitigate pests and diseases (Zhang et al., 2019; Chai et al., 2021). In this study, we addressed the responses of soil microbial communities to *T. grandis* inter-cropping with *P. sibiricum*, and compared the microbial community disparities between bulk and rhizosphere soil samples.

4.1 *Torreya-Polygonatum* inter-cropping improved the soil microbial diversity and communities

Intercropping has the potential to modulate the diversity of soil microbial communities. Previous studies showed that maize inter-cropping with peanut leads to an increase of soil beneficial microbial abundance and diversity (Du et al., 2020; He et al., 2013). Li and Wu (2018) disclosed that wheat inter-cropping with cucumber or mustard with cucumber can enhance the richness of operational microbial taxonomic in soil. In this study, PCoA results revealed that there were distinct variations in bacterial and fungal communities (Figure 4). Compared to mono-cropping, indices of Chao1, Shannon, Shannoneven, and PD using α-diversity analysis were increased both for bulk and rhizosphere soil samples of *T. grandis* inter-cropping with *P. sibiricum* (Figure 2). The study conducted by Deng et al. (2022) found no statistically significant differences in bacterial community richness (Chao1) and diversity (Shannon) between *T. grandis* inter-cropping with *P. sibiricum*

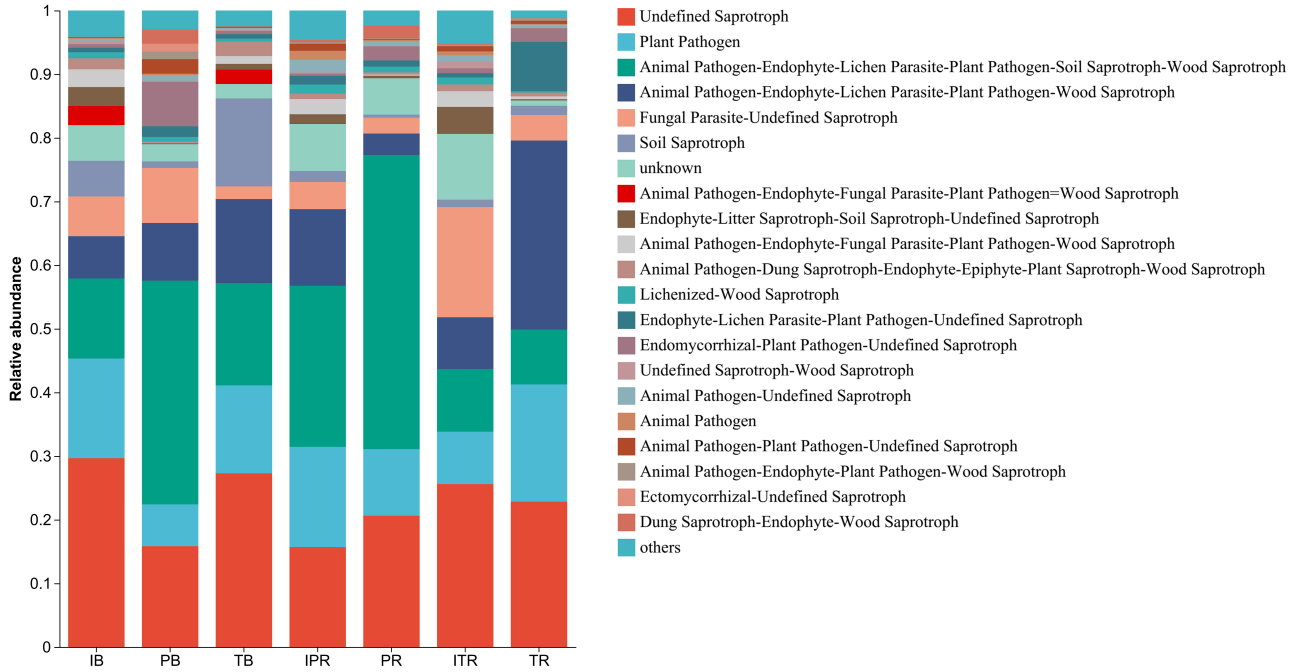

FIGURE 8
Compositions and relative abundance of assigned fungal functional groups (guild) inferred by FUNGuild. IB: the bulk soil of the *T. grandis* inter-cropping with *P. sibiricum*, PB: the bulk soil for mono-cropping of *P. sibiricum*, TB: the bulk soil for mono-cropping of *T. grandis*, IPR: the *P. grandis* rhizosphere soil of the *T. grandis* inter-cropping with *P. sibiricum*, PR: the rhizosphere soil for mono-cropping of *P. sibiricum*, ITR: the *T. grandis* rhizosphere soil of the *T. grandis* inter-cropping with *P. sibiricum*, and TR: the rhizosphere soil for mono-cropping of *T. grandis*.

and mono-cropping of *T. grandis* (ITR and TR). However, this study revealed a significant variation in the richness and diversity of bacteria and fungi in the rhizosphere soil of *T. grandis* after inter-cropping, while having minimal impact on the composition of bacterial communities in the rhizosphere soil of *P. sibiricum*. Our findings differ from Deng's observations in *T. grandis* plantation, potentially attributed to variations in sampling points (Deng et al., 2022).

4.2 *Torreya-Polygonatum* inter-cropping enhanced the roles of key microbial communities

Bacterial phyla of Actinobacteriota, Proteobacteria, Acidobacteriota, Firmicutes, and Chloroflexi were predominant within all samples here (Figure 5). Our results align with previous studies conducted in pure *T. grandis* forest (Feng et al., 2019; Deng et al., 2022) with the exception of Firmicutes. The most predominant phylum Actinobacteriota (33.2%) had significantly higher abundance within *T. grandis* rhizosphere soil after inter-cropping, compared to mono-cropping. The Actinobacteria taxa mainly consist of copiotrophs that strategically thrive on carbon availability and are actively involved with organic matter decomposition and cycling (Liu et al., 2017). Further, *T. grandis* inter-cropping with *P. sibiricum* resulted in relatively elevated presence of Acidobacteriota and Chloroflexi. Taxa residing these two phyla are known to plays crucial roles in polysaccharide degradation as well as the decomposition of non-degradable organic matter (Moghimian et al., 2017; Li et al., 2020). However, the relative abundance of Proteobacteria (represented by *Burkholderia*) and Firmicutes (represented by *Bacillus*) applying inter-cropping was decreased (Figure 6), which is in agreement of previous studies (Gao et al., 2019; Deng et al., 2022).

Inter-cropping known for effectively modulating the soil microbial community can be applied for disease management through reducing pathogen abundance (Zhang et al., 2023). *Cladosporium* speices are crucial plant pathogens responsible for stem rot and leaf spot diseases (Mohamed and Ibrahim, 2021), and in this study, the abundance of *Cladosporium* in the rhizosphere soil of *T. grandis* was significantly decreased following *T. grandis* inter-cropping with *P. sibiricum* (Figure 6d). *Fusarium* is a significant causative agent of root rot in *T. grandis* and *P. sibiricum* (Zhang et al., 2016; Li and Guo, 2019). The similar trend was found on *Fusarium* pathogen within the *P. sibiricum* (Figure 6d). The abundance of the opportunistic pathogen *Neocosmospora* known to induce canker disease, stem and root rot, as well as cane wilt (Zeng and Zhuang, 2023) was also substantially decreased as the result of inter-cropping (Figure 6d). Therefore, it is hypothesized that *T. grandis* inter-cropping with *P. sibiricum* may reduce the abundance of certain pathogens.

Inter-cropping, on the other side, can enhance plant resistance to pathogens and promote plant growth by recruiting beneficial microbial communities (Mendes et al., 2011; Latz et al., 2012; Dhar Purkayastha et al., 2018; Humphrey et al., 2020; Shalev et al., 2022). Xanthobacteraceae comprises a cluster of bacteria closely associated with the carbon cycle, and some species within

this group exhibit a facultatively chemolithoautotrophic lifestyle, enabling them to both assimilate and generate carbon dioxide (Kappler et al., 2012). Gemmatimonadaceae species are a group of nitrogen removal bacteria associated with the nitrogen cycle that play a key role in efficient phytic acid mineralization in different ecosystems (Jia et al., 2023). In this study, *T. grandis* inter-cropping with *P. sibiricum* significantly increased the abundance of Xanthobacteraceae and Gemmatimonadaceae in the rhizosphere soil of *T. grandis* (Figure 6c). Based on the analysis and prediction results from FAPROTAX, it can be inferred that intercropping has the potential to enhance the soil microbial communities' capacity for carbon and nitrogen cycling, thereby facilitating nutrient circulation within plants. The probiotic Saitozyma present in soil and plant rhizosphere exhibits the potential to enhance plant growth and disease management (Das et al., 2023). In this study, the rhizosphere soil of *T. grandis* was significantly improved after inter-cropping practice, suggesting its ability to recruit beneficial microorganisms for growth and disease control.

4.3 The influence of *Torreya-Polygonatum* inter-cropping on potential microbial function alteration

Changes in microbial community structure can result in microbial functional alterations (Preston-Mafham et al., 2002). FAPROTAX was employed to predict the functional profiles of soil bacteria under different samples. The results revealed that chemoheterotrophy (33.6%) and aerobic chemoheterotrophy (33.3%) were the predominant enriched functions, consistent with previous findings (Rocha et al., 2020; Wang et al., 2023). Previous studies disclosed that inter-cropping significantly enhanced soil microbial function associated with nutrient cycling and exhibited a consistent increase in the relative abundance of nitrogen-cycling and carbon-cycling bacteria (Zhong et al., 2022; Marcos-Pérez et al., 2023). In our study, we found that genes involved in carbon cycling (phototrophy, photoheterotrophy, photoautotrophy, and anoxygenic_photoautotrophy) and nitrogen cycling (nitrate_respiration, nitrite_denitrification, nitrite_respiration, and nitrogen_respiration) exhibited significantly higher abundance in the ITR sample compared to TR. These results suggest that *T. grandis* inter-cropping with *P. sibiricum* may enhance nutrient cycling in soil through its influence on bacterial functionality and alteration of soil bacterial community composition. This could be attributed to feedback cycles facilitated by C-cycle bacteria (Xanthobacteraceae) and N-cycle bacteria (Gemmatimonadaceae), which showed a significant increase under the inter-cropping samples.

FUNGuild was used to achieve fungal functional determination (Song et al., 2017; Nguyen et al., 2016). Undefined saprotrophs as the most abundant fungal functional group, may be attributed to the high prevalence of ascomycetes in each sample group, given that a significant portion of fungi within this phylum are associated with organic decomposition processes (Nguyen et al., 2016). Inter treatment comparisons reveal a lower prevalence of plant pathogen guild in the intercropped sample ITR compared to the TR, which aligns with the reduced abundance of pathogenic fungi such as *Cladosporium*, *Gibberella*, and *Neocosmospora*in in ITR, further contributes to mitigating soil-borne plant pathogens, thereby enhancing crop yield and disease resistance.

5 Conclusion

This study focused the impact of *T. grandis* inter-cropping with *P. sibiricum* and mono-cropping on soil microbial diversity and function. The results demonstrate that *T. grandis* inter-cropping with *P. sibiricum* significantly increases the abundance and diversity of soil fungal and bacterial communities comparing to mono-cropping. Moreover, this agricultural practice also enhanced the microbial functionality pertaining to nitrogen and carbon cycles, thereby potentially facilitating nutrient uptake by plants while concurrently reducing the prevalence of specific pathogens. The findings arisen from the study are helpful for agroforestry sustainable development and effective management.

Data availability statement

The datasets presented in this study can be found in online repositories. The names of the repository/repositories and accession number(s) can be found at: https://www.ncbi.nlm.nih.gov/, PRJNA1150097.

Author contributions

QW: Data curation, Formal analysis, Writing – original draft, Writing – review & editing, Conceptualization, Methodology. XP: Conceptualization, Data curation, Formal analysis, Investigation, Methodology, Writing – original draft. YY: Data curation, Formal analysis, Investigation, Methodology, Writing – review & editing. XZ: Conceptualization, Funding acquisition, Writing – original draft, Writing – review & editing. JH: Formal analysis, Funding acquisition, Project administration, Validation, Writing – review & editing. HW: Data curation, Project administration, Writing – original draft, Writing – review & editing.

Funding

The author(s) declare financial support was received for the research, authorship, and/or publication of this article. This work was supported by Department of Science and Technology of Zhejiang Province, China (2022C02009) and the Launching Funds for Talents of Zhejiang A & F University (2020FR036), China.

Conflict of interest

The authors declare that the research was conducted in the absence of any commercial or financial relationships that could be construed as a potential conflict of interest.

Publisher's note

All claims expressed in this article are solely those of the authors and do not necessarily represent those of

their affiliated organizations, or those of the publisher, the editors and the reviewers. Any product that may be evaluated in this article, or claim that may be made by its manufacturer, is not guaranteed or endorsed by the publisher.

Supplementary material

The Supplementary Material for this article can be found online at: https://www.frontiersin.org/articles/10.3389/fmicb.2024.1487619/full#supplementary-material

References

Bai, Y. X., Wang, G., Cheng, Y. D., Shi, P. Y., Yang, C. C., Yang, H. W., et al. (2019). Soil acidification in continuously cropped tobacco alters bacterial community structure and diversity via the accumulation of phenolic acids. *Sci. Rep.* 9:12499. doi: 10.1038/s41598-019-48611-5

Berg, G., and Smalla, K. (2009). Plant species and soil type cooperatively shape the structure and function of microbial communities in the rhizosphere. *FEMS Microbiol. Ecol.* 68, 1–13. doi: 10.1111/j.1574-6941.2009.00654.x

Chai, Q., Nemecek, T., Liang, C., Zhao, C., Yu, A., Coulter, J. A., et al. (2021). Integrated farming with intercropping increases food production while reducing environmental footprint. *Proc. Natl. Aca. Sci. U. S. A.* 118:e2106382118. doi: 10.1073/pnas.2106382118

Chen, X., and Chen, H. (2021). Comparing environmental impacts of Chinese torreya plantations and regular forests using remote sensing. *Environ. Dev. Sustainabil.* 23, 133–150. doi: 10.1007/s10668-019-00570-7

Chen, X., and Jin, H. (2019). Review of cultivation and development of Chinese torreya in China. *For. Trees Livelih.* 28, 68–78. doi: 10.1080/14728028.2018.1553690

Das, S., Rabha, J., and Narzary, D. (2023). Assessment of soil yeasts *Papiliotrema laurentii* S-08 and *Saitozyma podzolica* S-77 for plant growth promotion and biocontrol of *Fusarium wilt* of brinjal. *J. Appl. Microbiol.* 134:lxad252. doi: 10.1093/jambio/lxad252

Deng, P., Fan, W., Wang, H., Ti, J., and Xu, X. (2022). Chinese Torreya agroforestry alters the rhizosphere soil bacterial communities and potential functions. *Appl. Soil Ecol.* 177:104504. doi: 10.1016/j.apsoil.2022.104504

Dhar Purkayastha, G., Mangar, P., Saha, A., and Saha, D. (2018). Evaluation of the biocontrol efficacy of a Serratia marcescens strain indigenous to tea rhizosphere for the management of root rot disease in tea. *PLoS ONE* 13:e0191761. doi: 10.1371/journal.pone.0191761

Du, L. T., Huang, B. J., Du, N. S., Guo, S. R., Shu, S., and Sun, J. (2017). Effects of garlic/cucumber relay intercropping on soil enzyme activities and the microbial environment in continuous cropping. *HortScience* 52, 78–84. doi: 10.21273/HORTSCI11442-16

Du, Q., Zhou, L., Chen, P., Liu, X. M., Song, C., Yang, F., et al. (2020). Relay-intercropping soybean with maize maintains soil fertility and increases nitrogen recovery efficiency by reducing nitrogen input. *Crop J.* 8, 140–152. doi: 10.1016/j.cj.2019.06.010

Feng, Y., Hu, Y., Wu, J., Chen, J., Yrjälä, K., and Yu, W. (2019). Change in microbial communities, soil enzyme and metabolic activity in a *Torreya grandis* plantation in response to root rot disease. *For. Ecol. Manag.* 432, 932–941. doi: 10.1016/j.foreco.2018.10.028

Gao, L., Liu, X. M., Du, Y. M., Zong, H., and Shen, G. M. (2019). Effects of tobacco-peanut relay intercropping on soil bacteria community structure. *Ann. Microbiol.* 69, 1531–1536. doi: 10.1007/s13213-019-01537-9

Haichar, F. E. Z., Marol, C., Berge, O., Rangel-Castro, J. I., Prosser, J. I., Balesdent, J., et al. (2008). Plant host habitat and root exudates shape soil bacterial community structure. *ISME J.* 2, 1221–1230. doi: 10.1038/ismej.2008.80

He, Y., Ding, N., Shi, J., Wu, M., Liao, H., and Xu, J. (2013). Profiling of microbial PLFAs: implications for interspecific interactions due to intercropping which increase phosphorus uptake in phosphorus limited acidic soils. *Soil Biol. Biochem.* 57, 625–634. doi: 10.1016/j.soilbio.2012.07.027

Hinsinger, P., Bengough, A. G., Vetterlein, D., and Young, I. M. (2009). Rhizosphere: biophysics, biogeochemistry and ecological relevance. *Plant Soil* 321, 117–152. doi: 10.1007/s11104-008-9885-9

Humphrey, P. T., Satterlee, T. T., and Whiteman, N. K. (2020). Competitive hierarchies, antibiosis, and the distribution of bacterial life history traits in a microbiome. *BioRxiv 2020–06*. doi: 10.1101/2020.06.15.152272

Jia, L., Cheng, X., Fang, L., and Huang, X. (2023). Nitrogen removal in improved subsurface wastewater infiltration system: mechanism, microbial indicators and the limitation of phosphorus. *J. Environ. Manag.* 335:117456. doi: 10.1016/j.jenvman.2023.117456

Kappler, U., Davenport, K., Beatson, S., Lucas, S., Lapidus, A., Copeland, A., et al. (2012). Complete genome sequence of the facultatively chemolithoautotrophic and methylotrophic alpha proteobacterium *Starkeya novella* type strain (ATCC 8093T). *Stand. Genom. Sci.* 7, 44–58. doi: 10.4056/sigs.3006378

Kato, A., Miura, T., Yano, H., Masuda, K., Ishida, H., and Seino, Y. (1994). Suppressive effects of polygonati rhizoma on hepatic glucose output, GLUT2 mRNA expression and its protein content in rat liver. *Endocr. J.* 41, 139–144. doi: 10.1507/endocrj.41.139

Latz, E., Eisenhauer, N., Rall, B. C., Allan, E., Roscher, C., Scheu, S., et al. (2012). Plant diversity improves protection against soil-borne pathogens by fostering antagonistic bacterial communities. *J. Ecol.* 100, 597–604. doi: 10.1111/j.1365-2745.2011.01940.x

Li, D. L., and Guo, M. (2019). First report of *Fusarium oxysporum* causing root rot on *Polygonatum sibiricum* in Chizhou, China. *Plant Dis.* 103, 2956–2956. doi: 10.1094/PDIS-05-19-0922-PDN

Li, L., Li, S. M., Sun, J. H., Zhou, L. L., Bao, X. G., Zhang, H. G., et al. (2007). Diversity enhances agricultural productivity via rhizosphere phosphorus facilitation on phosphorus-deficient soils. *Proc. Natl. Acad. Sci. U. S. A.* 104, 11192–11196. doi: 10.1073/pnas.0704591104

Li, S., and Wu, F. (2018). Diversity and co-occurrence patterns of soil bacterial and fungal communities in seven intercropping systems. *Front. Microbiol.* 9:1521. doi: 10.3389/fmicb.2018.01521

Li, Y. Y., Feng, J., Zheng, L., Huang, J. B., Yang, Y., and Li, X. H. (2020). Intercropping with marigold promotes soil health and microbial structure to assist in mitigating tobacco bacterial wilt. *J. Plant Pathol.* 102:731. doi: 10.1007/s42161-020-00490-w

Liu, X., Cong, J., Lu, H., Xue, Y., Wang, X., Li, D., et al. (2017). Community structure and elevational distribution pattern of soil Actinobacteria in alpine grasslands. *Acta Ecol. Sin.* 37, 213–218. doi: 10.1016/j.chnaes.2017.02.010

Louca, S., Parfrey, L. W., and Doebeli, M. (2016). Decoupling function and taxonomy in the global ocean microbiome. *Science* 353:1272. doi: 10.1126/science.aaf4507

Luo, C., Li, W., Chun, Z., and Wu, Y. (2018). Discriminating five Polygonatum medical materials and monitoring their chemical changes associated with traditional process by FT-IR spectroscopy coupled with multivariate analysis. *Vibrat. Spectrosc.* 99, 104–112. doi: 10.1016/j.vibspec.2018.08.016

Luo, Y., Zhang, X., She, X. S., Zhuang, M., Su, M., Hu, C. Y., et al. (2023). Effects of compounds plantations of *Torreya grandis* on soil nutrient conservation in mountainous areas of Southern Anhui Province. *Chin. Agricult. Sci. Bullet.* 39, 51–59. doi: 10.11924/j.issn.1000-6850.casb2022-0595

Lv, J., Dong, Y., Dong, K., Zhao, Q., Yang, Z., and Chen, L. (2020). Intercropping with wheat suppressed *Fusarium wilt in* faba bean and modulated the composition of root exudates. *Plant Soil* 448, 153–164. doi: 10.1007/s11104-019-04413-2

Machado, S., Petrie, S., Rhinhart, K., and Qu, A. (2007). Long-term continuous cropping in the Pacific Northwest: tillage and fertilizer effects on winter wheat, spring wheat, and spring barley production. *Soil Till. Res.* 94, 473–481. doi: 10.1016/j.still.2006.09.007

Marcos-Pérez, M., Sánchez-Navarro, V., and Zornoza, R. (2023). Intercropping systems between broccoli and fava bean can enhance overall crop production and improve soil fertility. *Scient. Horticult.* 312:111834. doi: 10.1016/j.scienta.2023.111834

McPherson, M. R., Wang, P., Marsh, E. L., Mitchell, R. B., and Schachtman, D. P. (2018). Isolation and analysis of microbial communities in soil, rhizosphere, and roots in perennial grass experiments. *J. Visual. Exp.* 2018:137. doi: 10.3791/57932-v

Mendes, R., Kruijt, M., de Bruijn, I., Dekkers, E., van der Voort, M., Schneider, J. H. M., et al. (2011). Deciphering the rhizosphere microbiome for disease-suppressive bacteria. *Science* 332, 1097–1100. doi: 10.1126/science.1203980

Moghimian, N., Hosseini, S. M., Kooch, Y., and Darki, B. Z. (2017). Impacts of changes in land use/cover on soil microbial and enzyme activities. *Catena* 157, 407–414. doi: 10.1016/j.catena.2017.06.003

Mohamed, G. A., and Ibrahim, S. R. (2021). Untapped potential of marine-associated *Cladosporium* species: an overview on secondary metabolites, biotechnological relevance, and biological activities. *Mar. Drugs* 19:645. doi: 10.3390/md19110645

Nguyen, N. H., Song, Z., Bates, S. T., Branco, S., Tedersoo, L., Menke, J., et al. (2016). FUNGuild: an open annotation tool for parsing fungal community datasets by ecological guild. *Fung. Ecol.* 20, 241–248. doi: 10.1016/j.funeco.2015.06.006

Pervaiz, Z. H., Iqbal, J., Zhang, Q., Chen, D., Wei, H., and Saleem, M. (2020). Continuous cropping alters multiple biotic and abiotic indicators of soil health. *Soil Syst*. 4:59. doi: 10.3390/soilsystems4040059

Preston-Mafham, J., Boddy, L., and Randerson, P. F. (2002). Analysis of microbial community functional diversity using sole-carbon-source utilisation profiles-a critique. *FEMS Microbiol. Ecol*. 42, 1–14. doi: 10.1111/j.1574-6941.2002.tb00990.x

Rocha, S. M. B., Mendes, L. W., de Souza Oliveira, L. M., Melo, V. M. M., Antunes, J. E. L., Araujo, F. F., et al. (2020). Nodule microbiome from cowpea and lima bean grown in composted tannery sludge-treated soil. *Appl. Soil Ecol*. 151:103542. doi: 10.1016/j.apsoil.2020.103542

Shalev, O., Ashkenazy, H., Neumann, M., and Weigel, D. (2022). Commensal Pseudomonas protect *Arabidopsis thaliana* from a coexisting pathogen via multiple lineage-dependent mechanisms. *ISME J*. 16, 1235–1244. doi: 10.1038/s41396-021-01168-6

Song, C., Wang, W., Gan, Y., Wang, L., Chang, X., Wang, Y., et al. (2022). Growth promotion ability of phosphate-solubilizing bacteria from the soybean rhizosphere under maize-soybean intercropping systems. *J. Sci. Food Agricult*. 102, 1430–1442. doi: 10.1002/jsfa.11477

Song, Z., Kennedy, P. G., Liew, F. J., and Schilling, J. S. (2017). Fungal endophytes as priority colonizers initiating wood decomposition. *Funct. Ecol*. 31, 407–418. doi: 10.1111/1365-2435.12735

Tedersoo, L., Bahram, M., and Zobel, M. (2020). How mycorrhizal associations drive plant population and community biology. *Science* 367:eaba1223. doi: 10.1126/science.aba1223

Toju, H., Tanabe, A. S., Yamamoto, S., and Sato, H. (2012). High-coverage ITS primers for the DNA-based identification of ascomycetes and basidiomycetes in environmental samples. *PLoS ONE* 7:e40863. doi: 10.1371/journal.pone.0040863

Van Der Heijden, M. G., Bardgett, R. D., and Van Straalen, N. M. (2008). The unseen majority: soil microbes as drivers of plant diversity and productivity in terrestrial ecosystems. *Ecol. Lett*. 11, 296–310. doi: 10.1111/j.1461-0248.2007.01139.x

Wagg, C., Bender, S. F., Widmer, F., and Van Der Heijden, M. G. (2014). Soil biodiversity and soil community composition determine ecosystem multifunctionality. *Proc. Natl. Acad. Sci. U. S. A*. 111, 5266–5270. doi: 10.1073/pnas.1320054111

Wang, G., Bei, S., Li, J., Bao, X., Zhang, J., Schultz, P. A., et al. (2021). Soil microbial legacy drives crop diversity advantage: linking ecological plant-soil feedback with agricultural intercropping. *J. Appl. Ecol*. 58, 496–506. doi: 10.1111/1365-2664.13802

Wang, Z. H., Xu, M. Z., Li, F., Bai, Y., Hou, J. F., Li, X. Q., et al. (2023). Changes in soil bacterial communities and functional groups beneath coarse woody debris across a subalpine forest successional series. *Glob. Ecol. Conserv*. 43:e02436. doi: 10.1016/j.gecco.2023.e02436

Xian, Y. F., Lin, Z. X., Xu, X. Y., Su, Z. R., Chen, J. N., Lai, X. P., et al. (2012). Effect of Rhizoma Polygonati on 12-O-tetradecanoylphorbol-acetate-induced ear edema in mice. *J. Ethnopharmacol*. 142, 851–856. doi: 10.1016/j.jep.2012.06.013

Xu, N., Tan, G., Wang, H., and Gai, X. (2016). Effect of biochar additions to soil on nitrogen leaching, microbial biomass and bacterial community structure. *Eur. J. Soil Biol*. 74, 1–8. doi: 10.1016/j.ejsobi.2016.02.004

Yu, H., Chen, S., Zhang, X., Zhou, X., and Wu, F. (2019). Rhizosphere bacterial community in watermelon-wheat intercropping was more stable than in watermelon monoculture system under *Fusarium oxysporum* f. sp. niveum invasion. *Plant Soil* 445, 369–381. doi: 10.1007/s11104-019-04321-5

Yu, Y., Yang, J., Zeng, S., Wu, D., Jacobs, D. F., and Sloan, J. L. (2017). Soil pH, organic matter, and nutrient content change with the continuous cropping of *Cunninghamia lanceolata* plantations in South China. *J. Soils Sediment*. 17, 2230–2238. doi: 10.1007/s11368-016-1472-8

Zeng, J. R., Liu, J. Z., Lu, C. H., Ou, X. H., Luo, K. K., Li, C. M., et al. (2020). Intercropping with turmeric or ginger reduce the continuous cropping obstacles that affect *Pogostemon cablin* (patchouli). *Front. Microbiol*. 11:579719. doi: 10.3389/fmicb.2020.579719

Zeng, Z. Q., and Zhuang, W. Y. (2023). New species of Neocosmospora (Ascomycota) from China as evidenced by morphological and molecular data. *Life* 13:1515. doi: 10.3390/life13071515

Zhang, C. C., Dong, Y., Tang, L., Zheng, Y., Makowski, D., Yu, Y., et al. (2019). Intercropping cereals with faba bean reduces plant disease incidence regardless of fertilizer input; a meta-analysis. *Eur. J. Plant Pathol*. 154, 931–942. doi: 10.1007/s10658-019-01711-4

Zhang, C. Q., Zhang, S. Y., Chen, X. L., Qi, Q. Q., and Lou, H. Z. (2016). First report of *Fusarium crown* and root rot on *Torreya grandis* caused by Fusarium oxysporum species complex in China. *Plant Dis*. 100, 1500–1500. doi: 10.1094/PDIS-12-15-1514-PDN

Zhang, H., Yang, Y., Mei, X., Li, Y., Wu, J., Li, Y., et al. (2020). Phenolic acids released in maize rhizosphere during maize-soybean intercropping inhibit Phytophthora blight of soybean. *Front. Plant Sci*. 11:886. doi: 10.3389/fpls.2020.00886

Zhang, H. C., Wang, R., Chen, S., Qi, G. F., He, Z. L., and Zhao, X. Y. (2017). Microbial taxa and functional genes shift in degraded soil with bacterial wilt. *Sci. Rep*. 7:39911. doi: 10.1038/srep39911

Zhang, Y., Yang, Y., Lu, X., Wang, A., Xue, C., Zhao, M., et al. (2023). The effects and interrelationships of intercropping on Cotton *Verticillium wilt* and soil microbial communities. *BMC Microbiol*. 23, 1–15. doi: 10.1186/s12866-023-02780-6

Zhong, Y., Liang, L., Xu, R., Xu, H., Sun, L., and Liao, H. (2022). Intercropping tea plantations with soybean and rapeseed enhances nitrogen fixation through shifts in soil microbial communities. *Front. Agricult. Sci. Eng*. 9, 344–355. doi: 10.15302/J-FASE-2022451

frontiers | Frontiers in Microbiology

TYPE Original Research
PUBLISHED 16 December 2024
DOI 10.3389/fmicb.2024.1479580

OPEN ACCESS

EDITED BY
Dongdong Yan,
Chinese Academy of Agricultural Sciences (CAAS), China

REVIEWED BY
Waqar Ahmed,
South China Agricultural University, China
Shu Wang,
Southwest Forestry University, China

*CORRESPONDENCE
Guozhuang Zhang
✉ gzzhang@icmm.ac.cn
Linlin Dong
✉ lldong@icmm.ac.cn

†These authors have contributed equally to this work

RECEIVED 12 August 2024
ACCEPTED 03 December 2024
PUBLISHED 16 December 2024

CITATION
Shi L, Yang M, Wei G, Wei X, Hong F, Ma J, Wu Z, Zheng Y, Yang M, Chen S, Zhang G and Dong L (2024) Understanding the influence of plant genetic factors on rhizosphere microbiome assembly in *Panax notoginseng*. *Front. Microbiol.* 15:1479580.
doi: 10.3389/fmicb.2024.1479580

Understanding the influence of plant genetic factors on rhizosphere microbiome assembly in *Panax notoginseng*

Liping Shi[1†], Mingming Yang[1†], Guangfei Wei[1], Xiuye Wei[1,2], Fei Hong[3], Jiaxiang Ma[1], Zhe Wu[1], Yuqing Zheng[3], Miyi Yang[1], Shilin Chen[1,2], Guozhuang Zhang[1*] and Linlin Dong[1*]

[1]State Key Laboratory for Quality Ensurance and Sustainable Use of Dao-di Herbs, Institute of Chinese Materia Medica, China Academy of Chinese Medical Sciences, Beijing, China, [2]Institute of Herbgenomics, Chengdu University of Traditional Chinese Medicine, Chengdu, Sichuan, China, [3]Zhangzhou Pien Tze Huang Pharmaceutical Co., Ltd., Zhangzhou, China

Introduction: Functional rhizosphere microbiomes (FRM) are critical for plant health and yield. However, the ecological succession of FRM and their links to plant genetic factors across the life cycle of perennial plants remain poorly understood.

Methods: This study profiled FRM, including plant-beneficial bacteria (PBB) and fungal plant pathogens (FPP), across different developmental stages of *Panax notoginseng*.

Results: The biodiversity of both PBB and FPP were significantly higher in rhizosphere compared with farmland soil, and exhibited different succession patterns with plant growth. The relative abundance of PBB, but not FPP, decreased after plant cultivation. There were significantly negative correlations between FPP and PBB, particularly the biocontrol subgroup ($\rho = -0.56$, $p < 0.001$). The antagonistic effects of biocontrol bacteria against fungal pathogens were further validated by *in vitro* assays. The fitting of neutral community model indicated that the deterministic assembly of PBB, especially the biocontrol subgroup, was the strongest at the 3rd-year root growth stage of *P. notoginseng*. Plant genes involved in protein export, biosynthesis of alkaloids and amino acids were identified as drivers of the deterministic assembly of biocontrol subcommunity by RNA-Seq analysis. Additionally, a total of 13 transcription factors potentially regulating the expression of these biosynthesis genes were identified through co-expression network. In summary, this study unveils the succession patterns of FRM throughout the life cycle of *P. notoginseng* and the underlying plant genetic mechanisms, providing valuable insights for developing new plant disease management strategies by manipulating microbes.

KEYWORDS

rhizosphere soil, functional microbiomes, biocontrol bacteria, fungal plant pathogens, community succession, plant genetic network

1 Introduction

The rhizosphere, the soil region closely surrounding plant roots, is a unique habitat teeming with a diverse array of microbes, both beneficial and harmful to the host plant (Tan et al., 2017). These complex microbial communities and their interactions, such as antagonism and mutualism, significantly impact plant development, health, and yield (Bulgarelli et al., 2012; Etesami and Glick, 2020; Li et al., 2021). In recent years,

plant-beneficial bacteria (PBB)[1] in the rhizosphere have garnered increasing attention due to their potential role in sustainable agriculture (Haskett et al., 2021; Nerva et al., 2022). Functionally, PBB can be categorized into various subgroups, including biocontrol taxa (Bioc)[2] that antagonize pathogens, plant-growth-promoting taxa (PGP)[3] that enhance nutrient absorption in host plants, and stress resistance provision taxa (SR)[4] capable of alleviating plant abiotic stress (Banerjee and van der Heijden, 2023; Li et al., 2023). Extensive studies on the taxonomy, functions, and geographic distribution of PBB have improved our understanding of their functional mechanisms and global community structures (Haskett et al., 2021; Li et al., 2023). However, the assembly mechanisms of PBB in the rhizosphere and their succession across different developmental stages of the host plant, particularly perennial species, remain elusive. This understanding is crucial for effectively utilizing PBB to enhance plant performance in complex environments and achieving sustainable agriculture (Cordovez et al., 2019). Conversely, soil-borne fungal pathogens are the primary cause of plant diseases and yield reduction (Peng et al., 2023). For many plant species, especially under continuous monoculture, there is a tendency for the accumulation of specialized fungal plant pathogens (FPP)[5] in the rhizosphere, leading to increased disease incidence (Fones et al., 2020). Thus, understanding the assembly and succession of these harmful taxa is also vital for developing targeted and environment-friendly control strategies to maintain plant health (Bai et al., 2022).

During plant development, the succession of rhizosphere functional microbiomes, such as PBB and FPP, is influenced by a combination of host plant genetic factors, biotic interactions, environmental conditions, and stochastic forces (Cordovez et al., 2019). For example, plants can contribute to microbiome succession by altering edaphic properties and soil nutrient availability (Hannula et al., 2021; Xun et al., 2024). Antagonistic interactions between Bioc taxa and pathogens exemplify the biotic interplays affecting microbial community assembly (Perez-Gutierrez et al., 2013). Additionally, continuous dispersion, birth, and death of microbes are significant drivers of microbial dynamics, even in plant-associated habitats (Zhang et al., 2022). In summary, functional microbes can colonize the rhizosphere soil through dispersal from soil, air, and plants, forming a specific and dynamic community under the integrative effects of host and biotic factors, environmental conditions, and ecological stochasticity (Berendsen et al., 2018; Li et al., 2023; Song et al., 2021). Although the extreme complexity of influencing factors presents a major challenge in studying rhizosphere functional microbiome succession, research from an ecological assembly perspective can provide valuable insights into the interplay between plant development and the functional microbiome (Cordovez et al., 2019). From a metacommunity viewpoint, microbial community assembly results from both deterministic and stochastic processes, with the relative importance of these processes varying across space and time (Zhang et al., 2021). Deterministic processes include ecological selection imposed by biotic interactions and abiotic factors, such as environmental filtering, while stochastic processes encompass dispersal events, random birth-death events, and ecological drifts (Jiao et al., 2020; Xie et al., 2022). These ecological forces collectively shape the succession patterns of rhizosphere functional groups (e.g., PBB, FPP) during plant development. Various mathematical models, including neutral theory-based neutral models and null-model based NST (Ning et al., 2019; Sloan et al., 2006), have been developed to assess the relative contribution of different ecological processes to microbial community assembly. These models, widely used in diverse ecosystems, including plant-associated habitats, have provided critical insights into the assembly and succession mechanisms of ecologically important microbial communities (Zhou and Ning, 2017).

Another challenge in functional microbiome studies is identifying microbial members that are beneficial or harmful to the host plant. Traditional approaches rely on culturing and isolating microbes, followed by *in vivo* and *in vitro* validation experiments. However, due to technical limitations, not all microorganisms inhabiting plant-associated niches can be cultured and isolated (Compant et al., 2019). Sampling only local communities, such as limited rhizosphere soil samples, often fails to represent the entire species pool of the corresponding niche (Leibold et al., 2004). Additionally, some microbial functions related to plant phenotypes are only expressed in specific environments, such as with opportunistic plant pathogens (Brown et al., 2012). Recently, significant efforts have been made to assign functional characteristics to microbial taxa. For instance, the PBB database includes soil bacteria with experimentally verified plant-beneficial functions across three mechanisms: biocontrol, growth promotion, and stress resistance (Li et al., 2023). In the realm of fungi, Põlme et al. (2021) introduced the FungalTraits database, which amalgamates pre-existing databases and expert knowledge. These resources provide promising avenues for deciphering functional microbiomes.

Panax notoginseng (Burk.) F. H. Chen is a renowned and valuable perennial medicinal plant, highly esteemed for its medicinal and economic value (Zhang et al., 2021). Typically, *P. notoginseng* is cultivated for a minimum of 3 years before harvesting, with annual vegetative, flowering, and root inflation stages (Wang et al., 2016). Our previous studies have shown that the rhizosphere microbial community of *P. notoginseng* undergoes significant changes during its growth, particularly in the third year of root inflation growth, where the variations of microbial community were active (Wei et al., 2022). The variations in functional rhizosphere microbiomes during plant growth might contribute to the soil-borne disease occurrence. For example, *Fusarium oxysporum*-induced root rot was often attributed to the disruption of soil microbiome homeostasis (Li et al., 2022). The introduction of beneficial microbial communities was expected to recover the imbalance of micro-ecology to a state of relative health, thus reducing the abundance of plant pathogens and plant mortality (Zhang et al., 2020). However, the succession of the functional rhizosphere microbial community during growth stages is still unclear. Understanding the assembly mechanisms and succession patterns of rhizosphere functional groups alongside *P. notoginseng*'s development can offer insights into the dynamics of the rhizosphere microbiome in relation to plant health and lay the groundwork for developing microbe-based agricultural management strategies. In this study, we identified the rhizosphere functional microbial communities of

1 Plant-beneficial bacteria
2 Biocontrol taxa
3 Plant-growth-promoting taxa
4 Stress resistance provision taxa
5 Fungal plant pathogens

P. notoginseng at different developmental stages with the goals of: (i) revealing the succession patterns of distinct functional groups, including PBB and FPP, and their potential interactions; (ii) quantifying the relative contribution of various ecological processes to the assembly of functional microbiomes; and (iii) linking the succession of beneficial groups to root transcriptional regulation network throughout the development of *P. notoginseng*. Considering the functional potential of PBB and the biological characteristics of *P. notoginseng*, we hypothesize that: (i) the relative abundance of PBB, especially Bioc taxa, shows negative correlations with that of FPP, indicating potential antagonistic effects; (ii) the 3-year root inflation stage of *P. notoginseng* exerts strong selection on functional rhizosphere microbiomes; (iii) biosynthesis-related plant functions drive the succession of functional microbial communities.

2 Materials and methods

2.1 Collection of rhizosphere soil of *P. notoginseng* across different developmental stages

The quality of *P. notoginseng* root was strongly affected by cultivation area, with Wenshan Prefecture, Yunnan Province being the core production area of high-quality medicinal materials. For a better description of general patterns of rhizosphere functional microbiomes, the present study collected rhizosphere soil of *P. notoginseng* in five fields of three sites across the Wenshan Prefecture, including Pingba (23°14′29.5" N, 104°5′3.0″ E; PBA, PBB, and PBC), Yanshan (23°34′56.22" N, 104°19′49.05″ E; YS), and Qiubei (23°49′46.99″ N, 104°06′12.99″ E; QB). As described in the previous study (Wei et al., 2022), soil samples were collected during a 2-year growth from early 2016 to the end of 2017. In brief, 1-year-old seedlings were transplanted into each field and then cultivated according to Good Agricultural Practices (GAP) (Zhang et al., 2021). In each field and each sampling, three separated plots (1.4 m^2 × 8.0 m^2) were randomly selected as biological replicates, from each the rhizosphere soil was collected from 10 individual plants following with mixing. Specifically, 10 randomly selected healthy plants in each plot were gently dug out using a sterilized shovel and represented one sample, and bulk soil was removed by shaking the plants (Ahmed et al., 2022). Rhizosphere soil sample was collected through gentle shaking and squeezing in a sterile ziplock bag (Zhang et al., 2023). Before transplanting, bulk soil (BL) was also collected from 10 randomly selected locations in each plot. Rhizosphere soil samples were collected from three developmental stages of *P. notoginseng* each year, including vegetative growth stage (2-year and 3-year vegetative, 2YV and 3YV), flowering stage (2YF and 3YF), and root inflation stage (2YR and 3YR). A total of 105 soil samples were obtained (seven stages * 5 fields * 3 plots). After sampling, soil was sieved (2 mm) and stored at −80°C for further analysis.

2.2 Soil DNA extraction and amplicon sequencing

Total DNA was extracted from soil samples using the FastDNA SPIN Kit for soil (MoBio Laboratories, Inc., United States), and extracted DNA was stored at −80°C for future use (Zhang et al., 2021). The V4-V5 region of bacterial 16S rRNA gene was amplified using 515F (5′-GTGCCAGCMGCCGCGG-3′) and 907R (5′-CCGTCAATTCMTTTRAGTTT-3′) primer pair. Fungal ITS region was amplified using ITS1F (5′-CTTGGTCATTTAGAGGAAGTAA-3′) and ITS2R (5′- GCTGCGTTCTTCATCGATGC-3′) primer pair (Wei et al., 2022). Sequencing was performed on Illumina MiSeq PE 250 platform (Shanghai Biozeron Co., Ltd., China). Raw FASTQ files were demultiplexed, quality filtered, and denoised to generate amplicon sequence variants (ASVs) using the QIIME2-DADA2 pipeline (Bolyen et al., 2019; Callahan et al., 2016). The representative sequences of ASVs were taxonomically classified using the machine-learning-based classification methods implemented in QIIME2. Bayes-trained classifiers based on SILVA (v138) and UNITE (v8.0) were used to assign bacterial and fungal ASVs, respectively (Nilsson et al., 2019; Pruesse et al., 2007). Bacterial ASVs assigned to plant chloroplast and mitochondria were removed to eliminate host contamination. Low-abundance ASVs (total reads <10) were also removed to reduce the impact of potential sequencing error on results (Jiao and Lu, 2020). Bacterial and fungal feature tables were rarefied to an even library size of 2,339 and 3,827 reads, respectively. A total of 5,938 and 1,245 bacterial and fungal ASVs were obtained. The raw sequence data supporting amplicon analysis could be downloaded from the NCBI Sequence Read Archive (SRA) under the Bioproject number PRJNA559079.

2.3 RNA-seq and transcript assembly

Roots of 2-year and 3-year-old *P. notoginseng* at different developmental stages corresponding to rhizosphere soil samples were collected from Wenshan Prefecture (Wei et al., 2020). The entire root was dug out, washed, and ground into powder using liquid nitrogen. Total plant RNA was extracted from bulk root using plant RNA Isolation Mini Kit (BioTeke, Beijing, China). The RNA-Seq library was prepared according to the Illumina instruction. Sequencing was performed on Illumina HiSeq platform. After quality filtered, the FASTQ data was aligned to reference genome of *P. notoginseng* using HiSAT2 (Jiang et al., 2021; Kim et al., 2019). The abundance of transcripts was counted using featureCounts (Liao et al., 2014). The transcript abundance was normalized as fragments per kilobase per transcript per million mapped reads (FPKM values). Raw sequencing data could be downloaded from NCBI (PRJNA488357) and NGDC (PRJCA024789).

2.4 Isolation of FPP and rhizosphere biocontrol bacteria as well as antagonism test

The fungal pathogen *Fusarium oxysporum* has been reported as the major pathogen associated with the root rot of *P. notoginseng* (Ma et al., 2013). The *F. oxysporum* strain was isolated from *P. notoginseng* plant suffered from root rot in Yunnan Province and was used as the target for antagonism test. Rhizosphere bacteria isolates were obtained by inoculating soil suspension on 1/10 TSA plates (Zhou et al., 2022). The obtained bacterial strains were identified by reconstructing Neighbor-Joining phylogenetic tree based on 16S rDNA sequences.

Antagonism test was conducted to estimate the inhibitory ability against *F. oxysporum* of potential biocontrol bacteria (Zhou et al., 2022).

2.5 Statistical analysis

All statistical analyses were conducted in R environment (v4.2.2).[6] R codes used for statistical analyses are available at: https://github.com/githubzgz.

PBB were identified based on the PBB database (Li et al., 2023). Briefly, bacterial ASVs belonging to genus with beneficial functions, including biocontrol, stress resistance, and plant-growth-promoting capabilities, were identified as PBB taxa. Potential fungal plant pathogens were identified on the basis of "Plant pathogenic capacity" term in the FungalTraits database (Põlme et al., 2021). Alpha diversity indices of functional microbiomes, including richness, Chao1, and Shannon, were calculated using the vegan package (Dixon, 2003). The distribution of microbial abundance data is skewed, which does not meet the conditions of normal distribution. Kruskal-Wallis test, Nemenyi test, and nonparametric ANOVA (PERMANOVA) do not rely on the assumption of data distribution (Weiss et al., 2017). Therefore, Kruskal-Wallis test was used to evaluate the α-diversity differences among distinct growth stages, followed by the Nemenyi test for multiple comparisons using the PMCMRplus package (Pohlert, 2021). PERMANOVA was used to assess the explanatory power of developmental stages and sampling sites on microbial community variations represented by Bray-Curtis dissimilarities. This analysis was conducted using the adonis2 function in vegan package (Dixon, 2003). β-dispersal of microbial communities at different growth stages were calculated using the vegan package. Contributions of ASVs to the overall β-diversities were calculated using the simper function in vegan package. The abundance successions of the top 15 ASVs that were most important to community variations were fitted using local polynomial regression. Community variations were visualized by principal coordinates analysis using the vegan package.

Spearman correlations were calculated between the richness and relative abundance of PBB and FPP, aiming to explore the potential antagonism between functional groups. For each developmental stage, the spearman correlations between the relative abundance of FPP and widespread ASVs (occurring in more than half of samples) were also calculated and mapped on the phylogenetic tree constructed by FastTree. The phylogeny was visualized using the ggtree package (Yu et al., 2016).

To evaluate the relative importance of stochastic and deterministic processes in community assembly of rhizosphere functional microbiomes, we applied the Sloan's neutral model (Sloan et al., 2006) and the null model-based NST method (Ning et al., 2019). In Sloan's neutral model, the neutral taxa ratio (NTR) was calculated to represent the relative importance of neutral process to community assembly (Ji et al., 2020; Sloan et al., 2006). Normalized stochasticity ratio (NST) was used to quantify the contribution of ecological stochasticity to the assembly of functional microbial communities. NST analysis was performed using the NST package (Ning et al., 2019).

For linking root transcriptome profiles to the succession of community assembly of rhizosphere Bioc taxa, the transcripts were grouped into different clusters using fuzzy c-means algorithm with the Mfuzz package (Kumar and Futschik, 2007). Clusters exhibiting similar trends with the deterministic assembly of Bioc taxa were further analysed. Enrichment analysis of genes in different clusters was conducted using the clusterProfiler package (Wu et al., 2021). For cluster2 with expression trend similar to the deterministic assembly of Bioc taxa, a gene co-expression network was constructed using spearman correlation analysis (Spearman $\rho > 0.9$; BH adjusted $p < 0.001$). Genes belonging to the enriched biosynthesis pathways were extracted, and a subnetwork comprising these genes and connected genes was visualized using the Cytoscape platform (Shannon et al., 2003). Direct connections between transcription factors (TF) and biosynthesis-related genes were also extracted and visualized.

3 Results

3.1 Identification of functional microbial communities in the rhizosphere of *P. notoginseng*

In the primary cultivation area of *P. notoginseng* in Yunnan Province, a total of 15 bulk soil and 90 rhizosphere soil samples were collected at various plant growth stages. These stages included farmland (BL), two-year and three-year vegetation (2YV and 3YV), flowering (2YF and 3YF), and root inflation (2YR and 3YR). Following quality control measures, chimera filtering, and low-abundance filtering, we successfully identified 5,938 bacterial and 1,245 fungal amplicon sequence variants (ASVs). From these, based on the PBB database, 1,075 bacterial ASVs were identified as PBB. These comprised 1,023 ASVs associated with plant-growth-promoting characteristics, 438 ASVs related to biocontrol characteristics, and 180 ASVs linked to stress resistance traits. A total of 153 bacterial taxa demonstrated all three plant-beneficial characteristics (Figure 1A). At the phylum level, the PBB communities were primarily composed of Proteobacteria, which represented 37.6% of the total PBB ASV count, followed by Bacteroidetes, Actinobacteria, Firmicutes, Gemmatimonadetes, and Acidobacteria (Figure 1B). Additionally, we identified 330 FPP ASVs in the rhizosphere soil, which accounted for approximately 27% of the total fungal ASV count (Figure 1C). The potential FPP communities were predominantly Ascomycota, constituting 84.2% of the total FPP ASV count, with Basidiomycota and Macoromycota following (Figure 1D). These findings indicate that the rhizosphere of host plants is rich in both PBB and FPP.

3.2 PBB and FPP showed different succession patterns in terms of biodiversity and community composition

The communities of potential PBB and FPP exhibited significant shifts across the developmental stages of *P. notoginseng*, both in terms of α-diversities (Figures 2A,B) and community compositions (Figures 2C,D). The α-diversity of PBB in the rhizosphere soil was notably higher than in bulk land (BL) soil (Kruskal-Wallis followed by

6 http://www.r-project.org/

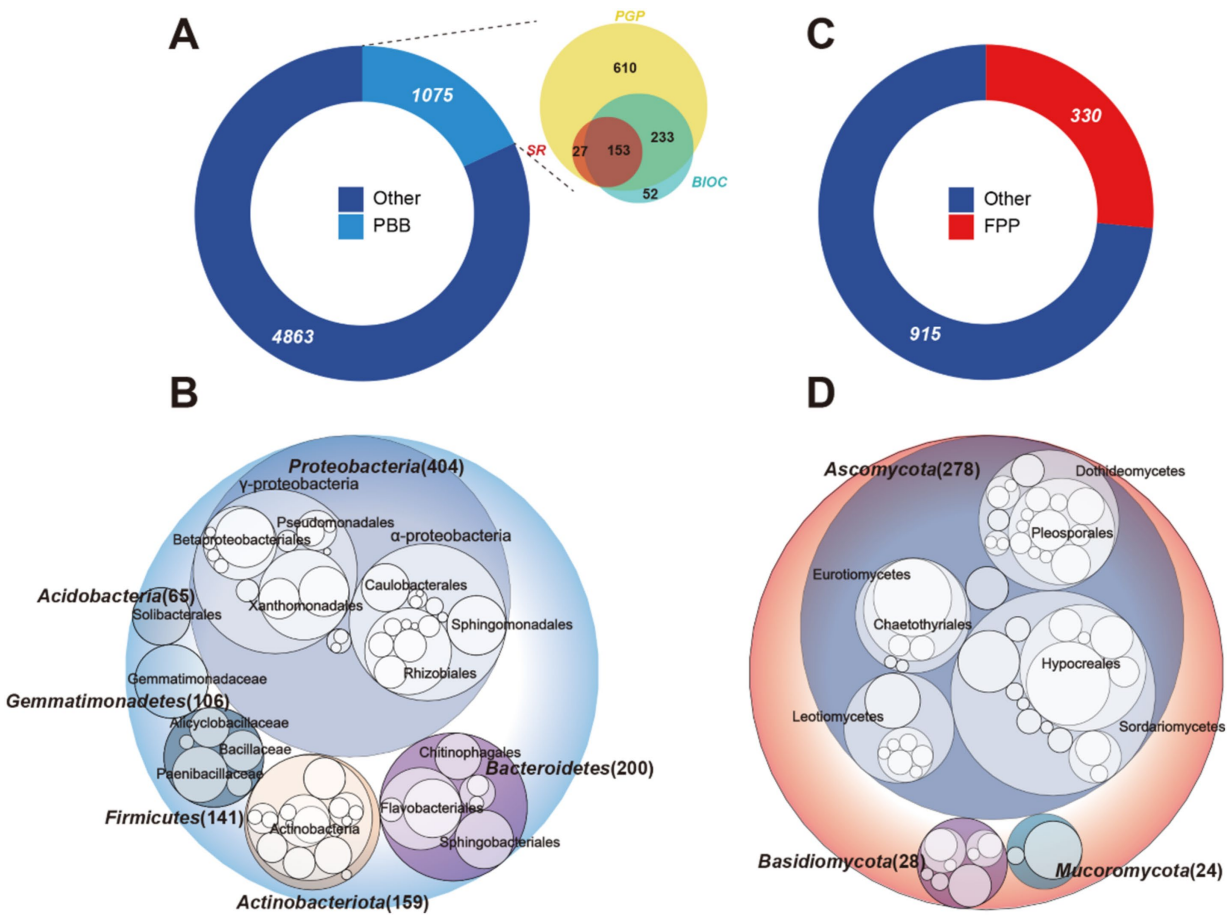

FIGURE 1
Potential PBB and FPP in the rhizosphere of *P. notoginseng*. Donut plots displayed the number of ASVs in PBB **(A)**, FPP **(C)**, and provided information on the number of subclasses outside the circular plot. Numbers represented the number of ASVs. Circular packing showed PBB ASVs **(B)** and FPP ASVs **(D)** at the phylum level, the color of the circle represented different phylum, with the diameter of the circle being proportional to the number of ASVs. PBB, plant-beneficial bacteria; FPP, fungal plant pathogens; PGP, plant-growth-promoting taxa; BIOC, biocontrol taxa; SR, stress resistance provision taxa.

Nemenyi test, $p < 0.05$) (Figure 2A; Supplementary Figure S1). Within the rhizosphere, PBB biodiversity decreased from the 2YV to the 3YV stages, then significantly increased, reaching a peak at the 3YR stage. The dynamic succession pattern of α-diversities was similar for both PBB and its subgroup communities (Supplementary Figure S2). However, the relative abundance of PBB was lower in the rhizosphere soil compared to BL (Figure 2C; Supplementary Figure S2). The trend in PBB relative abundance from 2YV to 3YR mirrored that of the PBB α-diversity, with a marked increase observed from the 3YF to 3YR stages. Regarding community composition, the relative abundance of Proteobacteria and Firmicutes in PBB was substantially lower in the rhizosphere soil compared to BL (Figure 2C). At the 3YR harvest stage, the relative abundance of Proteobacteria and Gemmatimonadetes increased significantly compared to other growth stages (Figure 2C).

Similarly, the α-diversity of FPP in the *P. notoginseng* rhizosphere was significantly higher than in BL (Figure 2B). After planting, FPP biodiversity in the rhizosphere gradually decreased from 2YV to 3YR (Figure 2B). The pattern of FPP relative abundance was consistent between the two-year and three-year stages, with an increase in relative abundance from the vegetation to root inflation stages each year (Figure 2D). Sordariomycetes was the dominant fungal class throughout the sampling period (Figure 2D). These findings underscore the distinct succession patterns of rhizosphere functional microbiomes across *P. notoginseng*'s developmental stages, highlighting the divergence in biodiversity and community composition between PBB and FPP.

3.3 Temporal dynamics of PBB and FPP community structures across *P. notoginseng* developmental stages

PERMANOVA revealed that the developmental stages significantly drove the community structure variations in PBB ($R^2 = 0.289$, $p = 0.001$) and FPP ($R^2 = 0.143$, $p = 0.001$) as measured by Bray-Curtis dissimilarities (Figures 3A,B). A distinct separation among PBB collected from different stages was showed by PCoA, and the 3YR samples could be separated from others (Figure 3A). PCoA of FPP also showed significant separation between BL and rhizosphere soil samples (Figure 3B). To quantify the community variations within each developmental stage, the βdispersion represented by the mean

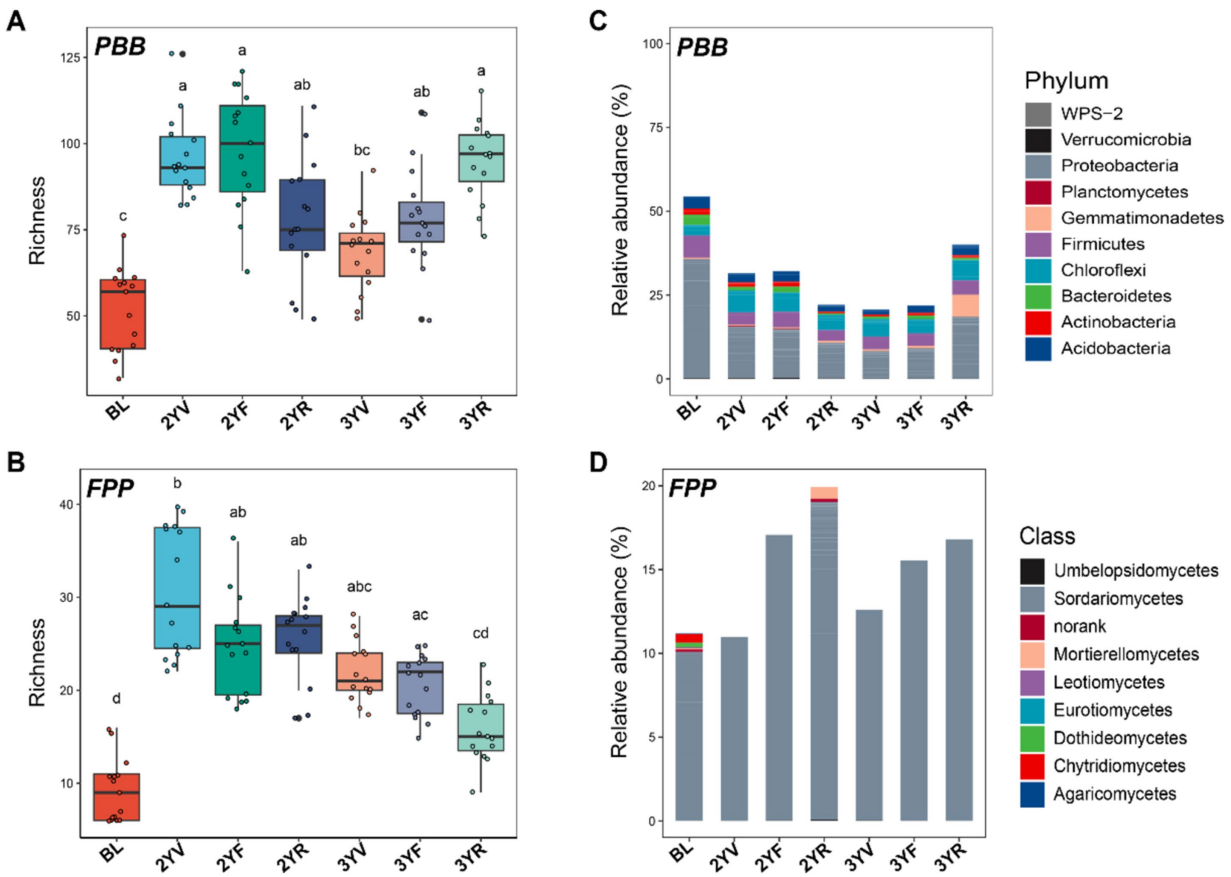

FIGURE 2
Changes in α-diversities and composition of PBB and FPP communities with *P. notoginseng* growth. PBB **(A)** and FPP **(B)** α-diversities at different growth stages were represented by ASV richness index. Different letters above the boxes indicate a significant difference determined by Kruskal-Wallis followed by Nemenyi test ($p < 0.05$). Shifts in the compositions of PBB **(C)** and FPP **(D)** communities with *P. notoginseng* growth. BL, 2YV, 2YF, and 2YR represent bulk soils and the 2-year vegetative, flowering, and root growth stages, respectively. 3YV, 3YF, and 3YR denote the 3-year vegetative, flowering, and root growth stages, respectively. PBB, plant-beneficial bacteria; FPP, fungal plant pathogens.

distances to group centroid were calculated and compared (Figures 3A,B). Although no statistically significant differences exhibited among different developmental stages, the β dispersion of both PBB and FPP showed apparent succession patterns. For PBB, the β dispersion firstly increased from BL to 2YV, then decreased from 3YF to 3YR (Figure 3A). In contrast to PBB, the β dispersion of FPP showed a trend of first decreasing and then increasing along the developmental stage (Figure 3B). These results revealed that the community structure variations of PBB and FPP communities were active at the 3YR stage.

To identify ASVs important for community variations, the contributions of ASVs to β diversities were calculated and the succession patterns of top 15 bacterial and fungal ASVs were fitted (Figures 3C,D). The relative abundance of 8 PBB ASVs showed decreasing tendency with plant growth, including members of *Bacillus*, *Mucilaginibacter*, *Actinoallomurus*, and *Rhodanobacter*. While the relative abundance of ASVs belonging to *Pseudomonas*, *Novosphingobium* and *Sphingobium* increased from BL to 3YR stage (Figure 3C). Most of the top 15 FPP ASVs showed an uprush from BL to 2YV, following with a stable abundance from 2YV to 3YR, mainly including members of *Trichoderma* (Figure 3D). However, the relative abundance of fungal ASV73 (*Volutella*) exhibited continuous growth after planting, and the uprush of fungal ASV11 (*Cadophora*) occurred from 3YF to 3YR (Figure 3D). These results identified different succession patterns of functional taxa that were critical for microbiome variations.

3.4 Rhizosphere biocontrol bacteria exhibited the strongest antagonistic interactions with FPP during *P. notoginseng* growth

The relationships between PBB and FPP in terms of the biodiversity and relative abundance were further evaluated. A significant and positive correlation between the richness of PBB and FPP was observed (Spearman rank correlation, $\rho = 0.429$, $p < 0.001$), with the correlation coefficients varies at different growth stages (Figure 4A). However, the relative abundance of PBB was significantly and negatively correlated with that of FPP ($\rho = 0.399$, $p < 0.001$) (Figure 4B). Across different sampling stages, the PBB-FPP negative correlations varied, with the strongest negative correlations observed in the 3YV and 3YF stages (Figure 4C). In PBB subgroups, Bioc exhibited the strongest negative correlations with FPP ($\rho = -0.564$,

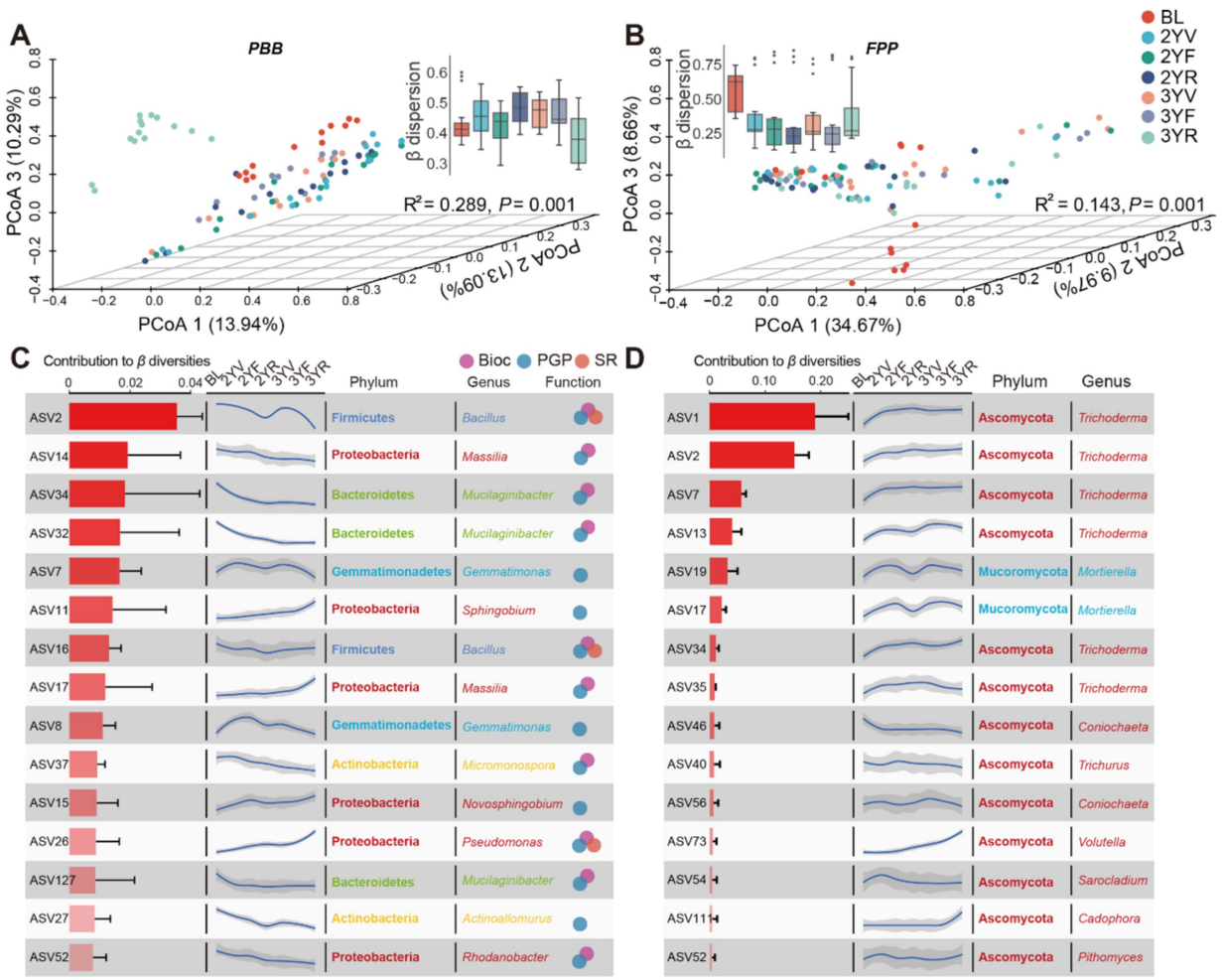

FIGURE 3
Changes in community structures of PBB and FPP across developmental stages of *P. notoginseng*. Principal coordinates analysis (PCoA) based on Bray-Curtis distances displaying significant differences among distinct sampling stages of PBB (R^2 = 0.289, p = 0.001, PERMANOVA) **(A)** and FPP (R^2 = 0.143, p = 0.001, PERMANOVA). **(B)** The inside boxplots represented β dispersion of two functional communities, respectively. The top 15 bacterial **(C)** and fungal **(D)** ASVs that were important to the community variations. Bar plots indicated the contributions of ASVs to β-diversities; curve graphs were obtained by fitting the relative abundance of ASVs to developmental stages. Dots on the right of **(C)** represented different functional subgroups in PBB. PBB, plant-beneficial bacteria; FPP, fungal plant pathogen.

$p < 0.001$) (Figures 4B,C), while the strengths of potential antagonism to FPP were lower for PGP ($\rho = -0.391$, $p < 0.001$) and SR ($\rho = -0.465$, $p < 0.001$) subgroups (Supplementary Figure S3).

The correlations between widespread ASVs and FPP were estimated for each development stage using spearman correlation analysis (Figure 4D). Bacterial taxa potentially antagonistic to FPP mainly belonged to Firmicutes, and exhibited the biocontrol function (Figure 4D). Only eight ASVs showed significant and negative correlations with FPP across at least three sampling stages, belonging to *Bacillus*, *Blastococcus*, *Phenylobacterium*, *Sphingobium*, *Pseudomonas*, and *Gemmatimonas* (Figure 4D).

To confirm the antagonistic effect of the Bioc group against fungal pathogens in the rhizosphere of *P. notoginseng*, bacteria were isolated from the rhizosphere soil of *P. notoginseng*. According to the PBB database, five strains potentially exhibiting biocontrol capability were isolated, one belonging to *Flavobacterium*, three to *Bacillus*, and one to *Gottfriedia* (a new taxonomic group separated from *Bacillus*) (Figure 5). In which, the three representative isolates all could inhibit the growth of root rot pathogen *F. oxysporum* as indicated by the antagonism test, confirming the antagonistic effect of Bioc group in *P. notoginseng* rhizosphere (Figure 5). These results showed that potential antagonism effects exhibited between FPP and PBB especially the Bioc group, and the antagonism strength varied with plant growth. Simultaneously, the antagonistic experiment also verified the reliability of screening rhizosphere functional bacteria based on PBB database.

3.5 The relative contribution of deterministic and stochastic processes to the assembly of functional microbiomes varied with plant growth

The clear succession of PBB and FPP in the rhizosphere soil of *P. notoginseng* were driven by the underlying dynamics of ecological assembly processes. The occurrence and abundance of ASVs in different functional microbiomes sampled at distinct developmental

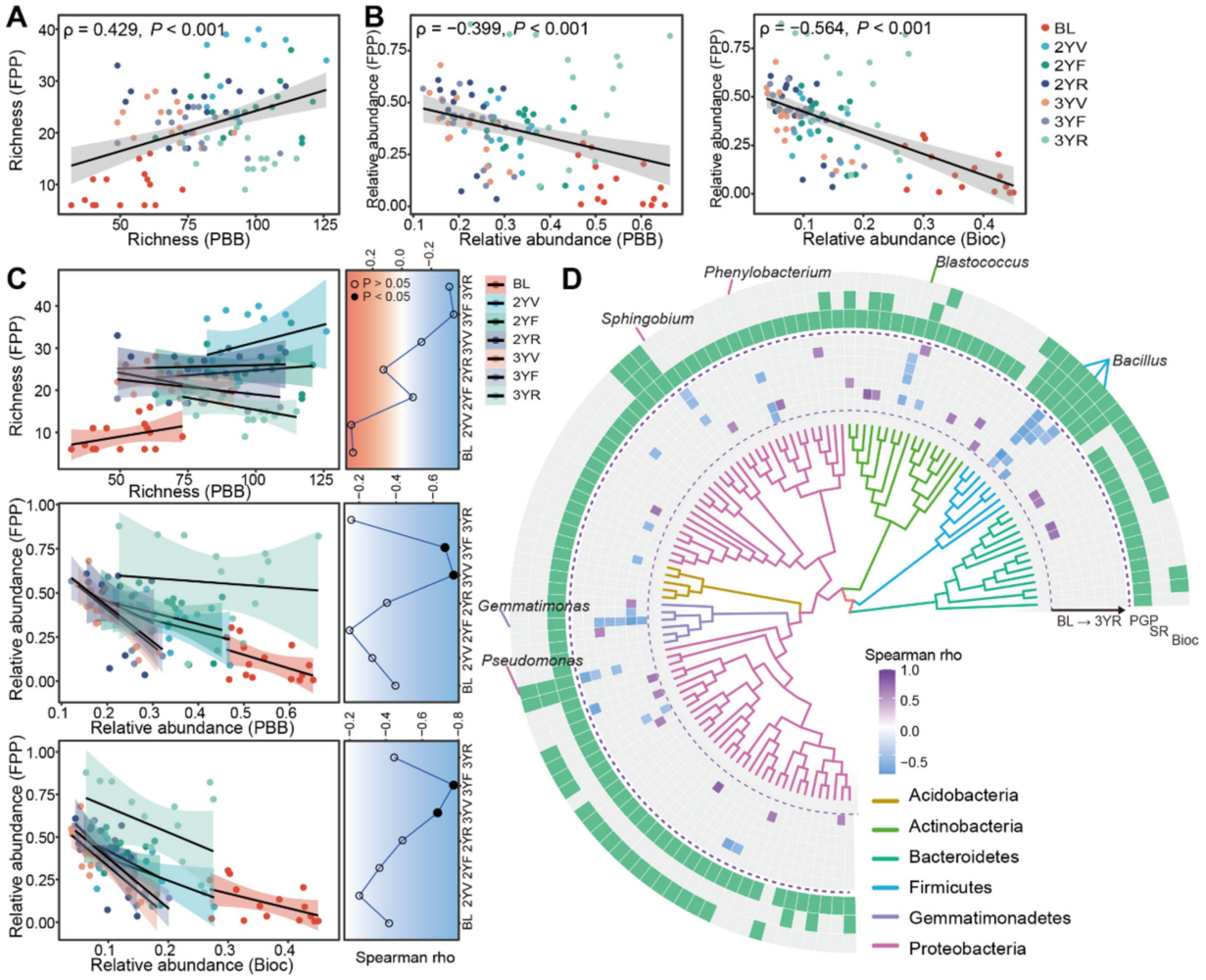

FIGURE 4
The potential antagonism effects between PBB and FPP and the succession patterns. **(A)** Correlations between the richness of PBB and FPP. **(B)** The correlation between the relative abundance of FPP and the relative abundance of PBB and Bioc communities, respectively. **(C)** Correlations between the indicators of PBB, Bioc, and FPP at different developmental stages. Line charts summarized the succession of correlation coefficients across plant developmental stages. Solid and hollow dots represented significant ($p < 0.05$) and non-significant ($p > 0.05$) correlations, respectively. **(D)** Significant correlations (BH adjusted $p < 0.05$) between widespread PBB ASVs (occurred in more than half of samples in different sampling stages) and the relative abundance of corresponding FPP community. The inside track represented phylogenetic tree of these bacterial ASVs constructed using FastTree. The heatmap in middle track represented the correlation coefficients. While the outside track indicated the functional subgroups of bacterial ASVs (i.e., PGP, SR, or Bioc). The genus-level taxonomic information was annotated for ASVs with negative and significant correlations with FPP across at least three sampling stages. PBB, FPP, PGP, Bioc, and SR represent plant-beneficial bacteria, fungal plant pathogens, plant-growth-promoting taxa, biocontrol taxa, and stress resistance provision taxa, respectively.

stages were thus fitted using Sloan's neutral model to evaluate the community assembly mechanisms (Figure 6; Supplementary Figures S4–7). The neutral model fitted well for FPP, PBB, and PBB subgroups, indicating the important role of stochastic processes to the assembly of functional microbiomes. AIC of neutral models were generally lower compared to corresponding binomial models, emphasizing the importance of dispersal limitation in shaping community structure (Figure 6A; Supplementary Figures S4–7).

The neutral taxa ratio was calculated to quantify the relative contributions of neutral (stochastic) and non-neutral (deterministic) processes to community assembly (Figure 6B). Compared with BL, the relative contribution of neutral process to the assembly of functional microbiomes showed a trend of first increasing and then decreasing. From the 3YV stage to the 3YR stage, the effects of deterministic processes increased for PBB and its subgroup communities, and the impact on FPP communities slightly increased. The null model-based NST analysis also confirmed the strong effects of deterministic processes at the 3YR period (Supplementary Figure S8). Notably, the NTR of non-PBB bacterial subcommunities did not change obviously across the growth period (Figure 6B). These results demonstrated that the succession of community assembly forces of functional microbiomes during the development stages of *P. notoginseng*.

3.6 Linking plant genetic network to the assembly of Bioc communities across plant development stages

As mentioned above, the Bioc taxa exhibited the strongest negative correlations with FPP, implying their potential in controlling

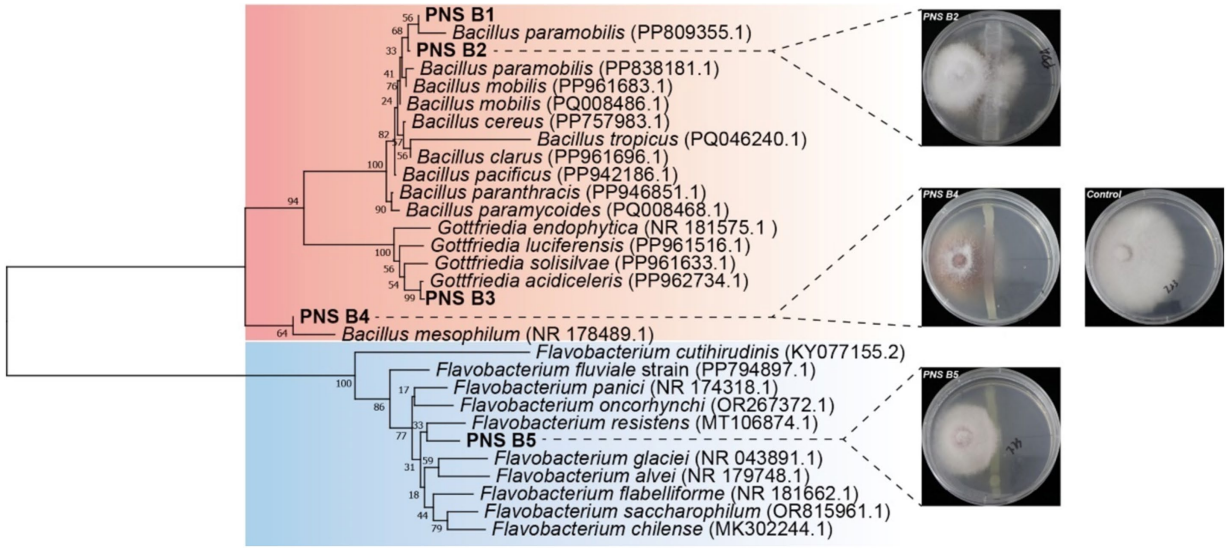

FIGURE 5
Evaluation of the role of Bioc's antagonistic effect against *F. oxysporum*. Neighbor-joining tree showing the phylogenetic relationship among the isolated Bioc group strains obtained in this study (in bold). Accession numbers of isolates obtained from the NCBI database are displayed in regular letters. The middle pictures display the *in vitro* inhibitory effects of the three representative isolates on *F. oxysporum* using PDA assay. The picture on the right shows the control *F. oxysporum* culture medium without bacterial inoculation.

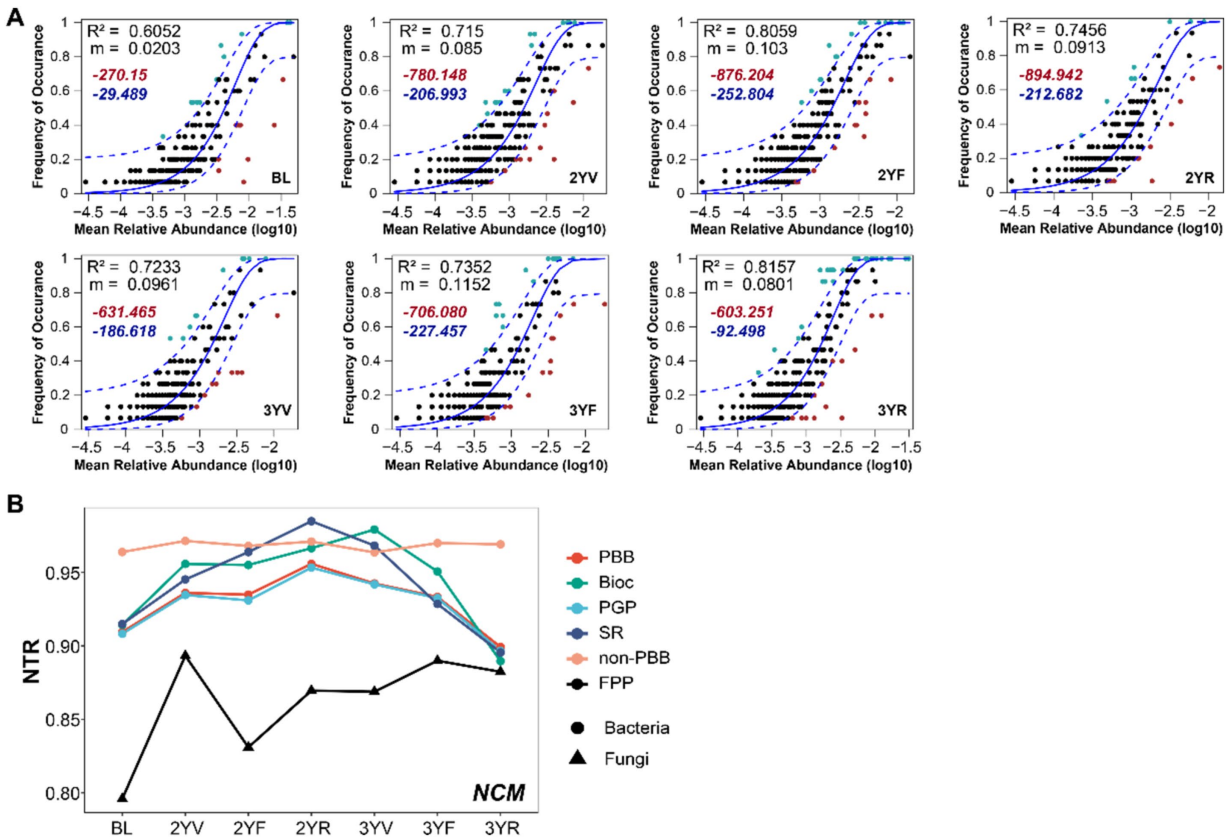

FIGURE 6
The ecological assembly mechanisms of rhizosphere functional microbiomes at different developmental stages of *P. notoginseng*. **(A)** Fit of the neutral community model with the community assembly of PBB. The solid blue line represents the best-fitting neutral model. The dashed line represents the 95% confidence intervals (CIs) around the best-fitting neutral model. m indicates the estimated migration rate, and R^2 indicates the fit to the neutral model. Red and blue numbers denote the AIC of the neutral model and the binomial model, respectively. **(B)** The neutral taxa ratio (NTR) for the functional community. PBB, plant-beneficial bacteria; non-PBB, bacteria without plant-beneficial characteristics; FPP, fungal plant pathogens; PGP, plant-growth-promoting taxa; BIOC, biocontrol taxa; SR, stress resistance provision taxa.

fungal diseases. The links between plant root activities and the community assembly mechanisms of Bioc were thus investigated during plant growth. For the description of root activities, we collected root samples of *P. notoginseng* and performed RNA-seq analysis. In total, the expression of 39,238 genes in roots were quantified. K-means clustering analysis was performed on genes with annotated information, which were divided into five categories (Figure 7A). Cluster 2 showed a consistent trend with the relative contribution of deterministic processes on Bioc community, suggesting that these genes may be involved in the recruitment of Bioc community (Figure 7B). The KEGG pathway enrichment analysis results showed that cluster 2 was significantly enriched by functions related to the biosynthesis, metabolism, and exudation of metabolites in plants, including tropane, piperidine and pyridine alkaloid biosynthesis, N-glycan biosynthesis, lysine biosynthesis, isoquinoline alkaloid biosynthesis, folate biosynthesis, vitamin B6 metabolism, alanine, aspartate and glutamate metabolism and protein export (Figure 7C; Supplementary Table S1).

A co-expression network was then constructed for genes in cluster 2. Transcripts involved with the enriched biosynthesis pathways were extracted and visualized (Figure 7D). Genes related to the N-glycan biosynthesis and folate biosynthesis exhibited more connections compared to other functional genes (Figure 7D), indicating that their expression might be modulated by complex processes. Given the important role of transcription-level regulation in the expression of biosynthesis genes, the transcription factors (TF) connected to these genes were further extracted (Figure 7D). Thirteen TFs belonging to bHLH (g68387), NAC (g60683, g57420), MADS (g10954), MYB (g26310, g92383), bZIP (g50830), ARF (g51046), IFRD1 (g12290, g12289), GRF (g92796), TFIIA (g54428), and TFIIH

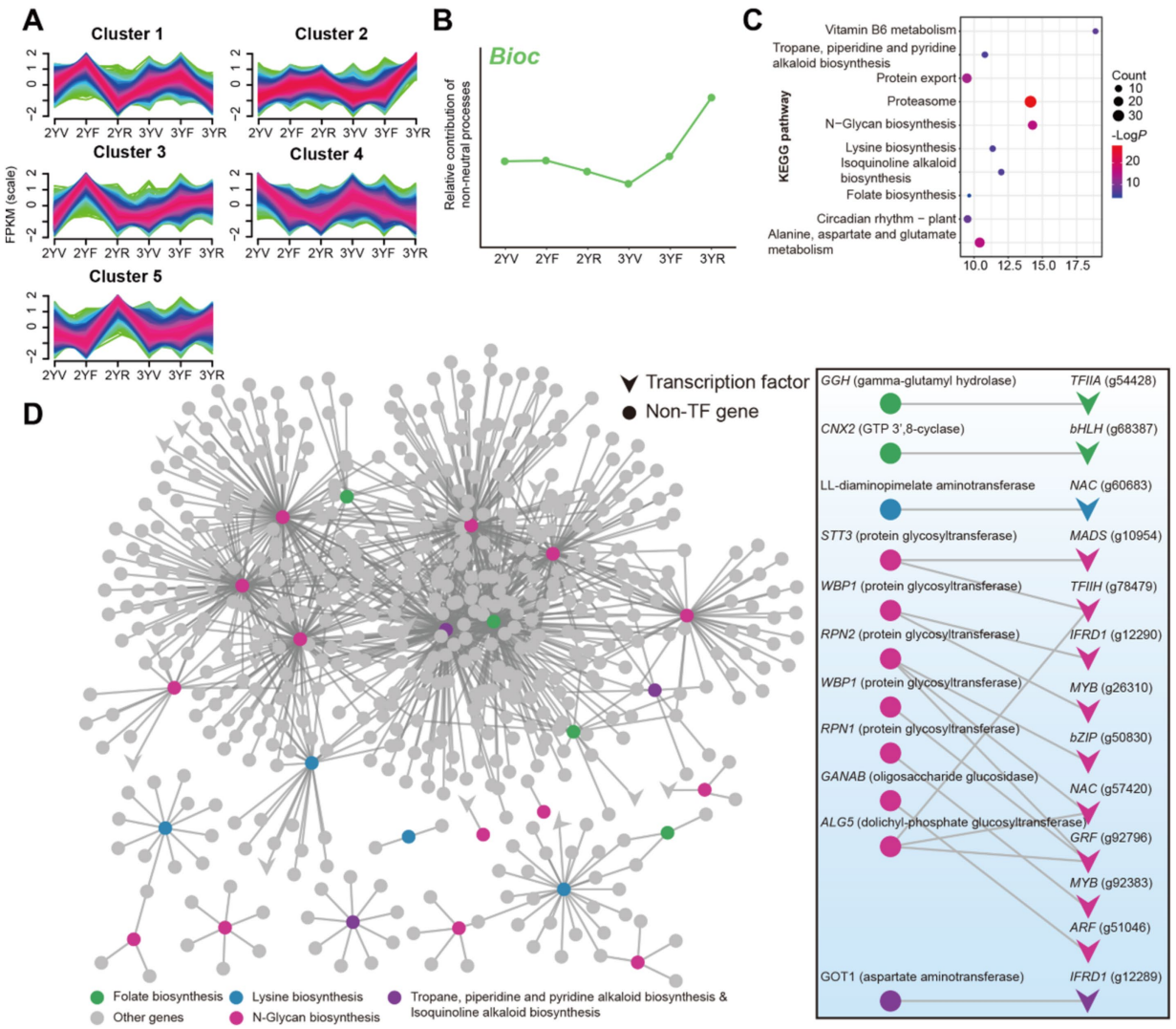

FIGURE 7
Gene expression analysis of *P. notoginseng* root at different developmental stages. **(A)** K-means-based gene clusters calculated using gene FPKM value. **(B)** The relative contribution of non-neutral processes to Bioc community assembly. **(C)** KEGG enrichment analysis of Clusters 2. Node size represents the number of genes within the pathway, and color represents the statistical significance. **(D)** Partial co-expression network of genes in cluster 2. Triangle and round nodes represented transcription factor (TF) and non-TF genes. The binary network on the right displayed the direct connections between TF and genes involved in enriched biosynthesis pathways. Gene symbols were labeled for biosynthesis-related genes, while TF families and annotation numbers were labeled for TFs.

(g78479) families were identified as potential regulators of biosynthesis pathways that might be related to the recruitment of Bioc taxa. These results revealed plant functions and regulators potentially related to the community assembly succession of rhizosphere Bioc community.

4 Discussion

Although extensive research has been conducted on rhizosphere functional microorganisms—both beneficial and harmful to the host plant—in terms of functional mechanisms, plant-microorganism interplays, and biogeographic distribution (Haskett et al., 2021; Li et al., 2023; Peng et al., 2023), their succession patterns, community assembly mechanisms, and links to plant genetic networks during the life cycle of perennial plants remain largely unexplored, which are critical for utilizing these functional microorganisms for sustainable agriculture. Dramatic physiological changes occur during plant development, such as resource allocation across organs, specific metabolite biosynthesis, and the balance between growth and defense (Chaparro et al., 2014; Major et al., 2017; Mathieu et al., 2009). These physiological variations, in conjunction with changing environmental conditions and ecological stochasticity, have significant impacts on rhizosphere functional microbiomes. Therefore, longitudinal studies encompassing different plant developmental stages, rather than merely cross-sectional analyses, are vital for a comprehensive understanding of plant-functional microorganism interactions and the effective utilization of microbes in sustainable agriculture (Russ et al., 2023; Xun et al., 2024). In the present study, the succession patterns of rhizosphere PBB and FPP in terms of biodiversity, relative abundance, and community structure across the life cycle of *P. notoginseng*, as well as the underlying assembly mechanisms were explored. The potential antagonism between PBB and FPP, as well as the links between the variations in root transcriptome and the deterministic assembly of beneficial microbial subcommunities were further investigated.

4.1 The succession patterns of rhizosphere functional microbiomes reflect the dynamic effects of host development

The biodiversity of both PBB and FPP in the rhizosphere of *P. notoginseng* was significantly higher than in unplanted bulk soil, aligning with findings from studies on other species like *Ranunculus glacialis* (Philippot et al., 2013). This increase can likely be attributed to the rhizodeposit effects of the host plant (Philippot et al., 2013). Rhizodeposits, including low-molecular-mass compounds exuded by roots, polymerized sugars, and root border cells, create diverse niches for rhizosphere functional microbes, thereby promoting species coexistence (Kraft et al., 2014). The niche-based promotion of species coexistence seems to be nonspecific to either PBB or FPP, as evidenced by significant and positive correlations between their α-diversities.

The biodiversity and relative abundance of PBB in the rhizosphere of *P. notoginseng* decreased and then increased throughout the plant's development, reflecting the dynamic influence of the plant on its beneficial microbial inhabitants. An enhancement of rhizosphere effects with plant growth, similar to that observed in species like foxtail millet (Wang et al., 2022), suggests that plant requirements for and effects on beneficial bacteria might be minimal during the early slow growth stages (the 2nd year) but increase significantly in the 3rd year, especially during the root inflation stage (3YR). The specific rise in the relative abundance of PBB at 3YR may indicate plant recruitment of beneficial bacteria for essential functions such as nutrient uptake. For example, a notable increase in the relative abundance of Gemmatimonadetes at 3YR suggests their potential role in enhancing nitrogen supply to the host plant, as supported by metagenome-based studies (Kalam et al., 2022). This theory is further corroborated by neutral model findings, which shows a stronger relative contribution of selection processes to the assembly of PBB at the 3YR stage compared to earlier stages, a pattern not observed for non-PBB subcommunities. Similarly, both the relative abundance and deterministic assembly of FPP increased at 3YR, indicating that active root physiology at this stage attracts not only beneficial bacteria but also potentially pathogenic fungi. Prior research has highlighted the crucial roles of root exudates in plant defense against pathogens, such as coumarins and benzoxazinoids (Pascale et al., 2019). However, the specifics of which root-derived molecules attract plant pathogens remain largely unexplored and warrant further investigation (van Griethuysen et al., 2024).

Another critical period is the 3YV stage, during which the relative abundance of both functional microbiomes, including PBB and FPP, were at their lowest. During the winter between the 2YR and 3YV stages, the reduced physiological activities of the plant, due to leaf abscission and root dormancy, likely lead to diminished effects on the functional microbiomes. Consequently, these microorganisms, heavily reliant on plant-derived carbon resources, might struggle to compete with other microbial taxa in the absence of plant support (Russ et al., 2023). This observation underscores the significance of continuous carbon input from the plant in maintaining rhizosphere functional microbiomes.

4.2 The potential antagonism in the rhizosphere reduces at the rapid growth stage of host plant

This study's findings align with our hypothesis, revealing significant and negative correlations between the relative abundance of FPP and PBB, particularly within the Bioc subgroup. The finding was also supported by the isolation-based antagonism test experiments. Biocontrol bacteria are known to suppress FPP proliferation through various mechanisms, including host immune induction, antibiosis compound production, and competition for scarce resources (Kohl et al., 2019). These complex interactions likely contribute to the strong negative correlations observed in our study. *Bacillus* spp. and *Pseudomonas* spp. are bacteria in the Bioc subgroup that show significant and negative correlations with FPP. Both genera have been well studied and their abilities to protect plants against pathogens have been widely described (Bernal et al., 2017; Molina-Santiago et al., 2019). The Bioc subgroup identified here presents a promising avenue for microbe isolation and validation for agricultural applications.

A strong succession patterns of the potential antagonism interactions were also observed during *P. notoginseng* growth. The potential antagonism continuously strengthened from 2YV to 3YV, as indicated by the negative correlation coefficients, implying the increasing regulation of plant on Bioc bacteria for protection against

pathogens. However, at the 3YR stage, there was a marked weakening of this antagonistic strength. Previous research has focused on the "growth-defense trade-offs," particularly in terms of genetic regulatory networks in plants involving diverse hormones, pathogen pattern recognition, and immune responses (He et al., 2022; Major et al., 2017). Our finding of diminished rhizosphere antagonism during rapid plant growth suggests that microbe-dependent rhizosphere defense might be an overlooked aspect of this trade-off. During periods of accelerated root biomass accumulation, plant physiological activities might prioritize primary metabolism and nutrient uptake, potentially at the expense of root defense, including microbe-assisted pathogen antagonism. Another possibility is that plant roots release more resources at the 3YR stage, weakening the resource competition-based antagonism in the rhizosphere. This insight underscores the importance of monitoring rhizosphere antagonistic interactions within agricultural ecosystems, especially during critical growth phases.

4.3 Plant genetic networks potentially related to the deterministic assembly of rhizosphere Bioc bacterial subcommunity

Genetically determined rhizodeposits are crucial for shaping the structure and function of the rhizosphere microbial community (Philippot et al., 2013). Thus, understanding the genetic basis of beneficial bacterial community dynamics is essential for breeding *P. notoginseng* varieties that are optimized for rhizosphere microbiome assistance (Trivedi et al., 2020; Xun et al., 2024). The exudation of proteins might be involved in important signaling molecules regulating the interaction between plants and microorganism, affecting the formation of beneficial rhizosphere microbial communities (Galloway et al., 2020; Sasse et al., 2018). N-glycan is an important protein modification (Ruiz-May et al., 2012), and our research has determined that the functional pathway of N-glycan biosynthesis in *P. notoginseng* is related to the deterministic assembly of Bioc community. The biosynthesis of other compounds, including different types of alkaloids, amino acid, and folate, were also linked to the assembly of rhizosphere Bioc community. The root exudation of these compounds has been extensively reported (Afridi et al., 2024; Chaparro et al., 2014). These complex groups of compounds can collectively shape beneficial rhizosphere microbiomes through multiple mechanisms, including chemotaxis and microenvironment regulation (Afridi et al., 2024). More importantly, transcription factors belonging to various families including MADS, TFII, IFRD1, MYB, bZIP, NAC, GRF and ARF, were identified as potential regulators controlling the biosynthesis of these compounds, potentially regulating the assembly and succession of FRM communities. For example, transcription factors MYB72 and MYB72-controlled β-glucosidase BGLU42 play a key role in regulating beneficial rhizosphere bacteria-induced systemic resistance (ISR) and by modulating the secretion of coumarin to inhibit soil-borne fungal pathogens (Stringlis et al., 2018). The plant functional pathways and regulators identified in this study offer valuable insights into the molecular mechanisms that underlie the interactions between plants and beneficial microbes in the rhizosphere, and provide clues for further molecular verification.

4.4 Fully understanding plant-rhizosphere interactions in the agricultural system of perennial plants: future directions

Although this study revealed the rhizosphere functional microorganisms, PBB-FPP interactions, the succession of beneficial microbial ecological construction processes during *P. notoginseng* growth, as well as the related plant genetic factors, more efforts are still needed to fully understand the interactions between plants and rhizosphere in perennial plant agricultural systems, in order to achieve microbial-based sustainable agricultural practices. Firstly, the candidate plant gene list was obtained through correlation analysis. Further validation studies using genetic manipulation techniques such as gene editing will confirm the functions of these candidate genes, providing targets for plant breeding aimed at healthy rhizosphere microbial communities. Secondly, although sampling was conducted at various developmental stages of *P. notoginseng* in this study, the rhizosphere exhibited complex dynamic changes, and the sampling frequency may not be sufficient to capture the complete dynamic patterns. Hence, more intensive sampling of both plants and the rhizosphere should be included in future studies. Third, the dynamics of the rhizosphere microbiome throughout the entire growth cycle of model plants and crops (such as *Arabidopsis*, rice, etc.) (Chaparro et al., 2014; Zhang et al., 2018) had been extensively studied, but the study of the succession patterns of the rhizosphere microbial communities during the developmental stages of perennial plants is relatively scarce. In future studies, more well-designed plant-rhizosphere microbe interaction studies on perennial plants are needed to help improve agricultural practices for perennials.

5 Conclusion

In conclusion, the plant developmental stage was a significant driving force affecting the rhizosphere functional microbiomes. The relative impact of deterministic processes on the assembly of functional microbial communities showed a trend of first increasing and then decreasing during plant growth, reflecting the adaptability of plant functional microbial communities to plant developmental changes. The genetic regulation networks, functional pathways, and potential molecular regulators related to the deterministic assembly of biocontrol rhizosphere microbiomes were also identified. This work provides a comprehensive understanding of the assembly and succession of rhizosphere functional microbiomes, as well as their links to plant genetic networks across the life cycle of perennial *P. notoginseng*, which is vital for utilizing microbial resources to achieve sustainable agriculture of medicinal plant.

Data availability statement

The original contributions presented in the study are included in the article/Supplementary material, further inquiries can be directed to the corresponding authors.

Author contributions

LS: Formal analysis, Validation, Visualization, Writing – original draft, Writing – review & editing. MinY: Formal analysis, Visualization, Writing – original draft. GW: Data curation, Resources, Validation,

Writing – review & editing. XW: Investigation, Validation, Writing – original draft. FH: Investigation, Resources, Writing – original draft. JM: Validation, Writing – review & editing. ZW: Methodology, Writing – original draft. YZ: Data curation, Writing – review & editing. MiyY: Visualization, Writing – review & editing. SC: Conceptualization, Funding acquisition, Writing – review & editing. GZ: Conceptualization, Formal analysis, Funding acquisition, Resources, Writing – original draft. LD: Funding acquisition, Resources, Supervision, Writing – original draft, Writing – review & editing.

Funding

The author(s) declare that financial support was received for the research, authorship, and/or publication of this article. This work was supported by the National Key Research and Development Program (2022YFC3501802, 2022YFC3501803 and 2022YFC3501804), Scientific and Technological Innovation Project of China Academy of Chinese Medical Sciences (CI2023E002), Specific research fund of The Innovation Platform for Academicians of Hainan Province (YSPTZX202137), National Natural Science Foundation of China (82304663), and Fundamental Research Funds for the Central Public Welfare Research Institutes (ZXKT22001, ZXKT22052, ZXKT22060, ZXKT23018, ZZ13-YQ-049, ZZ16-XRZ-072 and ZZ17-YQ-025).

Conflict of interest

FH and YZ were employed by the Zhangzhou Pien Tze Huang Pharmaceutical Co., Ltd.

The remaining authors declare that the research was conducted in the absence of any commercial or financial relationships that could be construed as a potential conflict of interest.

Publisher's note

All claims expressed in this article are solely those of the authors and do not necessarily represent those of their affiliated organizations, or those of the publisher, the editors and the reviewers. Any product that may be evaluated in this article, or claim that may be made by its manufacturer, is not guaranteed or endorsed by the publisher.

Supplementary material

The Supplementary material for this article can be found online at: https://www.frontiersin.org/articles/10.3389/fmicb.2024.1479580/full#supplementary-material

References

Afridi, M. S., Kumar, A., Javed, M. A., Dubey, A., de Medeiros, F. H. V., and Santoyo, G. (2024). Harnessing root exudates for plant microbiome engineering and stress resistance in plants. *Microbiol. Res.* 279:127564. doi: 10.1016/j.micres.2023.127564

Ahmed, W., Dai, Z., Zhang, J., Li, S., Ahmed, A., Munir, S., et al. (2022). Plant-microbe interaction: mining the impact of native *Bacillus amyloliquefaciens* WS-10 on tobacco bacterial wilt disease and rhizosphere microbial communities. *Microbiol. Spectr.* 10:e0147122. doi: 10.1128/spectrum.01471-22

Bai, B., Liu, W., Qiu, X., Zhang, J., Zhang, J., and Bai, Y. (2022). The root microbiome: community assembly and its contributions to plant fitness. *J. Integr. Plant Biol.* 64, 230–243. doi: 10.1111/jipb.13226

Banerjee, S., and van der Heijden, M. G. A. (2023). Soil microbiomes and one health. *Nat. Rev. Microbiol.* 21, 6–20. doi: 10.1038/s41579-022-00779-w

Berendsen, R. L., Vismans, G., Yu, K., Song, Y., de Jonge, R., Burgman, W. P., et al. (2018). Disease-induced assemblage of a plant-beneficial bacterial consortium. *ISME J.* 12, 1496–1507. doi: 10.1038/s41396-018-0093-1

Bernal, P., Allsopp, L. P., Filloux, A., and Llamas, M. A. (2017). The *Pseudomonas putida* T6SS is a plant warden against phytopathogens. *ISME J.* 11, 972–987. doi: 10.1038/ismej.2016.169

Bolyen, E., Rideout, J. R., Dillon, M. R., Bokulich, N. A., Abnet, C. C., Al-Ghalith, G. A., et al. (2019). Reproducible, interactive, scalable and extensible microbiome data science using QIIME 2. *Nat. Biotechnol.* 37, 852–857. doi: 10.1038/s41587-019-0209-9

Brown, S. P., Cornforth, D. M., and Mideo, N. (2012). Evolution of virulence in opportunistic pathogens: generalism, plasticity, and control. *Trends Microbiol.* 20, 336–342. doi: 10.1016/j.tim.2012.04.005

Bulgarelli, D., Rott, M., Schlaeppi, K., Loren, V., van Themaat, E., Ahmadinejad, N., et al. (2012). Revealing structure and assembly cues for Arabidopsis root-inhabiting bacterial microbiota. *Nature* 488, 91–95. doi: 10.1038/nature11336

Callahan, B. J., McMurdie, P. J., Rosen, M. J., Han, A. W., Johnson, A. J., and Holmes, S. P. (2016). DADA2: high-resolution sample inference from Illumina amplicon data. *Nat. Methods* 13, 581–583. doi: 10.1038/nmeth.3869

Chaparro, J. M., Badri, D. V., and Vivanco, J. M. (2014). Rhizosphere microbiome assemblage is affected by plant development. *ISME J.* 8, 790–803. doi: 10.1038/ismej.2013.196

Compant, S., Samad, A., Faist, H., and Sessitsch, A. (2019). A review on the plant microbiome: ecology, functions, and emerging trends in microbial application. *J. Adv. Res.* 19, 29–37. doi: 10.1016/j.jare.2019.03.004

Cordovez, V., Dini-Andreote, F., Carrion, V. J., and Raaijmakers, J. M. (2019). Ecology and evolution of plant microbiomes. *Ann. Rev. Microbiol.* 73, 69–88. doi: 10.1146/annurev-micro-090817-062524

Dixon, P. (2003). VEGAN, a package of R functions for community ecology. *J. Veg. Sci.* 14, 927–930. doi: 10.1111/j.1654-1103.2003.tb02228.x

Etesami, H., and Glick, B. R. (2020). Halotolerant plant growth–promoting bacteria: prospects for alleviating salinity stress in plants. *Environ. Exp. Bot.* 178:104124. doi: 10.1016/j.envexpbot.2020.104124

Fones, H. N., Bebber, D. P., Chaloner, T. M., Kay, W. T., Steinberg, G., and Gurr, S. J. (2020). Threats to global food security from emerging fungal and oomycete crop pathogens. *Nat. Food* 1, 332–342. doi: 10.1038/s43016-020-0075-0

Galloway, A. F., Akhtar, J., Marcus, S. E., Fletcher, N., Field, K., and Knox, P. (2020). Cereal root exudates contain highly structurally complex polysaccharides with soil-binding properties. *Plant J.* 103, 1666–1678. doi: 10.1111/tpj.14852

Hannula, S. E., Heinen, R., Huberty, M., Steinauer, K., De Long, J. R., Jongen, R., et al. (2021). Persistence of plant-mediated microbial soil legacy effects in soil and inside roots. *Nat. Commun.* 12:5686. doi: 10.1038/s41467-021-25971-z

Haskett, T. L., Tkacz, A., and Poole, P. S. (2021). Engineering rhizobacteria for sustainable agriculture. *ISME J.* 15, 949–964. doi: 10.1038/s41396-020-00835-4

He, Z., Webster, S., and He, S. Y. (2022). Growth-defense trade-offs in plants. *Curr. Biol.* 32, R634–R639. doi: 10.1016/j.cub.2022.04.070

Ji, M., Kong, W., Stegen, J., Yue, L., Wang, F., Dong, X., et al. (2020). Distinct assembly mechanisms underlie similar biogeographical patterns of rare and abundant bacteria in Tibetan plateau grassland soils. *Environ. Microbiol.* 22, 2261–2272. doi: 10.1111/1462-2920.14993

Jiang, Z., Tu, L., Yang, W., Zhang, Y., Hu, T., Ma, B., et al. (2021). The chromosome-level reference genome assembly for Panax notoginseng and insights into ginsenoside biosynthesis. *Plant Commun.* 2:100113. doi: 10.1016/j.xplc.2020.100113

Jiao, S., and Lu, Y. (2020). Abundant fungi adapt to broader environmental gradients than rare fungi in agricultural fields. *Glob. Chang. Biol.* 26, 4506–4520. doi: 10.1111/gcb.15130

Jiao, S., Yang, Y., Xu, Y., Zhang, J., and Lu, Y. (2020). Balance between community assembly processes mediates species coexistence in agricultural soil microbiomes across eastern China. *ISME J.* 14, 202–216. doi: 10.1038/s41396-019-0522-9

Kalam, S., Basu, A., and Podile, A. R. (2022). Difficult-to-culture bacteria in the rhizosphere: the underexplored signature microbial groups. *Pedosphere* 32, 75–89. doi: 10.1016/s1002-0160(21)60062-0

Kim, D., Paggi, J. M., Park, C., Bennett, C., and Salzberg, S. L. (2019). Graph-based genome alignment and genotyping with HISAT2 and HISAT-genotype. *Nat. Biotechnol.* 37, 907–915. doi: 10.1038/s41587-019-0201-4

Kohl, J., Kolnaar, R., and Ravensberg, W. J. (2019). Mode of action of microbial biological control agents against plant diseases: relevance beyond efficacy. *Front. Plant Sci.* 10:845. doi: 10.3389/fpls.2019.00845

Kraft, N. J. B., Adler, P. B., Godoy, O., James, E. C., Fuller, S., Levine, J. M., et al. (2014). Community assembly, coexistence and the environmental filtering metaphor. *Funct. Ecol.* 29, 592–599. doi: 10.1111/1365-2435.12345

Kumar, L., and Futschik, M. E. (2007). Mfuzz: a software package for soft clustering of microarray data. *Bioinformation* 2, 5–7. doi: 10.6026/97320630002005

Leibold, M. A., Holyoak, M., Mouquet, N., Amarasekare, P., Chase, J. M., Hoopes, M. F., et al. (2004). The meta community concept: a framework for multi-scale community ecology. *Ecol. Lett.* 7, 601–613. doi: 10.1111/j.1461-0248.2004.00608.x

Li, Z., Bai, X., Jiao, S., Li, Y., Li, P., Yang, Y., et al. (2021). A simplified synthetic community rescues *Astragalus mongholicus* from root rot disease by activating plant-induced systemic resistance. *Microbiome* 9:217. doi: 10.1186/s40168-021-01169-9

Li, J., Bao, Y., Wang, Z., Yang, Q., and Cui, X. (2022). Research progress in diseases of *Panax notoginseng*. *Physiol. Mol. Plant Pathol.* 121:101878. doi: 10.1016/j.pmpp.2022.101878

Li, P., Tedersoo, L., Crowther, T. W., Dumbrell, A. J., Dini-Andreote, F., Bahram, M., et al. (2023). Fossil-fuel-dependent scenarios could lead to a significant decline of global plant-beneficial bacteria abundance in soils by 2100. *Nat. Food* 4, 996–1006. doi: 10.1038/s43016-023-00869-9

Liao, Y., Smyth, G. K., and Shi, W. (2014). Feature counts: an efficient general purpose program for assigning sequence reads to genomic features. *Bioinformatics* 30, 923–930. doi: 10.1093/bioinformatics/btt656

Ma, L., Cao, Y. H., Cheng, M. H., Huang, Y., Mo, M. H., Wang, Y., et al. (2013). Phylogenetic diversity of bacterial endophytes of *Panax notoginseng* with antagonistic characteristics towards pathogens of root-rot disease complex. *Antonie Van Leeuwenhoek* 103, 299–312. doi: 10.1007/s10482-012-9810-3

Major, I. T., Yoshida, Y., Campos, M. L., Kapali, G., Xin, X. F., Sugimoto, K., et al. (2017). Regulation of growth-defense balance by the JASMONATE ZIM-DOMAIN (JAZ)-MYC transcriptional module. *New Phytol.* 215, 1533–1547. doi: 10.1111/nph.14638

Mathieu, A., Cournede, P. H., Letort, V., Barthelemy, D., and de Reffye, P. (2009). A dynamic model of plant growth with interactions between development and functional mechanisms to study plant structural plasticity related to trophic competition. *Ann. Bot.* 103, 1173–1186. doi: 10.1093/aob/mcp054

Molina-Santiago, C., Pearson, J. R., Navarro, Y., Berlanga-Clavero, M. V., Caraballo-Rodriguez, A. M., Petras, D., et al. (2019). The extracellular matrix protects *Bacillus subtilis* colonies from Pseudomonas invasion and modulates plant co-colonization. *Nat. Commun.* 10:1919. doi: 10.1038/s41467-019-09944-x

Nerva, L., Sandrini, M., Moffa, L., Velasco, R., Balestrini, R., and Chitarra, W. (2022). Breeding toward improved ecological plant-microbiome interactions. *Trends Plant Sci.* 27, 1134–1143. doi: 10.1016/j.tplants.2022.06.004

Nilsson, R. H., Larsson, K. H., Taylor, A. F. S., Bengtsson-Palme, J., Jeppesen, T. S., Schigel, D., et al. (2019). The UNITE database for molecular identification of fungi: handling dark taxa and parallel taxonomic classifications. *Nucleic Acids Res.* 47, D259–D264. doi: 10.1093/nar/gky1022

Ning, D., Deng, Y., Tiedje, J. M., and Zhou, J. (2019). A general framework for quantitatively assessing ecological stochasticity. *Proc. Natl. Acad. Sci.* 116, 16892–16898. doi: 10.1073/pnas.1904623116

Pascale, A., Proietti, S., Pantelides, I. S., and Stringlis, I. A. (2019). Modulation of the root microbiome by plant molecules: the basis for targeted disease suppression and plant growth promotion. *Front. Plant Sci.* 10:1741. doi: 10.3389/fpls.2019.01741

Peng, Z., Liu, Y., Qi, J., Gao, H., Li, X., Tian, Q., et al. (2023). The climate-driven distribution and response to global change of soil-borne pathogens in agroecosystems. *Glob. Ecol. Biogeogr.* 32, 766–779. doi: 10.1111/geb.13662

Perez-Gutierrez, R. A., Lopez-Ramirez, V., Islas, A., Alcaraz, L. D., Hernandez-Gonzalez, I., Olivera, B. C., et al. (2013). Antagonism influences assembly of a Bacillus guild in a local community and is depicted as a food-chain network. *ISME J.* 7, 487–497. doi: 10.1038/ismej.2012.119

Philippot, L., Raaijmakers, J. M., Lemanceau, P., and van der Putten, W. H. (2013). Going back to the roots: the microbial ecology of the rhizosphere. *Nat. Rev. Microbiol.* 11, 789–799. doi: 10.1038/nrmicro3109

Pohlert, T. (2021). PMCMRplus: Calculate pairwise multiple comparisons of mean rank sums extended. R package version 1.9. 6. Available at: https://cran.r-project.org/web/packages (Accessed February 15, 2023).

Põlme, S., Abarenkov, K., Henrik Nilsson, R., Lindahl, B. D., Clemmensen, K. E., Kauserud, H., et al. (2021). FungalTraits: a user-friendly traits database of fungi and fungus-like stramenopiles. *Fungal Divers.* 105, 1–16. doi: 10.1007/s13225-020-00466-2

Pruesse, E., Quast, C., Knittel, K., Fuchs, B. M., Ludwig, W., Peplies, J., et al. (2007). SILVA: a comprehensive online resource for quality checked and aligned ribosomal RNA sequence data compatible with ARB. *Nucleic Acids Res.* 35, 7188–7196. doi: 10.1093/nar/gkm864

Ruiz-May, E., Kim, S. J., Brandizzi, F., and Rose, J. K. (2012). The secreted plant N-glycoproteome and associated secretory pathways. *Front. Plant Sci.* 3:117. doi: 10.3389/fpls.2012.00117

Russ, D., Fitzpatrick, C. R., Teixeira, P. J. P. L., and Dangl, J. L. (2023). Deep discovery informs difficult deployment in plant microbiome science. *Cell* 186, 4496–4513. doi: 10.1016/j.cell.2023.08.035

Sasse, J., Martinoia, E., and Northen, T. (2018). Feed your friends: do plant exudates shape the root microbiome? *Trends Plant Sci.* 23, 25–41. doi: 10.1016/j.tplants.2017.09.003

Shannon, P., Markiel, A., Ozier, O., Baliga, N. S., Wang, J. T., Ramage, D., et al. (2003). Cytoscape: a software environment for integrated models of biomolecular interaction networks. *Genome Res.* 13, 2498–2504. doi: 10.1101/gr.1239303

Sloan, W. T., Lunn, M., Woodcock, S., Head, I. M., Nee, S., and Curtis, T. P. (2006). Quantifying the roles of immigration and chance in shaping prokaryote community structure. *Environ. Microbiol.* 8, 732–740. doi: 10.1111/j.1462-2920.2005.00956.x

Song, Y., Wilson, A. J., Zhang, X.-C., Thoms, D., Sohrabi, R., Song, S., et al. (2021). FERONIA restricts Pseudomonas in the rhizosphere microbiome via regulation of reactive oxygen species. *Nat. Plants* 7, 644–654. doi: 10.1038/s41477-021-00914-0

Stringlis, I. A., Yu, K., Feussner, K., de Jonge, R., Van Bentum, S., Van Verk, M. C., et al. (2018). MYB72-dependent coumarin exudation shapes root microbiome assembly to promote plant health. *Proc. Natl. Acad. Sci. U. S. A.* 115, E5213–E5222. doi: 10.1073/pnas.1722335115

Tan, Y., Cui, Y., Li, H., Kuang, A., Li, X., Wei, Y., et al. (2017). Diversity and composition of rhizospheric soil and root endogenous bacteria in Panax notoginseng during continuous cropping practices. *J. Basic Microbiol.* 57, 337–344. doi: 10.1002/jobm.201600464

Trivedi, P., Leach, J. E., Tringe, S. G., Sa, T., and Singh, B. K. (2020). Plant-microbiome interactions: from community assembly to plant health. *Nat. Rev. Microbiol.* 18, 607–621. doi: 10.1038/s41579-020-0412-1

van Griethuysen, P. A., Redeker, K. R., MacFarlane, S. A., Neilson, R., and Hartley, S. E. (2024). Virus-induced changes in root volatiles attract soil nematode vectors to infected plants. *New Phytol.* 241, 2275–2286. doi: 10.1111/nph.19518

Wang, T., Guo, R., Zhou, G., Zhou, X., Kou, Z., Sui, F., et al. (2016). Traditional uses, botany, phytochemistry, pharmacology and toxicology of Panax notoginseng (Burk.) F.H. Chen: a review. *J. Ethnopharmacol.* 188, 234–258. doi: 10.1016/j.jep.2016.05.005

Wang, Y., Wang, X., Sun, S., Jin, C., Su, J., Wei, J., et al. (2022). GWAS, MWAS and mGWAS provide insights into precision agriculture based on genotype-dependent microbial effects in foxtail millet. *Nat. Commun.* 13:5913. doi: 10.1038/s41467-022-33238-4

Wei, G., Li, M., Zhang, G., Chen, Z., Wei, F., Jiao, S., et al. (2022). Temporal dynamics of rhizosphere communities across the life cycle of Panax notoginseng. *Front. Microbiol.* 13:853077. doi: 10.3389/fmicb.2022.853077

Wei, G., Yang, F., Wei, F., Zhang, L., Gao, Y., Qian, J., et al. (2020). Metabolomes and transcriptomes revealed the saponin distribution in root tissues of Panax quinquefolius and Panax notoginseng. *J. Ginseng Res.* 44, 757–769. doi: 10.1016/j.jgr.2019.05.009

Weiss, S., Xu, Z. Z., Peddada, S., Amir, A., Bittinger, K., Gonzalez, A., et al. (2017). Normalization and microbial differential abundance strategies depend upon data characteristics. *Microbiome* 5:27. doi: 10.1186/s40168-017-0237-y

Wu, T., Hu, E., Xu, S., Chen, M., Guo, P., Dai, Z., et al. (2021). clusterProfiler 4.0: a universal enrichment tool for interpreting omics data. *Innovation* 2:100141. doi: 10.1016/j.xinn.2021.100141

Xie, Y., Ouyang, Y., Han, S., Se, J., Tang, S., Yang, Y., et al. (2022). Crop rotation stage has a greater effect than fertilisation on soil microbiome assembly and enzymatic stoichiometry. *Sci. Total Environ.* 815:152956. doi: 10.1016/j.scitotenv.2022.152956

Xun, W., Liu, Y., Ma, A., Yan, H., Miao, Y., Shao, J., et al. (2024). Dissection of rhizosphere microbiome and exploiting strategies for sustainable agriculture. *New Phytol.* 242, 2401–2410. doi: 10.1111/nph.19697

Yu, G., Smith, D. K., Zhu, H., Guan, Y., Lam, T. T. Y., and McInerny, G. (2016). Ggtree: an r package for visualization and annotation of phylogenetic trees with their covariates and other associated data. *Methods Ecol. Evol.* 8, 28–36. doi: 10.1111/2041-210x.12628

Zhang, G., Shi, L., Liu, C., Huang, Z., Zheng, Y., and Dong, L. (2023). Rhizosphere effects on the microbial community: specificity and conservatism across geographically disjunct Panax species. *Appl. Soil Ecol.* 192:105075. doi: 10.1016/j.apsoil.2023.105075

Zhang, G., Wei, F., Chen, Z., Wang, Y., Jiao, S., Yang, J., et al. (2022). Evidence for saponin diversity-mycobiome links and conservatism of plant-fungi interaction patterns across Holarctic disjunct Panax species. *Sci. Total Environ.* 830:154583. doi: 10.1016/j.scitotenv.2022.154583

Zhang, G., Wei, G., Wei, F., Chen, Z., He, M., Jiao, S., et al. (2021). Dispersal limitation plays stronger role in the community assembly of Fungi relative to Bacteria in rhizosphere across the arable area of medicinal plant. *Front. Microbiol.* 12:713523. doi: 10.3389/fmicb.2021.713523

Zhang, J., Wei, L., Yang, J., Ahmed, W., Wang, Y., Fu, L., et al. (2020). Probiotic consortia: reshaping the Rhizospheric microbiome and its role in suppressing root-rot disease of Panax notoginseng. *Front. Microbiol.* 11:701. doi: 10.3389/fmicb.2020.00701

Zhang, J., Zhang, N., Liu, Y. X., Zhang, X., Hu, B., Qin, Y., et al. (2018). Root microbiota shift in rice correlates with resident time in the field and developmental stage. *Sci. China Life Sci.* 61, 613–621. doi: 10.1007/s11427-018-9284-4

Zhou, J., and Ning, D. (2017). Stochastic community assembly: does it matter in microbial ecology? *Microbiol. Mol. Biol. Rev.* 81:e00002-17. doi: 10.1128/MMBR.00002-17

Zhou, X., Wang, J., Liu, F., Liang, J., Zhao, P., Tsui, C. K. M., et al. (2022). Cross-kingdom synthetic microbiota supports tomato suppression of fusarium wilt disease. *Nat. Commun.* 13:7890. doi: 10.1038/s41467-022-35452-6

frontiers | Frontiers in Microbiology

TYPE Original Research
PUBLISHED 11 February 2025
DOI 10.3389/fmicb.2025.1538093

OPEN ACCESS

EDITED BY
Dongdong Yan,
Chinese Academy of Agricultural Sciences (CAAS), China

REVIEWED BY
Farjana Sultana,
International University of Business Agriculture and Technology, Bangladesh
Xiaodong Wang,
Hebei Agricultural University, China
Huaigu Chen,
Jiangsu Academy of Agricultural Sciences (JAAS), China

*CORRESPONDENCE
Yuxing Wu
✉ wyx1209@163.com

RECEIVED 02 December 2024
ACCEPTED 27 January 2025
PUBLISHED 11 February 2025

CITATION
Wang Y, Feng J, Gao J, Han S, Li Q, Kong L and Wu Y (2025) The occurrence of wheat crown rot correlates with the microbial community and function in rhizosphere soil. *Front. Microbiol.* 16:1538093.
doi: 10.3389/fmicb.2025.1538093

The occurrence of wheat crown rot correlates with the microbial community and function in rhizosphere soil

Yajiao Wang[1], Jian Feng[2], Jianhai Gao[3], Sen Han[1], Qiusheng Li[1], Lingxiao Kong[1] and Yuxing Wu[1]*

[1]Institute of Plant Protection, Hebei Academy of Agricultural and Forestry Sciences, Baoding, China, [2]Plant Protection Plant Inspection Station of Baoding City, Baoding, China, [3]Cangxian Agriculture and Rural Bureau, Cangxian, China

Wheat crown rot (WCR) is a significant soil-borne disease affecting wheat production worldwide. Understanding the impact of wheat crown rot on the structure and function of microbial communities in the wheat rhizosphere soil can provide a theoretical basis for the mining biological control resources against WCR. In this study, rhizosphere soils with varying WCR severities (light, moderate, severe) were analyzed for chemical properties, microbial community composition and functions using high-throughput sequencing. The results revealed that WCR decreased rhizosphere soil pH, the content of available nitrogen and phosphorus, and the abundance of beneficial taxa such as *Bacillus* and *Streptomyces*. Additionally, functional predictions showed that microbial communities adapted to WCR by enhancing signaling pathways and reducing their anabolic activity. From soil with light WCR occurrence, we isolated *Bacillus velezensis* BF-237, whose abundance was reduced by WCR. Greenhouse experiments demonstrated that BF-237 achieved a control efficiency of 56.61% against WCR in artificially inoculated sterilized soil and 53.32% in natural soil. This study clarifies the impact of wheat crown rot on the community structure, and function of rhizosphere soil microorganisms, alongside identifying a promising biocontrol agent. These findings contribute to understanding WCR pathogenesis and offer practical resources for its management.

KEYWORDS

wheat crown rot, soil chemical properties, rhizosphere microbial community, *Bacillus velezensis*, biological control

1 Introduction

Wheat crown rot (WCR) is a significant soil-borne disease affecting wheat production, primarily caused by the pathogens *Fusarium pseudograminearum*, *F. graminearum*, *F. culmorum*, *etc.* (Kazan and Gardiner, 2018). In China, the predominant pathogen responsible for WCR is *F. pseudograminearum* (Deng et al., 2020; Zhang et al., 2024). These pathogens primarily infect the stem base of wheat, disrupting the water and nutrient transport system of the plant, and eventually causing browning and rotting at the stem base. During the grain-filling stage, this infection can result in white heads, severely impacting wheat yield and quality (Ozdemir et al., 2020). Wheat crown rot is prevalent worldwide, it is especially widespread and damaging in countries such as Australia, South Africa, the United States, and Canada, where in typical years, wheat crown rot can reduce wheat yield by approximately 9.5% on average, and in epidemic years, losses can reach as high as 35% (Kazan and Gardiner, 2018). In China, wheat crown rot caused by *F. pseudograminearum* was first reported in 2012, and its impact

now spans various winter wheat-growing regions nationwide (Li et al., 2012). Due to excessive fertilization, straw continued to return to the field and poor resistance of varieties, the disease showed a trend of increasing and spreading in the main wheat producing areas of Huang-Huai in China (Wang et al., 2023). Therefore, the prevention and control of wheat crown rot is urgent.

Currently, the primary methods for controlling WCR include agricultural practices (Moya-Elizondo and Jacobsen, 2016), resistant varieties (Liu and Ogbonnaya, 2015), chemical control (Zhang et al., 2022), and biological control (Feng et al., 2023). Management strategies such as removing crop residues, crop rotation, delayed sowing, and balanced fertilization can effectively reduce the incidence of WCR (Wang et al., 2023), though their control efficacy is relatively low. Planting resistant varieties is one of the simplest and most effective strategies (Rahman et al., 2021), however, the availability of resistant varieties is currently limited. Moreover, the prolonged and excessive use of chemical agents not only causes environmental pollution but also increases the resistance of pathogens to these chemicals (Zhang et al., 2023). Environmentally friendly and efficient biological control has emerged as a key approach for managing WCR. Although several biocontrol agents have been reported (Feng et al., 2023; Li et al., 2022; Xu et al., 2022), only a limited number are currently in widespread use. This is due to challenges such as the poor environmental adaptability of biocontrol agents, insufficient formulation stability, and high development costs. To promote the extensive application of biocontrol agents for WCR, it is necessary to screen strains with high efficacy and strong environmental adaptability.

Soil microorganisms play a crucial role in the occurrence and suppression of crop diseases (Yuan et al., 2020). On one hand, soil microorganisms act as an important reservoirs for biological control agents against crop diseases. Microorganisms in the soil, such as *Bacillus* spp. and *Streptomyces* spp., can inhibit the growth of pathogens by secreting antimicrobial compounds, competing for ecological niches, or inducing systemic resistance in plants (Saxena et al., 2020). On the other hand, a rich diversity of soil microorganisms contributes to a stable and complementary ecosystem that effectively suppresses the spread and proliferation of pathogens. Conversely, low microbial diversity may allow pathogens to dominate ecological niches, leading to disease outbreaks (Jayaraman et al., 2021). Following the occurrence of crop diseases, the extensive proliferation of pathogens can alter the structure of soil microbial communities, characterized by an increase in pathogen abundance and a decrease in the abundance of beneficial microorganisms (Shi et al., 2019). This may even reduce the overall diversity and functionality of soil microorganisms. Such changes can further exacerbate disease occurrence. Previous studies have shown that the occurrence of tomato *Fusarium* wilt disease decreases the pH of rhizosphere soil and the alpha diversity of rhizosphere bacteria, and reduced the abundance of beneficial bacteria such as *Bacillus* and *Lysinibacillus* (Yang et al., 2024). Similarly, the occurrence of banana wilt disease significantly decreases the microbial diversity in banana rhizosphere soil and alters the microbial community structure (Zhou et al., 2019). However, to date, no studies have investigated the relationship between the occurrence of wheat crown rot and soil microbial communities.

Understanding the disruption mechanisms of crop diseases on soil microbial communities and the adaptive strategies of rhizosphere microbial communities under disease stress is crucial for developing effective disease control measures. In this study, rhizosphere soils were collected from wheat fields with varying levels of WCR severity (light, moderate, and severe). The effects of disease occurrence on the chemical properties of wheat rhizosphere soil was measured, and the community structure and functions of bacteria and fungi were analyzed using Illumina MiSeq high-throughput sequencing technology. This study provides insights into the interactions between WCR and soil microorganisms, offering new perspectives for the targeted selection of beneficial microorganisms antagonistic to wheat crown rot and for disease management strategies.

2 Materials and methods

2.1 Site description and sample collection

The experimental site was located in a wheat farm in Ningjin County, Xingtai City, Hebei Province, China (37° 37' N, 114° 53′ E, 18 m a.s.l.), which has a subtropical monsoon climate. The area has an average annual temperature of 12.5°C and an average annual rainfall of 1,150–1,550 mm. Winter wheat is rotated with summer maize. The winter wheat variety used was Jimai 22, and the maize variety was Xianyu 335. In 2022, during the wheat filling stage (mid-May), three plots (200 m^2) with different severities of wheat crown rot—light (L), moderate (M), and severe (S) were selected from the wheat farm. Following the "W" multiple-point sampling method, wheat rhizosphere soil was collected. For each plot, soil samples were collected in three replicates, with each replicate including 10 sampling points, and 20 wheat plants per sampling point. Using a sampling spade, the entire wheat root system was carefully excavated, loose soil was shaken off and collected for greenhouse experiment, then whole wheat roots were subsequently placed in sterilized PBS buffer and shaked for 30 min, finally the rhizosphere soil was collected by centrifugation at 12,000 g for 5 min (Wu et al., 2024). The remaining wheat plants were used to investigate the incidence of wheat crown rot. A portion of the soil sample was stored at −80°C for DNA extraction, and the remainder was stored at 4°C for analyses of soil chemical properties.

2.2 Evaluation of the occurrence of wheat crown rot and quantitative detection of *Fusarium pseudograminearum* in the rhizosphere soil

Disease severity of WCR at the filling stage was rated on a 0–4 scale based on the symptoms observed on the crown (Zhang et al., 2022). 0: completely healthy; 1: light browning on the crown, less than 25% necrosis; 2: 25–50% necrosis; 3: 51–75% necrosis; 4: greater than 75% necrosis, or show symptoms of dried white ears or complete plant death. A disease index was then calculated as $\sum$ (Number of diseased plants with each score × Highest score)/(Total number of plants × Highest score) × 100%.

Genomic DNA from 0.5 g rhizosphere soil was extracted using the E.Z.N.A. Soil DNA Kit (Omega Bio-TEK, Norcross, GA, United States) following the protocol provided by the manufacturer. DNA concentration was assessed with a TBS-380 Mini-Fluorometer (Turner Biosystems, CA, United States) and its purity was assessed with NanoDrop 2000 UV–Vis spectrophotometer (Thermo Scientific,

Wilmington, DE, United States). DNA quality was confirmed using 1.2% agarose gel electrophoresis. To assess the titers of *F. pseudograminearum* in the rhizosphere soil, qPCR was conducted using primers Fptri3eF (5'-CAAGTTTGATCCAGGGTAATCC-3′) and Fptri3eR (5'-GCTG TTTCTCTTAGTCTTCCTCA-3′) as described by Obanor and Chakraborty (2014). A 20 μL reaction mixture was prepared using 1 μL of template DNA, following the protocol provided by TaKaRa Ex Taq HS DNA Polymerase. Amplification conditions included an initial denaturation at 95°C for 30 s, followed by 40 cycles of 95°C for 5 s and 60°C for 34 s, performed on an ABI7500 Real-Time PCR system. Each reaction was run in triplicate. Genome copies of *F. pseudograminearum* were quantified based on a standard curve generated from a recombinant plasmid containing the target DNA sequence.

2.3 Soil chemical property analysis

Rhizosphere soil samples were dried, ground and sieved before soil analysis. Soil chemical property was measured with the methods of Wang et al. (2021). Soil pH was measured using the potentiometric method with a soil-to-water ratio of 1:5 (mass-to-volume ratio). Soil organic carbon was determined using the potassium dichromate oxidation method with dilution and heating. Available phosphorus was measured using the acid-soluble molybdenum-antimony colorimetric method, and available potassium was determined by the ammonium acetate extraction method with flame photometry.

2.4 Illumina Miseq sequencing

The bacterial V3–V4 region of the 16S rDNA was amplified using specific primers 338F (5'-ACTCCTACGGGAGGCAGCAG-3′) and 806R (5'-GGACTACHVGGGTWTCTAA T-3′), and the fungal internal transcribed spacer-1 (ITS-1) region was amplified using specific primers primers ITS1F (5'-CTTGGTCATTTAGAGG AAGTAA--3′) and ITS2R (5'-GCTGCGTTCTTCATCGATGC--3′). The PCR amplification system was set up in a 20 μL reaction volume: 4 μL of 5 × FastPfu buffer, 2 μL of 2.5 mmol·L^{-1} dNTPs, 0.8 μL of each primer (5 μmol/L), 0.4 μL of FastPfu polymerase, and 1 μL of DNA template (20 ng/μL), with ddH_2O added to a final volume of 20 μL. The PCR cycling conditions were as follows: an initial denaturation at 95°C for 3 min, followed by 27 cycles of denaturation at 95°C for 30 s, annealing at 55°C for 30 s, and extension at 72°C for 30 s, with a final extension at 72°C for 10 min. PCR products were checked by 1.5% agarose gel electrophoresis, recovered, and purified. Samples were then sent to Shanghai Majorbio Bio-Pharm Technology Co., Ltd. for library construction and high-throughput sequencing on the Illumina MiSeq platform (Illumina, San Diego, United States) according to standard protocols.

2.5 Processing of sequencing data

Raw sequencing data were quality-controlled using Trimmomatic software, and sequences were assembled with FLASH software (Magoc and Salzberg, 2011). (1) A 50 bp sliding window was applied, and bases in the trailing sequence were trimmed when the average quality score within the window was below 20. Sequences shorter than 50 bp after quality control were removed. (2) Paired-end reads were merged based on overlapping regions with a minimum overlap length of 10 bp and a maximum mismatch rate of 0.2; unmergeable reads were discarded. (3) Sequences were demultiplexed based on barcodes and primers, with sequences containing ambiguous bases being removed. This process produced high-quality sequences for subsequent analysis. The raw sequences used in this study have been deposited in the NCBI (National Center for Biotechnology Information) database under the Sequence Read Archive (SRA) accession number PRJNA881807.

2.6 Isolation and identification

A total of 1 g of rhizosphere soil with slight occurrence of wheat crown rot was subjected to serial dilution and plated on LB agar (tryptone 10 g, yeast extract 5 g, NaCl 10 g, agar 15 g, ddH_2O up to 1 L, pH 7.0), followed by incubation at 37°C. Bacterial colonies with different colony characteristics were isolated and maintained on LB agar for further analysis. To assess the inhibition of *F. pseudograminearum* mycelial growth, a 5 mm agar plug of the fungus was placed in the center of a PDA plate (potato infusion 200 g, glucose 20 g, agar 15 g, ddH_2O up to 1 L), bacterial isolates (ddH_2O was used as control) inoculated 2.5 cm away from the fungal plug. After incubation at 28°C for 5 days, the inhibition zone between fungal and bacterial colonies was measured. The reaction to Gram staining were tested (Li et al., 2021). Genomic DNA of BF-237 was extracted using the MiniBEST Bacterial Genomic DNA Extraction Kit Ver. 3.0 (Takara, Beijing, China). The gene of *gyrB* was amplified with primers UP-1S and UP-2Sr (Dong et al., 2023) and sequenced (Tsingke Biotechnology, Beijing, China). The resulting *gyrB* sequence was analyzed using blastn against the NCBI nr database to identify similarities. Additionally, 12 other *gyrB* sequences were selected for phylogenetic analysis.

2.7 Biocontrol effect of BF-237 on wheat crown rot and growth promotion on wheat

In a greenhouse experiment, the biocontrol effect of BF-237 on wheat crown rot in sterilized field soil and in untreated field soil were investigated. Bulk soil with severe wheat crown rot was collected as described in method 2.1. Half of the collected soil was directly used for greenhouse experiment, the remaining half of the soil was autoclaved before use. The soil was autoclaved using the liquid cycle for 30 min at 121°C, then cooled at room temperature, then we repeated this procedure, sterilized soil was stored at 4°C until use. Soak wheat seeds in 2% sodium hypochlorite for 5 min, then rinse three times with water. Surface sterilized wheat seeds (Shixin 828) were soaked in 10^9 bacterial cells/mL BF-237 for 4 h at 28°C. *F. pseudograminearum* was grown in the sodium carboxymethyl cellulose medium (CMC, carboxymethyl cellulose 10 g, KH_2PO4 1 g, $MgSO_4{\cdot}7H_2O$ 0.5 g, $FeSO_4{\cdot}7H_2O$ 0.01 g, NaCl 0.5 g, yeast extract 1 g, ddH_2O up to 1 L) broth at 28°C and 180 rpm for 5 days to produce spores. Five treatments were set up, (1): SCK1, sterilized seeds were planted in sterile soil; (2): SCK2, sterilized seeds were planted in sterile soil with *F. pseudograminearum* (10^5 spores/g soil); (3): SB237, seeds soaked with BF-237 were planted in sterile soil with *F. pseudograminearum* (10^5 spores/g soil); (4): FCK, sterilized seeds were planted in field soil;

and (5): FB237, seeds soaked with BF-237 were planted in field soil. There were 4 replicates per treatment, 5 pots per replicate, and 20 seeds per pot. The pots were placed in a greenhouse with 16 h light/8 h dark at 25°C. At 21 days after sowing, wheat height was measured, and the severity and severity index of wheat crown rot were classified and calculated as described in method 2.2.

2.8 Statistical analyses

The alpha diversity (Shannon and Simpson indices) of the bacterial and fungal community were calculated by Mothur v.1.30[1] and the vegan package in R. Beta diversity was examined by Principal Coordinate Analysis (PCoA) based on Bray-Curtis distances in R. Redundancy analysis (RDA) was executed in R to analyze the relationship between dominant taxa of microorganisms and soil properties. Correlation networks were constructed to investigate the relationships among environmental factors, bacterial diversity indices, and wheat crown rot, employing the igraph and psych packages in R. All data underwent normality checks with the Shapiro–Wilk test prior to statistical analysis in SPSS v.16.0 (SPSS, Chicago, IL, United States). For non-normally distributed data, including alpha diversity indices, wheat crown rot, and the relative abundance of key genera, we applied the Kruskal-Wallis test for significance, using SPSS v.16.0.

3 Results

3.1 Wheat crown rot incidence and rhizosphere soil chemical properties

According to field survey results, the disease indices of wheat crown rot in light (L), moderate (M), and severe (S) plots were 2.4, 14.2, and 41.6, respectively (Figure 1A). The quantity of *F. pseudograminearum* in the rhizosphere soil for the L, M, and S plots was 5.58×10^3 copies/g, 2.25×10^4 copies/g, and 3.26×10^5 copies/g (Figure 1B), indicating a positive correlation between the incidence of wheat crown rot and the concentration of *F. pseudograminearum* in the rhizosphere soil. Following the occurrence of wheat crown rot, the contents of organic matter, available phosphorus, and available potassium in the wheat rhizosphere soil showed a decreasing trend. Compared to the L, these three indicators in the M rhizosphere soil decreased by 0.37, 8.18, and 23.77%, respectively. While in S, the reductions reached 2.59, 29.84, and 24.63%, respectively. Additionally, soil pH gradually decreased with the progression of wheat crown rot. The pH in the S plot was 7.46, which significantly lower than in the L pot (7.88) (Table 1).

3.2 Effects of wheat crown rot on rhizosphere microbial diversity

In this study, sequencing data were rarefied to the minimum sample size for alpha diversity index analysis. Results showed that coverage rates for all treatments exceeded 98%, indicating that the bacterial and fungal sequences obtained in this study achieved good coverage and that the sequencing depth was sufficient for analyzing bacterial and fungal diversity. The number of bacterial and fungal OTUs decreased as the disease index of wheat crown rot increased. The Sob, Chao, and Shannon indices for bacteria showed no significant change between L and M levels but were significantly lower in S, which increased by 11.61, 7.10, and 14.34%, respectively. For fungi, the Sob, Chao, and Shannon indices decreased with increasing disease index; compared to L, these indices in M decreased by 13.99, 10.72, and 10.62%, respectively, and in S by 27.97, 20.87, and 24.78%, respectively (Table 2). These results indicate that the occurrence of wheat crown rot reduced the alpha diversity of bacteria and fungi in the wheat rhizosphere soil.

1 http://www.mothur.org/

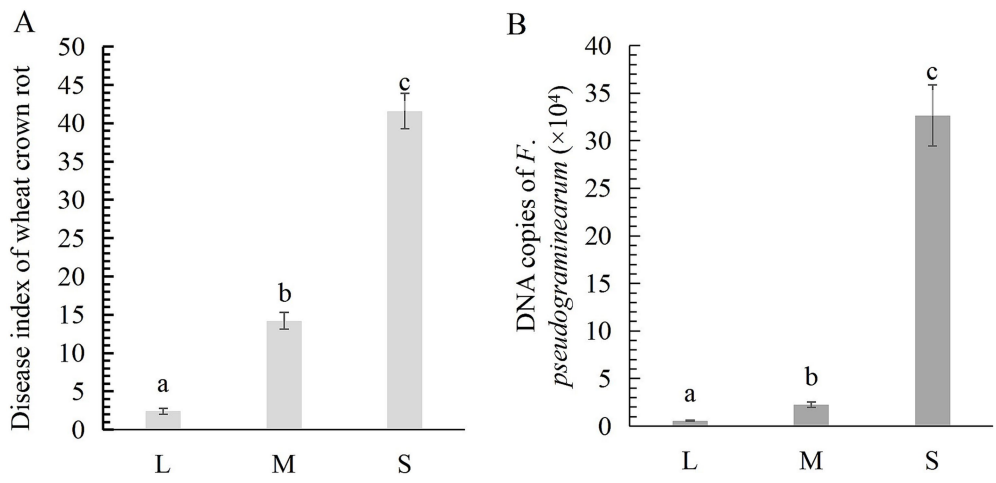

FIGURE 1
The disease index of wheat crown rot **(A)** and the abundance of *F. pseudograminearum* in wheat rhizosphere soil **(B)**. Data for the same disease with different letters above bars differed significantly ($p < 0.05$) according to Kruskal-Wallis test. L, M, and S: soil with different severities of wheat crown rot—light (L), moderate (M), and severe (S).

TABLE 1 The occurrence of wheat crown rot and soil physical and chemical properties.

Treatment	Organic matter g/kg	Available phosphorus mg/kg	Available potassium mg/kg	pH
L	27.0 ± 0.66a	439.9 ± 8.2a	345.0 ± 3.6a	7.88 ± 0.02a
M	26.9 ± 0.13a	404.5 ± 10.1b	263.3 ± 17.6b	7.82 ± 0.02ab
S	26.3 ± 0.56a	308.4 ± 9.7c	259.7 ± 6.9b	7.46 ± 0.05b

Different lowercases after the data indicate significant difference (p<0.05). L, M, and S: soil with different severities of wheat crown rot—light (L), moderate (M), and severe (S).

The effect of wheat crown rot on the beta diversity of bacterial and fungal communities in the wheat rhizosphere soil was analyzed using PCoA. For bacteria (Figure 2A), the PCoA results indicated that the PC1 and PC2 axes explained 50.18 and 11.65% of the variance in the bacterial community, respectively. Between L and M, there was little difference in bacterial community structure on the PC1 axis, with a 0.16 difference on the PC2 axis. However, in S, the bacterial community structure showed a significant difference on the PC1 axis compared to L and M, with a variance of approximately 0.3 (Supplementary Table S1). For fungi (Figure 2B), the PCoA results showed that the PC1 and PC2 axes explained 55.31 and 33.25% of the variance, respectively. In L and M, fungal community structure had a minor difference of 0.18 on the PC1 axis and a difference of 0.37 on the PC2 axis. In contrast, in S, fungal community structure showed significant differences on the PC1 axis compared to L and M, with differences of 0.32 and 0.50, respectively (Supplementary Table S1). These results demonstrate that wheat crown rot significantly altered the bacterial and fungal community structure in wheat rhizosphere soil on the PC1 axis.

3.3 Effects of wheat crown rot on rhizosphere microbial communities

Phylum-level analysis of bacterial community composition in wheat rhizosphere soil revealed 10 dominant phyla with relative abundance >1%, including Actinobacteria, Proteobacteria, Acidobacteria, Chloroflexi, Bacteroidetes, Gemmatimonadetes, Saccharibacteria, Firmicutes, Nitrospirae, and Verrucomicrobia (Figure 3A). In L, M, and S, the relative abundances of Actinobacteria (33.30, 33.56, 40.67%), Chloroflexi (9.21, 9.97, 11.85%), Saccharibacteria (1.71, 1.94, 1.95%), and Verrucomicrobia (0.96, 1.03, 1.09%) increased with the rise in wheat crown rot disease index. In contrast, the relative abundances of Acidobacteria (12.56, 11.80, 11.14%), Bacteroidetes (6.66, 6.37, 5.25%), and Nitrospirae (2.17, 1.45, 0.91%) decreased with the rise in wheat crown rot disease index. At the genus level (Figure 3B), grouping bacteria with <1% abundance and unclassified groups as "Other," we found that the dominant genera with relative abundance >1% displayed varied trends. In L, M, and S, *Bacillus* (1.26, 1.34, 0.87%), *Streptomyces* (2.12, 1.74, 1.56%), *Nitrospira* (2.17, 1.45, 0.91%), *Nonomuraea* (1.21, 1.65, 0.20%), and *Gaiella* (1.45, 0.90, 0.76%) decreased with the rise in wheat crown rot disease index. However, *Blastococcus*, *Sphingomonas*, *Skermanella*, *Pedobacter*, *Roseiflexus*, *Massilia*, and *Rubrobacter* increased with the rise in wheat crown rot disease index.

At the phylum level (Figure 3C), the composition of the wheat rhizosphere fungal community was analyzed, and the results showed that the dominant phyla were Ascomycota, Zygomycota, and Basidiomycota. Their relative abundances ranged from 89.18 to 95.20%, 3.17 to 9.27%, and 0.32 to 1.08%, respectively. Compared to L, there were no significant differences in the relative abundance of these three phyla in M. However, in S, the relative abundance of Ascomycota decreased by 6.31%, while the relative abundance of Zygomycota and Basidiomycota increased by 1.92 and 2.38 times, respectively. At the genus level (Figure 3D), fungal groups with a relative abundance of less than 1% and unclassified groups were categorized as "others." In L, M, and S, the relative abundances of *Alternaria* (12.47, 13.15, 27.55%), *Rhizopus* (3.32, 3.02, 8.82%), *Oedocephalum* (0.001, 1.40, 5.51%), *Gibberella* (4.19, 5.28, 5.44%), and *Cyphellophora* (0.2, 0.49, 1.04%) increased with the rise in wheat crown rot disease index. In contrast, the relative abundance of *Mycosphaerella* (31.65, 21.13, 21.55%), *Pyrenochaetopsis* (8.18, 6.34, 5.23%), *Acremonium* (4.50, 4.86, 3.04%), *Myrothecium* (2.48, 1.05, 0.96%), *Myrmecridium* (1.86, 0.41, 0.24%), and *Preussia* (3.06, 0.11, 0.05%) decreased with the rise in wheat crown rot disease index.

3.4 Correlation between environmental factors and rhizosphere microbial communities

The analysis of the relationship between environmental factors and genus-level bacterial changes in the rhizosphere soil showed that the first principal component (RDA1) and the second principal component (RDA2) explained 49.35 and 15.49% of all variables, respectively (Figure 4A). The bacterial community structure in the rhizosphere soil of wheat was partially overlapping between fields with light and moderate wheat crown rot, indicating similarity in community structure. However, in fields with severe wheat crown rot, the bacterial community structure in the rhizosphere soil was located further away on the RDA2 axis compared to fields with light and moderate wheat crown rot, with no overlap, suggesting a significant change in bacterial community structure in heavily affected fields. Additionally, RDA revealed that different environmental variables had varying impacts on the overall bacterial community. Available phosphorus ($r^2 = 0.937$; $p = 0.003$) had a highly significant effect on soil bacterial community composition ($p < 0.01$), while wheat crown rot ($r^2 = 0.820$; $p = 0.017$) had a significant effect ($p < 0.05$) (Supplementary Table S2). VPA analysis showed that wheat crown rot occurrence and changes in soil chemical properties explained 64.36% of the variation in soil bacterial diversity, with wheat crown rot accounting for 54.76%, soil chemical properties accounting for 54.36%, and their interaction accounting for 44.76%. Among soil chemical properties, available phosphorus had the highest explanatory power, at 45.81% (Figure 4C).

The analysis of the relationship between environmental factors and genus-level fungal changes in the rhizosphere soil indicated that the first principal component (RDA1) and the second principal component (RDA2) explained 48.74 and 35.38% of all variables,

TABLE 2 Statistics of alpha diversity of bacterial and fungal community.

		Otus	Sobs	Shannon	Chao	Coverage
Bacteria	L	2,897 ± 60a	2,423 ± 51.58a	6.64 ± 0.06a	2,847 ± 54.27a	0.985 ± 0.001a
	M	2,893 ± 54a	2,463 ± 33.98a	6.65 ± 0.04a	2,813 ± 52.19a	0.990 ± 0.002a
	S	2,528 ± 22b	2,171 ± 42.40b	6.20 ± 0.13b	2,490 ± 62.79b	0.986 ± 0.002a
Fungi	L	394 ± 13a	286 ± 21.57a	3.45 ± 0.12a	339 ± 18.20a	0.998 ± 0.000a
	M	374 ± 18a	246 ± 18.57b	3.08 ± 0.18b	303 ± 14.99b	0.998 ± 0.000a
	S	288 ± 18b	206 ± 13.89c	2.73 ± 0.10c	255 ± 19.93c	0.998 ± 0.000a

Different lowercases after the data indicate significant difference (p<0.05). L, M, and S: soil with different severities of wheat crown rot—light (L), moderate (M), and severe (S).

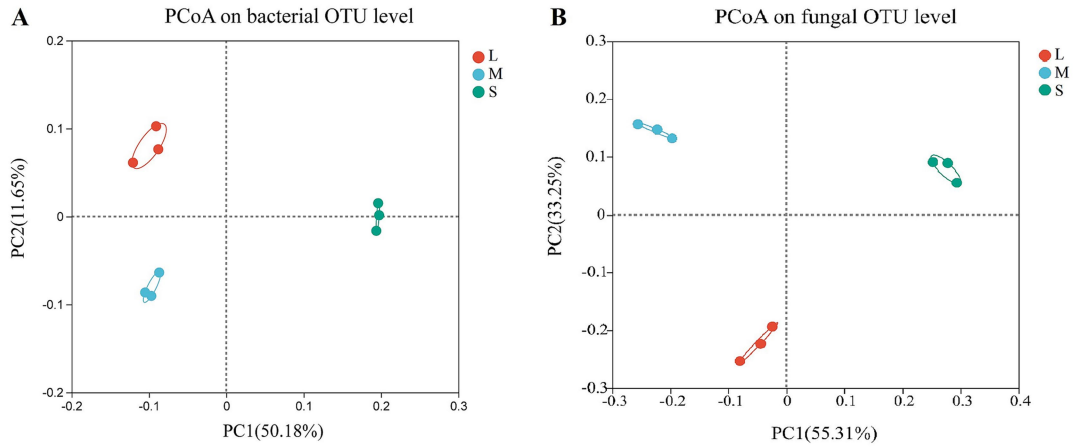

FIGURE 2
Principal coordinate analysis (PCoA) of wheat rhizosphere soil bacterial **(A)** and fungal **(B)** community. The X-axis and Y-axis represent the two selected principal coordinate axes, and the percentage represents the explanatory value of the principal coordinate axes to the difference in sample composition. L, M, and S: soil with different severities of wheat crown rot—light (L), moderate (M), and severe (S).

respectively (Figure 4B). The fungal community structure in the rhizosphere soil of wheat showed no overlap among fields with light, moderate, and severe wheat crown rot, indicating that the occurrence of crown rot altered the fungal community structure in the rhizosphere soil. Furthermore, RDA revealed that various environmental variables had distinct effects on the overall fungal community composition. Available phosphorus ($r^2 = 0.936$; $p = 0.009$) and pH ($r^2 = 0.846$; $p = 0.004$) had highly significant impacts on soil fungal community composition ($p < 0.01$), while wheat crown rot ($r^2 = 0.821$; $p = 0.017$) and available potassium ($r^2 = 0.926$; $p = 0.027$) had significant effects ($p < 0.05$) (Supplementary Table S2). VPA analysis showed that the occurrence of wheat crown rot and changes in soil chemical properties accounted for 77.51% of the variation in fungal diversity in the rhizosphere soil, with wheat crown rot explaining 35.61%, soil chemical properties explaining 74.01%, and their interaction explaining 32.11%. Among soil chemical properties, available phosphorus had the highest explanatory power at 32.34% (Figure 4D).

3.5 Effects of wheat crown rot on the functions of rhizosphere microorganisms

Based on the KEGG database, the PICRUSt2 tool was used to functionally predict bacterial 16S OTU information, identifying six primary metabolic pathways: metabolism, genetic information processing, environmental information processing, cellular processes, organismal systems, and human diseases. Within the metabolism pathway, 11 Level 2 functional groupings were identified (Figure 5A). The relative abundances of these 11 metabolic genes showed no significant differences between fields with light (L) and moderate (M) wheat crown rot incidence. However, compared to L, fields with severe (S) wheat crown rot had higher relative abundances of genes associated with xenobiotic degradation and metabolism, amino acids, secondary metabolite synthesis, and carbon metabolism, decreasing by 6.16, 3.24, 3.88, and 3.36%, respectively. In contrast, the relative abundances of genes related to glycine synthesis and signal transduction significantly increased, with reductions of 2.51 and 12.12%, respectively, compared to L.

According to functional predictions by FUNGuild, fungal functional classifications in the samples were identified (Figure 5B), showing that the fungal community could be divided into seven categories: plant pathogens, animal pathogens, dung saprotrophs, undefined saprotrophs, endophytes, mycorrhizal fungi, and unclassified fungi. The relative abundance of plant pathogens showed no significant difference between fields with light (L) and moderate (M) wheat crown rot incidence. However, in field with severe (S) wheat crown rot, the relative abundance of plant pathogens increased by 17.22 and 18.66% compared to L and M, respectively. The relative abundance of dung saprotrophs and undefined saprotrophs gradually decreased with the severity of wheat crown rot. Compared to L and

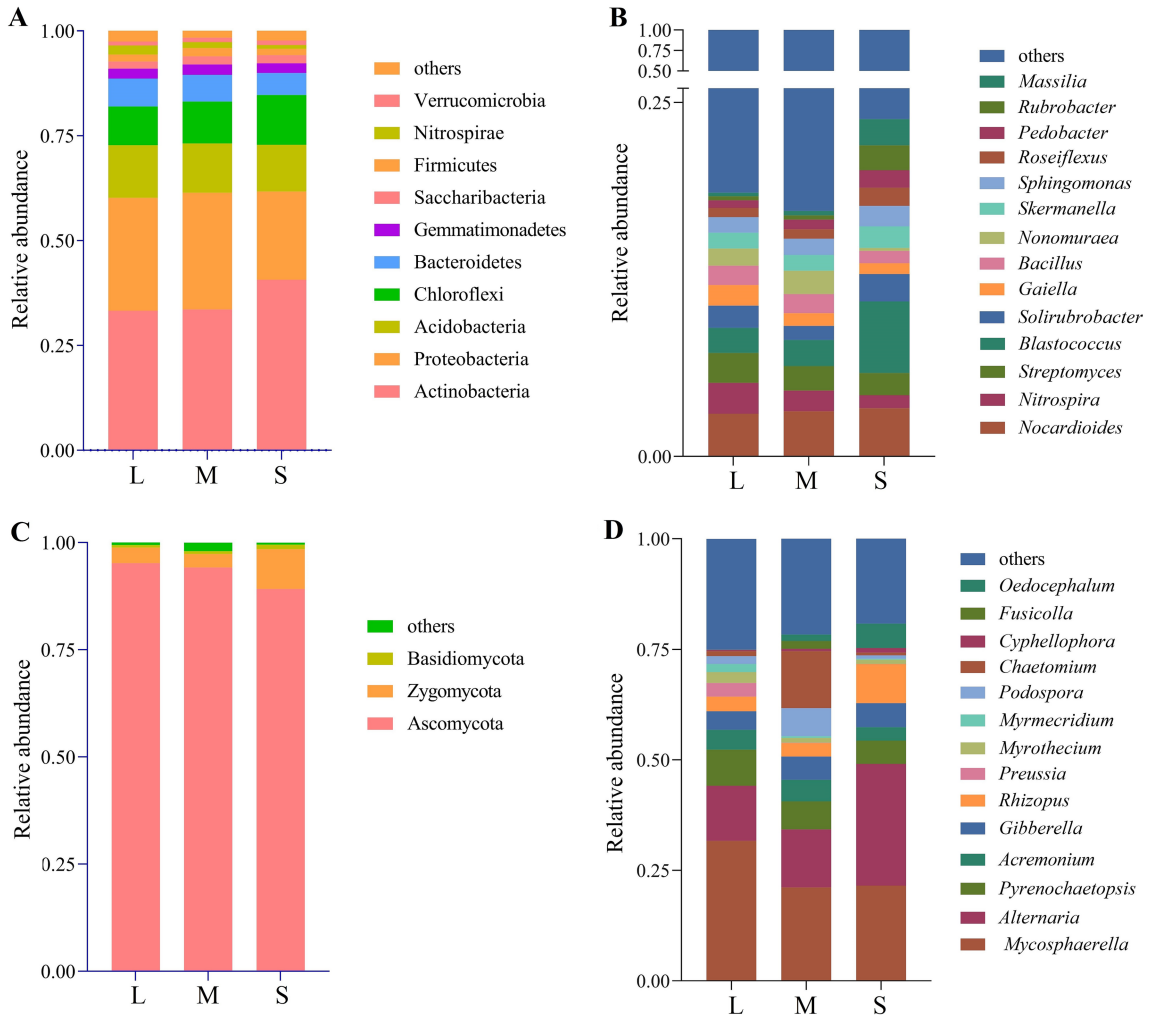

FIGURE 3
Relative abundances of wheat rhizosphere soil bacterial phyla **(A)**, bacterial genera **(B)**, fungal phyla **(C)** and fungal genera **(D)**. L, M, and S: soil with different severities of wheat crown rot—light (L), moderate (M), and severe (S).

M, the relative abundance of dung saprotrophs in S fields decreased by 25.25 and 7.92%, respectively, while that of undefined saprotrophs decreased by 25.28 and 21.60%, respectively. These results indicate that wheat crown rot increases the abundance of plant pathogens in the wheat rhizosphere while reducing the abundance of saprotrophic fungi.

3.6 Biocontrol effect of BF-237 on wheat crown rot

Of 128 bacterial strains isolated from wheat rhizosphere soil, BF-237 showed the largest zone of growth inhibition (9 mm). BF-237 colonies were milky white, convex, round, with uneven edges, wet surface and large folds on LB agar at 24 h at 37°C. BF-237 clustered with *Bacillus velezensis* based on genome comparisons with 11 other *Bacillus* species (Supplementary Figure S1), BF-237 also had the highest ANI value of 98.69% with *B. velezensis* OR683507.1. Thus, BF-237 was identified as a strain of *B. velezensis*. The greenhouse experiment showed that BF-237 had 56.61% control effect on wheat crown rot and 14.18% growth promotion effect on wheat in sterilized soil (Figure 6A). While, in natural soil BF-237 had 53.32% control effect on wheat crown rot and 11.50% growth promotion effect on wheat (Figure 6B).

4 Discussion

The occurrence of crop diseases usually significantly alters the chemical properties of the rhizosphere soil (Walters and Bingham, 2007). These chemical changes are often the result of plant-microbe interactions and the metabolic activities of pathogens triggered by disease. In our study, we found that the occurrence of wheat crown rot decreased the contents of organic matter, available nitrogen, and available phosphorus in wheat rhizosphere soil. When the pathogenic fungi grow and reproduce in the soil, they can restrict root growth, reducing the secretion of root metabolites and, consequently, reduce the carbon sources and organic matter available to soil microorganisms (Canarini et al., 2019). The microbial community in diseased soil also changes, potentially reduce the population of

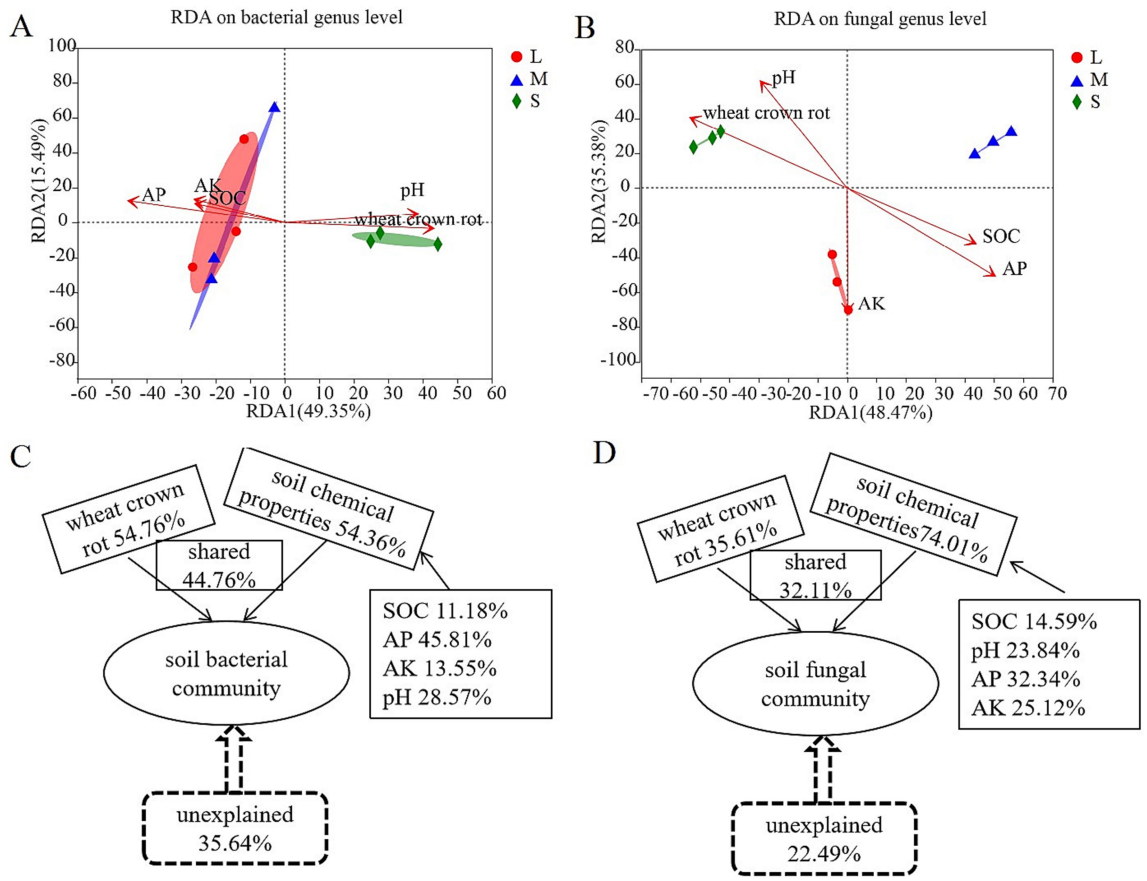

FIGURE 4
Correlation analysis of environmental factors with wheat rhizosphere soil bacterial and fungal community compositions. Redundancy analysis showing the influence of environmental factors on bacterial **(A)** and fungal **(B)** community at genus level. Analysis of contribution of environmental factors to changes in wheat rhizosphere soil bacterial **(C)** and fungal **(D)** community. L, M, and S: soil with different severities of wheat crown rot—light (L), moderate (M), and severe (S).

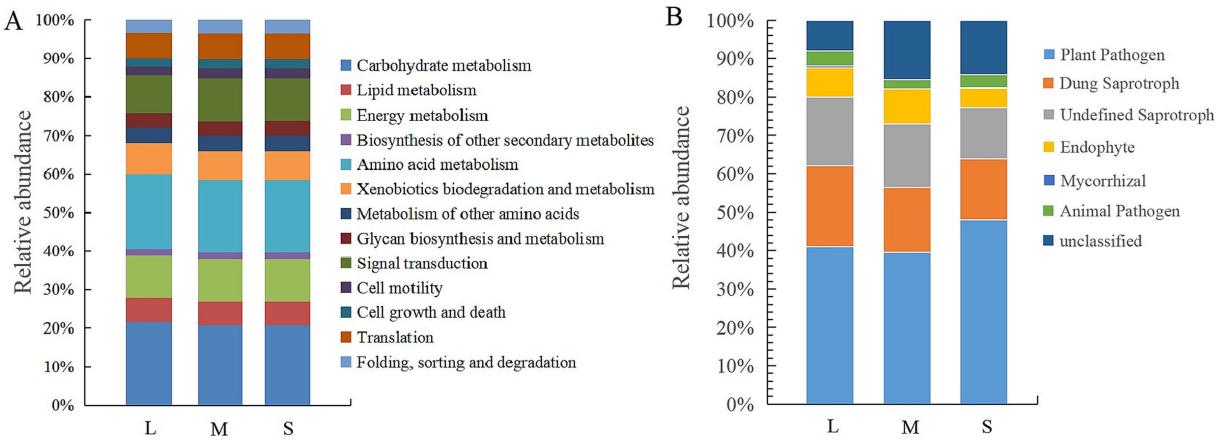

FIGURE 5
Functional analysis of bacteria **(A)** and fungi **(B)** in wheat rhizosphere soil. L, M, and S: soil with different severities of wheat crown rot—light (L), moderate (M), and severe (S).

beneficial microorganisms involved in carbon and nitrogen metabolism, resulting in an overall decrease in the content of carbon and nitrogen (Shi et al., 2019). The occurrence of wheat disease decreases the organic matter and available nutrient levels in the rhizosphere soil. This series of changes not only negatively impacts wheat growth by reducing the nutrients absorbed by plant roots,

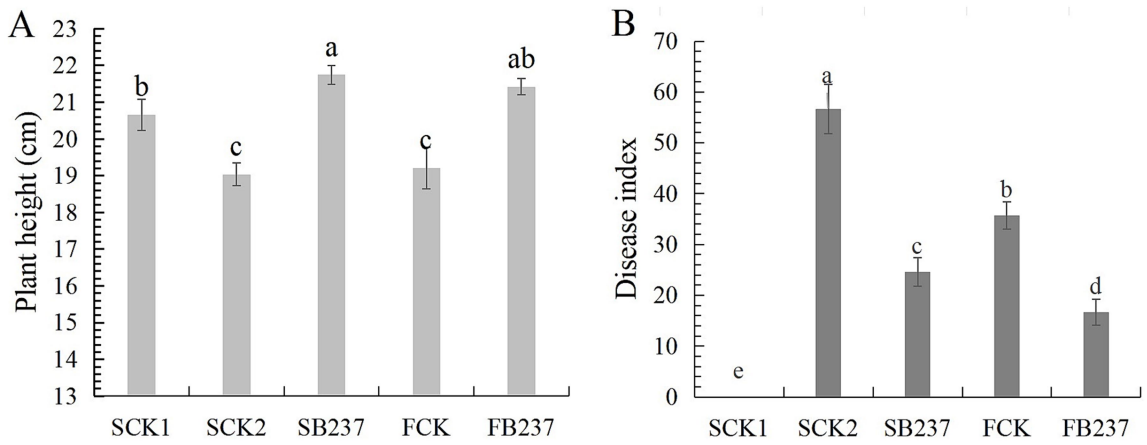

FIGURE 6
Growth promotion of BF-237 on wheat **(A)** and biocontrol effect on wheat crown rot **(B)**. SCK1: sterilized seeds were planted in sterile soil; SCK2: sterilized seeds were planted in sterile soil with *F. pseudograminearum* (10^5 spores/g soil); SB237: seeds soaked with BF-237 were planted in sterile soil with *F. pseudograminearum* (105 spores/g soil); FCK: sterilized seeds were planted in field soil; FB237: seeds soaked with BF-237 were planted in field soil.

which can make plants weaker and more susceptible to further disease, but it also weakens the health and stability of the soil ecosystem. Therefore, maintaining soil nutrients and microbial diversity is crucial for supporting crop health and soil ecological balance. In the process of disease prevention and control, improving soil physicochemical properties and promoting the recovery of beneficial microorganisms can help reduce the negative impacts of disease on both soil and plants.

Soil microbial diversity is an essential indicator of soil health and a foundation for maintaining ecological functions of the soil (Gupta et al., 2022). Studies have shown that soil microbial community diversity is closely linked to the occurrence of plant diseases (Shi et al., 2019; Todorović et al., 2023). Our study found that the bacterial and fungal diversity in wheat rhizosphere soil in field with severe WCR was significantly lower than that with light WCR, indicating that the occurrence of WCR reduces the bacterial and fungal diversity in the wheat rhizosphere soil. When crop diseases occur, pathogens rapidly proliferate in the rhizosphere, occupying ecological niches, forming dominant populations. Through competitive exclusion mechanisms, they suppress the growth of other microorganisms, leading to an overall reduction in diversity (Zhou et al., 2019). Moreover, diseases trigger a reduction in plant metabolism, such as a decrease in the secretion of nutrients from the roots (e.g., amino acids, carbon sources, etc.) (Berger et al., 2007; Rojas et al., 2014). This reduction in available resources for soil microorganisms, leading to a decline in the number of microorganisms that depend on these nutrients, thereby lowering microbial community diversity (Ma et al., 2022). A diverse microbial community can enhance the soil's ability to suppress soil-borne diseases, primarily because a rich microbial community can maintain functional diversity and stability, providing a healthy and stable environment for plant growth (Jayaraman et al., 2021).

The occurrence of WCR have altered the soil microbial community structure, mainly characterized by an increase in the abundance of some pathogens and a decrease in the abundance of some beneficial microorganisms. In fields with severe WCR, the abundance of *F. pseudograminearum* in wheat rhizosphere soil is 58 times higher than in healthy soil. Additionally, the relative abundance of *Alternaria* (pathogen of cabbage black spot, etc.) (Patel et al., 2023) and *Gibberella* (pathogen of maize stalk rot, etc.) (Liu et al., 2023) shows an upward trend, increasing by 120 and 30%, respectively. Furthermore, our study revealed that in the field with severe WCR, the relative abundance of *Streptomyces* and *Bacillus* in the wheat rhizosphere soil decreased. *Streptomyces* and *Bacillus* are two major groups of biocontrol bacteria and are the most widely used biocontrol agents in commercial production and field applications (Khan et al., 2021, 2023). *Streptomyces* can produce a variety of secondary metabolites, and over 90% of known antibiotics are derived from Streptomyces. It has been widely used in the biological control of WCR (Winter et al., 2019), rice blast disease (Chaiharn et al., 2020) and tomato root rot (Hassanisaadi et al., 2021). *Bacillus* can produce various antagonistic compounds, including peptides, lipopeptides, polyketides, siderophores, and bacteriocins which have been widely used in the biological control of WCR (Dong et al., 2023; Guo et al., 2024; Li et al., 2022). We hypothesize that during the occurrence of crop diseases, pathogens inhibit the growth of beneficial bacteria by competing for resources or by altering the soil environment through the production of toxins and other secondary metabolites.

The occurrence of crop diseases can trigger adjustments in soil microbial functions such as nutrient metabolism, defense, and signal transduction (Shi et al., 2019). These changes represent the microbial community's adaptation mechanisms to disease pressure, helping microorganisms maintain community stability in adverse environments and protect plant health. Our study found that after the occurrence of WCR, the abundance of signal transduction-related genes in the rhizosphere soil microbiome significantly increased. Soil microorganisms sense and respond to changes in the environment through signal transduction mechanisms that enable them to receive external stimuli, process information, and regulate their physiological activities to adapt to the complex soil ecological environment (Islam et al., 2020). So, we speculate that under the stress of WCR, pathogen rapidly proliferate in the soil, posing a threat to the microbial community. In response, microorganisms can quickly sense environmental

changes and recognize the presence of pathogens through signal transduction mechanisms, such as quorum sensing and signaling molecule communication, coordinating their defense responses. The enhancement of signal transduction helps the microbial community form a collective response when facing pathogens, improving overall disease resistance.

Our study also found that following the occurrence of WCR, the abundance of carbon metabolism, amino acid metabolism related genes in the rhizosphere soil microbiome significantly decreased. It is speculated that after the occurrence of crop disease, pathogens multiply rapidly in the soil, which inhibits the abundance of some microorganisms, especially those involved in nutrient metabolism, and ultimately leads to the reduction of nutrient metabolism capacity of soil microorganisms (Wang et al., 2022). Additionally, the occurrence of crop disease can reduce the nutrient content of crop rhizosphere soil (Walters and Bingham, 2007), leading to a nutrient-deficient environment in the soil. This results in reduced metabolic activity, allowing microorganisms to conserve resources and avoid excessive energy consumption. This strategy enables them to survive under nutrient-limited conditions and adapt to changes in the soil environment. After the occurrence of WCR, soil microorganisms reduce biosynthetic metabolism and enhance signal transduction as an important adaptive strategy to cope with environmental stress. This change allows microorganisms to allocate resources more effectively to cope with competition and pressure from pathogens, promoting cooperation within the microbial community and providing additional protection to plants. These functional adaptations have profound implications for the health of agricultural ecosystems and provides important theoretical support for soil management and disease control.

5 Conclusion

This study aimed to address the interactions between the occurrence of wheat crown rot and the wheat rhizosphere soil microbiome, and it confirmed that the occurrence of wheat crown rot decreased the pH of the rhizosphere soil and the contents of organic matter, available nitrogen, and available phosphorus. Additionally, it reduced bacterial and fungal diversity in the wheat rhizosphere soil, increased the abundance of plant pathogens such as *Fusarium pseudograminis*, *Alternaria*, and *Gibberella*, while reduced the abundance of beneficial bacteria such as *Streptomyces* and *Bacillus*. After the occurrence of wheat crown rot disease, soil microorganisms reduced their anabolic activity and enhanced signaling pathways to cope with the competition and pressure from pathogens, promoting collaboration within the microbial community and strengthening the community's ability to inhibit pathogens. A strain of *B. velezensis*, whose abundance was reduced due to the occurrence of wheat crown rot, was successfully isolated. Greenhouse experiments revealed that strain BF-237 significantly decreased the incidence of wheat crown rot. These findings further confirm that wheat crown rot reduces the abundance of beneficial bacteria in the soil. Field application of such beneficial bacteria has the potential to effectively mitigate wheat crown rot incidence. Our study broadens the understanding of the relationships between the occurrence of wheat crown rot and the soil microbiome and provides novel insights into wheat crown rot occurrence.

Data availability statement

The datasets presented in this study can be found in online repositories. The names of the repository/repositories and accession number(s) can be found in the article/Supplementary material.

Author contributions

YaW: Conceptualization, Writing – original draft. JF: Data curation, Investigation, Writing – original draft. JG: Data curation, Investigation, Writing – original draft. SH: Methodology, Software, Writing – original draft. QL: Data curation, Investigation, Writing – original draft. LK: Conceptualization, Writing – review & editing. YuW: Conceptualization, Funding acquisition, Visualization, Writing – review & editing.

Funding

The author(s) declare that financial support was received for the research, authorship, and/or publication of this article. This work was supported by Talents construction project of science and technology innovation, Hebei Academy of Agriculture and Forestry Sciences (C23R1009), Hebei Province backbone talents project return platform (B2024030), and the HAAFS Agriculture Science and Technology Innovation Project (2022KJCXZX-ZBS-7).

Conflict of interest

The authors declare that the research was conducted in the absence of any commercial or financial relationships that could be construed as a potential conflict of interest.

Generative AI statement

The authors declare that no Gen AI was used in the creation of this manuscript.

Publisher's note

Supplementary material

The Supplementary material for this article can be found online at: https://www.frontiersin.org/articles/10.3389/fmicb.2025.1538093/full#supplementary-material

References

Berger, S., Sinha, A. K., and Roitsch, T. (2007). Plant physiology meets phytopathology: plant primary metabolism and plant-pathogen interactions. *J. Exp. Bot.* 58, 4019–4026. doi: 10.1093/jxb/erm298

Canarini, A., Kaiser, C., Merchant, A., Richter, A., and Wanek, W. (2019). Root exudation of primary metabolites: mechanisms and their roles in plant responses to environmental stimuli. *Front. Plant Sci.* 10:157. doi: 10.3389/fpls.2019.00157

Chaiharn, M., Theantana, T., and Pathom-Aree, W. (2020). Evaluation of biocontrol activities of streptomyces spp. against rice blast disease fungi. *Pathogens* 9:126. doi: 10.3390/pathogens9020126

Deng, Y. Y., Li, W., Zhang, P., Sun, H. Y., Zhang, X. X., Zhang, A. X., et al. (2020). *Fusarium pseudograminearum* as an emerging pathogen of crown rot of wheat in eastern China. *Plant Pathol.* 69, 240–248. doi: 10.1111/ppa.13122

Dong, Q., Liu, Q., Goodwin, P. H., Deng, X., Xu, W., Xia, M., et al. (2023). Isolation and genome-based characterization of biocontrol potential of *Bacillus siamensis* YB-1631 against wheat crown rot caused by *Fusarium pseudograminearum*. *J. Fungi* 9:547. doi: 10.3390/jof9050547

Feng, C., Xu, F., Li, L., Zhang, J., Wang, J., Li, Y., et al. (2023). Biological control of *Fusarium* crown rot of wheat with *Chaetomium globosum* 12XP1-2-3 and its effects on rhizosphere microorganisms. *Front. Microbiol.* 14, 1–14. doi: 10.3389/fmicb.2023.1133025

Guo, S., Tariq, A., Liao, J., Yang, A., Jiang, X., Yin, Y., et al. (2024). Identification and antagonistic potential of *Bacillus atrophaeus* against wheat crown rot caused by *Fusarium pseudograminearum*. *Agronomy* 14:2135. doi: 10.3390/agronomy14092135

Gupta, A., Singh, U. B., Sahu, P. K., Paul, S., Kumar, A., Malviya, D., et al. (2022). Linking soil microbial diversity to modern agriculture practices: a review. *Int. J. Environ. Res. Public Health* 19:3141. doi: 10.3390/ijerph19053141

Hassanisaadi, M., Shahidi Bonjar, G. H., Hosseinipour, A., Abdolshahi, R., Barka, E. A., and Saadoun, I. (2021). Biological control of *Pythium aphanidermatum*, the causal agent of tomato root rot by two streptomyces root symbionts. *Agronomy* 11, 1–19. doi: 10.3390/agronomy11050846

Islam, W., Noman, A., Naveed, H., Huang, Z., and Chen, H. Y. H. (2020). Role of environmental factors in shaping the soil microbiome. *Environ. Sci. Pollut. Res.* 27, 41225–41247. doi: 10.1007/s11356-020-10471-2

Jayaraman, S., Naorem, A. K., Lal, R., Dalal, R. C., and Chaudhari, S. K. (2021). Disease suppressive soils beyond food production: a critical review. *Plant Nutr.* 21, 1437–1465. doi: 10.1007/s42729-021-00451-x

Kazan, K., and Gardiner, D. M. (2018). *Fusarium* crown rot caused by *Fusarium pseudograminearum* in cereal crops: recent progress and future prospects. *Mol. Plant Pathol.* 19, 1547–1562. doi: 10.1111/mpp.12639

Khan, M., Salman, M., Ahmad Jan, S., and Khan Shinwari, Z. (2021). Biological control of fungal phytopathogens: a comprehensive review based on *Bacillus* species. *MOJ Biol. Med.* 6, 90–92. doi: 10.15406/mojbm.2021.06.00137

Khan, S., Srivastava, S., Karnwal, A., and Malik, T. (2023). *Streptomyces* as a promising biological control agents for plant pathogens. *Front. Microbiol.* 14:1285543. doi: 10.3389/fmicb.2023.1285543

Li, B., Kong, L., Qiu, D., Francis, F., and Wang, S. (2021). Biocontrol potential and mode of action of entomopathogenic bacteria *Xenorhabdus budapestensis* C72 against *Bipolaris maydis*. *Biol. Control* 158:104605. doi: 10.1016/j.biocontrol.2021.104605

Li, S., Xu, J., Fu, L., Xu, G., Lin, X., Qiao, J., et al. (2022). Biocontrol of wheat crown rot using *Bacillus halotolerans* QTH8. *Pathogens* 11:595. doi: 10.3390/pathogens11050595

Li, H. L., Yuan, H. X., Fu, B., Xing, X. P., Sun, B. J., and Tang, W. H. (2012). First report of *Fusarium pseudograminearum* causing crown rot of wheat in Henan, China. *Plant Dis.* 96:1065. doi: 10.1094/PDIS-01-12-0007-PDN

Liu, C., and Ogbonnaya, F. C. (2015). Resistance to *Fusarium* crown rot in wheat and barley: a review. *Plant Breed.* 134, 365–372. doi: 10.1111/pbr.12274

Liu, M., Sui, Y., Yu, C., Wang, X., Zhang, W., Wang, B., et al. (2023). Coronatine-induced maize defense against *Gibberella* stalk rot by activating antioxidants and phytohormone signaling. *J. Fungi* 9:1155. doi: 10.3390/jof9121155

Ma, W., Tang, S., Dengzeng, Z., Zhang, D., Zhang, T., and Ma, X. (2022). Root exudates contribute to belowground ecosystem hotspots: a review. *Front. Microbiol.* 13, 1–19. doi: 10.3389/fmicb.2022.937940

Magoc, T., and Salzberg, S. L. (2011). FLASH: fast length adjustment of short reads to improve genome assemblies. *Bioinformatics* 27, 2957–2963. doi: 10.1093/bioinformatics/btr507

Moya-Elizondo, E. A., and Jacobsen, B. J. (2016). Integrated management of *Fusarium* crown rot of wheat using fungicide seed treatment, cultivar resistance, and induction of systemic acquired resistance (SAR). *Biol. Control* 92, 153–163. doi: 10.1016/j.biocontrol.2015.10.006

Obanor, F., and Chakraborty, S. (2014). Aetiology and toxigenicity of *Fusarium graminearum* and *F. Pseudograminearum* causing crown rot and head blight in Australia under natural and artificial infection. *Plant Pathol.* 63, 1218–1229. doi: 10.1111/ppa.12200

Ozdemir, F., Koc, N. K., Paulitz, T., Nicol, J. M., Schroeder, K. L., and Poole, G. (2020). Determination of *Fusarium* crown rot resistance in wheat to *Fusarium culmorum* and *Fusarium pseudogramineaum* using real time PCR. *Crop Prot.* 135:105204. doi: 10.1016/j.cropro.2020.105204

Patel, S. N., Kumar, P., Raghuvanshi, V. V., Patel, S. K., Siddharth, P., Singh, A., et al. (2023). Morphological characterization and pathogenicity test of *Alternaria* leaf spot of Chinese cabbage (*Brassica chinensis L.*). *Int. J. Plant Soil Sci.* 35, 1616–1625. doi: 10.9734/ijpss/2023/v35i193707

Rahman, M. M., Davies, P., Bansal, U., Pasam, R., Hayden, M., and Trethowan, R. (2021). Relationship between resistance and tolerance of crown rot in bread wheat. *Field Crops Res.* 265:108106. doi: 10.1016/j.fcr.2021.108106

Rojas, C. M., Senthil-Kumar, M., Tzin, V., and Mysore, K. S. (2014). Regulation of primary plant metabolism during plant-pathogen interactions and its contribution to plant defense. *Front. Plant Sci.* 5, 1–12. doi: 10.3389/fpls.2014.00017

Saxena, A. K., Kumar, M., Chakdar, H., Anuroopa, N., and Bagyaraj, D. J. (2020). *Bacillus* species in soil as a natural resource for plant health and nutrition. *J. Appl. Microbiol.* 128, 1583–1594. doi: 10.1111/jam.14506

Shi, W., Li, M., Wei, G., Tian, R., Li, C., Wang, B., et al. (2019). The occurrence of potato common scab correlates with the community composition and function of the geocaulosphere soil microbiome. *Microbiome* 7:14. doi: 10.1186/s40168-019-0629-2

Todorović, I., Moënne-Loccoz, Y., Raičević, V., Jovičić-Petrović, J., and Muller, D. (2023). Microbial diversity in soils suppressive to Fusarium diseases. *Front. Plant Sci.* 14, 1–24. doi: 10.3389/fpls.2023.1228749

Walters, D. R., and Bingham, I. J. (2007). Influence of nutrition on disease development caused by fungal pathogens: implications for plant disease control. *Ann. Appl. Biol.* 151, 307–324. doi: 10.1111/j.1744-7348.2007.00176.x

Wang, Z., Wang, Z., Ma, L., Lv, X., Meng, Y., and Zhou, Z. (2021). Straw returning coupled with nitrogen fertilization increases canopy photosynthetic capacity, yield and nitrogen use efficiency in cotton. *Eur. J. Agron.* 126:126267. doi: 10.1016/j.eja.2021.126267

Wang, Y., Wu, Y., Cao, C., Han, S., Zhao, W., Li, Q., et al. (2023). Effects of fertilizer reduction coupled with straw returning on soil fertility, wheat root endophytic bacteria,and the occurrence of wheat crown rot. *Front. Microbiol.* 14:1143480. doi: 10.3389/fmicb.2023.1143480

Wang, Z., Zhang, Y., Bo, G., Zhang, Y., Chen, Y., Shen, M., et al. (2022). *Ralstonia solanacearum* infection disturbed the microbiome structure throughout the whole tobacco crop niche as well as the nitrogen metabolism in soil. *Front. Bioeng. Biotechnol.* 10, 1–16. doi: 10.3389/fbioe.2022.903555

Winter, M., Samuels, P. L., Otto-Hanson, L. K., Dill-Macky, R., and Kinkel, L. L. (2019). Biological control of *Fusarium* crown and root rot of wheat by *Streptomyces* isolates – It's complicated. *Phytobiomes J.* 3, 52–60. doi: 10.1094/PBIOMES-11-18-0052-R

Wu, N., Shi, W., Zhang, L., Wang, H., Liu, W., Ren, Y., et al. (2024). Dynamic alterations and ecological implications of rice rhizosphere bacterial communities induced by an insect-transmitted reovirus across space and time. *Microbiome* 12:189. doi: 10.1186/s40168-024-01910-0

Xu, W., Yang, Q., Xie, X., Goodwin, P. H., Deng, X., Zhang, J., et al. (2022). Genomic and phenotypic insights into the potential of *Bacillus subtilis* YB-15 isolated from rhizosphere to biocontrol against crown rot and promote growth of wheat. *Biology (Basel)* 11:778. doi: 10.3390/biology11050778

Yang, L., Han, W., Tan, B., Wu, Y., Li, S., and Yi, Y. (2024). Effects of nutrient accumulation and microbial community changes on tomato *Fusarium* wilt disease in greenhouse soil. *Sustain. For.* 16:7756. doi: 10.3390/su16177756

Yuan, J., Wen, T., Zhang, H., Zhao, M., Penton, C. R., Thomashow, L. S., et al. (2020). Predicting disease occurrence with high accuracy based on soil macroecological patterns of *Fusarium* wilt. *ISME J.* 14, 2936–2950. doi: 10.1038/s41396-020-0720-5

Zhang, N., Xu, Y., Zhang, Q., Zhao, L., Zhu, Y., Wu, Y., et al. (2023). Detection of fungicide resistance to fludioxonil and tebuconazole in *Fusarium pseudograminearum*, the causal agent of *Fusarium* crown rot in wheat. *PeerJ* 11, 1–14. doi: 10.7717/peerj.14705

Zhang, N., Yuan, S., Zhang, Q., Liu, W., Zhou, Y., and Yang, W. (2022). Screening fungicides for controlling wheat crown rot caused by *Fusarium pseudograminearum* across Hebei Province in China. *Agriculture* 12:1643. doi: 10.3390/agriculture12101643

Zhang, J. Z., Zhang, J. H., Wang, J., Zhang, M., Li, C., Wang, W., et al. (2024). Population genetic analyses and trichothecene genotype profiling of *Fusarium pseudograminearum* causing wheat crown rot in Henan, China. *J. Fungi* 10:240. doi: 10.3390/jof10040240

Zhou, D., Jing, T., Chen, Y., Wang, F., Qi, D., Feng, R., et al. (2019). Deciphering microbial diversity associated with *Fusarium* wilt-diseased and disease-free banana rhizosphere soil. *BMC Microbiol.* 19, 161–113. doi: 10.1186/s12866-019-1531-6

frontiers | Frontiers in Microbiology

TYPE Original Research
PUBLISHED 05 March 2025
DOI 10.3389/fmicb.2025.1521064

OPEN ACCESS

EDITED BY
Jose Ignacio Marín-Guirao,
IFAPA Centro La Mojonera, Spain

REVIEWED BY
Wensheng Fang,
Chinese Academy of Agricultural Sciences, China
Hongguang Liu,
Jiangxi Academy of Water Science and Engineering, China

*CORRESPONDENCE
Jiayao Zhuang
✉ nlzjiayao@njfu.edu.cn

RECEIVED 01 November 2024
ACCEPTED 12 February 2025
PUBLISHED 05 March 2025

CITATION
Liu Z, Luo C, Zheng K, Sun Y, Ru J, Ma Y, Zhang X, Zhou Y and Zhuang J (2025) Native mixed microbe inoculants (M1H) optimize soil health to promote *Cajanus cajan* growth: the soil fungi are more sensitive than bacteria. *Front. Microbiol.* 16:1521064.
doi: 10.3389/fmicb.2025.1521064

Native mixed microbe inoculants (M1H) optimize soil health to promote *Cajanus cajan* growth: the soil fungi are more sensitive than bacteria

Zexun Liu[1], Chengcheng Luo[1], Kang Zheng[1], Yongtao Sun[2], Jie Ru[2], Yaner Ma[3], Xinru Zhang[1], Yong Zhou[4] and Jiayao Zhuang[1]*

[1]Collaborative Innovation Center of Sustainable Forestry in Southern China of Jiangsu Province, Nanjing Forestry University, Nanjing, China, [2]East China Academy of Inventory and Planning of NFGA, Hangzhou, China, [3]National Forestry and Grassland Bureau Forest and Grass Survey Planning Institute, Beijing, China, [4]Beijing Liangshui River Administration Office, Beijing, China

Microbial inoculant is widely used in plant growth and crop production. However, the effect of native mixed microbial inoculants on soil microbiota and plant growth remain to be elucidated. Here, we used pot experiment for 5 months to determine the microbial inoculants treatments with growth-promoting effect on *Cajanus cajan*, such as M1P (*Serratia marcescens*) treatment and M1H treatment: the mixture of M1P and M45N (*Paenibacillus polymyxa*), and investigate the effect of these inoculants on the capacity of soil nutrients and rhizosphere microbiomes in promoting *C. cajan* growth. Further, the adaptability of these strains to environmental stress (temperature and pH) was determined by using stress-resistant growth experiment. The results showed that M1H treatment resulted in soil nutrients consumption and led to substantial alterations in the microbial community that were more effective in promoting *C. cajan* growth. The enhanced plant growth observed with M1H inoculation may be due to its impact on the soil micro-environment, particularly through increasing beneficial genera (e.g., *Cunninghamella*, *Mortierella*, *Chryseolinea*, and *Bacillus*) and decreasing potential genera (e.g., *Zopfiella* and *Podospora*). In addition, at the genus level (top 10), the effect of M1H inoculation on soil fungal community was higher than that of bacteria, which shows that the change of soil fungal community after M1H inoculation was more sensitive than that of bacteria. Spearman correlation analysis further revealed that the abundance of *Cunninghamella*, *Mortierella*, *Chryseolinea*, *Zopfiella* and *Podospora* were the key factors affecting *C. cajan* growth. Moreover, FUNGuild function prediction clearly indicated distinct differences in the fungal functions of CK, MIP and M1H treatment, in which a lower relative abundance of saprotroph fungi in M1H treatment compared to CK, these results may confirmed the possibility of decreasing the abundance of *Zopfiella* and *Podospora* under M1H treatment. Taken together, our findings highlight the role of M1H inoculant in promoting *C. cajan* growth and ameliorating soil health, and providing valuable insight of using native mixed microbial inoculants to cultivate *C. cajan* and optimize soil micro-environment.

KEYWORDS

***Cajanus cajan*, growth promoting effect, soil nutrients, soil fungal and bacterial communities, FUNGuild**

1 Introduction

Cajanus cajan is a perennial woody plant, which belongs to the subfamily Papilionidae of Leguminosa (Gnanesh et al., 2011). It is widely consumed as food due to its high nutritional value (Rao et al., 2002). In addition, *C. cajan* has a high tolerance to different stresses, such as barren resistance, salt tolerance, drought tolerance, and so on. Thus, it is regarded as a pioneer tree species for the prevention and control of soil erosion. These characteristics have increased the utilization rate of *C. cajan* worldwide (Lazcano et al., 2021). Due to the rapid decline of the available land and the sharp decline in soil fertility, it is necessary to improve both land utilization rates and plant growth rates, which is crucial given the current situation (Dastager et al., 2010). The application of chemical fertilizer is the most common method to promote plant growth and increase crop yield. The rapid development of agriculture has increased the dependency of agriculture on chemical fertilizers. Chemical fertilizers increase plant growth and crop yield in a short time but adversely affect the soil environment, resulting in abnormal levels of soil nutrients and a decreased abundance of beneficial microbes, and in turn, aggravating soil degradation and posing a potential threat to human health (Liu et al., 2023; Tian et al., 2021). Thus, microbial fertilizer containing beneficial microbes has become the hot spot of agricultural research studies as it is stable and eco-friendly.

Soil microbes are a vital part of the soil ecosystem (Baldock and Skjemstad, 2000; Wang et al., 2017). They play an important role in the soil nutrient cycle, such as the decomposition of organic matter and regulation of soil nutrient levels (Semchenko et al., 2022). Certain soil microbes improve soil quality and the soil micro-ecological environment by dissolving insoluble nutrients and secreting plant hormones. Besides, they also increase plant's soil nutrient consumption and promote plant growth (Li et al., 2022; Tian et al., 2021).

Previous studies have shown that application of microbial inoculant could affect soil microbial diversity and community structure and directly or indirectly promote plant growth. For instance, *Trichoderma harzianum* and *Bacillus* inoculants increased the abundance of beneficial soil microbes and inhibited the growth of pathogenic bacteria resulting in increased tomato yield (Cheng et al., 2020, 2021). Chen et al. (2020) reported that beneficial microbial fertilizer effectively inhibited the accumulation of soil pathogens and ameliorated the rhizospheric microbial community structure, resulting in increased growth of *Chrysanthemum*. Zhuang et al. (2021) reported that *Penicillium*. NL-Z1 fungal inoculants induced and increased the abundance of *Mortierella*, increasing growth of *Acanthopanax* sp. Li et al. (2022) reported that the application of microbial fertilizer containing *Bacillus* inoculant increased the abundance of beneficial microbes, such as *Bacillus* (is included in the phylum *Firmicutes*) and *Actinomadura* (is included in the phylum *Actinobacteria*), and decreased the abundance of pathogenic fungi, such as *Fusarium* and *Phytophthora* in the rhizospheric soil of strawberry plants, increasing the yield of strawberries. Till now, numerous studies have investigated the effects of single microbial inoculants on plant growth and soil micro-ecological environment (El-Sharkawy et al., 2021). However, how native mixed microbial inoculants can help us to promote plant growth, understand the correlation and of soil nutrients, soil microbial community structure, and plant growth remain unclear.

Soil microbial community structure is an important biological index to evaluate plant growth (Mapelli et al., 2012; Tian et al., 2021; Zhu et al., 2014). The interspecific correlations among microbes, including induction, transformation, coexistence, and antagonism, play a significant role in shaping the structure and diversity of the soil microbial community, thereby affecting plant growth. Previous studies have shown that optimizing the soil microbial community structure could directly or indirectly determine the adaptability of plants to the environment (Kos et al., 2009; Samaddar et al., 2021; Stefan et al., 2021), especially the altered abundance of beneficial and pathogenic microbes in the soil, which could reflect the soil's health. This also demonstrates that understanding the altered microbial community structure of plant growth is crucial. Thus, understanding the changes in microbial community structure will help us to unravel microbial mechanisms concerning plant growth. Although the well-studied nature of single microbial inoculants, there are few studies on the effects of inoculation with microbial inoculants from *C. cajan* rhizosphere, such as *Serratia marcescens* and *Paenibacillus polymyxa*, especially the effects of the mixed microbial inoculants of *S. marcescens* and *P. polymyxa* on the growth of *C. cajan* is unknown. Therefore, it is essential to study the external benefits of mixed microbial inoculants of *S. marcescens* and *P. polymyxa* and the internal relationships between microbes.

In this study, we conducted a pot experiment on *C. cajan* plant for 5 months using native microbial inoculants, i.e., *P. polymyxa* (M45N) and *S. marcescens* (M1P), which were isolated from the rhizospheric soil of *C. cajan*. We also used high-throughput Illumina MiSeq (ITS and 16S) sequencing technology to investigate taxonomic changes in the soil's bacterial and fungal communities in response to different microbial inoculants. We hypothesized that (1) soil nutrients and microbial community structure in the rhizosphere would be affected by different microbial inoculants; (2) mixed microbial inoculants would have a stronger growth-promoting effect on *C. cajan* than single microbial inoculants; and (3) changes in the microbial community could be a potential factor affecting this ability. Consequently, these characteristics would further unveil the underlying mechanisms of microbial inoculants on *C. cajan* growth. In conjunction with the premise of the rational use of space resources, the specific objectives of this study were (1) to assess the effect of different microbial inoculants on growth indexes (plant height, plant ground diameter and dry weight), soil nutrients, soil microbial diversity, microbial community structure, and function, and (2) to evaluate the environmental factors influence the fungal and bacterial communities composition. This study assessed and confirmed the feasibility and effectiveness of native mixed microbial inoculants in promoting plant growth, providing a theoretical basis and sustainable management for the cultivation and development of *C. cajan*.

2 Materials and methods

2.1 The source, isolation and screening of rhizosphere microbes, and preparation of microbial inoculants

Cajanus cajan seeds were purchased from a flower seed market in Jiujiang City, Jiangxi province, China, and were planted in the Baguazhou experimental field in Qixia District, Nanjing in mid-May

2022. At the end of November, the soil rhizospheric samples from healthy *C. cajan* were collected in the experimental field. The soil samples were stored in a 4°C ice box and brought back to the soil and water conservation laboratory of Nanjing Forestry University for microbial screening experiments.

The microbial screening experiments step as follows: A 10-fold serial dilution of soil samples was smeared on NA (nutrient agar, for cultivating bacteria: 3 g of beef extract, 10 g of peptone, 5 g of NaCl, 20 g of agar, and 1,000 mL of deionized water, pH 7.0–7.2) and PDA (potato dextrose agar, for cultivating fungi: 6 g of potato flour, 20 g of glucose, 18 g of agar, and 1,000 mL of deionized water, pH 7.0–7.2) to isolate bacteria and fungi, respectively. The agar plates were incubated at 28°C for 3 days. Morphologically distinct colonies were subjected to purification following subculturing. Seven purified strains were obtained, namely M1N, M2N, M3N, M45N, M1P, M2P, and M45P. Among these, M1N, M2N, M3N, M45N, M1P, and M2P were bacterial isolates (NA) and M45P was a fungal isolates (PDA) (Supplementary Figure S1). Purified strains were prepared into microbial inoculants with the values of 0.8–1.2 under OD600 (equivalent to $0.8–1.2 \times 10^8$ cfu/mL), and 60 mL of them was applied to the rhizosphere soil for the pot experiment of *C. cajan*.

2.2 Pot experiment

The experiment was conducted in a greenhouse at Baguazhou, Nanjing Province, China. The temperature of the greenhouse was maintained at 30 ± 5°C, a relative humidity of 65%, and with adequate sunlight exposure. The initial farmland soil was air-dried, screened by a 5 mm mesh, and mixed with vermiculite and perlite in a ratio of 3:1:1. The mixed soils were filled with 2.5 kg per pot (30 cm in diameter, 25 cm in depth). The initial soil properties are determined in Supplementary Table S1.

On April 29, 2023, *C. cajan* seeds were pretreated prior to the pot experiment. Firstly, we soaked *C. cajan* seeds in distilled water for 12 h, filtered the water, and then soaked them in a 0.5% sodium hypochlorite solution for 1 min to disinfect the seeds (Solorzano and Malvick, 2011). Later, the disinfected seeds were washed with pure water and later kept in the seedling cup to germinate for 2 week. The seeds germinated into seedlings by May 15, and the seedlings with similar height growth (about 6-8 cm in height) were transplanted into pots with 2.5 kg soil. One healthy seedling was planted in each pot. Nine treatments with five replicates were designed, thus a total of 45 pots were designed in this study. The main treatments were as follows: (1) CK: contained sterile LB culture solution (without strain derivatives); (2) M1P: *S. marcescens* inoculant; (3) M1H: inoculants of the mixture contained M45N (*P. polymyxa*) and M1P; (4) Other treatments, including M1N, M2N, M3N, M2P, M45N, and M45P treatments, had no growth-promoting effect on *C. cajan* growth (Supplementary Figure S2). Thus, only the treatments with significant differences compared to CK, such as M1P and M1H treatments, were analyzed in the subsequent fungal and bacterial communities analysis.

One week after the seedlings were transplanted (on May 22), microbial inoculants with an OD600 of 0.8–1.2 were prepared, and 60 mL of them was applied to the rhizosphere soil in each treatment. The first day of microbial inoculants application were recorded as day one of the experiment, and inoculation was repeated every other month (on May 22, June 22, July 22, August 22, and September 22). Samples were taken after 5 months, from May 22 to October 22, 2019. During the whole experimental period, potted plants were randomly placed in the greenhouse and rearranged every other month. Identical agronomic management measures were then implemented across all treatments for the study.

2.3 Stress-resistant growth experiment

The stress-resistant growth experiment was conducted in the Soil and Water Conservation Laboratory of Nanjing Forestry University and included temperature and pH stress resistance tests. For the temperature stress resistance test, derivatives of M1P (1-mm-diameter disk), M45N (1-mm-diameter disk), and M1H (0.5-mm diameter disk of M1P and M45N, respectively) purified through multiple generations were inoculated into 250 mL conical flasks containing 100 mL of LB culture medium. The LB medium was prepared with 10 g of peptone, 5 g of yeast extract, 5 g of NaCl, and 1,000 mL of deionized water, adjusted to pH 7.2. The cultures were shaken evenly and incubated at temperature gradients of 10, 20, 30, 40, 50, and 60°C for 3 days, with three replicates per temperature condition. Strain concentrations in the culture solutions were measured every 12 h using an ultraviolet–visible spectrophotometer at OD600, and these values represented the strain concentrations. For the pH stress resistance test, sulfuric acid and sodium hydroxide were used to adjust the pH of solutions to values of 5, 6, 7, 8, 9, and 10. LB culture media were prepared by replacing deionized water with these pH-adjusted solutions. Derivatives of M1P, M45N, and M1H were inoculated into 250 mL conical flasks containing 100 mL of the pH-adjusted LB culture medium. The cultures were incubated at 35°C ± 0.2°C for 3 days, with three replicates for each pH condition. Strain concentrations were measured every 12 h using an ultraviolet–visible spectrophotometer at OD600. The experiment was designed with two primary factors (temperature and pH), six secondary factors (six temperature gradients and six pH gradients), three biological replicates, and three strains, resulting in a total of 108 conical flasks. This setup ensured a comprehensive assessment of microbial stress resistance under varying environmental conditions.

The strains of M1P and M45N were ascertained based on microbial screening experiments (Supplementary Figure S3) and pot experiments (Supplementary Figures S2, S4). Besides, the strain of M45N and M1P were identified based on morphological characteristics and 16S rDNA analysis, which were identified *P. polymyxa* and *S. marcescens*, respectively. The preparation of microbial inoculants step as follows: To prepare inoculants of M45N, M1P, and their mixture (M1H), purified isolates were inoculated on NA plates, respectively, until their derivatives covered half of the plate. Derivatives were inoculated into a 250 mL Erlenmeyer flask containing 100 mL LB (Luria Bertani) medium. Cultures were incubated at 25°C and 200 rpm for 48 h. After 48 h, the cultivating bacteria of the suspension was measured (UV-8000T, Shanghai Metash Instruments Co., Ltd.) at OD600 using a UV–visible spectrophotometer. The values of OD600 in the bacterial solutions was ensured to be in the range of 0.8–1.2 by dilution or continuous culturing. Microbial inoculants were prepared by diluting the culture 100 times. These microbial inoculants were used in *C. cajan* pot experiment.

2.4 Plant and soil sampling

The pot experiment was concluded after 5 months, and the samples of plants and rhizospheric soil in the pot were collected for indexes measurement. For plant, vernier calipers and tape were utilized to measure the plant ground diameter and plant height of the seedlings, as the growth indexes of *C. cajan*. Plant height and plant ground diameter were measured before each harvest. The dry weight of plant was determined after drying at 60°C for 24 h until constant weight in oven. For soil, rhizospheric soils adhered to the roots of plants from the range of 0–20 cm were collected by shaking method (Gently swing by hand for 2 min, with a frequency of about 60 times/min), and the fine roots in rhizosphere soils were completely removed with tweezers to reduce the influence on the experimental determination. Thus, a total of 15 rhizospheric soil samples were collected, and each of which was about 100 g. The soil samples were stored in the self-sealing bags. Each soil sample was divided into two parts and brought back to the laboratory on ice. One part of the sample was stored at a − 80°C for soil microbial community analysis, and the other part of the sample was air-dried to determine for the chemical properties analyses of the soil.

2.5 Soil chemical properties analyses

The levels of total nitrogen (TN), total potassium (TK), hydrolyzed nitrogen (AN), and available potassium (AK) were determined by using the Semi-micro Kjeldahl method (De Falco et al., 2004; J et al., 1984), sodium hydroxide melting flame photometry, alkaline hydrolysis diffusion method, and flame photometry with NH_4OAc extraction, respectively. The level of soil organic carbon (OC) was determined using external heating with concentrated sulfuric acid and potassium dichromate. Besides, a 10 g soil sample into a 50 mL beaker, add distilled water with no CO_2 according to the water-soil ratio of 2.5:1, stir it with a stirrer for 1 min, and let it stand for 30 min, then determine it with a pH meter.

2.6 Soil DNA extraction, PCR amplification, and high-throughput gene sequencing

A total of 0.25 g of rhizosphere soil from each potted soil samples were used for DNA extraction. The complete genomic DNA of potted soil samples was extracted using the e.z n.a.® Soil DNA Kit (Omega Bio-Tek, Norcross, GA, United States) and detailed steps were referred to the built-in instructions. The concentration of extracted DNA was detected by Nanodrop RND-2000 (NanoDrop Technologies, Wilmington, DE, United States). After extraction, the extracted genomic DNA was detected on using 1% agarose gel electrophoresis. Then, two universal primers 338F (5'-ACTCCTACGGGAGCAGCAG-3′) - 806R (5'-GGACTACHGGGTWTCTAAT-3′) (Ma et al., 2020) and ITS1F (5′-GATGAAGA ACGYAGYRAA-3′) - ITS2R (5'-GCTGCGTTCT TCAT CATGATGC-3′) (Adams et al., 2013) were used to perform PCR amplification and MiSeq sequencing on the V3–V4 region of the bacterial 16SrRNA gene and the fungal ITS1 region. The PCR reaction consisted of 12.5 μL 2 × Premix Taq™ (TaKaRa. Bio Inc. Shiga, Japan), 1 μL of each primer (10 μm), 2 μL of DNA extract (5–20 ng), and 9 μL of dd H_2O to a final volume of 25 μL. The PCR amplification conditions as follows: denaturated at 95°C for 3 min, followed by 35 cycles of denaturation at 95°C for 30 s, annealing at 55°C for 30 s, annealing at 55°C for 30 s, and a final extension step at 72°C for 10 min. The PCR products of the same samples were mixed and detected by using 2% agarose gel electrophoresis and purified by using an AxyPrepDNA gel recovery kit (Axygen Biosciences, U.S.). Referring to the preliminary quantitative results of electrophoresis, the PCR products were quantified using QuantiFluor™-ST blue fluorescence quantitative system (Promega company). The DNA samples were quantified and mixed according to the sequencing quantity requirements of each sample. The DNA samples were sequenced using Mothur (V.1.36.1). The columns were filtered to remove the chimera to obtain the optimized sequence. The workflow as follows: FASTP v. 0.19.6 was used to perform quality control on the original sequences to remove low-quality reads, and FLASH v. 1.2.11 was used for splicing to obtain longer sequences (Magoč and Salzberg, 2011; Callahan et al., 2016). UPARSE v. 11 was used for operational taxonomic unit (OTU) clustering after quality control splicing, and the chimeras were removed according to 97% similarity to acquire the optimized DNA sequences, which were divided into operational classification units (OTUs) (Edgar et al., 2011). MiSeq sequences of purified amplicons were high-throughput sequenced by Guangzhou Jidi'ao Technology Service Co., Ltd. (Guangzhou, China) using Illumina® MiSeq sequencer (Illumina, San Diego, CA, United States).

2.7 Bioinformatics analysis and statistical analysis

Statistical analysis of the soil's chemical properties and growth indexes of *C. cajan* was carried out by applying one-way analysis of variance (ANOVA) and the new multiple range method to the data. All analyses were conducted with SPSS statistical software package, version 20.0 (IBM, United States). The significance for statistical tests was accepted at $p < 0.05$.

Microbial (fungal and bacterial) diversity indexes including the Chao1 and Shannon indexes were calculated using the "vegan" R package[1]. R's default ggplot2 (v3.5) package was used to make species composition analysis graphs and the vegan package for environmental correlation analysis to detect the relationship between environmental factors, samples, and microbial community. Besides, Welch's *t*-test was used to compare differences in the relative abundance of the microbial phylum and genus level between treatments. The correlations between the environmental factors, samples, and microbial community were evaluated via redundancy analysis (RDA) using Canoco software (version 4.5). Prior to conducting the RDA analysis, we standardized the units of physicochemical parameters using R's default vegan package to ensured uniformity and consistency in the data. Spearson's correlation coefficient was employed to correlate the physical and chemical properties of soil and microbial communities in soil. Moreover, the "Vegan" package was used for principal coordinates analysis (PCoA) to determine the beta diversity of microbial communities based on Bray–Curtis dissimilarity, and the first two axes were then plotted using R package "ggplot2 (v3.5). For

1 https://cran.r-project.org/

TABLE 1 Effect of application of microbial inoculants on the growth of *Cajanus cajan*.

Indexes	CK	M45N	M1P	M1H
Height/cm	87.30 ± 4.36a	92.57 ± 5.86ab	108.17 ± 4.06b	118.37 ± 2.11c
Plant ground diameter/mm	6.15 ± 0.25a	6.80 ± 0.31ab	7.14 ± 0.20bc	7.61 ± 0.22c
Dry weight/g	654.72 ± 8.34a	684.56 ± 6.38ab	756.32 ± 5.42b	827.65 ± 7.33c
Aboveground-dry weight/g	438.66 ± 6.12a	449.07 ± 5.08a	513.71 ± 3.22b	564.46 ± 5.13c
Underground-dry weight/g	216.06 ± 4.22a	235.49 ± 5.20b	242.61 ± 5.20c	263.19 ± 6.20d

Different lowercase letters indicate the significant differences ($p < 0.05$).

fungi (ITS gene data), based on their putative life history following ecological guild assignment sensu FUNGuild, the functional categories were assigned with the confidence of highly probable and probable (Nguyen et al., 2016). FUNGuild is a database for the comparison of fungal functions and linking fungal gene sequencing information with the ecological functions of fungi, as well as identifying the nutrient types used by fungi at the genus level and conducting the specific functional classifications. It was also used to study the fungal ecological functions in ecosystems (Tanunchai et al., 2023). For bacteria (16S gene data), the FAPROTAX v. 1.1 (functional annotation of transgenic taxa) database was used to perform rapid functional screening and grouping of 16S bacterial data from terrestrial ecosystems (Sansupa et al., 2021). Based on the OTU classification table of bacterial 16S, the FAPROTAX database was used to predict the potential biogeochemical cycling process of soil samples for functional annotation (Louca et al., 2016). All biological information analysis was carried out using the dynamic real-time interactive online data analysis platform[2].

The isolates of M45N and M1P were deposited in the China Center for Type Culture Collection with the deposit numbers are M20221840 and M20221841, respectively. Additionally, the obtained sequences were uploaded to the NCBI database, and the registration numbers are OR976060 and OR976061, respectively.

3 Results

3.1 Growth of *C. cajan*

Compared with the control (CK), M1P and M1H treatments significantly increased the plant growth of *C. cajan*, including plant height, plant ground diameter, and dry weight, while M45N treatment had no significant differences (Table 1). Among these, M1H treatment as the optimal treatment, significantly increased the plant height, plant ground diameter, and dry weight by 35.58, 23.74, and 26.41% ($p < 0.05$), respectively. Specifically, the aboveground dry weight increased by 28.68%, while the underground dry weight increased by 21.81%, all showing statistically significant differences compared to CK ($p < 0.05$). Besides, M1P treatment exhibited similar effects on plant growth as M1H treatment in plant growth, and the growth-increasing effect of M1H treatment was greater than that of M1P treatment. Additionally, refer to Supplementary Figure S1 for the other treatments that had no growth-promoting effect on *C. cajan* growth.

3.2 Changes in soil properties under different microbial inoculants

As shown in Figure 1, compared with CK, M1P and M1H treatments alleviated soil acidification to a certain extent, and their pH values were 6.31 and 6.61, respectively, and significantly decreased the contents of OC, TN, AN, and AK in the soil ($p < 0.05$). Specifically, M1P and M1H treatments significantly decreased the OC content by 17.14 and 21.89% ($p < 0.05$), respectively, compared to CK, and significantly decreased the TN content by 26.13 and 19.23%, respectively. Moreover, decreasing the TN content did not increase the AN content, and significantly decreased it by 19.08 and 19.71% ($p < 0.05$) under M1P and M1H treatments, respectively. Besides, the contents of TK and AK showed a similar trend to that of TN and AN under M1P and M1H treatments.

3.3 Analysis of soil fungal and bacterial diversity

The fungal and bacterial communities of 15 rhizospheric soil samples were analyzed using high-throughput Illumina MiSeq sequencing technology. A total of 1,662,391 fungal and 1,122,625 bacterial sequences were obtained from all samples, which were clustered into 6,176 fungal OTUs and 59,291 bacterial OTUs, and with an average sequencing coverage rate of 98% (Supplementary Figure S5). The OTUs dilution curve of the samples tended to be flat, indicating high-quality sequencing data were reasonable and reliable. The alpha diversity of fungal and bacterial communities in the rhizosphere soil samples was assessed using the Chao1 and Shannon indexes. Among then, Chao1 index represent the richness and uniformity of OTUs, and Shannon index represent the diversity and uniformity of microbial community (Figures 2A,B). The results showed that M1H treatment had significant effect on the alpha diversity of soil fungi and bacteria ($p < 0.05$), while M1P treatment had no significant effect, compared to CK. Specifically, Chao 1 index of soil fungi and bacteria were significantly increased by 10.34 and 9.41% under M1H treatment ($p < 0.05$), respectively, and by 6.61 and 2.67% to Shannon index, respectively (Figures 2A,B). In contrast, M1P treatment decreased the Chao 1 and Shannon indexes of soil fungi, and decreased Shannon index of soil bacteria, compared to CK. The findings reveal the influence of the fungal and bacterial alpha diversity changes caused by M1P and M1H treatments on *C. cajan* (see discussion section for details). The PCoA showed that the five replicates in each treatment in the fungal and bacterial communities were clustered together, indicating good repeatability between samples, and M1P and M1H treatments result in obviously deviated in the composition of the soil

2 http://www.omicsmart.com

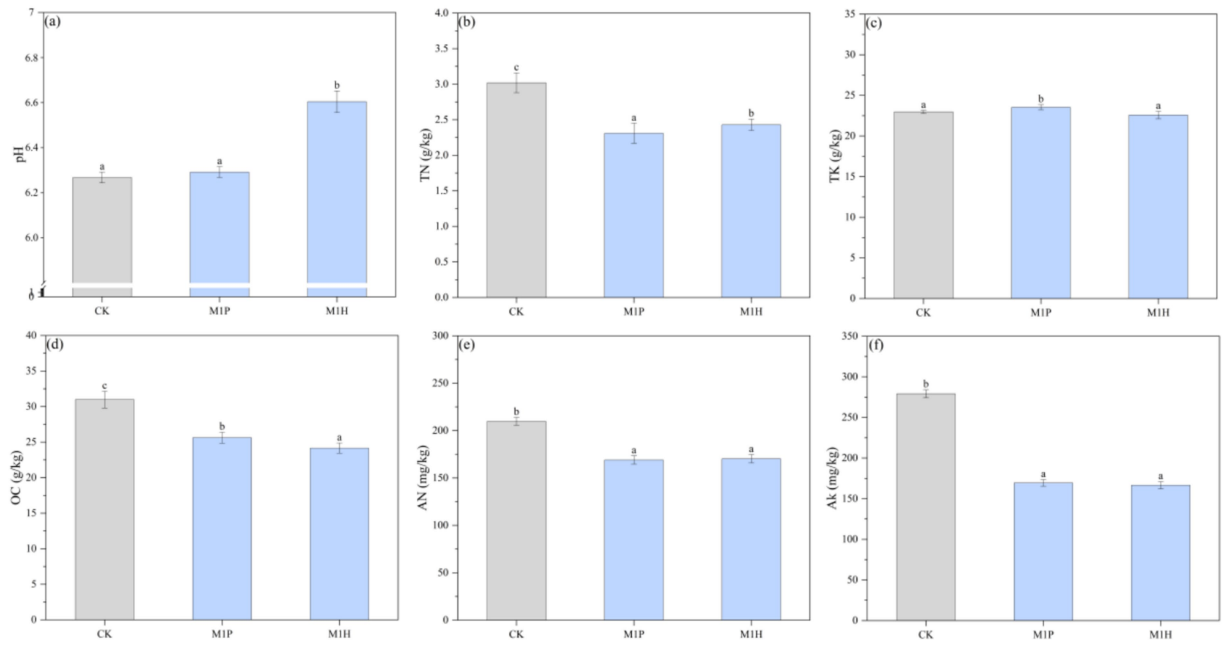

FIGURE 1
Variation in soil properties (soil pH **(A)**, TN **(B)**, TK **(C)**, OC **(D)**, AN **(E)**, and AK **(F)**) under different microbial inoculants. Here, OC, TN, AN, TK, and AK represent organic matter, total nitrogen, available nitrogen, total potassium, and available potassium, respectively. Different lowercase letters indicate the significant differences ($p < 0.05$).

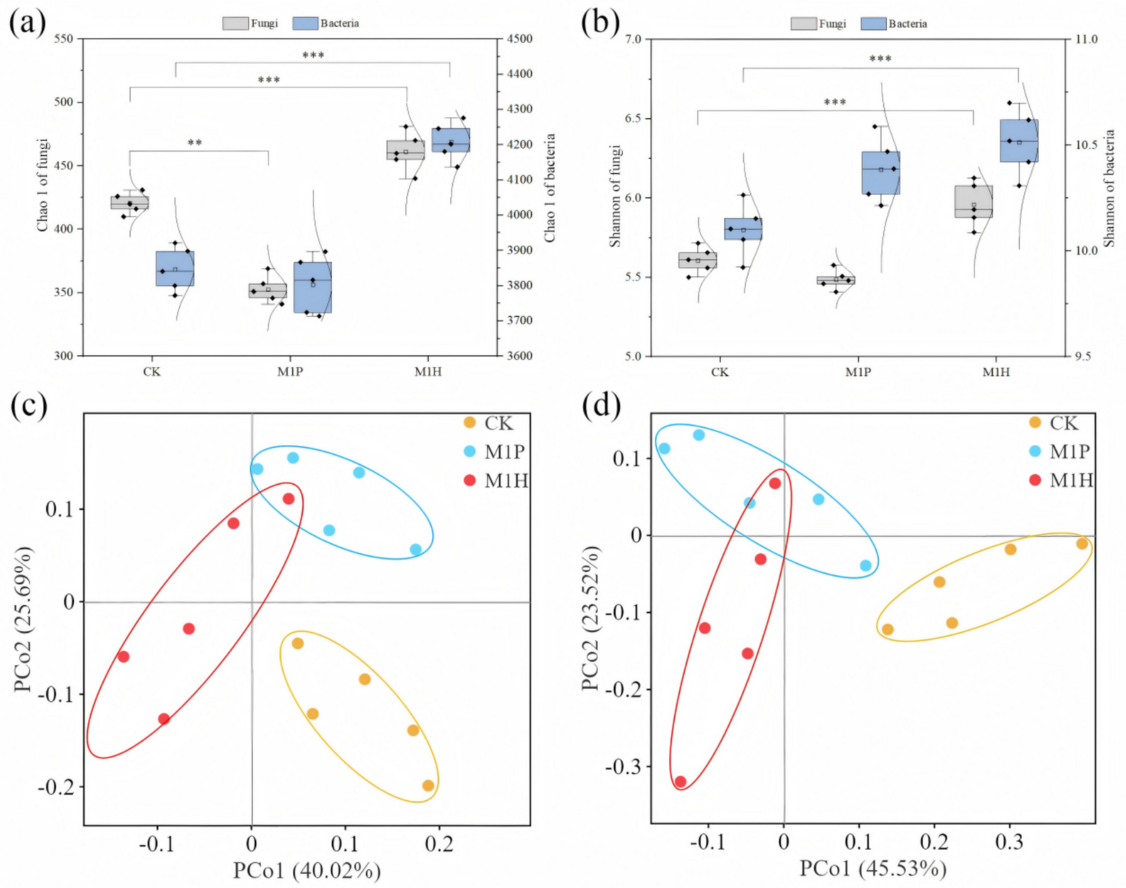

FIGURE 2
Variation in the alpha diversity **(A,B)** and principal coordinate analysis (PCoA) **(C,D)** of soil fungi **(A,C)** and bacteria **(B,D)** under different microbial inoculants. Here, *, ** and *** denote a significant difference between the different treatments at $p < 0.05$, $p < 0.01$ and $p < 0.001$, respectively.

fungal and bacterial communities (Figures 2C,D). Specifically, the contribution rates of PCo1 and PCo2 to the differences in fungal species composition between treatments were 40.02 and 25.69%, and 45.53 and 23.52% to bacteria species composition, respectively.

3.4 Distribution of microbial community structures

The shifts in fungal and bacterial (phylum and genus) communities compositions across all the treatments were investigated based on internal transcribed spacer region (ITS1) gene and the hyper-variable V3–V4 region (16S rDNA) of the 16S rRNA gene sequencing. Figures 3A,C demonstrate the fungal community at the phylum and genus levels in the soil samples. Of these phyla, *Ascomycota, Mucoromycota, Ciliophora, Mortierellomycota*, *Chytridiomycota* and *Basidiomycota* were the dominant phyla in fungal communities (relative abundance of these species exceeded 1% in all treatments). Compared to CK, the relative abundance of *Ascomycota* and *Chlorophyta* were significantly decreased by 32.00% ($p = 0.001$) and 79.79% ($p = 0.003$) under M1H treatment, respectively, while significantly increased the relative abundance of *Mucoromycota* ($p = 0.016$) and *Mortierellomycota* ($p < 0.001$) by 30.47 and 173.99%, respectively. Importantly, *Mucoromycota* (34.59%) replaced *Ascomycota* (31.80%) as the most abundant phylum under M1H treatment, which increased from 26.51 to 34.59%. M1P treatment had no significantly effected to the relative abundance of *Ascomycota*, *Mucoromycota* and *Chytridiomycota*. Besides, M1P and M1H treatments significantly increased the relative abundance of *Mortierellomycota* by 59.41% ($p = 0.002$) and 173.99% ($p < 0.001$), respectively. Meanwhile, as is shown in Figure 4A, the relative abundance of *Ascomycota* and *Mortierellomycota* had significantly different between M1P and M1H treatments. The relative abundance of *Ascomycota* were 31.80 and 43.78% ($p = 0.003$), respectively, and *Mortierellomycota* were 7.11 and 12.22% ($p = 0.002$), respectively, under M1P and M1H treatments. Other phyla were present at low levels. In addition, we further analyzed the changes of the top 10 species of fungal communities at the genus level (Figure 3C). Among then, *Cunninghamella*, *Mortierella*, *Fusarium*, *Penicillium*, *Zopfiella*, and *Podospora* were the top six fungal species in the genus level, which were the dominant genera in the fungal communities across all soil samples, and these species mainly belong to *Mucoromycota* (*Cunninghamella*), *Mortierellomycota* (*Mortierella*) and *Ascomycota* (*Fusarium*, *Penicillium*, *Zopfiella*, and *Podospora*). Compared to CK, M1P and M1H treatments significantly increased the relative abundance of *Cunninghamella* by 17.83% ($p = 0.008$) and 45.44% ($p = 0.005$), respectively, the relative abundance of *Mortierella* by 44.16% ($p = 0.042$) and 262.69% ($p = 0.002$), respectively. Besides, the relative abundance of *Penicillium* was significantly decreased by 13.77% ($p = 0.032$) and 32.12% ($p = 0.009$), respectively. Meanwhile, as is shown in Figure 4C, the relative abundance of *Cunninghamella*, *Mortierella*, *Penicillium*, *Zopfiella*, and *Podospora* had significantly different between M1P and M1H treatments. Compared to M1P treatment, M1H treatment significantly increased the relative abundance of *Cunninghamella* and *Mortierella* by 23.43% ($p = 0.014$) and 151.59% ($p = 0.001$), respectively, while significantly decreased relative abundance of *Penicillium*, *Zopfiella* and *Podospora* by 21.28% ($p = 0.044$), 60.39% ($p = 0.002$) and 58.86% ($p = 0.004$), respectively.

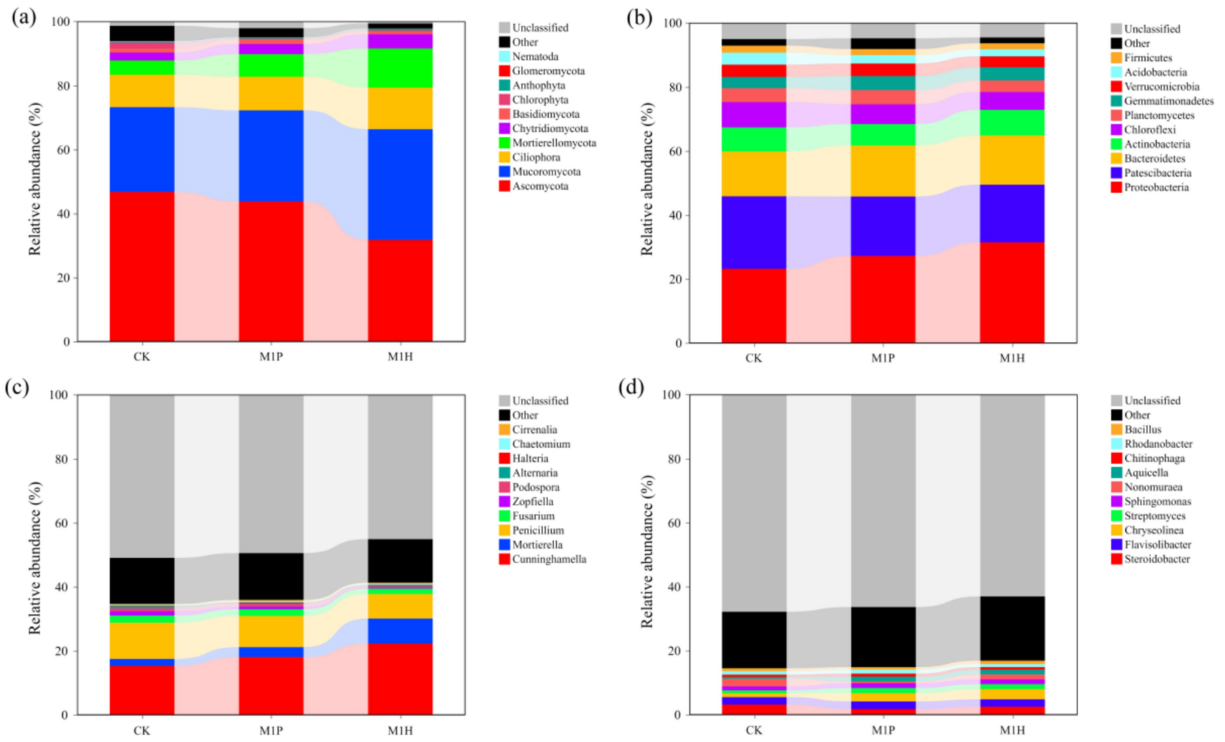

FIGURE 3
Relative abundance of fungal **(A,C)** and bacterial **(B,D)** communities at phylum **(A,B)** and genus **(B,C)** levels under different microbial inoculants.

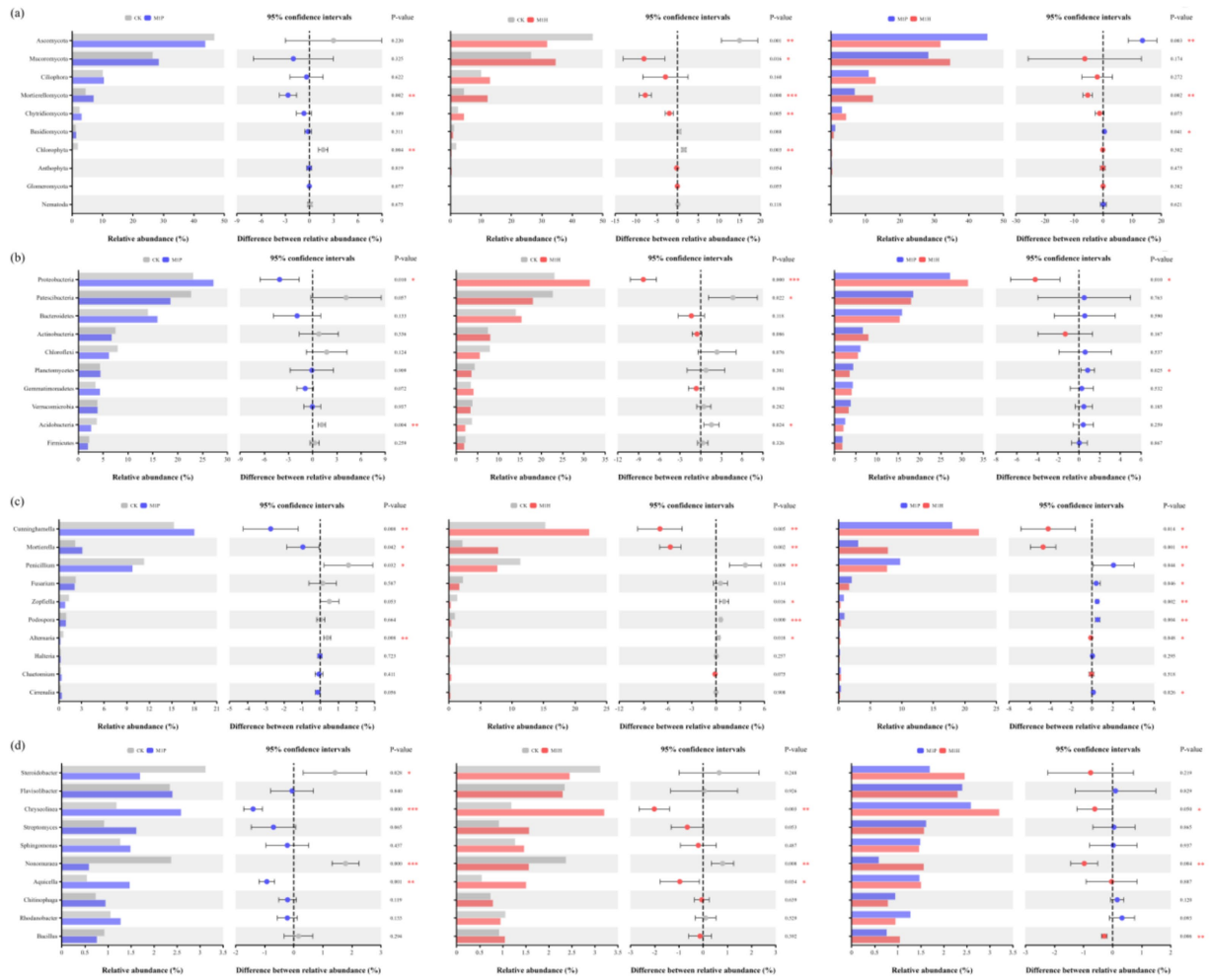

FIGURE 4
Student's *t*-test bar plot on fungal **(A,C)** and bacterial **(B,D)** communities at phylum **(A,B)** and genus **(B,C)** levels with 95% confidence intervals. Here, *, ** and *** denote a significant difference between the two treatments at $p < 0.05$, $p < 0.01$ and $p < 0.001$, respectively. At the phylum and genus level, all phyla and genera with effective sequence abundances within the top 10 were screened for analysis. The abscissa is the species, and the ordinate is the relative abundance percentage and confidence intervals.

For bacteria, Figures 3B, 4B demonstrate the bacterial community at the phylum and genus levels in the soil samples. Of these phyla, *Proteobacteria*, *Patescibacteria*, *Bacteroidetes*, *Actinobacteria*, *Chloroflexi*, *Planctomycetes*, *Gemmatimonadetes*, *Verrucomicrobia*, *Acidobacteria*, and *Firmicutes* were considered dominant (contributed an average of 1% or more to total community composition) and were differentiated in all treatments. Compared to CK, M1P treatment significantly affected the relative abundance of *Proteobacteria* and *Acidobacteria*, and M1P treatment significantly affected the relative abundance of *Proteobacteria*, *Patescibacteria*, and *Acidobacteria*. Besides, *Proteobacteria* was the most dominant bacterial phyla in all the treatments. Compared to CK, M1P and M1H treatments significantly increased the relative abundance of *Proteobacteria* by 17.68% ($p = 0.010$) and 35.88% ($p < 0.001$), respectively. M1H treatment significantly increased the relative abundance of *Proteobacteria* by 15.49% ($p = 0.010$) compared with M1P treatment. Moreover, compared to CK, M1P and M1H treatments decreased the relative abundance of *Patescibacteria* by 18.29 and 20.54% ($p = 0.022$), respectively. In addition, we further analyzed the changes of bacterial community at the genus level (Figures 3D, 4D). Compared to CK, M1P and M1H treatments significantly affected the relative abundance of the relative abundance of *Steroidobacter*, *Chryseolinea*, *Nonomuraea*, and *Aquicella*. Compared to CK, M1P and M1H treatments significantly increased the relative abundance of *Chryseolinea* by 118.07% ($p < 0.001$) and 169.81% ($p = 0.003$), respectively, and M1H treatment increased the relative abundance of *Bacillus* by 13.51%. Differently, compared to M1P treatment, M1H treatment significantly increased the relative abundance of *Chryseolinea*, *Nonomuraea* and *Bacillus* by 13.73% ($p = 0.050$), 165.66% ($p = 0.004$) and 37.69% ($p = 0.006$), respectively.

3.5 Interaction between microbial communities and environmental variables in rhizosphere soil

We analyzed the influence of soil properties on microbial community structure. As per the outcomes of RDA (Figure 5), the

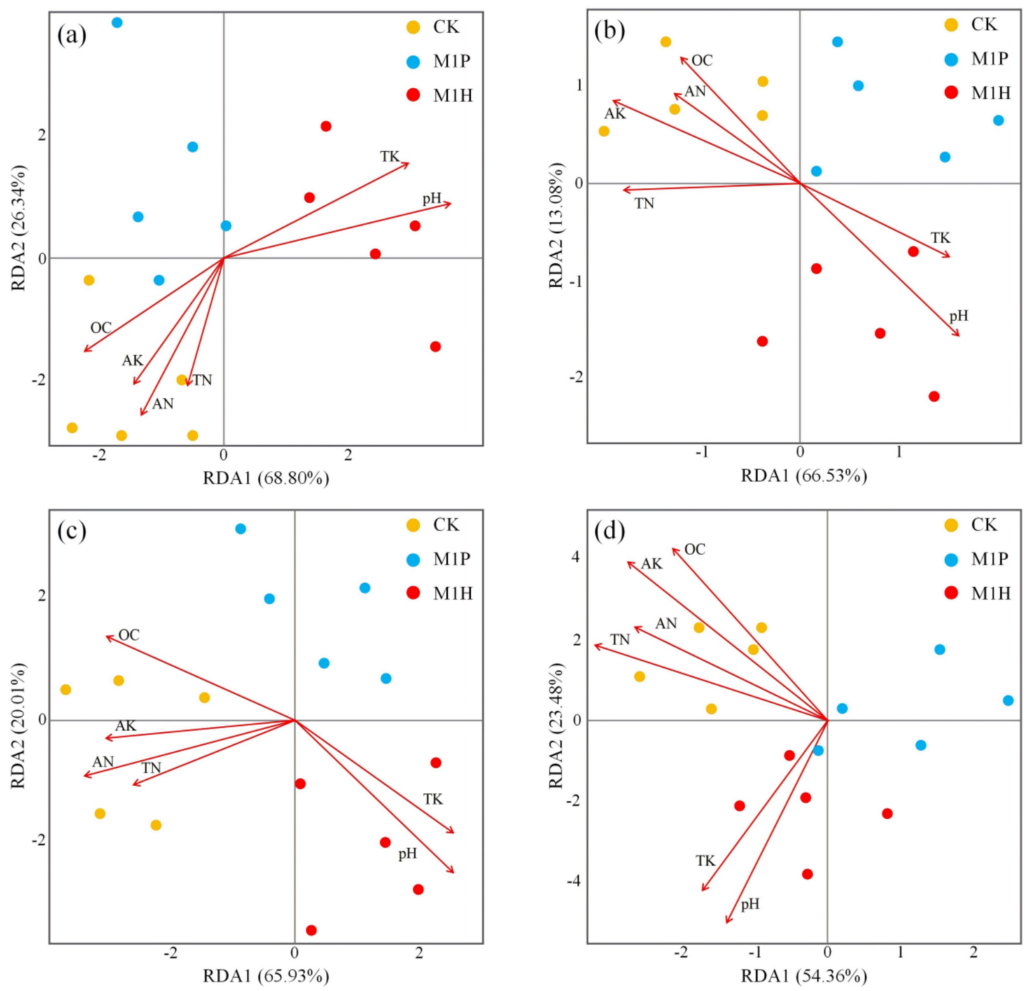

FIGURE 5
Redundancy Analysis (RDA) of the soil nutrients, soil samples, and phylum **(A,B)** and genus **(C,D)** of soil fungal **(A,C)** and bacterial **(B,D)** communities. Here, OC, TN, AN, TK, and AK represent organic matter, total nitrogen, available nitrogen, total potassium, and available potassium, respectively.

RDA of the soil fungal and bacterial communities explained the total variance of 95.14% (Figure 5A) and 79.61% (Figure 5B) at the phylum levels, respectively. Besides, the RDA of the soil fungal and bacterial communities explained the total variance of 85.94% (Figure 5C) and 76.84% (Figure 5D) at the genus levels, respectively. These indicated the reliability of the RDA, and microbial inoculants addition resulted in apparent changes in the soil microbial community structure. In addition, the fungal and bacterial community in CK treatment was positively correlated with OC, TN, AN, and AK, and negatively correlated with pH and TK (Figure 5). In contrast, the fungal and bacterial community in M1H treatment was negatively correlated with OC, TN, AN, and AK, and positively correlated with pH and TK (Figure 5).

Spearman correlation analysis further showed that fungi were more closely related to environmental factors than bacteria in the rhizospheric soil of *C. cajan*. Specifically, *Ascomycota* that the main fungal phyla, was significantly negatively correlated with pH ($p = 0.028$, $R = -0.761$), HG ($p = 0.031$, $R = -0.752$), and DW ($p = 0.035$, $R = -740$), while was significantly positively correlated with AN ($p = 0.022$, $R = 0.766$) and TN ($p = 0.030$, $R = 0.749$), respectively (Figure 6A). *Mortierellomycota* and *Mucoromycota* were significantly positively correlated with plant growth indexes, while *Mortierellomycota* was significantly negatively correlated with AK ($p = 00.021$, $R = -783$), AN ($p = 0.013$, $R = -820$) and TN ($p = 0.004$, $R = -0.880$), respectively (Figure 6A). At the genus level (Figure 6C), *Mortierella* was significantly positively correlated with plant growth indexes ($p < 0.05$) and pH ($p = 0.012$, $R = 0.824$), whereas *Mortierella* ($p = 0.049$, $R = -0.688$) and *Penicillium* ($p = 0.020$, $R = 0.786$) were significantly correlated with OC. Besides, soil pathogenic fungi, such as *Zopfiella* and *Podospora*, were significantly positively correlated with TN and AN, while significantly negatively correlated with DW. In the bacterial phylum community (Figures 6B,D), *Proteobacteria* was significantly negatively correlated with OC ($p = 0.043$, $R = -0.692$), while was significantly positively correlated with DW ($p = 0.041$, $R = 0.698$). Besides, *Acidobacteria* was significantly positively correlated with AN ($p = 0.036$, $R = 0.700$) and TN ($p = 0.030$, $R = 0.712$), respectively. At the genus level (Figure 6D), *Steroidobacter* belong to *Proteobacteria*, was positively correlated with pH, TK, HG, and DW. *Nonomuraea* was significantly positively correlated with AK ($p = 0.039$, $R = 0.693$), TN ($p = 0.026$, $R = 0.727$), and AN ($p = 0.025$, $R = 0.733$). *Bacillus* was not significantly correlated with soil environmental variables.

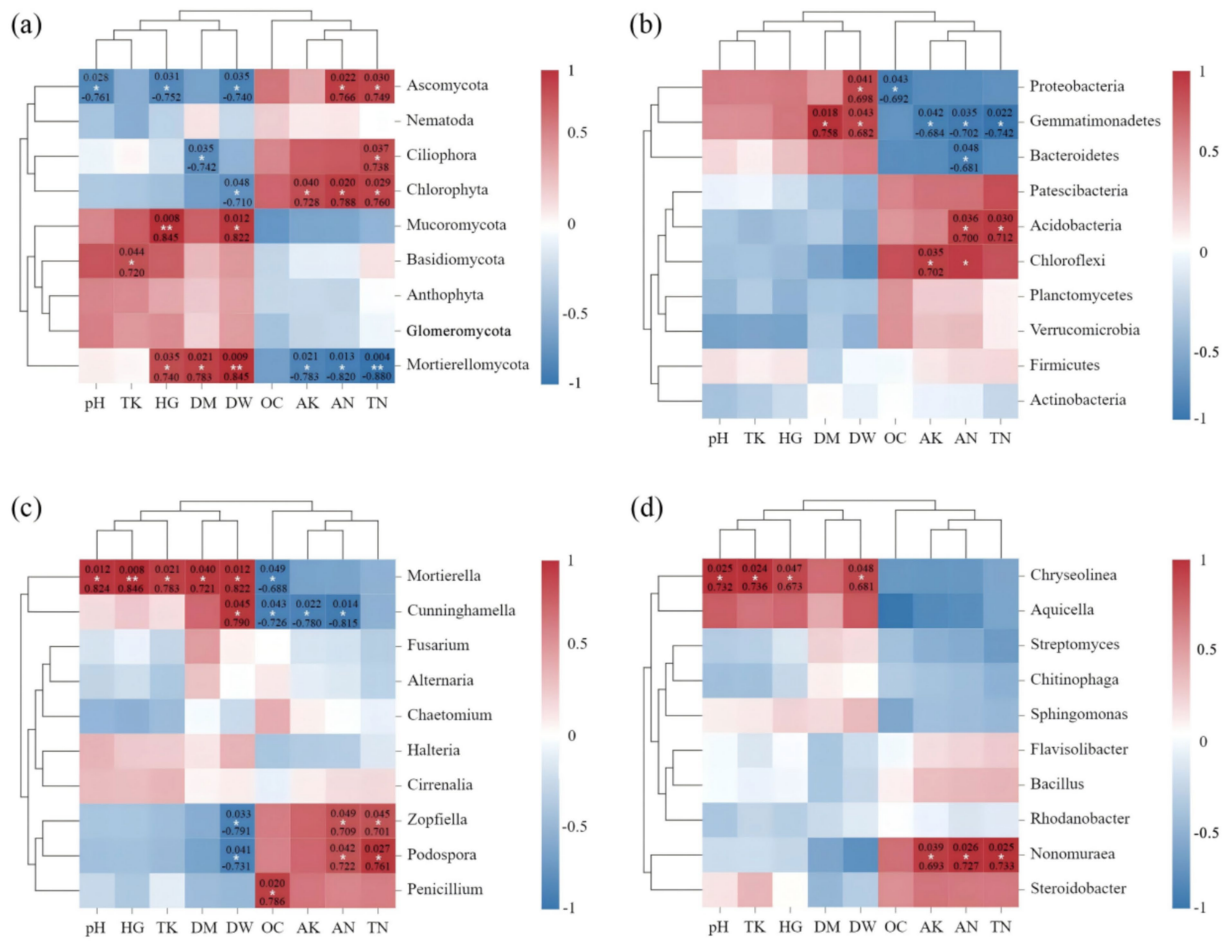

FIGURE 6
Heat map analysis of the correlation between the species composition of soil fungi **(A,C)** and bacteria **(B,D)** at the phylum **(A,B)** and genus **(C,D)** levels and soil nutrients and plant growth index. Here, OC, TN, AN, TK, AK HG, DM, and DW represent organic matter, total nitrogen, available nitrogen, total potassium, available potassium plant height, plant ground diameter, and dry weight, respectively. The legend on the right is the color interval for different *R* values. The number of asterisks indicates the degree of correlation ($p < 0.05$): *$p \leq 0.05$, **$0.05 < p \leq 0.01$, ***$p \leq 0.001$.

3.6 Prediction of fungal (FunGuild) and bacterial (FAPROTAX) ecological functions

The functional abundance of fungal communities of *C. cajan* rhizospheric soil from two treatments and the CK group were identified using ITS rDNA gene amplicon data and FunGuild (Figure 7). At the trophic level, the functional types of soil fungal communities could be divided into seven categories, including Saprotroph, Pathotroph-Saprotroph-Symbiotroph, Saprotroph-Symbiotroph, Symbiotroph, Pathotroph, Pathotroph-Saprotroph, and Pathotroph-Symbiotroph. Compared with CK, M1P and M1H treatments significantly increased the function of Unassigned, increasing by 8.23 and 8.89%, respectively. Meanwhile, Saprotroph, emerged as the most dominant soil fungal community, was significantly decreased by 9.89 and 9.35% under M1P and M1H treatment, respectively. Besides, Pathtroph-saprotrophs-symbiote, emerged as the second most dominant function of the soil fungal community, increasing its abundance under M1P and M1H treatments. The other functional abundance of fungal communities was less than 1%. At the guild level (Figure 8), the functional abundance of undefined Saprotroph, Dung Saprotroph, and Dung Saprotroph-Plant Saprotroph in saprotroph altered significantly. Compared with CK, M1P and M1H treatments decreased the Undefined Saprotroph by 2.01% ($R = -0.33$) and 2.67% ($R = -0.80$), respectively. Meanwhile, Dung Saprotroph abundance decreased by 7.05% ($R = -0.60$) and 6.87% ($R = -0.55$). The M1P treatment significantly decreased Dung Saprotroph-Plant Saprotroph by 0.54% ($R = -1.04$), while M1H treatment significantly increased it by 0.42% ($R = 0.96$), which could be one of the reasons for the difference in the M1P and M1H treatments. Moreover, M1P and M1H treatments increased the functional abundance of Animal Pathogen-Endophyte-Lichen Parasite-Plant Pathogen-Soil Saprotroph-Wood Saprotroph in Pathotroph-Saprotroph-Symbiotroph by 1.59% ($R = 1.15$) and 0.13% ($R = -0.50$). Meanwhile, the functional abundance of Animal Pathogen-Endophyte-Plant Pathogen-Undefined Saprotroph decreased by 1.32 and 1.40%, respectively under M1P and M1H treatments.

The FAPROTAX functional prediction revealed differences in microbial functions between the CK treatment and the two inoculant treatments (M1P and M1H) (Figures 9, 10). The functional types of soil bacterial communities were categorized into seven categories, including chemoheterotrophy (9.30% ~ 10.32%), aerobic_chemoheterotrophy

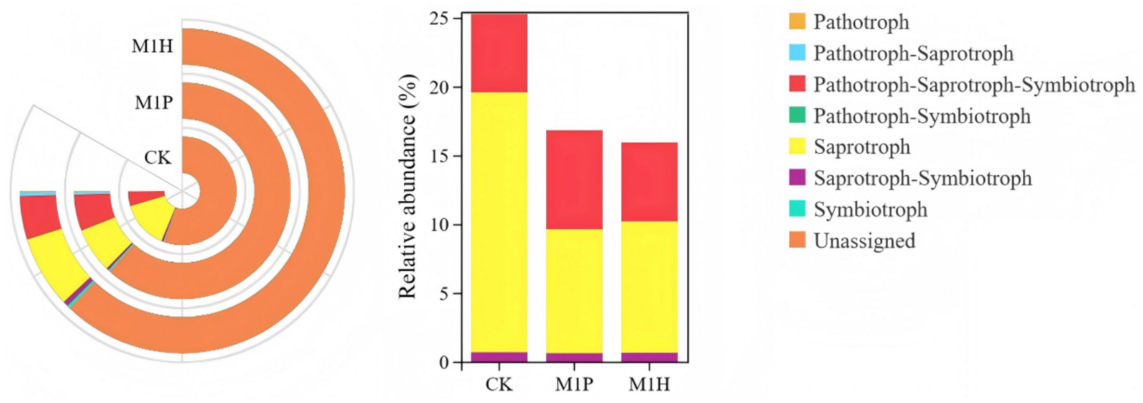

FIGURE 7
Functional differences of soil fungal communities with different microbial inoculants at trophic level.

(8.14% ~ 8.75%), nitrate_reduction (1.03% ~ 1.46%), intracellular_parasites (0.89% ~ 1.04%), fermentation (0.78% ~ 1.11%), predatory_or_exoparasitic (0.42% ~ 0.57%), chloroplasts (0.11% ~ 1.14%), aromatic_compound_degradation (0.39% ~ 0.57%), and methylotrophy (0.33% ~ 0.34%) (Figure 9). Among these, chemoheterotrophy and aerobic_chemoheterotrophy were identified as the most dominant types of bacterial functions across all treatments. Notably, the abundance of chemoheterotrophy and aerobic_chemoheterotrophy was higher in the M1P and M1H treatments compared to the CK. In contrast, the abundance of the remaining five functions of bacterial community was less than 2% across all treatments.

Functional thermogram of analysis of the bacterial community (Figure 10) showed that M1P treatment showed enrichment in nitrate_reduction, aromatic_compound_degradation, intracellular_parasites, fermentation, and chloroplasts ($R > 1.00$). M1H treatment was enriched in methylotrophy and predatory_or_exoparasitic ($R > 1.00$). These results indicated that native microbial inoculation significantly affects the functional profile of the bacterial community in the rhizosphere soil of *C. cajan*. The enhanced microbial functions in the M1P and M1H treatments highlight the potential of these inoculants to modulate soil microbial activity effectively.

4 Discussion

4.1 Effect of M1H applied on soil properties

Soil nutrients, a basic index to evaluate soil fertility, could be used to determine the overall level of soil quality, which affects the structure of the soil microbial community, and finally affects the plant's growth (Shao et al., 2020; Yin et al., 2021). Some reports indicated that microbial inoculants containing beneficial microbes can directly or indirectly modify soil physicochemical properties (Wei et al., 2018; Zhuang et al., 2021). For instance, soil pH is one of the most critical environmental factors affecting soil quality (Zheng et al., 2022). Previous studies shown that *Bacillus*-containing microbial inoculants significantly alleviated the alkalization of strawberry rhizosphere soil, increased the biomass, and improved fruit quality (Li et al., 2022). Similarly, in the current study, the native *S. marcescens* (M1P) and the native mixed microbe inoculants (M1H) alleviated soil acidification, and increased soil pH, in line with previous findings (Zheng et al., 2022). This effect could be attributed to decreased availability of available nutrients, such as AK, and AN likely caused by the activity of proton-coupled solute transporters and the anion uptake, which increase soil acidification (Hinsinger and Jaillard, 2010; Wong et al., 2008). Moreover, the application of microbial inoculants increase the consumption of soil carbon by microbial communities and plants, improve microbial metabolic activities, and regulate the stability of soil pH (Yin et al., 2021). Previous studies suggests that the application of organic inoculants and microbial inoculants improve the plant absorption of soil nutrients, decrease the contents of available nutrients in soil, (e.g., AK, AN, and AP), and thereby promote plant growth (Li Q. et al., 2019; Li Y. et al., 2019; Virk et al., 2022). In this study, we observed that M1H treatment significantly decreased AK and AN contents in the soil by 40.31 and 18.84%, respectively, and promoting the growth of *C. cajan* (plant height, plant ground diameter and dry weight). This reduction in available nutrients may result from microbial inoculants altering the soil microbial community structure, enhancing the microbial metabolic process, and increasing nutrient uptake by plants, consistent with previous findings (Li et al., 2022; Soong et al., 2018). Furthermore, Soussana and Lemaire (2014) and Wang C. et al. (2016) reported that microbial inoculants intake increased the underground carbon distribution in plants and soil carbon absorption, decreasing the OC content. Consistent with these studies. M1H treatment in this study significantly decreased the content of OC by 21.89% compared to CK, indicating increased the consumption and distribution of underground carbon sources by *C. cajan*, in line with previous findings (Li et al., 2022; Soussana and Lemaire, 2014; Wang C. et al., 2016). Interestingly, while the M1H treatment decreased TN and TK contents, potentially affecting AN and AK levels, the M1P treatment showed lower AN and AK contents than the CK treatment. The OC content in the soil showed a similar trend with AN and AK under M1H treatment. In addition, She et al. (2017) and Yin et al. (2013) reported that *Bacillus* can transform insoluble nutrients into effective nutrients needed by plant growth, and improve nutrient availability in the soil. However, the application of *Bacillus* also increases nutrient consumption of by microbes and plants, reflecting the true nutrient dynamics in the soil. These findings highlight the importance of native mixed microbial inoculants (M1H) in increasing the growth of *C. cajan* and provide insights into the mechanisms by which M1H affects soil nutrient dynamics. This study highlights the

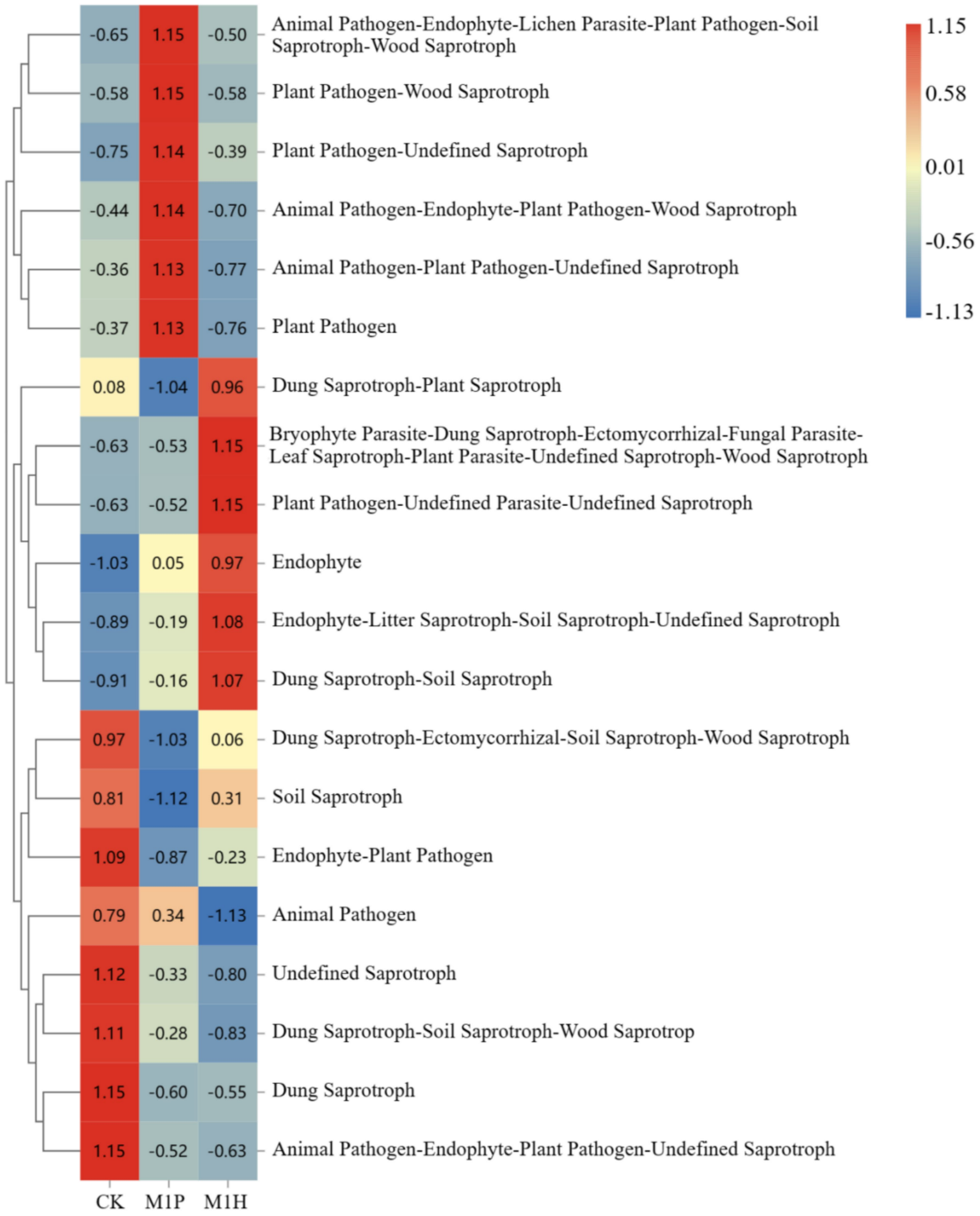

FIGURE 8
Analysis of community function heat map based on FunGuild at guild level. The legend on the right is the color interval for different R values. The number in the square indicates the specific *R* values.

potential of microbial inoculants in sustainable agricultural practices, particularly for plant development.

Indeed, exogenous microbial inoculants have been employed to correlate plants growth to soil nutrients (Li et al., 2022; Zhuang et al., 2021). However, in the current research, most annotations focus on the promotion effect of soil nutrient enrichment on plant growth, but ignore the research on the balance relationship between plant absorption and soil eutrophication by exogenous strains. Moreover, *C. cajan*, as pioneer tree species for the prevention and control of soil erosion, but has received relatively less research attention (Lazcano et al., 2021). In our study, the relationship between the decrease of soil nutrients in *C. cajan* rhizosphere after M1H treatment and the benefit of plant growth confirmed the improvement of *Cajanus cajanus*' ability to absorb soil nutrients to some extent. Additionally, due to the

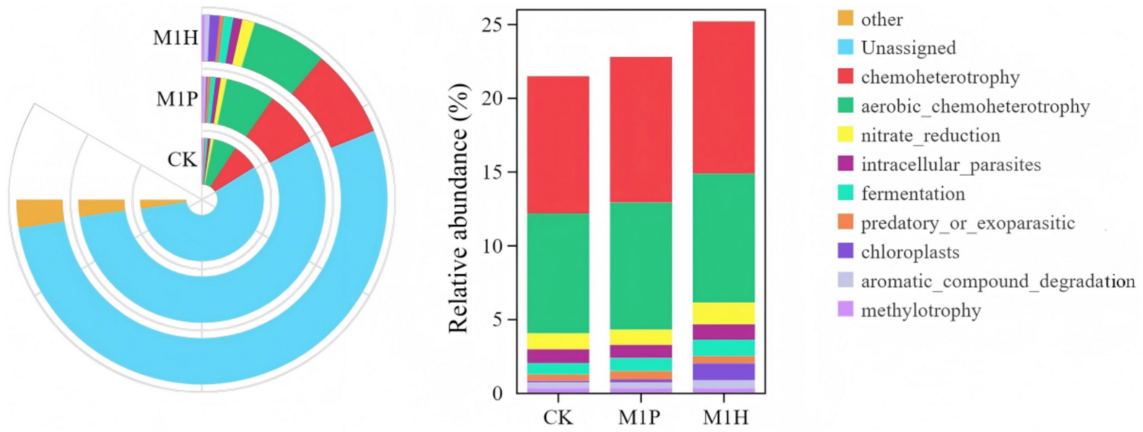

FIGURE 9
Functional differences of soil bacterial communities with different microbial inoculants.

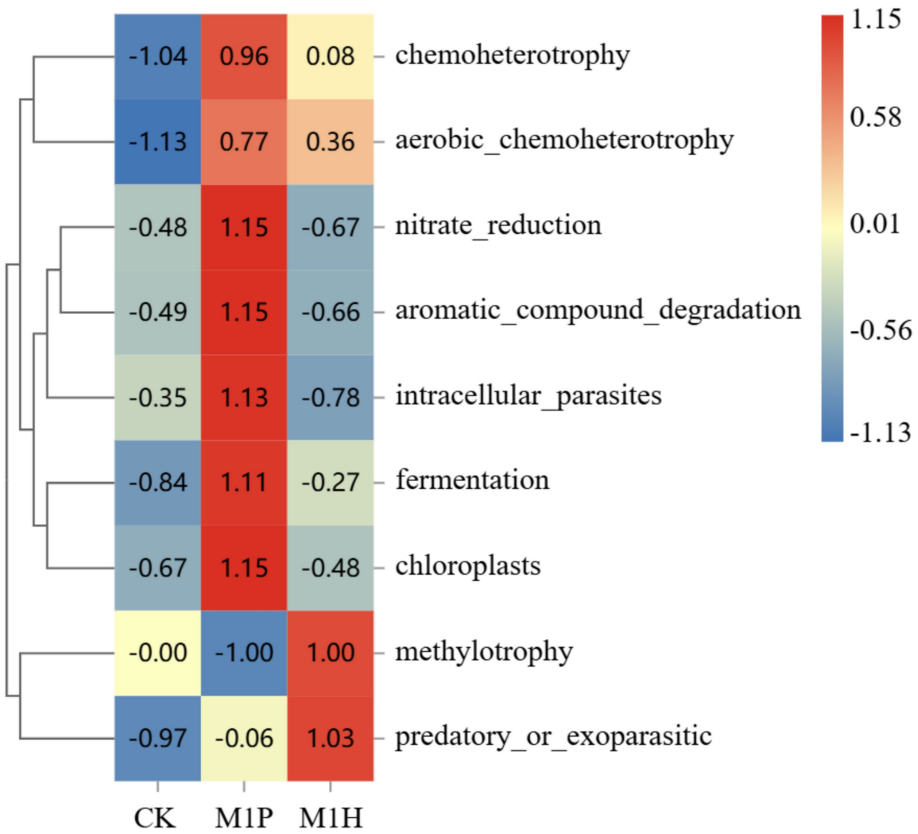

FIGURE 10
Analysis of community function heat map based on FAPROTAX. The legend on the right is the color interval for different *R* values. The number in the square indicates the specific *R* values.

relative dearth of relevant data, and considering that the internal relationship between endogenous microbes and nutrient absorption of *C. cajan* has not been involved in the current research, this limitation hinders the current research, especially the changes of nutrients in *Cajanus cajanus* plants. Therefore, it is necessary to explore the changes of nutrients in *C. cajan* under M1H treatment to confirm the viewpoint and provide scientific protection for this study.

4.2 Effect of M1H on fungal and bacterial communities' structure and function

Soil microbes are a vital part of the soil ecosystem, playing crucial roles in promoting plant growth and maintaining the micro-ecological environment of the soil (Liu et al., 2018; Luo et al., 2017; Song et al., 2022). In this study, it was observed that M1P and M1H

treatments showed different trends in soil diversity indexes. Some previous studies showed that the application of microbial inoculants stimulated or induced the development of rhizosphere soil microbes, and thereby enriched the richness and diversity of soil microbial communities (Li et al., 2022; Zhuang et al., 2021), while others reported that although the application of microbial inoculants promoted plant growth and crop yield, it may simultaneously lead to a reduction in the diversity and richness of soil microbes. This reduction occurs because exogenous microbial inoculants, as an aggregate of the same microbe, intensifying competition among soil microbes within a short time, making the microbes with weak adaptability unable to cope with environmental changes, ultimately resulting in the reduction of soil richness and diversity (Cheng et al., 2021; Yao et al., 2003). These findings highlight that the variable and multi-directional effects of exogenous microbial inoculants on soil microbial communities. Understanding the potential functions of native microbial inoculants, particularly their effect on rhizosphere microbial diversity, offers a pathway to optimizing plant growth.

We then sought to understand the mechanism behind the ability of the rhizosphere microbiome to promoting the growth ability of *C. cajan* under inoculation with M1P and M1H inoculants. In this study, we observed that different microbial inoculants did alter the soil fungal community structure. *Ascomycota*, *Mucoromycota*, *Ciliophora*, *Mortierellomycota*, and *Chytridiomycota* were still the dominant phyla in the soil fungal community, and their abundances changed significantly, in line with previous findings (Wang H. et al., 2016; Zhou et al., 2015). Notably, *Mucoromycota* instead of *Ascomycota* emerged as the most abundant fungal phylum under M1H treatment, whereas the M1P treatment did not show this trend. This due to showed that *Ascomycota* and *Mucoromycota* could be significantly greatly influenced by the level of soil nutrients, mainly by OC, TN and AN, and *Mucoromycota* was negatively correlated with AN ($p = 0.013$, $R = -0.820$) and TN ($p = 0.004$, $R = -0.880$), respectively, and was positively correlated with plant growth indexes by using Spearman analysis (Figure 6A). Besides, some studies showed that the affects of *Mucoromycota* not always depend on high nutrient levels in the soil environment, but also on the nutrient content of the background soil (Nie et al., 2018). Nguyen et al. (2016) further reported that the abundance of *Mucoromycota* in soil was significantly different under different N levels and high N levels significantly restrained the abundance of *Mucoromycot* (Nguyen et al., 2016; Nie et al., 2018). In this study, the results showed that M1H treatment significantly decreased *Ascomycota* abundance in the soil, and the soil nutrient contents, including TN, TK, AN, and AK, corroborating previous findings (Nguyen et al., 2016). Furthermore, FunGuild analysis indicated that the application of M1P and M1H microbial inoculants significantly decreased the Saprotrophs abundance in the soil fungal community. This reduction was likely due to decreased *Ascomycot*a abundance in the soil resulting from the decreased level of soil nutrients after the addition of microbial inoculants, as *Ascomycota* contains a large number of microbial communities involved in saprophytic or symbiotic functions (Abbasi et al., 2021; Cheng et al., 2021). The reduction in soil nutrients following microbial inoculant application contributed to this shift in fungal community structure. These results suggest that applying native microbial inoculants, coupled with careful management of soil N levels, promotes the transformation of dominant soil microorganisms, improving the growth of *C. cajan*.

According to previous reports, beneficial microbial inoculants can optimize soil community structure, improve the soil micro-environment, and promote plant growth (Kaur and Garg, 2020; Li et al., 2022). For instance, the application of microbial inoculants containing *Penicillium* have been shown to significantly increase the abundance of *Mortierella*, thereby promote the growth of *I. matsum* (Zhuang et al., 2021). Similarly, *Bacillus*-containing inoculants can increase the abundance of beneficial microbes, such as *Firmicutes*, *Chloroflexi*, *Bacillus,* and *Actinomadura*, while inhibiting the abundance of pathogenic fungi, like *Fusarium* and *Phytophthora* in soil, and increasing strawberry yield (Li et al., 2022). While these studies highlight the contributions of microbial inoculants to soil community structure and the soil microbial environment, research on compound microbial inoculants combining *S. marcescens* and *P. polymyxa* remains limited. In this study, we observed that the application of M1H significantly increased the abundance of beneficial microbes, particularly *Cunninghamella* in the soil, which was positively correlated with the growth of *C. cajan*. The increased abundance of *Cunninghamella* likely contributed to enhanced nutrient consumption by *C. cajan*. Moreover, foreign microbial inoculants are known to induce changes in the structure of the soil microbial community structure. In this study, the most significant changes in the fungal community were the a decrease in the relative abundance of *Ascomycota* and an increase in *Mortierellomycota*, with M1H treatment significantly altered these relative abundances of *Ascomycota* and *Mortierellomycota* by 32.00 and 42.16%. Previous studies have indicated that *Ascomycota* is often more abundant in diseased soils, whereas *Mortierellomycota* is associated with healthy soils, and the relative abundance of *Mortierellomycota* was confirmed to have a significant relationship with *Penicillium* (Yuan et al., 2020; Zhuang et al., 2021). The genetic characteristics of *Mortierella* highlight its ability to degrade toxic organic matter, contributing to soil health (Zhuang et al., 2021); Furthermore, *Mortierella* has been shown to increase the level of indole acetic acid levels in plants, thereby enhancing plant biomass. These findings strongly support the role of *Mortierella* as a beneficial microorganism that promotes soil improvement and plant growth. The observed increase in *Mortierella* abundance following M1H application represents a positive shift in the soil microbial community, further validating the effectiveness of the M1H microbial inoculant in improving soil health and supporting the growth of *C. cajan*.

In this study, we further investigated the effects of native mixed microbial inoculants on potential microbial communities, as they may represent an important factor affecting the growth of *C. cajan*. The abundance of *Zopfiella* and *Podospora* (both belong to *Ascomycota*) were significantly decreased under M1H treatment, and were negatively correlated with plant growth indexes indices based on Spearman analysis (Figure 6C). *Zopfiella* and *Podospora* belong to *Chaetomiaceae* and *Lasiosphaeriaceae*, respectively, and both belong to Ascomycota, widely exist in soil feces contain important pathogens or saprophytic fungi that can may negatively impact plant growth (Li Q. et al., 2019; Li Y. et al., 2019). Furthermore, Ma et al. (2024), by analyzing 82 animal feces samples from different sources, reported that *Zopfiella* and *Podospora* in wild budgerigar feces showed pathogenic characteristics, while pathogenic effects of

Zopfiella and *Podospora* in feces from other sources were less apparent. These findings suggest that the M1H microbial inoculant can optimize the soil microenvironment by promoting, the abundance of beneficial microbes while suppressing the abundance of potentially microbes, aligning with previous studies (Kaur and Garg, 2020; Li et al., 2022). RDA revealed that *Zopfiella* and *Podospora* were positively correlated with TN and AN levels, indicating that high soil nitrogen levels could elevate the abundance of pathogenic microbes (Wei et al., 2018). Moreover, the soil pH value ($R = 0.012$, $p = 0.824$) and TK ($R = 0.021$, $p = 0.783$) were identified as key factors affecting the abundance of *Mortierella*. In this study, M1H treatment significantly decreased the abundance of genes associated with the saprotroph function of soil flora and the relative abundance of *Zopfiella* and *Podospora*, both members of *Ascomycota*. This reduction suggests that *Zopfiella* and *Podospora* may play a primary role in saprotrophic functions. However, the observed changes in the abundance of these fungi in the rhizosphere soil of *C. cajan* do not provide evidence regarding their potential to cause disease or the overall disease status of the soil. While the roles of *Zopfiella* and *Podospora* in the rhizosphere remain unclear, their correlation with plant growth indices suggests that they may act as potential factors affecting the growth of *C. cajan* (Figure 6C). Therefore, these fungi have been classified as potential soil microbes in this study. Despite the observed associations, a lack of targeted research limits the understanding of the pathogenicity and mechanisms of *Zopfiella* and *Podospora* in the context of *C. cajan* physiology. While this study establishes a foundation by highlighting the relationship between their abundance and plant growth, further research is needed to confirm their pathogenic roles and explore their mechanisms of action. The findings presented here offer a new perspective for future investigations into the potential pathogenicity of *Zopfiella* and *Podospora*. In summary, the application of M1H inoculants altered the relative abundance of beneficial and potentially harmful microbes in the soil, improving the soil microenvironment and explaining changes in soil nutrient factors. Compared to studies on single microbial inoculants, this research marks a significant advancement by demonstrating the broader impacts of mixed microbial inoculants on soil microbial communities and plant growth.

4.3 Internal factors affecting the growth-promoting ability of M1H

The application of microbial inoculants has been shown to affect the soil nutrients, alter the soil microbial community structures, and impact plant growth (Cheng et al., 2020; Li et al., 2022; Zhang et al., 2019). In this study, we observed that the addition of M1H inoculants significantly affected the microbial diversity and community structure of *C. cajan* rhizosphere soil, with a greater impact observed on soil fungi compared to bacteria. This suggests that fungi may play a key role in the analyzed soil environment in promoting the growth of *C. cajan*. At the genus level, the abundances of *Cunninghamella*, *Zopfiella*, and *Podospora* were significantly changed under the M1H treatment compared to CK. Notably, the abundance of *Cunninghamella* was positively associated with *C. cajan* growth, while *Zopfiella* and *Podospora* showed negative correlations. OC and AN were identified as the primary environmental factors affecting the abundance of these genera. Moreover, while no significant differences were observed in the abundances of *Zopfiella* and *Podospora* between M1H and M1P treatments, *Cunninghamella* abundance was significantly higher in the M1H treatment. This increase corresponded with enhanced growth of *C. cajan*, indicating that the superior growth-promoting effects of M1H compared to M1P may be attributed to the increased abundance of *Cunninghamella*. Differences were also observed at the bacterial genus level between M1H and M1P treatments, with genera such as *Chryseolinea*, *Nonomuraea,* and *Chitinophaga* showing significant variations. This may be related to the role of trace elements in promoting interactions between microbes (Fang et al., 2020; Toffa et al., 2021). Previous studies have demonstrated that host microbes usually exist in plants and the nutrient-rich rhizospheric soil environments increase the absorption of soil nutrients through roots. It is conducive to the decomposition of organic matter and the absorption of available nutrients, thereby promoting the growth and development of plants (Ingram et al., 2005; Li et al., 2022; Soong et al., 2018). These findings align with our study, which highlights the potential roles of *Cunninghamella*, *Zopfiella*, and *Podospora* in the growth of *C. cajan*. The results suggest that inoculating the soil micro-ecological environment with native microbial inoculants can reduce biological competition, optimize soil conditions, and promote plant growth. This highlights the importance of localized microbial inoculation strategies in improving plant performance and soil health.

5 Conclusion

Our research examined the impact on *C. cajan* growth, soil nutrients and soil rhizosphere microbiomes by pot experiment with different native microbial inoculants. The results showed that both M1P and M1H treatments significantly promoted the growth of *C. cajan*, but M1H treatment showed a higher growth-promoting ability than M1P treatment, and increased the consumption capacity of soil OC, AN, and AK contents. Meanwhile, M1H treatment led to substantial alterations in the soil microbial community that were more effective in promoting *C. cajan* growth, particularly through increasing beneficial genera (e.g., *Cunninghamella*, *Mortierella*, *Chryseolinea*, *Chrysolina*, and *Bacillus*) and decreasing potential genera (e.g., *Zopfiella* and *Podospora*). Among then, *Cunninghamella*, *Zopfiella*, and *Podospora* were the key bioindicators for influencing *C. cajan* growth by Spearman correlation analysis. The study also proved that OC, AK, AN, and TN were the key environmental factors influencing *Cunninghamella*, *Zopfiella*, and *Podospora*. Notably, the effect of M1H inoculation on soil fungal community was higher than that of bacterial community at the genus levels, which indicates that the change of soil fungal community after M1H inoculation was more active than that of bacteria. In summary, the native mixed microbial inoculants (M1H) enhanced the consumption of soil nutrients by *C. cajan*, purified the soil micro-environment, and thereby promoted the growth of *C. cajan*. This study confirmed the feasibility and effectiveness of mixed microbial inoculants in promoting plant growth, which provides a theoretical basis and sustainable management strategy for the cultivation of *C. cajan* and the development of the agriculture husbandry industry.

Data availability statement

The datasets presented in this study can be found in online repositories. The names of the repository/repositories and accession number(s) can be found in the article/Supplementary material.

Author contributions

ZL: Data curation, Formal analysis, Investigation, Methodology, Software, Supervision, Validation, Writing – original draft, Writing – review & editing. CL: Investigation, Methodology, Writing – original draft. KZ: Data curation, Investigation, Writing – original draft. YS: Conceptualization, Data curation, Formal analysis, Supervision, Writing – original draft. JR: Investigation, Methodology, Resources, Writing – original draft. YM: Conceptualization, Data curation, Formal analysis, Investigation, Methodology, Software, Writing – original draft. XZ: Data curation, Formal analysis, Software, Writing – original draft. YZ: Supervision, Validation, Writing – original draft. JZ: Conceptualization, Data curation, Formal analysis, Funding acquisition, Investigation, Methodology, Project administration, Resources, Software, Supervision, Validation, Visualization, Writing – review & editing.

Funding

The author(s) declare that no financial support was received for the research, authorship, and/or publication of this article.

Conflict of interest

The authors declare that the research was conducted in the absence of any commercial or financial relationships that could be construed as a potential conflict of interest.

Generative AI statement

The authors declare that no Gen AI was used in the creation of this manuscript.

Publisher's note

All claims expressed in this article are solely those of the authors and do not necessarily represent those of their affiliated organizations, or those of the publisher, the editors and the reviewers. Any product that may be evaluated in this article, or claim that may be made by its manufacturer, is not guaranteed or endorsed by the publisher.

Supplementary material

The Supplementary material for this article can be found online at: https://www.frontiersin.org/articles/10.3389/fmicb.2025.1521064/full#supplementary-material

References

Abbasi, S., Sadeghi, A., Omidvari, M., and Tahan, V. (2021). The stimulators and responsive genes to induce systemic resistance against pathogens: an exclusive focus on tomato as a model plant. *Biocatal. Agric. Biotechnol.* 33:101993:101993. doi: 10.1016/j.bcab.2021.101993

Adams, R. I., Miletto, M., Taylor, J. W., and Bruns, T. D. (2013). Dispersal in microbes: fungi in indoor air are dominated by outdoor air and show dispersal limitation at short distances. *ISME J.* 7, 1262–1273. doi: 10.1038/ismej.2013.28

Baldock, J. A., and Skjemstad, J. O. (2000). Role of the soil matrix and minerals in protecting natural organic materials against biological attack. *Org. Geochem.* 31, 697–710. doi: 10.1016/S0146-6380(00)00049-8

Callahan, B. J., McMurdie, P. J., Rosen, M. J., Han, A. W., Johnson, A., and Holmes, S. (2016). DADA2: high-resolution sample inference from Illumina amplicon data. *Nat. Methods* 13, 581–583. doi: 10.1038/nmeth.3869

Chen, H., Zhao, S., Zhao, J., Zhang, K., Jiang, J., Guan, Z., et al. (2020). Deep tillage combined with biofertilizer following soil fumigation improved chrysanthemum growth by regulating the soil microbiome. *Microbiol Open* 9:e1045:e1045. doi: 10.1002/mbo3.1045

Cheng, H., Zhang, D., Huang, B., Song, Z., Ren, L., Hao, B., et al. (2020). Organic fertilizer improves soil fertility and restores the bacterial community after 1, 3-dichloropropene fumigation. *Sci. Total Environ.* 738:140345:140345. doi: 10.1016/j.scitotenv.2020.140345

Cheng, H., Zhang, D., Ren, L., Song, Z., Li, Q., Wu, J., et al. (2021). Bio-activation of soil with beneficial microbes after soil fumigation reduces soil-borne pathogens and increases tomato yield. *Environ. Pollut.* 283:117160:117160. doi: 10.1016/j.envpol.2021.117160

Dastager, S. G., Deepa, C. K., and Pandey, A. (2010). Isolation and characterization of novel plant growth promoting Micrococcus sp NII-0909 and its interaction with cowpea. *Plant Physiol. Biochem.* 48, 987–992. doi: 10.1016/j.plaphy.2010.09.006

De Falco, G., Magni, P., Teräsvuori, L. M. H., and Matteucci, G. (2004). Sediment grain size and organic carbon distribution in the Cabras lagoon (Sardinia, Western Mediterranean). *Chem. Ecol.* 20, 367–377. doi: 10.1080/02757540310001629189

Edgar, R. C., Haas, B. J., Clemente, J. C., Quince, C., and Knight, R. (2011). UCHIME improves sensitivity and speed of chimera detection. *Bioinformatics.* 27, 2194–2200. doi: 10.1093/bioinformatics/btr381

El-Sharkawy, H., Abbas, M. S., Soliman, A. S., Ibrahim, S. A., and El-Nady, I. (2021). Synergistic effect of growth-promoting microorganisms on bio-control of *Fusarium oxysporum* f. sp. pisi, growth, yield, physiological and anatomical characteristics of pea plants. *Pestic. Biochem. Physiol.* 178:104939:104939. doi: 10.1016/j.pestbp.2021.104939

Fang, W., Song, Z., Tao, S., Zhang, D., Huang, B., Ren, L., et al. (2020). Biochar mitigates the negative effect of chloropicrin fumigation on beneficial soil microorganisms. *Sci. Total Environ.* 738:139880. doi: 10.1016/j.scitotenv.2020.139880

Gnanesh, B. N., Bohra, A., Sharma, M., Byregowda, M., Pande, S., Wesley, V., et al. (2011). Genetic mapping and quantitative trait locus analysis of resistance to sterility mosaic disease in pigeonpea [*Cajanus cajan* (L.) Millsp.]. *Field Crop Res.* 123, 53–61. doi: 10.1016/j.fcr.2011.04.011

Hinsinger, P., and Jaillard, B. (2010). Root-induced release of interlayer potassium and vermiculitization of phlogopite as related to potassium depletion in the rhizosphere of ryegrass. *J. Soil Sci.* 44, 525–534. doi: 10.1111/j.1365-2389.1993.tb00474.x

Ingram, L. J., Schuman, G. E., Stahl, P. D., and Spackman, L. K. (2005). Microbial respiration and organic carbon indicate nutrient cycling recovery in reclaimed soils. *Soil Sci. Soc. Am. J.* 69, 1737–1745. doi: 10.2136/sssaj2004.0371

J, D., F, F., and Agl. (1984). Physical and chemical method of soil and water analysis.

Kaur, H., and Garg, N. (2020). Interactive effects of zinc-arbuscular mycorrhizal (AM) Fungi on cadmium uptake, rubisco, Osmolyte synthesis and yield in *Cajanus cajan* (L.) Millsp. *Int. J. Sustain. Agric. Res.* 8, 17–42. doi: 10.18488/journal.70.2021.81.17.42

Kos, M., van Loon, J. J. A., Dicke, M., and Vet, L. E. M. (2009). Transgenic plants as vital components of integrated pest management. *Trends Biotechnol.* 27, 621–627. doi: 10.1016/j.tibtech.2009.08.002

Lazcano, C., Boyd, E., Holmes, G., Hewavitharana, S., Pasulka, A., and Ivors, K. (2021). The rhizosphere microbiome plays a role in the resistance to soil-borne pathogens and nutrient uptake of strawberry cultivars under field conditions. *Sci. Rep.* 11:3188. doi: 10.1038/s41598-021-82768-2

Li, Q., Fang, W., Yan, D., Wang, Q., and Cao, A. (2019). Research progress on the effect of fumigants on soil microorganisms. *Chin. J. Pestic. Sci.* 21, 780–786. doi: 10.16801/j.issn.1008-7303.2019.0091

Li, Y., Li, Y., Zhang, H., Wang, M., and Chen, S. (2019). Dizotrophic *Paenibacillus beijingensis* BJ-18 provides nitrogen for plant and promotes plant growth, nitrogen uptake and metabolism. *Front. Microbiol.* 10:1119. doi: 10.3389/fmicb.2019.01119

Li, Q., Zhang, D., Song, Z., Ren, L., Jin, X., Fang, W., et al. (2022). Organic fertilizer activates soil beneficial microorganisms to promote strawberry growth and soil health after fumigation. *Environ. Pollut.* 295:118653:118653. doi: 10.1016/j.envpol.2021.118653

Liu, D., Huang, Y., Sun, H., and An, S. (2018). The restoration age of *Robinia pseudoacacia* plantation impacts soil microbial biomass and microbial community structure in the loess plateau. *Catena* 165, 192–200. doi: 10.1016/j.catena.2018.02.001

Liu, Z., Wu, Z., Tian, F., Liu, X., Li, T., He, Y., et al. (2023). Phosphate-solubilizing microorganisms regulate the release and transformation of phosphorus in biochar-based slow-release fertilizer. *Sci. Total Environ.* 869:161622:161622. doi: 10.1016/j.scitotenv.2023.161622

Louca, S., Parfrey, L. W., and Doebeli, M. (2016). Decoupling function and taxonomy in the global ocean microbiome. *Science* 353, 1272–1277. doi: 10.1126/science.aaf4507

Luo, D., Liu, S., Shi, Z. M., Feng, Q. H., Liu, Q. L., Zhang, L., et al. (2017). Soil microbial community structure in picea asperata plantations with different ages in subalpine of western Sichuan, Southwest China. *Chin. J. Appl. Ecol.* 28, 519–527. doi: 10.13287/j.1001-9332.201702.028

Ma, X. P., Li, Z. G., Cai, L. J., Xiao, M., He, F., Liu, Z., et al. (2024). Analysis of fungal diversity in the gut feces of wild takin (*Budorcas taxicolor*). *Front. Microbiol.* 15:1364486. doi: 10.3389/fmicb.2024.1364486

Ma, H., Wei, M., Wang, Z., Hou, S., Li, X., and Xu, H. (2020). Bioremediation of cadmium polluted soil using a novelcadmium immobilizing plant growth promotion strain Bacillus sp. TZ5 loaded on biochar. *J. Hazard. Mater.* 388:122065. doi: 10.1016/j.jhazmat.2020.122065

Magoč, T., and Salzberg, S. L. (2011). FLASH: fast length adjustment of short reads to improve genome assemblies. *Bioinformatics* 27, 2957–2963. doi: 10.1093/bioinformatics/btr507

Mapelli, F., Marasco, R., Balloi, A., Rolli, E., Cappitelli, F., Daffonchio, D., et al. (2012). Mineral–microbe interactions: biotechnological potential of bioweathering. *J. Biotechnol.* 157, 473–481. doi: 10.1016/j.jbiotec.2011.11.013

Nguyen, N. H., Song, Z., Bates, S. T., Branco, S., Tedersoo, L., Menke, J., et al. (2016). FUNGuild: An open annotation tool for parsing fungal community datasets by ecological guild. *Fungal Ecol.* 20, 241–248. doi: 10.1016/j.funeco.2015.06.006

Nie, S. A., Lei, X., Zhao, L., Brookes, P. C., Wang, F., Chen, C., et al. (2018). Fungal communities and functions response to long-term fertilization in paddy soils. *Appl. Soil Ecol.* 130, 251–258. doi: 10.1016/j.apsoil.2018.06.008

Rao, S. C., Coleman, S. W., and Mayeux, H. S. (2002). Forage production and nutritive value of selected Pigeonpea ecotypes in the southern Great Plains. *Crop Sci.* 42, 1259–1263. doi: 10.2135/cropsci2002.1259

Samaddar, S., Schmidt, R., Tautges, N. E., and Scow, K. (2021). Adding alfalfa to an annual crop rotation shifts the composition and functional responses of tomato rhizosphere microbial communities. *Appl. Soil Ecol.* 167:104102. doi: 10.1016/j.apsoil.2021.104102

Sansupa, C., Wahdan, S. F., Hossen, S., Disayathanoowat, T., Wubet, T., and Purahong, W. (2021). Can we use functional annotation of prokaryotic taxa (FAPROTAX) to assign the ecological functions of soil bacteria? *Appl. Sci.* 11:688. doi: 10.3390/app11020688

Semchenko, M., Leff, J. W., Lozano, Y. M., Saar, S., Davison, J., Wilkinson, A., et al. (2022). Fungal diversity regulates plant-soil feedbacks in temperate grassland. *Sci. Adv.* 4:eaau4578. doi: 10.1126/sciadv.aau4578

Shao, T., Zhao, J., Liu, A., Long, X., and Rengel, Z. (2020). Effects of soil physicochemical properties on microbial communities in different ecological niches in coastal area. *Appl. Soil Ecol.* 150:103486:103486. doi: 10.1016/j.apsoil.2019.103486

She, S., Niu, J., Zhang, C., Xiao, Y., Chen, W., Dai, L., et al. (2017). Significant relationship between soil bacterial community structure and incidence of bacterial wilt disease under continuous cropping system. *Arch. Microbiol.* 199, 267–275. doi: 10.1007/s00203-016-1301-x

Solorzano, C. D., and Malvick, D. K. (2011). Effects of fungicide seed treatments on germination, population, and yield of maize grown from seed infected with fungal pathogens. *Field Crop Res.* 122, 173–178. doi: 10.1016/j.fcr.2011.02.011

Song, J.-J., Xu, X.-Y., Bai, J.-Z., Yu, Q., Cheng, B., Feng, Y., et al. (2022). Effects of straw returning and fertilizer application on soil nutrients and winter wheat yield. *Environ. Sci.* 43, 4839–4847. doi: 10.13227/j.hjkx.202112043

Soong, J. L., Marañon-Jimenez, S., Cotrufo, M. F., Boeckx, P., Bodé, S., Guenet, B., et al. (2018). Soil microbial CNP and respiration responses to organic matter and nutrient additions: evidence from a tropical soil incubation. *Soil Biol. Biochem.* 122, 141–149. doi: 10.1016/j.soilbio.2018.04.011

Soussana, J.-F., and Lemaire, G. (2014). Coupling carbon and nitrogen cycles for environmentally sustainable intensification of grasslands and crop-livestock systems. *Agric. Ecosyst. Environ.* 190, 9–17. doi: 10.1016/j.agee.2013.10.012

Stefan, L., Hartmann, M., Engbersen, N., Six, J., and Schöb, C. (2021). Positive effects of crop diversity on productivity driven by changes in soil microbial composition. *Front. Microbiol.* 12:2021. doi: 10.3389/fmicb.2021.660749

Tanunchai, B., Ji, L., Schroeter, S. A., Wahdan, S. F. M., Hossen, S., Delelegn, Y., et al. (2023). FungalTraits vs. FUNGuild: comparison of ecological functional assignments of leaf- and needle-associated Fungi across 12 temperate tree species. *Microb. Ecol.* 85, 411–428. doi: 10.1007/s00248-022-01973-2

Tian, D., Su, M., Zou, X., Zhang, L., Tang, L., Geng, Y., et al. (2021). Influences of phosphate addition on fungal weathering of carbonate in the red soil from karst region. *Sci. Total Environ.* 755:142570:142570. doi: 10.1016/j.scitotenv.2020.142570

Toffa, J., Loko, Y. L. E., Kpindou, O. K. D., Zanzana, K., Adikpeto, J., Gbenontin, Y., et al. (2021). Endophytic colonization of tomato plants by Beauveria bassiana Vuillemin (Ascomycota: Hypocreales) and leaf damage in Helicoverpa armigera (Hübner) (Lepidoptera: Noctuidae) larvae. *Egypt. J. Biol. Pest Control* 31:82. doi: 10.1186/s41938-021-00431-4

Virk, Z. A., Farraj, D. A. A., Iqbal, M., Lewinska, K., and Hussain, S. (2022). Noculation with the pH lowering plant growth promoting bacterium *Bacillus* sp. ZV6 enhances Ni Phytoextraction by *Salix alba* from a Ni-polluted soil receiving effluents from Ni electroplating industry. *Sustain. For.* 14:6975. doi: 10.3390/su14126975

Wang, H., Guo, C. L., Yang, C. F., Lu, G. N., Chen, M. Q., Dang, Z., et al. (2016). Distribution and diversity of bact-erial communities and sulphate-reducing bacteria in a paddy soil irrigated with acid-mine drainage. *J. Appl. Microbiol.* 121, 196–206. doi: 10.1111/j-am.13143

Wang, Y., Li, C., Tu, C., Hoyt, G. D., DeForest, J. L., Hu, S., et al. (2017). Long-term no-tillage and organic input management enhanced the diversity and stability of soil microbial community. *Sci. Total Environ.* 609, 341–347. doi: 10.1016/j.scitotenv.2017.07.053

Wang, C., Wang, G., Wang, Y., Rafique, R., Ma, L., Hu, L., et al. (2016). Fire alters vegetation and soil microbial Community in Alpine Meadow. *Land Degrad. Dev.* 27, 1379–1390. doi: 10.1002/ldr.2367

Wei, W., Yang, M., Liu, Y., Huang, H., Ye, C., Zheng, J., et al. (2018). Fertilizer N application rate impacts plant-soil feedback in a sanqi production system. *Sci. Total Environ.* 633, 796–807. doi: 10.1016/j.scitotenv.2018.03.219

Wong, V. N. L., Dalal, R. C., and Greene, R. S. B. (2008). Salinity and sodicity effects on respiration and microbial biomass of soil. *Biol. Fertil. Soils* 44, 943–953. doi: 10.1007/s00374-008-0279-1

Yao, H., Xu, J., and Huang, C. (2003). Substrate utilization pattern, biomass and activity of microbial communities in a sequence of heavy metal-polluted paddy soils. *Geoderma* 115, 139–148. doi: 10.1016/S0016-7061(03)00083-1

Yin, C., Hulbert, S., Schroeder, K., Mavrodi, O., Mavrodi, D., Dhingra, A., et al. (2013). Role of bacterial communities in the natural suppression of *Rhizoctonia solani* bare patch disease of wheat (*Triticum aestivum* L.). *Appl. Environ. Microbiol.* 79, 7428–7438. doi: 10.1128/AEM.01610-13

Yin, X., Zhao, L., Fang, Q., and Ding, G. (2021). Differences in soil physicochemical properties in different-aged *Pinus massoniana* plantations in Southwest China. *Forests* 12:987. doi: 10.3390/f12080987

Yuan, J., Wen, T., Zhang, H., Zhao, M. L., Penton, C. R., Thomashow, L. S., et al. (2020). Predicting disease occurrence with high accuracy based on soil macroecological patterns of Fusarium wilt. *ISME J.* 14, 2936–2950. doi: 10.1038/s41396-020-0720-5

Zhang, D., Yan, D., Fang, W., Huang, B., Wang, X., Wang, X., et al. (2019). Chloropicrin alternated with biofumigation increases crop yield and modifies soil bacterial and fungal communities in strawberry production. *Sci. Total Environ.* 675, 615–622. doi: 10.1016/j.scitotenv.2019.04.222

Zheng, C., Kong, K., Zhang, Y., Yang, W., Wu, L., Munir, M., et al. (2022). Differential response of bacterial diversity and community composition to different tree ages of pomelo under red and paddy soils. *Front. Microbiol.* 13:958788. doi: 10.3389/fmicb.2022.958788

Zhou, J., Guan, D., Zhou, B., Zhao, B., Ma, M., Qin, J., et al. (2015). Influence of 34-years of fertilization on bacterial communities in an intensively cultivated black soil in Northeast China. *Soil Biol. Biochem.* 90, 42–51. doi: 10.1016/j.soilbio.2015.07.005

Zhu, Y., Duan, G., Chen, B., Peng, X., Chen, Z., and Sun, G. X. (2014). Mineral weathering and element cycling in soil-microorganism-plant system. *Science* 57, 888–896. doi: 10.1007/s11430-014-4861-0

Zhuang, J., Liu, C., Wang, X., Xu, T., and Yang, H. (2021). Penicillium simplicissimum NL-Z1 induced an imposed effect to promote the leguminous plant growth. *Front. Microbiol.* 12:738734. doi: 10.3389/fmicb.2021.738734

frontiers | Frontiers in Microbiology

TYPE Original Research
PUBLISHED 08 May 2025
DOI 10.3389/fmicb.2025.1544479

OPEN ACCESS

EDITED BY
Jose Ignacio Marín-Guirao,
IFAPA Centro La Mojonera, Spain

REVIEWED BY
Arthur Prudêncio De Araujo Pereira,
Federal University of Ceara, Brazil
Setu Bazie Tagele,
University of California, Riverside,
United States

*CORRESPONDENCE
Chuntao Yin
✉ chuntao.yin@usda.gov

RECEIVED 12 December 2024
ACCEPTED 15 April 2025
PUBLISHED 08 May 2025

CITATION
Yin C, Lahr N and Zhou R (2025)
Cyanobacterium *Nostoc* species mitigate soybean cyst nematode infection on soybean by shaping rhizosphere microbiota.
Front. Microbiol. 16:1544479.
doi: 10.3389/fmicb.2025.1544479

Cyanobacterium *Nostoc* species mitigate soybean cyst nematode infection on soybean by shaping rhizosphere microbiota

Chuntao Yin[1]*, Nathan Lahr[1] and Ruanbao Zhou[2]

[1]North Central Agricultural Research Laboratory, US Department of Agriculture, Agricultural Research Service (USDA-ARS), Brookings, SD, United States, [2]Department of Biology and Microbiology, South Dakota State University, Brookings, SD, United States

Soybean cyst nematode (SCN, *Heterodera glycines* Ichinohe) is the most devastating and yield-limiting pathogen that threatens soybean production globally. Sustainable SCN disease management strategies are needed. In this study, a cyanobacterial strain was isolated from SCN-infected soybean soil and identified as *Nostoc punctiforme* using the cyanobacterial 16S rRNA gene sequence. When susceptible soybean plants were grown in the SCN-inoculated soil, *N. punctiforme* inoculants significantly reduced the total number of SCN eggs and second-stage juveniles (J2s), compared to the control with SCN inoculation only. Further microbial analysis showed that *N. punctiforme* inoculants changed the bacterial and fungal communities in the soybean rhizospheres and significantly increased the relative abundance of several bacterial and fungal species with potential nematicidal activities, suggesting the changes of soybean rhizosphere microbiota may partially contribute to the activity of *N. punctiforme* inoculants against SCN. However, *N. punctiforme* inoculants did not directly induce soybean defense reactions against SCN. Thus, *N. punctiforme* may be a potential microbial source against SCN invasion in soybean.

KEYWORDS

cyanobacteria, soybean cyst nematode, nematicidal activity, microbiota, plant defense system

Introduction

Soybean [*Glycine max* (L.) Merr.], an economically important oilseed crop worldwide, provides protein and oil for humans and animals (SoyStats, 2020) and is considered an important contributor to meet the global food demand expected to double by 2050 (Hunter et al., 2017). However, a variety of phytopathogens cause significant yield loss and quality reduction that threaten soybean production. Soybean cyst nematode (SCN, *Heterodera glycines* Ichinohe) is the most damaging pathogen of soybean worldwide (Allen et al., 2017; Bent, 2022). SCN is widely distributed in nearly all major soybean production areas of the United States (Tylka and Marett, 2021) and causes 10–30% yield losses annually (ca. $1.5 billion) (Bandara et al., 2020; Koenning and Wrather, 2010; Tylka and Marett, 2021; Winter et al., 2006). Due to the longevity of SCN cysts in soil and unnoticeable aboveground symptoms, it is challenging to eliminate SCN from the field completely once a soybean field is infected (Arjoune et al., 2022). Genetic resistance and rotation to nonhost crops are considered primary management strategies. However, repeated monoculture of the same genetic resistance, introgressed from plant introduction (PI) 88788 and PI 548402 (Peking)

(Tylka et al., 2022), has led to the evolution of SCN that overcomes the resistance (Bent, 2022). Nematicides are the other control options for soybean producers, but the negative environmental effects (Desaeger et al., 2020) and the emergence of nematicide resistance (Wram et al., 2022) have encouraged the development of eco-friendly alternatives.

Cyanobacteria, widely distributed in both aquatic and terrestrial environments, are known for their beneficial roles in agricultural ecosystems (Lee and Ryu, 2021; Parmar et al., 2023; Sithole et al., 2023). Cyanobacteria have been used for stimulating plant growth (Alvarez et al., 2024; Suresh et al., 2019) and/or for managing plant diseases (Kim, 2006; Righini et al., 2022). For example, root-drench application of cyanobacteria, *Anabaena variabilis*, *A. torulosa*, and *Calothrix* sp., reduced damping-off symptoms caused by soilborne pathogens like *Fusarium oxysporum*, *Pythium debaryanum*, and *Rhizoctonia solani* in tomato and cotton (Chaudhary et al., 2012; Prasanna et al., 2013; Righini et al., 2022). Recently, the use of cyanobacteria-based biostimulants to combat plant-parasitic nematodes has gained attention (Sithole et al., 2023). *Synechococcus nidulans* increased nematode J2 mortality and inhibited egg hatching of multiple nematodes, including *Meloidogyne graminicola*, *M. incognita, Heterodera cajani*, *H. avenae*, and *Rotylenchulus reniformis* (Holajjer et al., 2012). *Anabaena oryzae* had nematicidal activity against *Meloidogyne incognita* on banana (*Musa acuminata*) plants (Hamouda and El-Ansary, 2017). The aqueous and methanolic extracts of cyanobacteria *Oscillatoria* sp. were demonstrated to decrease the volume of galls, eggs, and adult female root-knot nematode (*M. incognita*) in soybean roots and number of J2s in soil (Ghareeb et al., 2022). Studies on the suppression of cyanobacteria on plant pathogenic nematodes are still in their infancy, despite very promising results being reported.

Some cyanobacterial species can protect host plants against pathogenic nematodes via nematocidal activity (Choleva et al., 2007; Ghareeb et al., 2022; Hamouda and El-Ansary, 2017). Holajjer et al. (2013) noted that cyanobacteria produce cyanotoxins to alter nematode behavior or disrupt egg hatching process. Previous studies have revealed that the phytoactive metabolites of cyanobacteria, such as amides, alkaloids, saponins, and carotenoids, slowed the life cycle of *Caenorhabditis elegans* (Asimakis et al., 2022; Biondi et al., 2004). Ghareeb et al. (2022) found that *Oscillatoria* sp. activated soybean defense system against invasion of *M. incognita*. However, the detailed mode of action of cyanobacteria on root pathogens is largely unexplored.

Several studies have shown that cyanobacterial inoculants influenced soil- and plant-associated microbes. Cyanobacterium (*Calothrix elenkenii*) increased the population densities of culturable microbiome members from plant tissues, with about 60% culturable bacterial isolates belong to *Bacillaceae* (Priya et al., 2015). Foliar and soil drench of *Bacillus* sp. and *Nostoc-Anabaena* consortium altered *nifH* and bacterial *amoA* gene abundances (Thapa et al., 2021). Cyanobacteria-green microalgae consortia inoculants shifted bacterial and fungal communities of chili plants, with some microbial taxa (Firmicutes, Chloroflexi, Planctomycetes, Proteobacteria, Bacillariophyta, Basidiomycota, and Glomeromycotan) dominating in the consortia-treated soils, while others (Actinobacteria, Bacteroidetes, and Streptomycota) dominating in untreated soils (Jose et al., 2024). Surprisingly, little information is available on cyanobacteria-mediated microbiota against soilborne pathogens.

In the present study, we isolated a cyanobacterium from SCN-infected soybean soil and identified it to be *Nostoc punctiforme* using the cyanobacterial 16S rRNA gene-specific primers. The objectives of this study were: 1. to evaluate the effect of the isolated *N. punctiforme* on SCN infestation; 2. to examine the effect of *N. punctiforme* inoculants on soybean rhizosphere microbiota; and 3. to assess the ability of *N. punctiforme* to induce soybean systemic resistance against SCN. We hypothesized that *N. punctiforme* inoculants would mitigate SCN damage to soybean by changing soybean rhizosphere microbiota and inducing soybean systemic resistance.

Materials and methods

Plant, soil, and soybean cyst nematode

Soybean cultivar "Williams 82," susceptible to SCN, was used in this study. Soil was collected from the field plots with a maize-soybean rotation since 2018 at the Eastern South Dakota Soil and Water Research Farm (44°19′N, 96°46′W) in Brookings, SD. Soil was collected at a depth of 0 to 20 cm using a shovel in the fall of 2021 after crop harvest and before ground freezing and transferred to the lab. The soil was mixed thoroughly and sieved through a 5 mm aperture sieve to remove plant debris and rocks, and then stored at 4°C for further use. The collected field soil was mixed with sterile quartz sand (4030 silica sand, 0.45–0.55 mm diameter, Unimin Minnesota Corp, Le Sueur, MN) and calcined clay (Turface All Sport Pro, Profile Products, Buffalo Grove, IL) in a ratio of 1:1:1 (w/w/w) for SCN population increase. Soybean seeds were sterilized by exposure to chlorine gas [25:1 (v/v) 10% sodium hypochlorite and 12 N HCl] for 16 h (Chen et al., 2018), planted in the mixed soil, and grown in a growth chamber with a 16 h photoperiod (light intensity 1,000 $\mu E\ m^{-2} s^{-1}$) at 26 ± 2°C. SCN HG type 7 was initially isolated from the soybean field in Brookings, SD, and multiplied on "Williams 82" in a growth chamber as previously described (Yin et al., 2024). SCN Cysts and eggs were collected from the soybean roots and soil according to the technique of Shepherd (1970) with modifications as previously described (Yin et al., 2024).

Cyanobacterial strain isolation and culture conditions

Among the planting pots for SCN population increase, one pot with lower SCN populations displayed blue-green color in the soil that appears to be cyanobacterial-like microbe under a compound microscope (Leica Microsystems Inc., Deerfield, IL). To isolate the blue-green organism, 100 μl of SCN egg extracts were spread over the surface of BG11 medium, a cyanobacterial selection medium (Ferris and Hirsch, 1991), in petri dishes, and then incubated in a growth chamber with a 16 h photoperiod at 26 ± 2°C. After the growth of the blue-green cultures, a series of successive streaking

(5–6 times) of the blue-green cultures was performed in BG11 medium and the purity of the culture was ensured by regular observation under a compound microscope (Wang et al., 2018). The blue-green organism was then re-streaked in $BG11_0$ medium (no combined nitrogen in BG11 medium) for 3–4 times. The blue-green strain was able to reproducibly grow well in $BG11_0$ medium, suggesting that it has nitrogen-fixing ability.

Genomic DNA extraction and cyanobacterium identification

Genomic DNA (gDNA) of the isolated culture was extracted following the protocol of cyanobacterial gDNA extraction as previously described (Qiu et al., 2019). Briefly, 200 ml of cultures (OD_{720} = 0.4) were centrifuged and 500 μl of the sterilized 10% sucrose buffer (50 mM Tris-HCl, pH 8.0, 10 mM EDTA), 50 μl of 125 mg ml^{-1} lysozyme (MilliporeSigma, Rockville, MD), 150 μl of 10% (w/w) SDS, and 10 μl of RNase (10 mg ml^{-1}) were added to suspend/wash the cell pellets. The suspension was incubated at 37°C for 1 h. Then the saturated phenol and chloroform solution was used to extract gDNA. The gDNA was dissolved in sterile ddH_2O for further use.

The 16S rRNA gene fragment was amplified from the extracted gDNA using cyanobacterial-specific primers (CYA106F 5′-CGGACGGGTGAGTAACGCGTGA-3′ and CYA781R 5′-GACTACWGGGGTATCTAATCCCWTT-3′) as previously described (Boutte et al., 2006; Nübel et al., 1997). PCR reaction consisted of 1 μl of gDNA (50 ng), 10 μl of 2x Phusion master mix (ThermoFisher Scientific Inc., MA), and 0.25 μM of each primer in a total volume of 20 μl. PCR was performed as follows: 98°C for 30 s; 30 cycles of 98°C for 10 s, 55°C for 10 s, and 72°C for 45 s; final extension at 72°C for 10 min. The PCR products were analyzed on a 1.5% agarose gel, purified with the GeneJET PCR purification kit (ThermoFisher Scientific Inc., MA), and sequenced from both ends at Elim Biopharm (Hayward, CA). The sequences were subjected to a BLAST analysis at NCBI database and the assembled sequence was deposited in NCBI database (accession number: PQ740210).

SCN inhibition assay

The efficacy of the isolated cyanobacterium against SCN HG type 7 in soybean "Williams 82" was examined in a growth chamber. The collected field soil was mixed with sterile quartz sand in a ratio of 2:3 [w(fresh weight)/w(dry weight)]. Plastic cones (40 mm in diameter and 210 mm long) were filled with 120 g of mixed soil. One pre-germinated "Williams 82" seed was sown in each cone, followed by a 15 ml aliquot of the isolated cyanobacterial culture suspended in sterile ddH_2O. Cyanobacterial culture was added with high concentration (OD_{720} = 0.5) or low concentration (5x dilution, OD_{720} = 0.1). Finally, 4,000 SCN eggs (Haarith et al., 2021) were added in a 3 cm deep hole around the soybean plant. Sterile ddH_2O or sterile ddH_2O and SCN were used as controls. Each treatment had four replicates. Cones were arranged in a randomized complete block design in plastic racks and maintained in the controlled conditions (16 h photoperiod, 26 ± 2°C). Each cone received 10 ml of water daily in the first 3 weeks, then 10 ml of water twice a day in the final 2 weeks. After 35 days, the soybean plants were uprooted gently and washed free of adhering soil. Plant parameters, including shoot length and fresh shoot weight, were measured. The SCN eggs and J2s were extracted from the soil and half of plant roots (Shepherd, 1970), and the number of eggs and J2s was counted using a Leica DML compound microscope at 100 x magnification (Leica Microsystems Inc., Deerfield, IL). The other half of the roots were used for rhizosphere soil preparation as described previously (Yin et al., 2021). The roots after washing off rhizosphere soil were stored at −80°C for RNA extraction. The experiment was repeated three times and the rhizosphere DNA and root RNA were prepared from one experiment with four replicates.

Soil DNA extraction and amplicon sequencing of rhizosphere microbiota

Amplicon sequencing was used to evaluate whether the cyanobacterial inoculants affect the rhizosphere microbiota in soybean plants grown in the SCN-inoculated soil. Rhizosphere soil DNA was extracted using a DNeasy PowerSoil kit (Qiagen, Carlsbad, CA) and a bead beater SPEX 1600 MiniG (Spex SamplePrep, Metuchen, NJ) at 1,500 Hz for 1 min. The DNA was quantified using a Nanodrop spectrophotometer (Thermo Fisher Scientific, Waltham, MA) and sent to the University of Minnesota Genomics Center for amplification and sequencing. For bacterial amplicon sequencing, v4 hypervariable region of the 16S rRNA gene was amplified using forward primer 515f (GTGYCAGCMGCCGCGGTAA) and reverse primer 806r (GGACTACNVGGGTWTCTAAT) (Caporaso et al., 2011). For fungal amplicon sequencing, fungal internal transcribed spacer 1 (ITS1) region was amplified using a two-step dual-indexed amplification (Gohl et al., 2016a,b). The fungal ITS1 region was amplified in the first set of PCR using primers ITS1∗_Nextera (5′-TCGTCGGCAGCGTCAGATGTGTATAAGAGACAG**CTTGGTCATTTAGAGGAAG∗TAA**-3′) and ITS2 (5′-GTCTCGTGGGCTCGGAGATGTGTATAAGAGACAG**GCTGCGTTCTTCATCGA∗TGC**-3′) (ITS-specific sequences in bold, "*" indicates the position of a phosphorothioate bond) (Gohl et al., 2016b). PCR assays were carried out using KAPA HiFi PCR kit (Roche, Indianapolis, IN, USA) and an initial denaturing at 95°C for 5 min, followed by 25 cycles of denaturation at 98°C for 20 s, annealing at 55°C for 15 s, and extension at 72°C for 1 min, with a final extension at 72°C for 5 min. PCR products were diluted to 1:100, and 5 μl of diluted PCR product was included in a second round of PCR using forward indexing primer (5′-AATGATACGGCGACCACCGAGATCTACACTCGTCGGCAGCGTC-3′) and reverse indexing primer (5′-CAAGCAGAAGACGGCATACGAGATGTCTCGTGGGCTCGG-3′) (Gohl et al., 2016b). The second PCR consisted of an initial denaturation at 95°C for 5 min, followed by 10 cycles of 98°C for 20 s, 55°C for 15 s, and 72°C for 1 min, with a final extension at 72°C for 5 min. Then, the amplicons were pooled, size selected,

spiked with 20% PhiX, and sequenced (2 × 300 paired-end, V3 chemistry) on the Illumina MiSeq platform.

Amplicon sequence processing

The sequence processing was conducted using USEARCH (v11) (Edgar, 2010, 2018) to denoise sequences and define zero-radius operational taxonomic units (ZOTUs, 100% identity threshold). Briefly, primer and barcode sequences were removed along with 10 and 55 bp for bacterial sequences and 30 and 85 bp for fungal sequences from forward and reverse reads, respectively. Reads were paired with 15 maximum differences and an 80% identity threshold. To generate high-quality reads for denoising, reads were filtered with a maximum expected error rate of 1, singletons were removed, and sequences were denoised using the "unoise3" algorithm (Edgar, 2016). Processed reads were then mapped to ZOTU representatives to generate a ZOTU abundance table. Taxonomy was assigned to ZOTUs using the SINTAX algorithm with an 80% confidence threshold to the Ribosomal Database Project reference database (v18, Cole et al., 2014) for bacterial sequence and the UNITE reference database (v7, Tedersoo et al., 2018) for fungal sequence. ZOTUs identified as non-bacteria or non-fungi were discarded, and ZOTU tables that were rarefied were subsampled in place of rarefied sequences for all analyses unless otherwise noted. The sequencing data was deposited in NCBI Sequence Read Archive with the project PRJNA1196987 and available after the acceptance of the manuscript.

RNA extraction from soybean roots, cDNA synthesis, and quantitative PCR assay

To examine whether the isolated cyanobacteria inoculants induce plant defense system against SCN in soybean roots, the expression of five defense-related genes (*PR1*, *PR2*, *PR3*, *PR5*, and PR10) was measured by RT-quantitative PCR (qPCR) using gene-specific primers and the soybean ubiquitin gene was used as a reference (Supplementary Table 1). Total RNA was extracted from the soybean roots using RNeasy plant kit (Qiagen, Carlsbad, CA) according to manufacturer's instruction. All RNA samples were digested with DNase I (New England Biolabs, Ipswich, MA) following the manufacturer's instruction prior to synthesizing cDNA. The absence of gDNA contamination was subsequently confirmed by the lack of PCR amplification of RNA samples with primers designed for soybean ubiquitin gene. First-strand cDNA was synthesized using ProtoScript first strand cDNA synthesis kit (New England Biolabs, Ipswich, MA). qPCR was performed using SsoAdvanced Universal SYBR Green Supermix kit (Bio-Rad, Hercules, CA). qPCR reaction consisted of 10 μl PCR reaction by mixing 5 μl of SYBR Green Supermix (2x), 0.4 μl of each primer (10 μM), and 4.2 μl of diluted cDNA. qPCR was conducted on CFX Opus Real-Time PCR system (Bio-Rad, Hercules, CA) using the following conditions: for the first cycle, samples were initially incubated for 30 s at 94°C, followed by 45 cycles at 94°C for 15 s, and 60°C for 20 s, followed by a melt curve of 65–95°C with 0.5°C increments every 5 s.

Statistical analysis and data visualization

The effect of the isolated cyanobacterium on the number of SCN eggs and J2s extracted from soil and soybean roots was evaluated using Kruskal-Wallis's test followed by Wilcoxon *post hoc* tests in JMP Pro 15.1.0 (SAS Institute, Cary, NC). Microbiome data analysis was performed in R version 4.3.2 using multiple packages, including vegan (v2.6.8, Oksanen et al., 2024), pheatmap (v 1.0.12, Kolde, 2015), and ggplot2 (v3.5.1, Wickham, 2016). Microbial alpha diversity was calculated using the "diversity" function of the vegan package. After normality and homogeneity of variance testing (Shapiro-Wilks and Levene's test), the difference in diversity index among treatments was examined with Kruskal-Wallis test, followed by a *post hoc* Dunn's test using the FSA package. Nonmetric multidimensional scaling (NMDS) was used to visualize the similarity of microbial community among rhizosphere samples based on Bray-Curtis distances. Permutational multivariate analysis of variance (PERMANOVA) was performed to determine microbial differences due to cyanobacteria and SCN inoculation. DESeq2 (v1.46.0, Love et al., 2014) was performed to identify microbial ZOTUs that differed in the rhizosphere samples between cyanobacteria-treated and -untreated samples with ZOTUs tables. Briefly, the ZOTUs tables were filtered to remove rare taxa (<10 total sequences). Those ZOTUs were kept that had normalized counts >10 and that were present in three or more samples. Wald's test was used to contrast ZOTUs from cyanobacterium-treated and -untreated samples or from high concentration of cyanobacterium and low concentration of cyanobacterium. ZOTUs were considered differentially abundant if they had a base mean >20, FDR adjusted $p < 0.1$, and estimated log2-fold change >1. Relative abundance of differential ZOTUs was then plotted in a heatmap using DESeq2 normalized log (x + 1) transformed counts.

Results

Identification of the isolated cyanobacterium

The isolated cyanobacterium grew well autotrophically in the nitrogen-free medium $BG11_0$, which suggested it is capable of nitrogen fixation. Under microscopic observation, the isolated cyanobacterium is a filamentous organism (Supplementary Figure 1) and can produce heterocyst cells (Supplementary Figure 1B). The 16S rRNA gene was amplified from the extracted gDNA of the cyanobacterial cultures using cyanobacterial-specific primers and sequenced. The 16S rRNA gene fragment was 641 bp in length and was deposited in GenBank (accession number: PQ740210). BLAST results showed that the sequence of the isolated cyanobacterium was 99.68% identical to *Nostoc punctiforme* (Sequence ID: MH090930.1).

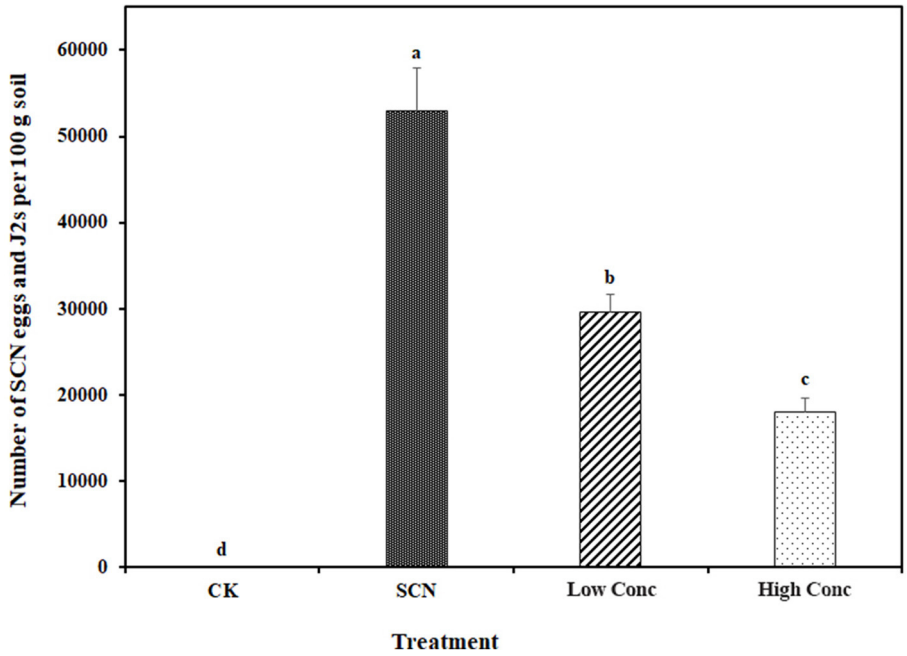

FIGURE 1
Effect of *Nostoc punctiforme* inoculants on soybean cyst nematode. CK: control without SCN (HG type 7) and *N. punctiforme* inoculation, SCN: SCN inoculation, Low Conc: SCN and low concertation *N. punctiforme* inoculation, High Conc: SCN and high concertation *N. punctiforme* inoculation. Different letters indicate a statistically significant difference between treatments within an experiment as determined by Kruskal-Wallis's test ($p \leq 0.05$, $n = 4$).

Effect of *Nostoc punctiforme* on SCN population and soybean growth

After soybean plants grew in the SCN and *N. punctiforme* inoculated soil for 35 days, *N. punctiforme* inoculants significantly reduced the total number of SCN eggs and J2s, compared to SCN inoculation only. But the number of SCN eggs and J2s was still significantly higher than the control without SCN infestation (Figure 1 and Supplementary Figure 2). Additionally, the inoculation concentration of *N. punctiforme* appeared to affect the SCN suppression (Figure 1). However, we did not observe that *N. punctiforme* inoculants significantly improved soybean plant growth in the experimental conditions, with plant shoot length and fresh weight similar to that of the SCN infestation (Supplementary Figure 3).

Effect of *Nostoc punctiforme* on soybean rhizosphere microbiota

Bacterial and fungal communities from the soybean roots across all samples were characterized. Bacterial communities in the soybean rhizosphere were dominated by phyla Proteobacteria (35.53%), Actinobacteria (26.59%), and Acidobacteria (10.97%) (Supplementary Figure 4A). The most abundant fungal phyla in the soybean rhizosphere were Ascomycota (50.38%), followed by Basidiomycota (38.45%), Chytridiomycota (5.18%), and Mortierellomycota (4.22%) (Supplementary Figure 4B).

The *N. punctiforme* inoculants did not influence the alpha diversity indexes of bacterial community in the soybean rhizosphere, including Shannon, richness, and inverse Simpson, except for the low concentration of *N. punctiforme* inoculants effects on inverse Simpson. In contrast, the *N. punctiforme* inoculants significantly decreased the Shannon diversity of fungal community, regardless of the inoculation concentration, and decreased the richness of fungal community in the low concentration inoculation (Supplementary Table 2) with no effects on inverse Simpson indexes.

Non-metric multidimensional scaling (NMDS) analysis revealed that the *N. punctiforme* inoculants changed the bacterial and fungal communities in the soybean rhizosphere (Figures 2A, B). Bacterial community clustered by *N. punctiforme* inoculation treatments, regardless of inoculation concentration. *N. punctiforme* inoculants and their concentration separated fungal community. Further permutational multivariate analysis of variance (PERMANOVA) supported the effect of the *N. punctiforme* inoculants on soybean rhizosphere microbiota (Table 1). The *N. punctiforme* inoculants had significant effects on the bacterial ($p = 0.005$) and fungal communities ($p = 0.017$), explaining 24.9% of the overall variation in the bacterial community and 35.3% in the fungal community, respectively (Table 1).

Most interestingly, the *N. punctiforme* inoculants significantly increased the relative abundance of four bacterial species (ZOTUs), including ZOTU17 belonging to genus *Ohtaekwangia*, ZOTU22 (family Rhizobiaceae), ZOTU42 (genus *Nostoc*), and unidentified bacterial species ZOTU4, compared to SCN inoculation only, regardless of the *N. punctiforme* inoculation concentration

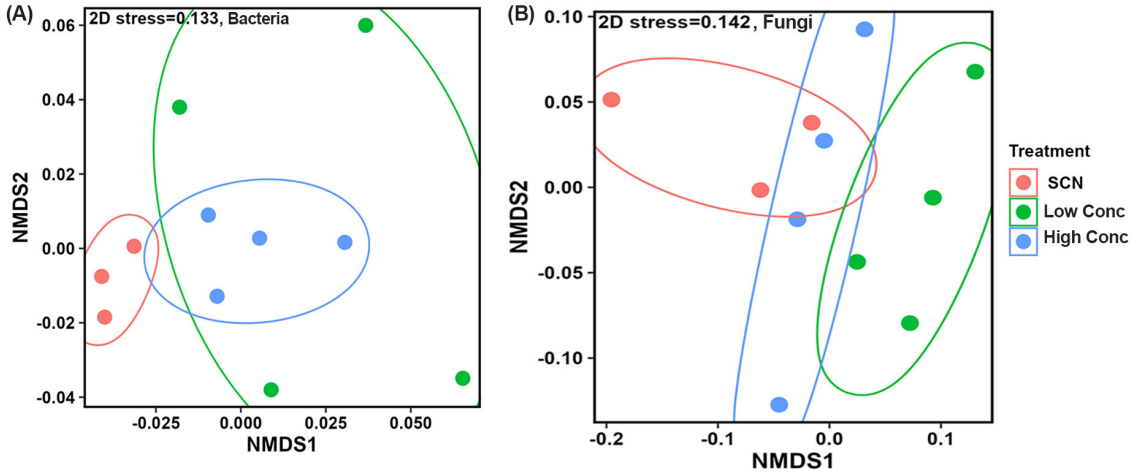

FIGURE 2
Nonmetric multidimensional scaling (NMDS) plots of Bray-Curtis distances among soybean rhizosphere microbiota following SCN and *N. punctiforme* inoculation. Samples are colored by SCN and *N. punctiforme* inoculation. **(A)** bacterial community, **(B)**. fungal community. SCN: SCN inoculation, Low Conc: SCN and low concertation *N. punctiforme* inoculation, High Conc: SCN and high concertation *N. punctiforme* inoculation. The different groups are highlighted by ellipses showing a 95% confidence range for the variation within each group.

TABLE 1 PERMANOVA of impacts of cyanobacteria inoculation on soybean rhizosphere microbiota.

Microbiome	Factor	*F* value	r^2	*p* value[a]
Bacterial community	Cyanobacteria	1.490	0.249	**0.005**
Fungal community	Cyanobacteria	2.184	0.353	**0.017**

[a] Values in bold represent factors with a significant effect ($p < 0.05$).

(Figure 3). Furthermore, the relative abundance of three fungal species was higher in the *N. punctiforme* inoculated soybean rhizosphere than that without *N. punctiforme* inoculants, and they were ZOTU55 classified as genus *Arthrobotrys* (family Orbiliaceae), ZOTU138 belonging to genus *Hirsutella* (family Ophiocordycipitaceae), and unidentified fungal species ZOTU3, regardless of the *N. punctiforme* inoculation concentration (Figure 4).

Effect of *N. punctiforme* inoculants on expression of soybean defense-related genes

SCN inoculation significantly increased the expression of three soybean defense-related genes, including *PR3*, *PR5*, and *PR10*, but did not affect the expression of *PR1* and *PR2*, compared to no SCN inoculation. However, we did not observe that *N. punctiforme* inoculants significantly impact the expression of all five tested *PR* genes, compared to SCN inoculation only (Figure 5).

Discussion

In this study, a cyanobacterium was isolated from the SCN-infected soybean soil and further identified as *Nostoc punctiforme* using cyanobacterial-specific 16S rRNA gene sequence. The *N. punctiforme* inoculants significantly reduced SCN population when soybean "Williams 82" was grown in the SCN-infested soil, compared to the control (no *N. punctiforme* additions). The results suggested that the isolated *N. punctiforme* may have antagonistic activity and could be considered as a potential microbial candidate for enhancing soybean plants against SCN. Prokaryotic cyanobacteria possessing beneficial traits, such as fixing atmospheric nitrogen, promoting plant growth, and increasing soil pores by producing adhesive substances (Kuraganti et al., 2020), are abundant in agricultural soils. Some cyanobacteria have been utilized as biofertilizers to enhance soil fertility and to promote crop growth in cropping systems (Joshi et al., 2020; Ramakrishnan et al., 2023). However, adding the isolated *N. punctiforme* cultures into the soil did not significantly increase soybean seedling biomass or promote the growth of wheat and maize plants compared to no *N. punctiforme* inoculants (data not shown).

The insecticidal properties of several cyanobacteria and their extracts have been used as environmentally friendly approaches in integrated pest management for pest control (Asimakis et al., 2022; Ghareeb et al., 2022). Although numerous studies demonstrated that inoculating soil-friendly microorganisms, like biocontrol microbial strains (*Bacillus* spp. and *Trichoderma* spp.), altered microbial diversities and activities (Li et al., 2022; Saravanakumar et al., 2017; Senkovs et al., 2021), there was little information about cyanobacterial inoculant effects on microbiomes. In this study, we found that *N. punctiforme* inoculants significantly shifted rhizosphere microbial communities in soybean grown in the SCN inoculated soil. Notably, *N. punctiforme* inoculants significantly increased the relative abundance of four bacterial species (ZOTU4, ZOTU17, ZOTU22, and ZOTU42) and three fungal species (ZOTU55, ZOTU138, and ZOTU3), regardless of the inoculation concentration. High abundance of ZOTU42, which belongs to genus *Nostoc*, in the *N. punctiforme* inoculated samples was expected. ZOTU17 and ZOTU22 belong to bacterial genus *Ohtaekwangia* (family Cytophagaceae) and family Rhizobiaceae, respectively. The two bacterial species are involved in soil

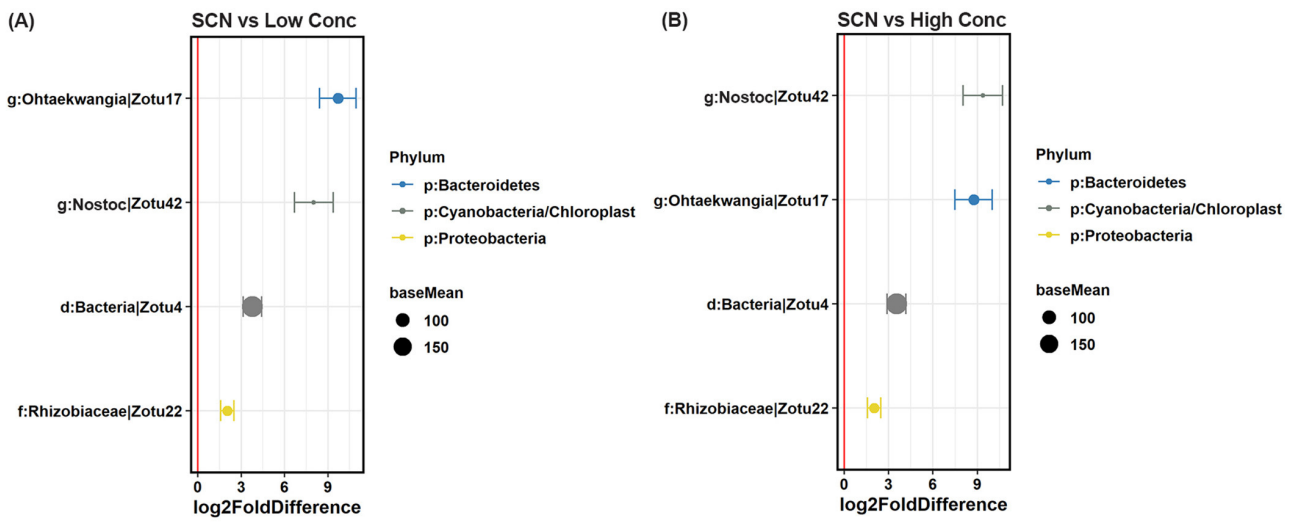

FIGURE 3
Differentially abundant bacterial ZOTUs identified in the soybean rhizosphere by SCN and *N. punctiforme* inoculations (FDR adjusted $p < 0.1$, Wald's test). **(A)** Bacterial ZOTUs in the SCN and low concertation *N. punctiforme* inoculation, **(B)** bacterial ZOTUs in the SCN and high concertation *N. punctiforme* inoculation. SCN: SCN inoculation, Low Conc: SCN and low concertation *N. punctiforme* inoculation, High Conc: SCN and high concertation *N. punctiforme* inoculation. Values on the x-axis presented the DESeq2-estimated log2-fold difference. The red vertical line represents a zero-fold change, where ZOTUs to the right of the line (positive values) are increased in relative abundance in *N. punctiforme* inoculation, and those to the left of the line (negative values) are more abundant in no *N. punctiforme* inoculation. Dots indicate ZOTUs, where the size of the dot is scaled by its mean abundance among all samples (base mean ≥ 20) and its color represents the phylum to which that ZOTUs belongs.

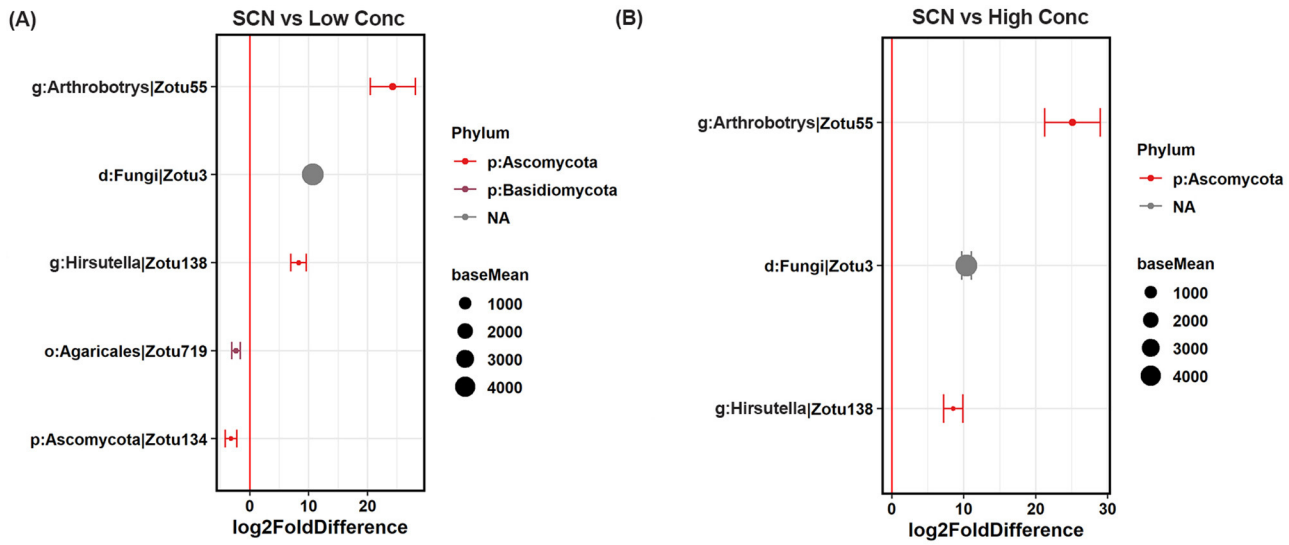

FIGURE 4
Differentially abundant fungal ZOTUs identified in the soybean rhizosphere by SCN and *N. punctiforme* inoculations (FDR adjusted $p < 0.1$, Wald's test). **(A)** Fungal ZOTUs in the SCN and low concertation *N. punctiforme* inoculation, **(B)** fungal ZOTUs in the SCN and high concertation *N. punctiforme* inoculation. SCN: SCN inoculation, Low Conc: SCN and low concertation *N. punctiforme* inoculation, High Conc: SCN and high concertation *N. punctiforme* inoculation. Values on the x-axis presented the DESeq2-estimated log2-fold difference. The red vertical line represents a zero-fold change, where ZOTUs to the right of the line (positive values) are increased in relative abundance in *N. punctiforme* inoculation, and those to the left of the line (negative values) are more abundant in no *N. punctiforme* inoculation. Dots indicate ZOTUs, where the size of the dot is scaled by its mean abundance among all samples (base mean ≥ 20) and its color represents the phylum to which that ZOTUs belongs.

nitrogen cycling (Alves et al., 2014; Rodríguez-Caballero et al., 2017). It is interesting to note that *Ohtaekwangia* can produce marinoquinoline, a chemical compound with antibiotic, antifungal, and insecticidal activities that could protect plants from pathogens and predators (Okanya et al., 2011). Further, Deng et al. (2021) found that *Ohtaekwangia* was the dominant bacterial genus in the suppressive soil against pathogenic fungal *Fusarium oxysporum* and Ou et al. (2019) showed that OTU belonging to genus *Ohtaekwangia* was negatively correlated with the relative abundance of *F. oxysporum*, demonstrating

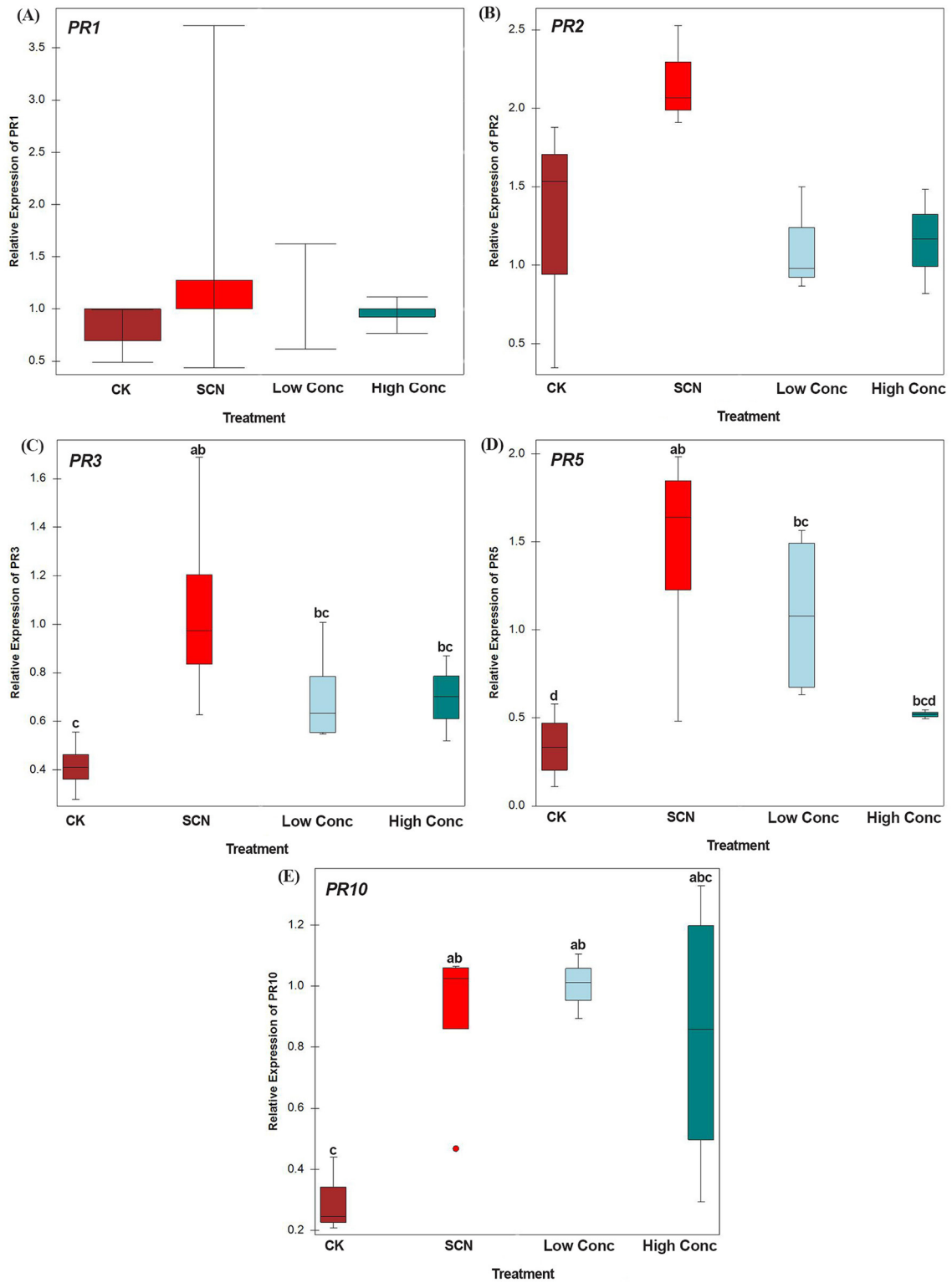

FIGURE 5
RT-qPCR analysis of the expression of pathogenesis-related genes. **(A)** Relative expression of *PR1*, **(B)** Relative expression of *PR2*, **(C)** Relative expression of *PR3*, **(D)** Relative expression of *PR5*, **(E)** Relative expression of *PR10*. Gene expression levels were analyzed from four treatments: CK: control without SCN and *N. punctiforme* inoculations, SCN: SCN inoculation, Low Conc: SCN and low concertation *N. punctiforme* inoculations, High Conc: SCN and high concertation *N. punctiforme* inoculations. Data are normalized by the ubiquitin reference gene and relative transcript levels in comparison with those of CK. Error bars represent standard error of the mean values of two technical replicates from four biological replicates. Differences in expression levels were tested by analysis of variance (ANOVA) and Tukey test. For each gene, bars with different letters indicate statistically significant differences between treatments.

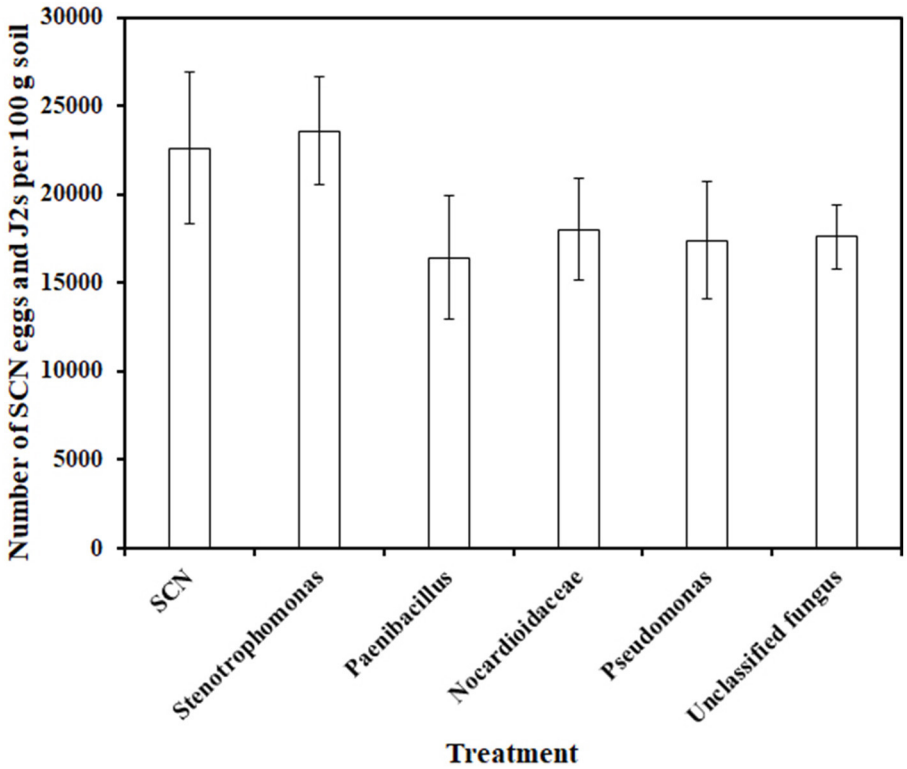

FIGURE 6
Effect of *N. punctiforme* co-existing microbial inoculants on soybean cyst nematode. SCN: SCN inoculation, Stenotrophomonas: SCN and *Stenotrophomonas maltophilia* inoculation, Paenibacillus: SCN and *Paenibacillus lactis* inoculation, Nocardioides: SCN and *Nocardioides zeae* inoculation, Pseudomonas: SCN and *Pseudomonas sp.* inoculation, Unclassified fungus: SCN and unclassified fungus inoculation (Kruskal-Wallis's test, $p = 0.72$, $n = 4$).

Ohtaekwangia being involved in fungal disease suppression. ZOTU55 and ZOTU138 belong to fungal genus *Arthrobotrys* (family Orbiliaceae) and *Hirsutella* (family Ophiocordycipitaceae), respectively. *Arthrobotrys* spp. are a well-known nematode-trapping fungus with biocontrol potential against root-knot nematodes (Eken et al., 2023; Yu et al., 2014). *Arthrobotrys* spp. can immobilize nematodes remotely through secreting specific nematotoxic metabolites (Nordbring-Hertz, 2004). *Arthrobotrys* spp. widely distribute in most habitats due to their adaptability and flexible lifestyles, thus they are considered excellent agents for controlling plant parasitic nematodes (Eken et al., 2023; Soliman et al., 2021). But there is no report that *Arthrobotrys* spp. can inhibit soybean cyst nematodes. *Hirsutella* spp. are another most discussed fungi for their biological control of nematodes, including SCN (Chen and Liu, 2007; Haarith et al., 2021; Sun et al., 2024). Among them, two species, *H. rhossiliensis* and *H. minnesotensis,* have been extensively studied on their SCN control abilities (Chen and Liu, 2007). *H. minnesotensis* was detected in 14% of soybean fields in Minnesota, South Dakota, and Michigan in the US (Chen and Liu, 2007; Mwaheb et al., 2017) and parasitizes SCN juveniles and other vermiform motile stages using adhesive conidia that penetrate and eventually kill the nematodes (Chen and Liu, 2007). ZOTU4 and ZOTU3 are unclassified bacterial and fungal species, respectively, and whether they are involved in SCN suppression needs further investigation. Additionally, we found that *N. punctiforme* inoculants significantly reduced the Shannon index of fungal community but had minimal effects on the bacterial diversities. The reduction of the Shannon index of fungal community may be attributed to the high abundance of some fungal taxa in the cyanobacteria inoculated samples, compared to the controls. Taken together, the changes in microbial communities and the increase in relative abundance of these potential parasitical microbial taxa in the soybean rhizosphere by *N. punctiforme* inoculants may contribute to the reduction of SCN population. But the suppressive functions of the specific bacterial and fungal species need further investigation.

Previous research showed that beneficial microorganisms, including cyanobacteria, generally elicit plant defense against biotic challenges (Abdelaziz et al., 2022; Molinari and Leonetti, 2019). The extracts of *Oscillatoria* sp., a cyanobacterium, regulated pathogenesis-related genes linked with plant defense and immunity against soybean root-rot nematode (Ghareeb et al., 2022). Belton et al. (2021) reported that *N. punctiforme* induced defense genes against programmed cell death in *Arabidopsis thaliana*. However, in this study, the expression levels of five soybean *PR* genes were examined by qPCR in the soybean roots of *N. punctiforme* and SCN treated, SCN only, and the controls without *N. punctiforme* and SCN inoculations. The results showed that *N. punctiforme* inoculants did not significantly upregulate or downregulate the five *PR* genes compared with SCN-treated only, suggesting *N. punctiforme* -enhanced soybean resistance to SCN may not be directly associated with the induction of soybean defense system.

However, our current data does not exclude the possibility of indirect interaction with other soil microbes that might activate plant defenses.

Many filamentous cyanobacteria possess a complex multilayer envelope around the cells, making it difficult to isolate single filaments that are free of other associated microbes (Fernandez-Valenzuela et al., 2021). Due to *N. punctiforme* generally being wrapped by extracellular polysaccharide sheaths (Sharma et al., 2009), obtaining axenic cultures of *N. punctiforme* is challenging. In this study, we did not successfully obtain axenic cultures of *N. punctiforme,* although several available methods were used, including repeated transfer of cells (Rippka et al., 1981), antibiotic, thermal, and sonication treatments (Han et al., 2014; Meixner et al., 2022), and treating akinetes with sodium hypochlorite (Šulčius et al., 2017; Vaz et al., 2014). To examine whether these co-existing microbes influence SCN population, one fungal and four bacterial strains were isolated from the *N. punctiforme* cultures using tryptic soy agar and potato dextrose agar media, respectively. Those microbial strains were identified as *Stenotrophomonas maltophilia*, *Paenibacillus lactis*, *Nocardioides zeae, Pseudomonas* sp., and unclassified fungus, respectively, using 16S rRNA and ITS primers (Yin et al., 2024). The cultures of single bacterial and fungal strain inoculations did not significantly change the total number of SCN eggs and J2s associated with susceptible "Williams 82" compared with the SCN inoculation only (Figure 6), indicating the SCN suppression activity of *N. punctiforme*. However, we cannot exclude the potential role of consortium of *N. punctiforme* and coexisting microbes in SCN infection.

The establishment and persistence of the introduced microbes in soil are important for functioning effectively. The microbial data in this study showed that ZOTU42 was more abundant in *N. punctiforme*-treated samples than in the controls (SCN inoculation only). The v4 hypervariable region of 16S rRNA sequence of ZOTU42 shows 100% query cover and identity to the sequence of *N. punctiforme* suggesting that the presence of inoculated cyanobacterial strain in the soil 5 weeks post inoculation. However, *N. punctiforme* grows relatively slowly (about 4 weeks to reach $OD_{720} = 0.5$) in the test condition that may limit the application of *N. punctiforme* on a large scale in fields.

Data availability statement

The datasets presented in this study can be found in online repositories. The names of the repository/repositories and accession number(s) can be found below: https://www.ncbi.nlm.nih.gov/, PQ740210 and project PRJNA1196987.

Author contributions

CY: Conceptualization, Funding acquisition, Investigation, Methodology, Project administration, Resources, Software, Supervision, Validation, Visualization, Writing – original draft, Writing – review & editing. NL: Data curation, Investigation, Methodology, Validation, Writing – review & editing. RZ: Methodology, Resources, Writing – review & editing.

Funding

The author(s) declare that financial support was received for the research and/or publication of this article. This work was supported by USDA-ARS in-house funds.

Acknowledgments

We thank USDA-ARS in house funding support. We thank Sharon Schneider for critical reading of the manuscript.

Conflict of interest

The authors declare that the research was conducted in the absence of any commercial or financial relationships that could be construed as a potential conflict of interest.

Generative AI statement

The author(s) declare that no Gen AI was used in the creation of this manuscript.

Publisher's note

All claims expressed in this article are solely those of the authors and do not necessarily represent those of their affiliated organizations, or those of the publisher, the editors and the reviewers. Any product that may be evaluated in this article, or claim that may be made by its manufacturer, is not guaranteed or endorsed by the publisher.

Author disclaimer

Mention of trade names or commercial products in this publication is solely for the purpose of providing specific information and does not imply recommendation or endorsement by the U.S. Department of Agriculture. USDA is an equal opportunity provider and employer.

Supplementary material

The Supplementary Material for this article can be found online at: https://www.frontiersin.org/articles/10.3389/fmicb.2025.1544479/full#supplementary-material

SUPPLEMENTARY FIGURE 1
Cyanobacterium isolation and purification. **(A)** *Nostoc punctiforme* growth in BG11 liquid media, **(B)** The filamentous and heterocytes of *N. punctiforme* under 100 x microscopy. Red arrows indicate heterocytes.

SUPPLEMENTARY FIGURE 2
Effect of *Nostoc punctiforme* inoculants on soybean cyst nematode. **(A)** Independent experiment 1, **(B)** Independent experiment 2. CK: control without SCN (HG type 7) and *N. punctiforme* inoculation, SCN: SCN inoculation, Low Conc: SCN and low concertation *N. punctiforme* inoculation, High Conc: SCN and high concertation *N. punctiforme*

inoculation. Different letters indicate a statistically significant difference between treatments within an experiment as determined by Kruskal-Wallis's test ($p \leq 0.05$, $n = 4$).

SUPPLEMENTARY FIGURE 3
Effect of *Nostoc punctiforme* inoculants on soybean growth. **(A)** soybean shoot length, **(B)** soybean shoot fresh weight. CK: control without SCN and *N. punctiforme* inoculations, SCN: SCN inoculation, Low Conc: SCN and low concertation *N. punctiforme* inoculations, High Conc: SCN and high concertation *N. punctiforme* inoculations. Different letters indicate a statistically significant difference between treatments within an experiment as determined by the Kruskal-Wallis's test ($p \leq 0.05$, $n = 4$).

SUPPLEMENTARY FIGURE 4
Microbial taxonomic assignments at the phyla level and their percentage contribution (abundance) in the soybean rhizosphere. **(A)** bacterial phyla, **(B)** fungal phyla. SCN: SCN inoculation, Low Conc: SCN and low concertation *N. punctiforme* inoculations, High Conc: SCN and high concertation *N. punctiforme* inoculations.

References

Abdelaziz, A. M., Attia, M. S., Salem, M. S., Refaay, D. A., Alhoqail, W. A., and Senousy, H. H. (2022). Cyanobacteria-mediated immune responses in pepper plants against *Fusarium Wilt*. *Plants* 11:2049. doi: 10.3390/plants11152049

Allen, T. W., Bradley, C. A., Sisson, A. J., Byamukama, E., Chilvers, M. I., Coker, C. M., et al. (2017). Soybean yield loss estimates due to diseases in the United States and Ontario, Canada, from 2010 to 2014. *Plant Health Prog.* 18, 19–27. doi: 10.1094/PHP-RS-16-0066

Alvarez, A. L., Weyers, S. L., and Gardner, R. D. (2024). Cyanobacteria-based soil amendments in the soil-plant system: effects of inoculations on soil nutrient and microbial dynamics under spring wheat growth. *Algal Res.* 77:103326. doi: 10.1016/j.algal.2023.103326

Alves, L. C., De Souza, J. A. M., de Mello Varani, A., and de Macedo Lemos, E. G. (2014). "The Family Rhizobiaceae," in *The Prokaryotes eds.* E. Rosenberg, E. F. DeLong, S. Lory, et al. (Berlin, Heidelberg: Springer), 419–437. doi: 10.1007/978-3-642-30197-1_297

Arjoune, Y., Sugunaraj, N., Peri, S., Nair, S. V., Skurdal, A., Ranganathan, P., et al. (2022). Soybean cyst nematode detection and management: a review. *Plant Methods* 18:110. doi: 10.1186/s13007-022-00933-8

Asimakis, E., Shehata, A. A., Eisenreich, W., Acheuk, F., Lasram, S., Basiouni, S., et al. (2022). Algae and their metabolites as potential bio-pesticides. *Microorganisms* 10:307. doi: 10.3390/microorganisms10020307

Bandara, A. Y., Weerasooriya, D. K., Bradley, C. A., Allen, T. W., and Esker, P. D. (2020). Dissecting the economic impact of soybean diseases in the United States over two decades. *PLoS One* 15:e0231141. doi: 10.1371/journal.pone.0231141

Belton, S., McCabe, P. F., and Ng, C. K. (2021). The cyanobacterium, *Nostoc punctiforme* can protect against programmed cell death and induce defence genes in *Arabidopsis thaliana*. *J. Plant Interact.* 16, 64–74. doi: 10.1080/17429145.2021.1891306

Bent, A. F. (2022). Exploring soybean resistance to soybean cyst nematode. *Annu. Rev. Phytopathol.* 60, 379–409. doi: 10.1146/annurev-phyto-020620-120823

Biondi, N., Piccardi, R., Margheri, M. C., Rodolfi, L., Smith, G. D., and Tredici, M. R. (2004). Evaluation of *Nostoc* strain ATCC 53789 as a potential source of natural pesticides. *Appl. Environ. Microbiol.* 70, 3313–3320. doi: 10.1128/AEM.70.6.3313-3320.2004

Boutte, C., Grubisic, S., Balthasart, P., and Wilmotte, A. (2006). Testing of primers for the study of cyanobacterial molecular diversity by DGGE. *J.Microbiol. Methods* 65, 542–550. doi: 10.1016/j.mimet.2005.09.017

Caporaso, J. G., Lauber, C. L., Walters, W. A., Berg-Lyons, D., Lozupone, C. A., Turnbaugh, P. J., Noah Fierer, N., and Knight, R. (2011). Global patterns of 16S rRNA diversity at a depth of millions of sequences per sample. *Proc. Natl. Acad. Sci. U.S.A.* 108, 4516–4522. doi: 10.1073/pnas.1000080107

Chaudhary, V., Prasanna, R., Nain, L., Dubey, S., Gupta, V., Singh, R., et al. (2012). Bioefficacy of novel cyanobacteria-amended formulations in suppressing damping off disease in tomato seedlings. *World J. Microbiol. Biotechnol.* 28, 3301–3310. doi: 10.1007/s11274-012-1141-z

Chen, L., Cai, Y., Liu, X., Guo, C., Sun, S., Wu, C., et al. (2018). Soybean hairy roots produced *in vitro* by *Agrobacterium rhizogenes*-mediated transformation. *Crop J.* 6, 162–171. doi: 10.1016/j.cj.2017.08.006

Chen, S., and Liu, S. (2007). Effects of tillage and crop sequence on parasitism of *Heterodera glycines* juveniles by *Hirsutella* spp. and on juvenile population density. *Nematropica* 37, 93–106. Available online at: https://journals.flvc.org/nematropica/article/view/64419

Choleva, B., Bileva, T., and Tsvetkov, J. (2007). Organo-biological means and methods for control of plant parasitic nematodes as alternative of agrochemicals. *Ecol. Fut.* 6, 43–49. Available online at: https://www.cabidigitallibrary.org/doi/pdf/10.5555/20103006862

Cole, J.R., Wang, Q., Fish, J.A., Chai, B., McGarrell, D.M., Sun, Y., et al. (2014). Ribosomal database project: data and tools for high throughput rRNA analysis. *Nucleic Acids Res.* 42(D1), D633-D642. doi: 10.1093/nar/gkt1244

Deng, X., Zhang, N., Shen, Z., Zhu, C., Liu, H., Xu, Z., et al. (2021). Soil microbiome manipulation triggers direct and possible indirect suppression against *Ralstonia solanacearum* and *Fusarium oxysporum*. *NPJ Biofilms Microbiomes* 7:33. doi: 10.1038/s41522-021-00204-9

Desaeger, J., Wram, C., and Zasada, I. (2020). New reduced-risk agricultural nematicides-rationale and review. *J. Nematol.* 52, 1–16. doi: 10.21307/jofnem-2020-091

Edgar, R. C. (2010). Search and clustering orders of magnitude faster than BLAST. *Bioinformatics* 26, 2460–2461. doi: 10.1093/bioinformatics/btq461

Edgar, R. C. (2016). *UNOISE2: Improved error-correction for Illumina 16S and ITS amplicon sequencing.* BioRxiv. doi: 10.1101/081257

Edgar, R. C. (2018). Updating the 97% identity threshold for 16S ribosomal RNA OTUs. *Bioinformatics* 34, 2371–2375. doi: 10.1093/bioinformatics/bty113

Eken, C., Uysal, G., Demir, D., Çalişkan, S., Sevindik, E., and Çaglayan, K. (2023). Use of *Arthrobotrys* spp. *in biocontrol of the root-knot nematode Meloidogyne incognita. Eur. J. Biol. Res.* 13, 173–180. doi: 10.5281/zenodo.10015641

Fernandez-Valenzuela, S., Chávez-Ruvalcaba, F., Beltran-Rocha, J. C., San Claudio, P. M., and Reyna-Martínez, R. (2021). Isolation and culturing axenic microalgae: Mini-review. *Open Microbiol. J.* 15, 111–119. doi: 10.2174/1874285802115010111

Ferris, M. J., and Hirsch, C. (1991). Method for isolation and purification of cyanobacteria. *Appl. Environ. Microbiol.* 57, 1448–1452. doi: 10.1128/aem.57.5.1448-1452.1991

Ghareeb, R. Y., Abdelsalam, N. R., El Maghraby, D. M., Ghozlan, M. H., El-Argawy, E., and Abou-Shanab, R. A. (2022). *Oscillatoria* sp. as a potent anti-phytopathogenic agent and plant immune stimulator against root-knot nematode of Soybean cv. Giza 111. *Front. Plant Sci.* 13:870518. doi: 10.3389/fpls.2022.870518

Gohl, D. M., MacLean, A., Hauge, A., Becker, A., Walek, D., and Beckman, K. B. (2016b). An optimized protocol for high-throughput amplicon-based microbiome profiling. *Protoc. Exch.* doi: 10.1038/protex.2016.030

Gohl, D. M., Vangay, P., Garbe, J., MacLean, A., Hauge, A., Becker, A., et al. (2016a). Systematic improvement of amplicon marker gene methods for increased accuracy in microbiome studies. *Nat. Biotech.* 34, 942–949. doi: 10.1038/nbt.3601

Haarith, D., Kim, D. G., Chen, S., and Bushley, K. E. (2021). Growth chamber and greenhouse screening of promising *in vitro* fungal biological control candidates for the soybean cyst nematode (*Heterodera glycines*). *Biol. Control.* 160:104635. doi: 10.1016/j.biocontrol.2021.104635

Hamouda, R. A., and El-Ansary, M. S. M. (2017). Potential of plant-parasitic nematode control in banana plants by microalgae as a new approach towards resistance. *Egypt. J. Biol. Pest Control* 27, 165–172. Available online at: https://www.cabidigitallibrary.org/doi/pdf/10.5555/20173278343

Han, P. P., Jia, S. R., Sun, Y., Tan, Z. L., Zhong, C., Dai, Y. J., et al. (2014). Metabolomic approach to optimizing and evaluating antibiotic treatment in the axenic culture of cyanobacterium *Nostoc flagelliforme*. *World J. Microbiol. Biotechnol.* 30, 2407–2418. doi: 10.1007/s11274-014-1666-4

Holajjer, P., Kamra, A., Gaur, H. S., and Dhar, D. W. (2012). *In vitro* nematicidal activity of a terrestrial cyanobacterium, *Synechococcus nidulans*, towards plant-parasitic nematodes. *Nematology* 14, 85–92. doi: 10.1163/138855411X578879

Holajjer, P., Kamra, A., Gaur, H. S., and Manjunath, M. (2013). Potential of cyanobacteria for biorational management of plant-parasitic nematodes: a review. *Crop Protect.* 53, 147–151. doi: 10.1016/j.cropro.2013.07.005

Hunter, M. C., Smith, R. G., Schipanski, M. E., Atwood, L. W., and Mortensen, D. A. (2017). Agriculture in 2050: recalibrating targets for sustainable intensification. *Bioscience* 67, 386–391. doi: 10.1093/biosci/bix010

Jose, S., Malla, M. A., Renuka, N., Bux, F., and Kumari, S. (2024). Cyanobacteria-green microalgae consortia enhance soil fertility and plant growth by shaping the native soil microbiome of *Capsicum annuum*. *Rhizosphere* 30:100892. doi: 10.1016/j.rhisph.2024.100892

Joshi, H., Shourie, A., and Singh, A. (2020). "Cyanobacteria as a source of biofertilizers for sustainable agriculture," in *Advances in*

cyanobacterial biology (Cambridge, MA: Academic Press), (pp. 385–396). doi: 10.1016/B978-0-12-819311-2.00025-5

Kim, J. D. (2006). Screening of cyanobacteria (blue-green algae) from rice paddy soil for antifungal activity against plant pathogenic fungi. *Mycobiology* 34, 138–142. doi: 10.4489/MYCO.2006.34.3.138

Koenning, S. R., and Wrather, J. A. (2010). Suppression of soybean yield potential in the continental United States by plant diseases from 2006 to 2009. *Plant Health Prog.* 11:5. doi: 10.1094/PHP-2010-1122-01-RS

Kolde, R. (2015). *R pheatmap: Pretty Heatmaps.* R package version 1.0.8. Available online at: http://CRAN.R-project.org/package=pheatmap (accessed December 11, 2015).

Kuraganti, G., Edla, S., and Pallaval, V. B. (2020). "Cyanobacteria as biofertilizers: current research, commercial aspects, and future challenges," in Advances in Plant Microbiome and Sustainable Agriculture. Microorganisms for Sustainability eds. A. Yadav, A. Rastegari, N. Yadav, D. Kour (Singapore: Springer). doi: 10.1007/978-981-15-3204-7_11

Lee, S. M., and Ryu, C. M. (2021). Algae as new kids in the beneficial plant microbiome. *Front. Plant Sci.* 12:599742. doi: 10.3389/fpls.2021.599742

Li, H., Toh, R., Wei, Y., Wang, Y., Hu, J., An, S., et al. (2022). Microbiomes across root compartments are shaped by inoculation with a fungal biological control agent. *Appl. Soil Ecol.* 170:104230. doi: 10.1016/j.apsoil.2021.104230

Love, M. I., Huber, W., and Anders, S. (2014). Moderated estimation of fold change and dispersion for RNA-seq data with DESeq2. *Genome Biol.* 15, 1–21. doi: 10.1186/s13059-014-0550-8

Meixner, K., Daffert, C., Bauer, L., Drosg, B., and Fritz, I. (2022). PHB producing cyanobacteria found in the neighborhood-their isolation, purification and performance testing. *Bioengineering* 9:178. doi: 10.3390/bioengineering9040178

Molinari, S., and Leonetti, P. (2019). Bio-control agents activate plant immune response and prime susceptible tomato against root-knot nematodes. *PloS One* 14:e0213230. doi: 10.1371/journal.pone.0213230

Mwaheb, M. A., Hussain, M., Tian, J., Zhang, X., Hamid, M. I., El-Kassim, N. A., et al. (2017). Synergetic suppression of soybean cyst nematodes by chitosan and *Hirsutella minnesotensis* via the assembly of the soybean rhizosphere microbial communities. *Biol. Control* 115, 85–94. doi: 10.1016/j.biocontrol.2017.09.011

Nordbring-Hertz, B. (2004). Morphogenesis in the nematode-trapping fungus *Arthrobotrys oligospora*-An extensive plasticity of infection structures. *Mycologist* 18, 125–133. doi: 10.1017/S0269915X04003052

Nübel, U., Garcia-Pichel, F., and Muyzer, G. (1997). PCR primers to amplify 16S rRNA genes from cyanobacteria. *Appl. Environ. Microbiol.* 63, 3327–3332. doi: 10.1128/aem.63.8.3327-3332.1997

Okanya, P. W., Mohr, K. I., Gerth, K., Jansen, R., and Müller, R. (2011). Marinoquinolines A- F, pyrroloquinolines from *Ohtaekwangia kribbensis* (Bacteroidetes). *J. Nat. Prod.* 74, 603–608. doi: 10.1021/np100625a

Oksanen, J., Blanchette, F. G., Kindt, R., Legendre, P., McGlinn, P. R., O'Hara, R. B., et al., (2024). *Vegan: Community ecology package.* Available online at: https://cran.r-project.org/web/packages/vegan/index.html (accessed August 28, 2024).

Ou, Y., Penton, C.R., Geisen, S., Shen, Z., Sun, Y., Lv, N., et al. (2019). Deciphering underlying drivers of disease suppressiveness against pathogenic *Fusarium oxysporum*. *Front. Microbiol.* 10:2535. doi: 10.3389/fmicb.2019.02535

Parmar, P., Kumar, R., Neha, Y., and Srivatsan, V. (2023). Microalgae as next generation plant growth additives: Functions, applications, challenges and circular bioeconomy based solutions. *Front. Plant Sci.* 14:1073546. doi: 10.3389/fpls.2023.1073546

Prasanna, R., Chaudhary, V., Gupta, V., Babu, S., Kumar, A., Singh, R., et al. (2013). Cyanobacteria mediated plant growth promotion and bioprotection against *Fusarium wilt* in tomato. *Eur. J. Plant Pathol.* 136, 337–353. doi: 10.1007/s10658-013-0167-x

Priya, H., Prasanna, R., Ramakrishnan, B., Bidyarani, N., Babu, S., Thapa, S., et al. (2015). Influence of cyanobacterial inoculation on the culturable microbiome and growth of rice. *Microbiol. Res.* 171, 78–89. doi: 10.1016/j.micres.2014.12.011

Qiu, Y., Gu, L., Tian, S., Sidhu, J., Gibbons, J., Van Den Top, T., et al. (2019). *Developmentally regulated genome editing in terminally differentiated n2-fixing heterocysts of Anabaena cylindrica ATCC 29414.* BioRxiv 629832. doi: 10.1101/629832

Ramakrishnan, B., Maddela, N. R., Venkateswarlu, K., and Megharaj, M. (2023). Potential of microalgae and cyanobacteria to improve soil health and agricultural productivity: a critical view. *Environ. Sci. Adv.* 2, 586–611. doi: 10.1039/D2VA00158F

Righini, H., Francioso, O., Martel Quintana, A., and Roberti, R. (2022). Cyanobacteria: a natural source for controlling agricultural plant diseases caused by fungi and oomycetes and improving plant growth. *Horticulturae* 8:58. doi: 10.3390/horticulturae8010058

Rippka, R., Waterbury, J. B., and Stanier, R. Y. (1981). "Isolation and purification of cyanobacteria: some general principles," in *The prokaryotes. A handbook on habitats, isolation and identification of bacteria,* eds. M. P. Starr, H. Stolp, H. G. Truper, A. Balows, H. C. Schlegel (New York: Spring-Verlag), 212–220. doi: 10.1007/978-3-662-13187-9_8

Rodríguez-Caballero, G., Caravaca, F., Alguacil, M. M., Fernández-López, M., Fernández-González, A. J., and Roldán, A. (2017). Striking alterations in the soil bacterial community structure and functioning of the biological N cycle induced by *Pennisetum setaceum* invasion in a semiarid environment. *Soil Biol. Biochem.* 109, 176–187. doi: 10.1016/j.soilbio.2017.02.012

Saravanakumar, K., Li, Y., Yu, C., Wang, Q.Q., Wang, M., Sun, J., et al. (2017). Effect of *Trichoderma harzianum* on maize rhizosphere microbiome and biocontrol of Fusarium Stalk rot. *Sci. Rep.* 7:1771. doi: 10.1038/s41598-017-01680-w

Senkovs, M., Nikolajeva, V., Makarenkova, G., and Petrina, Z. (2021). Influence of *Trichoderma asperellum* and *Bacillus subtilis* as biocontrol and plant growth promoting agents on soil microbiota. *Ann. Microbiol.* 71, 1–10. doi: 10.1186/s13213-021-01647-3

Sharma, M., Rani, N., Kamra, A., Kaushik, A., and Bala, K. (2009). Growth, exopolymer production and metal bioremoval by *Nostoc punctiforme* in Na and Cr (VI) spiked medium. *J. Environ. Res. Dev.* 4:372. Available online at: https://www.academia.edu/11937063/GROWTH_EXOPOLYMER_PRODUCTION_AND_METAL_BIOREMOVAL_BY_Nostoc_punctiforme_IN_Na_AND_Cr_VI_SPIKED_MEDIUM

Shepherd, A. M. (1970). "Extraction and estimation of *Heterodera,*" in Laboratory Methods for Work with Plant and Soil Nematodes. eds. J. F. Southey (Technical Bulletin 2. Ministry of Agriculture, Fisheries, and Food: London), 23–33.

Sithole, N., Gupta, S., Dube, Z., Ogbe, A., and Van Staden, J. (2023). Algae and cyanobacteria-based biostimulants in controlling plant-parasitic nematodes: a sustainable approach for crop protection. *Phytoparasitica* 51, 803–813. doi: 10.1007/s12600-023-01094-7

Soliman, M. S., El-Deriny, M. M., Ibrahim, D. S. S., Zakaria, H., and Ahmed, Y. (2021). Suppression of root-knot nematode *Meloidogyne incognita* on tomato plants using the nematode trapping fungus *Arthrobotrys oligospora* Fresenius. *J. Appl. Microbiol.* 131, 2402–2415. doi: 10.1111/jam.15101

SoyStats (2020). 2018 Soy Highlights. Available online at: http://soystats.com/2018-highlights

Šulčius, S., Slavuckytė, K., Januškaitė, M., and Paškauskas, R. (2017). Establishment of axenic cultures from cyanobacterium *Aphanizomenon flos-aquae* akinetes by micromanipulation and chemical treatment. *Algal Res.* 23, 43–50. doi: 10.1016/j.algal.2017.01.006

Sun, X., Liao, J., Lu, J., Lin, R., Zou, M., Xie, B., et al. (2024). Parasitism of *Hirsutella rhossiliensis* on different nematodes and its endophytism promoting plant growth and resistance against root-knot nematodes. *J. Fungi* 10:68. doi: 10.3390/jof10010068

Suresh, A., Soundararajan, S., Elavarasi, S., Oscar, F. L., and Thajuddin, N. (2019). Evaluation and characterization of the plant growth promoting potentials of two heterocystous cyanobacteria for improving food grains growth. *Biocatal. Agric. Biotechnol.* 17, 647–652. doi: 10.1016/j.bcab.2019.01.002

Tedersoo, L., Sánchez-Ramírez, S., Koljalg, U., Bahram, M., Döring, M., Schigel, D., et al. (2018). High-level classification of the Fungi and a tool for evolutionary ecological analyses. *Fungal Divers.* 90, 135–159. doi: 10.1007/s13225-018-0401-0

Thapa, S., Prasanna, R., Ramakrishnan, B., Mahawar, H., Bharti, A., Kumar, A., et al. (2021). Microbial inoculation elicited changes in phyllosphere microbial communities and host immunity suppress *Magnaporthe oryzae* in a susceptible rice cultivar. *Physiol. Mol. Plant Pathol.* 114:101625. doi: 10.1016/j.pmpp.2021.101625

Tylka, G. L., Gebhart, G. D., Marett, C. C., Mullaney, M. P., and Rasmussen, J. (2022). *2022 Evaluation of Iowa soybean varieties resistant to soybean cyst nematode.* Iowa State University, Extension and Outreach. Available online at: https://books.google.com/books?id=aE2mzwEACAAJ

Tylka, G. L., and Marett, C. C. (2021). Known distribution of the soybean cyst nematode, *Heterodera glycines*, in the United States and Canada in 2020. *Plant Health Prog.* 22, 72–74. doi: 10.1094/PHP-10-20-0094-BR

Vaz, M.G.M.V., Bastos, R.W., Milanez, G.P., Moura, M.N., Ferreira, E.G., Perin, C., et al. (2014). Use of sodium hypochlorite solutions to obtain axenic cultures of *Nostoc* strains (Cyanobacteria). *Braz. J. Botany* 37, 115–120. doi: 10.1007/s40415-014-0055-4

Wang, N., Tian, S., Gu, L., Xu, L., Qiu, Y., Van Den Top, T., et al. (2018). Isolation of potential photosynthetic N 2-fixing microbes from topsoil of native grasslands in South Dakota. In *Proceedings of the South Dakota Academy of Science* (Vol. 97, p. 117). South Dakota State University, 272. Available omline at: https://openprairie.sdstate.edu/nrm_pubs/272

Wickham, H. (2016). *Ggplot2: Elegant graphics for data analysis.* New York, NY: Springer-Verlag. doi: 10.1007/978-3-319-24277-4_9

Winter, S. M. J., Rajcan, I., and Shelp, B. J. (2006). Soybean cyst nematode: challenges and opportunities. *Can. J. Plant Sci.* 86, 25–32. doi: 10.4141/P05-072

Wram, C. L., Hesse, C. N., and Zasada, I. A. (2022). Transcriptional changes of biochemical pathways in *Meloidogyne incognita* in response to non-fumigant nematicides. *Sci. Rep.* 12:9875. doi: 10.1038/s41598-022-14091-3

Yin, C., Casa Vargas, J. M., Schlatter, D. C., Hagerty, C. H., Hulbert, S. H., and Paulitz, T. C. (2021). Rhizosphere community selection reveals bacteria associated with reduced root disease. *Microbiome* 9, 1–18. doi: 10.1186/s40168-020-00997-5

Yin, C., Larson, M., Lahr, N., and Paulitz, T. (2024). Wheat rhizosphere-derived bacteria protect soybean from soilborne diseases. *Plant Dis.* doi: 10.1094/PDIS-08-23-1713-RE

Yu, Z., Mo, M., Zhang, Y., and Zhang, K. Q. (2014). "Taxonomy of nematode-trapping fungi from *Orbiliaceae*, Ascomycota," in *Nematode Trapping Fungi.* eds. K. Q. Zhang, and K. D. Hyde (Dordrecht: Springer), 41–210. doi: 10.1007/978-94-017-8730-7_3

frontiers | Frontiers in Microbiology

TYPE Original Research
PUBLISHED 14 May 2025
DOI 10.3389/fmicb.2025.1520443

OPEN ACCESS

EDITED BY
Paola Grenni,
National Research Council, Italy

REVIEWED BY
Setu Bazie Tagele,
University of California, Riverside,
United States
Junli Cao,
Shanxi Agricultural University, China

*CORRESPONDENCE
Wensheng Fang
✉ fangwensheng@caas.cn
Zhoubin Liu
✉ hnlzb2020@hunau.edu.cn
Bozhi Yang
✉ yangy_1223@163.com

RECEIVED 31 October 2024
ACCEPTED 25 March 2025
PUBLISHED 14 May 2025

CITATION
Tian W, Wang Q, Cao A, Yan D, Li Y, Liu Z, Yang B and Fang W (2025) Genotype-dependent responses of pepper endophytes to soil microbial community shifts induced by allyl isothiocyanate fumigation.
Front. Microbiol. 16:1520443.
doi: 10.3389/fmicb.2025.1520443

Genotype-dependent responses of pepper endophytes to soil microbial community shifts induced by allyl isothiocyanate fumigation

Wenfeng Tian[1,2], Qiuxia Wang[2], Aocheng Cao[2], Dongdong Yan[2], Yuan Li[2], Zhoubin Liu[1]*, Bozhi Yang[1]* and Wensheng Fang[2]*

[1]Engineering Research Center for Horticultural Crop Germplasm Creation and New Variety Breeding, Ministry of Education, Key Laboratory of Vegetable Biology of Hunan Province, College of Horticulture, Hunan Agricultural University, Changsha, Hunan, China, [2]State Key Laboratory for Biology of Plant Diseases and Insect Pests, Institute of Plant Protection, Chinese Academy of Agricultural Sciences, Beijing, China

Introduction: Allyl isothiocyanate (AITC) has demonstrated efficacy as a soil fumigant, effectively controlling soil-borne pathogens and nematodes. Although AITC has a significant effect on soil microbial communities, whether fumigation affects the production of crop endophytes is unclear.

Methods: In this study, AITC was used to fumigate the soil, and the response of endophytic bacteria (in roots, stems, and leaves) in different pepper genotypes (Xiangla359, La Xuan, Shuang Jiao) was investigated.

Results: Fumigation with AITC significantly increased soil microbial diversity, stimulated the growth of Actinomycetota, and inhibited Pseudomonadota. However, the effects on endophytic bacteria varied among pepper varieties. Specifically, fumigation significantly reduced microbial diversity in the roots and leaves of Xiangla359, but had no significant effect on La Xuan and Shuang Jiao. Furthermore, the growth-promoting effect of AITC was most pronounced in Xiangla359.

Conclusion: Our results suggest that while AITC fumigation significantly alters soil microbial diversity and composition, its effects on crop endophytes are genotype-dependent. These findings provide insight into the complex interactions between soil microbial communities and crop endophytes in response to soil fumigation.

KEYWORDS

soil fumigation, endophyte, soil microorganism, AITC, genotype, pepper

1 Introduction

Peppers (*Capsicum annuum L.*), esteemed for their piquant flavor and robust nutritional profile, belong to the Solanaceae family and are renowned for their abundant polyphenols, capsaicinoids, ascorbic acid, and other phytochemicals (Barboza et al., 2022). In China, peppers are among the most extensively cultivated vegetables, with the 2021 cultivated area exceeding 213 ha, representing approximately 10% of the total vegetable

cultivation acreage. The expansion of protected cultivation has driven a remarkable surge in vegetable yields; however, this progress has been paralleled by the accumulation of soil pathogens and exacerbation of soil-borne diseases, thereby impeding agricultural advancement (Ren et al., 2018). Consequently, addressing the persistent crop disorders in peppers and enhancing their yield constitute pivotal concerns in contemporary agricultural practices.

Soil fumigation represents the most direct and effective strategy for addressing the challenges associated with crop recolonization (Mao et al., 2014). Among the various fumigants, allyl isothiocyanate (AITC) stands out as a high-quality, plant-derived agent known for its efficacy in preventing and eradicating a range of soil-borne pathogenic nematodes (Dahlin and Hallmann, 2020; Ren et al., 2018), pathogenic fungi (Yu et al., 2019) and weeds (Zhang Y. et al., 2023). Additionally, AITC effectively inhibits pests during storage (Wu et al., 2009) and mitigates postharvest diseases (Otoni et al., 2014; Ugolini et al., 2014) all while maintaining a high safety profile and leaving no pesticide residues.

Recent studies have demonstrated that AITC significantly inhibits the development of gray mold in tomatoes, thereby extending their storage life (Barea-Ramos et al., 2024). Furthermore, AITC has been shown to effectively mitigate postharvest quality deterioration in edible mushrooms and raspberries (Park et al., 2023; Zou et al., 2024). Yu et al.'s (2022) research revealed that the inhibitory effect of AITC on C. heterostrophus was linked to the downregulation of genes associated with energy metabolism, oxidoreductase activity, melanin biosynthesis, and cell wall-degrading enzymes, resulting in a significant reduction in melanin production in C. heterostrophus. Moreover, AITC has been proven to effectively inhibit various pathogenic bacteria, including Rhizoctonia solani, Fusarium graminearum, Ralstonia solanacearum, P. aphanidermatum, Fusarium spp., and Phytophthora spp (Ashiq et al., 2022; Handiseni et al., 2017; Ren et al., 2018).

Soil microorganisms play a crucial role in environmental processes and are pivotal in maintaining the stability of soil ecosystems (Wu et al., 2024). The non-targeted nature of the fumigant led to a notable reduction in the population of detrimental soil microorganisms, such as Fusarium oxysporum and Mycobacterium avium. The application of AITC fumigation resulted in a transient decline in the overall microbial abundance in the soil, which gradually recovered over a one-month period (Castellano-Hinojosa et al., 2022). Furthermore, a significant increase in beneficial soil bacteria was observed following AITC fumigation (Tagele et al., 2021). AITC soil fumigation was also found to enhance the population of aerobic denitrifying bacteria (Li et al., 2023). Moreover, AITC fumigation and its degradation products demonstrated effective inhibition of soil manganese oxidation, leading to an increase in the bioavailable manganese content in the soil (Wang et al., 2024).

The diversity of inter-root microorganisms is intricately modulated by factors such as pH, effective phosphorus levels, and organic matter content (Zhou et al., 2021). Additionally, the species composition and abundance of the rhizosphere microbiome are influenced by the developmental stages of plants and the specific plant species present (Chen et al., 2022). Disparities in the distribution and abundance of inter-root and endophytic microorganisms significantly impact various physiological processes in plants, including growth regulation, disease resistance, and hormonal signaling pathways (Hartmann and Six, 2023; Yang et al., 2023). Endophytic microorganisms represent a category of microbes that engage in mutually beneficial symbiotic relationships with their host plants. Due to their prolonged coexistence within the unique plant environment, these microorganisms are recognized as valuable microbial resources that significantly contribute to the growth, development, and stress resilience of crops (Compant et al., 2019). Endophytes facilitate plant growth by providing essential nutrients or conferring protection against pathogenic challenges. The potential of plant endophytic microorganisms to enhance crop resistance and stimulate yield gains has attracted considerable research attention (Afzal et al., 2019; Sessitsch et al., 2012). Among these microorganisms, endophytic fungi have emerged as a focal point of investigation. Several studies have demonstrated that endophytic fungi play a significant role in enhancing crop nitrogen utilization (Yang et al., 2014). Notably, the presence of the endophytic bacterium Paenibacillus exerts a profound influence on the metabolic profile of isolated cultivated poplar plants (Scherling et al., 2009). Several bacterial and fungal genomes, such as those of Penicillium, Fusarium, Phytophthora, Dendrobacter, and *Streptomyces*, contain genes associated with nitrogen metabolism, hormone biosynthesis, phosphate utilization, and root colonization mechanisms (Huang et al., 2022; Shah et al., 2022). These Microorganisms play a crucial role in providing essential nutrients to plants, thereby facilitating growth promotion through mechanisms such as nitrogen fixation and enhanced access to phosphorus and iron (Liu et al., 2022; Phurailatpam et al., 2022).

Although the interactions between soil microbiota and crop endophytes are acknowledged to be crucial for plant health, the specific mechanisms underlying these interactions remain unclear. It has been demonstrated that soil microbial diversity and composition significantly impact plant growth and health, thereby influencing the dynamics of endophytic flora. However, changes in soil microbial communities do not invariably lead to shifts in crop endophytes, as the distinct habitats of endophytes are primarily shaped by the plant's internal environment. Soil management practices, such as fertilization, microbial inoculation, and fumigation treatments, can modulate microbial diversity and abundance in the soil, subsequently influencing the microbial communities within the plant's root system and above-ground structures, including endophyte populations. In this investigation, we employed HiSeq2500 high-throughput sequencing technology to explore variations in microbial community diversity and the structural composition of endophytes in different pepper varieties following AITC fumigation. Our study aims to elucidate the potential impact of changes in soil microbial communities on crop endophyte communities.

2 Materials and methods

2.1 Indoor soil fumigation experiment

The experimental soil used in this study was sourced from Yanqing, Beijing (115°44'–116°34'E, 40°16'–40°47'N) and is classified as alkaline tidal soil. Prior to use, the soil was sieved

through a 2 mm mesh. A total of 12 kg of the test soil was weighed and placed into a 20 L plastic bucket. A 20% water emulsion of propylene isothiocyanate (AITC), obtained from Beijing Agronon Bio-Pharmaceutical Co., Ltd., was thoroughly mixed with the soil. Immediately after mixing, the bucket was sealed tightly with a transparent plastic cover and securely wrapped with transparent tape. The mixture was then incubated at 28°C in a light-free environment for a duration of 10 days. A control group without the addition of AITC was also included. Following the fumigation period, the soil was left uncovered in a well-ventilated area for one week to ensure the complete dispersion of any remaining fumigant. Subsequently, 30 g of the soil was collected and stored at −80°C for macrogenomic sequencing.

2.2 Pepper planting

The pepper seeds were pre-soaked and allowed to germinate for 3 days prior to sowing. Subsequently, the seeds were evenly distributed in the soil, covered with approximately 1 cm of loose soil, watered once, and maintained at a constant temperature of around 28°C. Regular watering was carried out to ensure soil moisture levels were optimal. Each experimental group consisted of 42 plants. The incubation room was set to a temperature of 28°C, with a relative humidity of 60% and a photoperiod of L//D = 12H//12H.

2.3 Sample collection

Sampling was conducted on the 55th day after pepper transplantation to assess plant height, stem thickness, and chlorophyll content. Chlorophyll levels were measured using a handheld chlorophyll meter. On the same day, rhizosphere soil samples were collected. During the sampling process, the peppers were carefully uprooted, and any loose soil attached to the root system was gently shaken off. Tightly adhered soil was then collected using a brush. A portion of the soil was stored at 4°C for the evaluation of physicochemical indices, while another portion was stored at −80°C for high-throughput sequencing.

The preparation of pepper samples involved washing the roots, stems, and leaves with distilled water to remove impurities. After washing, the roots, stems, and leaves were cut and soaked in 75% ethanol for 2 min, followed by a 5-min wash with a 2% sodium hypochlorite solution. Subsequently, the samples were transferred to 75% ethanol for 1 min and rinsed three times with sterile water, repeating this process three times. The samples were then dried, placed in self-sealing bags, and stored at −80°C for high-throughput sequencing (Ren et al., 2019). Each set of trials was conducted in triplicate.

2.4 Physicochemical properties of soil

Soil physicochemical parameters were analyzed following the method established by Li Sheik Kai. Nitrate nitrogen and ammonium nitrogen were extracted using KCl and quantified using a flow analyzer. Effective phosphorus was extracted with $NaHCO_3$ and measured using a flow analyzer, while fast-acting potassium was extracted with CH_3COONH_4 and quantified using a flame spectrophotometer. pH was determined using a 2.5:1 water-to-soil ratio and potentiometric method, and electrical conductivity was measured using a 2.5:1 water-to-soil ratio and conductivity probe. Organic matter content was assessed through potassium dichromate titration.

2.5 Metagenomic sequencing

0.2 g of soil material was used to extract total genomic DNA with the E.Z.N.A.® soil DNA Kit (Omega Bio-tek, Norcross, GA, USA) according to manufacturer's instructions. Concentration and purity of extracted DNA was determined with SynergyHTX and NanoDrop2000, respectively. DNA quality was checked on 1% agarose gel.

DNA extract was fragmented to an average size of about 350 bp using Covaris M220 (Gene Company Limited, China) for paired-end library construction. Paired-end library was constructed using NEXTFLEX Rapid DNA-Seq (Bioo Scientific, Austin, TX, USA). Paired-end sequencing was performed on Illumina NovaSeq™ X Plus (Illumina Inc., San Diego, CA, USA) at Majorbio Bio-Pharm Technology Co., Ltd (Shanghai, China) using NovaSeq X Series 25B Reagent Kit according to the manufacturer's instructions.[1]

2.6 DNA extraction, PCR amplification, and high-throughput sequencing

DNA extraction from treated plant samples was performed utilizing the Qiagen magnetic bead method, while total DNA from soil samples was isolated using the E.Z.N.A.® Soil DNA Kit. Following extraction, the purity and concentration of DNA were evaluated using the Scandrop200 and confirmed by 1% agarose gel electrophoresis, respectively. Primers were tailed with PacBio barcode sequences to distinguish each sample. Amplification reactions (20-μL volume) consisted of 5 × FastPfu buffer 4 μL, 2.5 mM dNTPs 2 μL, forward primer (5 μM) 0.8 μL, reverse primer (5 μM) 0.8 μL, FastPfu DNA Polymerase 0.4 μL, template DNA 10 ng and DNase-free water. The PCR amplification was performed as follows: initial denaturation at 95°C for 3 min, followed by 27 cycles of denaturing at 95°C for 30 s, annealing at 60°C for 30 s and extension at 72°C for 45 s, and single extension at 72°C for 10 min, and end at 4°C (T100 Thermal Cycler PCR thermocycler, BIO-RAD, USA). After electrophoresis, The PCR products were purified using the AMPure® PB beads (Pacifc Biosciences, CA, USA) and quantified with Qubit 4.0 (Thermo Fisher Scientific, USA). For amplification of the 16S rRNA gene in pepper root, stem, and leaf samples, primers 779F (AACMGGATTAGATACCCKG) and 1193R (ACGTCATCCCCACCTTCC) were employed, whereas primers 338F (ACTCCTACGGGAGGCAGCA) and 806R (GGACTACHVGGGTWTCTAAT) were utilized for soil samples. Subsequent high-throughput and macro-genome sequencing were conducted by Shanghai Meiji Biotechnology Co., Ltd.

1 www.illumina.com

2.7 Statistical analyses

The purified amplicons were pooled in equimolar and paired-end sequenced (2 × 300) on an Illumina MiSeq platform (Illumina, San Diego, USA). The original sequences were sequenced, spliced, quality controlled, and filtered to obtain optimized sequences (Magoc and Salzberg, 2011), clustered into operable taxonomic units (OTUs) according to similarity levels. The optimized sequences were compared with the Silva (SSU123)16S rRNA Database. A confidence threshold of 0.7 was chosen to combine with the RDP classifier Bayesian algorithm v2.21 to taxonomically analyze (Magoc and Salzberg, 2011), OTU sequences at 97% similarity level to obtain species annotation information for OTUs. The best-hit taxonomy of non-redundant genes was obtained by aligning them against the NCBI NR database by DIAMOND[6] (version 2.0.13)[2] with an e-value cutoff of 1e-5. Similarly, the functional annotation (GO, KEGG, eggNOG, CAZy, CARD, PHI) of non-redundant genes was obtained. Based on the taxonomic and functional annotation and the abundance profile of non-redundant genes, the differential analysis was carried out at each taxonomic, functional, or gene-wise level by Kruskal–Wallis test. The experimental data was organized using Microsoft Excel 2010 software. The comparison of means between groups was conducted using SPSS 26 for independent samples *t*-test and one-way ANOVA. The significance level was set at $\alpha = 0.05$. PcoA was generated using the Bray Curtis algorithm, and community composition and variability analyses were performed using the Meguiar's Cloud platform. Graphing was carried out using Origin 2017. The Welch *t*-test method was used to calculate the confidence interval. The stats package (version 3.3.1) of R and the scipy package (version 1.0.0) of Python were used. The linear discriminant analysis (LDA) effect size (LEfSe)[3] was performed to identify the significantly abundant taxa (phylum to genera) of bacteria among the different groups (LDA score > 3.8, $P < 0.05$).

3 Results

3.1 Effects of allyl isothiocyanate on soil microorganisms and functions

Gene-based species taxonomic annotations were compared with the NR database to extract species and abundance information across various taxonomic levels, including domain, kingdom, phylum, order, family, genus, and species for each sample. A total of 244 phyla, 501 orders, 1,003 families, 1,966 genera, and 30,841 species were identified through NR species annotation. The results of the bacterial community alpha diversity index (Table 1) demonstrate that AITC fumigation significantly enhanced the richness of the soil microbial community.

A comparative analysis of soil microorganisms before and after allyl isothiocyanate (AITC) fumigation revealed shifts in the top ten microorganisms at the phylum level within the soil microbial community (Figure 1A). The predominant phyla identified were Actinomycetota, Pseudomonadota, Acidobacteriota, Chloroflexota, Gemmatimonadota, Nitrososphaerota, Verrucomicrobiota, Planctomycetota, Candidatus Dormibacteraeota, and unclassified d_Bacteria. Notably, the relative abundance of Actinomycetota showed a significant increase ($P < 0.01$) post-fumigation. Conversely, there was a marked decrease in the relative abundance of Pseudomonadota and Bacteroidota ($P < 0.01$), indicating that Actinomycetota exhibited a significant increase ($P < 0.01$) (Figures 2A–C).

TABLE 1 Alpha diversity index of soil microbial community fumigated by allyl isothiocyanate.

Sample	Ace	Shannon	Simpson
CK	8.5 ± 0.50	1.95 ± 0.002	0.14 ± 0.009
AITC	12.33 ± 0.67	2.30 ± 0.08	0.11 ± 0.005

At the genus level (Figure 1B), the top ten microorganisms in relative abundance in the soil microbial community were *Sphingomonas*, *unclassified_p_Acidobacteriota*, *unclassified_c_Actinomycetes*, *unclassified_p_Actinomycetota*, *unclassified_p_Chloroflexota*, *Nocardioides*, *unclassified_p_Gemmatimonadota*, *Bradyrhizobium*, *unclassified_c_Terriglobia*, *Streptomyces*. Of which, *Sphingomonas*, *Lysobacter*, *Nitrososphaera*, *Marmoricola*, *Candidatus_Nitrosocosmicus*, *Phycicoccus*, *Nitrosopumilus* showed significant reduction in relative abundance after fumigation, *Arthrobacter*, *Blastococcus*, *Pseudarthrobacter*, *Actinacidiphila*, *Catenulispora*, *Mycobacterium*, *Pseudonocardia*, and *Trebonia* increased significantly in relative abundance (Figures 2D–I).

By comparing the results with the KEGG database, the top three annotations at Level 1 (Figure 3A) in soil samples were identified as Metabolism, Environmental Information Processing, and Genetic Information Processing. The known gene functions with the top 10 abundances were analyzed using ANOVA. The analysis of variance revealed that the Metabolism function was significantly higher in fumigated soil compared to unfumigated soil ($P < 0.05$), while Genetic Information Processing, Cellular Processes, and Human Diseases were significantly lower in the fumigated soil ($P < 0.05$). At Level 2 (Figure 3B), metabolic pathways were also significantly higher in the soil samples than in the unfumigated soil, with significant increases observed in the following pathways: Biosynthesis of Secondary Metabolites, Microbial Metabolism in Diverse Environments, Carbon Metabolism, Quorum Sensing, ABC Transporters, and Pyruvate Metabolism ($P < 0.05$). The top 10 pathways annotated at the Pathway classification level that exhibited significant differences (Figure 3C) included Biosynthesis of Secondary Metabolites, Microbial Metabolism in Diverse Environments, Carbon Metabolism, Biosynthesis of Cofactors, Two-Component System, Quorum Sensing, ABC Transporters, Pyruvate Metabolism, and Purine Metabolism.

3.2 Effects of allyl isothiocyanate on the growth of peppers and soil physicochemical indexes

Allyl isothiocyanate (AITC) fumigation exerts a positive effect on the growth and development of peppers, although varietal

2 http://ab.inf.uni-tuebingen.de/software/diamond/
3 http://huttenhower.sph.harvard.edu/lefse

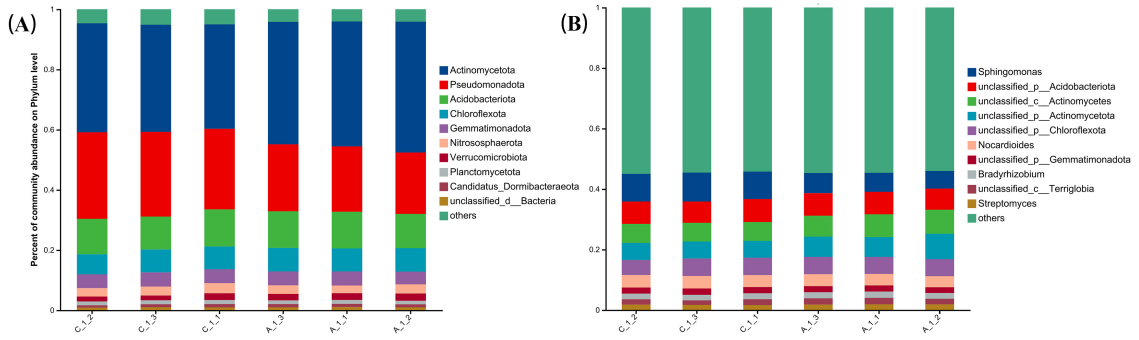

FIGURE 1
Bar chart showing changes in the relative abundance of the top ten bacterial communities at the phylum level **(A)** and genus level **(B)** in soil samples.

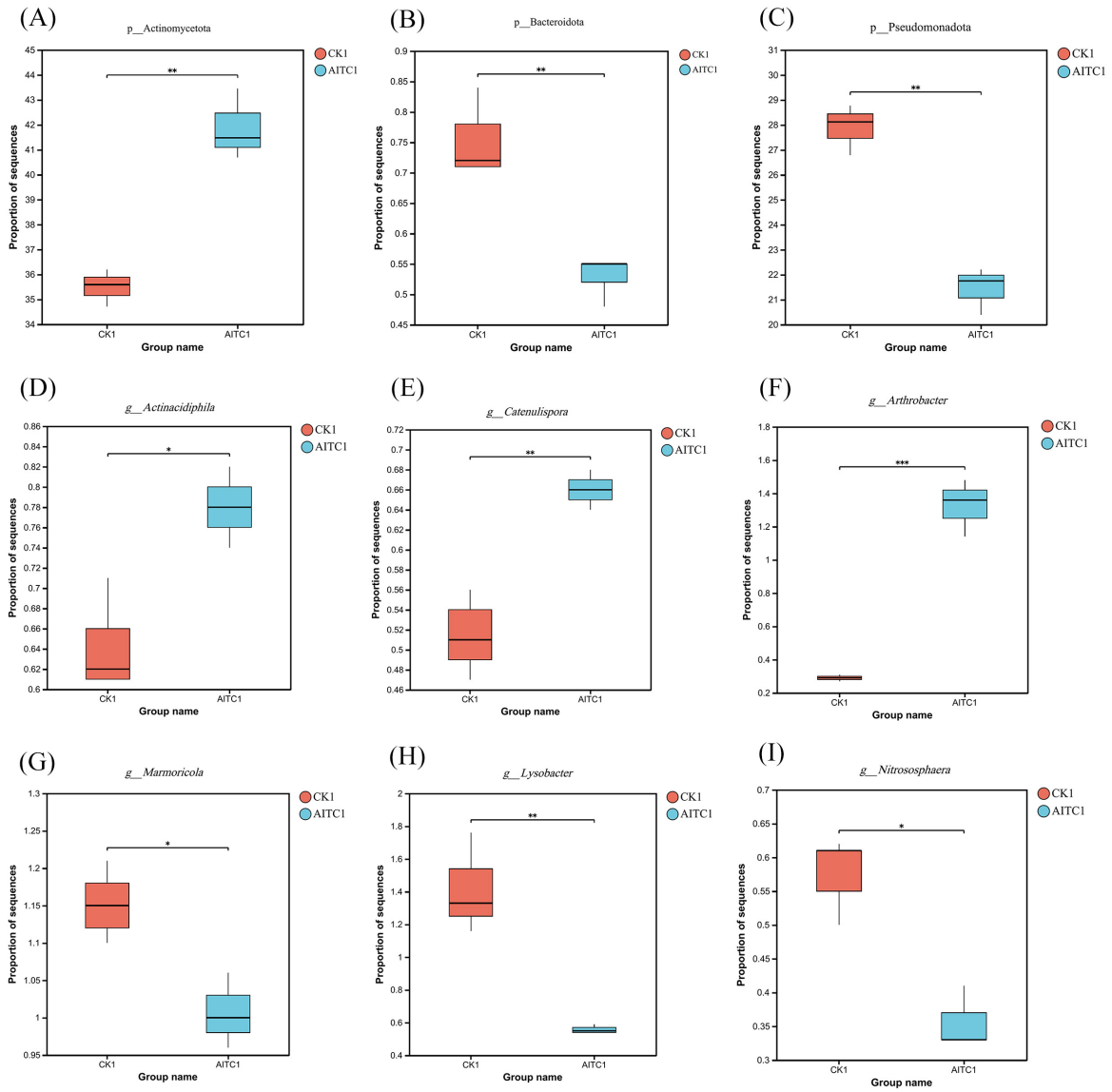

FIGURE 2
Microorganisms with significant differences in soil microorganisms at the phylum level **(A–C)** and genus level **(D–I)** after AITC fumigation. *$0.01 < p \leq 0.05$, **$0.001 < p \leq 0.01$.

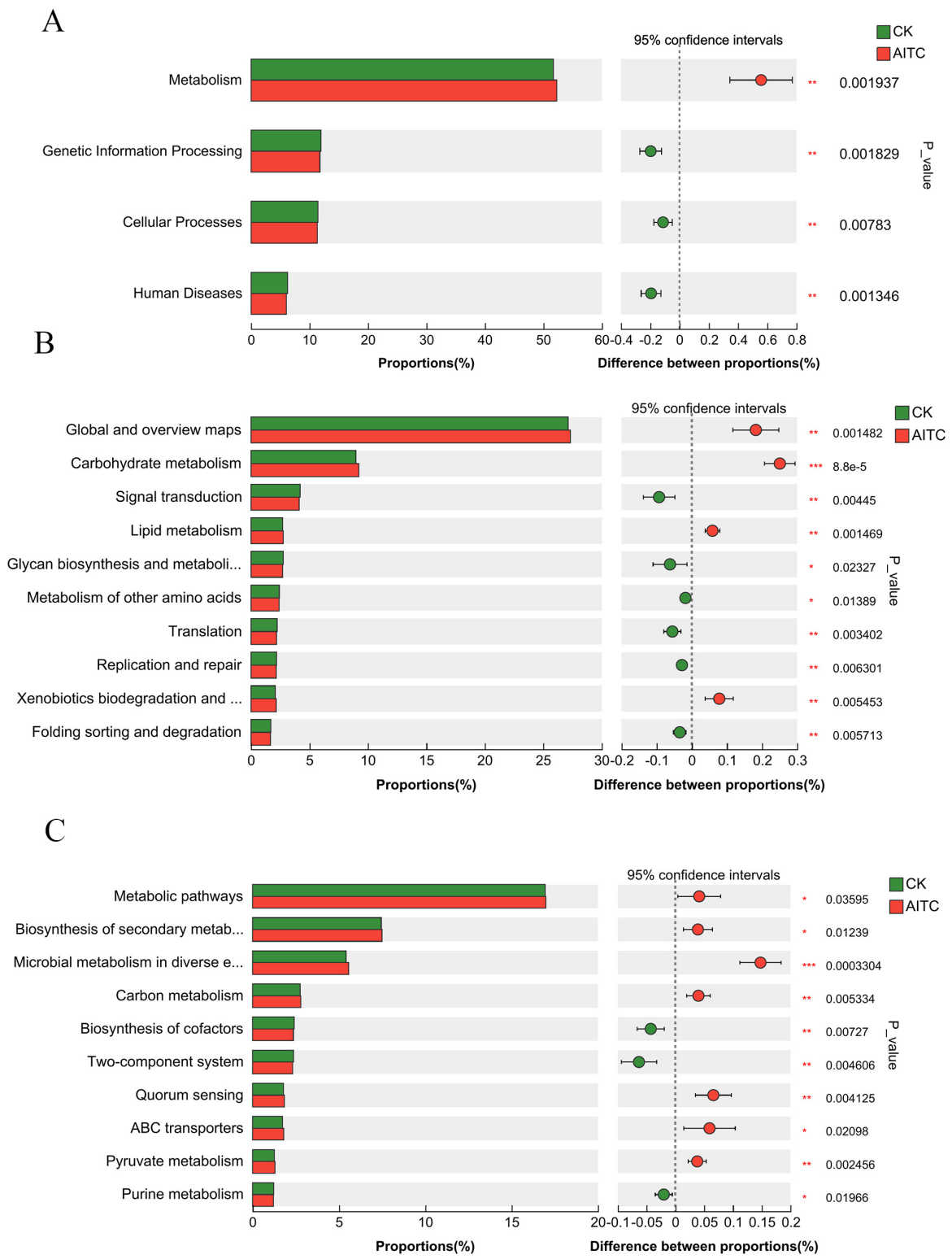

FIGURE 3
The KEGG functional levels of soil microorganisms after AITC fumigation were significantly different. **(A)** Pathway level 1. **(B)** Pathway level 2. **(C)** Pathway level 3.

discrepancies are evident (Figure 4). By the 55th day post-planting, fumigation significantly enhanced the plant height of Xiangla359 and Shuang Jiao, as well as the stem thickness of Shuang Jiao. Specifically, in the treatment group, the plant height of Xiangla359 exhibited a significant increase of 28.2%, accompanied by a notable 10.4% increase in stem thickness. Moreover, La Xuan demonstrated a growth of 12.5% in plant height, while Shuang Jiao exhibited a substantial rise of 25.9%. As depicted in Table 2, the impacts of

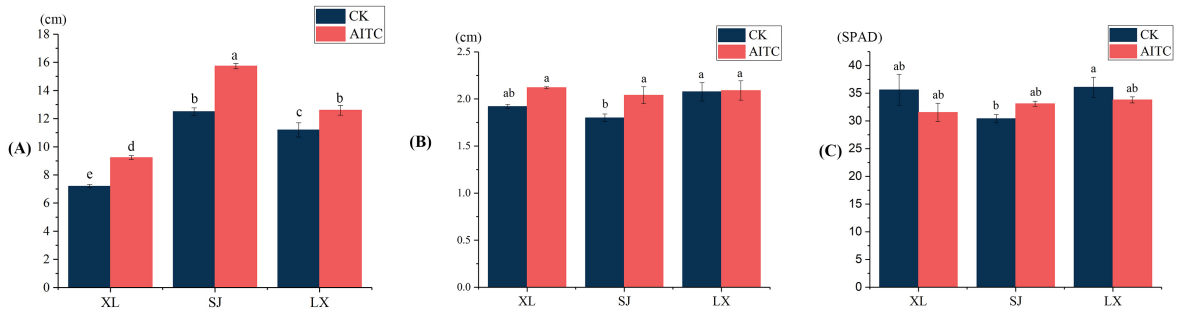

FIGURE 4
The impact of AITC fumigation on the growth of pepper plants. **(A)** Height of pepper plants under different treatments. **(B)** Stem diameter of chili pepper plants under different treatments. **(C)** Chlorophyll content of chili pepper leaves under different treatments. All results are expressed as mean ± standard deviation (SD), and the same letters indicate no statistical difference (P = 0.05) according to Duncan's new multiple range test.

TABLE 2 **Effect of soil fumigation with allyl isothiocyanate on physicochemical indexes of rhizosphere soil of different varieties of capsicum.**

	Conductivity (μs/cm)	pH	Organic matter (mg/kg)	Available *P* (mg/kg)	Available K (mg/kg)	NH_4^+-N (mg/kg)	NO_3^--N (mg/kg)
CK-XL	252.33 ± 20.36a	7.88 ± 0.11a	25.01 ± 1.30a	334.36 ± 4.88a	260 ± 6.62b	19.69 ± 13.67a	23.73 ± 0.01a
AI-XL	297.33 ± 11.88a	7.66 ± 0.03a	26.39 ± 1.16a	350.88 ± 4.63a	335 ± 42.57ab	16.70 ± 4.70a	23.75 ± 0.03a
CKLX	250.33 ± 18.13a	7.61 ± 0.005a	26.88 ± 0.79a	353.62 ± 3.43a	284.17 ± 34.69ab	20.16 ± 9.79a	23.77 ± 0.04a
AI-LX	245 ± 25.97a	7.55 ± 0.02a	25.72 ± 1.27a	444.92 ± 96.79a	260.83 ± 3.34b	31.91 ± 15.54a	23.75 ± 0.04a
CK-SJ	306.33 ± 27.77a	7.78 ± 0.005a	25.94 ± 0.44a	349.89 ± 12.30a	360 ± 31.26ab	16.70 ± 5.09a	24.33 ± 0.62a
AI-SJ	278 ± 17.69a	7.62 ± 0.07a	26.74 ± 0.11a	373.51 ± 5.35a	381.67 ± 52.19a	10.95 ± 2.63a	23.71 ± 0.001a

All results are expressed as mean ± standard deviation (SD), and the same letters indicate no statistical difference (P = 0.05) according to Duncan's new multiple range test.

soil fumigation with AITC on the physicochemical indicators of the rhizosphere soil for various chili pepper cultivars varied; however, these variations were not deemed statistically significant.

3.3 Effect of soil fumigation with allyl isothiocyanate on the diversity index of the bacterial community of pepper

Significant variations in the bacterial community diversity index (ACE) were observed among different parts of the pepper plant, including inter-root, intra-root, intra-stem, and intra-leaf regions, regardless of the fumigation treatment (Figure 5A). These findings suggest that tissue variability remained consistent even after fumigation. However, 80 days post-fumigation, the ACE values for intra-root and intra-leaf bacterial diversity were significantly reduced by allyl isothiocyanate (AITC), while no significant impact was observed on inter-root and intra-stem bacterial diversity. This indicates that the stimulating effect of AITC on soil microbial community diversity diminished over time but continued to significantly influence microbial diversity within the roots and leaves of the crop.

Further analysis of the responses of bacterial communities in the root, stem, and leaf tissues of three pepper varieties revealed distinct spatial characteristics and significant differences in the effects of allyl isothiocyanate (AITC) fumigation on endophytic bacteria. Inter-root bacterial diversity showed no significant differences among Xiangla359 (XL), Shuang Jiao (SJ), and La Xuan (LX). However, AITC fumigation significantly increased the inter-root bacterial diversity index (ACE) in Xiangla359 (Figure 5B). Within the roots, both Xiangla359 and Shuang Jiao exhibited significantly higher bacterial diversity compared to La Xuan. Nevertheless, AITC fumigation resulted in a significant decrease in bacterial diversity within the roots of Xiangla359, with no significant differences observed among the three varieties after fumigation (Figure 5C). Conversely, La Xuan displayed significantly higher bacterial diversity in the stems compared to Xiangla359 and Shuang Jiao. However, AITC fumigation led to a significant reduction in bacterial diversity in the stems of La Xuan, with no significant differences among the three varieties after fumigation (Figure 5D). In terms of leaf tissues, Xiangla359 exhibited significantly higher bacterial diversity compared to Shuang Jiao and La Xuan. AITC fumigation significantly reduced bacterial diversity in the leaves of Xiangla359 but had no significant effect on Shuang Jiao and La Xuan (Figure 5E). Overall, the impact of AITC fumigation on endophytes in pepper roots and leaves was more pronounced than in stems, resulting in a significant reduction in microbial diversity in the roots and leaves of Xiangla359, while showing no significant effects on Shuang Jiao and La Xuan.

3.4 Effect of allyl isothiocyanate on the structure of the bacterial community of chili peppers

In the unfumigated treatment, both tissue site and genotype significantly influenced the structure of the endophytic bacterial community in pepper, accounting for 22% ($p < 0.01$) and 19%

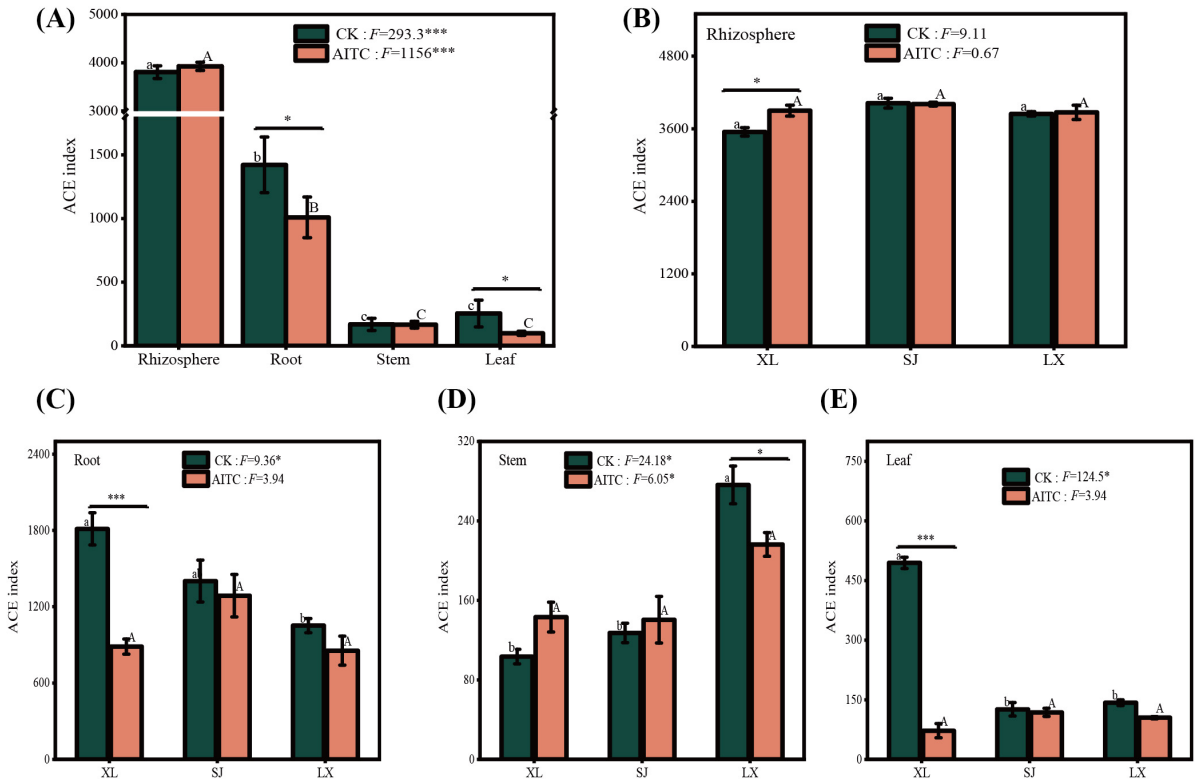

FIGURE 5
The impact of AITC fumigation on the microbial diversity index of chili plants: **(A)** overall effect on different tissues; **(B)** response of rhizosphere bacteria; **(C)** response of endophytic fungi in roots; **(D)** response of endophytic bacteria in stems; **(E)** response of endophytic bacteria in leaves. *$0.01 < p \leq 0.05$, ***$p \leq 0.001$.

($p < 0.01$) of the variation, respectively (Figure 6A). Conversely, allyl isothiocyanate (AITC) fumigation markedly enhanced the contribution of genotype to the endophytic bacterial community structure in pepper, increasing it to 58% ($p < 0.001$) while concurrently reducing the contribution of tissue site (Figure 6B).

Consequently, we conducted a detailed analysis of the bacterial community structure across various tissues (roots, stems, and leaves) of different pepper cultivars. Following to AITC fumigation, the impact of genotypes on inter-root and intra-stem bacterial community structures was found to be statistically insignificant. However, there was a notable increase in the explanatory power of the bacterial community structure in roots (23 vs. 33%, $p < 0.05$), accompanied by a corresponding decrease in leaves (44 vs. 33%, $p < 0.05$) (Figures 6C, D). It is evident that allyl isothiocyanate (AITC) fumigation primarily influences the bacterial community structure in roots and leaves of pepper and is closely associated with the genotype of the plant.

Linear discriminant analysis effect size (LEfSe) was employed to identify species with significant differences across various parts of pepper plants. The LEfSe species hierarchy chart (LDA > 3.8) was used to identify groups exhibiting significant variations. As shown in the distribution plots (Figures 7A–C) with LDA scores exceeding 3.8, significant differences were observed in the microbial communities enriched in different parts of the pepper plant under various treatments.

At the genus level, untreated Xiangla359 roots exhibited a marked predominance of *Streptomyces*, *Sphingomonas*, *Sphingobium*, *Methylophilus*, *Neorhizobium*, and *Flavobacterium*. In contrast, the stems showed a significant increase in Prevotella, *Lactobacillus*, and *Aeromonas*, while the leaves were predominantly dominated by *Rickettsia*. Following AITC treatment, the roots displayed a significant abundance of *Cellvibrio*, *Massilia*, *Caulobacter*, and *Allorhizobium-Neorhizobium-Pararhizobium-Rhizobium*. In the stems, *Pleomorphomonas*, *Corynebacterium*, and *Cloacibacterium* were notably abundant.

Untreated Shuang Jiao roots demonstrated substantial concentrations of *Streptomyces*, *Sphingobium*, *Neorhizobium*, *Massilia*, *Acidovorax*, and *Allorhizobium-Neorhizobium-Pararhizobium-Rhizobium*. The stems were notably enriched with *Actinoplanes*, *Prevotella*, *Paludibacter*, *Pleomorphomonas*, *Aeromonas*, *Cloacibacterium*, *Dysgonomonas*, and *Flavobacterium*, while *Bacillus* and *Leifsonia* were primarily concentrated in the leaves. After AITC treatment, the roots of Shuang Jiao displayed a notable rise in *Subgroup_10*, *Steroidobacter*, *Sphingomonas*, *Ohtaekwangia*, *Herpetosiphon*, *Cellvibrio*, *Acetobacter*, and *Devosia*. In the stems, *Corynebacterium*, *Lactobacillus*, and *Microbacterium* were significantly more abundant.

In untreated La Xuan roots, *Streptomyces*, *Sphingomonas*, *Sphingobium*, *Pseudomonas*, *Neorhizobium*, *Flavobacterium*, *Massilia*, and *Actinoplanes* were notably abundant. The stems exhibited significant accumulation of *Corynebacterium* and *Pleomorphomonas*. Following AITC treatment, the roots displayed a marked increase in *Cellvibrio*, *Acidovorax*,

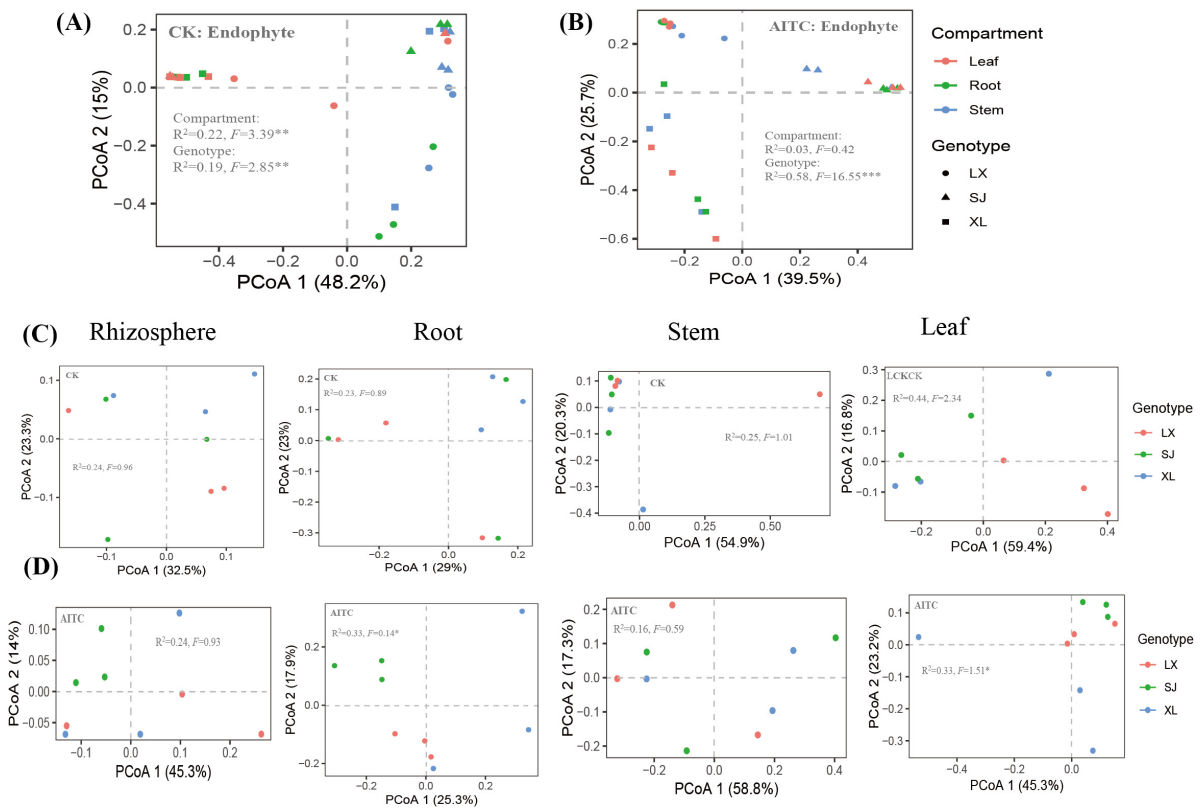

FIGURE 6
Based on the Bray Curtis algorithm PCoA (Principal Co-ordinates Analysis), **(A)** PCoA of endophytic bacteria in untreated samples; **(B)** PCoA of endophytic bacteria treated with AITC (Allyl isothiocyanate); **(C)** PCoA of rhizosphere, endophytic, stem, and leaf bacteria in untreated samples; **(D)** PCoA of rhizosphere, endophytic, stem, and leaf bacteria in treated samples. PERMANOVA method was used to calculate statistical differences.

Caulobacter, and *Allorhizobium-Neorhizobium-Pararhizobium-Rhizobium*. In the stems, *Dysgonomonas*, *Aeromonas*, *Cloacibacterium*, and *Bacteroidota* were significantly more prevalent, while Rickettsia was predominantly concentrated in the leaves.

In the rhizosphere of pepper plants, the predominant bacterial phyla included *Actinobacteriota*, *Proteobacteria*, *Acidobacteriota*, *Chloroflexi*, *Firmicutes*, *Gemmatimonadota*, *Bacteroidota*, and *Myxococcota* (Supplementary Figure 1A). Fumigation with allyl isothiocyanate (AITC) significantly increased the relative abundance of *Armatimonadota* and enhanced the presence of *Acidobacteriota* in the inter-root region of Shuang Jiao. At the genus level, the primary taxa identified included *Streptomyces*, *Allorhizobium-Neorhizobium-Pararhizobium-Rhizobium*, *Pseudomonas*, *Massilia*, *Flavobacterium*, *Actinoplanes*, *Methylophilus*, and *Sphingobium* (Supplementary Figure 1B). Moreover, fumigation led to a substantial rise in the relative abundance of *Pseudarthrobacter* (34.21%) and *RB41* (62.21%), while reducing the abundance of *Gaiella* (41.09%) in the inter-root soil of Shuang Jiao.

In the root systems of pepper plants, the predominant bacterial phyla identified were *Proteobacteria*, *Actinobacteriota*, *Firmicutes*, *Bacteroidota*, *Myxococcota*, *Bdellovibrionota*, *Chloroflexi*, *Acidobacteriota*, *Gemmatimonadota*, and *Verrucomicrobiota* (Supplementary Figure 2A). Fumigation with AITC significantly increased the relative abundance of *Myxococcota*, while simultaneously decreasing *Actinobacteriota* in the roots of Shuang Jiao. At the genus level, the major taxa present in pepper roots included *Streptomyces*, *Allorhizobium-Neorhizobium-Pararhizobium-Rhizobium*, *Pseudomonas*, *unclassified_f_Alcaligenaceae*, *Massilia*, *Flavobacterium*, *Actinoplanes*, *Methylophilus*, *Sphingobium*, and *unclassified_f_Oxalobacteraceae* (Supplementary Figure 2B). AITC fumigation notably enhanced the relative abundance of *Cloacibacterium* (356.38%) and led to significant increases in *Allorhizobium-Neorhizobium-Pararhizobium-Rhizobium* (221.94%), *Bacillus* (141.51%), *Pseudomonas* (191.47%), and *Corynebacterium* (209.91%) within the roots of Xiangla359. In contrast, fumigation reduced the abundance of *Cloacibacterium* (61.78%), *Streptomyces* (63.76%), *Pseudomonas* (88.80%), and *Massilia* (70.26%) in Shuang Jiao roots, while increasing that of *Corynebacterium* (148.74%) and *Bacillus* (13.88%). Similarly, in La Xuan roots, fumigation led to an increase in the relative abundance of *Cloacibacterium* (75.37%), *Allorhizobium-Neorhizobium-Pararhizobium-Rhizobium* (80.11%), and *Corynebacterium* (23.56%), while reducing *Streptomyces* (59.55%) and *Massilia* (40.36%) (Figure 8).

.

In pepper stems, the predominant bacterial phyla identified included *Proteobacteria*, *Firmicutes*, *Bacteroidota*, *Actinobacteriota*, *Deinococcota*, *Cyanobacteria*, *Gemmatimonadota*, *Myxococcota*, *Bdellovibrionota*, and *Verrucomicrobiota* (Supplementary

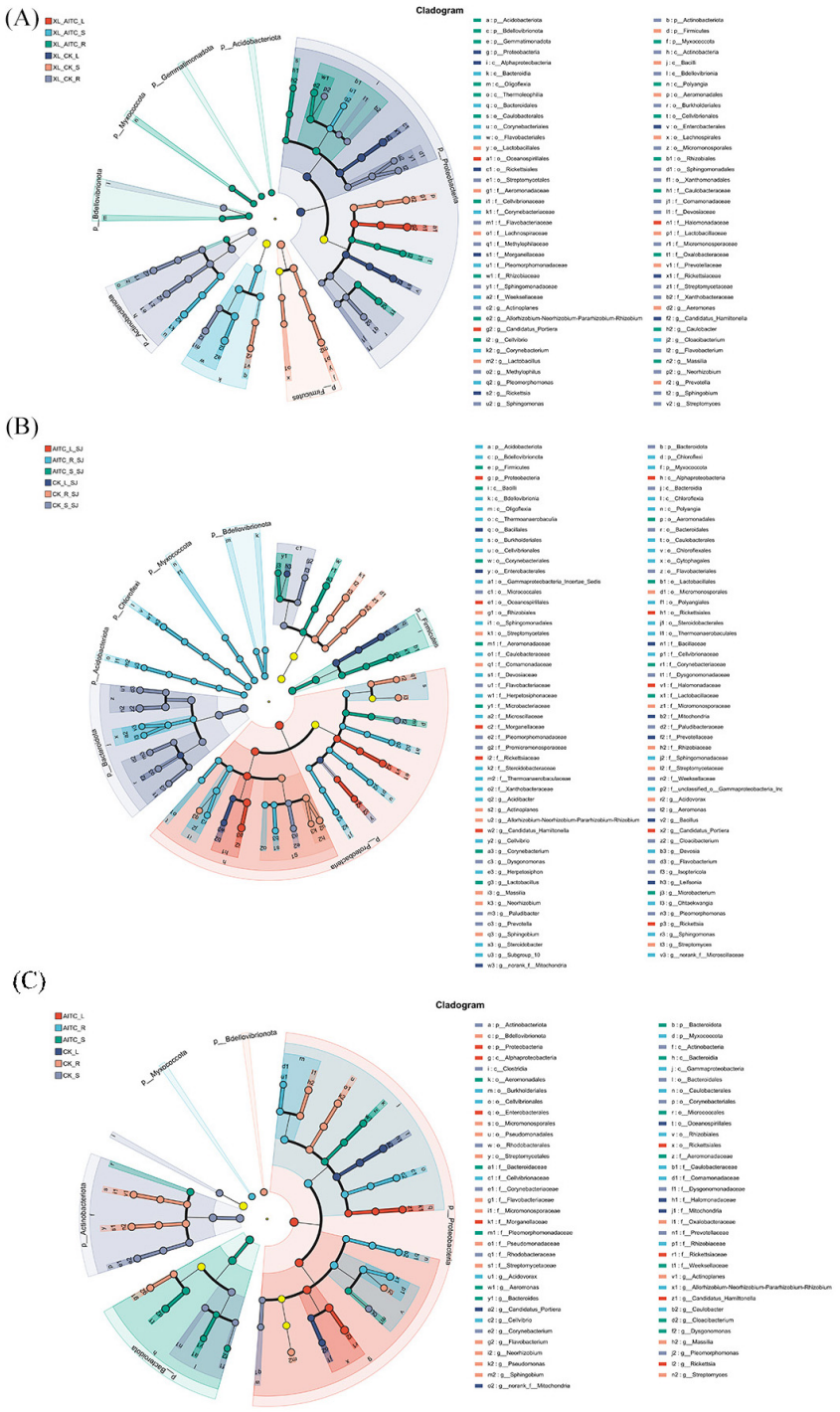

FIGURE 7
LEfSe cladogram analysis of endophytic microbial community (LDA = 3.8) in pepper after soil fumigation (P = 0.05). The five rings in the cladogram represent the phylum, class, order, family and genus, respectively, when read from the inside. The different color nodes (except yellow) on the ring represent significant changes in taxonomic composition due to the treatments. **(A)** Xiangla359; **(B)** Shuangjiao; **(C)** Laxuan.

Figure 3A). At the genus level, the dominant taxa were *Cloacibacterium*, *Corynebacterium*, *Bacillus*, *Aeromonas*, *Lactobacillus*, *Flavobacterium*, *Paludibacter*, *Prevotella*, and the *Allorhizobium-Neorhizobium-Pararhizobium-Rhizobium* group (Supplementary Figure 3B). Following fumigation, the *Allorhizobium-Neorhizobium-Pararhizobium-Rhizobium* group in Xiangla359 stems showed a significant increase in relative abundance (637.21%), accompanied by a 50.10% increase in *Corynebacterium*. In contrast, *Massilia* and *Pseudomonas* saw a decline in relative abundance by 63.85% and 24.61%, respectively. In the La Xuan stem microbiome, fumigation resulted in increased abundances of *Cloacibacterium* (153.46%), *Corynebacterium* (60.77%), *Bacillus* (94.50%), and *Allorhizobium-Neorhizobium-Pararhizobium-Rhizobium* (82.45%). Meanwhile,

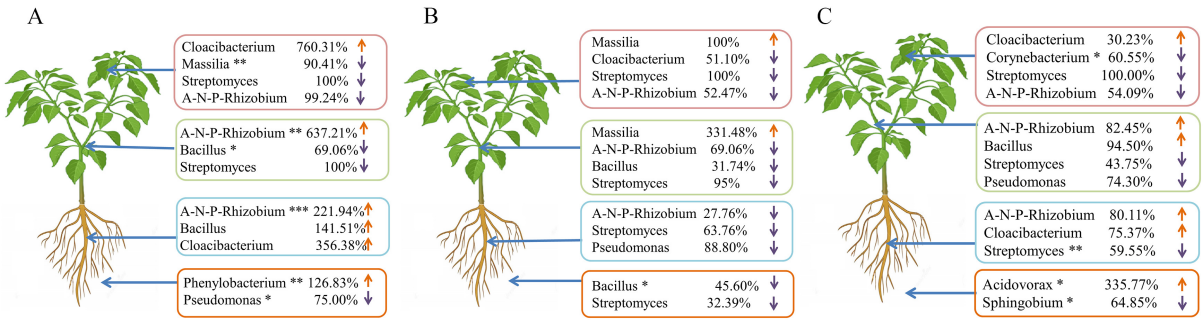

FIGURE 8
Changes in microorganisms in the roots, stems, leaves, and rhizosphere soil of different varieties of pepper plants. **(A)** Xiangla359; **(B)** Shuang Jiao; **(C)** La Xuan; A-N-P-Rhizobium: *Allorhizobium-Neorhizobium-Pararhizobium-Rhizobium* (*$p < 0.05$, ** < 0.01, *** < 0.001).

Massilia, *Pseudomonas*, and *Streptomyces* decreased by 94.50, 74.30, and 43.75%, respectively. In another cultivar, fumigation led to a 331.48% increase in *Massilia*, while relative abundances of *Cloacibacterium*, *Allorhizobium-Neorhizobium-Pararhizobium-Rhizobium*, and *Streptomyces* decreased by 38.02, 69.06, and 95%, respectively, within the stem microbiome (Figure 8).

In pepper leaves, the predominant bacterial phyla identified included *Proteobacteria*, *Firmicutes*, *Bacteroidota*, *Actinobacteriota*, *Deinococcota*, *Cyanobacteria*, *Gemmatimonadota*, *Myxococcota*, *Bdellovibrionota*, and *Verrucomicrobiota* (Supplementary Figure 4A). At the genus level, *Bacillus*, *Cloacibacterium*, *Corynebacterium*, *Prevotella*, and *Lactobacillus* were the most abundant genera (Supplementary Figure 4B). Fumigation with allyl isothiocyanate (AITC) induced notable shifts in these microbial communities, particularly increasing the relative abundance of *Cloacibacterium* (760.31%) in Xiangla359 leaves, while significantly decreasing *Massilia* (90.41%), *Pseudomonas* (48.43%), *Streptomyces* (100%), and *Allorhizobium-Neorhizobium-Pararhizobium-Rhizobium* (99.24%). In Shuang Jiao leaves, AITC treatment led to a 100% increase in *Massilia*, while *Corynebacterium* (52.47%), *Streptomyces* (100%), *Bacillus* (73.76%), and the *Allorhizobium-Neorhizobium-Pararhizobium-Rhizobium* group (52.47%) were reduced. Similarly, in La Xuan leaves, AITC exposure resulted in substantial increases in *Massilia* (1,209.09%) and *Pseudomonas* (144.73%), alongside reductions in *Corynebacterium* (60.55%), *Streptomyces* (100%), *Bacillus* (55.90%), and the *Allorhizobium-Neorhizobium-Pararhizobium-Rhizobium* group (54.09%) (Figure 8).

The traceability analysis results revealed that AITC fumigation significantly altered the distribution of the source and sink of the pepper microbiome across sub-compartments (soil, roots, stems, and leaves), particularly in Xiangla359 varieties. Compared to the non-fumigated group, the fumigation treatment promoted the accumulation of microorganisms in the roots, stems, and leaves of Xiangla359 peppers, while enhancing the enrichment of endophytic bacteria in the stems and roots of Laxuan pepper and Shuangjiao pepper respectively. This shift indicated that fumigation not only influenced the overall structure of the microbial community but also regulated the dynamic balance between source and sink by altering the migration and distribution of microorganisms. However, the extent of this regulation varied across genotypes (Figure 9).

4 Discussion

The microbial community structure in the rhizosphere of peppers shows considerable variability, with a notable degree of specificity in the interaction between plant genotypes and microbial composition (Weinert et al., 2011). Certain plant genotypes can selectively accumulate beneficial microorganisms, thereby enhancing plant defenses against pathogens (Berendsen et al., 2012). In this study, we observed significant differences in bacterial community diversity across different regions of the pepper plant, including inter-root, intra-root, intra-stem, and intra-leaf areas, independent of fumigation treatments. Furthermore, the variability in microbial composition within these tissues remained stable, irrespective of fumigation. Distinct plant genotypes appear to promote specific microbial enrichments, likely influenced by root-secreted compounds, inter-root environmental conditions, and additional biochemical factors (Cordovez et al., 2019). Moreover, AITC fumigation significantly altered soil metabolic processes, leading to changes in root distribution and inter-root exudation patterns.

The modification of soil microbial community structure by AITC fumigation influences microbial composition within the roots, stems, and leaves of peppers through various mechanisms: (1) Nutrient availability: AITC fumigation alters soil nutrient cycling, particularly by enhancing nitrogen and phosphorus mineralization, which significantly increases the availability of these nutrients for plant uptake (Fang et al., 2022; Huang et al., 2020; Li et al., 2023). Additionally, nutrient release from organic matter following fumigation—likely due to the suppression of specific microbial taxa—supports root nourishment. Compounds generated through these processes act as nutrient sources for soil microorganisms, selectively promoting the growth of particular microbial populations in the rhizosphere. This selective enrichment subsequently affects microbial community composition within the plant's stems and leaves. (2) Microbial interaction: Interactions among soil microorganisms are intricate, involving both competitive and symbiotic relationships. Beneficial

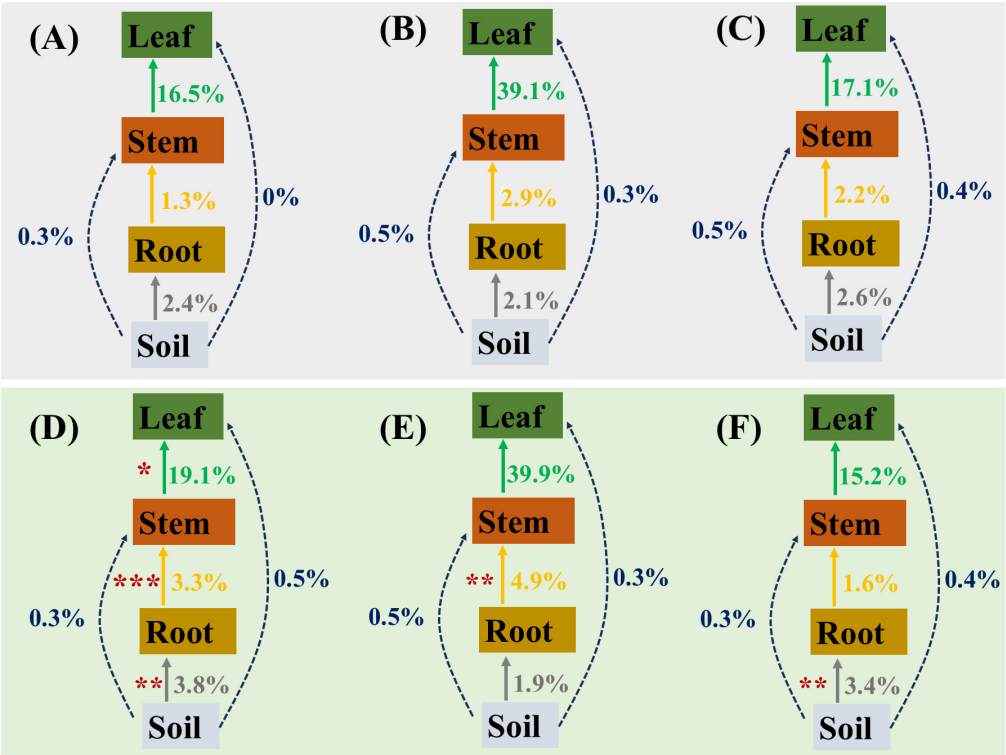

FIGURE 9
Traceability analysis of microorganisms in different genotypes of pepper across various sub-chambers (soil, root, stem, leaf) in the unfumigated **(A,B)** and AITC fumigated **(D–F)** groups. **(A,D)**: Xiangla359; **(B,E)**: Laxuan; **(C,F)**: Shuang Jiao. The values to the right of the arrows represent the percentage from source to sink, and the asterisk to the left of the arrows indicates a significant difference between the fumigated and control groups.

microorganisms are essential for enhancing plant resistance to pathogens, while harmful microorganisms can detrimentally impact plant health. The balance of these interactions strongly influences the microbial community composition within plant tissues. For example, allyl isothiocyanate (AITC) fumigation has been shown to increase soil microbial diversity and promote the growth of beneficial bacteria, such as Bacillus species. These beneficial microorganisms can colonize plant roots from the soil and subsequently move through the vascular system to the stems and leaves. This translocation process introduces novel microbial species and reshapes the existing microbial communities across different plant tissues. (3) Soil health: Prior to fumigation, soils generally exhibit low quality, often characterized by nutrient imbalances, degraded soil structure, and an unbalanced microbial community. Fumigation can significantly improve soil health by enhancing nutrient cycling and restructuring the microbial community (Cordovez et al., 2019). Healthy soils support high microbial diversity, which promotes vigorous plant growth. This robust plant growth stimulates the development of an extensive root system, thereby sustaining a diverse array of microorganisms within the roots and influencing microbial communities in the stems and leaves.

Fumigation with allyl isothiocyanate (AITC) induces significant shifts in soil microbial communities and functions, subsequently affecting the populations of beneficial bacteria in the roots, stems, and leaves of various pepper cultivars. AITC fumigation promotes the proliferation of diverse beneficial microorganisms, each with specialized biological functions. For example, *Allorhizobium-Neorhizobium-Pararhizobium-Rhizobium* species and nitrogen-fixing (Guo et al., 2024; Zhang W. et al., 2023), and *Streptomyces* strains play crucial roles in enhancing plant nutrient uptake (Olenska et al., 2020). Additionally, plant growth-promoting rhizobacteria (PGPR) such as *Pseudomonas* and the inter-root probiotic *Massilia* contribute to increased plant vigor and resilience (He et al., 2024). Cellulolytic activities are associated with *Cellvibrio* and *Sphingomonas*, while *Devosia* species are linked to inter-root exudates (Chen et al., 2019).

5 Conclusion

In this study, we investigated the effects of allyl isothiocyanate (AITC) soil fumigation on the endophytic bacterial communities associated with different pepper genotypes (Xiangla359, La Xuan, and Shuang Jiao). Our findings revealed that AITC fumigation predominantly influenced bacterial community structure in both roots and leaves, with a strong correlation to the genetic characteristics of the pepper cultivars. Notably, AITC fumigation led to a significant reduction in microbial diversity within the roots and leaves of Xiangla359, while having no substantial impact on La Xuan and Shuang Jiao.

Moreover, the growth-promoting effects of AITC fumigation varied among the three pepper varieties, with Xiangla359 exhibiting

the most pronounced enhancement. This variation appears to be attributable to differential fumigation effects on beneficial bacterial populations across the roots, stems, and leaves of each cultivar. For instance, the *Allorhizobium-Neorhizobium-Pararhizobium-Rhizobium* increased in the roots and stems of Xiangla359 and La Xuan but decreased in Shuang Jiao. Similarly, *Bacillus* populations increased in the roots of Xiangla359 but declined in La Xuan and Shuang Jiao, while *Streptomyces* consistently decreased in the roots across all pepper varieties.

These results indicate that AITC fumigation significantly alters the diversity and structural composition of soil microbial communities; however, its effects on endophytic communities in pepper plants are highly dependent on the plant genotype.

Data availability statement

The raw sequence data reported in this paper have been deposited in the Genome Sequence Archive (Genomics, Proteomics & Bioinformatics 2021) in National Genomics Data Center (Nucleic Acids Res 2022), China National Center for Bioinformation / Beijing Institute of Genomics, Chinese Academy of Sciences (GSA: CRA025577) that are publicly accessible at https://ngdc.cncb.ac.cn/gsa.

Author contributions

WT: Writing – original draft, Writing – review and editing. QW: Writing – original draft. AC: Writing – original draft. DY: Writing – original draft. YL: Writing – original draft. ZL: Writing – original draft. BY: Writing – original draft. WF: Writing – original draft.

Funding

The authors declare that financial support was received for the research and/or publication of this article. This work was supported by the National Key Research and Development Program of China (2021YFD1600300-4, 2023YFD1701200), Special Project of Biological Seed Industry and Fine and Deep Processing of Agricultural Products (202202AE090031), and Innovation Program of Chinese Academy of Agricultural Sciences (CAAS-CSAL-202401).

Conflict of interest

The authors declare that the research was conducted in the absence of any commercial or financial relationships that could be construed as a potential conflict of interest.

Generative AI statement

The authors declare that no Generative AI was used in the creation of this manuscript.

Publisher's note

All claims expressed in this article are solely those of the authors and do not necessarily represent those of their affiliated organizations, or those of the publisher, the editors and the reviewers. Any product that may be evaluated in this article, or claim that may be made by its manufacturer, is not guaranteed or endorsed by the publisher.

Supplementary material

The Supplementary Material for this article can be found online at: https://www.frontiersin.org/articles/10.3389/fmicb.2025.1520443/full#supplementary-material

References

Afzal, I., Shinwari, Z. K., Sikandar, S., and Shahzad, S. (2019). Plant beneficial endophytic bacteria: Mechanisms, diversity, host range and genetic determinants. *Microbiol. Res.* 221, 36–49. doi: 10.1016/j.micres.2019.02.001

Ashiq, S., Edwards, S. G., Fatukasi, O., Watson, A., and Back, M. A. (2022). In vitro activity of isothiocyanates against Fusarium graminearum. *Plant Pathol.* 71, 594–601. doi: 10.1111/ppa.13505

Barboza, G. E., Garcia, C. C., de Bem Bianchetti, L., Romero, M., and Scaldaferro, M. (2022). Monograph of wild and cultivated chili peppers (Capsicum L., Solanaceae). *PhytoKeys* 200, 1–423. doi: 10.3897/phytokeys.200.71667

Barea-Ramos, J. D., Rodriguez, M. J., Calvo, P., Melendez, F., Lozano, J., and Martin-Vertedor, D. (2024). Inhibition of Botrytis cinerea in tomatoes by allyl-isothiocyanate release from black mustard (Brassica nigra) seeds and detection by E-nose. *Food Chem.* 432:137222. doi: 10.1016/j.foodchem.2023.137222

Berendsen, R. L., Pieterse, C. M. J., and Bakker, P. A. H. M. (2012). The rhizosphere microbiome and plant health. *Trends Plant Sci.* 17, 478–486. doi: 10.1016/j.tplants.2012.04.001

Castellano-Hinojosa, A., Boyd, N. S., and Strauss, S. L. (2022). Impact of fumigants on non-target soil microorganisms: A review. *J. Hazard. Mater.* 427:128149. doi: 10.1016/j.jhazmat.2021.128149

Chen, J., Feng, W., Yan, H., Liu, P., Zhou, G., Guo, S., et al. (2022). Explore the interaction between root metabolism and rhizosphere microbiota during the growth of Angelica sinensis. *Front. Plant Sci.* 13:1005711. doi: 10.3389/fpls.2022.1005711

Chen, S., Waghmode, T. R., Sun, R., Kuramae, E. E., Hu, C., and Liu, B. (2019). Root-associated microbiomes of wheat under the combined effect of plant development and nitrogen fertilization. *Microbiome* 7:136. doi: 10.1186/s40168-019-0750-2

Compant, S., Samad, A., Faist, H., and Sessitsch, A. (2019). A review on the plant microbiome: Ecology, functions, and emerging trends in microbial application. *J. Adv. Res.* 19, 29–37. doi: 10.1016/j.jare.2019.03.004

Cordovez, V., Dini-Andreote, F., Carrion, V. J., and Raaijmakers, J. M. (2019). Ecology and evolution of plant microbiomes. *Annu. Rev. Microbiol.* 73:69. doi: 10.1146/annurev-micro-090817-062524

Dahlin, P., and Hallmann, J. (2020). New insights on the role of Allyl isothiocyanate in controlling the root knot nematode meloidogyne hapla. *Plants* 9:603. doi: 10.3390/plants9050603

Fang, W., Wang, Q., Li, Y., Hua, J., Jin, X., Yan, D., et al. (2022). Microbial regulation of nitrous oxide emissions from chloropicrin-fumigated soil amended with biochar. *J. Hazard. Mater.* 429:128060. doi: 10.1016/j.jhazmat.2021.128060

Guo, T., Yao, X., Wu, K., Guo, A., and Yao, Y. (2024). Response of the rhizosphere soil microbial diversity to different nitrogen and phosphorus application rates in a hulless barley and pea mixed-cropping system. *Appl. Soil Ecol.* 195:105262. doi: 10.1016/j.apsoil.2023.105262

Handiseni, M., Zhou, X., and Jo, Y. (2017). Soil amended with Brassica juncea plant tissue reduces sclerotia formation, viability and aggressiveness of Rhizoctonia solani AG1-IA towards rice. *Crop Prot.* 100, 77–80. doi: 10.1016/j.cropro.2017.06.009

Hartmann, M., and Six, J. (2023). Soil structure and microbiome functions in agroecosystems. *Nat. Rev. Earth Environ.* 4, 4–18. doi: 10.1038/s43017-022-00366-w

He, X., Wang, D., Jiang, Y., Li, M., Delgado-Baquerizo, M., Mclaughlin, C., et al. (2024). Heritable microbiome variation is correlated with source environment in locally adapted maize varieties. *Nat. Plants* 10, 598–617. doi: 10.1038/s41477-024-01654-7

Huang, B., Yan, D., Wang, Q., Fang, W., Song, Z., Cheng, H., et al. (2020). Effects of dazomet fumigation on soil phosphorus and the composition of phoD -harboring microbial communities. *J. Agric. Food. Chem.* 68, 5049–5058. doi: 10.1021/acs.jafc.9b08033

Huang, X., Zeng, Z., Chen, Z., Tong, X., Jiang, J., He, C., et al. (2022). Deciphering the potential of a plant growth promoting endophyte Rhizobium sp. WYJ-E13, and functional annotation of the genes involved in the metabolic pathway. *Front. Microbiol.* 13:1035167. doi: 10.3389/fmicb.2022.1035167

Li, Y., Lu, D., Xia, Y., Xu, X., Huang, H., Mei, X., et al. (2023). Effects of allyl isothiocyanate fumigation on medicinal plant root knot disease control, plant survival, and the soil bacterial community. *BMC Microbiol.* 23:278. doi: 10.1186/s12866-023-02992-w

Liu, T., Liao, Q. H., Yu, F. Q., Zi, S. H., Tian, S. H., and Fan, L. Y. (2022). Plant growth - promoting activities of bacterial endophytes isolated from the medicinal plant Pairs polyphylla var. Yunnanensis. *World J. Microbiol. Biotechnol.* 38:15. doi: 10.1007/s11274-021-03194-0

Magoc, T., and Salzberg, S. L. (2011). Flash: Fast length adjustment of short reads to improve genome assemblies. *Bioinformatics* 27, 2957–2963. doi: 10.1093/bioinformatics/btr507

Mao, L., Wang, Q., Yan, D., Ma, T., Liu, P., Shen, J., et al. (2014). Evaluation of chloropicrin as a soil fumigant against Ralstonia solanacarum in ginger (Zingiber officinale Rosc.) production in China. *PLoS One* 9:e91767. doi: 10.1371/journal.pone.0091767

Olenska, E., Malek, W., Wojcik, I., Swiecicka, I., Thijs, S., and Vangronsveld, J. (2020). Beneficial features of plant growth-promoting rhizobacteria for improving plant growth and health in challenging conditions: A methodical review. *Sci. Total Environ.* 743:140682. doi: 10.1016/j.scitotenv.2020.140682

Otoni, C. G., de Fatima Ferreira, Soares, N., Silva, W. A. D., Medeiros, E. A. A., and Junior, J. C. B. (2014). Use of Allyl isothiocyanate-containing sachets to reduce aspergillus flavus sporulation in peanuts. *Packag. Technol. Sci.* 27, 549–558. doi: 10.1002/pts.2063

Park, D., Park, S., Liu, K., and Ku, K. (2023). Optimal allyl isothiocyanate concentration on Botrytis cinerea during the postharvest storage of blackberries and mechanism of blackberry color changes at high concentration of allyl isothiocyanate. *Postharvest Biol. Technol.* 199:112292. doi: 10.1016/j.postharvbio.2023.112292

Phurailatpam, L., Gupta, A., Sahu, P. K., and Mishra, S. (2022). Insights into the functional potential of bacterial endophytes from the ethnomedicinal plant, Piper longum L. *Symbiosis* 87, 165–174. doi: 10.1007/s13199-022-00864-x

Ren, F., Dong, W., and Yan, D. (2019). Organs, cultivars, soil, and fruit properties affect structure of endophytic mycobiota of pinggu peach trees. *Microorganisms* 7:322. doi: 10.3390/microorganisms7090322

Ren, Z., Li, Y., Fang, W., Yan, D., Huang, B., Zhu, J., et al. (2018). Evaluation of allyl isothiocyanate as a soil fumigant against soil-borne diseases in commercial tomato (Lycopersicon esculentum Mill.) Production in China. *Pest Manag. Sci.* doi: 10.1002/ps.4911 Online ahead of print.

Scherling, C., Ulrich, K., Ewald, D., and Weckwerth, W. (2009). A metabolic signature of the beneficial interaction of the endophyte paenibacillus sp. Isolate and in vitro-grown poplar plants revealed by metabolomics. *Mol. Plant. Microbe. Interact.* 22, 1032–1037. doi: 10.1094/MPMI-22-8-1032

Sessitsch, A., Hardoim, P., Doring, J., Weilharter, A., Krause, A., Woyke, T., et al. (2012). Functional characteristics of an endophyte community colonizing rice roots as revealed by metagenomic analysis. *Mol. Plant. Microbe. Interact.* 25, 28–36. doi: 10.1094/MPMI-08-11-0204

Shah, S., Shah, B., Sharma, R., Rekadwad, B., Shouche, Y. S., Sharma, J., et al. (2022). Colonization with non-mycorrhizal culturable endophytic fungi enhances orchid growth and indole acetic acid production. *BMC Microbiol.* 22:101. doi: 10.1186/s12866-022-02507-z

Tagele, S. B., Kim, R., and Shin, J. (2021). Interactions between brassica biofumigants and soil microbiota: Causes and impacts. *J. Agric. Food. Chem.* 69, 11538–11553. doi: 10.1021/acs.jafc.1c03776

Ugolini, L., Martini, C., Lazzeri, L., D'Avino, L., and Mari, M. (2014). Control of postharvest grey mould (Botrytis cinerea Per.: Fr.) On strawberries by glucosinolate-derived allyl-isothiocyanate treatments. *Postharvest Biol. Technol.* 90, 34–39. doi: 10.1016/j.postharvbio.2013.12.002

Wang, X., Wang, Q., Zhang, D., Liu, J., Fang, W., Li, Y., et al. (2024). Fumigation alters the manganese-oxidizing microbial communities to enhance soil manganese availability and increase tomato yield. *Sci. Total Environ.* 919:170882. doi: 10.1016/j.scitotenv.2024.170882

Weinert, N., Piceno, Y., Ding, G., Meincke, R., Heuer, H., Berg, G., et al. (2011). PhyloChip hybridization uncovered an enormous bacterial diversity in the rhizosphere of different potato cultivars: Many common and few cultivar-dependent taxa. *FEMS Microbiol. Ecol.* 75, 497–506. doi: 10.1111/j.1574-6941.2010.01025.x

Wu, H., Cui, H., Fu, C., Li, R., Qi, F., Liu, Z., et al. (2024). Unveiling the crucial role of soil microorganisms in carbon cycling: A review. *Sci. Total Environ.* 909:168627. doi: 10.1016/j.scitotenv.2023.168627

Wu, H., Zhang, G. A., Zeng, S., and Lin, K. C. (2009). Extraction of allyl isothiocyanate from horseradish (Armoracia rusticana) and its fumigant insecticidal activity on four stored-product pests of paddy. *Pest Manag. Sci.* 65, 1003–1008. doi: 10.1002/ps.1786

Yang, B., Wang, X., Ma, H., Jia, Y., Li, X., and Dai, C. (2014). Effects of the fungal endophyte Phomopsis liquidambari on nitrogen uptake and metabolism in rice. *Plant Growth Regul.* 73, 165–179. doi: 10.1007/s10725-013-9878-4

Yang, K., Fu, R., Feng, H., Jiang, G., Finkel, O., Sun, T., et al. (2023). RIN enhances plant disease resistance via root exudate-mediated assembly of disease- suppressive rhizosphere microbiota. *Mol. Plant.* 16, 1379–1395. doi: 10.1016/j.molp.2023.08.004

Yu, H., Jia, W., Zhao, M., Le, Li, Liu, J., et al. (2022). Antifungal mechanism of isothiocyanates against Cochliobolus heterostrophus. *Pest Manag. Sci.* 78, 5133–5141. doi: 10.1002/ps.7131

Yu, J., Vallad, G. E., and Boyd, N. S. (2019). Evaluation of allyl isothiocyanate as a soil fumigant for tomato (Lycopersicon esculentum Mill.) production. *Plant Dis.* 103, 2764–2770. doi: 10.1094/PDIS-11-18-2013-RE

Zhang, W., Mao, G., Zhuang, J., and Yang, H. (2023). The co-inoculation of Pseudomonas chlororaphis H1 and Bacillus altitudinis Y1 promoted soybean [Glycine max (L.) Merrill] growth and increased the relative abundance of beneficial microorganisms in rhizosphere and root. *Front. Microbiol.* 13:1079348. doi: 10.3389/fmicb.2022.1079348

Zhang, Y., Fang, W., Yan, D., Ji, Y., Chen, X., Guo, A., et al. (2023). Comparison of drip-irrigated or injected allyl isothiocyanate against key soil-borne pathogens and weeds. *Pest Manag. Sci.* 79, 3860–3870. doi: 10.1002/ps.7590

Zhou, N., Mu, M., Xie, H., Wu, Y., Zhou, Y., and Li, W. (2021). Rhizospheric fungal diversities and soil biochemical factors of fritillaria taipaiensis over five cultivation years. *Horticulturae* 7:560. doi: 10.3390/horticulturae7120560

Zou, Y., Zhang, Y., Zheng, E., Zhou, H., Qu, H., and Yang, H. (2024). Integration of transcriptomics and metabolomics to reveal the mechanism of allyl isothiocyanate delaying postharvest quality deterioration of Coprinus comatus. *Postharvest Biol. Technol.* 216:113075. doi: 10.1016/j.postharvbio.2024.113075

frontiers | Frontiers in Microbiology

TYPE Original Research
PUBLISHED 18 June 2025
DOI 10.3389/fmicb.2025.1496701

OPEN ACCESS

EDITED BY
Jesus Fernandez Bayo,
University of Granada, Spain

REVIEWED BY
Xu Liu,
Nanjing Agricultural University, China
Ren Bai,
Chinese Academy of Sciences (CAS), China
Hao Tan,
Sichuan Academy of Agricultural Sciences, China

*CORRESPONDENCE
Qingyun Zhao
✉ qingyun_022@catas.cn
Yizhang Xing
✉ xyz615@catas.cn

RECEIVED 15 September 2024
ACCEPTED 16 April 2025
PUBLISHED 18 June 2025

CITATION
Hong S, Xing Y, Yang J, Zhao Q, Su F, Zhuang H, Wang H, Wu Z and Chen Y (2025) Pandan–vanilla rotation mitigates *Fusarium* wilt disease in vanilla: insights from rhizosphere microbial community shifts. *Front. Microbiol.* 16:1496701. doi: 10.3389/fmicb.2025.1496701

Pandan–vanilla rotation mitigates *Fusarium* wilt disease in vanilla: insights from rhizosphere microbial community shifts

Shan Hong[1,2,3,4], Yizhang Xing[5]*, Jinming Yang[6], Qingyun Zhao[5]*, Fan Su[5], Huifa Zhuang[5], Hui Wang[5], Zhuangsheng Wu[1] and Yisong Chen[1,4]

[1]Sanya Institute, Hainan Academy of Agricultural Sciences/Hainan Key Laboratory of Vegetable Biology, The Institute of Vegetables, Hainan Academy of Agricultural Sciences, Sanya, Hainan Province, China, [2]State Key Laboratory of Plant Genomics, Institute of Genetics and Developmental Biology, Chinese Academy of Sciences, Beijing, China, [3]Hainan Seed Industry Laboratory, Sanya, Hainan Province, China, [4]National Nanfan Research Institute (Sanya), Chinese Academy of Agricultural Sciences, Sanya, Hainan Province, China, [5]Spice and Beverage of Institute, Chinese Academy of Tropical Agricultural Sciences/Key Laboratory of Genetic Resources Utilization of Spice and Beverage Crops, Ministry of Agriculture and Rural Affairs/Hainan Provincial Key Laboratory of Genetic Improvement and Quality Regulation for Tropical Spice and Beverage Crops, Wanning, Hainan Province, China, [6]The Sanya Institute of Nanjing Agricultural University, Nanjing Agricultural University, Sanya, Hainan Province, China

Introduction: Vanilla monoculture often leads to *Fusarium* wilt disease, affecting the industry globally.

Methods: Here, we evaluated the effects of vanilla–black pepper, –pandan, and –sweet rice tea rotations (i.e., growing vanilla in soil previously planted with these crops) on *Fusarium oxysporum* abundance and rhizosphere microbial communities using real-time quantitative PCR and high-throughput sequencing.

Results: Pandan rotation, in particular, reduced disease incidence to 17% and decreased *F. oxysporum* copy numbers; sweet rice tea showed similar suppressive effects. Crop rotation significantly increased fungal diversity and richness. Different cropping systems, including fallow, monoculture and crop rotation, significantly influenced fungal and bacterial community development, with cropping system and rotated crops being the main drivers of rhizosphere community assembly. The black pepper and pandan rotations specifically enriched certain fungal OTUs, such as OTU1_*Thermomyces*, OTU37_*Arthrobotrys*, and OTU18_*Arthrobotrys*, which serve as biomarkers for the presence of *F. oxysporum*. After pandan rotation, microbial interactions within the rhizosphere intensified, with notable enrichment of core bacterial taxa, including OTU22_*Nitrosospira*, OTU56_*Lacibacterium*, and OTU178_*Actinospica*. Soil pH was identified as a significant factor influencing microbial community assembly. The fungal community structure, along with core OTU22_*Nitrosospira* and soil pH, was pivotal in curbing pathogen growth, explaining 25.19%, 8.61%, and 20.45% of the variance, respectively.

Conclusion: This study revealed that incorporating pandan into crop rotation may effectively alleviate soil-borne diseases during vanilla production.

KEYWORDS

crop rotation, vanilla, pandan, microbial community, rhizosphere microbiome

Introduction

Vanilla (*Vanilla planifolia*), a member of the Orchidaceae family and the *Vanilla* genus, is an herbaceous perennial vine in tropical and subtropical regions (Minoo et al., 2008; Koyyappurath et al., 2016). It is highly acclaimed for its distinctive aroma and flavor. However, it is prone to *Fusarium* wilt disease caused by the soil-borne pathogen *Fusarium oxysporum* f. sp. *vanillae*, which results in severe replanting issues, reduced yield, and inferior quality (Pinaria et al., 2010; Mosquera-Espinosa et al., 2022). Our previous study elucidated how different durations of monoculture affect the soil microbial community structure and composition in vanilla cultivation systems. We discovered that long-term monoculture intensifies the incidence of *Fusarium* wilt disease (DI) in vanilla due to alterations in the soil microbial community, particularly due to decreases in beneficial microbes and the growth of *F. oxysporum* pathogens (Xiong et al., 2015).

Rhizosphere microbial communities are essential for enhancing the disease resistance and stress tolerance of crops (Trivedi et al., 2020). The diversity of these communities is intricately connected to the overall health of crops (Pedrinho et al., 2024). Research has shown that high diversity in functional soil microbes can improve crop resistance to diseases and stress tolerance by facilitating nutrient uptake and the synthesis of antimicrobial substances (Romero et al., 2023). Rhizosphere microbes, particularly fungi, are crucial for forming and maintaining soil structure, suppressing pathogens, and enhancing crop disease resistance (Yarzábal Rodríguez et al., 2024). Beneficial fungi compete with pathogens for nutrients and living space in the soil (Wang and Kuzyakov, 2024). By rapidly occupying specific ecological niches in the rhizosphere and forming stable microbial community structures, they limit the invasion and growth of pathogens (Li et al., 2022). Upon interacting with plant roots, some fungi can activate plant systemic resistance mechanisms (Rabari et al., 2023). Additionally, there is a complex synergistic relationship between fungi and bacteria in the inhibition of pathogens. Bacteria can promote the growth of fungi, while the metabolic products produced by fungi can enhance the antibacterial capabilities of bacteria (Napitupulu, 2025). Similar to those in the rhizosphere, mycosphere microbial communities are also effective in alleviating fungal pathogens of mushrooms (Yu et al., 2025), demonstrating the shared principles of microbiome biocontrol capabilities. Furthermore, agricultural management strategies such as crop rotation significantly influence the composition and functionality of soil microbial communities, thereby positively affecting crop health and productivity (Yang et al., 2020; Longepierre et al., 2021).

Crop rotation is an effective strategy for managing soil health through the modulation of the abundance and diversity of the soil microbial community, ensuring the health of both the soil and crops (Iheshiulo et al., 2023). This approach is environmentally friendly and economically viable for controlling soil-borne diseases (Zhou et al., 2023). We developed crop rotation systems, including black pepper (*Piper nigrum* L.) rotation with vanilla and coffee (*Coffea* L.) rotation with vanilla, and reported that black pepper–vanilla rotation significantly stimulated beneficial fungal genera such as *Trichoderma* and *Penicillium* (Xiong et al., 2016). However, as black pepper is a perennial crop, creating additional crop rotation systems is essential for addressing vanilla replanting problems and achieving high economic returns on limited arable land, which is crucial for the sustainable development of the vanilla industry (Yang et al., 2024).

Core rhizosphere microbes, as key indicator species, regulate microbial community structures through plant–microbe interactions or through interactions among microbes (Toju et al., 2018; Hong et al., 2023). Our preliminary research indicated that in long-term vanilla monoculture systems, changes in fungal communities are closely related to the suppression of *Fusarium* wilt disease, with the core disease-suppressing microbe *Mortierella* being predominant. It accounted for 37% of the total fungal sequences and may serve as an indicator of *Fusarium* wilt disease suppression in vanilla (Xiong et al., 2017). Moreover, soil physicochemical properties, particularly pH changes, significantly impact microbial community structure and core rhizosphere microbe abundance (Hong et al., 2020). Soil pH significantly regulates microbial community structure and pathogen suppression efficacy through both direct and indirect pathways. In terms of direct effects, pH modulates the catalytic activity and substrate-binding capacity of microbial extracellular enzymes (e.g., urease and phosphatase) and intracellular enzymes by altering their ionization states. Regarding indirect mechanisms, neutral to slightly alkaline environments (pH 6.5–7.5) enhance the quorum sensing efficiency of antagonistic microbial communities (e.g., *Pseudomonas* spp.), which restricts pathogens' iron acquisition or suppresses the expression of virulence genes by modulating the synthesis of siderophores and antibiotics. Concurrently, pH-driven shifts in nutrient availability further shape microbial competitive interactions. Hence, integrating soil physicochemical property analysis with microbial community analysis is essential for understanding how crop rotation effectively suppresses soil-borne *Fusarium* wilt disease in vanilla (Hermans et al., 2020; Philippot et al., 2024).

Previous research on the role of crop rotation in enhancing disease resistance in vanilla has been focused mainly on perennial crops, with an emphasis on disease suppression mechanisms mediated by soil fungal communities. However, there is a significant gap in the analysis of soil bacterial communities and in the comprehensive examination of the interplay between soil microbes and physicochemical properties. To fill this gap and meet evolving industrial needs, in this study, we identified two characteristic tropical spice crops—pandan (*Pandanus amaryllifolius*) and sweet rice tea (*Strobilanthes tonkinensis Lindau*)—for the first time for crop rotation with vanilla. Both are herbaceous plants with 6-month production cycles. They require minimal field management, thus keeping labor costs low, yet yield an output valued at $7,500 to $9,600 per hectare, making them popular among local farmers. Accordingly, soil that had been under rotation with pepper, pandan, and sweet rice tea for 1 year was collected and replanted with vanilla. Using qPCR combined with high-throughput sequencing, we focused on assessing the disease-suppressive effects of the rotations on vanilla and impact on the rhizosphere soil microbial community postrotation under greenhouse conditions. In this research, we aim to provide theoretical insights for developing effective crop

rotation strategies to suppress soil-borne *Fusarium* wilt disease in vanilla cultivation.

Materials and methods

Experiment description

The pot experiment was conducted from May 2023 to April 2024 in the greenhouse of the Spice and Beverage Research Institute at the Chinese Academy of Tropical Agricultural Sciences. Greenhouse conditions were maintained at 22–25°C during the daytime, 20–25°C at nighttime, with 72% relative humidity and 75% light transmittance. The soil used in the pot experiments was naturally infested soil collected from a vanilla plantation at the Spice and Beverage Research Institute, located in Longxing Town, Wanning City, Hainan Province, China (110°19′E−110°22′E, 18°12′N−18°16′N). This site has been continuously cultivated with vanilla for over 10 years, with an annual *Fusarium* wilt disease incidence of 65%. The soil texture was classified as sandy loam, with the following physicochemical properties: pH 5.58, organic matter (OM) 25.82 g-kg^{-1}, alkali-hydrolyzable nitrogen (AN) 100.32 mg-kg^{-1}, available phosphorus (AP) 20.46 mg-kg^{-1}, and available potassium (AK) 150.46 mg-kg^{-1}.

Prior to the experiment, all soil was transported to the greenhouse and sieved through a 2-mm mesh. The soils were under rotation with black pepper, pandan, and sweet rice tea. After 1 year of crop rotation, the soils were collected and vanilla was planted. The soils cropped with black pepper, pandan, and sweet rice tea were designated as black pepper–vanilla rotation (H), pandan–vanilla rotation (B), and sweet rice tea–vanilla rotation (C), respectively. Soils with vanilla monoculture were labeled as X, while fallow soils served as controls (CK). Notably, this study specifically focused on evaluating the disease suppression capacity of vanilla replanted after crop rotation. Therefore, the post-rotation soils were excluded from subsequent analysis.

The vanilla variety tested was Mexican vanilla (*Vanilla planifolia Andrews*). Vanilla is propagated asexually, so we planted 60 cm long mature stems from high-quality parent plants. The experiment was based on a randomized block design. Each treatment was replicated three times to ensure the reliability of the results. Each replicate consisted of six pots, with three plants per pot. Each pot was filled with 15 kg of soil, and the pot dimensions were 32 cm × 25 cm, ensuring sufficient space between each plant and independence to avoid potential cross-contamination. Each pot received 90 g of organic fertilizer, which was carefully mixed with the soil using a small shovel to ensure even distribution. The organic fertilizer had a pH of 7.51 and contained 1.33% nitrogen (N), 2.54% P_2O_5, and 1.23% K_2O. The chemical fertilizer application was based on traditional agricultural practices. Soil samples were collected from the rhizosphere compartment after 12 months of cultivation. Notably, this experiment was focused on evaluating the disease suppression effects of vanilla replanted after crop rotation. Therefore, the soils after crop rotation were not subjected to further research. The disease incidence (DI) of vanilla due to *Fusarium* wilt was statistically assessed on the basis of typical symptoms and was calculated as the percentage of affected plants out of the total surveyed (Xiong et al., 2016).

Soil sampling and DNA extraction

Seven pots were randomly selected from each treatment, and the three vanilla plants in each pot were combined to form one sample. Each treatment resulted in seven composites soil samples. The vanilla plants were carefully removed from the soil, immediately preserved in an ice box at 4°C, and transported promptly to the laboratory. The soil closely associated with the root system was dislodged by gently shaking the plant roots, and this soil was designated rhizosphere soil (Chen et al., 2020). In total, 35 rhizosphere soil samples were obtained. Each sample was accurately weighed to 0.4 grams for DNA extraction using the PowerSoil DNA Isolation Kit from QIAGEN/MoBio (MoBio Laboratories, Carlsbad, CA, USA). The extraction was performed according to the manufacturer's protocol, ensuring meticulous and error-free execution of the procedure. The extracted DNA samples were subsequently stored at −70°C for future analysis.

Soil physicochemical analysis

In accordance with our previous report (Hong et al., 2020), soil pH was measured in a soil–water suspension (1:2.5 w/v) via a glass electrode attached to a pH meter after shaking for 30 min. The organic matter (OM) content was determined using the potassium dichromate titration method, where potassium dichromate oxidizes organic carbon, and the organic matter content is calculated by titrating the dichromate remaining. Available nitrogen (AN) was measured using the alkaline diffusion method, where sodium hydroxide is used to treat the soil, and the resulting ammonia is absorbed by boric acid, followed by titration with standard acid. Available phosphorus (AP) was extracted with sodium bicarbonate and determined by the molybdenum blue method. Available potassium (AK) was extracted with ammonium acetate and measured using flame photometry.

Quantification of *F. oxysporum*

The overall abundance of *F. oxysporum* in the rhizosphere soil of vanilla was ascertained via real-time quantitative PCR (qPCR), employing the pathogen-specific primer sets AFP308R (CGAATTAACGCGAGTCCCAAC) and ITS1F (CTTGGTCATTTAGAGGAAGTAA) as previously described (Xiong et al., 2017). A standard curve was constructed via a serial dilution method using a plasmid harboring the internal transcribed spacer (ITS) region of *F. oxysporum*. Quantitative PCR was performed on the Applied Biosystems QuantStudio 7 Flex, following a standardized protocol for template amplification. The PCR mixture had a final volume of 20 μl, containing 10 μl of SYBR® Premix Ex Taq™ (2×), 0.4 μl of each primer (final concentration of 10 μM), 0.4 μl of ROX Reference Dye II (50×), 1 μl of DNA template (∼20 ng/μl), and nuclease-free water to the full volume. The performance of PCR amplification was assessed by examining the dissociation curve and determining the amplification efficiency. Triplicate analyses were conducted for each sample, and the data were log-transformed to express

the results as log-transformed copy numbers per gram of dry soil.

Sequencing of amplicons

The V4 region of the 16S rRNA gene from soil bacteria was amplified using the primers 520F (AYTGGGYDTAAAGNG) and 802R (TACNVGGGTATCTAATCC; Caporaso et al., 2011). For soil fungi, the ITS1 region was amplified with the primers ITS5F (GGAAGTAAAAGTCGTAACAAGG) and ITS1R (GCTGCGTTCTTCATCGATGC; Schoch et al., 2012). Unique barcodes/linkers and adapters were incorporated during the amplification process to prepare samples for sequencing. The PCR mixture, totaling 25 μl, included 5× reaction buffer (5 μl), 5× GC buffer (5 μl), 10 μM primers (1 μl), template DNA (2 μl), 100 mM dNTPs (5 μl), and nuclease-free water to the full volume. The PCR amplification parameters consisted of initial denaturation at 98°C for 2 min, followed by 28 to 30 cycles of denaturation at 98°C for 15 s, annealing at 55°C for 30 s for bacteria and at 50°C for 30 s for fungi, with extension at 72°C for 30 s.

Following PCR amplification, the resulting products were purified using the QIAquick PCR Purification Kit (QIAGEN, Germany). The concentration of the purified DNA samples was measured using a Qubit® 2.0 fluorometer (Invitrogen, USA). The sequencing libraries were prepared from equimolar pooled samples using the NEBNext® Ultra™ DNA Library Prep Kit for Illumina (New England Biolabs, UK), after which they were read for sequencing. The quality of the constructed libraries was assessed and verified via an Agilent 2,100 Bioanalyzer (Agilent Technologies, USA) and a KAPA Library Quantification Kit (KAPA Biosystems, USA). After library construction, the library was loaded onto the flow cell of the Illumina MiSeq sequencer. The flow cell surface underwent bridge PCR amplification to form numerous DNA clusters. During sequencing, the sequencer sequentially added nucleotides labeled with fluorescent markers to the DNA chains. Each incorporated nucleotide emitted a specific fluorescent signal, and the DNA sequence was determined by detecting the order of these signals. The entire process from library construction to sequencing was executed and completed by Shanghai Personal Biotechnology Co., Ltd.

Bioinformatics analysis

The raw sequencing data were subjected to initial quality filtering with Trimmomatic (version 0.33) to exclude low-quality sequences. The primer sequences were removed via Cutadapt (version 1.9.1) (Martin, 2011). USEARCH (version 10) was used to merge paired-end sequences (Edgar, 2013), and UCHIME (version 8.1) was used to remove chimeras (Edgar et al., 2011), ensuring high-quality sequences for further analysis. Denoising of quality-controlled data was performed using the DADA2 algorithm (Callahan et al., 2016) in QIIME2 (2020.6 version) (Bolyen et al., 2019), with a 0.005% threshold to filter anomalous sequences. Operational taxonomic units (OTUs) were clustered at a 97% sequence similarity threshold and taxonomically classified using the RDP classifier against the RDP Bacterial 16S rRNA (Wang et al., 2007) and UNITE Fungal ITS (Kõljalg et al., 2013) databases.

After quality control, 12,250 bacterial and 3,756 fungal OTUs were identified. The Chao 1 and Shannon indices were used to assess species richness and community diversity, respectively. Beta diversity was analyzed using principal coordinate analysis (PCoA), multiple regression tree (MRT; De'Ath, 2002), and heatmap clustering on the basis of the Bray–Curtis distance. Permutational multivariate analysis of variance (PERMANOVA) and analysis of similarity (ANOSIM) were used to test for differences in community structure. Hellinger standardization was performed on the rarefied OTU table before beta diversity was analyzed. The relative abundance of each OTU per sample was calculated as the number of sequences affiliated with the target OTU divided by the total number of sequences. Structural equation models (SEMs), constructed with the GGally, lavaan, and semPlot packages, were used to evaluate the influence of bacterial and fungal communities on pathogens (Mamet et al., 2019). In the structural equation model, soil microbial community structure (PCoA1 scores) and diversity (Shannon index) were included as measured variables, with the abundance of *F. oxysporum* as the response variable.

Identification of the core microbiome

We first applied linear discriminant analysis effect size (LEfSe) with a threshold of scores ≥3 to identify differential microbial biomarkers across various spice crops (Hong et al., 2020). Subsequently, the predictive importance of these biomarkers in suppressing *F. oxysporum* was evaluated using a random forest model implemented through the R package randomForest (Wen et al., 2023b). We subsequently identified hub OTUs among the rotated crops. The psych package in R was used for graphical representation, and data points with correlation coefficients above 0.8 and $P < 0.05$ were selected to construct a bacterial–fungal co-occurrence network (Revelle and Revelle, 2015). The topological properties of this network were assessed using GEPHI software for visualization (Bastian et al., 2009). A high average degree of nodes indicated increased network complexity, implying a more intricate interplay among microbial species. Hub OTUs was identified on the basis of a customized threshold reflecting node characteristics: a degree > 7 and closeness centrality > 0.6, which accounted for <15% of all nodes in the network (Costello et al., 2012; Agler et al., 2016; Banerjee et al., 2018). Ultimately, the core microbiome was identified via the intersection of biomarker microbes identified through LEfSe and random forest analysis with hub microbes identified through network analysis (Hong et al., 2023).

Statistical analysis

A comparison of pathogen abundance, microbial diversity, taxonomic composition, and soil physicochemical factors was conducted using Duncan's multiple range test in the agricolae package of R. We employed the vegan package in R to conduct both linear and nonlinear regression analyses, thereby investigating the relationship between pathogen abundance and microbial diversity.

The rdacca.hp R package was employed to evaluate the relative importance of soil physicochemical factors as explanatory variables influencing bacterial and fungal microbial communities (Lai et al., 2022). Furthermore, we applied a general linear model (GLM) using the relaimpo package in R to evaluate the contributions of bacterial and fungal communities, core microbes, and physicochemical factors to pathogen suppression (Shen et al., 2019).

Sequence accession numbers

The sequences have been submitted to the Sequence Read Archive (SRA) of the National Center for Biotechnology Information under the accession number PRJNA1126394.

Results

Disease incidence, pathogen abundance, and rhizosphere microbial structure

After a decade of continuous vanilla cultivation, a rotation with black pepper, pandan, and sweet rice tea was performed before replanting with vanilla. We found that the DI of vanilla was 55% with continuous cultivation, but it significantly decreased to 27% after rotation with black pepper, 22% with sweet rice tea, and 17% with pandan (Figure 1A). *F. oxysporum* abundance was significantly lower in the pandan–vanilla and sweet rice tea–vanilla rotation systems ($P < 0.05$), with no significant difference between the two treatments (Figure 1B).

Compared with the vanilla monoculture, crop rotation with black pepper, sweet rice tea, or pandan did not significantly affect soil bacterial richness or diversity, but both richness and diversity were significantly greater in the rotations than those in the fallow treatment (Supplementary Figures S1A, B). The richness and diversity of the fungal community significantly increased with rotation (Supplementary Figures S1C, D) and were significantly negatively correlated with pathogen abundance (Supplementary Figures S1G, H). Principal coordinate analysis (PCoA) based on Bray–Curtis distances clearly revealed significant differences in the soil fungal communities among the fallow, vanilla monoculture, and crop rotation treatments (Figure 1C, left). However, no distinct separation was observed among the rotations of black pepper, pandan, and sweet rice tea. This finding was confirmed by PERMANOVA (Figure 1C, $R^2 = 0.38$, $P = 0.001$) and ANOSIM (Supplementary Table S1, $P = 0.001$). Moreover, the fungal community (PCoA1) was significantly negatively correlated with the abundance of *F. oxysporum* (Figure 1C, middle). Further cluster heatmap analysis indicated that fallow and vanilla monoculture could be clustered separately, whereas the rotations of pepper, pandan and sweet rice tea had similar community structures and were clustered together (Supplementary Figure S2B). The trend in the soil bacterial community structure was consistent with that of the fungal community structure (Figure 1D).

ITS sequencing revealed that, compared with vanilla monoculture, crop rotation with pepper, pandan and sweet rice tea significantly increased the relative abundance of the phylum *Ascomycota* (Figure 1C, right) and was significantly negatively correlated with *F. oxysporum* abundance (Supplementary Table S2). The genera *Thermomyces* and *Arthrobotrys* were significantly more abundant after rotation, with *Arthrobotrys* increasing 9.8-fold after pandan rotation, and both genera were negatively correlated with the pathogen (Supplementary Table S3). 16S rRNA gene sequencing revealed that crop rotation significantly increased the abundance of *Proteobacteria*, *Gemmatimonadetes*, and *Latescibacteria* (Figure 1D, right), which was also negatively correlated with *F.*

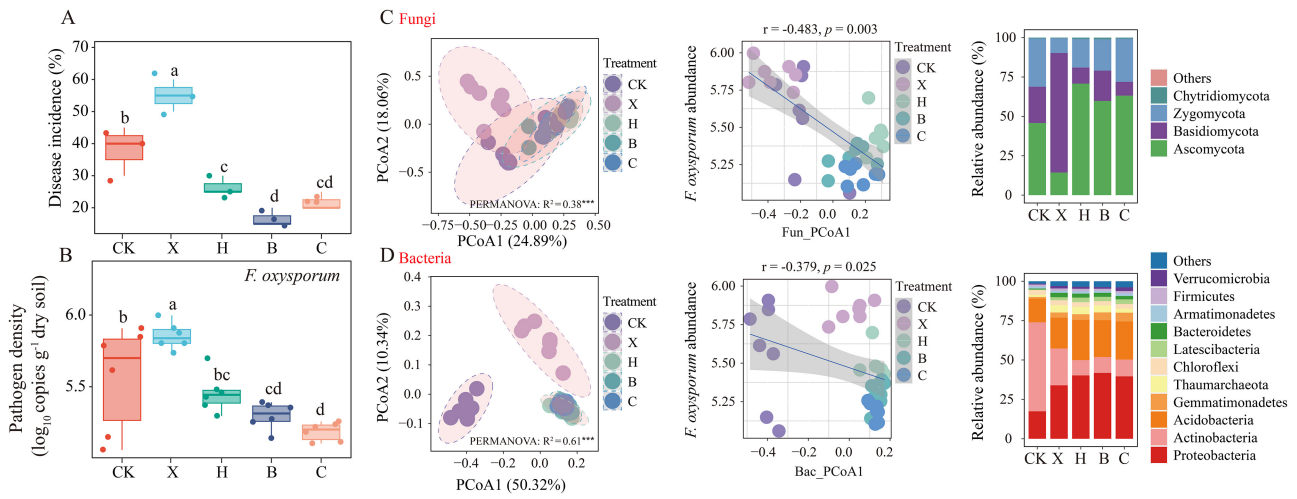

FIGURE 1
Impact of crop rotation on disease incidence and *Fusarium oxysporum* abundance in vanilla rhizosphere soil. Effects of crop rotation on **(A)** disease incidence and **(B)** *Fusarium oxysporum* abundance. Changes in rhizosphere soil **(C)** fungal and **(D)** bacterial community structure and composition across crops. Linear regression analysis of community structure and *F. oxysporum* abundance. Statistical significance was assessed via Duncan's test (mean ± SD). Different letters denote a significant difference at the $P < 0.05$ level. CK, fallow; X, vanilla monoculture; H, black pepper–vanilla rotation; B, pandan–vanilla rotation; C, sweet rice tea–vanilla rotation.

oxysporum abundance (Supplementary Table S2). At the genus level, *Nitrosospira*, *Gemmatimonas*, and *Gp17* were significantly more abundant in rotation systems, particularly those involving pandan and sweet rice tea, and were negatively associated with the pathogen (Supplementary Table S4).

Disease suppression by rhizosphere microbial communities

MRT analysis revealed that cropping system was the main factor shaping rhizosphere fungi, explaining 26.81% of the variance, whereas crops in rotation were secondary factors, accounting for 9.29% of the variance (Figure 2A). For bacteria, crop rotation was the primary factor, explaining 61.23% of the variance (Figure 2B).

A general linear model (GLM) was used to assess the impact of fungal and bacterial community structure and diversity on the suppression of *F. oxysporum* abundance, quantified via qPCR-based absolute quantification (Figure 2C). Both the fungal and bacterial principal coordinate axes significantly reduced pathogen abundance, with the fungal community being the major factor, accounting for 24.95% of the variance. The second axis of the bacterial community also significantly contributed, accounting for 13% of the variance. SEM revealed that bacterial community structure and diversity positively influence fungal community structure ($r = 0.22$ for structure, $r = 0.40$ for diversity), which in turn significantly decreased the abundance of *F. oxysporum* quantified via qPCR ($r = -0.79$; Figure 2D).

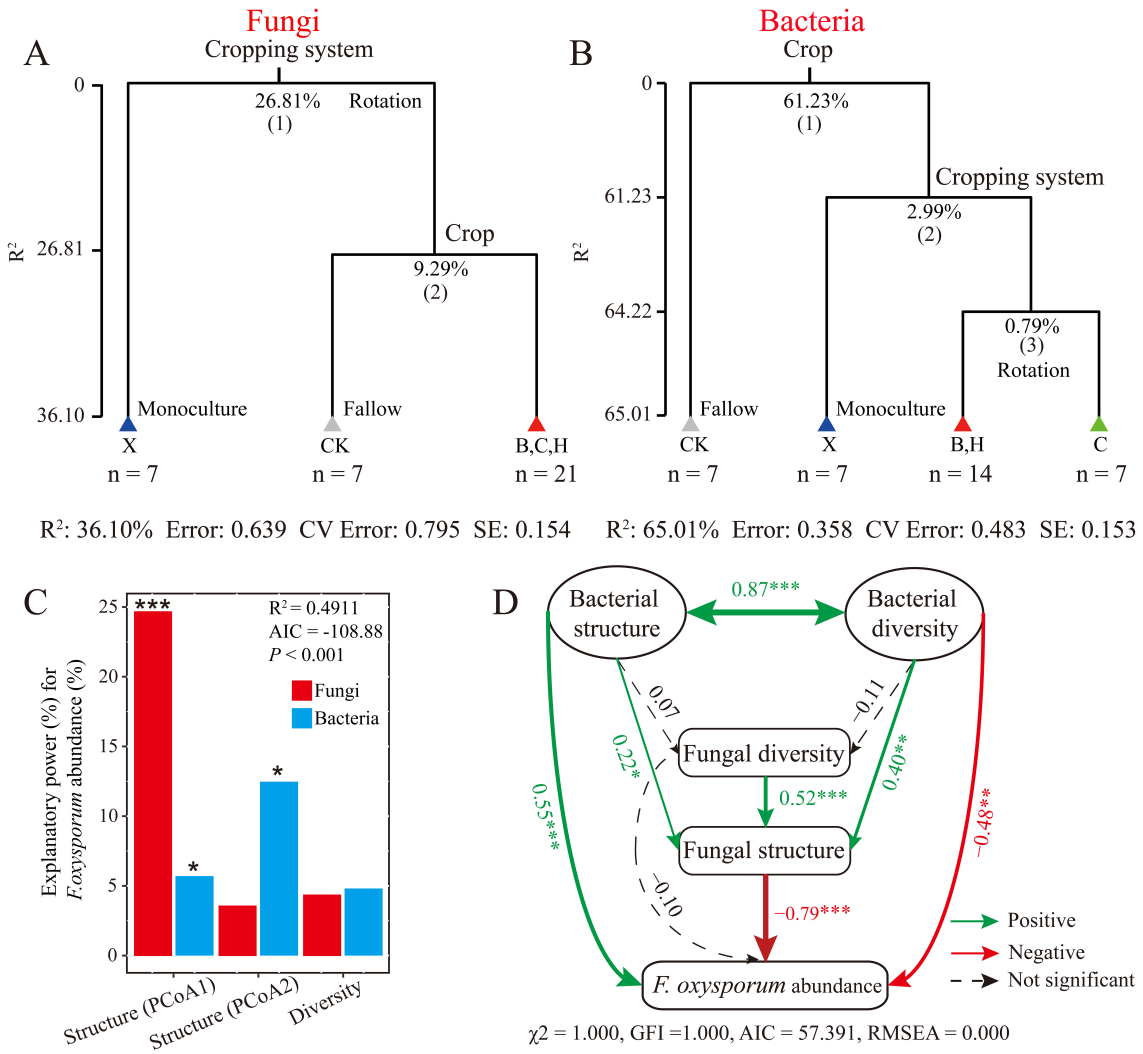

FIGURE 2
Analyses of soil microbial community structure and pathogen inhibitory effects. Multiple regression tree (MRT) analysis of soil microbial **(A)** fungal and **(B)** bacterial community structure; **(C)** relative importance of community structure in pathogen inhibition; **(D)** structural equation modeling (SEM) analysis of pathogen inhibition correlations, with solid arrows indicating significant ($P < 0.05$) and dashed arrows indicating non-significant correlations. The R-squared values indicate the correlation strength and direction. Positive values indicate positive correlations, and negative values indicate negative correlations. CK, fallow; X, vanilla monoculture; H, black pepper–vanilla rotation; B, pandan–vanilla rotation; C, sweet rice tea–vanilla rotation.

Identification of disease-suppressive biomarkers

We used a more stringent LDA score threshold of ≥3 to identify biomarkers between groups. We then displayed the top 20 fungal (Figure 3A) and bacterial (Figure 3B) OTU taxa by relative abundance. Among fungi, 20 biomarkers were identified (Supplementary Table S5). Specifically, the fallow treatment enriched 5 biomarkers, mainly from the phyla *Ascomycota* and *Basidiomycota*; vanilla monoculture enriched 1 *Ascomycota* biomarker; black pepper rotation enriched 8 biomarkers, primarily from the phyla *Ascomycota* and *Zygomycota*; pandan rotation enriched 3 *Zygomycota* biomarkers; and sweet rice tea rotation enriched 3 biomarkers from the phyla *Ascomycota* and *Zygomycota*. Notably, black pepper rotation significantly enriched OTU1_*Thermomyces* ($F = 4.682$, $P = 0.005$) and OTU37_*Arthrobotrys* ($F = 4.188$, $P = 0.008$), pandan rotation significantly enriched OTU18_*Arthrobotrys* ($F = 3.326$, $P = 0.023$), and sweet rice tea rotation significantly enriched OTU16_*Mortierella* ($F = 2.800$, $P = 0.044$). The relative abundances of these biomarkers were significantly negatively correlated with *F. oxysporum* abundance ($P < 0.05$).

For bacteria, we identified a total of 147 biomarkers (Supplementary Table S6). Specifically, the fallow treatment enriched 27 biomarkers, mainly from the phyla *Proteobacteria* and *Actinobacteria*; vanilla monoculture enriched 22 biomarkers, primarily from the phyla *Proteobacteria* and *Actinobacteria*; black pepper rotation enriched 26 biomarkers, mainly from the phyla *Proteobacteria* and *Acidobacteria*; pandan rotation enriched 34 biomarkers, primarily from the phyla *Proteobacteria* and *Acidobacteria*; and sweet rice tea rotation enriched 38 biomarkers, predominantly from the phylum *Proteobacteria*.

Random forest models identified significant predictors of *F. oxysporum* response. In the fungal model (Figure 4A, $R^2 = 0.331$, $P < 0.01$), black pepper–vanilla rotation enriched OTU1_*Thermomyces* and OTU37_*Arthrobotrys*, and pandan–vanilla rotation enriched OTU18_*Arthrobotrys* significantly. For bacteria (Figure 4B), the black pepper–vanilla rotation model ($R^2 = 0.314$, $P < 0.01$) highlighted OTU235_*Gp16*, OTU145_*Gp11*, and OTU158_*Gp17* as predictors. In the pandan–vanilla rotation model ($R^2 = 0.625$, $P < 0.01$), multiple bacterial OTUs were identified as predictors, including OTU11_*Gp6*, OTU5794_*Magnetospirillum*, OTU78_*Zoogloea*, OTU33_*Lacibacterium*, OTU22_*Nitrosospira*, and OTU109_*Latescibacteria*. The sweet rice tea–vanilla rotation model ($R^2 = 0.465$, $P < 0.01$) also revealed several significant bacterial predictors, such as OTU200_*Methylibium*, OTU113_*Roseisolibacter*, OTU178_*Actinospica*, OTU56_*Lacibacterium*, OTU18_*Nitrospira*, and OTU90_*Micromonospora*. Compared with those in the fallow and vanilla monoculture treatment, the relative abundances of the identified biomarkers significantly increased (Supplementary Figure S3, $P < 0.05$).

Identification of hub taxa

Co-occurrence network analysis of rhizosphere bacteria and fungi revealed distinct structures under fallow, vanilla monoculture, and rotation treatments (Figure 5). The pandan–vanilla rotation network had the highest node and connection counts, with 96% positive correlations, and the highest average node degree was 2.78, indicating strong microbial interactions (Supplementary Table S7). On the basis of node degree and closeness centrality (Table 1), in the pandan–vanilla rotation, 8 bacterial hub taxa, such as OTU31, OTU99, OTU178, OTU10, OTU14, OTU22, OTU56, and OTU130, were uniquely identified. The 8 identified hub taxa had relative abundances >0.2%, with values of 0.53%, 0.27%, 0.28%, 1.26%, 0.87%, 1.01%, 0.27%, and 0.38%, respectively. Notably, OTU22, OTU56, and OTU178,

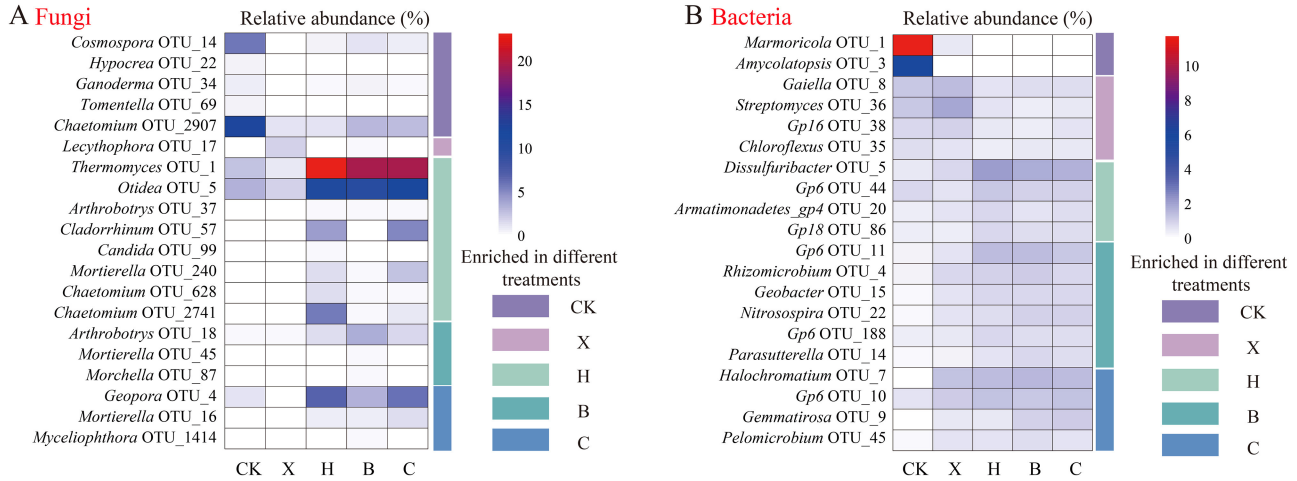

FIGURE 3
Relative abundance of biomarkers of rhizosphere microbiomes in different spice crops identified by linear discriminant analysis (LDA). Identification of **(A)** fungal and **(B)** bacterial biomarkers via LDA. Different lowercase letters denote significance at $P < 0.05$. CK, fallow; X, vanilla monoculture; H, black pepper–vanilla rotation; B, pandan–vanilla rotation; C, sweet rice tea–vanilla rotation.

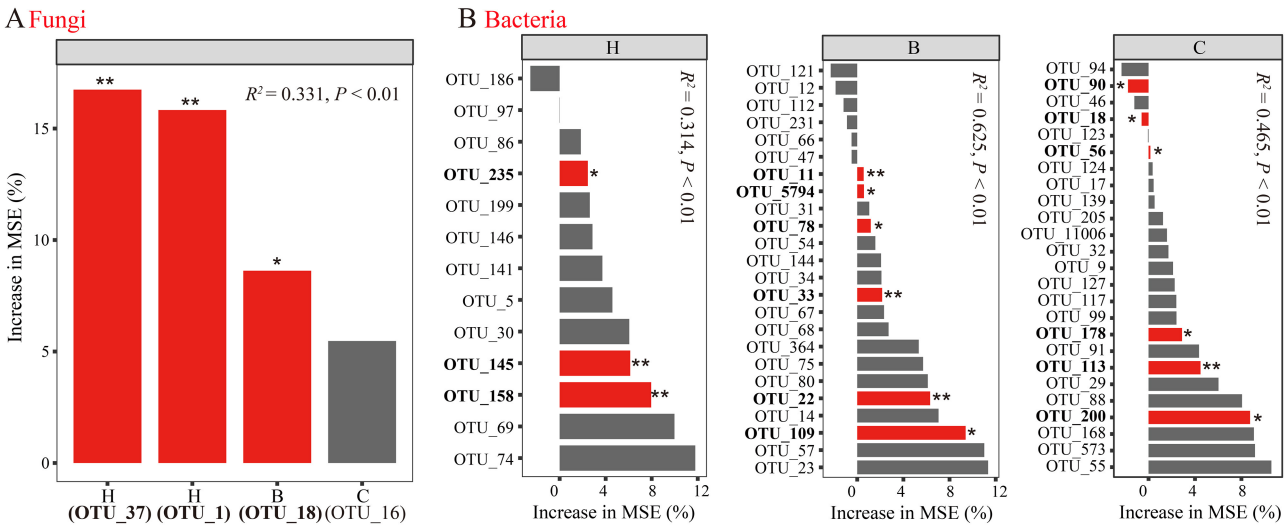

FIGURE 4
Assessment of **(A)** fungal and **(B)** bacterial biomarker responses to *F. oxysporum* with random forest. Different lowercase letters denote significance at $P < 0.05$. CK, fallow; X, vanilla monoculture; H, black pepper–vanilla rotation; B, pandan–vanilla rotation; C, sweet rice tea–vanilla rotation.

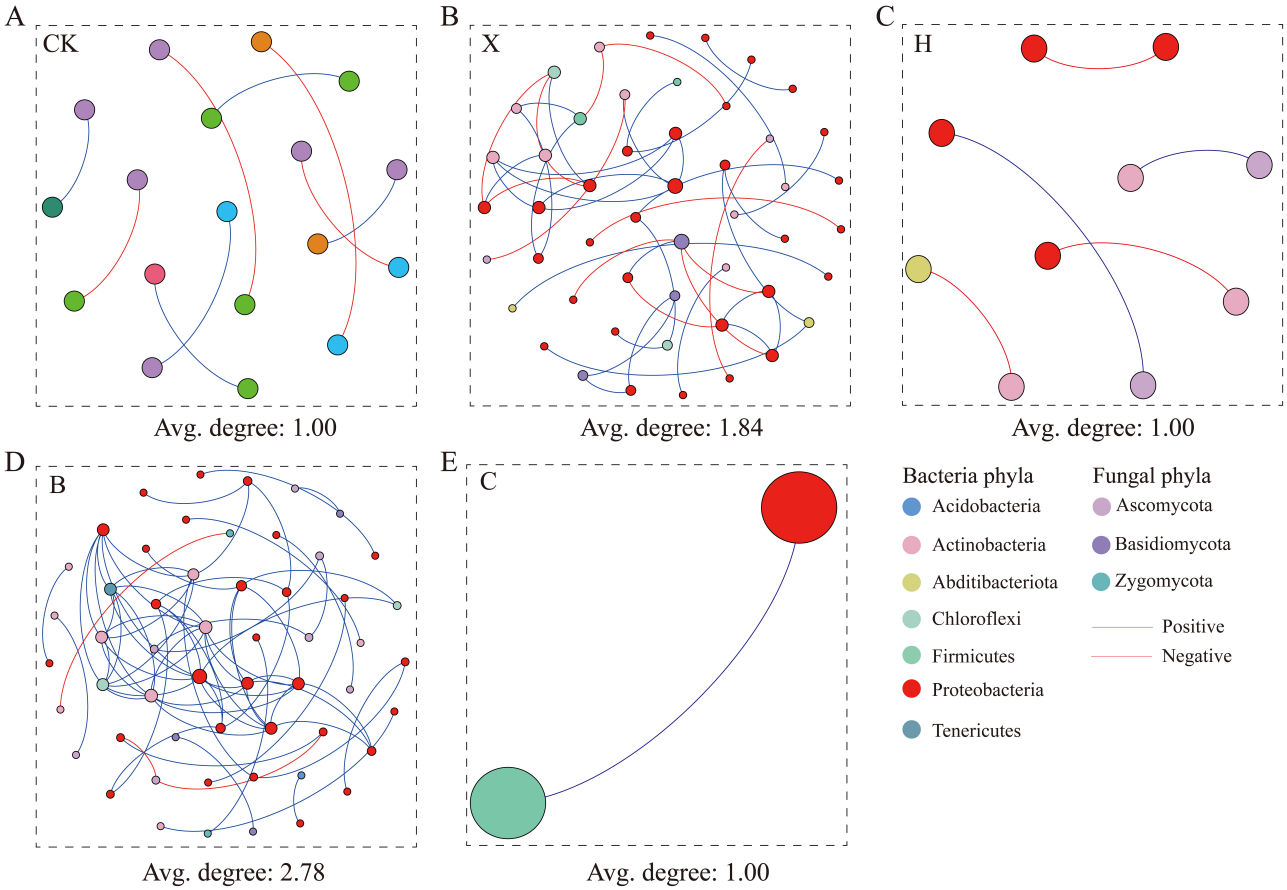

FIGURE 5
Assessing microbial co-occurrence networks in the rhizospheres of rotated spice crops. Complexity of bacterial–fungal interactions reflected by network node connectivity. A higher average degree of nodes indicates a more complex network, suggesting more extensive synergistic interactions between microbiomes. **(A)** CK = fallow; **(B)** X = vanilla monoculture; **(C)** H = black pepper-vanilla rotation; **(D)** B = pandan-vanilla rotation; **(E)** C = sweet rice tea-vanilla rotation.

TABLE 1 Identification of hub nodes in bacterial–fungal microbial co-occurrence networks after rotation with various spice crops.

Network	Sample ID[b]	Phylum	Genus	RA%[c]	Degree[d]	Closeness[e] centrality
B_network[a]	B_OTU31	*Acidobacteria*	*Gp6*	0.53%	10	0.6
	B_OTU99	*Nitrospirae*	*Nitrospira*	0.27%	8	0.6
	B_OTU178	*Actinobacteria*	*Actinospica*	0.28%	8	0.6
	B_OTU10	*Acidobacteria*	*Gp6*	1.26%	7	0.6
	B_OTU14	*Proteobacteria*	*Parasutterella*	0.87%	7	0.6
	B_OTU22	*Proteobacteria*	*Nitrosospira*	1.01%	7	0.6
	B_OTU56	*Tenericutes*	*Lacibacterium*	0.27%	7	0.6
	B_OTU130	*Acidobacteria*	*Gp6*	0.38%	7	0.6

[a] The B_network refers to the bacterial-fungal microbial co-occurrence network in the rhizosphere soil of pandan. According to our network node characteristic criteria for identifying hub nodes (i.e., degree and closeness centrality), the rhizosphere microbial co-occurrence networks of other spice crops exhibited no hub nodes meeting these established standards.
[b] B_OTUs denote bacterial taxa.
[c] RA (relative abundance) refers to the percentage representation of each bacterial taxon within the microbial community of pandan.
[d/e] Hub OTUs were identified based on a customized threshold reflecting node characteristics: a degree > 7 and a closeness centrality > 0.6. These hub OTUs accounted for <15% of all nodes in the network.

identified as enriched biomarkers by random forest analysis, also qualified as hubs in the network analysis, designating them as core microbiota. OTU22, specifically, emerged as a pandan–vanilla rotation-enriched, host-specific core microbe.

Predicting pathogen-suppressive indicators

Following crop rotation with spice crops, we measured soil physicochemical properties and found that, compared with those under vanilla monoculture cultivation, soil pH, OM, AN, AP, and AK significantly increased under spice rotation (Figure 6A, $P < 0.05$). However, soil pH and OM did not differ significantly between the pandan and sweet rice tea rotation systems. Soil pH and OM significantly influenced both fungal and bacterial communities, with soil pH being the primary factor, explaining 10.8% and 42.2% of the variance in fungal and bacterial communities, respectively (Figures 6B, C).

A general linear model was used to evaluate the potential of microbial communities, core microbiota and physicochemical properties in suppressing pathogens. The model explained 71.02% of the variation in pathogen suppression (Table 2, $P < 0.001$). Key factors included fungal community structure, the core microbial species OTU22, and soil pH, with individual explanatory contributions of 18.71%, 7.59%, and 17.83%, respectively ($P < 0.05$ for all).

Discussion

Vanilla, an herbaceous perennial vine, is particularly susceptible to continuous cropping obstacles. Our previous research revealed that rotation with black pepper can effectively regulate the soil fungal community, thereby increasing vanilla disease resistance (Xiong et al., 2016). In this study, we conducted pot experiments by replanting vanilla in soils previously rotated with black pepper, pandan and sweet rice tea. The results indicated that rotation with pepper, pandan, or sweet rice tea not only reduced the DI but also significantly decreased the copy number of *F. oxysporum* (Figure 1). This aligns with our previous findings on crop rotation systems. For example, cultivation methods such as pepper–banana rotation (Hong et al., 2020), eggplant–banana rotation (Hong et al., 2023) and pineapple–banana rotation (Yuan et al., 2021) effectively improved banana disease suppression. These findings suggest that reducing the abundance of *F. oxysporum* may be key to enhancing vanilla disease suppression. However, owing to the high cost of planting and managing vanilla, we opted for pot experiments over field trials. Although the experiment was conducted in a controlled environment, we adjusted parameters such as temperature and humidity to mimic natural microenvironments, ensuring the reliability, stability and reproducibility of our results. In addition, pandan and sweet rice tea are short-cycle spice crops that have been widely applied in tropical production in recent years. The production cycle of these plants is 6 months, whereas that of black pepper is 30 months. Therefore, considering the planting cycles of black pepper, pandan and sweet rice tea, we selected a planting time that was in between these two cycles for our pot experiment. Specifically, we replanted vanilla in the soil after a 12-month rotation to evaluate disease-suppression effects. Although our current study has certain limitations, we plan to conduct further long-term research to explore the differences in disease-suppression effects across various rotation cycles.

The diversity and richness of the soil microbiome are pivotal for alleviating the negative impacts of environmental stress on plants, offering protection against biotic challenges and assisting in the plant recovery process (Trivedi et al., 2020). Our study revealed that the adoption of a crop rotation regime that included black pepper, pandan, or sweet rice tea markedly improved the richness and diversity of the soil fungal community. This finding corroborates the outcomes of our previous research, indicating a pronounced increase in the richness and diversity of fungal populations when black pepper and coffee were under rotation with vanilla (Xiong et al., 2016). These results highlight the diverse impacts of different crop rotation strategies on the bacterial and fungal constituents of the soil microbiome. Specific rotational crops appear to stimulate the proliferation of beneficial microbial groups, thereby shaping the

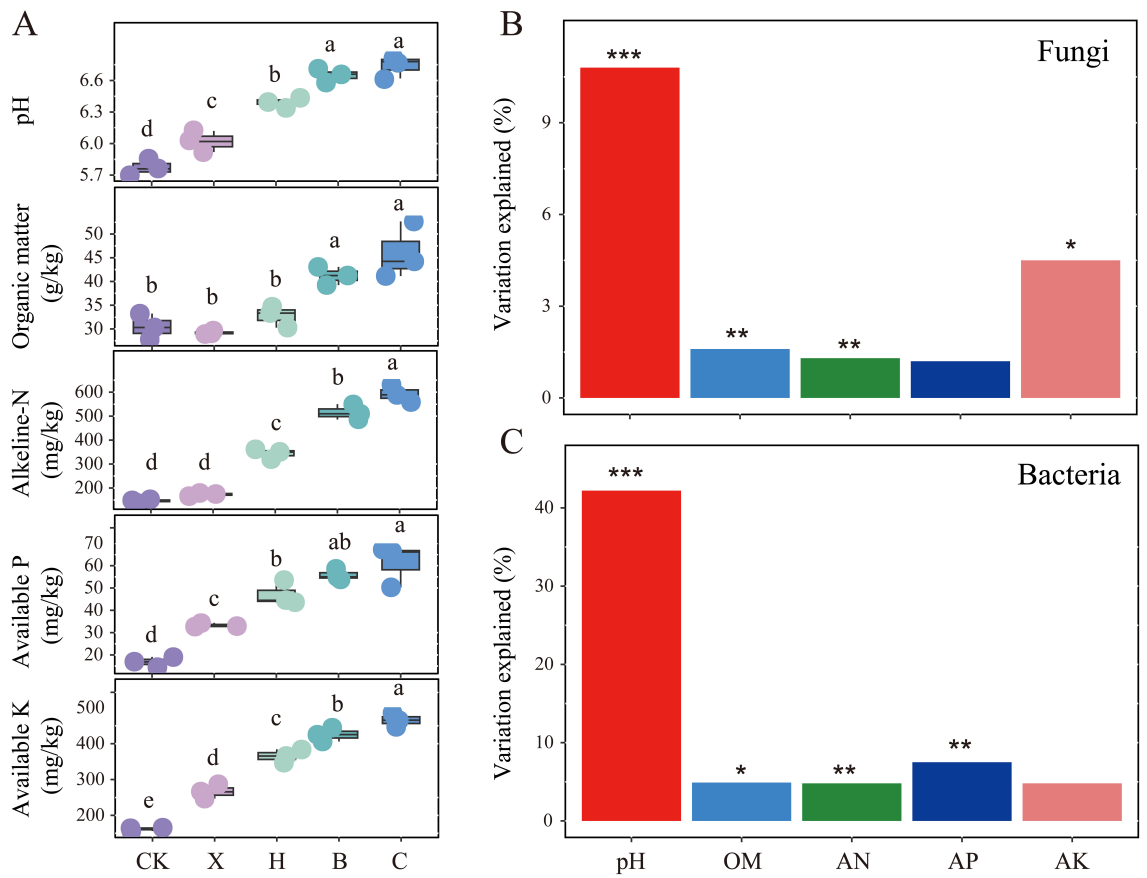

FIGURE 6
Variations in **(A)** soil physicochemical properties and the impact of these environmental factors on the composition of **(B)** fungal and **(C)** bacterial communities after rotation with different spice crops. CK, fallow; X, vanilla monoculture; H, black pepper–vanilla rotation; B, pandan–vanilla rotation; C, sweet rice tea–vanilla rotation. OM, organic matter; NA, alkali-hydrolysable, AP, available phosphorus; AK, available potassium. * represents $P < 0.05$, ** represents $P < 0.01$ and *** represents $P < 0.001$.

structure of the soil microbial community. These microbes compete with pathogens for niche resources at the root interface, limiting pathogen access to nutrients and effectively controlling the spread of the pathogens (Wen et al., 2023a).

Studies indicate that the structure and composition of microbial communities after long-term crop rotation significantly differ from those in monoculture systems (Zhou et al., 2023; Cerecetto et al., 2024). In this study, both fungal and bacterial community structures were clearly distinguishable among fallow, monoculture and crop rotation treatments, resulting in three distinct community configurations. However, the community structures of the black pepper, pandan and sweet rice tea groups were notably similar and indistinguishable. This similarity suggests that crop rotation alters soil resource distribution and environmental conditions, allowing different functional microbial communities to coexist simultaneously, leading to overlapping communities. Essentially, the soil microbial communities that establish following rotation with black pepper, pandan and sweet rice tea likely contain beneficial microbes that compete with pathogens for limited rhizosphere resources. Therefore, future research should be focused on elucidating the mechanisms of community assembly to better understand how crop rotation affects the composition of soil microbial communities, thereby enhancing crop health.

In this study, we conducted a comparative analysis of microbes identified as biomarkers by LDA and random forest analysis and identified hub taxa from co-occurrence networks, defining core microbes as those common to both. We discovered that replanting vanilla in soils previously subjected to rotation with black pepper, pandan, and sweet rice tea specifically activated certain fungal biomarker taxa, such as OTU1_*Thermomyces*, OTU18_*Arthrobotrys*, and OTU37_*Arthrobotrys*, as well as core bacterial microbes, such as OTU22_*Nitrosospira*, OTU56_*Lacibacterium*, and OTU178_*Actinospica*. Our previous research indicated that black pepper–vanilla rotation could significantly enrich antagonistic core fungal taxa, such as *Trichoderma* and *Penicillium* (Xiong et al., 2016). This implies that different rotation crops possess distinct rhizosphere metabolites, which, during the vanilla season, differentially enrich specific core microbiota (Wen et al., 2023b). Additionally, the duration of crop rotation significantly influences the assembly of core microbial communities (Iheshiulo et al., 2023). Existing studies have demonstrated that fungal taxa, such as *Thermomyces* and *Arthrobotrys*, may contribute positively to disease suppression

10.3389/fmicb.2025.1496701

TABLE 2 Linear modeling to identify the microbial and soil physicochemical factors associated with the reduction in *Fusarium oxysporum* abundance in vanilla.

F. oxysporum abundance	df	*F* value	*P*-value	*t*	RI (%)
Fungal structure	**1**	**42.373**	**0.001**	**−1.939**	**18.71%**
Bacterial structure	1	0.240	0.628	3.259	8.48%
OTU_18 (*Arthrobotrys*)	1	1.023	0.321	0.244	2.45%
OTU_37 (*Arthrobotrys*)	1	0.593	0.447	−1.058	6.88%
OTU_11 (*Gp6*)	1	0.402	0.531	−0.345	3.97%
OTU_22 (*Nitrosospira*)	**1**	**10.835**	**0.002**	**−2.096**	**7.59%**
OTU_56 (*Lacibacterium*)	1	0.476	0.496	−0.310	2.48%
OTU_178 (*Actinospica*)	1	0.197	0.663	0.504	2.63%
pH	**1**	**5.132**	**0.032**	**−2.265**	**17.83%**
Residuals	27				
Model summary: $R^2 = 0.7102$, AIC = −116.23, $p < 0.001$					
Proportion of variance explained by model: 71.02%					

RI, relative importance. *P*-values were calculated via ANOVA. Bolded lines in the table represent factors exhibiting a statistically significant correlation with decreased pathogen abundance ($P < 0.05$).

(Nagai et al., 2020), but there is currently insufficient evidence to assert that core bacterial microbes, such as *Nitrosospira*, *Lacibacterium*, and *Actinospica*, have direct disease resistance functions. Nevertheless, the core microbes identified in this study are integral components of the soil microbial community (Yue et al., 2024). Different members of these core groups may suppress diseases through various mechanisms, including antibiotic production (Li et al., 2016; Kusuma et al., 2022; Banerjee and van der Heijden, 2023), nutrient competition, or physical barrier formation. Moreover, these core taxa may indirectly influence pathogen growth through synergistic interactions with other microbes (Li et al., 2016; Banerjee and van der Heijden, 2023).

Research has shown that crop rotation, for example, introducing chili peppers in banana plantations, can restructure the soil microbiome by increasing pH, leading to increased proliferation of beneficial *Pseudomonas* that improve disease resistance in crops (Hong et al., 2020). Our study corroborates these findings, demonstrating that intercropping vanilla with spice crops significantly increases rhizosphere soil pH and impacts fungal and bacterial communities. Crop rotation effectively mitigates the acidification trend induced by monoculture practices through mechanisms including (1) modulating the chemical properties of crop residues, (2) optimizing nutrient uptake balance, (3) reshaping microbial functional profiles, and (4) enhancing soil buffering capacity. The pronounced sensitivity of soil microbial communities to pH variations indicates that agricultural practices can be leveraged to increase crop disease resistance (Tamburini et al., 2020; Wittwer et al., 2021). For example, amending the soil pH with peanut crop residues can increase the activity of the antagonistic soil microbiome (Watanabe et al., 2011). The pH level directly influences the enzymatic activity and physiological processes within *Fusarium*, thereby regulating their growth and metabolism. Additionally, pH significantly and directly affects the toxin-producing capacity of *Fusarium*. pH modulates the composition of plant root exudates (e.g., organic acids and phenolic compounds), indirectly altering the host plant's chemical defense efficacy against *Fusarium*. Furthermore, increasing the soil pH can regulate the soil microbial community by enriching beneficial bacteria and suppressing pathogens, thereby alleviating soil-borne diseases in *Panax notoginseng* (Deng et al., 2024). Through a general linear model, we determined that fungal community structure, particularly the core taxon OTU2, and soil pH are key determinants of pathogen suppression, with fungal structure being the predominant factor. This underscores the need to consider the collective influence of soil microbial communities on the health of crops rather than focusing solely on individual microbiota (Wagg et al., 2019; Delgado-Baquerizo et al., 2021).

In summary, intercropping spice crops, particularly pandan, with orchards susceptible to soil-borne diseases effectively reduces the incidence of disease and the level of *F. oxysporum* while increasing fungal community diversity. This approach selectively enriches for key fungal and bacterial taxa, such as OTU1_*Thermomyces*, OTU18_*Arthrobotrys*, OTU37_*Arthrobotrys*, OTU22_*Nitrosospira*, OTU56_*Lacibacterium*, and OTU178_*Actinospica*, reshaping the soil microbiome. The resulting increase in soil pH is believed to reorganize microbial communities, particularly fungal communities, thereby suppressing pathogen abundance. These results suggest that the modulation of soil pH and restructuring of microbial communities are pivotal for enhancing vanilla resistance to diseases through the pandan–vanilla rotation strategy.

Data availability statement

The datasets presented in this study can be found in online repositories. The names of the repository/repositories and accession number(s) can be found in the article/Supplementary material.

Author contributions

SH: Data curation, Methodology, Writing – original draft. YX: Writing – review & editing. JY: Data curation, Writing – review & editing. QZ: Supervision, Writing – review & editing. FS: Software, Writing – review & editing. HZ: Methodology, Writing – review & editing. HW: Project administration, Writing – review & editing. ZW: Methodology, Visualization, Writing – review & editing. YC: Methodology, Software, Writing – review & editing.

Funding

The author(s) declare that financial support was received for the research and/or publication of this article. The study was funded by the Hainan Provincial Natural Science Foundation of China (322QN404, 321QN326), Hainan Seed Industry Laboratory (B23C1000419), Hainan Provincial Postdoctoral

Research Project (B25B10005), Hainan Province South China Sea New-Star Science and Technology Innovation Talent Platform Project (NHXXRCXM202331), Talent Start-up Funding of Hainan Academy of Agricultural Sciences (HAAS2023RCQD24) and Key Research and Development Project of Hainan Province (ZDYF2022XDNY268).

Conflict of interest

The authors declare that the research was conducted in the absence of any commercial or financial relationships that could be construed as potential conflicts of interest.

The reviewer XL declared a shared affiliation with the author JY to the Handling Editor at the time of review.

Publisher's note

All claims expressed in this article are solely those of the authors and do not necessarily represent those of their affiliated organizations, or those of the publisher, the editors and the reviewers. Any product that may be evaluated in this article, or claim that may be made by its manufacturer, is not guaranteed or endorsed by the publisher.

Supplementary material

The Supplementary Material for this article can be found online at: https://www.frontiersin.org/articles/10.3389/fmicb.2025.1496701/full#supplementary-material

References

Agler, M. T., Ruhe, J., Kroll, S., Morhenn, C., Kim, S. T., Weigel, D., et al. (2016). Microbial hub taxa link host and abiotic factors to plant microbiome variation. *PLoS Biol.* 14, 1–31. doi: 10.1371/journal.pbio.1002352

Banerjee, S., Schlaeppi, K., and van der Heijden, M. G. A. (2018). Keystone taxa as drivers of microbiome structure and functioning. *Nat. Rev. Microbiol.* 16, 567–576. doi: 10.1038/s41579-018-0024-1

Banerjee, S., and van der Heijden, M. G. A. (2023). Soil microbiomes and one health. *Nat. Rev. Microbiol.* 21, 6–20. doi: 10.1038/s41579-022-00779-w

Bastian, M., Heymann, S., and Jacomy, M. (2009). Gephi: an open source software for exploring and manipulating networks. *Icwsm* 8, 361–362. doi: 10.1609/icwsm.v3i1.13937

Bolyen, E., Rideout, J. R., Dillon, M. R., Bokulich, N. A., Abnet, C. C., Al-Ghalith, G. A., et al. (2019). Reproducible, interactive, scalable and extensible microbiome data science using QIIME 2. *Nat. Biotechnol.* 37, 852–857. doi: 10.1038/s41587-019-0209-9

Callahan, B. J., McMurdie, P. J., Rosen, M. J., Han, A. W., Johnson, A. J. A., and Holmes, S. P. (2016). DADA2: High-resolution sample inference from Illumina amplicon data. *Nat. Methods* 13, 581–583. doi: 10.1038/nmeth.3869

Caporaso, J. G., Lauber, C. L., Walters, W. A., Berg-Lyons, D., Lozupone, C. A., Turnbaugh, P. J., et al. (2011). Global patterns of 16S rRNA diversity at a depth of millions of sequences per sample. *Proc. Natl. Acad. Sci. USA.* 108, 4516–4522. doi: 10.1073/pnas.1000080107

Cerecetto, V., Leoni, C., Jurburg, S. D., Kampouris, I. D., Smalla, K., and Babin, D. (2024). Pasture-crop rotations modulate the soil and rhizosphere microbiota and preserve soil structure supporting oat cultivation in the Pampa biome. *Soil Biol. Biochem.* 195:109451. doi: 10.1016/j.soilbio.2024.109451

Chen, Y., Bonkowski, M., Shen, Y., Griffiths, B. S., Jiang, Y., Wang, X., et al. (2020). Root ethylene mediates rhizosphere microbial community reconstruction when chemically detecting cyanide produced by neighbouring plants. *Microbiome* 8:4. doi: 10.1186/s40168-019-0775-6

Costello, E. K., Stagaman, K., Dethlefsen, L., Bohannan, B. J. M., and Relman, D. A. (2012). The application of ecological theory toward an understanding of the human microbiome. *Science* 336, 1255–1262. doi: 10.1126/science.1224203

De'Ath, G. (2002). Multivariate regression trees: a new technique for modeling species–environment relationships. *Ecology* 83, 1105–1117. doi: 10.1890/0012-9658(2002)083[1105:MRTANT]2.0.CO;2

Delgado-Baquerizo, M., Eldridge, D. J., Liu, Y. R., Sokoya, B., Wang, J. T., Hu, H. W., et al. (2021). Global homogenization of the structure and function in the soil microbiome of urban greenspaces. *Sci. Adv.* 7:eabg5809. doi: 10.1126/sciadv.abg5809

Deng, W., Gong, J., Peng, W., Luan, W., Liu, Y., Huang, H., et al. (2024). Alleviating soil acidification to suppress Panax notoginseng soil-borne disease by modifying soil properties and the microbiome. *Plant Soil* 502, 653–669. doi: 10.1007/s11104-024-06577-y

Edgar, R. C. (2013). UPARSE: highly accurate OTU sequences from microbial amplicon reads. *Nat. Methods* 10, 996–999. doi: 10.1038/nmeth.2604

Edgar, R. C., Haas, B. J., Clemente, J. C., Quince, C., and Knight, R. (2011). UCHIME improves sensitivity and speed of chimera detection. *Bioinformatics* 27, 2194–2200. doi: 10.1093/bioinformatics/btr381

Hermans, S. M., Buckley, H. L., Case, B. S., Curran-Cournane, F., Taylor, M., and Lear, G. (2020). Using soil bacterial communities to predict physico-chemical variables and soil quality. *Microbiome* 8:79. doi: 10.1186/s40168-020-00858-1

Hong, S., Jv, H. L., Lu, M., Wang, B. B., Zhao, Y., and Ruan, Y. Z. (2020). Significant decline in banana Fusarium wilt disease is associated with soil microbiome reconstruction under chilli pepper-banana rotation. *Eur. J. Soil Biol.* 97:103154. doi: 10.1016/j.ejsobi.2020.103154

Hong, S., Yuan, X., Yang, J., Yang, Y., Jv, H., Li, R., et al. (2023). Selection of rhizosphere communities of diverse rotation crops reveals unique core microbiome associated with reduced banana Fusarium wilt disease. *New Phytol.* 238, 2194–2209. doi: 10.1111/nph.18816

Iheshiulo, E. M.-A., Larney, F. J., Hernandez-Ramirez, G., St. Luce, M., Liu, K., and Chau, H. W. (2023). Do diversified crop rotations influence soil physical health? A meta-analysis. *Soil Tillage Res.* 233:105781. doi: 10.1016/j.still.2023.105781

Kõljalg, U., Nilsson, R. H., Abarenkov, K., Tedersoo, L., Taylor, A. F. S., Bahram, M., et al. (2013). Towards a unified paradigm for sequence-based identification of fungi. *Mol. Ecol.* 22, 5271–5277. doi: 10.1111/mec.12481

Koyyappurath, S., Atuahiva, T., Le Guen, R., Batina, H., Le Squin, S., Gautheron, N., et al. (2016). Fusarium oxysporum f. sp. radicis-vanillae is the causal agent of root and stem rot of vanilla. *Plant Pathol.* 65, 612–625. doi: 10.1111/ppa.12445

Kusuma, A. B., Putra, K. E., Vanggy, L. R., Loh, J., Nouioui, I., and Goodfellow, M. (2022). Actinospica acidithermotolerans sp. nov., a novel actinomycete isolated from sediment from an Indonesian hot spring. *Arch. Microbiol.* 204:518. doi: 10.1007/s00203-022-03058-7

Lai, J., Zou, Y., Zhang, J., and Peres-Neto, P. R. (2022). Generalizing hierarchical and variation partitioning in multiple regression and canonical analyses using the rdacca.hp R package. *Methods Ecol. Evol.* 13, 782–788. doi: 10.1111/2041-210X.13800

Li, F., Jin, Z., Wang, Z., Liao, Y., Yu, L., and Li, X. (2022). Host plant selection imprints structure and assembly of fungal community along the soil-root continuum. *mSystems* 7:e0036122. doi: 10.1128/msystems.00361-22

Li, L., Yang, M., Luo, J., Qu, Q., Chen, Y., Liang, L., et al. (2016). Nematode-trapping fungi and fungus-associated bacteria interactions: the role of bacterial diketopiperazines and biofilms on Arthrobotrys oligospora surface in hyphal morphogenesis. *Environ. Microbiol.* 18, 3827–3839. doi: 10.1111/1462-2920.13340

Longepierre, M., Widmer, F., Keller, T., Weisskopf, P., Colombi, T., Six, J., et al. (2021). Limited resilience of the soil microbiome to mechanical compaction within four growing seasons of agricultural management. *ISME Commun.* 1:44. doi: 10.1038/s43705-021-00046-8

Mamet, S. D., Redlick, E., Brabant, M., Lamb, E. G., Helgason, B. L., Stanley, K., et al. (2019). Structural equation modeling of a winnowed soil microbiome identifies how invasive plants re-structure microbial networks. *ISME J.* 13, 1988–1996. doi: 10.1038/s41396-019-0407-y

Martin, M. (2011). Cutadapt removes adapter sequences from high-throughput sequencing reads. *EMBnet J.* 17, 10–12. doi: 10.14806/ej.17.1.200

Minoo, D., Jayakumar, V., Veena, S., Vimala, J., Basha, A., Saji, K., et al. (2008). Genetic variations and interrelationships in Vanilla planifolia and few related species as expressed by RAPD polymorphism. *Genet. Resour. Crop Evol.* 55, 459–470. doi: 10.1007/s10722-007-9252-3

Mosquera-Espinosa, A. T., Bonilla-Monar, A., Flanagan, N. S., Rivas, Á., Sánchez, F., Chavarriaga, P., et al. (2022). *In vitro* evaluation of the development of fusarium in vanilla accessions. *Agronomy* 12:2831. doi: 10.3390/agronomy12112831

Nagai, K., Mori, Y., Ishikawa, S., Furuta, T., Gamuyao, R., Niimi, Y., et al. (2020). Antagonistic regulation of the gibberellic acid response during stem growth in rice. *Nature* 584, 109–114. doi: 10.1038/s41586-020-2501-8

Napitupulu, T. P. (2025). Agricultural relevance of fungal mycelial growth-promoting bacteria: mutual interaction and application. *Microbiol. Res.* 290:127978. doi: 10.1016/j.micres.2024.127978

Pedrinho, A., Mendes, L. W., de Araujo Pereira, A. P., Araujo, A. S. F., Vaishnav, A., Karpouzas, D. G., et al. (2024). Soil microbial diversity plays an important role in resisting and restoring degraded ecosystems. *Plant Soil* 500, 325–349. doi: 10.1007/s11104-024-06489-x

Philippot, L., Chenu, C., Kappler, A., Rillig, M. C., and Fierer, N. (2024). The interplay between microbial communities and soil properties. *Nat. Rev. Microbiol.* 22, 226–239. doi: 10.1038/s41579-023-00980-5

Pinaria, A. G., Liew, E. C. Y., and Burgess, L. W. (2010). Fusarium species associated with vanilla stem rot in Indonesia. *Australas. Plant Pathol.* 39, 176–183. doi: 10.1071/AP09079

Rabari, A., Ruparelia, J., Jha, C. K., Sayyed, R. Z., Mitra, D., Priyadarshini, A., et al. (2023). Articulating beneficial rhizobacteria-mediated plant defenses through induced systemic resistance: a review. *Pedosphere* 33, 556–566. doi: 10.1016/j.pedsph.2022.10.003

Revelle, W., and Revelle, M. W. (2015). *Package 'Psych'. The Comprehensive R Archive Network,* 337–338.

Romero, F., Hilfiker, S., Edlinger, A., Held, A., Hartman, K., Labouyrie, M., et al. (2023). Soil microbial biodiversity promotes crop productivity and agro-ecosystem functioning in experimental microcosms. *Sci. Total Environ.* 885:163683. doi: 10.1016/j.scitotenv.2023.163683

Schoch, C. L., Seifert, K. A., Huhndorf, S., Robert, V., Spouge, J. L., Levesque, C. A., et al. (2012). Nuclear ribosomal internal transcribed spacer (ITS) region as a universal DNA barcode marker for Fungi. *Proc. Natl. Acad. Sci. USA*. 109, 6241–6246. doi: 10.1073/pnas.1117018109

Shen, Z., Xue, C., Penton, C. R., Thomashow, L. S., Zhang, N., Wang, B., et al. (2019). Suppression of banana Panama disease induced by soil microbiome reconstruction through an integrated agricultural strategy. *Soil Biol. Biochem.* 128, 164–174. doi: 10.1016/j.soilbio.2018.10.016

Tamburini, G., Bommarco, R., Wanger, T. C., Kremen, C., van der Heijden, M. G. A., Liebman, M., et al. (2020). Agricultural diversification promotes multiple ecosystem services without compromising yield. *Sci. Adv.* 6:eaba1715. doi: 10.1126/sciadv.aba1715

Toju, H., Peay, K. G., Yamamichi, M., Narisawa, K., Hiruma, K., Naito, K., et al. (2018). Core microbiomes for sustainable agroecosystems. *Nature Plants* 4, 247–257. doi: 10.1038/s41477-018-0139-4

Trivedi, P., Leach, J. E., Tringe, S. G., Sa, T. M., and Singh, B. K. (2020). Plant-microbiome interactions: from community assembly to plant health. *Nat. Rev. Microbiol.* 18, 607–621. doi: 10.1038/s41579-020-0412-1

Wagg, C., Schlaeppi, K., Banerjee, S., Kuramae, E. E., and van der Heijden, M. G. A. (2019). Fungal-bacterial diversity and microbiome complexity predict ecosystem functioning. *Nat. Commun.* 10:4841. doi: 10.1038/s41467-019-12798-y

Wang, C., and Kuzyakov, Y. (2024). Mechanisms and implications of bacterial-fungal competition for soil resources. *ISME J.* 18:wrae073. doi: 10.1093/ismejo/wrae073

Wang, Q., Garrity, G. M., Tiedje, J. M., and Cole, J. R. (2007). Naive Bayesian classifier for rapid assignment of rRNA sequences into the new bacterial taxonomy. *Appl. Environ. Microbiol.* 73, 5261–5267. doi: 10.1128/AEM.00062-07

Watanabe, K., Matsui, M., Honjo, H., Becker, J. O., and Fukui, R. (2011). Effects of soil pH on rhizoctonia damping-off of sugar beet and disease suppression induced by soil amendment with crop residues. *Plant Soil* 347, 255–268. doi: 10.1007/s11104-011-0843-6

Wen, T., Ding, Z., Thomashow, L. S., Hale, L., Yang, S., Xie, P., et al. (2023a). Deciphering the mechanism of fungal pathogen-induced disease-suppressive soil. *New Phytol.* 238, 2634–2650. doi: 10.1111/nph.18886

Wen, T., Xie, P., Liu, H., Liu, T., Zhao, M., Yang, S., et al. (2023b). Tapping the rhizosphere metabolites for the prebiotic control of soil-borne bacterial wilt disease. *Nat. Commun.* 14:4497. doi: 10.1038/s41467-023-40184-2

Wittwer, R. A., Bender, S. F., Hartman, K., Hydbom, S., Lima, R. A. A., Loaiza, V., et al. (2021). Organic and conservation agriculture promote ecosystem multifunctionality. *Sci. Adv.* 7:eabg6995. doi: 10.1126/sciadv.abg6995

Xiong, W., Li, R., Ren, Y., Liu, C., Zhao, Q. Y., Wu, H. S., et al. (2017). Distinct roles for soil fungal and bacterial communities associated with the suppression of vanilla Fusarium wilt disease. *Soil Biol. Biochem.* 107, 198–207. doi: 10.1016/j.soilbio.2017.01.010

Xiong, W., Zhao, Q., Zhao, J., Xun, W., Li, R., Zhang, R., et al. (2015). Different continuous cropping spans significantly affect microbial community membership and structure in a vanilla-grown soil as revealed by deep pyrosequencing. *Microb. Ecol.* 70, 209–218. doi: 10.1007/s00248-014-0516-0

Xiong, W., Zhao, Q. Y., Xue, C., Xun, W. B., Zhao, J., Wu, H. S., et al. (2016). Comparison of fungal community in black pepper-vanilla and vanilla monoculture systems associated with vanilla Fusarium wilt disease. *Front. Microbiol.* 7:117. doi: 10.3389/fmicb.2016.00117

Yang, T., Siddique, K. H. M., and Liu, K. (2020). Cropping systems in agriculture and their impact on soil health-a review. *Glob. Ecol. Conserv.* 23:e01118. doi: 10.1016/j.gecco.2020.e01118

Yang, X., Xiong, J., Du, T., Ju, X., Gan, Y., Li, S., et al. (2024). Diversifying crop rotation increases food production, reduces net greenhouse gas emissions and improves soil health. *Nat. Commun.* 15:198. doi: 10.1038/s41467-023-44464-9

Yarzábal Rodríguez, L. A., Álvarez Gutiérrez, P. E., Gunde-Cimerman, N., Ciancas Jiménez, J. C., Gutiérrez-Cepeda, A., Ocaña, A. M. F., et al. (2024). Exploring extremophilic fungi in soil mycobiome for sustainable agriculture amid global change. *Nat. Commun.* 15:6951. doi: 10.1038/s41467-024-51223-x

Yu, Y., Kang, X., Liu, T., Wang, Y., Tang, J., Peng, W., et al. (2025). Inoculation of the Morchella importuna mycosphere with *Pseudomonas chlororaphis* alleviated a soil-borne disease caused by *Paecilomyces penicillatus*. *Biol. Fertil. Soils* 61, 141–161. doi: 10.1007/s00374-024-01874-1

Yuan, X., Wang, B., Hong, S., Xiong, W., Shen, Z., Ruan, Y., et al. (2021). Promoting soil microbial-mediated suppressiveness against Fusarium wilt disease by the enrichment of specific fungal taxa via crop rotation. *Biol. Fertil. Soils* 57, 1137–1153. doi: 10.1007/s00374-021-01594-w

Yue, H., Sun, X., Wang, T., Zhang, A., Han, D., Wei, G., et al. (2024). Host genotype-specific rhizosphere fungus enhances drought resistance in wheat. *Microbiome* 12:44. doi: 10.1186/s40168-024-01770-8

Zhou, Y., Yang, Z., Liu, J., Li, X., Wang, X., Dai, C., et al. (2023). Crop rotation and native microbiome inoculation restore soil capacity to suppress a root disease. *Nat. Commun.* 14, 8126–8126. doi: 10.1038/s41467-023-43926-4

frontiers | Frontiers in Microbiology

TYPE Original Research
PUBLISHED 27 June 2025
DOI 10.3389/fmicb.2025.1484219

OPEN ACCESS

EDITED BY
Anil K. H. Raghavendra,
Elizabeth Macarthur Agricultural Institute,
Australia

REVIEWED BY
Wensheng Fang,
Chinese Academy of Agricultural Sciences,
China
Rafael Hernández Maqueda,
University of Almeria, Spain
Ana M. Pastrana,
University of California, Agriculture and
Natural Resources, United States

*CORRESPONDENCE
Jose Ignacio Marín-Guirao
✉ josei.marin@juntadeandalucia.es
Miguel de Cara-García
✉ franciscom.cara@juntadeandalucia.es

RECEIVED 21 August 2024
ACCEPTED 10 June 2025
PUBLISHED 27 June 2025

CITATION
Marín-Guirao JI and de Cara-García M (2025)
Native bacteria from a Mediterranean
greenhouse associated to soil health and
suppressiveness.
Front. Microbiol. 16:1484219.
doi: 10.3389/fmicb.2025.1484219

Native bacteria from a Mediterranean greenhouse associated to soil health and suppressiveness

Jose Ignacio Marín-Guirao* and Miguel de Cara-García*

Andalusian Institute of Agricultural and Fisheries Research Training (IFAPA) La Mojonera, Almería, Spain

This study, conducted over two consecutive seasons in an organic-certified Mediterranean tomato greenhouse, aimed to assess the dynamics of soil bacterial composition at pre-planting phase following the incorporation of fresh sheep manure and subsequent solarisation (biosolarisation), as well as at the end of the crop cycle. Gene sequencing using 16S rRNA, and plate culture methods were applied. Additionally, dual culture tests were performed to evaluate the antagonistic activity of 95 soil-isolated bacteria against five soilborne pathogenic fungi and five beneficial fungi sourced from commercial products. Culturable and thermophilic bacterial populations shifted over time, but showed no clear trend. However, alpha diversity was lower at pre-planting phase and increased by the end of the cropping seasons. Significant shifts in beta diversity were also observed across sampling times. Firmicutes showed higher relative abundance at pre-planting phase, while Proteobacteria were consistently more abundant at the end of the cropping season. The genera *Bacillus* and *Thauera* were identified as biomarkers, with *Bacillus* associated with the pre-planting phase and *Thauera* with the end of the cropping seasons (LDA score > 4.5). Among the 52 ecological pathways detected via FAPROTAX database, nitrogen-related functions showed higher presence at the end of the cropping seasons. Isolates with antagonistic activity were detected at all sampling times. The 37.9% of the isolates showed antagonism, 31.6% against phytopathogenic fungi, 20.0% against beneficial fungi, and 12.6% against both. *Colletotrichum gloeosporioides* and *Botrytis cinerea* were the pathogens to which the highest number of isolates showed antagonism, while *Trichoderma asperellum* and *T. atroviride* were among the beneficial ones. Among the native antagonistic bacteria, *Streptomyces* spp. was the dominant genus followed by *Bacillus*. This information highlights how the functional diversity of native bacteria communities from biosolarised soils, may impact the performance of introduced biocontrol microorganisms, as well as the development of natural soil suppressiveness.

KEYWORDS

agroecology, antagonism, biosolarisation, FAPROTAX, DNA metabarcoding, organic amendment, sustainability, *Trichoderma*

1 Introduction

The current trend on intensification in organic and conventional horticultural production systems, underscores the need for effective crop protection and production methods that ensure environmental sustainability (Lal, 2020). In this regard, disease-suppressive soils (DSS) represent a significant achievement toward sustainability. It refers to soils where disease

progression remains minimal, even when soil-borne pathogens and susceptible host plants are present (Baker and Cook, 1974; Schneider, 1982), and is mainly influenced by the intrincate interactions among soil, plant, microbiome and environmental factors (Gómez Expósito et al., 2017; Jayaraman et al., 2021; Sagova-Mareckova et al., 2023). Although the abiotic factors of the soil are believed to play a role, soil biodiversity strongly influences the phenomena through diverse biological mechanisms which are summarized as (Hoitink and Boehm, 1999; Mazzola, 2002; Garbeva et al., 2006; Adesina et al., 2007; Jayaraman et al., 2021): (i) parasitism against pathogens, (ii) production of metabolites, toxins and antibiotics, (iii) competition for nutrients, resources and/or substrates, (iv) activation of disease-resistant genes in the host plant, and (v) improvement of plant nutrition and soil health. In this way, soil microbial community plays a crucial role in the DSS since it is involved in the above mentioned mechanisms (Alabouvette et al., 1993; Mazzola, 2002; Weller et al., 2002; Garbeva et al., 2004; Mazzola and Freilich, 2016; Siegel-Hertz et al., 2018).

Among the native soil microbiota, soil bacteria, including thermophilic bacteria, have been reported as main actors in the suppressiveness of soil-borne diseases in different agricultural soils (Mendes et al., 2011; Gómez Expósito et al., 2017; Schlatter et al., 2017). The composition of the bacterial community is one of the major factors in the mechanism of disease suppression (Hemkemeyer et al., 2024; Kang et al., 2024; Ni et al., 2022), and several bacterial genera including *Bacillus*, *Pseudomonas* and *Streptomyces*, among others, have been proposed as key players in disease suppressiveness of soils (Hoitink et al., 1997; Chng et al., 2015; Xiong et al., 2015; Eberlein et al., 2016). These microorganisms are actively involved in the transformation and decomposition of organic matter (Pankhurst and Lynch, 1995), and the incorporation of organic amendments (OA) can positively impact their communities, improving soil health and enhancing soil disease suppressiveness (Bonanomi et al., 2007, 2010, 2018; Postma and Schilder, 2015; Akanmu et al., 2021), as well as allowing to achieve greenhouse sustainability (Giagnocavo et al., 2022). In addition, OA incorporation impacts on physical and chemical factors that also has an influence on the mechanisms of soil suppressiveness (Amir and Alabouvette, 1993), as well as in greenhouse soil fertility (García-Raya et al., 2019; Marín-Guirao et al., 2019a, 2023a; Castillo-Díaz et al., 2021, 2022). In this regard, the incorporation of fresh organic matter followed by solarisation (i.e., biosolarisation) is an increasing practice in Mediterranean greenhouses, reaching 4.6% of producers in south-eastern Spain during campaign 2019/2020 (García et al., 2024). Biosolarisation is mainly practiced as a soil disinfection technique, but also to promote the decomposition of organic material, what helps to prevent potential phytotoxicity issues that can occur when seedlings are transplanted with fresh, insuficciently decomposed material.

Understanding the impact of soil biosolarisation on the native bacterial community is crucial, as it directly influences community structure and functionality. It is essential to appraises the extent of this impact, and to determine whether bacteria with suppressive properties against phytopathogenic fungi may emerge, following the implementation of such practices. Additionally, evaluating the persistence of these bacteria at the end of consecutive crop cycles is essential, as it is a highly relevant aspect in maintaining crop health (Mendes et al., 2011; Gómez Expósito et al., 2017). Furthermore, given the rising utilization of commercial products containing biological control organisms (BCO) and other beneficial microorganisms for crops, it is highly pertinent to study whether native soil bacteria might also exhibit a suppressive effect on these microorganisms. This currently limited understanding holds substantial significance and is crucial for the efficacy of such products when applied into the soil.

The present study was conducted for two consecutive years in an organic-certified greenhouse with tomato crops. The study aimed to assess the dynamics of soil bacterial composition at pre-planting phase following the incorporation of fresh sheep manure in summer and subsequent solarization (biosolarisation), as well at the finalization of the crop cycle, using 16S rRNA gene sequencing and plate culture methods on soil microbial composition. Additionally, dual culture tests were performed to evaluate the antagonistic activity of 95 soil-isolated bacteria collected at the start and end of the tomato crops against five soilborne pathogenic fungi and five beneficial fungi sourced from commercial products.

2 Materials and methods

2.1 Experimental greenhouse and soil management

The present study was conducted for two consecutive years (the 2019/2020 and 2020/2021 seasons) at the Andalusian Institute for Research and Training in Agriculture and Fisheries (IFAPA) in Almería, Spain (36°48′N, 2°41′W; altitude 142 m), the largest cropping region for Mediterranean greenhouses. The climate in the area is Mediterranean semi-arid, characterized by mild winters and hot summers with no rainfall. The experimental greenhouse, certified for organic production by the Andalusian Organic Farming Committee (C. A. A. E.) since 2006, covered 832 m^2 and was representative of the "raspa y amagado" Mediterranean greenhouse. Two subsequent winter cycles of "Valenciano type" tomato plants (*Solanum lycopersicum* L.), grafted onto Armstrong® rootstock (Syngenta, Basel, Switzerland), were cultivated during 2019/20 and 2020/21 seasons, referred to as season 1 and season 2, respectively. Four-week-old tomato plants were planted on September 17th, 2019, and September 25th, 2020, in seasons 1 and 2, respectively. Prior to planting in both years, fresh sheep manure was uniformly incorporated into the greenhouse soil at a rate of 4 kg m^{-2} in July. Incorporation involved mixing the manure with the soil using a rotavator. Next, drip lines were deplyed and, with the aim of favoring manure's decomposition, the soil was covered with transparent polyethylene film (30 μm TIF Desinfección DS®, Sotrafa, Almería, Spain) for a period of 2 months, after a single irrigation application to reach saturation at 15 cm depth. The maximum, minimum, and average temperatures at 20 cm soil depth during biosolarisation in 2020 were 44.8 ± 0.9, 31.8 ± 0.6, and 39.3 ± 0.3, respectively. Planting occurred 2 days after removing the film. Crop management and pest control practices were adhered to Regulation (EU) 2018/848 on organic production. At the start of the study, the soil consisted of 19% clay, 13% silt, and 68% sand. Soil pH was 8.57, electrical conductivity (EC) 6.19 dS m^{-1}, organic matter content 1.20%, total carbonates (HCO_3^-) 14.33%, active limestone 5.67%, nitric-nitrogen (N) 157 mg L^{-1}, total nitrogen 0.04%, phosphorus Olsen (P Olsen) 19 meq L^{-1}, interchangeable calcium (Ca^{+2}) 1,253 mg L^{-1}, interchangeable sodium (Na^+) 37 mg L^{-1}, interchangeable magnesium

(Mg^{+2}) 261 mg L^{-1}, interchangeable potassium (K^{+}) 1,841 mg L^{-1}, and C/N ratio 20. The soil had no history of soilborne pathogens.

2.2 Soil collection

Soil samples were taken at four different sampling times. During the 2-year study period, samples were collected 2 days before planting (i.e., Start Season 1, 15th September 2019, and Start Season 2, 23rd September 2020) and at the conclusion of the tomato crop season (i.e., End Season 1, 3rd April 2020, and End Season 2, 23rd April 2021). At Start Season 1, soil sampling was conducted in three designated areas of the greenhouse immediately preceding the planting of tomato seedlings. In subsequent sampling times, systematic soil samples were taken in 12 uniformly distributed plots within the greenhouse. The samples were taken with an auger at a depth of 0–30 cm. Three subsamples were randomly taken from cultivation lines and then mixed and homogenized to ensure representativeness in each sample. For each soil sample, one subsample was air-dried and sieved (<0.2 mm) for microbiological analysis through the plate culture method, and another subsample was frozen at −80°C for DNA extraction used in the assessment of bacterial microbiota through DNA metabarcoding.

2.3 Quantification and isolation of soil culturable bacteria and soil thermophilic bacteria

The preparation of soil samples included a drying, grinding, and sieving process, following the method described by Tello et al. (1991). Drying was conducted at room temperature (20–25°C) for a period of 7–10 days, until soil humidity was constant and homogenous. A porcelain mortar was used for grinding, and a 200 μm mesh-size sieve was used for sieving. Both the mortar and sieve were thoroughly washed and disinfected between samples by covering them with alcohol and lighting it. Then, the soil culturable bacteria and thermophilic bacteria were analyzed by means of the serial dilution method (Tello et al., 1991). The culture medium used for bacteria evaluation was nutrient agar (NA, Oxoid, Basingtoke, U. K.). In the case of thermophilic bacteria, soil samples were previously subjected to a heat treatment in an oven at 70°C for 1 h, using a semi-selective medium for actinobacteria (Crawford et al., 1993). This technique was applied to isolate the live thermophilic culturable fraction and to allow the study of its antagonistic activity (see Section 2.5.). In both cases, five subreplicates (9 cm-diameter Petri dishes) of each soil sample were analised at 10^{-5} and 10^{-6} dilutions. The Petri dishes were incubated at 25°C for 7 days. Subsequently, total colony forming units (CFU) of bacteria and thermophilic bacteria were quantified, eventually expressing the results as CFU/g dry soil.

2.4 Assessment of bacterial microbiota through DNA metabarcoding

2.4.1 Soil DNA extraction, amplicon high-throughput sequencing, and processing of sequencing data

DNA from soil samples was isolated using the DNeasy PowerSoil Pro DNA isolation kit (Qiagen, Hilden, Germany), strictly following the manufacturer's instructions. An extraction blank for cross-contamination was included. DNA was quantified using the Qubit High Sensitivity dsDNA Assay (Thermo Fisher Scientific, Waltham, MA, United States). For bacterial library preparation, a fragment of the 16S genomic region (of about 460 bp) was amplified using the primers Bakt_341F (5′ CCT ACG GGN GGC WGC AG 3′) and Bakt_805R (5′ GAC TAC HVG GGT ATC TAA TCC 3′) (Herlemann et al., 2011). Illumina sequencing primers were attached to these primers at their 5′ ends. Polymerase chain reactions (PCRs) were carried out in a final volume of 12.5 μL, containing 1.25 μL of template DNA, 0.5 μM of the primers, 3.25 μL of Supreme NZYTaq 2x Green Master Mix (NZYTech, Lisbon, Portugal), and ultrapure water up to 12.5 μL. The reaction mixture was incubated as follows: an initial denaturation step at 95°C for 5 min, followed by 25 cycles of 95°C for 30 s, 50°C for 45 s, 72°C for 45 s, and a final extension step at 72°C for 7 min. A negative control that contained no DNA (BPCR) was included in every PCR round to check for contamination during library preparation. The libraries were run on a 2% agarose gel stained with GreenSafe (NZYTech) and imaged under UV light to verify the library size. Libraries were purified using the Mag-Bind RXNPure Plus magnetic beads (Omega Biotek, Beijing, China), following the instructions provided by the manufacturer. Then, libraries were pooled in equimolar amounts according to the quantification data provided by the Qubit dsDNA HS Assay (Thermo Fisher Scientific). This pool also contained a testimonial amount (1 μL) of the PCR blank and DNA extraction blank (Bex). The pool was sequenced in the MiSeq PE300 run (Illumina). DNA metabarcoding analyses were carried out by AllGenetics & Biology S. L. (La Coruña, Spain; www.allgenetics.eu). Illumina paired-end raw forward (R1) and reverse (R2) FASTQ reads were stored in separate files. The quality of the FASTQ files was checked with the software (v0.11.9) FastQC (Andrews, 2010) and the output was summarized using MultiQC (Ewels et al., 2016). The obtained amplicon reads were processed using QIIME 2 (release 2022.2) (Bolyen et al., 2019). Specifically, the tool DADA2 (Callahan et al., 2016) (implemented in QIIME 2) was used to remove the PCR primers, filter low-quality reads, denoise, merge the forward and reverse reads, remove the chimeric reads, and cluster the resulting sequences into amplicon sequence variants (ASVs). The resulting output of the DADA2 pipeline was a table containing the number of occurrences of every observed ASV in each sample. The taxonomic assignment of ASVs was conducted using a pre-trained classifier of the SILVA reference database (Quast et al., 2013) (updated in August 2020). Specifically, the feature-classifier classify-sklearn approach implemented in QIIME 2 (Bokulich et al., 2018) was employed. The following ASVs were excluded: singletons (i.e., ASVs containing only one member sequence in the whole dataset), ASVs occurring at a frequency below 0.01%, non-bacterial ASVs such as eukaryotic sequences of chloroplast (Moore et al., 2019) and mitochondrial (Emelyanov, 2001) origin, unidentified sequences, and sequences assigned only at the kingdom level. The final filtered ASV table was converted into a Biological Observation Matrix (biom) file that was directly imported into R 3.6.1 (R-Team-Core, 2019) using the package phyloseq 1.24.2 (McMurdie and Holmes, 2013). The final filtered ASV and the biom file were used for further analysis and plotting.

2.4.2 Bacterial community description and data processing

Four indexes of biodiversity were selected to study the alpha diversity of the bacterial community of each sample: Margalef genus

richness (d) (Margalef, 1958); the Shannon–Wiener diversity index (H′) log basis (Shannon and Weaver, 1949); Pielou's evenness (J) (Pielou, 1969) of the distribution of individuals among genera; and Simpson's dominance (D) (Simpson, 1949). All calculations were carried out with the software PRIMER version 6.0 (Primer-E Ltd., Plymouth, U. K.) for Windows (Clarke and Gorley, 2006). Regarding beta diversity, bacterial community data at the operational taxonomic unit (OTU) level through DNA metabarcoding evaluation method, were compared among sampling times using permutational analysis of variance (PERMANOVA). Also, pairwise PERMANOVA comparisons were performed. These tests calculate Pseudo-F statistics to obtain *p*-values (Anderson, 2001). All PERMANOVA tests used 9,999 permutations from unrestricted permutations of raw data. Previously, data were square root transformed. The calculation of similarity matrices in the PERMANOVA analysis was based on Bray–Curtis distance. In addition, principal coordinate analysis (PCoA) was used to visualize the potential differences in the soil bacterial community structure among sampling times or within sampling times. PERMANOVA and PCoA analyses were performed using the multivariate statistical software package PRIMER-6 with the PERMANOVA+ extension (Primer-E Ltd., Plymouth, UK) for Windows. The linear discriminant analysis effect size (LEfSe) algorithm (Segata et al., 2011) was generated from Python (version 3.12) and used to identify and compare unique bacterial taxa significantly related to any of the four sampling times (Start Season 1, End Season 1, Start Season 2, End Season 2). In addition, data from Start Season 1 and Start Season 2, as well as those from End Season 1 and End Season 2, were pooled in order to identify and compare unique bacterial taxa significantly related to Start Season and End Season, respectively. The threshold for the logarithmic linear discriminant analysis (LDA) score was established at 4.5 and the Wilcoxon *p*-value was set at 0.05.

Bacterial functional potential was investigated using Functional Annotation of Prokaryotic Taxa (FAPROTAX) database (Louca et al., 2016). FAPROTAX is a database that categorizes bacterial taxa into recognized metabolic or ecologically significant groups (considered as functional groups), utilizing current literature on cultured strains as a reference. Following the procedure of Vido et al. (2024), previously bacterial ASVs was filtered to reduce noise (i.e., removal of those with <10 counts). In addition, filtering was completed by removing functional groups with reads abundances ≤100. The abundances of each taxa assigned to an functional group were pooled to form a total relative abundance count for each group, and the abundances of unassigned taxa were excluded. Then, the diversity and composition of ecological groups within each sampling time were compared and contrasted using the same method outlined for taxonomy beta diversity. Thus, PERMANOVA, pairwise PERMANOVA and PCoA were conducted on the top 15 ecological groups to focus on the most relevant ecological pathways. In addition, LEfSe was performed to detect differentially abundant ecological pathways across groups of soil samples depending on sampling time (LDA score established at 3).

2.5 *In vitro* antagonism toward phytopathogenic and beneficial fungi

2.5.1 Strains isolation and target fungi

The isolates used in the antagonism assays were obtained from the thermophilic bacteria analyses described in section 2.3. Following the evaluation specified in that section, colonies from soil samples taken at different sampling times were randomly selected and isolated on Petri dishes with 15 mL of NA medium. Eleven isolates from Start Season 1, 51 from End Season 1, and 33 from Start Season 2 were selected. Thus, the antagonistic activity of 95 soil-isolated bacteria against nine fungi and one oomycete (*Phytophthora capsici*), referred to as fungi throughout the rest of the document, was studied. Specifically, the evaluations were conducted against five soilborne pathogenic fungi, as well as five beneficial fungi sourced from commercial products (Table 1).

2.5.2 Dual culture protocol

Dual culture tests on Potato Glucose Agar (PGA, Oxoid, Basingtoke, U. K.) were performed to evaluate the antagonistic activity of soil-isolated bacteria against the ten target fungi (Table 1). Plates (9 cm diameter), which contained 15 mL of PGA, were inoculated with strain culture by streak and incubated at 25 ± 1°C in the dark for 8 days. Later, a 5-mm-diameter disk of the target fungi was placed at an equidistant distance between the bacteria and the edge of the plate. The disk was obtained from the edge of the colony where the growth is most active. The initial distance between the bacteria and the fungus was 3.25 cm, and the bacteria were streaked up to 2 cm from the edge of the plate. The plates containing the bacteria and the fungus in confrontation were sealed and incubated at 25 ± 1°C in darkness until the fungus reached the edge of the plate opposite to the bacteria. At this point, measurements were performed. The distance between the edge of the bacterial growth and the edge of the fungal colony (inhibition distance) was measured. The approximate incubation times varied depending on the target fungus: 3–4 days for *Botrytis cinerea*, *Trichoderma longibrachiatum*, *Trichoderma harzianum* T-22, and *Trichoderma atroviride*, 7–8 days for *Fusarium oxysporum* f. sp. *radicis-cucumerinum* (FORC), *Fusarium proliferatum*, *Colletotrichum gloeosporioides*, and *Trichoderma asperellum*, and 7–10 days for *Phytophthora capsici*, while *Paecilomyces lilacinus* exhibited the slowest growth, taking 20–30 days until measurement. Antagonistic activity

TABLE 1 Phytopathogenic and beneficial fungi used in dual culture tests and origin of the strains.

Target fungi used in the *in vitro* antagonism assays	Code	Origin
Pathogenic fungi		
Colletotrichum gloeosporioides	Cg	Marín-Guirao et al. (2023b)
Fusarium proliferatum	Fp	Brizuela et al. (2020)
Fusarium oxysporum f. sp. *radicis-cucumerinum*	Forc	Águila-Carricondo et al. (2024)
Botrytis cinerea	Bc	Marín-Guirao et al. (2023b)
Phytophthora capsici	Pc	Águila-Carricondo et al. (2024)
Beneficial fungi		
Trichoderma harzianum T-22	Th	Koppert B. V.
Trichoderma longibrachiatum	Tl	BIOMIP S. L.
Trichoderma asperellum	Ta1	Certis Europe B. V.
Trichoderma atroviride	Ta2	Certis Europe B. V.
Paecilomyces lilacinus	Paec	Certis Europe B. V.

was considered when the inhibition distance was equal to or greater than 4 mm to any of the target fungus, and additionally, the growth of the target fungi did not continue after the 5-day observation period. Five replicates were prepared for each combination bacteria-fungi.

2.5.3 Identification of soil-isolated bacteria with suppressive properties

The isolates that showed antagonistic activity were analyzed by means of PCR sequencing of amplicons of the 16S rRNA gene using the primers 27F-1492R (Condori et al., 2019) and subsequent database searches using BLASTN software, based on the consensus sequences created by aligning the forward and reverse sequences of the target isolates. The PCR conditions were 5 min at 94°C, 35 cycles of 1 min at 94°C, 1 min at 55°C, 2 min at 72°C, and a final elongation of 7 min at 72°C. Purified PCR products were sequenced using the Sanger sequencing method (Instituto de Biología Molecular y Celular de Plantas, Valencia, Spain) and edited via base calling on the BioEdit program (Hall, 1999).

2.6 Statistical analysis

Data on the total culturable bacteria and thermophilic culturable bacteria populations, sequencing depth for the 16S library, the relative abundance of dominant bacterial phyla and genera, and the indices of biodiversity were analyzed via an analysis of variance (one-way ANOVA) to compare differences among sampling times. Previously, normality and homoscedasticity were tested using the Shapiro–Wilk and Levene tests, respectively. The Kruskal–Wallis one-way non-parametric test ($p = 0.05$) was performed when normality or homoscedasticity of data was not evident ($p < 0.05$ Shapiro–Wilk or Levene tests, respectively). Arcsine square root transformation was applied to percentages before analyses. Duncan's *post hoc* test was then applied to perform a pairwise comparison between sampling times at a 95% confidence level. These statistical analyses were carried out using the statistical software package Statgraphics Centurion XIX (Statgraphics Technologies, Inc., The Plains, VA, United States) for Windows (Microsoft Corporation, WA, United States).

3 Results

3.1 Taxonomic compositions of the bacterial communities

The total culturable bacteria population exhibited values ranging from 2,920,000 to 24,200,000 CFU/g dry soil depending on the sampling time (Figure 1). The highest values were observed at the end of Season 1, which showed significant differences ($p < 0.001$) compared to the other sampling times. For thermophilic culturable bacteria, the population ranged from 2,170,000 to 11,300,000 CFU/g dry soil. In this case, the population was lower at the beginning of Season 1 ($p < 0.05$) compared to the other sampling times (Figure 1).

Figure 2 illustrates the relative abundance of different microbial phyla (Figures 2A,B) and genera (Figures 2C,D) at the start and at the end of the two seasons. Regarding phyla, Proteobacteria dominated in both start and end seasons, with a significant increase ($p < 0.001$) from 28.6% at the start to 52.3% at the end in season 1, and from 17.6% at the start to 32.6% at the end in season 2. Firmicutes showed an increase from 7.8% in start season 1 to 30.1% in start season 2, followed by a decrease to 16.3% in end season 2 ($p < 0.001$). Actinobacteriota also showed fluctuations ($p < 0.001$), peaking at 13.5% in end season 2. Acidobacteriota, Gemmatimonadota, Methylomirabilota, and Myxococcota showed the highest relative abundance in start season 1 ($p < 0.001$). Other phyla, such as Bacteroidota, Planctomycetota, Patescibacteria, Chlorofexi displayed varying patterns but maintained presence throughout the two seasons.

Similarly, the relative abundance of bacterial genera varied across seasons (Figure 2D). *Thauera* experienced increase in both seasons, rising from 0.09 to 18.55% in Season 1 and from 0.03 to 7.80% in Season 2. In contrast, *Bacillus* showed decrease, dropping from 5.74 to 0.69% in Season 1 and from 19.68 to 8.36% in Season 2. Other notable trends include MND1, which increased from 1.00 to 2.00% in Season 1. Some genera, like *Pseudomonas*, exhibited notable fluctuations, with a peak of 2.26% in End Season 1. Others, such as *Streptomyces, Dongia* and SWB02 showed sporadic occurrences throughout the seasons, with values ranging from 0.09 to 1.09%. All genera, except *Acidibacter*, showed significant differences among sampling times ($p \leq 0.01$) with no common pattern among them.

3.2 Alpha diversity of soil bacterial community

Generally, the alpha diversity indices showed significant differences among different sampling times ($p < 0.01$), except for the Dominance-Simpson index (Figures 3A–D). Thus, species richness (Margalef index) was higher at the end of the crop in both years compared to values at the start of the crops ($p = 0.0000$), with average values ranging from 53.30 ± 7.01 to 37.59 ± 3.99 (Figure 3A). The Evenness-Pielou Index did not offer this trend, showing higher values at the start and end of the study compared to values at the start of the second year ($p = 0.0064$), although these differences were not detected at the end of the crop in year 1. In the case of the Diversity-Shannon index, values were lower at the start of the crop in year 2 compared to

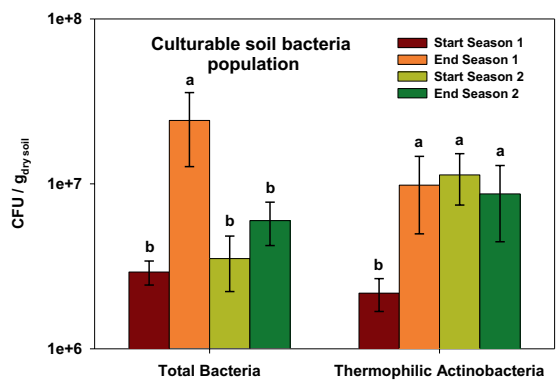

FIGURE 1
Total Colony Forming Units (CFU) of soil culturable bacteria and thermophilic bacteria at the start and at the end of season 1 (2019/20) and season 2 (2020/2021). In each case, different letters denote significant differences between sampling times at $p \leq 0.05$ (Duncan's test).

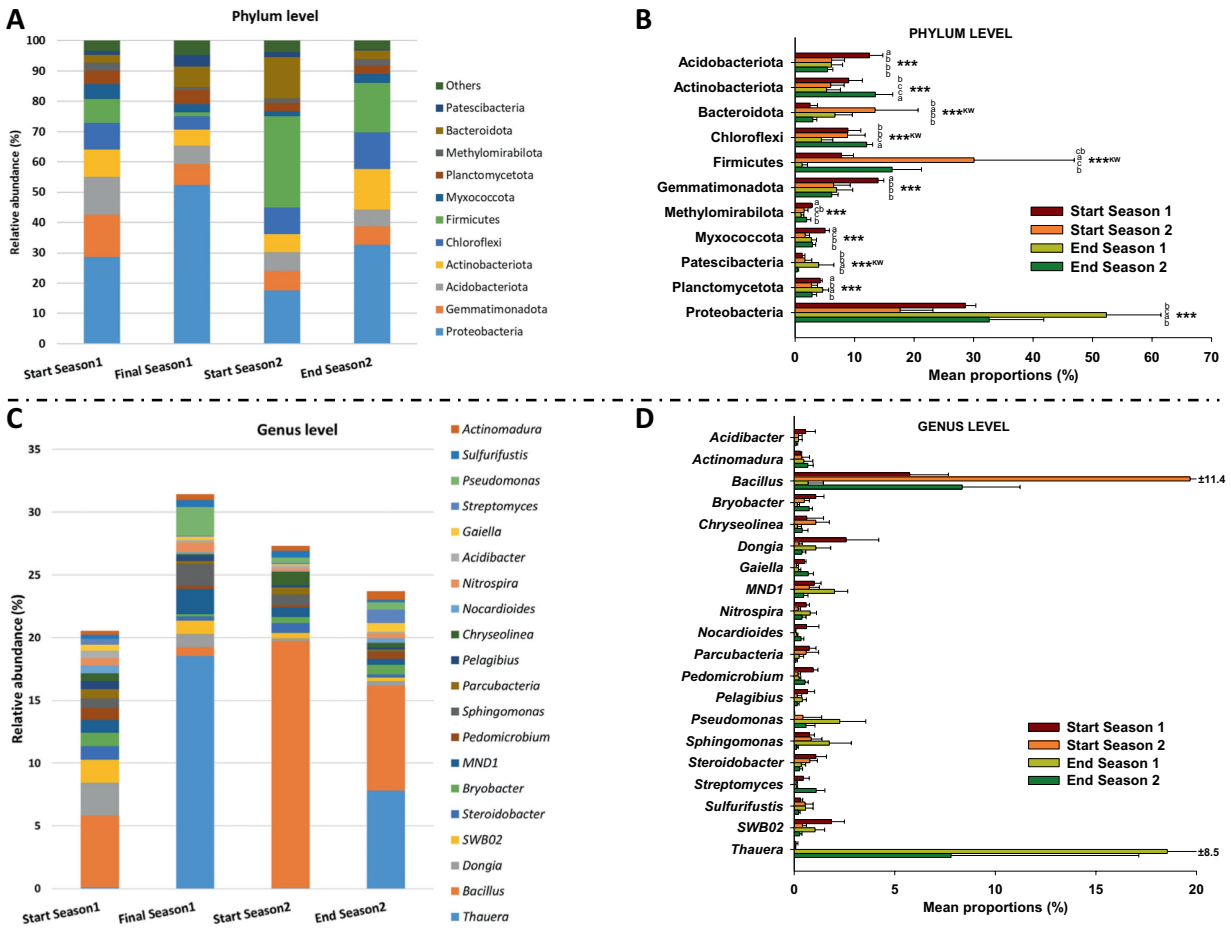

FIGURE 2
Bacterial community data found in the soil by 16S RNA sequencing. Relative abundance (%) of dominant bacterial phyla **(A,B)** and genera **(C,D)** divided into the start and end of the 2 years (seasons). "***" indicates significance at $p \leq 0.001$ (Duncan's test). "KW" p-value through the Kruskal–Wallis non-parametric test. Note: All genera in **(D)**, except *Acidibacter* sp., showed significance at $p \leq 0.01$ through the Kruskal–Wallis non-parametric test.

the other time points considered ($p = 0.0007$), with average values ranging from 4.35 ± 0.41 to 5.07 ± 0.35.

3.3 Beta diversity of soil bacterial community. Comparison of soil bacterial community structure among sampling times

The global PERMANOVA test indicated a significant effect (Pseudo-$F = 9.6531$, $p < 0.0001$) of the sampling time on bacterial communities' beta diversity. In addition, pairwise tests revealed significant differences between bacterial communities across different seasons (Supplementary Table S1). Notably, comparisons between the start and end of each year exhibit considerable dissimilarities ($p < 0.003$). However, comparisons between the different sampling times highlight significant variations in bacterial composition in all cases ($p < 0.0001$).

Principal coordinates analysis (PCoA) further supports the statistical findings of the PERMANOVA analysis. The PCoA results show that the PCoA1 and PCoA2 explained 29.6 and 13.2% of the difference in the compositions of the bacterial communities among samples (Figure 4). The results of PCoA showed that the bacterial communities in the samples of the four different sampling time had a discrete distribution, with relatively large distances among the samples of each moment and a clear clustering of samples from each time.

3.4 Compositional differences and biomarkers of the bacterial communities

LEfSe analysis identified biomarkers that caused significant differences among the four sampling times (Figure 5). A total of 5, 10, 5, and 2 biomarkers (LDA score > 4.5) were identified in the soil bacterial community analyzed by means of DNA metabarcoding at the Start Season 1, Start Season 2, End Season 1 and End Season 2, respectively.

When data from the 2 years of study are pooled based on whether they come from soil samples taken at the start or at the end of the seasons, a total of 9 and 5 biomarkers were identified at the beginning and end of the crop, respectively (Figure 6). Thus, the phylum Firmicutes, class Bacilli, order Bacillales, family Bacillaceae, and genus

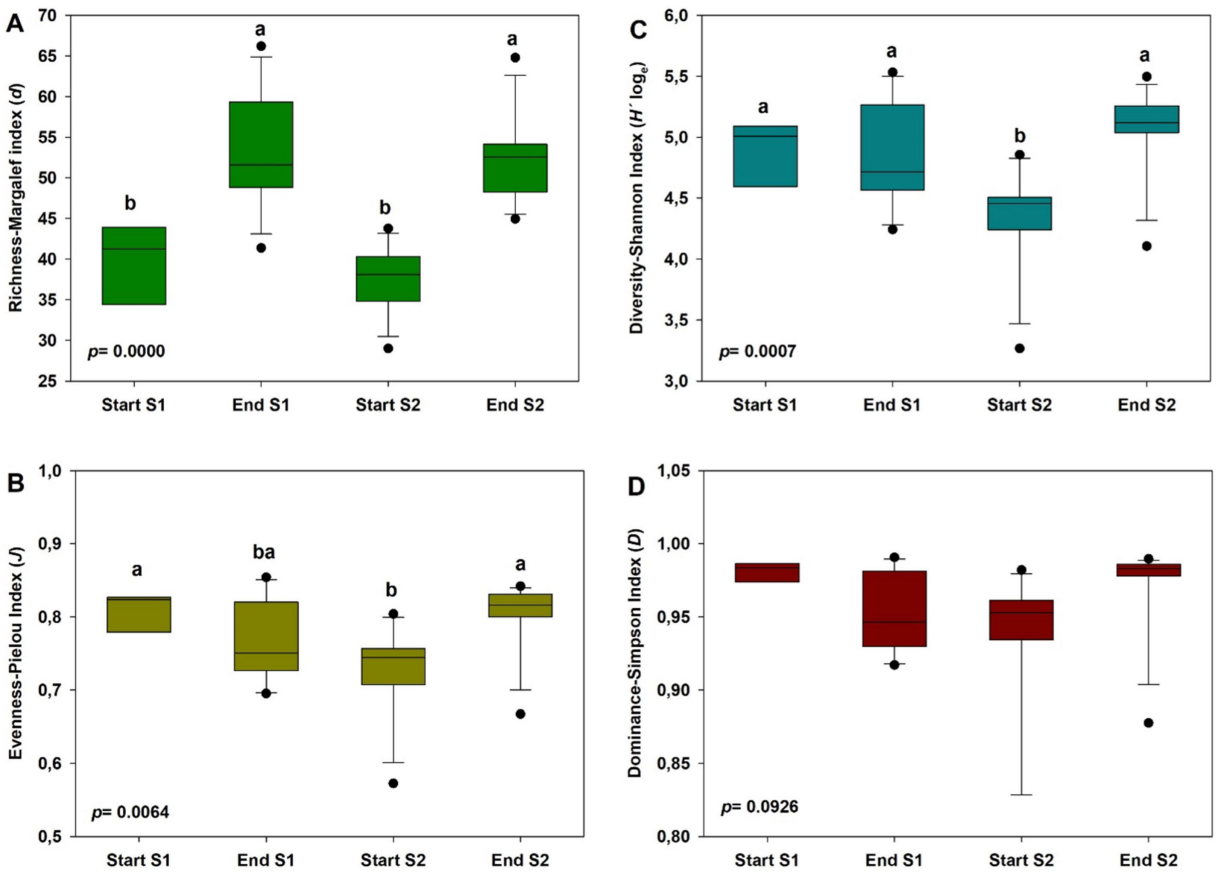

FIGURE 3
Alpha diversity indices of soil bacterial community at the start and at the end of season 1 (S1; 2019/20) and season 2 (S2; 2020/2021): Margalef richness index **(A)**, Shannon–Wiener diversity index **(B)**, Pielou's evenness index **(C)** and Simpson's dominance index. In each case, different letters denote significant differences between sampling times at $p \leq 0.01$ (Duncan's test).

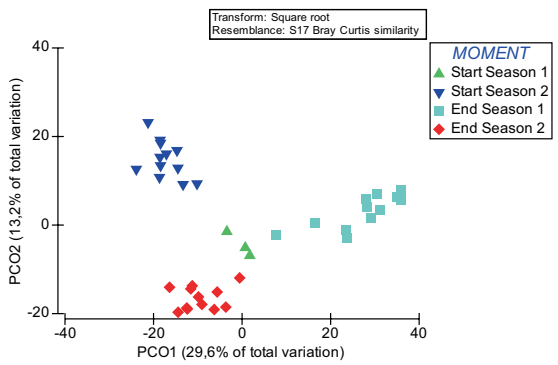

FIGURE 4
Principal coordinate analysis (PCoA) of the influence of sampling time on the beta diversity of soil bacterial communities. Over the 2 years of the study, soil samples were taken at the start of the crop (Start Season: after incorporating fresh sheep manure in summer followed by solarisation) and at the end (End Season).

Bacillus, along with the class Rhodothermia, order Rhodothermales, family Rhodothermaceae, and an uncultured genus, were the biomarkers identified at the start of the crop. Whereas at the end of the crop, they were the phylum Proteobacteria, class Gammaproteobacteria, order Burkholderiales, family Rhodocyclaceae, and genus *Thauera*.

3.5 Soil bacterial function prediction

The abundances of different bacterial functional pathways were predicted using the FAPROTAX database.

3.5.1 Functional annotation overview based on 16S rRNA data

From a total sequencing reads average per sample of 56,976, an average of 29,763 reads per sample received functional assignment to any of the 52 functional groups detected via FAPROTAX database. This represents 45 ± 23.4% of the total sequencing reads. Considering the percentage of readings assigned to functionality at the different sampling times, the highest value was observed in the End Season 1 (68.9 ± 15.7%), which showed differences compared to the other sampling moments ($p \leq 0.001$; Duncan's test), including End Season 2, which presented an average value of 50.4 ± 14.4%. It is noteworthy that the lowest values were detected at the Start Season in both years of study, with values of 22.0 ± 4.2% and 21.4 ± 5.8% in Season 1 and Season 2, respectively.

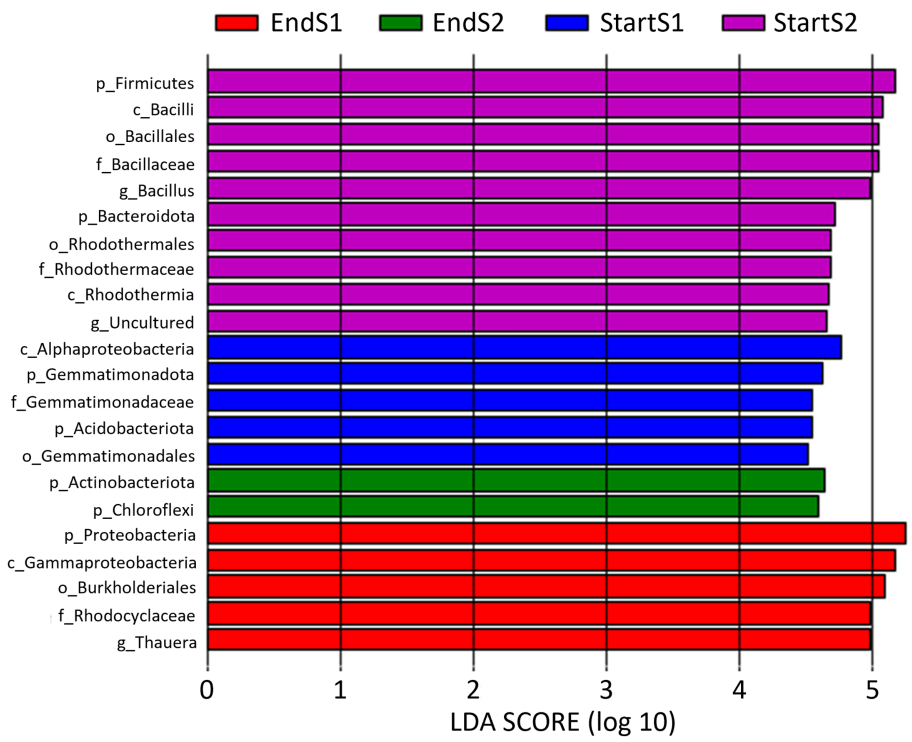

FIGURE 5
Linear discriminant analysis (LDA) to detect differentially abundant taxa across groups of soil samples depending on sampling time: start and end of season 1 (S1; 2019/20) and season 2 (S2; 2020/2021). Only taxa with an LDA score >4.5 ($p < 0.05$) are shown.

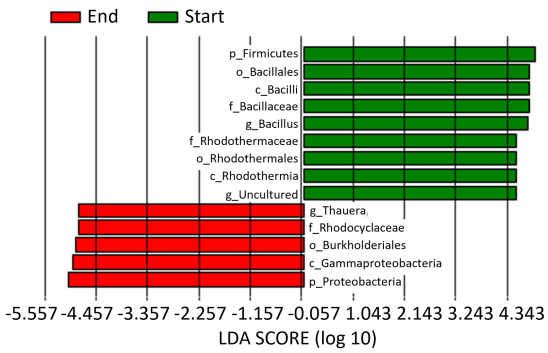

FIGURE 6
Linear discriminant analysis (LDA) to detect differentially abundant taxa across groups; only taxa with an LDA score >4.5 ($p < 0.05$) are shown. Data from the 2 years of study are pooled based on whether they come from soil samples taken at the start (Start) or at the end (End) of the seasons.

3.5.2 Dominant functional groups and their temporal distribution

Based on the FAPROTAX database, the top 15 functional groups which represented an average of 97.1 ± 2.2%, 87.2 ± 15.5%, 95.2 ± 2.7% and 92.7 ± 6.3% of the total sequencing reads assigned to functionality of Start Season 1, Start Season 2, End Season 1 and End Season 2 soil samples, respectively, were obtained. The relative proportion (i.e., percentage) of these top 15 functional groups across all sampling times is showed as a heatmap (Figure 7). In all sampling times, chemoheterotrophy emerges as the primary ecological pathway, representing more than 20% of the sequences in all cases, and surpassing 50% in some of them. This is followed by aerobic chemoheterotrophy, which similarly exhibits values above or close to 20%. It is remarkable that no entry was found for group "plant pathogen." Figure 7 represents similarities in the relative abundance of the 15 bacterial functional groups within the soil bacterial communities at each sampling time, particularly between Start Season 1 and Start Season 2, as well as between End Season 1 and End Season 2. Nitrogen respiration, nitrate respiration, nitrite respiration, and nitrate reduction are observed with higher relative abundance in the samples from End Season 1 and End Season 2, whereas Fermentation emerges as the ecological pathway that appears to be more relevant in the samples from Start Season 1 and Start Season 2. In this regard, When the global PERMANOVA test was conducted, a significant main effect (Pseudo-$F = 31.467$, $p < 0.0001$) of sampling time on the composition of functional groups was detected (Supplementary Table S2). However, the only case where pairwise PERMANOVA tests did not find significant differences was between the samples from Start Season 1 and Start Season 2. Principal Coordinates Analysis supported the statistical findings of the PERMANOVA analysis. In this case, the PCoA results indicated that PCoA1 and PCoA2 explained 80.3 and 7.5% of the differences in compositions and diversity of the bacterial functional groups (Figure 8). The results of PCoA showed that the functional bacterial groups in the samples of the four different sampling time had a discrete distribution, with relatively large distances among the samples of each moment and a clear clustering of samples from each sampling time, except for the samples from Start Season 1 and Start Season 2, which exhibited mixing. Although pairwise PERMANOVA tests found differences between End Season 1 and End Season 2, the PCoA

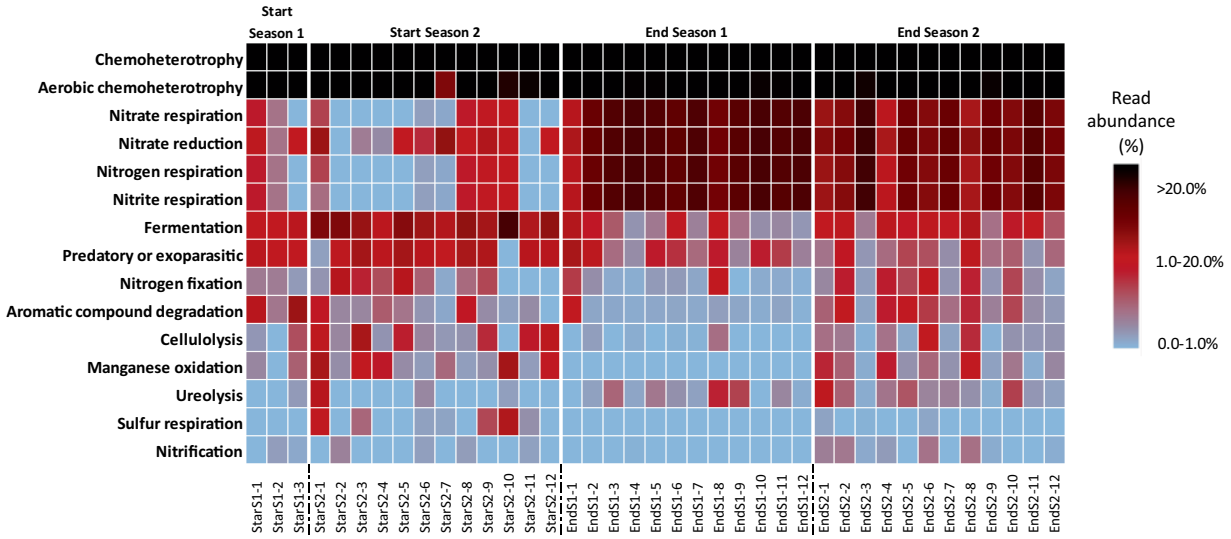

FIGURE 7
Relative abundance heat map showing the relative abundance of 15 bacterial functional groups within the bacterial communities found in the soil at each sampling time. Functional groups were normalized within each sample via total sum scaling resulting in a color scale denoting the proportion within each sample.

results showed all samples from End Season of both years separated from those of Start Season of both years along PCoA1.

3.5.3 Differential functional pathways identified by LEfSe

LEfSe analysis identified a total of 13 functional pathways that caused significant differences (LDA score > 3) among the four sampling times (Figure 9): Aromatic compound degradation, Chemoheterotrophy and aerobic chemoheterotrophy at Start Season 1; fermentation, predatory or exoparasitic, manganese oxidation, cellulolysis y Sulfur respiration at Start Season 2, nitrogen, nitrate and nitrite respiration and nitrate reduction at End Season 1, and ureolysis at End Season 2.

When data from the 2 years of study are pooled based on whether they come from soil samples taken at the start or at the end of the seasons, a total of 6 and 5 markers were identified at the start and end of the season, respectively (Figure 10). Thus, Chemoheterotrophy, fermentation, predatory or exoparasitic, manganese oxidation, cellulolysis and sulfur respiration were the biomarkers identified at Start Season, while nitrogen, nitrate and nitrite respiration, nitrate reduction and ureolysis at End Season.

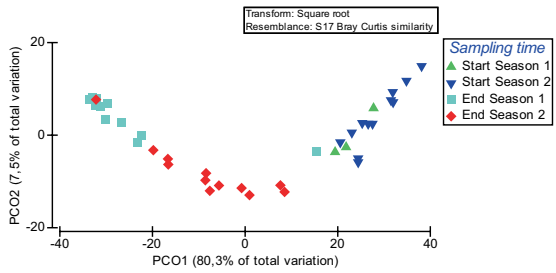

FIGURE 8
Principal coordinate analysis (PCoA) of the influence of sampling time on the composition and diversity of the top 15 bacterial functional groups. Over the 2 years of the study, soil samples were taken at the start of the crop (Start Season: after incorporating fresh sheep manure in summer followed by solarisation) and at the end (End Season).

3.6 Antagonistic bacteria against the *in vitro* growth of phytopathogenic and beneficial fungi

In total, out of the 95 isolates tested, 36 of them (37.9%) showed antagonism, 30 (31.6%) against phytopathogenic fungi, 19 (20.0%) against beneficial fungi, and 12 (12.6%) against both (Table 2; Figure 11). *Colletotrichum gloeosporioides* and *Botrytis cinerea* were the pathogenic fungi against which the highest number of isolates showed antagonism, with 58.3 and 41.7% of the isolates showing antagonism, respectively. Meanwhile, *Trichoderma asperellum* and *T. atroviride* were prominent among the beneficial fungi, with 33.3 and 25.0% of the isolates, respectively. Only 8.3% exhibited antagonism against *F. proliferatum* and Forc, while *T. longibrachiatum* and *Paecilomyces lilacinus* were the fungi with the least antagonistic response, with only 1 and 2 isolates (2.8 and 5.6%), respectively. Depending on the sampling time, 36.4% of the isolates from Start Season 1, 54.9% of the isolates from End Season 1, and 22.2% of the isolates from Start Season 2 exhibited antagonism against target fungi. All isolates were identified through PCR (16S rRNA): *Streptomyces* spp. (26), *Bacillus* spp. (4), *Brevundimonas* spp. (2), *Pseudochrobactrum* spp. (2), *Stenotrophomonas* sp. (1), *Alcaligenes* sp. (1).

4 Discussion

In this study, the total culturable bacterial populations and thermophilic culturable bacteria experienced shifts depending on the

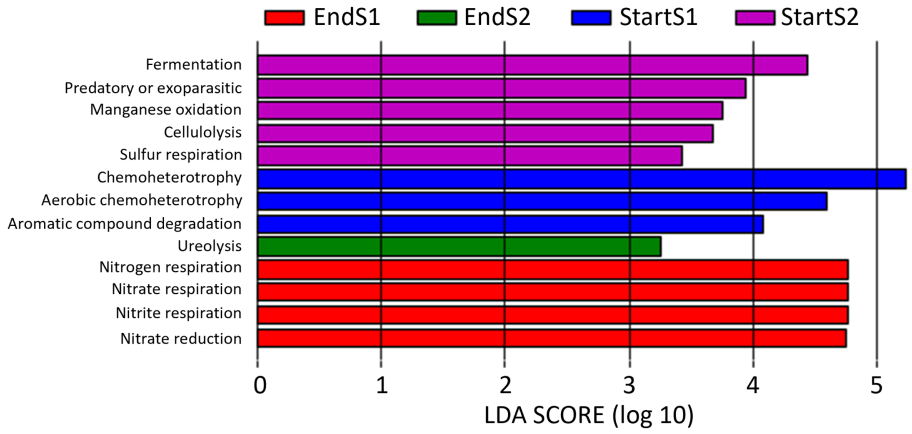

FIGURE 9
Linear discriminant analysis (LDA) to detect differentially abundant ecological pathways across groups of soil samples depending on sampling time: start and end of season 1 (S1; 2019/20) and season 2 (S2; 2020/2021). Only ecological pathways with an LDA score >3 ($p < 0.05$) are shown.

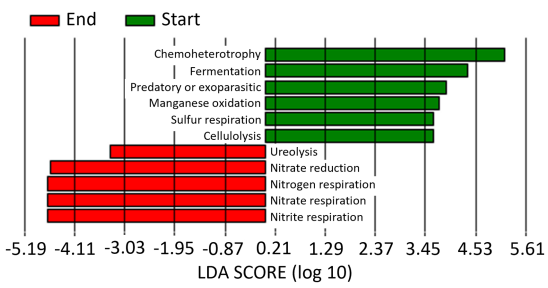

FIGURE 10
Linear discriminant analysis (LDA) to detect differentially abundant ecological pathways across groups; only ecological pathways with an LDA score >3 ($p < 0.05$) are shown. Data from the 2 years of study are pooled based on whether they come from soil samples taken at the start (Start) or at the end (End) of the seasons.

sampling time, but no clear trend was observed and the impact on these bacterial fractions population cannot be conclusively attributed to the treatments. In this regard, it's important to consider that changes in soil quality parameters and sampling time are factors that highly influence microbial variations, particularly in cultivated and amended soils (Li et al., 2018; Vido et al., 2024).

A noticeable outcome of the study is the dynamics of the bacterial communitys alpha diversity throughout the crop season. Primarily, species richness (Margalef index), but also Shannon diversity and Pielou's evenness indices, appeared lower at pre-planting phase (Start Season), meanwhile at the end of the cropping seasons, all alpha diversity indices tended to increase and consistently reach higher values. In addition, significant changes in bacterial community beta diversity were recorded across the different sampling times (PERMANOVA $p < 0.01$). In this sense, changes in the soil microbial community have been previously reported after the application of manure in crop fields (Hartmann et al., 2015; Sun et al., 2015; Tang et al., 2023), as well as after solarisation treatments when manure and other organic amendments had been previously incorporated (Achmon et al., 2020; Marín-Guirao et al., 2019b, 2023a; Shea et al., 2022). According to Vido et al. (2024) our results also highlight the dynamic nature of bacterial community composition over time at phylum and genus level when soils are amended with organic materials and organic crop management. In any case, Proteobacteria and Firmicutes were the most prevalent phyla in all sampling times. These two phyla, along with Actinobacteriota, are consistently associated with soil-borne disease suppression (Raaijmakers et al., 2009; Mendes et al., 2011).

In our study, the relative abundance of Firmicutes was higher at pre-planting phase (Start Season) compared to End Season, contrary to Proteobacteria, which consistently showed higher levels at the End Season in both years. Thus, *Bacillus* (phylum Firmicutes) was identified as a biomarker in Start Season, while *Thauera* (phylum Proteobacteria) was the biomarker at the genus level in End Season. These are biomarkers indicating a superior ability to discriminate between the studied conditions and a higher statistical significance and relevance for the study (LDA score >4.5). *Bacillus* is a widely studied genus for its suppressive properties against soil pathogens (Miljaković et al., 2020; Zhang et al., 2023). However, bacteria of the genus *Thauera* have been biotechnologically interesting for their ability to degrade aromatic compounds (Elder and Kelly, 1994; Philipp and Schink, 2000), and more recently for their role in the production of a promising alternative to non-degradable plastics (Koller et al., 2017). To the best of our knowledge, *Thauera* has not been reported to have capabilities for controlling soil pathogens. The observed changes in the abundances of these two genera may have been influenced by the high temperatures reached during the solarization process that followed the incorporation of the organic amendment (Pullman et al., 1981). While, *Bacillus* spp. are recognized thermophilic bacteria (Edwards et al., 1965; Bond and Favero, 1975), most *Thauera* species are recognized as mesophilic bacteria (Fida et al., 2016), although a thermophilic *Thauera* species has been also reported (Yang et al., 2018). In fact, the treatments did not completely eliminate *Thauera* bacteria but maintained a viable inoculum capable of recolonizing the soil during the crop season. In this regard, the incorporation of an organic amendment rich in nitrogen, such as fresh sheep manure, could favor the presence of these bacteria in the studied soil. Both bacteria genera are active

TABLE 2 Antagonistic activity of soil-isolated bacteria at different sampling times against phytopathogenic and beneficial fungi, and their identification through polymerase chain reaction (PCR) sequencing of amplicons of the 16S rRNA gene.

	Inhibition zone (mm)											
	Pathogenic fungi					Beneficial fungi						
Strain	Forc	Fp	Pc	Botry	Cg	Tl	Th	Ta1	Ta2	Paec	Soil sampling time origin	Identification
20/02-1								6.2 ± 1.6			Start S1	*Bacillus* sp.
20/02-4				5.4 ± 0.5				11.8 ± 1.3			Start S1	*Streptomyces* sp.
20/02-11								4.6 ± 1.1			Start S1	*Alcaligenes* sp.
20/02-22								4.8 ± 1.8			Start S1	*Stenotrophomonas* sp.
20/02-31								4.2 ± 1.6			End S1	*Bacillus* sp.
20/02-33				2.8 ± 0.8	3.0 ± 0.7			7.0 ± 1.2	6.2 ± 2.3		End S1	*Streptomyces* sp.
20/02-35								4.4 ± 1.1			End S1	*Streptomyces* sp.
20/02-39					6.8 ± 1.9			4.0 ± 1.4			End S1	*Streptomyces* sp.
20/02-41	4.6 ± 0.5	3.6 ± 0.9			5.4 ± 1.5						End S1	*Streptomyces* sp.
20/02-48	5.6 ± 0.9	4.0 ± 0.7			9.4 ± 2.3			3.2 ± 0.8		5.0 ± 1.9	End S1	*Streptomyces* sp.
20/02-54				5.0 ± 2.0	3.2 ± 0.8						End S1	*Streptomyces* sp.
20/07-2				8.6 ± 1.9							End S1	*Streptomyces* sp.
20/07-3					6.2 ± 0.8						End S1	*Streptomyces* sp.
20/07-4					2.6 ± 0.9			4.2 ± 0.8			End S1	*Streptomyces* sp.
20/07-9					4.4 ± 0.5						End S1	*Streptomyces* sp.
20/07-13				6.4 ± 0.9	12.8 ± 1.6						End S1	*Streptomyces* sp.
20/07-14				12.6 ± 0.9	8.2 ± 2.0						End S1	*Streptomyces* sp.
A47			6.3 ± 1.2	17.0 ± 1.2			10.4 ± 1.8		8.8 ± 1.1		End S1	*Streptomyces* sp.
A49				19.0 ± 2.5	5.0 ± 2.2		11.8 ± 1.9	7.6 ± 1.7	9.4 ± 0.9		End S1	*Streptomyces* sp.
A51				17.8 ± 0.8	7.6 ± 1.3				4.4 ± 0.5		End S1	*Pseudochrobactrum* sp.
A53				7.8 ± 1.9	6.6 ± 0.5				4.8 ± 0.4		End S1	*Streptomyces* sp.
A54		5.8 ± 2.4									End S1	*Streptomyces* sp.
A56			5.5 ± 1.3		11.0 ± 0.7		12.8 ± 1.3		11.0 ± 1.2		End S1	*Streptomyces* sp.
A57			4.5 ± 3.1		10.6 ± 0.5						End S1	*Brevundimonas* sp.
A60			7.6 ± 1.7		9.6 ± 0.9		12.4 ± 1.1		9.2 ± 0.8		End S1	*Brevundimonas* sp.
A61					4.8 ± 1.3						End S1	*Streptomyces* sp.

(Continued)

10.3389/fmicb.2025.1484219

TABLE 2 (Continued)

	Inhibition zone (mm)											
	Pathogenic fungi					Beneficial fungi						
Strain	Forc	Fp	Pc	Botry	Cg	Tl	Th	Ta1	Ta2	Paec	Soil sampling time origin	Identification
A62				6.8 ± 1.0	11.6 ± 1.5			4.4 ± 1.5			End S1	*Streptomyces* sp.
A63			4.0 ± 3.2		4.8 ± 1.8				6.2 ± 2.7		End S1	*Streptomyces* sp.
A83				5.8 ± 0.5	7.8 ± 1.0						Start S2	*Streptomyces* sp.
A88					8.4 ± 1.5						Start S2	*Streptomyces* sp.
A89				4.0 ± 1.7	8.6 ± 1.5						Start S2	*Streptomyces* sp.
A93				7.3 ± 1.5							Start S2	*Streptomyces* sp.
A94			9.0 ± 0.7								Start S2	*Bacillus* sp.
A95					8.4 ± 1.5						Start S2	*Streptomyces* sp.
A99				11.8 ± 1.3							Start S2	*Pseudochrobactrum* sp.
A100	9.8 ± 1.9	10.8 ± 1.5		18.0 ± 2.2	11.8 ± 1.9	13.4 ± 0.9		15.4 ± 0.5	15.8 ± 0.8	8.1 ± 3.0	Start S2	*Bacillus* sp.

Antagonistic activity was considered when the inhibition zone was ≥ 4 mm to any of the target fungus.

Cg: *Colletotrichum gloeosporioides*; Fp: *Fusarium proliferatum*; Forc: *Fusarium oxysporum f.* sp. *radicis-cucumerinum*; Bc: *Botrytis cinerea*; Pc: *Phytophthora capsici*; Th: *Trichoderma harzianum T-22*; Tl: *Trichoderma longibrachiatum*; Ta1: *Trichoderma asperellum*; Ta2: *Trichoderma atroviride*; Paec: *Paecilomyces lilacinus*; S1: season 1, 2019/2020; S2: season 2, 2020/2021.

10.3389/fmicb.2025.1484219

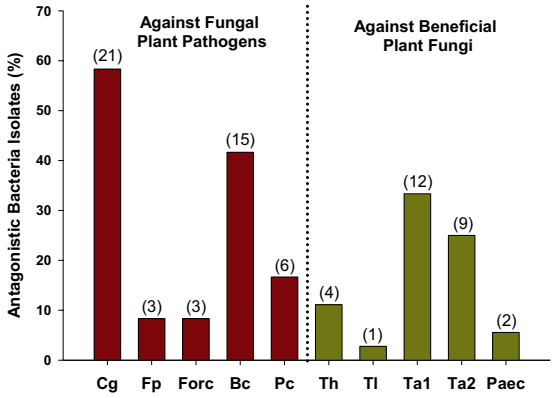

FIGURE 11
Soil-isolated bacteria with antagonism against the tested fungi. In total, 95 isolates were evaluated. Percentages expressed over the total bacteria that exhibited antagonism, which were 36. In brackets, the number of isolates with antagonism against each fungus. Only those with the inhibition distance equal to or greater than 4 mm to the target fungus were considered. Cg: *Colletotrichum gloeosporioides*; Fp: *Fusarium proliferatum*; Forc: *Fusarium oxysporum* f. sp. *radicis-cucumerinum*; Bc: *Botrytis cinerea*; Pc: *Phytophthora capsici*; Th: *Trichoderma harzianum* T-22; Tl: *Trichoderma longibrachiatum*; Ta1: *Trichoderma asperellum*; Ta2: *Trichoderma atroviride*; Paec: *Paecilomyces lilacinus*.

microorganisms involved in the nitrogen cycle and have been recognized as dominant denitrifiers in various environments, including soils (Fuka et al., 2007). In this regard, we identified ecological (functional) pathways related to the nitrogen cycle (nitrate and nitrite respiration, nitrate reduction, and ureolysis) that present a higher percentage of functional related sequences at the End of the Season compared to the Start of the Season, immediately after the treatments. As previously reported, alkeline hydrolyzable organic nitrogen content and soil organic carbon content are key factors that drive shifts in soil microbial composition and could also determine the observed changes in microbial functional communities formed at different successional stages (Dasgupta et al., 2024; Ding et al., 2024).

A relevant result of the present study is the presence of native bacteria with antagonistic properties against prevalent pathogenic fungi, but also against common beneficial fungi sourced from commercial products. Even a large number of these isolates exhibited antagonism against both pathogenic and beneficial fungi, thus highlighting the complexity of the edaphic system, an aspect often overlooked in agricultural soil management plans. In addition, isolates with antagonistic activity were detected at all sampling times throughout the study, both following the treatments performed and at the end of the crop season, which suggests that they are also present during the development of the crops. Among the native antagonistic bacteria (16S rRNA), *Streptomyces* was the dominant genus followed by *Bacillus*, while bacteria from the genera *Brevundimonas*, *Pseudochrobactrum*, *Stenotrophomonas*, and *Alcaligenes* also showed antagonism. Among them, *Streptomyces* spp. and *Bacillus* spp. are among the most studied biological control agents. Their role in the suppression of several plant pathogens has been well-documented and attributed to their production of a wide variety of bioactive secondary metabolites and enzymes, including antibiotics, bacteriocins, and volatile compounds (Alabouvette and Steinberg, 2006; Kunova et al., 2016; Zhang et al., 2023).

The evaluation of the specific soil management practices needed for developing and maintaining soil microbial functionality which favor DSS in cultivable lands is a highly complex issue that is difficult to decipher (Alabouvette and Steinberg, 2006). It must be considered that the complexity of the microbial interactions as well as the underlying mechanisms and microbial traits remain elusive for most disease suppressive soils (Gómez Expósito et al., 2017). In any case, in our study, isolates with antagonistic activity were detected at all sampling times, even after incorporating fresh sheep manure in summer followed by solarisation for 2 months. All the isolates used in the antagonism assays, were obtained from the thermophilic bacteria analyses performed in this study, and thus their presence is high in the evaluated soil, with populations ranging from millions to tens of millions of CFU/g dry soil. Thus, the soil management described in this study was compatible with, and possibly responsible for the high presence of these microorganisms in the soil of the greenhouse. This is a highly relevant information for the development of a soil suppressive to soil pathogens, but also for the use of certain commercial products containing BCO and other beneficial microorganisms for crops, as the presence of native bacteria with these properties can influence their effectiveness.

In conclusion, the results of this study show changes in the soil bacterial community and its functionality over the crop cycle following the application of sheep manure combined with summer solarisation in a Mediterranean greenhouse. The study reflects the presence of native bacteria with antagonistic properties inhabiting the mentioned biosolarised soils. Moreover, this fact also demonstrates the differential antagonistic ability of each isolate concerning the phytopathogenic or beneficial profile of the tested fungal species. These results are highly relevant for the application of agronomic soil management practices aimed at improving the natural suppressiveness of soils, to diseases caused by fungi and actinomycetes, as well as for the proper use of formulations based on beneficial fungi. However, further studies are necessary to elucidate whether the suppressive properties against soil-borne pathogens of the studied native bacteria are clearly manifested when considering the intricate interactions among soil, plant, microbiome, and environment. Additionally, these results should guide the development of commercial formulations with microorganisms that ensure farmers the establishment of these microorganisms in their soil and the derived benefits.

Data availability statement

The datasets and sequences from this study are available in the Zenodo open-access repository under the OPTIMSOIL project (PID2021-125545OR-C21): https://zenodo.org/records/15545241.

Author contributions

JM-G: Conceptualization, Data curation, Formal analysis, Investigation, Methodology, Software, Validation, Writing – original draft, Writing – review & editing. MC-G: Conceptualization, Funding acquisition, Investigation, Methodology, Project administration, Resources, Supervision, Validation, Writing – original draft, Writing – review & editing.

Funding

The author(s) declare that financial support was received for the research and/or publication of this article. Grant PID2021-125545OR-C21 funded by MICIU/AEI/10.13039/501100011033 and by "ERDF/EU."

Conflict of interest

The authors declare that the research was conducted in the absence of any commercial or financial relationships that could be construed as a potential conflict of interest.

Publisher's note

All claims expressed in this article are solely those of the authors and do not necessarily represent those of their affiliated organizations, or those of the publisher, the editors and the reviewers. Any product that may be evaluated in this article, or claim that may be made by its manufacturer, is not guaranteed or endorsed by the publisher.

Supplementary material

The Supplementary material for this article can be found online at: https://www.frontiersin.org/articles/10.3389/fmicb.2025.1484219/full#supplementary-material

References

Achmon, Y., Claypool, J. T., Fernández-Bayo, J. D., Hernandez, K., McCurry, D. G., Harrold, D. R., et al. (2020). Structural changes in bacterial and fungal soil microbiome components during biosolarization as related to volatile fatty acid accumulation. *Appl. Soil Ecol.* 153:103602. doi: 10.1016/j.apsoil.2020.103602

Adesina, M. F., Lembke, A., Costa, R., Speksnijder, A., and Smalla, K. (2007). Screening of bacterial isolates from various European soils for *in vitro* antagonistic activity towards *Rhizoctonia solani* and *fusarium oxysporum*: site- dependent composition and diversity revealed. *Soil Biol. Biochem.* 39, 2818–2828. doi: 10.1016/j.soilbio.2007.06.004

Águila-Carricondo, P., Román, R., Marín-Guirao, J. I., Cantón, Y., and de Cara, M. (2024). Native biocrust-cyanobacteria strains showing antagonism against three soilborne pathogenic fungi. *Pathogens* 13:579. doi: 10.3390/pathogens13070579

Akanmu, A. O., Babalola, O. O., Venturi, V., Ayilara, M. S., Adeleke, B. S., Amoo, A. E., et al. (2021). Plant disease management: leveraging on the plant-microbe-soil interface in the biorational use of organic amendments. *Front. Plant Sci.* 12:700507. doi: 10.3389/fpls.2021.700507

Alabouvette, C., Lemanceau, P., and Steinberg, C. (1993). Recent advances in the biological control of fusarium wilts. *Pestic. Sci.* 37, 365–373. doi: 10.1002/ps.2780370409

Alabouvette, C., and Steinberg, C. (2006). "The soil as a reservoir for antagonists to plant diseases" in An ecological and societal approach to biological control. eds. J. Eilenberg and H. M. T. Hokkanen, vol. *2* (Dordrecht the Netherlands: Springer), 123–144. doi: 10.1007/978-1-4020-4401-4_8

Amir, H., and Alabouvette, C. (1993). Involvement of soil abiotic factors in the mechanisms of soil suppressiveness to *fusarium* wilts. *Soil Biol. Biochem.* 25, 157–164. doi: 10.1016/0038-0717(93)90022-4

Anderson, M. J. (2001). A new method for non-parametric multivariate analysis of variance. *Austral Ecol.* 26, 32–46. doi: 10.1111/j.1442-9993.2001.01070

Andrews, S. (2010). FastQC: a quality control tool for high throughput sequence data; Cambridge: Babraham Bioinformatics, Babraham Institute. Available online at: http://www.bioinformatics.babraham.ac.uk/projects/fastqc/ (Accessed April 8, 2024).

Baker, K., and Cook, R. J. (1974). Biological control of plant pathogens. New York: WH Freeman and Company.

Bokulich, N. A., Kaehler, B. D., Rideout, J. R., Dillon, M., Bolyen, E., Knight, R., et al. (2018). Optimizing taxonomic classification of marker-gene amplicon sequences with QIIME 2's q2-feature-classifier plugin. *Microbiome* 6:90. doi: 10.1186/s40168-018-0470-z

Bolyen, E., Rideout, J. R., Dillon, M. R., Bokulich, N. A., Abnet, C. C., Al-Ghalith, G. A., et al. (2019). Reproducible, interactive, scalable and extensible microbiome data science using QIIME 2. *Nat. Biotechnol.* 37, 852–857. doi: 10.1038/s41587-019-0209-9

Bonanomi, G., Antignani, V., Capodilupo, M., and Scala, F. (2010). Identifying the characteristics of organic soil amendments that suppress soilborne plant diseases. *Soil Biol. Biochem.* 42, 136–144. doi: 10.1016/j.soilbio.2009.10.012

Bonanomi, G., Antignani, C., Pane, C., and Scala, F. (2007). Suppression of soil borne fungal diseases with organic amendments. *J. Plant Pathol.* 89, 311–324.

Bonanomi, G., Lorito, M., Vinale, F., and Woo, S. L. (2018). Organic amendments, beneficial microbes, and soil microbiota: toward a unified framework for disease suppression. *Annu. Rev. Phytopathol.* 56, 1–20. doi: 10.1146/annurev-phyto-080615-100046

Bond, W. W., and Favero, M. S. (1975). Thermal profile of a *Bacillus* species (ATCC 27380) extremely resistant to dry heat. *Appl. Microbiol.* 29, 859–860. doi: 10.1128/am.29.6.859-860.1975

Brizuela, A. M., De La Lastra, E., Marín-Guirao, J. I., Gálvez, L., De Cara-García, M., Capote, N., et al. (2020). Fusarium consortium populations associated with Asparagus crop in Spain and their role on field decline syndrome. *J. Fungi* 6:336. doi: 10.3390/jof6040336

Callahan, B. J., McMurdie, P. J., Rosen, M. J., Han, A. W., Johnson, A. J. A., and Holmes, S. P. (2016). DADA2: high-resolution sample inference from Illumina amplicon data. *Nat. Methods* 13, 581–583. doi: 10.1038/nmeth.3869

Castillo-Díaz, F. J., Belmonte-Ureña, L. J., Camacho-Ferre, F., and Tello Marquina, J. C. (2022). Biodisinfection as a profitable fertilization method for horticultural crops in the framework of the circular economy. *Agronomy* 12:521. doi: 10.3390/agronomy12020521

Castillo-Díaz, F. J., Marín-Guirao, J. I., Belmonte-Ureña, L. J., and Tello-Marquina, J. C. (2021). Effect of repeated plant debris reutilization as organic amendment on greenhouse soil fertility. *Int. J. Environ. Res. Public Health* 18:11544. doi: 10.3390/ijerph182111544

Chng, S., Cromey, M., Dodd, S., Stewart, A., Butler, R. C., and Jaspers, M. V. (2015). Take-all decline in New Zealand wheat soils and the microorganisms associated with the potential mechanisms of disease suppression. *Plant Soil* 397, 239–259. doi: 10.1007/s11104-015-2620-4

Clarke, K. R., and Gorley, R. N. (2006). Primer v6: User manual or tutorial. Plymouth, UK: Plymouth Marine Laboratory, 190.

Condori, S., Fernández, P., and Valderrama, M. R. (2019). Aislamiento y caracterización de *Streptomyces* spp. rizosféricos promotores del crecimiento vegetal. *Idesia* 37, 109–116. doi: 10.4067/S0718-34292019000200109

Crawford, D., Lynch, J., Whipps, J., and Ousley, M. (1993). Isolation and characterization of actinomycete antagonists of a fungal root pathogen. *Appl. Environ. Microbiol.* 59, 3899–3905. doi: 10.1128/aem.59.11.3899-3905.1993

Dasgupta, D., Richardson, A. E., Camuy-Vélez, L. A., Kirkby, C., Kirkegaard, J. A., and Banerjee, S. (2024). Microbial dynamics during in-situ organic matter decomposition reveals the importance of keystone taxa in the core microbiome. *Appl. Soil Ecol.* 199:105396. doi: 10.1016/j.apsoil.2024.105396

Ding, M., Dai, H., He, Y., Liang, T., Zhai, Z., Zhang, S., et al. (2024). Continuous cropping system altered soil microbial communities and nutrient cycles. *Front. Microbiol.* 15:1374550. doi: 10.3389/fmicb.2024.1374550

Eberlein, C., Heuer, H., Vidal, S., and Westphal, A. (2016). Microbial communities in *Globodera pallida* females raised in potato monoculture soil. *Phytopathology* 106, 581–590. doi: 10.1094/PHYTO-07-15-0180-R

Edwards, J. L. Jr., Busta, F. F., and Speck, M. L. (1965). Thermal inactivation characteristics of *Bacillus subtilis* spores at ultrahigh temperatures. *Appl. Microbiol.* 13, 851–857. doi: 10.1128/am.13.6.851-857.1965

Elder, D. J., and Kelly, D. J. (1994). The bacterial degradation of benzoic acid and benzenoid compounds under anaerobic conditions: unifying trends and new perspectives. *FEMS Microbiol. Rev.* 13, 441–468. doi: 10.1111/j.1574-6976.1994.tb00061.x

Emelyanov, V. V. (2001). Evolutionary relationship of Rickettsiae and mitochondria. *FEBS Lett.* 501, 11–18. doi: 10.1016/S0014-5793(01)02618-7

Ewels, P., Magnusson, M., Lundin, S., and Käller, M. (2016). MultiQC: summarize analysis results for multiple tools and samples in a single report. *Bioinformatics* 32, 3047–3048. doi: 10.1093/bioinformatics/btw354

Fida, T. T., Chen, C., Okpala, G., and Voordouw, G. (2016). Implications of limited thermophilicity of nitrite reduction for control of sulfide production in oil reservoirs. *Appl. Environ. Microbiol.* 82, 4190–4199. doi: 10.1128/AEM.00599-16

Fuka, M. M., Braker, S. H. G., and Philippot, L. (2007). "Molecular tools to assess the diversity and density of denitrifying Bacteria in their habitats" in Biology of the nitrogen cycle. eds. H. Bothe, S. J. Ferguson and W. E. Newton (Amsterdam, Netherlands: Elsevier), 313–330.

Garbeva, P., Postma, J., van Veen, J. A., and van Elsas, J. D. (2006). Effect of above-ground plant species on soil microbial community structure and its impact on suppression of *Rhizoctonia solani* AG3. *Environ. Microbiol.* 8, 233–246. doi: 10.1111/j.1462-2920.2005.00888.x

Garbeva, P., van Veen, J. A., and van Elsas, J. D. (2004). Microbial diversity in soil: selection microbial populations by plant and soil type and implications for disease suppressiveness. *Annu. Rev. Phytopathol.* 42, 243–270. doi: 10.1146/annurev.phyto.42.012604.135455

García, C., Céspedes, A. J., Páez, F. C., Cano, M., Martín, E., and Parra, S. (2024). Trends in soil disinfection in greenhouses in southeastern Spain. *Acta Hortic.* 1410, 51–56. doi: 10.17660/ActaHortic.2024.1410.8

García-Raya, P., Ruiz-Olmos, C., Marín-Guirao, J. I., Asensio-Grima, C., Tello-Marquina, J. C., and de Cara-García, M. (2019). Greenhouse soil Biosolarization with tomato plant debris as a unique fertilizer for tomato crops. *Int. J. Environ. Res. Public Health* 16:279. doi: 10.3390/ijerph16020279

Giagnocavo, C., de Cara-García, M., González, M., Juan, M., Marín-Guirao, J. I., Mehrabi, S., et al. (2022). Reconnecting farmers with nature through agroecological transitions: interacting niches and experimentation and the role of agricultural knowledge and innovation systems. *Agriculture* 12:137. doi: 10.3390/agriculture12020137

Gómez Expósito, R., de Bruijn, I., Postma, J., and Raaijmakers, J. M. (2017). Current insights into the role of rhizosphere Bacteria in disease suppressive soils. *Front. Microbiol.* 8:2529. doi: 10.3389/fmicb.2017.02529

Hall, T. A. (1999). Bioedit: a user-friendly biological sequence alignment editor and analysis program for windows 95/98/NT. *Nucleic Acids Symp. Ser.* 41, 95–98.

Hartmann, M., Frey, B., Mayer, J., Mader, P., and Widmer, F. (2015). Distinct soil microbial diversity under long-term organic and conventional farming. *ISME J.* 9, 1177–1194. doi: 10.1038/ismej.2014.210

Hemkemeyer, M., Schwalb, S. A., Berendonk, C., Geisen, S., Heinze, S., Joergensen, R. G., et al. (2024). Potato yield and quality are linked to cover crop and soil microbiome, respectively. *Biol. Fertil. Soils* 60, 525–545. doi: 10.1007/s00374-024-01813-0

Herlemann, D. P., Labrenz, M., Jürgens, K., Bertilsson, S., Waniek, J. J., and Andersson, A. F. (2011). Transitions in bacterial communities along the 2000 km salinity gradient of the Baltic Sea. *ISME J.* 5, 1571–1579. doi: 10.1038/ismej.2011.41

Hoitink, H. A. J., and Boehm, M. J. (1999). Biocontrol within the context of soil microbial communities: a substrate-dependent phenomenon. *Annu. Rev. Phytopathol.* 37, 427–446. doi: 10.1146/annurev.phyto.37.1.427

Hoitink, H. A. J., Stone, A. G., and Han, D. Y. (1997). Suppression of plant disease by composts. *HortScience* 32, 184–187.

Jayaraman, S., Naorem, A., Lal, R., Dalal, R. C., Sinha, R. K., Patra, A. K., et al. (2021). Disease-suppressive soils—beyond food production: a critical review. *J. Soil Sci. Plant Nutr.* 21, 1437–1465. doi: 10.1007/s42729-021-00451-x

Kang, H., Chai, A., Lin, Z., Shi, Y., Xie, X., Li, L., et al. (2024). Deciphering differences in microbial community diversity between Clubroot-diseased and healthy soils. *Microorganisms* 12:251. doi: 10.3390/microorganisms12020251

Koller, M., Maršálek, L., de Sousa Dias, M. M., and Braunegg, G. (2017). Producing microbial polyhydroxyalkanoate (PHA) biopolyesters in a sustainable manner. *New Biotechnol.* 37, 24–38. doi: 10.1016/j.nbt.2016.05.001

Kunova, A., Bonaldi, M., Saracchi, M., Pizzatti, C., Chen, X., and Cortesi, P. (2016). Selection of *Streptomyces* against soil borne fungal pathogens by a standardized dual culture assay and evaluation of their effects on seed germination and plant growth. *BMC Microbiol.* 16:272. doi: 10.1186/s12866-016-0886-1

Lal, R. (2020). Managing soil quality for humanity and the planet. *Front. Agricult. Sci. Eng.* 7, 251–253. doi: 10.15302/J-FASE-2020329

Li, L., Xu, M., Eyakub Ali, M., Zhang, W., Duan, Y., and Li, D. (2018). Factors affecting soil microbial biomass and functional diversity with the application of organic amendments in three contrasting cropland soils during a field experiment. *PLoS One* 13:e0203812. doi: 10.1371/journal.pone.0203812

Louca, S., Parfrey, L. W., and Doebeli, M. (2016). Decoupling function and taxonomy in the global ocean microbiome. *Science* 353, 1272–1277. doi: 10.1126/science.aaf4507

Margalef, D. R. (1958). Information theory in ecology. *Gen. Syst.* 3, 36–71.

Marín-Guirao, J. I., De Cara-García, M., Crisol-Martínez, E., Gómez-Tenorio, M. Á., García-Raya, P., and Tello-Marquina, J. C. (2019a). Association of plant development to organic matter and fungal presence in soils of horticultural crops. *Ann. Appl. Biol.* 174, 339–348. doi: 10.1111/aab.12501

Marín-Guirao, J. I., de Cara-García, M., and Tello-Marquina, J. C. (2019b). Effect of soil biodisinfection on soil fungal communities associated to horticultural crops. *Ecosistemas* 28, 63–72. doi: 10.7818/ECOS.1708

Marín-Guirao, J. I., García-García, M. C., Martín-Expósito, E., and de Cara-García, M. (2023a). Continued organic fertigation after basal manure application does not impact soil fungal communities, tomato yield or soil fertility. *Microorganisms* 11:1715. doi: 10.3390/microorganisms11071715

Marín-Guirao, J. I., Páez-Cano, F. C., García-García, M. C., Katsoulas, N., and de Cara-García, M. (2023b). Evaluation of copper-free alternatives to control grey mould in organic Mediterranean greenhouse tomato production. *Agronomy* 13:137. doi: 10.3390/agronomy13010137

Mazzola, M. (2002). Mechanisms of natural soil suppressiveness to soilborne diseases. *Antonie Van Leeuwenhoek* 81, 557–564. doi: 10.1023/A:1020557523557

Mazzola, M., and Freilich, S. (2016). Prospects for biological soil-borne disease control: application of indigenous versus synthetic microbiomes. *Phytopathology* 107, 256–263. doi: 10.1094/PHYTO-09-16-0330-RVW

McMurdie, P. J., and Holmes, S. (2013). Phyloseq: an R package for reproducible interactive analysis and graphics of microbiome census data. *PLoS One* 8:e61217. doi: 10.1371/journal.pone.0061217

Mendes, R., Kruijt, M., de Bruijn, I., Dekkers, E., van der Voort, M., and Schneider, J. H. M. (2011). Deciphering the rhizosphere microbiome for disease-suppressive bacteria. *Science* 332, 1097–1100. doi: 10.1126/science.1203980

Miljaković, D., Marinković, J., and Balešević-Tubić, S. (2020). The significance of *Bacillus* spp. in disease suppression and growth promotion of field and vegetable crops. *Microorganisms* 8:1037. doi: 10.3390/microorganisms8071037

Moore, K. R., Magnabosco, C., Momper, L. M., Gold, D. A., Bosak, T., and Fournier, G. P. (2019). An expanded ribosomal phylogeny of Cyanobacteria supports a deep placement of plastids. *Front. Microbiol.* 10:1612. doi: 10.3389/fmicb.2019.01612

Ni, H., Zong, R., Sun, J., Wu, Y., Yu, L., Liu, Y., et al. (2022). Response of bacterial community to the occurrence of Clubroot disease in Chinese cabbage. *Front. Microbiol.* 13:922660. doi: 10.3389/fmicb.2022.922660

Pankhurst, C. E., and Lynch, J. M. (1995). The role of soil microbiology in sustainable intensive agriculture. *Adv. Plant Pathol.* 11, 229–247.

Philipp, B., and Schink, B. (2000). Two distinct pathways for anaerobic degradation of aromatic compounds in the denitrifying bacterium *Thauera aromatica* strain AR-1. *Arch. Microbiol.* 173, 91–96. doi: 10.1007/s002039900112

Pielou, E. C. (1969). An introduction to mathematical ecology. New York: Wiley-Inter-Science.

Postma, J., and Schilder, M. T. (2015). Enhancement of soil suppressiveness against *Rhizoctonia solani* in sugar beet by organic amendments. *Appl. Soil Ecol.* 94, 72–79. doi: 10.1016/j.apsoil.2015.05.002

Pullman, G. S., De Vay, J. E., and Garber, R. H. (1981). Soil solarization and thermal death: algorithmic relationship between time and temperature for four soilborne plant pathogens. *Phytopathology* 71, 959–964.

Quast, C., Pruesse, E., Yilmaz, P., Gerken, J., Schweer, T., Yarza, P., et al. (2013). The SILVA ribosomal RNA gene database project: improved data processing and web-based tools. *Nucleic Acids Res.* 41, D590–D596. doi: 10.1093/nar/gks1219

Raaijmakers, J. M., Paulitz, T. C., Steinberg, C., Alabouvette, C., and Moenne-Loccoz, Y. (2009). The rhizosphere: a playground and battlefield for soilborne pathogens and beneficial microorganisms. *Plant Soil* 321, 341–361. doi: 10.1007/s11104-008-9568-6

R-Team-Core (2019). R: a language and environment for statistical computing. R Foundation for Statistical Computing, Vienna. Available online at: https://www.R-project.org/.

Sagova-Mareckova, M., Omelka, M., and Kopecky, J. (2023). The Golden goal of soil management: disease-suppressive soils. *Phytopathology* 113, 741–752. doi: 10.1094/PHYTO-09-22-0324-KD

Schlatter, D., Kinkel, L., Thomashow, L., Weller, D., and Paulitz, T. (2017). Disease suppressive soils: new insights from the soil microbiome. *Phytopathology* 107, 1284–1297. doi: 10.1094/PHYTO-03-17-0111-RVW

Schneider, R. W. (1982). Suppressive soils and plant disease. St Paul, MN: American Phytopathological Society.

Segata, N., Izard, J., Waldron, L., Gevers, D., Miropolsky, L., Garrett, W. S., et al. (2011). Metagenomic biomarker discovery and explanation. *Genome Biol.* 12:R60. doi: 10.1186/gb-2011-12-6-r60

Shannon, C. E., and Weaver, W. (1949). The mathematical theory of communication. Urbana, IL: University Illinois Press.

Shea, E. A., Fernández-Bayo, J. D., Hodson, A. K., Parr, A. E., Lopez, E., Achmon, Y., et al. (2022). Biosolarization restructures soil bacterial communities and decreases parasitic nematode populations. *Appl. Soil Ecol.* 172:104343. doi: 10.1016/j.apsoil.2021.104343

Siegel-Hertz, K., Edel-Hermann, V., Chapelle, E., Terrat, S., Raaijmakers, J. M., and Steinberg, C. (2018). Comparative microbiome analysis of a fusarium wilt suppressive soil and a fusarium wilt conducive soil from the Chateaurenard region. *Front. Microbiol.* 9:568. doi: 10.3389/fmicb.2018.00568

Simpson, E. H. (1949). Measurement of diversity. *Nature* 163:688. doi: 10.1038/163688a0

Sun, R., Zhang, X., Guo, X., Wang, D., and Chu, H. (2015). Bacterial diversity in soils subjected to long-term chemical fertilization can be more stably maintained with the addition of livestock manure than wheat straw. *Soil Biol. Biochem.* 88, 9–18. doi: 10.1016/j.soilbio.2015.05.007

Tang, T., Sun, X., Liu, Q., Dong, Y., and Zha, M. (2023). Treatment with organic manure inoculated with a biocontrol agent induces soil bacterial communities to inhibit tomato fusarium wilt disease. *Front. Microbiol.* 13:1006878. doi: 10.3389/fmicb.2022.1006878

Tello, J. C., Vares, F., and Lacasa, A. (1991). "Análisis de muestras" in Manual de Laboratorio. Diagnóstico de Hongos. Bacterias y Nematodos Fitopatógenos (Madrid: MAPA), 9–48.

Vido, J. J., Wang, X., Sale, P. W. G., Celestina, C., Shindler, A. E., and Hayden, H. L. (2024). Bacterial community shifts occur primarily through rhizosphere expansion in response to subsoil amendments. *Environ. Microbiol.* 26:e16587. doi: 10.1111/1462-2920.16587

Weller, D. M., Raaijmakers, J. M., Gardener, B. B., and Thomashow, L. S. (2002). Microbial populations responsible for specific soil suppressiveness. *Annu. Rev. Phytopathol.* 40, 309–348. doi: 10.1146/annurev.phyto.40.030402.110010

Xiong, W., Zhao, Q., Zhao, J., Xun, W., Li, R., Zhang, R., et al. (2015). Different continuous cropping spans significantly affect microbial community membership and structure in a vanilla-grown soil as revealed by deep pyrosequencing. *Microb. Ecol.* 70, 209–218. doi: 10.1007/s00248-014-0516-0

Yang, L., Muhadesi, J. B., Wang, M. M., Wang, B. J., Liu, S. J., and Jiang, C. Y. (2018). *Thauera hydrothermalis* sp. *nov.*, a thermophilic bacterium isolated from hot spring. *Int. J. Syst. Evol. Microbiol.* 68, 3163–3168. doi: 10.1099/ijsem.0.002960

Zhang, N., Wang, Z., Shao, J., Xu, Z., Liu, Y., Xun, W., et al. (2023). Biocontrol mechanisms of *Bacillus*: improving the efficiency of green agriculture. *Microb. Biotechnol.* 16, 2250–2263. doi: 10.1111/1751-7915.14348

Frontiers in Microbiology

Explores the habitable world and the potential of microbial life

The largest and most cited microbiology journal which advances our understanding of the role microbes play in addressing global challenges such as healthcare, food security, and climate change.

Discover the latest Research Topics

See more →

Frontiers

Avenue du Tribunal-Fédéral 34
1005 Lausanne, Switzerland
frontiersin.org

Contact us

+41 (0)21 510 17 00
frontiersin.org/about/contact